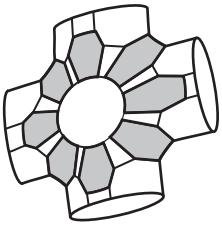

ARS MATHEMATICA CONTEMPORANEA

Volume 7, Number 2, Fall/Winter 2014, Pages 263–536

Covered by:
Mathematical Reviews
Zentralblatt MATH
COBISS
SCOPUS
Science Citation Index-Expanded (SCIE)
Web of Science
ISI Alerting Service
Current Contents/Physical, Chemical & Earth Sciences (CC/PC & ES)

The University of Primorska

The Society of Mathematicians, Physicists and Astronomers of Slovenia
The Institute of Mathematics, Physics and Mechanics

The publication is partially supported by the Slovenian Research Agency from the Call for co-financing of scientific periodical publications.

The curse of the impact factor

Last year our journal received the financial support of the Slovenian National Research Agency (ARRS). An important parameter in determining the level of support is the journal's impact factor for the previous year. Luckily, our official impact factor for the year 2012 was 0.67, which for the first time put AMC into the second quartile among mathematical journals covered by the ISI. The flow of manuscripts reaching our editorial office has increased significantly, and the acceptance rate of papers submitted to the AMC has dropped from over 75% in the initial years, to under 20% currently.

The careers of many young and emerging mathematicians around the world now depend on the bibliometric parameters of the journals in which their papers appear. In some cases, publishing in high impact factor journals brings substantial rewards to the authors. They climb more quickly and higher up the academic scale, they can obtain tenure earlier, their access to grants is secured, and the institutions they work for are financially rewarded.

Also in many jurisdictions, the large volume of applications and competition for money between different research fields has resulted in a modification of selection and ranking procedures, using bibliometric data in order to give a greater impression of objectivity. Unfortunately, in a large number of cases this reduces to a single parameter, which is the journal impact factor.

For these reasons we were anxious to see the release of the 2013 impact factor, which is announced in the Journal Citation Report. We were quite disappointed when we found out that the citation figures issued in the JCR did not appear to match the figures in the ISI database. The ISI database shows 27 citations in the year 2013 for AMC articles published in the years 2011 and 2012, but the JCR shows only 22. When we asked about the difference, we were advised that 5 citations (about 20% of the total) came in too late to be used. Apparently the JCR is taken as a snapshot in time, but does not give the true figure, as it omits citations made in publications in the given year but after the snapshot is taken. We noticed several problems with such a policy. The time when the snapshot is taken is not announced in advance. However it is certainly taken several months before the release of the JCR. Nevertheless it makes it impossible for an independent observer to check the correctness of figures published in the JCR. In our case the doubts of impartiality and objectivity of the published impact factors remain.

Let n denote the number of citations in the JCR and let N be the corresponding number of citations in the database. Define $\lambda = (N-n)/n$ to be the *JCR citation loss* of a journal. For ACM for the year 2013 the citation loss was $\lambda = 5/22 = 0.227$. We computed λ for several comparable journals from a well-known commercial publisher. And they were much lower. This questions the validity and reliability of the JCR and the impact factor itself, in an era when so many decisions have become so dependent on it.

Of course there are other well known (and well-documented) flaws in the use of citations and impact factors, stemming from the fact that they are not solely a measure of impact, but are influenced by so many other things such as citation culture in the discipline or sub-discipline, numbers of authors per paper, trends (and 'hot' topics), and even mistakes made and corrected. It seems that there is stronger correlation between impact and power than impact and quality.

We are trying to convince our sponsors that the impact factor should not be given too much weight in any formula or process for deciding on the amount of financial support for scientific publications. Our greater worry is that misuse of a flawed impact indicator managed by a profit-oriented private company may have unjustified impact on the evaluation of scientific quality in publicly funded research. We believe that learned societies should have greater role in this process. In mathematics, AMS with MathSciNet and EMS with Zentralblatt are more than adequate authorities to measure impact of research in mathematics. Unfortunately we are not aware of any learned society that would be able to offer comparable services for the science community at large.

Dragan Marušič and Tomaž Pisanski
Editors In Chief

Contents

Volume 7, Number 2, Fall/Winter 2014, Pages 263–536

ARS MATHEMATICA CONTEMPORANEA

Also available at http://amc-journal.eu
ISSN 1855-3966 (printed edn.), ISSN 1855-3974 (electronic edn.)
ARS MATHEMATICA CONTEMPORANEA 7 (2014) 263–280

Efficient enumeration of rooted maps of a given orientable genus by number of faces and vertices

Timothy R. S. Walsh

Department of Computer Science, University of Quebec in Montreal (UQAM), P.O. Box 8888, Station A, Montreal, Quebec, Canada, HC3-3P8

Alain Giorgetti *

Department of Computer Science for Complex Systems, FEMTO-ST Institute (UMR 6174), University of Franche-Comté (UFC), 16 route de Gray, 25030 Besançon, France

Received 11 February 2011, accepted 1 March 2013, published online 7 May 2013

Abstract

We simplify the recurrence satisfied by the polynomial part of the generating function that counts rooted maps of positive orientable genus g by number of vertices and faces. We have written an optimized program in C++ for computing this generating function and constructing tables of numbers of rooted maps, and we describe some of these optimizations here. Using this program we extended the enumeration of rooted maps of orientable genus g by number of vertices and faces to $g = 4$, 5 and 6 and by number of edges to $g = 5$ and 6 and conjectured a further simplification of the generating function that counts rooted maps by number of edges. Our program is documented and available on request, allowing anyone with a sufficiently powerful computer to carry the calculations even further.

Keywords: Efficient enumeration, rooted maps, orientable genus, generating functions

Math. Subj. Class.: 05C30, 05A15

1 Introduction: definitions and history

A *map* is defined topologically as a 2-cell imbedding of a connected graph, loops and multiple edges allowed, in a 2-dimensional surface. The *faces* of a map are the connected components of the complement of the graph in the surface. In this article the surface is

*Corresponding author.
E-mail addresses: walsh.timothy@uqam.ca (Timothy R. S. Walsh), alain.giorgetti@femto-st.fr (Alain Giorgetti)

assumed to be without boundary and orientable, with an orientation already attributed to it (clockwise, say), so that it is completely described by a non-negative integer g, its *genus*. For short, a map on a surface of genus g will be called a *genus-g map*. A *planar map* is a genus-0 map (a map on a sphere) and a *toroidal map* is a genus-1 map (a map on a torus or donut). If a map on a surface of genus g has v vertices, e edges and f faces, then by the Euler-Poincaré formula [7, chap. 9]

$$v - e + f = 2(1 - g). \tag{1.1}$$

Two maps are *equivalent* if there is an orientation-preserving homeomorphism between their imbedding surfaces that takes the vertices, edges and faces of one map into the vertices, edges and faces of the other. A *dart* of a map or graph is a semi-edge. A loop is assumed to be incident twice with the same vertex, so that every edge, whether or not it is a loop, is incident to two darts. The *degree* of a vertex is the number of darts incident to it. The face incident to a dart d is the face incident to the edge containing d and on the left of an observer on d facing away from the vertex incident to d and the degree of a face is the number of darts incident to it. A *rooted map* is a map with a distinguished dart, its *root*. Two rooted maps are equivalent if there is an orientation-preserving homeomorphism between their imbedding surfaces that takes the vertices, edges, faces and the root of one map into the vertices, edges, faces and the root of the other. A *combinatorial map* is a connected graph with a cyclic order imposed on the darts incident to each vertex, representing the order in which the darts of a (topological) map are encountered during a rotation around the vertex according to the orientation of the imbedding surface. The darts incident to a face are encountered by successive application of the following pair of actions: go from the current dart to the dart on the other end of the same edge and then to the next dart incident to the same vertex according to the cyclic order. In this way the faces of a combinatorial map can be counted, so that its genus can be calculated from (1.1). Two combinatorial maps are equivalent if they are related by a map isomorphism – a graph isomorphism that preserves this cyclic order – with an analogous definition for the equivalence of two rooted combinatorial maps.

It is worth noting that rooted combinatorial maps with e edges are in one-to-one correspondence with torsion-free subgroups of index $2e$ in the triangle group $\Delta(\infty, 2, \infty) = \langle x, y, z | y^2 = xyz = 1 \rangle \cong Z * Z_2$ [12]. Rooted combinatorial maps are indeed a permutation representation of these groups. Details about this correspondence may be found e.g. in [13].

By *enumerating* maps with a given set of properties, whether rooted or not, we mean counting the number of equivalence classes of maps with these properties. It was shown in [12] that each equivalence class of topological maps is uniquely defined by an equivalence class of combinatorial maps; so for the purposes of enumeration, the term "map" can be taken to mean "combinatorial map".

Let $m_g(v, f)$ be the number of rooted genus-g maps with v vertices and f faces. By face-vertex duality, this number is equal to the number $m_g(f, v)$ of rooted genus-g maps with f vertices and v faces. The generating function that counts rooted genus-g maps is the following formal power series in two variables u and w:

$$M_g(w, u) = \sum_{v,f \geq 1} m_g(v, f) w^v u^f. \tag{1.2}$$

Rooted maps were introduced in [15] because they are easier to count than unrooted

maps; this is because only the trivial map automorphism preserves the root [16], so that rooted maps can be counted without considering map automorphisms. In [15], W. T. Tutte found a closed-form formula for the number of rooted planar maps with n edges. In [16], he found a parametric system of equations defining $M_0(w,u)$. In [1] D. Arquès obtained the simpler expression

$$M_0(w,u) = pq(1-2p-2q) \tag{1.3}$$

with the parameters p and q defined by

$$w = p(1-p-2q) \tag{1.4}$$

and

$$u = q(1-2p-q), \tag{1.5}$$

where $p = q = 0$ when $w = u = 0$. In [16], a recursive formula was found for the number of rooted planar maps given the number of vertices, the number of edges, and the degree of the face containing the root; these numbers of maps were then added over all possible degrees of this face and the result expressed in terms of generating functions. In [17], the first author generalized this method to obtain a recursive formula for the number of maps of genus g with a distinguished dart in each vertex given the number of vertices and the degree of each one; these numbers were then multiplied by the appropriate factor and added over all possible non-increasing sequences of vertex-degrees summing to $2e$ to obtain the number of rooted maps of genus g with e edges and v vertices. A table of these numbers of maps with up to 14 edges appears in [17] (see [19] for a published account of this work and a table of maps with up to 11 edges) but no attempt was made there to express this result in terms of generating functions. We note here that a similar generalization in which the degrees of all the faces are known but only some of them have a distinguished edge on their boundary, and these faces must be of degree at least 3, appears in [8], where it is attributed to Tutte under the name of Tutte's recursion equations.

In [5] an improvement on the method of [17] was introduced: to count rooted genus-g maps it is sufficient to know the degree of the first $g+1$ vertices and to distinguish a dart of only the first vertex as the root, thus reducing the number of maps that have to be considered. Using doubly-rooted maps, D. Arquès [2] obtained the analogue of (1.3) for toroidal maps:

$$M_1(w,u) = \frac{pq\,(1-p-q)}{\left[(1-2p-2q)^2 - 4pq\right]^2}. \tag{1.6}$$

From this result, he obtained a closed-form formula for the number of rooted toroidal maps with e edges and another one for the number of rooted toroidal maps with v vertices and f faces. In [6] a generating function was obtained for the number of rooted maps of genus 2 and 3 with e edges.

In [9] the second author generalized (1.6) and obtained a general form for the generating function $M_g(w,u)$ counting rooted maps of any genus $g > 0$:

$$M_g(w,u) = \frac{pq\,(1-p-q)\,P_g(p,q)}{\left[(1-2p-2q)^2 - 4pq\right]^{5g-3}}, \tag{1.7}$$

where $P_g(p,q)$ is a symmetric polynomial in p and q of total degree bounded by $6g-6$ with integral coefficients (in what follows, unless otherwise specified, all the polynomials defined here are polynomials in p and q).

Let us now briefly explain the interest of this result for rooted map counting. In [3, 9] the polynomials $P_g[p,q]$ were calculated for $g = 2$ and 3. In this article we extend this calculation to $g = 4$, 5 and 6. To derive the generating function $M_g(w,u)$ from $P_g[p,q]$, we compute p and q as power series in w and u iteratively from (1.4) and (1.5) and then we replace p and q by their respective power series in (1.7) to obtain $M_g(w,u)$. By (1.2) the number of rooted maps of genus g with v vertices and f faces is the coefficient of $w^v u^f$ in $M_g(w,u)$. In this way we enumerate rooted maps of genus 4, 5 and 6 with v vertices and f faces for any v and f greater than or equal to 1.

The polynomial P_g in (1.7) is defined in terms of another polynomial T_g of degree bounded by $10g-8$ by

$$P_g = \frac{T_g}{(1-p)^{4g-2}}, \tag{1.8}$$

and that polynomial, in turn, is defined in terms of a family of polynomials $R_g(n_1,\dots,n_r)$ in p and q by

$$T_g = R_{g-1}(0,0) + \sum_{j=1}^{g-1} q(1-p-q)R_j(0)R_{g-j}(0). \tag{1.9}$$

The degree of the polynomial $R_g(n_1,\dots,n_r)$ is defined by the equation

$$\deg R_g(n_1,\dots,n_r) = 2(n_1+\dots+n_r) + 7r + 10g - 12. \tag{1.10}$$

The polynomials $R_g(n_1,\dots,n_r)$ are defined recursively in terms of several other families of polynomials and a recursively-defined family of rational functions of p and q. We have two finite families of polynomials in p alone defined by the following two sets of equations.

$$\begin{gathered} K_0(p) = -p; \qquad K_1(p) = -1-p; \qquad K_2(p) = -1; \\ K_m(p) = 0 \text{ for all } m \geq 3. \end{gathered} \tag{1.11}$$

$$\begin{gathered} L_0(p) = -p; \qquad L_1(p) = -1-2p; \\ L_2(p) = -2-p; \qquad L_3 = -1; \\ L_k(p) = 0 \text{ for all } k \geq 4. \end{gathered} \tag{1.12}$$

In what follows, the parameter p will be omitted, so that these polynomials will be referred to as K_m and L_k. We then have two polynomials H and J (in p and q) defined by

$$J = q(1-p-q) \tag{1.13}$$

and

$$H = (1-2p-2q)^2 - 4pq. \tag{1.14}$$

Finally we have an infinite family $(E_k)_{k\geq 1}$ of rational functions of p and q, all but the first two of which are polynomials, defined recursively by

$$\begin{gathered} E_1 = \frac{1}{2J(1-p)^2}; \\ E_2 = \frac{-p-4q+2p^2+4q^2+4pq}{2J(1-p)^2}; \\ E_3 = -1; \\ E_k = -J(1-p)^2 \textstyle\sum_{i=2}^{i=k-1} E_i E_{k+1-i} \text{ for all } k \geq 4. \end{gathered} \tag{1.15}$$

To make the recursive definition of the polynomials $R_g(n_1,\ldots,n_r)$ comprehensible, we first explain the abbreviations and conventions we use. For any positive integer r, $[r]$ denotes the sequence $(2,\ldots,r)$ if $r \geq 2$ and the empty sequence if $r = 1$. For any subsequence X of $[r]$, $[r]-X$ denotes the subsequence of the elements of $[r]$ that are not in X. For any sequence $(n_2,\ldots,n_r)$ of integers, N_X denotes the sequence of those n_i such that i is in X and N_j denotes the sequence $(n_2,\ldots,n_{j-1},n_{j+1},\ldots,n_r)$. By convention, a sum over an empty domain is equal to zero.

The polynomials $R_0(n_1)$ are not defined. The anchor of this recursive definition is

$$R_0(0,0) = (1-p)^2. \tag{1.16}$$

If $g = 0$ and $r = 2$ but $(n_1,n_2) \neq (0,0)$, then we have

$$\begin{aligned} R_0(n_1,n_2) &= (1-p)^2\left(-n_2 H E_{n_1+n_2+2} - (n_2+1)E_{n_1+n_2+3}\right) \\ &\quad +2J(1-p)^2 \sum_{\substack{i+j+k=n_1+1 \\ i>0,\, k<n_1}} (-1)^{j+1} H^j E_i R_0(k,n_2). \end{aligned} \tag{1.17}$$

We note that (1.16) is a special case of (1.17) where $n_1 = n_2 = 0$.

If $(g,r) \neq (0,2)$, then

$$R_g(n_1,\ldots,n_r) = \text{term}_1 + \text{term}_2 + \text{term}_3 + \text{term}_4, \tag{1.18}$$

where

$$\text{term}_1 = 2J(1-p)^2 \sum_{\substack{i+j+k=n_1+1 \\ i>0,\, k<n_1}} (-1)^{j+1} H^j E_i R_g(k,n_2,\ldots,n_r) \tag{1.19}$$

(we note that the second line of (1.17) is a special case of (1.19) where $g = 0$ and $r = 2$),

$$\text{term}_2 = J \sum_{\substack{k+l+m=n_1+1 \\ 0\leq j\leq g \\ X\subseteq[r] \\ (j,X)\neq(0,\emptyset) \\ (j,X)\neq(g,[r])}} K_m H^m R_j(k,N_X) R_{g-j}(l,N_{[r]-X}), \tag{1.20}$$

$$\text{term}_3 = \sum_{i+j+m=n_1+1} K_m H^m R_{g-1}(i,j,N_{[r]}) \tag{1.21}$$

and

$$\text{term}_4 = \sum_{j=2}^{r} \begin{pmatrix} n_j \sum_{k+l=n_1+n_j+2} L_k H^{k+1} R_g(l,N_j) \\ +(n_j+1)\sum_{k+l=n_1+n_j+3} L_k H^k R_g(l,N_j) \end{pmatrix}. \tag{1.22}$$

It was shown in [9] that each polynomial $R_g(n_1,\ldots,n_r)$ is symmetric in all its variables. This was made possible by distinguishing a dart incident to each of the vertices whose degree is considered, which increases the size of the coefficients but does not increase the number of polynomials that have to be calculated.

We note here that in the account of these results published in [3] formula (1.17) and the sum in (1.15) are missing; the formulas are presented correctly in [9]. At that time the second author, programming in Maple, calculated the polynomial P_g and the generating

function $M_g(w,u)$ for $g=2$ and $g=3$ (these results are published in [3]) and also computed the generating function that counts rooted maps of genus 4 by number of edges. This result was recently included in [13], where it was used to count both rooted and unrooted maps of genus 4 by number of edges.

Recently, the second author extended his enumeration results to genus 5. The first author, programming mainly in C, optimized the calculation of the polynomials $R_g(n_1,\ldots,n_r)$ and thus extended the enumeration by number of vertices and faces, as well as by number of edges, to genus 6. Although each author used a different algorithm and a different programming language, we both obtained the same answers, and the numbers of rooted maps we calculated agree with the tables in [17], providing evidence of the correctness of our results. An account of these extensions is given in Sections 2 and 3. Tables of rooted map numbers are given in Appendix A. A discussion of the enumeration of rooted genus-g maps by number of edges appears in Section 4 and the polynomial part of each of the corresponding generating functions appears in Appendix B. Finally, a discussion of some open problems appears in Section 5.

2 Results from the Maple program

A first version of the Maple code written in 1998 implemented recurrence relations between the rational functions introduced in [4] for the computation of the generating functions M_g. It was not designed for efficiency but for validating formulas from [4]. That code has also been used for validating the formulas from (1.2) through (1.22) for the first values of g, r and $n_1,\ldots,n_r$ (these formulas were first obtained from a long computation that was done by hand and is thus error-prone). When executed in 1998 with Maple V for computing $M_4(w,u)$ that code ran into a fundamental limitation (wired into the Maple kernel) of a maximal number of 65,535 terms in any polynomial.

That old code has been recently replaced by a simpler code implementing directly the recursion between polynomials described by the formulas from (1.2) through (1.22). The code is short (less than 400 lines) and resembles the mathematical formulas as much as possible in order to detect errors. All the results obtained by this new code match known results in rooted map enumeration. For all these reasons, it can be considered as a reference for the debugging of optimized implementations.

With a personal computer running under Windows XP with an Intel Core 2 Duo CPU at 2.19 GHz and 3.5 Gb of memory, and a Maple 14 release supporting larger objects, the next two generating functions $M_4(w,u)$ and $M_5(w,u)$ were successfully computed in 4 minutes and 5 hours, respectively. It was, however, not sensible to continue using this inefficient prototype for computing the next generating functions. A better idea was to write an independent implementation optimizing memory space and execution time.

3 Optimizations and the C program

Aside from the advantage in execution speed that C has over Maple, the first author optimized the calculation of the polynomials $R_g(n_1,\ldots,n_r)$. One of these optimizations was made possible by the following observation.

Proposition 3.1. *For any $(g,r)\neq(0,1)$ and any sequence $n_1,\ldots,n_r$, the polynomial $R_g(n_1,\ldots,n_r)$ is divisible by $(1-p)^2$.*

Proof. We use generalized induction on the degree of a polynomial of the form $R_g(n_1,\ldots,$

n_r), which we call an *R-polynomial*.

Basic step (degree 2). The only R-polynomial of degree 2 is $R_0(0,0) = (1-p)^2$: see (1.16).

Induction step. Suppose that the degree d of a given R-polynomial $R_g(n_1, \ldots, n_r)$, as defined by (1.10), is greater than 2 and that every R-polynomial of degree $< d$ is divisible by $(1-p)^2$. We show that $R_g(n_1, \ldots, n_r)$ is also divisible by $(1-p)^2$. Since every R-polynomial on the right side of equations (1.17), (1.19), (1.20), (1.21) and (1.22) is of degree $< d$, it follows from the induction hypothesis that each such polynomial is divisible by $(1-p)^2$. We examine each of these equations in turn.

Equation (1.17). The first line contains a factor $(1-p)^2$. The term $E_{n_1+n_2+3}$ is a polynomial for any non-negative n_1 and n_2. The term $E_{n_1+n_2+2}$ is a polynomial unless $n_1 = n_2 = 0$, but in this case $E_{n_1+n_2+2}$ is multiplied by $n_2 = 0$; so the first line of (1.17) is divisible by $(1-p)^2$. In the second line, each term of the sum contains a polynomial $R_0(k, n_2)$, which, by the induction hypothesis, is divisible by $(1-p)^2$. This factor of $(1-p)^2$ could be cancelled by E_1 or E_2, but the sum is nevertheless a polynomial, and the factor $(1-p)^2$ by which the sum is multiplied ensures that the second line of (1.17) too is divisible by $(1-p)^2$; so the right side of (1.17) is divisible by $(1-p)^2$.

Equation (1.19). By an argument similar to the one used for the second line of (1.17), the right side of (1.19) is divisible by $(1-p)^2$.

Equations (1.20)-(1.22). Each term in the sum contains at least one R-polynomial that is divisible by $(1-p)^2$; so the right side of each of these equations is divisible by $(1-p)^2$. It follows from (1.18) that $R_g(n_1, \ldots, n_r)$ is divisible by $(1-p)^2$, which completes the proof. □

We now modify equations (1.8)-(1.10), and (1.16)-(1.22) in the light of Proposition 3.1. We introduce a new family of polynomials (which we call *S-polynomials*) defined by

$$S_g(n_1, \ldots, n_r) = R_g(n_1, \ldots, n_r)/(1-p)^2 \tag{3.1}$$

and we also let

$$U_g = T_g/(1-p)^2. \tag{3.2}$$

Then U_g is a polynomial of degree $10(g-1)$ and (1.8)-(1.10) become (3.3)-(3.5), respectively.

$$P_g = \frac{U_g}{(1-p)^{4g-4}}, \tag{3.3}$$

$$U_g = S_{g-1}(0,0) + q(1-p-q)\,(1-p)^2 \sum_{j=1}^{g-1} S_j(0) S_{g-j}(0). \tag{3.4}$$

$$\deg S_g(n_1, \ldots, n_r) = 2(n_1 + \ldots + n_r) + 7(r-2) + 10g. \tag{3.5}$$

Also, (1.16)-(1.22) become (3.6)-(3.12), respectively.

$$S_0(0,0) = 1, \tag{3.6}$$

$$\begin{aligned} S_0(n_1,n_2) &= (-n_2HE_{n_1+n_2+2}-(n_2+1)E_{n_1+n_2+3}) \\ &\quad +2J(1-p)^2\sum_{\substack{i+j+k=n_1+1\\ i>0,\,k<n_1}}(-1)^{j+1}H^jE_iS_0(k,n_2). \end{aligned} \tag{3.7}$$

If $(g,r)\neq(0,2)$, then

$$S_g(n_1,\ldots,n_r)=\text{term}_5+\text{term}_6+\text{term}_7+\text{term}_8, \tag{3.8}$$

where

$$\text{term}_5=2J(1-p)^2\sum_{\substack{i+j+k=n_1+1\\ i>0,\,k<n_1}}(-1)^{j+1}H^jE_iS_g(k,n_2,\ldots,n_r), \tag{3.9}$$

$$\text{term}_6=J(1-p)^2\sum_{\substack{k+l+m=n_1+1\\ 0\le j\le g\\ X\subseteq[r]\\ (j,X)\neq(0,\emptyset)\\ (j,X)\neq(g,[r])}}K_mH^mS_j(k,N_X)S_{g-j}(l,N_{[r]-X}), \tag{3.10}$$

$$\text{term}_7=\sum_{i+j+m=n_1+1}K_mH^mS_{g-1}(i,j,N_{[r]}), \tag{3.11}$$

and

$$\text{term}_8=\sum_{j=2}^{r}\begin{pmatrix} n_j\sum_{k+l=n_1+n_j+2}L_kH^{k+1}S_g(l,N_j)\\ +(n_j+1)\sum_{k+l=n_1+n_j+3}L_kH^kS_g(l,N_j)\end{pmatrix}. \tag{3.12}$$

Since $R_g(n_1,\ldots,n_r)$ is symmetric in all its variables, so is $S_g(n_1,\ldots,n_r)$; so only those polynomials $S_g(n_1,\ldots,n_r)$ with $n_1\le\ldots\le n_r$ are treated. In all the S-polynomials on the right side of each of the equations (3.9)-(3.12), only the first two variables can violate these inequalities; so they are inserted into their proper slots among the remaining variables to preserve the inequalities. Also, equation (3.4) is symmetric in j and $g-j$, equation (3.10) is symmetric in k and l and equation (3.11) is symmetric in i and j; so the calculations there can be cut almost in half. In equation (3.12), each polynomial $S_g(l,N_j)$ is calculated only once and then used twice. The following easily proved observations can be used to avoid calculating a polynomial that is identically 0: $\text{term}_5=0$ if $n_1=0$, $\text{term}_6=0$ if $g+r\le 2$, $\text{term}_7=0$ if $g=0$, $\text{term}_8=0$ if $r=1$ or $(g,r)=(0,2)$. From these observations, it follows that the only term that could possibly contribute to $S_0(n_1)$ is term_5. From (3.9) it follows by generalized induction on n_1 that $S_0(n_1)=0$ for all $n_1\ge 0$; so these polynomials do not have to be defined.

All the S-polynomials are stored in a single one-dimensional array s. A preliminary recursion does not calculate any of these polynomials. Instead, it calculates all the quadruples (d,g,r,c) of parameters of the S-polynomials that will later be calculated, where $d=\deg S_g(n_1,\ldots,n_r)$ and c is an integer coding the sequence $(n_1,\ldots,n_r)$, and stores the list of quadruples in four parallel arrays, one array for each of the four parameters d, g, r, c and one element of all four arrays for each quadruple (d,g,r,c). The program then sorts the four parallel arrays by degree d using bucket sort, computes the number of S-polynomials that have to be calculated and the total number of terms in these polynomials and stores in two arrays the index in s and the one in the four parallel arrays of the first term for each degree d. Then the S-polynomials are calculated in increasing order of their

degree and stored in s. This can be done non-recursively because all the S-polynomials that need to be used will have already been stored and need only be found by searching the four parallel arrays, starting with the first index for the appropriate degree d, for the appropriate parameters, and adding $(d+1)(d+2)/2$ to the index in s each time the index in the four parallel arrays is increased by 1. Once the last polynomial $S_{g-1}(0,0)$ has been calculated, first (3.4) is used to calculate U_g and then (3.3) is used to calculate P_g and its coefficients are stored in a text file, which is available from the first author on request.

The number of S-polynomials that have to be calculated is roughly the total number of partitions of all the positive integers up to $10(g-1)$. For each of these polynomials, the most expensive calculation is term$_6$, because the sum there runs over all the partitions of the sequence $[r] = (2, \ldots, r)$, where r can be as great as $g+1$, and involves multiplying two S-polynomials. The time-complexity of calculating P_g is therefore exponential in g, but the optimizations made here nevertheless made it possible to calculate P_g for a greater value of g than was possible previously. Another program computes a table of numbers of rooted genus-g maps counted by number of vertices and faces by reading this file and using (1.2) if $g \geq 1$ or (1.3) if $g = 0$. Tables of numbers of rooted genus-g maps for any $g \leq 6$ and with up to any reasonable number of edges are available from the first author on request.

The programs were written mainly in C. The one that computes the polynomials is about 2000 lines long and the one that computes the tables is about 300 lines long. They both use the C++ library CLN to do arithmetic on big integers because CLN reads arithmetic expressions in C that use only addition, multiplication and subtraction; only statements involving quotients, remainders, input/output of big integers and file management had to be modified. Since CLN requires a GNU compiler, XCODE was downloaded and installed by Jerome Tremblay, a computer technician at UQAM, who also downloaded and installed CLN and wrote sample C++ statements for input/output of big numbers and file management.

The programs were executed on a 2004 Macintosh GR4 computer. The time taken to compute the polynomial P_g varied from run to run. In Table 1 we show, for each g from 1 to 6, the number of S-polynomials that were calculated, the total number of terms in all these S-polynomials, and a typical execution time. Once the S-polynomials had been computed and stored, it took the computer only 48 seconds to make a table of numbers of genus-6 maps with up to 42 edges counted by number of vertices and faces.

Source codes for both programs are included in release 0.3.2 and higher of the MAP project [11]. The polynomials P_2 and P_3 appear in [3]. The polynomials P_4, P_5 and P_6 are too large to be reproduced here. The coefficients of the polynomials $P_g[p,q]$ for $1 \leq g \leq 6$ are included in the MAP project and available from the first author on request. For $1 \leq g \leq 6$ tables of numbers of rooted genus-g maps up to 20 edges are given in Appendix A. More numbers of rooted genus-g maps for any $g \leq 6$ and with up to any reasonable number of edges can be obtained from code included in the MAP project and are available from the first author on request.

4 Counting by number of edges

To compute the generating function $M_g(z) = z^{2g-2} M_g(z,z)$ that counts rooted genus-g maps by number of edges alone, we use the substitution obtained in [13], which is a more compact form of the one obtained in [9] and published in [3]. Let

$$p = q = m, \tag{4.1}$$

g	number of S-polynomials	total number of terms	execution time
1	1	1	instantaneous
2	16	507	1 second
3	67	7407	10 seconds
4	205	49796	2 minutes
5	543	235410	20 minutes
6	1314	900114	3.5 hours

Table 1: Evaluation of the computation cost

where

$$z = m(1-3m) \text{ and } m = 0 \text{ when } z = 0. \tag{4.2}$$

By substituting from (4.1) into (1.4) and (1.5) to express w and u in terms of m and then substituting into (1.7), we obtain the following equation for $g \geq 1$:

$$M_g(z) = \frac{m^{2g}(1-3m)^{2g-2}P_g(m,m)}{(1-6m)^{5g-3}(1-2m)^{5g-4}}. \tag{4.3}$$

For $g = 0$, we substitute into (1.3) instead of (1.7) and obtain

$$M_0(z) = (1-3m)^{-2}(1-4m). \tag{4.4}$$

The first author computed $M_g(z)$ from the computed values of $M_g(w,u)$ for $g \leq 6$. The program divides the polynomial $P_g(m,m)$ by $1-2m$ as often as possible. The program then divides the resulting polynomial by 2 and by 3 as often as possible, extracts the appropriate constant factor and then stores the resulting generating function in another text file, also available from the first author. The second author computed $M_g(z)$ directly for $g \leq 6$. We then compared our formulas and verified that they agree. The formulas for $P_g(m,m)$ for $1 \leq g \leq 6$ appear in Appendix B. Now $P_g(m,m)$ is of degree $6g-6$, but we found experimentally in 2009 that for $1 \leq g \leq 6$, $P_g(m,m)$ is divisible by $(1-2m)^{2g-2}$, so that the quotient is only of degree $4g-4$, and we conjectured that this is the case for any positive integer g. In 2010, the second author proved that conjecture [10].

5 Some interesting open problems

The recurrences satisfied by the R- and S-polynomials both result from proofs by induction. After the right conjecture has been guessed by observing the first computed terms, these proofs are not difficult to find, but they are tedious and error-prone due to the length of the expressions involved. Thus they are good candidates for automation. We plan to develop a suitable formal framework for assisting this kind of proofs with a computer algebra system. The challenge is to shorten the chain of conjectures and proofs about the general pattern of generating functions for counting rooted maps.

Once the numbers of rooted maps of genus up to g are known, the number of unrooted maps up to genus g can be calculated using the methods presented in [14]. As was mentioned above, the second author collaborated with A. Mednykh to count rooted and unrooted maps of genus 4 by number of edges [13]. It would be interesting to count unrooted genus-g maps by number of vertices and faces for as many values of g as possible (see [18] for an account of the progress made on this problem).

6 Acknowledgments

The authors are grateful to Roman Nedela, Alexander Mednykh and the anonymous referees for helpful comments and suggestions.

References

[1] D. Arquès, Une relation fonctionnelle nouvelle sur les cartes planaires pointées, *J. Comb. Theory B* **39** (1985), 27–42.

[2] D. Arquès, Relations fonctionnelles et dénombrement des cartes pointées sur le tore, *J. Comb. Theory B* **43** (1987), 253–274.

[3] D. Arquès and A. Giorgetti, Énumération des cartes pointées de genre quelconque en fonction des nombres de sommets et de faces, *J. Comb. Theory B* **77** (1999), 1–24.

[4] D. Arquès and A. Giorgetti, Counting rooted maps on a surface, *Theor. Comput. Sci.* **234** (2000), 255–272.

[5] E. A. Bender and E. R. Canfield, The asymptotic number of rooted maps on a surface, *J. Comb. Theory A* **43** (1986), 244–257.

[6] E. A. Bender and E. R. Canfield, The number of rooted maps on an orientable surface, *J. Comb. Theory B* **53** (1991), 293–299.

[7] H. S. M. Coxeter, *Regular Polytopes*, 3rd ed., Dover, New York, 1973.

[8] B. Eynard and N. S. Orantin, Topological recursion in enumerative geometry and random matrices, *J. Phys. A-Math. Theor.* **42** (2009), 293001.

[9] A. Giorgetti, *Combinatoire bijective et énumérative des cartes pointées sur une surface*, PhD thesis, Université de Marne-la-Vallée, Institut Gaspard Monge, 1998, `http://tel.archives-ouvertes.fr/tel-00724977`.

[10] A. Giorgetti, Guessing a Conjecture in Enumerative Combinatorics and Proving It with a Computer Algebra System, in: T. Jebelean, M. Mosbah and N. Popov (eds.), *SCSS'10*, July 2010, pp. 5–18.

[11] A. Giorgetti, MAP project release 0.3.2, `https://sourceforge.net/projects/combi/files/map/`, January 2013.

[12] G. A. Jones and D. Singerman, Theory of maps on orientable surfaces, *Proc. London Math. Soc.* **37** (1978), 273–307.

[13] A. Mednykh and A. Giorgetti, Enumeration of genus four maps by number of edges, *Ars Math. Contemp.* **4** (2011), 351–361.

[14] A. Mednykh and R. Nedela, Enumeration of unrooted maps of a given genus, *J. Comb. Theory B* **96** (2006), 706–729.

[15] W. T. Tutte, A census of planar maps, *Canad. J. Math.* **15** (1963), 249–271.

[16] W. T. Tutte. On the enumeration of planar maps. *Bull. Amer. Math. Soc.* **74** (1968), 64–74.

[17] T. R. S. Walsh, *Combinatorial enumeration of non-planar maps*, PhD thesis, University of Toronto, 1971.

[18] T. R. S. Walsh, A. Giorgetti and A. Mednykh, Enumeration of unrooted orientable maps of arbitrary genus by number of edges and vertices, *Discrete Math.* **312** (2012), 2660–2671.

[19] T. R. S. Walsh and A. B. Lehman, Counting rooted maps by genus I, *J. Comb. Theory B* **13** (1972), 192–218.

Appendix A

Number $m_g(v, f)$ of rooted maps of genus g with e edges and v vertices, for $1 \leq g \leq 6$ and $2g \leq e \leq 20$. Lines whose column of v is empty give the total number $m_g(e)$ of rooted maps of genus g with e edges.

e	v	$g=1$	$g=2$	$g=3$
2	1	1		
2		1		
3	1	10		
3	2	10		
3		20		
4	1	70	21	
4	2	167		
4	3	70		
4		307	21	
5	1	420	483	
5	2	1720	483	
5	3	1720		
5	4	420		
5		4280	966	
6	1	2310	6468	1485
6	2	14065	15018	
6	3	24164	6468	
6	4	14065		
6	5	2310		
6		56914	27954	1485
7	1	12012	66066	56628
7	2	100156	258972	56628
7	3	256116	258972	
7	4	256116	66066	
7	5	100156		
7	6	12012		
7		736568	650076	113256
8	1	60060	570570	1169740
8	2	649950	3288327	2668750
8	3	2278660	5554188	1169740
8	4	3392843	3288327	
8	5	2278660	570570	
8	6	649950		
8	7	60060		
8		9370183	13271982	5008230
9	1	291720	4390386	17454580
9	2	3944928	34374186	66449432
9	3	17970784	85421118	66449432
9	4	36703824	85421118	17454580
9	5	36703824	34374186	
9	6	17970784	4390386	
9	7	3944928		
9	8	291720		
9		117822512	248371380	167808024
10	1	1385670	31039008	211083730

e	v	$g=1$	$g=2$	$g=3$
10	2	22764165	313530000	1171704435
10	3	129726760	1059255456	1955808460
10	4	344468530	1558792200	1171704435
10	5	472592916	1059255456	211083730
10	6	344468530	313530000	
10	7	129726760	31039008	
10	8	22764165		
10	9	1385670		
10		1469283166	4366441128	4721384790
11	1	6466460	205633428	2198596400
11	2	126264820	2583699888	16476937840
11	3	875029804	11270290416	40121261136
11	4	2908358552	22555934280	40121261136
11	5	5188948072	22555934280	16476937840
11	6	5188948072	11270290416	2198596400
11	7	2908358552	2583699888	
11	8	875029804	205633428	
11	9	126264820		
11	10	6466460		
11		18210135416	73231116024	117593590752
12	1	29745716	1293938646	20465052608
12	2	678405090	19678611645	196924458720
12	3	5593305476	106853266632	647739636160
12	4	22620890127	276221817810	945068384880
12	5	50534154408	375708427812	647739636160
12	6	65723863196	276221817810	196924458720
12	7	50534154408	106853266632	20465052608
12	8	22620890127	19678611645	
12	9	5593305476	1293938646	
12	10	678405090		
12	11	29745716		
12		224636864830	1183803697278	2675326679856
13	1	135207800	7808250450	174437377400
13	2	3550829360	140725699686	2079913241120
13	3	34225196720	925572602058	8789123742880
13	4	164767964504	2979641557620	17326957790896
13	5	448035881592	5235847653036	17326957790896
13	6	729734918432	5235847653036	8789123742880
13	7	729734918432	2979641557620	2079913241120
13	8	448035881592	925572602058	174437377400
13	9	164767964504	140725699686	
13	10	34225196720	7808250450	
13	11	3550829360		
13	12	135207800		
13		2760899996816	18579191525700	56740864304592
14	1	608435100	45510945480	1384928666550
14	2	18182708362	955708437684	19925913354061
14	3	201976335288	7454157823560	104395235785256
14	4	1137369687454	29079129795702	264477214235234
14	5	3682811916980	63648856688592	357391270819604
14	6	7302676928666	82234427131416	264477214235234
14	7	9145847808784	63648856688592	104395235785256
14	8	7302676928666	29079129795702	19925913354061
14	9	3682811916980	7454157823560	1384928666550
14	10	1137369687454	955708437684	
14	11	201976335288	45510945480	
14	12	18182708362		
14	13	608435100		
14		33833099832484	284601154513452	1137757854901806
15	1	2714556600	257611421340	10369994005800

e	v	$g=1$	$g=2$	$g=3$
15	2	91392185080	6216591472728	176357530955320
15	3	1156128848680	56532447160536	1115525500250760
15	4	7506901051000	261637840342860	3505018618003600
15	5	28442316247080	694146691745820	6087558311398000
15	6	67173739068760	1117259292848016	6087558311398000
15	7	102432266545800	1117259292848016	3505018618003600
15	8	102432266545800	694146691745820	1115525500250760
15	9	67173739068760	261637840342860	176357530955320
15	10	28442316247080	56532447160536	10369994005800
15	11	7506901051000	6216591472728	
15	12	1156128848680	257611421340	
15	13	91392185080		
15	14	2714556600		
15		413610917006000	4272100949982600	21789659909226960
16	1	12021607800	1422156202740	73920866362200
16	2	452077562620	38985279745230	1461629029629340
16	3	6447533938280	407653880116680	10933959720960760
16	4	47700234551918	2200626948631386	41491242915292306
16	5	208462422428152	6928413234959820	89390908732820144
16	6	576218752277476	13518984452463630	114899070275212424
16	7	1046677747672360	16842445235560944	89390908732820144
16	8	1274461449989715	13518984452463630	41491242915292306
16	9	1046677747672360	6928413234959820	10933959720960760
16	10	576218752277476	2200626948631386	1461629029629340
16	11	208462422428152	407653880116680	73920866362200
16	12	47700234551918	38985279745230	
16	13	6447533938280	1422156202740	
16	14	452077562620		
16	15	12021607800		
16		5046403030066927	63034617139799916	401602392805341924
17	1	52895074320	7683009544980	505297829133240
17	2	2205359390592	236923660397172	11460411934448048
17	3	35155923872640	2815913391715452	99727841192820016
17	4	293370096957504	17486142956133684	447708887118504600
17	5	1461307573813824	64232028100704156	1165172136542282424
17	6	4660202610532480	148755268498286436	1857975645023518752
17	7	9908748651241088	224686278407291148	1857975645023518752
17	8	14373136466094880	224686278407291148	1165172136542282424
17	9	14373136466094880	148755268498286436	447708887118504600
17	10	9908748651241088	64232028100704156	99727841192820016
17	11	4660202610532480	17486142956133684	11460411934448048
17	12	1461307573813824	2815913391715452	505297829133240
17	13	293370096957504	236923660397172	
17	14	35155923872640	7683009544980	
17	15	2205359390592		
17	16	52895074320		
17		61468359153954656	916440476048146056	7165100439281414160
18	1	231415950150	40729207226400	3331309741059300
18	2	10627956019245	1401097546161936	85694099173907510
18	3	187959014565840	18743188498056288	855779329367736840
18	4	1753945289216484	132344695964811720	4470547991985864322
18	5	9857665477085832	559373367462490656	13767319160210071404
18	6	35839052357422132	1511718920778951024	26522236056202555206
18	7	87930943305742512	2710382626755160416	32904419378927915376
18	8	149314477245194262	3286157560248860532	26522236056202555206
18	9	177882700353757460	2710382626755160416	13767319160210071404
18	10	149314477245194262	1511718920778951024	4470547991985864322
18	11	87930943305742512	559373367462490656	855779329367736840
18	12	35839052357422132	132344695964811720	85694099173907510
18	13	9857665477085832	18743188498056288	3331309741059300
18	14	1753945289216484	1401097546161936	
18	15	187959014565840	40729207226400	
18	16	10627956019245		
18	17	231415950150		

e	v	$g=1$	$g=2$	$g=3$
18		747672504476150374	13154166812674577412	124314235272290304540
19	1	1007340018300	212347275857640	21280393666593600
19	2	50668344988068	8089830217844928	614960028331370816
19	3	987658610225052	120789163612555200	6968569097113244096
19	4	10229201477344752	960323177351524512	41790549086980226368
19	5	64309102366765200	4616545437250956192	149789855223187292608
19	6	263868150558327376	14358354462488121408	34150541800882273132 8
19	7	738178726378902064	30044423965980553536	51189583141115492217 6
19	8	1446563778096423816	43241609165618454096	51189583141115492217 6
19	9	2017523504473479992	43241609165618454096	34150541800882273132 8
19	10	2017523504473479992	30044423965980553536	149789855223187292608
19	11	1446563778096423816	14358354462488121408	41790549086980226368
19	12	738178726378902064	4616545437250956192	6968569097113244096
19	13	263868150558327376	960323177351524512	614960028331370816
19	14	64309102366765200	120789163612555200	21280393666593600
19	15	10229201477344752	8089830217844928	
19	16	987658610225052	212347275857640	
19	17	50668344988068		
19	18	1007340018300		
19		9083423595292949240	186700695099591735024	2105172926498512761984
20	1	4365140079300	1090848505817070	132216351453357600
20	2	239250231713210	45732525474843801	4257157940494918160
20	3	5110652802256260	756589971284883792	54217755730994858080
20	4	58364244137596695	6716133365837116980	369061676845849000520
20	5	407372683115470800	36362952155187558600	1518921342035154605600
20	6	1870153808268516280	12865798319026864068	4031165546220945277040
20	7	5905479331377981200	30985988543975359 8768	7151648337964982801760
20	8	13196809961724011350	52051697802973651 8606	8640883781524178188980
20	9	21241931655650633720	61791046211171489 6820	7151648337964982801760
20	10	24868664942648145372	52051697802973651 8606	4031165546220945277040
20	11	21241931655650633720	30985988543975359 8768	1518921342035154605600
20	12	13196809961724011350	12865798319026864068	369061676845849000520
20	13	5905479331377981200	36362952155187558600	54217755730994858080
20	14	1870153808268516280	6716133365837116980	4257157940494918160
20	15	407372683115470800	756589971284883792	132216351453357600
20	16	58364244137596695	45732525474843801	
20	17	5110652802256260	1090848505817070	
20	18	239250231713210		
20	19	4365140079300		
20		110239596847544663002	2623742783421329300190	34899691847703927826500

e	v	$g=4$	$g=5$	$g=6$
8	1	225225		
8		225225		
9	1	12317877		
9	2	12317877		
9		24635754		
10	1	351683046	59520825	
10	2	792534015		
10	3	351683046		
10		1495900107	59520825	
11	1	7034538511	4304016990	
11	2	26225260226	4304016990	
11	3	26225260226		
11	4	7034538511		
11		66519597474	8608033980	
12	1	111159740692	158959754226	24325703325
12	2	600398249550	354949166565	
12	3	993494827480	158959754226	
12	4	600398249550		
12	5	111159740692		
12		2416610807964	672868675017	24325703325
13	1	1480593013900	4034735959800	2208143028375
13	2	10743797911132	14805457339920	2208143028375
13	3	2576235457300	14805457339920	
13	4	2576235457300	4034735959800	
13	5	10743797911132		
13	6	1480593013900		
13		75981252764664	37680386599440	4416286056750
14	1	17302190625720	79553497760100	100940771124360
14	2	160576594766588	420797306522502	223790013148500
14	3	517592962672296	691650582088536	100940771124360
14	4	750260619502310	420797306522502	
14	5	517592962672296	79553497760100	
14	6	160576594766588		
14	7	17302190625720		
14		2141204115631518	1692352190653740	425671555397220
15	1	182231849209410	1302772718028600	3130208769783780
15	2	2089035241981688	9220982517965400	11344028448443832
15	3	8615949311310872	21853758736216200	11344028448443832
15	4	16789118602155860	21853758736216200	3130208769783780
15	5	16789118602155860	9220982517965400	
15	6	8615949311310872	1302772718028600	
15	7	2089035241981688		
15	8	182231849209410		
15		55352670009315660	64755027944420400	28948474436455224
16	1	1763184571730010	18475997006212200	74520697707149580
16	2	24325590127655531	166713517116449940	387689146050297186
16	3	123981042854132536	528887751025584600	633832536898519848
16	4	309197871098871838	762684674663536626	387689146050297186
16	5	415691294404230748	528887751025584600	74520697707149580
16	6	309197871098871838	166713517116449940	
16	7	123981042854132536	18475997006212200	
16	8	24325590127655531		
16	9	1763184571730010		

e	v	$g=4$	$g=5$	$g=6$
16		1334226671709010578	2190839204960030106	1558252224413413380
17	1	15894791312284170	233454817237201560	1457897216520222060
17	2	258634264294653390	2595050050431235488	10115530661997850556
17	3	1587135819804394530	10499075716384241952	23746474580826741940
17	4	4892650539994184868	20269771718252599536	23746474580826741940
17	5	8419549939292302908	20269771718252599536	10115530661997850556
17	6	8419549939292302908	10499075716384241952	1457897216520222060
17	7	4892650539994184868	2595050050431235488	
17	8	1587135819804394530	233454817237201560	
17	9	258634264294653390		
17	10	15894791312284170		
17		30347730709395639732	67194704604610557072	70639804918689629112
18	1	134951136993773100	2682208751185413450	24464684545968004800
18	2	2548272396065512974	35801820369640556595	21581053828295469987 2
18	3	18451302662846918700	178505550201444784920	67587037009639932 9024
18	4	68503375296263488977	439591872915483185214	97055917759716295668 8
18	5	145737674581607574840	588564117958709029644	67587037009639932 9024
18	6	186553519919803261860	439591872915483185214	21581053828295469987 2
18	7	145737674581607574840	178505550201444784920	24464684545968004800
18	8	68503375296263488977	35801820369640556595	
18	9	18451302662846918700	2682208751185413450	
18	10	2548272396065512974		
18	11	134951136993773100		
18		657304672067357799042	1901727022434216910002	2802850363447807024080
19	1	1088243826731751690	28449551653853229900	362610922310040035940
19	2	23532893106071038404	447016944351510642564	393154776189896788952 0
19	3	197822824662547694148	2677324515710001081372	156588469108579930853 60
19	4	866831237081712285138	8127109896970086044280	300026919542323522776 08
19	5	222138141781843144801098	1388115304057219050151 2	300026919542323522776 08
19	6	351564703551118662741 6	1388115304057219050151 2	156588469108579930853 60
19	7	351564703551118662741 6	8127109896970086044280	393154776189896788952 0
19	8	222138141781843144801098	2677324515710001081372	362610922310040035940
19	9	866831237081712285138	447016944351510642564	
19	10	197822824662547694148	28449551653853229900	
19	11	23532893106071038404		
19	12	1088243826731751690		
19		136526073040627883957 88	503221078985152829992 56	999113950985987065768 56
20	1	8391311316938069520	2818581119980394769 00	484865567959207635057 0
20	2	205518653220527665304	513100899050048609625 0	630046002116167133522 27
20	3	197928188112611322537 6	361887831458012435589 00	308528931105126354302 392
20	4	100717576991552759068 24	131989618396827099239 715	751928550048308520251 566
20	5	304681002664809171477 60	277921666244135490925 320	100332632116336477849 5004
20	6	580899208975583528916 72	354556747218700475500 140	751928550048308520251 566
20	7	718233716129125338871 68	277921666244135490925 320	308528931105126354302 392
20	8	580899208975583528916 72	131989618396827099239 715	630046002116167133522 27
20	9	304681002664809171477 60	361887831458012435589 00	484865567959207635057 0
20	10	100717576991552759068 24	513100899050048609625 0	
20	11	197928188112611322537 6	281858111998039476900	
20	12	205518653220527665304		
20	13	8391311316938069520		
20		273469313030628783700080	125758261699722519409 4310	325994779525265210700 8514

Appendix B

Polynomial $P_g(m,m)/(1-2m)^{(2g-2)}$ in the generating function $M_g(z)$.

g	$P_g(m,m)/(1-2m)^{(2g-2)}$
1	1
2	$3\,(7-70m+295m^2-636m^3+588m^4)$
3	$3^2\left(\begin{array}{l}165-2596m+19835m^2-102138m^3+397742m^4\\ -1162744m^5+2360496m^6-2918016m^7+1642656m^8\end{array}\right)$
4	$3^2\left(\begin{array}{l}25025-465894m+4245462m^2-28633200m^3\\ +178608786m^4-1025233956m^5+4855070265m^6\\ -17709582732m^7+48202134300m^8-95026128096m^9\\ +128766120048m^{10}-107657028288m^{11}+41956066368m^{12}\end{array}\right)$
5	$3^2\left(\begin{array}{l}6613425-128153480m+1123286598m^2-7641539820m^3\\ +68489369190m^4-681945904584m^5+5453799804351m^6\\ -33175983024306m^7+157025924018370m^8\\ -590662433458296m^9+1778501684246544m^{10}\\ -4258112783048352m^{11}+7946769062433024m^{12}\\ -11156448512891520m^{13}+11087677481748480m^{14}\\ -6955529138076672m^{15}+2071316467035648m^{16}\end{array}\right)$
6	$3^3\left(\begin{array}{l}900951975-16624244750m+105922471285m^2\\ -402327939748m^3+9014122899102m^4\\ -183050473605084m^5+2152106046117936m^6\\ -17716916701552824m^7+113738504396139378m^8\\ -602051461456822740m^9+2694620167659984726m^{10}\\ -10264333975933057272m^{11}+33144207748349404248m^{12}\\ -89851078246171110912m^{13}+201700042332545251008m^{14}\\ -368052722019205320960m^{15}+531966143515513800960m^{16}\\ -586003188281237388288m^{17}+462270648384927677952m^{18}\\ -232608604432295245824m^{19}+56102738197832792064m^{20}\end{array}\right)$

ARS MATHEMATICA CONTEMPORANEA

Also available at http://amc-journal.eu
ISSN 1855-3966 (printed edn.), ISSN 1855-3974 (electronic edn.)
ARS MATHEMATICA CONTEMPORANEA 7 (2014) 281–291

On the lightness of chordal 4-cycle in 1-planar graphs with high minimum degree*

Xin Zhang †
Department of Mathematics, Xidian University, Xi'an 710071, P. R. China

Guizhen Liu ‡
School of Mathematics, Shandong Univeristy, Jinan 250100, P. R. China

Received 12 January 2012, accepted 8 February 2013, published online 7 May 2013

Abstract

A graph G is 1-planar if it can be drawn on the plane so that each edge is crossed by at most one other edge. The family of 1-planar graphs with minimum vertex degree at least δ and minimum edge degree at least ε is denoted by $\mathcal{P}_\delta^1(\varepsilon)$. In this paper, it is proved that every graph in $\mathcal{P}_7^1(14)$ (resp. $\mathcal{P}_6^1(13)$) contains a copy of chordal 4-cycle with all vertices of degree at most 10 (resp. 12).

Keywords: 1-planar graph, light graph, cycle, discharging.

Math. Subj. Class.: 05C75, 05C10

1 Introduction

All graphs considered in this paper are finite, undirected, loopless and without multiple edges. For a graph G, we use $V(G)$, $E(G)$, $\delta(G)$ and $\Delta(G)$ to denote the vertex set, the edge set, the minimum degree and the maximum degree of G, respectively. By $F(G)$, we denote the face set of G when G is a plane graph. If $uv \in E(G)$, then u is said to be the *neighbor* of v. We use $N_G(v)$ to denote the set of neighbors of a vertex v. The degree of a vertex $v \in V(G)$, denoted by $d_G(v)$, is the value of $|N_G(v)|$, and the degree of an edge $uv \in E(G)$, denoted by $d_G(uv)$, is the value of $d_G(u) + d_G(v)$. A k-, k^+- and k^--$vertex$ is a vertex of degree k, at least k and at most k, respectively. In this paper, C_k and P_k denotes a cycle and a path with k vertices and K_4^- denotes a chordal 4-cycle, which is a

*A project funded by Scientific Research Program of the Higher Education Institution of XinJiang (Grant No. XJEDU2012I38) and the Fundamental Research Funds for the Central Universities (Grant No. K5051370003).

†Supported in part by the National Natural Science Foundation of China (Grants No. 11101243, 11201440).

‡Supported in part by the National Natural Science Foundation of China (Grants No. 61070230).

E-mail addresses: xzhang@xidian.edu.cn (Xin Zhang), gzliu@sdu.edu.cn (Guizhen Liu)

graph obtained by removing an edge from a complete graph K_4. A cycle $C = [x_1 \cdots x_k]$ of a graph G is of the type $(d_1, \cdots, d_k)$ if $d_G(x_i) = d_i$ for $1 \leq i \leq k$. Similarly we can define cycles of the type $(\geq d_1, \cdots, \geq d_k)$, etc. For other undefined concepts we refer the readers to [2].

A graph is 1-*planar* if it can be drawn on the plane so that each edge is crossed by at most one other edge. The notion of 1-planarity was introduced by Ringel [16] while trying to simultaneously color the vertices and faces of a plane graph G such that any pair of adjacent/incident elements receive different colors. Note that we can construct, for given plane graph, a 1-planar graph G^1 whose vertex set is $V(G) \cup F(G)$ and any two vertices of G^1 are adjacent if and only if their corresponding elements in G are adjacent or incident.

Borodin proved that each 1-planar graph is 6-colorable (the bound 6 being sharp) [3, 4] which positively answered a conjecture raised by Ringel in [16], and that each 1-planar graph is acyclically 20-colorable [7]. The list analogue of vertex coloring of 1-planar graphs was investigated by Albertson and Mohar [1], and by Wang and Lih [18]. Zhang et al. showed that each 1-planar graph G with maximum degree Δ is Δ-edge-colorable if $\Delta \geq 10$ [25], or $\Delta \geq 9$ and G contains no chordal 5-cycles [19], or $\Delta \geq 8$ and G contains no chordal 4-cycles [20], or $\Delta \geq 7$ and G contains no 3-cycles [21], is $(\Delta + 1)$-edge-choosable and $(\Delta + 2)$-total-choosable if $\Delta \geq 16$ [27], is Δ-edge-choosable and $(\Delta + 1)$-total-choosable if $\Delta \geq 21$ [27]. Zhang et al. also showed that the $(p, 1)$-total labelling number of each 1-planar graph G is at most $\Delta(G) + 2p - 2$ if $\Delta(G) \geq 8p + 4$ [28], and the linear arboricity of each 1-planar graph G is exactly $\lceil \Delta(G)/2 \rceil$ if $\Delta(G) \geq 33$ [24].

Another topic concerning 1-planar graphs is to investigate their global and local structures. In [9], it is shown that each 1-planar graph with n vertices has at most $4n - 8$ edges and this upper bound is tight, which implies that the minimum vertex degree of any 1-planar graph is at most 7.

Let H be a connected graph and $\mathcal{G}$ be a family of graphs. If for any graph $G \in \mathcal{G}$, G contains a subgraph $K \simeq H$ such that

$$\max_{x \in V(K)} \{d_G(x)\} \leq t_h < +\infty \text{ and } \sum_{x \in V(K)} d_G(x) \leq t_w < +\infty, \tag{1.1}$$

then we say that H is $light$ in $\mathcal{G}$, and otherwise say that H is $heavy$ in $\mathcal{G}$. The smallest integers t_h and t_w satisfying (1.1) are called the $height$ and the $weight$ of H in the family $\mathcal{G}$, denoted by $h(H, \mathcal{G})$ and $w(H, \mathcal{G})$, respectively. By $\mathcal{L}(\mathcal{G})$, we denote the set of light graphs in the family $\mathcal{G}$. Throughout this paper, $\mathcal{P}^1_\delta(\varepsilon)$ (resp. $\mathcal{P}_\delta(\varepsilon)$) denotes the family of 1-planar graphs (resp. planar graphs) with minimum vertex degree at least δ and minimum edge degree at least ε. If $\varepsilon = 2\delta$, we use the natation $\mathcal{P}^1_\delta$ (resp. $\mathcal{P}_\delta$) for short to represent $\mathcal{P}^1_\delta(\varepsilon)$ (resp. $\mathcal{P}_\delta(\varepsilon)$). Note that for the parameter $\mathcal{P}^1_\delta(\varepsilon)$, we need to assume that $\delta \leq 7$ and $\varepsilon \geq 2\delta$.

The first complete description of the set of light graphs in the family of 1-planar graphs with high minimum degree was given in [9, 22]; there was proved that $\mathcal{L}(\mathcal{P}^1_4) = \{P_1, P_2, P_3\}$. Fabrici and Madaras [9], Zhang, Liu and Wu [22], and Dong [8] together proved that $\mathcal{L}(\mathcal{P}^1_5) = \{P_1, P_2, P_3, P_4, S_3\}$, where S_3 is a 3-star. For the lightness of some graphs in the family $\mathcal{P}^1_\delta$ where $6 \leq \delta \leq 7$, the readers can refer to [6, 9, 11, 10, 12, 13, 17, 22, 26, 23].

In this paper, we investigate the lightness of some graphs in $\mathcal{P}^1_\delta(\varepsilon)$ with not only $\varepsilon = 2\delta$ but also $\varepsilon > 2\delta$, the later case of which has not been considered for the family of 1-planar graphs even before. Our motivation comes from the analogical results for planar graphs

with minimum degree δ and minimum edge degree $2\delta+1$ where $\delta \in \{3,4\}$. For example, Borodin proved in [5] that $\mathcal{L}(\mathcal{P}_3(7)) = \{P_1, P_2, P_3\}$ (also proved in [14] by Madaras and Škrekovski), and Mohar et al. [15] presented some light subgraphs in the class $\mathcal{P}_4(9)$.

In what follows, we show in Section 2.3 that K_4^- is light in the family $\mathcal{P}_7^1$ as well as in its superfamily $\mathcal{P}_6^1(13)$, and its height is at most 10 and at most 12, respectively.

2 The lightness of chordal 4-cycle

2.1 Basic terms

In the following, we always assume that G is a 1-planar graph that has been drawn on a plane so that every edge is crossed by at most one another edge and the number of crossings is as small as possible. The *associated plane graph* $G^\times$ of G is the plane graph that is obtained from G by turning all crossings of G into new 4-vertices. A vertex in $G^\times$ is $false$ if it is not a vertex of G; otherwise, it is *true*. Similarly, by false (resp. true) face, we mean a face in $G^\times$ that is incident with at least one false (resp. no false) vertices. Let v and f be a vertex and a face in $G^\times$. The function $\zeta(v)$ (resp. $\zeta(f)$) denotes the number of false vertices that are adjacent to v (resp. incident with f) in $G^\times$.

For convenience, we introduce some specialized notations. Let v be a false vertex in $G^\times$ and let v_1, v_2, v_3, v_4 be its neighbors in a clockwise order. Define f_i to be the face incident with vv_i and vv_{i+1}, where subscripts are taken modulo 4. Note that if $d(f_i) = 3$, then $v_iv_{i+1} \in E(G)$. In this case, let f_i' be the other face incident with the edge v_iv_{i+1}. If $d(f_i') = 3$, then its third vertex will be denoted by v_i'. Thus v_i' is a false vertex if and only if f_i' is false, in which case we denote a neighbor of v_i (resp. v_{i+1}) in G to be v_i'' (resp. v_{i+1}''), so that v_iv_i'' and $v_{i+1}v_{i+1}''$ are two edges in G that crossed by each other at the point v_i'. Denote the face that is incident with the path $v_iv_i'v_{i+1}''$ (resp. $v_{i+1}v_i'v_i''$) in $G^\times$ by f_i^L (resp. f_i^R).

While proving the lightness of a graph in a given family of graphs, usually, the discharging method is used. In the proof of this paper, based on this method we consider a hypothetical counterexample G (a 1-planar graph) and then construct its associated plane graph $G^\times$. We first assign an initial charge c to each element $x \in V(G^\times)\bigcup F(G^\times)$ as follows:

$$c(x) = \begin{cases} \alpha d_{G^\times}(x) - 2(\alpha+\beta), & \text{if } x \in V(G^\times); \\ \beta d_{G^\times}(x) - 2(\alpha+\beta), & \text{if } x \in F(G^\times), \end{cases} \tag{2.1}$$

where α and β are some prescribed positive numbers. By combining the Euler formula $|V(G^\times)| - |E(G^\times)| + |F(G^\times)| = 2$ on $G^\times$ and the relation $\sum_{v\in V(G^\times)} d_{G^\times}(v) = \sum_{f\in F(G^\times)} d_{G^\times}(f) = 2|E(G^\times)|$, we have $\sum_{x\in V(G^\times)\bigcup F(G^\times)} c(x) = -4(\alpha+\beta) < 0$. We then redistribute the charge of the vertices and the faces of $G^\times$ according to some discharging rules, which only move charge around but do not affect the total charges so that, after discharging, the final charge c' of each element in $V(G^\times)\bigcup F(G^\times)$ is nonnegative. This leads to a contradiction that $\sum_{x\in V(G^\times)\bigcup F(G^\times)} c(x) = \sum_{x\in V(G^\times)\bigcup F(G^\times)} c'(x) \geq 0$ and completes the proof.

2.2 A key discharging lemma

Let G be a 1-planar graph and let v be a true vertex in its associated plane graph $G^\times$. Denote $F(v)$ to be the subgraph induced by the faces that are incident with v. Note that $F(v)$ can be decomposed into many parts, each of which is one of the five clusters in Figure

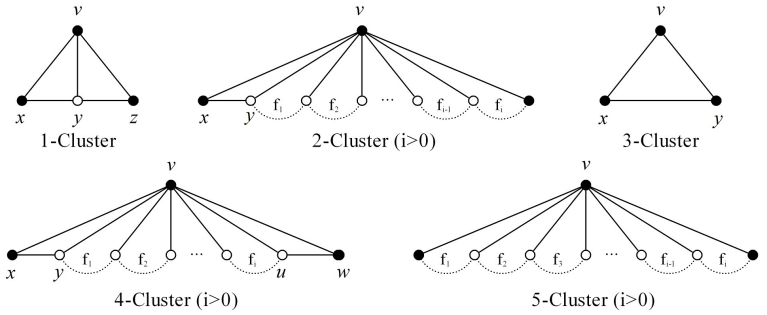

Figure 1: $F(v)$ can be decomposed into the combination of the above five clusters

1, and any two parts of which are adjacent only if they have a common edge vw such that w is a true vertex. The hollow vertices in Figure 1 are false and the solid ones are true, and all the faces marked by f_i are 4^+-faces.

Lemma 2.1. *Let v be a 6^+-vertex in the associated plane graph $G^\times$ of a 1-planar graph G. Assign v an initial charge $c(v) = \alpha d_{G^\times}(v) - 2(\alpha + \beta)$, where α and β are some prescribed positive numbers satisfying $2\alpha \geq \beta$. Suppose that v sends out charges only by the following three discharging rules:*

Rule A *v transfers a charge of $\frac{2\alpha-\beta}{3}$ to each incident 3-face in $G^\times$;*

Rule B *If v is incident with two adjacent 3-faces $f_1 = [xvz]$ and $f_2 = [yvz]$ so that z is a false vertex in $G^\times$, then v sends the charge λ to z;*

Rule C *If v is incident with a 3-face $f_1 = [xvz]$ sharing a common edge vz with a 4^+-face f_2 so that z is a false vertex in $G^\times$, then v sends the charge μ to z.*

Denote $c'(v)$ to be the final charge of v after applying the above rules. If $d_{G^\times}(v)$ is even with

$$\lambda \leq \left(\frac{2}{3} - \frac{4}{d_{G^\times}(v)}\right)(\alpha + \beta), \tag{2.2}$$

$$\mu = \frac{3}{4}\lambda, \tag{2.3}$$

or $d_{G^\times}(v) \geq 9$ is odd with

$$\lambda \leq \left(\frac{2d_{G^\times}(v) - 12}{3d_{G^\times}(v) - 3}\right)(\alpha + \beta), \tag{2.4}$$

$$\mu = \frac{1}{2}\lambda, \tag{2.5}$$

or $d_{G^\times}(v) = 7$ with

$$\lambda = \mu = \frac{\alpha + \beta}{12}, \tag{2.6}$$

then $c'(v) \geq 0$.

Proof. Denote n_i to be the number of i-clusters contained in $F(v)$ and m_i to be the charges sent out from v through an i-cluster. By their definitions, one can easily observe that

$$2n_1 + 2n_2 + n_3 + 3n_4 + n_5 \leq d_{G^\times}(v). \tag{2.7}$$

For the case when $d_{G^\times}(v)$ is even, by (2.7) and the choices of λ, μ as in (2.2) and (2.3), we have

$$\begin{aligned}
c'(v) &= c(v) - \frac{2\alpha-\beta}{3} d_{G^\times}(v) - \sum_{i=1}^{5} n_i m_i \\
&= \frac{\alpha+\beta}{3} d_{G^\times}(v) - 2(\alpha+\beta) - \lambda n_1 - \mu n_2 - 2\mu n_4 \\
&\geq \frac{\alpha+\beta}{3} d_{G^\times}(v) - 2(\alpha+\beta) - \frac{\lambda}{2}(2n_1 + 2n_2 + n_3 + 3n_4 + n_5) \\
&\geq \frac{\alpha+\beta}{3} d_{G^\times}(v) - 2(\alpha+\beta) - \frac{\lambda}{2} d_{G^\times}(v) \\
&\geq \frac{\alpha+\beta}{3} d_{G^\times}(v) - 2(\alpha+\beta) - \left(\frac{1}{3} - \frac{2}{d_{G^\times}(v)}\right)(\alpha+\beta) d_{G^\times}(v) \\
&= 0.
\end{aligned}$$

Now, we consider the case when $d_{G^\times}(v)$ is odd. Here, note that

$$n_2 + n_3 + n_4 + n_5 \geq 1 \tag{2.8}$$

since any copy of a 1-cluster consists even number of faces incident with v. By (2.7), (2.8) and the choices of λ, μ as in (2.4) and (2.5), we have

$$\begin{aligned}
c'(v) &= c(v) - \frac{2\alpha-\beta}{3} d_{G^\times}(v) - \sum_{i=1}^{5} n_i m_i \\
&= \frac{\alpha+\beta}{3} d_{G^\times}(v) - 2(\alpha+\beta) - \lambda n_1 - \mu n_2 - 2\mu n_4 \\
&= \frac{\alpha+\beta}{3} d_{G^\times}(v) - 2(\alpha+\beta) - \frac{\lambda}{2}(2n_1 + 2n_2 + n_3 + 3n_4 + n_5) + \\
&\quad \frac{\lambda}{2}(n_2 + n_3 + n_4 + n_5) \\
&\geq \frac{\alpha+\beta}{3} d_{G^\times}(v) - 2(\alpha+\beta) - \frac{\lambda}{2} d_{G^\times}(v) + \frac{\lambda}{2} \\
&\geq \frac{\alpha+\beta}{3} d_{G^\times}(v) - 2(\alpha+\beta) - \left(\frac{d_{G^\times}(v) - 6}{3 d_{G^\times}(v) - 3}\right)(\alpha+\beta)(d_{G^\times}(v) - 1) \\
&= 0.
\end{aligned}$$

For the particular case when $d_{G^\times}(v) = 7$, we can deduce from (2.7) that

$$n_1 + n_2 + 2n_4 = \left\lfloor \frac{2n_1 + 2n_2 + 3n_4}{2} \right\rfloor + \left\lceil \frac{1}{2} n_4 \right\rceil \leq \left\lfloor \frac{7}{2} \right\rfloor + \left\lceil \frac{1}{2} \left\lfloor \frac{7}{3} \right\rfloor \right\rceil = 4. \tag{2.9}$$

Thus by (2.9) along with the choices of λ and μ as in the equation (2.6), we have

$$\begin{aligned} c'(v) &= c(v) - \frac{2\alpha-\beta}{3}d_{G^\times}(v) - \sum_{i=1}^{5} n_i m_i \\ &= \frac{\alpha+\beta}{3} - \lambda n_1 - \mu n_2 - 2\mu n_4 \\ &= \frac{\alpha+\beta}{3} - \lambda(n_1+n_2+2n_4) \\ &\geq \frac{\alpha+\beta}{3} - 4\lambda \\ &= 0. \end{aligned}$$

Consequently, we complete the proof of this lemma. □

2.3 The height of chordal 4-cycle in $\mathcal{P}_6^1(13)$ and $\mathcal{P}_7^1$

Theorem 2.2. *Each 1-planar graph with minimum degree at least 6 contains at least one of the following configurations:*

- (a) *a pair of adjacent vertices of degree 6;*
- (b) *a 4-cycle $C = [x_1x_2x_3x_4]$ of the type $(6, \leq 12, \leq 8, \leq 12)$ with a chord x_1x_3;*
- (c) *a 4-cycle $C = [x_1x_2x_3x_4]$ of the type $(7, \leq 10, \leq 8, \leq 10)$ with a chord x_1x_3.*

Proof. The proof of the theorem is carried out by the discharging method as described in Section 2.1. Suppose G is a counterexample to the theorem. Consider the associated plane graph $G^\times$ of G. Assign the charges to each element $x \in V(G^\times) \cup F(G^\times)$ as mentioned in the inequation (2.1) of Section 2.1 by choosing $\alpha = 2$ and $\beta = 3$. If v is a true vertex in G, then $d_{G^\times}(v) = d_G(v)$, so in the following we use $d(v)$ for short to represent both of the two notions. A *big* vertex, *semi-big* vertex, *intermediate* vertex and *semi-intermediate* vertex refer to a vertex $v \in V(G^\times)$ with $d(v) \geq 13$, $d(v) \geq 11$, $6 \leq d(v) \leq 12$ and $6 \leq d(v) \leq 10$, respectively. Therefore, a true vertex in $G^\times$ is either big or intermediate, and an intermediate vertex in $G^\times$ is either semi-big or semi-intermediate. By *big* face, we denote a face $f \in F(G^\times)$ with degree at least 4. Now, we define the discharging rules as follows.

Rule 1 Each 6^+-vertex sends $\frac{1}{3}$ to each incident face;

Rule 2 Each 4-vertex sends $\frac{1}{3}$ to each incident false 3-face;

Rule 3 Each big face sends $\frac{11}{12}$ to each incident 4-vertex;

Rule 4 Let f be a big face having a common edge xy with a false 3-face $g = [xyz]$. If z is a 4-vertex, then f sends $\frac{5}{12}$ to z through xy;

Rule 5 Let f be a big face having a common edge xy with a false 3-face $g = [xyz]$. If x is a 4-vertex and yz is incident with another false 3-face $h = [yzu]$, then f sends $\frac{5}{24}$ to u through xy and yz;

Rule 6 Let $f = [xyz]$ be a true 3-face having a common edge yz with a false 3-face $g = [uyz]$. If $d(x) \geq 11$, then x sends $\frac{5}{12}$ to u through yz;

Rule 7 Let $f=[xyz]$ and $g=[uyz]$ be two adjacent false 3-faces, and let z be a 4-vertex. Suppose yu is incident with another false 3-face $h=[yuw]$ so that yy' crosses uu' in G at w. If at least one of the following four occasions appears in $G^\times$

- $d(x)\geq 13$, $\min\{d(u),d(y)\}=6$, $\max\{d(u),d(y)\}\leq 8$ and y,u,u' are all intermediate vertices with $yu'\in E(G^\times)$;
- $d(x)\geq 13$, $\min\{d(u),d(y)\}=6$, $\max\{d(u),d(y)\}\leq 8$ and y,u,y' are all intermediate vertices with $uy'\in E(G^\times)$;
- $d(x)\geq 11$, $\min\{d(u),d(y)\}=7$, $\max\{d(u),d(y)\}\leq 8$ and y,u,u' are all semi-intermediate vertices with $yu'\in E(G^\times)$;
- $d(x)\geq 11$, $\min\{d(u),d(y)\}=7$, $\max\{d(u),d(y)\}\leq 8$ and y,u,y' are all semi-intermediate vertices with $uy'\in E(G^\times)$,

then x sends $\frac{5}{24}$ to w through yz and yu;

Rule 8 Let $f=[xyz]$ and $g=[uyz]$ be two adjacent false 3-faces. If z is a 4-vertex, then y sends to z a charge of

$\frac{5}{12}$, if $d(y)=7$;
$\frac{5}{6}$, if $d(y)=8$;
$\frac{5}{4}$, if $9\leq d(y)\leq 12$;
$\frac{5}{3}$, if $d(y)\geq 13$;

Rule 9 Let $f=[xyz]$ be a false 3-face having a common edge yz with a big face β. If z is a 4-vertex, then y sends to z a charge of

$\frac{5}{12}$, if $d(y)=7$;
$\frac{5}{8}$, if $8\leq d(y)\leq 12$;
$\frac{5}{6}$, if $d(y)\geq 13$.

In the following, we estimate the final charge c' of vertices and faces after the charge redistribution and prove $c'(x)\geq 0$ for each $x\in V(G^\times)\bigcup F(G^\times)$. By Rules 1 and 2, any 3-face f in $G^\times$ receive $\frac{1}{3}$ from each of its incident vertices, which implies the final charge of f is exactly zero. For a big face f in $G^\times$ (recall that $\zeta(f)$ denotes the number of 4-vertices incident with f), it would send $\frac{11}{12}\zeta(f)$ to its incident 4-vertices by Rule 3. Besides, if f is incident with a 4-vertex v, then f send out $2\times\frac{5}{24}=\frac{5}{12}$ through uv and vw by Rule 5, where u and w denote the neighbors of v on the boundary of f. Since f is incident with $d(f)-2\zeta(f)$ true edges (namely, an edge of $G^\times$ containing no 4-vertex), by Rule 4, a total charge of $\frac{5}{12}(d(f)-2\zeta(f))$ would be sent out from f through the true edges incident with f. On the other hand, f receive $\frac{1}{3}$ from each of $d(f)-\zeta(f)$ true vertices incident with it. Since $\zeta(f)\leq\frac{d(f)}{2}$, $c'(f)\geq 3d(f)-10-\frac{11}{12}\zeta(f)-\frac{5}{12}\zeta(f)-\frac{5}{12}(d(f)-2\zeta(f))+\frac{1}{3}(d(f)-\zeta(f))=\frac{35}{12}d(f)-\frac{5}{6}\zeta(f)-10\geq\frac{5}{2}d(f)-10\geq 0$ for $d(f)\geq 4$.

By Lemma 2.1 along with Rules 1,8 and 9, one can check that $c'(v)\geq 0$ for all vertices of degree between 6 and 10. For a big vertex v in $G^\times$, denote $F(v)$ to be the subgraph induced by the faces that are incident with v. As we state at the beginning of Section 2.2, $F(v)$ can be decomposed into a combination of the five clusters in Figure 1. By n_i and m_i, we denote the number of i-clusters contained in $F(v)$ and the charges sent out from v through an i-cluster. If there is a 2-cluster in $F(v)$, then v send $\frac{5}{6}$ to y (see Figure 1) by Rule 9 and at most $\frac{5}{24}$ through xy by Rule 7, so $m_2\leq\frac{5}{6}+\frac{5}{24}=\frac{25}{24}$. Similarly, we can prove

that $m_3 \leq \frac{5}{12}$ by Rule 6, $m_4 \leq 2 \times \frac{5}{6} + 2 \times \frac{5}{24} = \frac{25}{12}$ by Rules 7, 9 and $m_5 = 0$. We now estimate the value of m_1 much more carefully. First, we show the following observation.

Observation. *If v is incident with a 1-cluster as in Figure 1 and has sent out some charge through xy by Rule 7, then it would not send out any charge through the edge yz.*

Proof. Denote u to be the neighbor of v in G such that uv crosses xz in G at the point y. Suppose, on the contrary, that v send out some charge through yz. By the definitions of the rules, uyz is a 3-face in $G^\times$ and z is an intermediate vertex in $G^\times$. Since v has sent out charge through xy by Rule 7, by the definition of Rule 7, we have $xu \in E(G^\times)$, $\min\{d(x), d(u)\} = 6$ and $\max\{d(x), d(u)\} \leq 8$. Furthermore, xu is also incident with a 3-cycle, say xuw, in G such that w is an intermediate vertex in $G^\times$ different from z. Now, the four distinct vertices x, z, u, w form a 4-cycle $[uwxz]$ in G with a chord ux, and therefore, the configuration (b) occurs in G. This contradiction verifies this observation. ‖

By Rules 7, 8 and the above observation, we immediately have $m_1 \leq \frac{5}{3} + \frac{5}{24} = \frac{15}{8}$. Therefore, by Rule 1 and the inequality (2.7) in Section 2.1, we have $c'(v) \geq 2d(v) - 10 - \frac{1}{3}d(v) - \frac{15}{8}n_1 - \frac{25}{24}n_2 - \frac{5}{12}n_3 - \frac{25}{12}n_4 \geq \frac{5}{3}d(v) - 10 - \frac{15}{16}(2n_1 + 2n_2 + n_3 + 3n_4 + n_5) + \frac{25}{48}(n_2 + n_3 + n_4 + n_5) \geq \frac{35}{48}d(v) - 10 + \frac{25}{48}(n_2 + n_3 + n_4 + n_5) > 0$ for $d(v) \geq 14$. If $d(v) = 13$, then by the inequality (2.8) in Section 2.1, we also have $c'(v) \geq \frac{35}{48}d(v) - 10 + \frac{25}{48} = 0$ in final. For vertices of degree 11 or 12 (they are semi-big but not big), we can also check the nonnegativity of their final charges. Proof of them are left to the readers, since they use the same argument as in the previous analysis on the big vertices.

Now, the only missed case is when v is a 4-vertex in $G^\times$ (namely, v is a false vertex). As we know, the initial charge of a 4-vertex v is -2, so if v is incident with at least three big faces, then by Rules 2 and 3, the final charge $c'(v)$ of v is at least $-2-\frac{1}{3}+3\times\frac{11}{12} = \frac{5}{12} > 0$. In the following, we discuss three other cases.

Case 1. v is incident with exactly two 3-faces.

First, suppose that f_1 and f_2 are 3-faces. Since no two 6-vertices are adjacent in G, at least two of v_1, v_2 and v_3 are 7^+-vertices. Thus by Rules 8 and 9, each of the two 7^+-vertices among v_1, v_2 and v_3 would send at least $\frac{5}{12}$ to v. Therefore, $c'(v) \geq -2 - 2 \times \frac{1}{3} + 2 \times \frac{11}{12} + 2 \times \frac{5}{12} = 0$ by Rules 2, 3, 8 and 9.

Second, suppose that f_1 and f_3 are 3-faces. In this case, one can also show that there are at least two 7^+-vertices among v_1, v_2, v_3 and v_4. Thus by Rules 2, 3, 8 and 9, we still have $c'(v) \geq -2 - 2 \times \frac{1}{3} + 2 \times \frac{11}{12} + 2 \times \frac{5}{12} = 0$.

Case 2. v is incident with exactly three 3-faces.

Without loss of generality, we assume that f_1, f_2, f_3 are 3-faces and f_4 is a 4^+-face (recall the definitions of f_i in Section 2.1). By Rule 3, f_4 shall send $\frac{11}{12}$ to v.

First, suppose that at least two of v_1, v_2, v_3 and v_4, say v_1 and v_4 (other cases can be dealt with similarly), are big vertices. Thus at least one of v_2 and v_3 must be 7^+-vertex since they are adjacent in G. Therefore, by Rules 2, 3 and 9, $c'(v) \geq -2-3\times\frac{1}{3}+2\times\frac{5}{6}+\frac{5}{12}+\frac{11}{12} = 0$.

Next, suppose that only one of v_1, v_2, v_3 and v_4 is big vertex. If v_2 or v_3, say v_2, is big, then at least one of v_1, v_3 and v_4 should be a 7^+-vertex since they three form a 3-path in G. By Rules 2, 3, 8 and 9, $c'(v) \geq -2 - 3 \times \frac{1}{3} + \frac{5}{3} + \frac{5}{12} + \frac{11}{12} = 0$. If v_1 or v_4, say v_1, is big, then all of v_2, v_3 and v_4 are intermediate. If they are all 7^+-vertices, then $c'(v) \geq -2 - 3 \times \frac{1}{3} + \frac{5}{6} + 3 \times \frac{5}{12} + \frac{11}{12} = 0$ by Rules 2, 8 and 9. Thus we assume that at

least one of v_2, v_3 and v_4 is a 6-vertex. Here, we only consider the case when $d(v_3) = 6$ and leave the discussions on the rest two cases to the readers, since they are quite similar. First, suppose $d(v_2) \geq 9$. By Rules 3 and 8, v_1, v_2 and f_4 shall send $\frac{5}{6}$, $\frac{5}{4}$ and $\frac{11}{12}$ to v, respectively, thus, $c'(v) \geq -2-3\times\frac{1}{3}+\frac{5}{6}+\frac{5}{4}+\frac{11}{12} = 0$. Second, suppose $d(v_2) \leq 8$. We now consider the face f_2' (recall its definition in Section 2.1). If f_2' is a big face in $G^\times$, then by Rule 4, f_2' sends $\frac{5}{12}$ to v through the edge v_2v_3. If f_2' is a true 3-face, then v_2' (recall the corresponding definition in Section 2.1) must be a big vertex, because otherwise the configuration (b) would appear in G, meanwhile, v receives $\frac{5}{12}$ from v_2' through the edge v_2v_3 by Rule 6. If f_2' is false 3-face, then we consider the faces f_2^L and f_2^R (recall their definitions in Section 2.1). If f_2^L is a big face, then by Rule 5, f_2^L sends $\frac{5}{24}$ to v through the edge v_2v_3. If f_2^L is a 3-face, then it must be false since it is incident with a false vertex v_2'. Since v_2, v_3, v_4 and v_3'' (recall the definitions of v_i'' in Section 2.1) form a chordal 4-cycle with a chord v_2v_3 in G, v_3'' must be a big vertex, and then v shall receive $\frac{5}{24}$ from v_3'' through the edge v_2v_3 by Rule 7. Similarly, v would receive another $\frac{5}{24}$ through the edge v_2v_3 from either the face f_2^R or the vertex v_2''. Hence, through the edge v_2v_3, v shall totally receive a charge of $2\times\frac{5}{24} = \frac{5}{12}$. Since neither v_2 nor v_4 can be a 6-vertex (because each of them is adjacent to the 6-vertex v_3 in G), each of v_2 and v_4 shall send $\frac{5}{12}$ to v by Rules 8 and 9. Thus, by Rules 2, 3 and 9, we still have $c'(v) \geq -2-3\times\frac{1}{3}+\frac{5}{12}+2\times\frac{5}{12}+\frac{5}{6}+\frac{11}{12} = 0$.

At last, suppose none of v_1, v_2, v_3 and v_4 is big. If v_2 or v_3, say v_2, is a 6-vertex, then v_1, v_3 and v_4 are 7^+-vertices since each of them is adjacent to v_2. Furthermore, $d(v_3) \geq 9$, because otherwise the configuration (b) would appear in G, so by Rules 2, 3, 8 and 9, we have $c'(v) \geq -2-3\times\frac{1}{3}+2\times\frac{5}{12}+\frac{5}{4}+\frac{11}{12} = 0$. We now assume $\min\{d(v_2), d(v_3)\} \geq 7$. If $\max\{d(v_2), d(v_3)\} \geq 9$ (without loss of generality, assume $d(v_3) \geq 9$), then by Rules 2, 3, 8 and 9, $c'(v) \geq -2-3\times\frac{1}{3}+2\times\frac{5}{4}+\frac{11}{12} > 0$ when $d(v_2) \geq 9$, $c'(v) \geq -2-3\times\frac{1}{3}+2\times\frac{5}{12}+\frac{5}{4}+\frac{11}{12} = 0$ when $d(v_2) \leq 8$ and $d(v_1) \geq 7$, and $c'(v) \geq -2-3\times\frac{1}{3}+\frac{5}{12}+\frac{5}{12}+\frac{5}{4}+\frac{11}{12} = 0$ when $d(v_2) \leq 8$ and $d(v_1) = 6$ (note that in this case, a charge of at least $\frac{5}{12}$ shall be transferred to v through the edge v_1v_2). Therefore, we assume $\max\{d(v_2), d(v_3)\} \leq 8$ in the following. First, suppose at least one of v_2 and v_3 is a 8-vertex. Without loss of generality, suppose $d(v_2) = 7$ and $d(v_3) = 8$. By Rule 8, v_2 and v_3 shall send $\frac{5}{12}$ and $\frac{5}{6}$ to v, respectively. By a similar argument as above, v shall also receive $\frac{5}{12}$ either from the vertex v_1 when $d(v_1) \geq 7$ or through the edge v_1v_2 when $d(v_{(1)} = 6$, and another $\frac{5}{12}$ either from the vertex v_4 when $d(v_4) \geq 7$ or through the edge v_3v_4 when $d(v_{(4)} = 6$. Thus, by Rules 2 and 3, we have $c'(v) \geq -2-3\times\frac{1}{3}+\frac{5}{12}+\frac{5}{6}+2\times\frac{5}{12}+\frac{11}{12} = 0$.

Second, suppose $d(v_2) = d(v_3) = 7$. Under this hypothesis, at least one of v_1 and v_4 should be semi-big, because otherwise a configuration (c) would appear in G. If v_1 and v_4 are 8^+-vertices, then by Rules 2, 3, 8 and 9, $c'(v) \geq -2-3\times\frac{1}{3}+2\times\frac{5}{12}+2\times\frac{5}{8}+\frac{11}{12} = 0$. If one of v_1 and v_4, say v_4, is a 7^--vertex, then by a similar argument as before, we can show that v receives $\frac{5}{12}$ through the edges v_1v_2 and another $\frac{5}{12}$ through the edges v_2v_3. Therefore, by Rules 2, 3, 8 and 9, we have $c'(v) \geq -2-3\times\frac{1}{3}+2\times\frac{5}{12}+\frac{5}{8}+2\times\frac{5}{12}+\frac{11}{12} > 0$.

Case 3. v is incident with four 3-faces.

If at least two of v_1, v_2, v_3 and v_4 are big vertices, then by Rules 2 and 8, $c'(v) \geq -2-4\times\frac{1}{3}+2\times\frac{5}{3} = 0$.

If only one of v_1, v_2, v_3, v_4, say v_1, is a big vertex, then we can assume that v_2, v_3 and v_4 are 7^+-vertices. Otherwise, without loss of generality, suppose $d(v_2) = 6$. Since no two 6-vertices are adjacent in G, $d(v_3) \geq 7$ and $d(v_4) \geq 7$. If v_3 and v_4 are 8^+-vertices, then $c'(v) \geq -2-4\times\frac{1}{3}+\frac{5}{3}+2\times\frac{5}{6} = 0$ by Rules 2 and 8. We now assume that one of v_3 and v_4, say v_3, is a 7-vertex. If now $d(v_4) \geq 9$, then $c'(v) \geq -2-4\times\frac{1}{3}+\frac{5}{3}+\frac{5}{12}+\frac{5}{4} = 0$

Rules 2 and 8. If $d(v_4) \leq 8$, then by a similar argument as in Case 1, we can show that v receives $\frac{5}{12}$ through the edges v_2v_3 and another $\frac{5}{12}$ through the edges v_3v_4. Therefore, by Rules 2 and 8, $c'(v) \geq -2 - 4 \times \frac{1}{3} + \frac{5}{3} + 2 \times \frac{5}{12} + 2 \times \frac{5}{12} = 0$. Hence, we can assume $\min\{d(v_2), d(v_3), d(v_4)\} \geq 7$. If at least one of v_2, v_3 and v_4 is a 8^+-vertex, then by Rules 2 and 8, $c'(v) \geq -2 - 4 \times \frac{1}{3} + 2 \times \frac{5}{12} + \frac{5}{6} = 0$. If $d(v_2) = d(v_3) = d(v_4) = 7$, then by a similar argument as in Case 1, one can show that a charge of $\frac{5}{12}$ would be transferred to v through each of the edges v_2v_3 and v_3v_4. Hence, by Rules 2 and 8, we have $c'(v) \geq -2 - 4 \times \frac{1}{3} + 3 \times \frac{5}{12} + 2 \times \frac{5}{12} > 0$.

We now consider the last case when v_1, v_2, v_3 and v_4 are intermediate vertices. If they all are 8^+-vertices, then by Rules 2 and 8, $c'(v) \geq -2 - 4 \times \frac{1}{3} + 4 \times \frac{5}{6} = 0$. If one of them, say v_1, is a 6-vertex, then v_2, v_3 and v_4 are 9^+-vertex, because otherwise the configuration (b) would appear in G. This implies that $c'(v) \geq -2 - 4 \times \frac{1}{3} + 3 \times \frac{5}{4} > 0$ by Rules 2 and 8. We now assume that $d(v_1) = 7$ and $\min\{d(v_2), d(v_3), d(v_4)\} \geq 7$. If at least two of v_2, v_3 and v_4 are 9^+-vertices, then by Rules 2 and 8, $c'(v) \geq -2 - 4 \times \frac{1}{3} + 2 \times \frac{5}{12} + 2 \times \frac{5}{4} = 0$. Thus, we assume that at least two of v_2, v_3, v_4, say v_2 and v_3, are 8^--vertices. In this case, v_4 should be a semi-big vertex because otherwise the configuration (c) would occur in G. If $d(v_2) = d(v_3) = 8$, then by Rules 2 and 8, $c'(v) \geq -2 - 4 \times \frac{1}{3} + \frac{5}{12} + 2 \times \frac{5}{6} + \frac{5}{4} = 0$. If $\min\{d(v_2), d(v_3)\} = 7$, then by a similar argument as in Case 1, one can prove that a charge of $\frac{5}{12}$ would be transferred to v through each of the edges v_1v_2 and v_2v_3. This implies that $c'(v) \geq -2 - 4 \times \frac{1}{3} + 3 \times \frac{5}{12} + 2 \times \frac{5}{12} + \frac{5}{4} = 0$.

Hence, we deduce that $\sum_{x \in V(G^\times) \bigcup F(G^\times)} c'(x) \geq 0$. This contradiction completes the proof. □

Corollary 2.3. *$K_4^- \in \mathcal{L}(\mathcal{P}_6^1(13))$ and $h(K_4^-, \mathcal{P}_6^1(13)) \leq 12$.*

Corollary 2.4. *$K_4^- \in \mathcal{L}(\mathcal{P}_7^1)$ and $h(K_4^-, \mathcal{P}_7^1) \leq 10$.*

Corollary 2.5. *$h(P_2, P_6^1) \leq 8$ and $w(P_2, P_6^1) \leq 15$.*

References

[1] M. O. Albertson and B. Mohar, Coloring vertices and faces of locally planar graphs. *Graph. Combinator.* **22** (2006), 289–295.

[2] J. A. Bondy and U. S. R. Murty, *Graph Theory with Applications*, North-Holland, New York, 1976.

[3] O. V. Borodin, Solution of Ringel's problems on the vertex-face coloring of plane graphs and on the coloring of 1-planar graphs (in Russian), *Diskret. Analiz* **41** (1984), 12–26.

[4] O. V. Borodin, A New Proof of the six Color Theorem, *J. Graph Theory* **19** (1995), 507–521.

[5] O.V. Borodin, Minimal vertex degree sum of a 3-path in plane maps, *Discuss. Math. Graph Theory* **17** (1997), 279–284.

[6] O. V. Borodin, I. G. Dmitriev and A. O. Ivanova, The height of a 4-cycle in triangle-free 1-planar graphs with minimum degree 5, *J. Appl. Industrial Math.* **3** (2009), 28–31.

[7] O. V. Borodin, A. V. Kostochka, A. Raspaud and E. Sopena, Acyclic colouring of 1-planar graphs, *Discrete Appl. Mat.* **114** (2001), 29–41.

[8] W. Dong, Light paths of 1-planar graphs with bounded minimum degree, manuscript.

[9] I. Fabrici and T. Madaras, The structure of 1-planar graphs, *Discrete Math.* **307** (2007), 854–865.

[10] D. Hudák and T. Madaras, On local structures of 1-planar graphs of minimum degree 5 and girth 4, *Discuss. Math. Graph Theory* **29** (2009), 385–400.

[11] D. Hudák and T. Madaras, On local properties of 1-planar graphs with high minimum degree, *Ars Math. Contemp.* **4** (2011), 245–254.

[12] V. P. Korzhik, Minimal non-1-planar graphs, *Discrete Math.* **308** (2008), 1319–1327.

[13] V. P. Korzhik and B. Mohar, Minimal obstructions for 1-immersions and hardness of 1-planarity test, *Springer Lect. Notes Comput. Sci.* **5417** (2009), 302–312, 2009.

[14] T. Madaras and R. Škrekovski, Heavy paths, light stars and big melons, *Discrete Math.* **286** (2004), 115–131.

[15] B. Mohar, R. Škrekovski and H.-J. Voss, Light subgraphs in planar graphs of minimum degree 4 and edge-degree 9, *J. Graph Theory* **44** (2003), 261–295.

[16] G. Ringel, Ein sechsfarbenproblem auf der Kugel (in German), *Abh. Math. Sem. Hamburg. Univ.* **29** (1965), 107–117.

[17] Y. Suzuki, Optimal 1-planar graphs which triangulate other surfaces, *Discrete Math.* **310** (2010), 6–11.

[18] W. Wang and K.-W. Lih, Coupled choosability of plane graphs, *J. Graph Theory* **58** (2008), 27–44.

[19] X. Zhang and G. Liu, On edge colorings of 1-planar graphs without chordal 5-cycles, *Ars Combin.* **104** (2012), 431–436.

[20] X. Zhang and G. Liu, On edge colorings of 1-planar graphs without adjacent triangles, *Inform. Process. Lett.* **112** (2012), 138–142.

[21] X. Zhang, G. Liu and J.-L. Wu, Edge coloring of triangle-free 1-planar graphs (in Chinese), *Journal of Shandong University (Natural Science)* **45** (2010), 15–17.

[22] X. Zhang, G. Liu and J.-L. Wu, Structural properties of 1-planar graphs and an application to acyclic edge coloring (in Chinese), *Scientia Sinica Mathematica* **40** (2010), 1025–1032.

[23] X. Zhang, G. Liu and J.-L. Wu, Light subgraphs in the family of 1-planar graphs with high minimum degree, *Acta Math. Sinica, English Series* **28** (2012), 1155–1168.

[24] X. Zhang, G. Liu and J.-L. Wu, On the linear arboricity of 1-planar graphs, *OR Transactions* **15** (2011), 38–44.

[25] X. Zhang and J.-L. Wu, Edge coloring of 1-planar graphs, *Inform. Process. Lett.* **111** (2011), 124–128.

[26] X. Zhang X, J.-L. Wu and G. Liu, New upper bounds for the heights of some light subgraphs in 1-planar graphs with high minimum degree, *Discrete Math. Theoret. Comp. Sc.* **13** (2011), 9–16.

[27] X. Zhang, J.-L. Wu, G. Liu, List edge and list total coloring of 1-planar graphs, *Front. Math. China* **7** (2012), 1005–1018.

[28] X. Zhang, Y. Yu and G. Liu, On $(p, 1)$-total labelling of 1-planar graphs, *Cent. Eur. J. Math.* **9** (2011), 1424–1434.

ARS MATHEMATICA CONTEMPORANEA

Also available at http://amc-journal.eu
ISSN 1855-3966 (printed edn.), ISSN 1855-3974 (electronic edn.)
ARS MATHEMATICA CONTEMPORANEA 7 (2014) 293–297

On the connectivity of Cartesian product of graphs*

Jelena Govorčin

Faculty of information studies
Ulica talcev 3, 8000 Novo mesto, Slovenia

Riste Škrekovski

Department of Mathematics, University of Ljubljana
Jadranska 19, 1000 Ljubljana, Slovenia

Received 29 February 2012, accepted 29 October 2012, published online 7 May 2013

Abstract

We give a new alternative proof of Liouville's formula which states that for any graphs G and H on at least two vertices, $\kappa(G\Box H) = \min\{\kappa(G)|H|,\ |G|\kappa(H),\ \delta(G)+\delta(H)\}$, where κ and δ denote the connectivity number and minimum degree of a given graph, respectively. The main idea of our proof is based on construction of a vertex-fan which connects a vertex from $V(G\Box H)$ to a subgraph of $G\Box H$. We also discuss the edge version of this problem as well as formula for products with more than two factors.

Keywords: Connectivity, Cartesian product.

Math. Subj. Class.: 05C40, 05C76

1 Introduction

The Cartesian product has been studied extensively since the 1950's. Despite of its simple definition, answering many underlying questions is far from being trivial. One such question refers to a connectivity of a Cartesian product and how it depends on invariants of its factors.

The first result of this type appeared in an article written by Sabidussi [5] in 1957. He proved that for arbitrary graphs G and H, $\kappa(G\Box H) \geq \kappa(G)+\kappa(H)$. In 1978, Liouville [4] conjectured that for graphs G and H on at least two vertices, $\kappa(G\Box H) = \min\{\kappa(G)|H|,\ |G|\kappa(H),\ \delta(G)+\delta(H)\}$, where κ and δ denote the connectivity number

*Partially supported by ARRS project L7-4119 and ARRS research programs P1-0383.
E-mail addresses: jelena.govorcin@fis.unm.si (Jelena Govorčin), skrekovski@gmail.com (Riste Škrekovski)

and minimum degree of a given graph, respectively. The result of Subidussi was improved by Xu and Yang [7]. They showed that $\kappa(G\Box H) \geq \min\{\kappa(G)+\delta(H), \kappa(H)+\delta(G)\}$, where G and H are connected undirected graphs. Finally, the Liouville's formula has been recently proved by Špacapan in [6]. For more information on the topic, see also [1, 2, 3].

We use the following terminology. The *Cartesian product* of two graphs G and H, denoted by $G\Box H$, is a graph with vertex set $V(G)\times V(H)$, where two vertices (g,h) and (g',h') are adjacent if $gg'\in E(G)$ and $h=h'$ or $g=g'$ and $hh'\in E(H)$. The graphs G and H are called the *factors* of $G\Box H$. For any $h\in V(H)$, we denote by G^h the subgraph of $G\Box H$ induced by $V(G)\times\{h\}$ and name it *G-fiber*. Similarly, we can define *H-fiber*.

For a graph G and $v\in V(G)$, the *degree* of a vertex v is denoted by $d_G(v)$, or simply $d(v)$ if the graph G is known from the context. Furthermore, we denote by $\delta(G)$ the minimum degree of a graph G. The minimum degree is additive under Cartesian products, i.e. $\delta(G\Box H)=\delta(G)+\delta(H)$. Recall that the symbol $N_G(v)$ denotes the set of neighbours of a vertex v in a graph G.

For a connected graph G a subset $S\subseteq V(G)$ is a *separating set* if $G-S$ has more than one component. The *connectivity* $\kappa(G)$ of G is the minimum size of $S\subseteq V(G)$ such that $G-S$ is disconnected or a single vertex. For any $k\leq\kappa(G)$, we say that G is *k-connected*. A subset of edges $S'\subseteq E(G)$ is *disconnecting set* if $G-S'$ has more than one component. The *edge-connectivity* $\lambda(G)$ of G is the maximum k for which G is k-edge-connected, i.e. every disconnecting set consists of at least k edges.

A set of (u,W)-paths, where $W\subset V(G)$ and $u\in V(G)\setminus W$, is called a *vertex-fan* (resp. an *edge-fan*) if any two of the considered paths have only vertex u in common (resp. edge-disjoint paths). We say that a vertex-fan *avoids a vertex* v if its paths do not contain v.

In this paper, we provide an alternative poof of Liouville's formula. Our approach to proving this result includes construction of a vertex-fan which connects a vertex from $V(G\Box H)$ to a subgraph of $G\Box H$. Namely, for every vertex $(a,b)\in V(G\Box H)$ there exists a vertex-fan of minimum size $d(a)+d(b)$ which connects a chosen vertex and a connected subgraph of $G\Box H$ comprised of a fiber of G and a fiber of H. We also discuss the edge version of this problem as well as formula for products with more than two factors.

2 Connectivity of Cartesian product

Here, we construct the fan.

Proposition 2.1. *Let G and H be connected graphs, $a,c\in V(G)$ and $b,d\in V(H)$ distinct vertices. Then, there exists a vertex-fan F from (a,b) to $G^d\cup{}^cH$ of size $d(a)+d(b)$ that avoids the vertex (c,d). Moreover $d(a)$ paths of F are ended in G^d and $d(b)$ paths of F are ended in ${}^cH$.*

Proof. Let $N_G(a)=\{a_1,a_2,\ldots,a_{d(a)}\}$ and $N_H(b)=\{b_1,b_2,\ldots,b_{d(b)}\}$. Let $P_G=ax_1x_2x_3\cdots x_k(=c)$ (resp. $P_H=by_1y_2y_3\cdots y_l(=d)$) be a shortest path that connects a and c in G (resp. b and d in H). Thus, x_1 (resp. y_1) is the only neighbour of a (resp. b) that is contained in P_G (resp. P_H). So, without loss of generality, we can assume that $x_1=a_1$ and $y_1=b_1$.

Now, we construct a vertex-fan F from (a,b) to $G^d\cup{}^cH$. First, we define $d(a)$ vertex-

disjoint paths that use copies of the path P_H to reach the fiber G^d:

$$\begin{array}{lll} (a,b)P_{^aH} & \text{where} & P_{^aH} = (a,y_1)(a,y_2)(a,y_3)\cdots(a,y_{l-1})(a,d), \\ (a,b)(a_i,b)P_{^{a_i}H} & \text{where} & P_{^{a_i}H} = (a_i,y_1)(a_i,y_2)(a_i,y_3)\cdots(a_i,y_{l-1})(a_i,d), \end{array}$$

$i = 2,3,\ldots,d(a)$. Furthermore, we construct $d(b)$ vertex-disjoint paths that use copies of the path P_G to reach the fiber ${}^cH$. For every $j = 2,3,\ldots,d(b)$ define:

$$\begin{array}{lll} (a,b)P_{G^b} & \text{where} & P_{G^b} = (x_1,b)(x_2,b)(x_3,b)\cdots(x_{k-1},b)(c,b), \\ (a,b)(a,b_j)P_{G^{b_j}} & \text{where} & P_{G^{b_j}} = (x_1,b_j)(x_2,b_j)(x_3,b_j)\cdots(x_{k-1},b_j)(c,b_j). \end{array}$$

As can be easily seen from the construction, defined paths are vertex disjoint and none contains the vertex (c,d).

□

Now, we prove the formula.

Theorem 2.2. *Let G and H be graphs on at least two vertices. Then,*

$$\kappa(G\Box H) = \min\{\kappa(G)|H|,\ |G|\kappa(H),\ \delta(G)+\delta(H)\}.$$

Proof. First we show that $\kappa(G\Box H)$ is at most the claimed minimum. Let S be a separating set of the graph G. Then $S\times V(H)$ is a separating set of $G\Box H$. Consequently, $\kappa(G\Box H) \leq \kappa(G)|H|$ and analogously, $\kappa(G\Box H) \leq \kappa(H)|G|$. Since $\kappa(G\Box H) \leq \delta(G\Box H) = \delta(G) + \delta(H)$, it follows that $\kappa(G\Box H) \leq \min\{\kappa(G)|H|,\ |G|\kappa(H),\ \delta(G)+\delta(H)\}$ and we have shown desired inequality.

Now, we show that $\kappa(G\Box H)$ is at least the claimed minimum. Suppose it is false and $G\Box H$ has a separating set S with $|S| < \min\{\kappa(G)|H|,\ |G|\kappa(H), \delta(G)+\delta(H)\}$. Then, there exist vertices $c \in V(G)$ and $d \in V(H)$ such that $|V(G^d)\cap S| < \kappa(G)$ and $|V({}^cH)\cap S| < \kappa(H)$. In particular, $G^d - S$ and ${}^cH - S$ are connected.

Notice that Proposition 2.1 implies that each vertex of $G\Box H - S$ is connected to $G^d \cup {}^cH$ by a path avoiding S. Hence, if $(c,d) \notin S$, then $G^d \cup {}^cH - S$ is connected, and so is $G\Box H - S$.

So assume $(c,d) \in S$. Then $G\Box H - S$ has at most two components, one containing $G^d - S$ and other containing ${}^cH - S$. Now we will find a vertex adjacent to both of these subgraphs, and this will imply connectedness of $G\Box H - S$.

If we can choose $c_1 \in N_G(c)$ and $d_1 \in N_H(d)$ such that none of vertices (c,d_1), (c_1,d_1), (c_1,d) belongs to S, then (c_1,d_1) connects $G^d - S$ and ${}^cH - S$ and hence connectedness of $G\Box H - S$ follows. Suppose that we cannot make such a choice. Let x (resp. y) be the number of neighbours of (c,d) in $G^d - S$ (resp. ${}^cH - S$). Then $x\,y$ vertices from $N_G(c)\times N_H(d)$ must be in S, because of the assumption. So there are at least $d_G(c) - x + d_H(d) - y + x\,y + 1$ vertices in S.

By the assumption on S, $d_G(c) - x + d_H(d) - y + x\,y + 1 < \delta(G) + \delta(H) < d_G(c) + d_H(d)$ and after simple transformation one can obtain $x\,y + 1 < x + y$. But the latter inequality holds if and only if $x = 0$ or $y = 0$. Since $\kappa(G) \leq \delta(G)$, this contradicts the assumptions that both fibers G^d and ${}^cH$ contain less than $\kappa(G)$ resp. $\kappa(H)$ vertices of S.

Hence, we showed that $G^d \cup {}^cH - S$ is connected, and so is $G\Box H - S$. Therefore, $|S| \geq \delta(G) + \delta(H)$. □

We discuss the edge version of this problem. A similar result for the edge-connectivity of the Cartesian product was proved by Xu and Yang [7] in 2006 using the edge version of Menger's theorem:

Theorem 2.3. *Let G and H be graphs on at least two vertices. Then,*

$$\lambda(G\Box H) = \min\{\lambda(G)|H|,\ |G|\lambda(H),\ \delta(G)+\delta(H)\}.$$

In 2008 new short version of the proof, avoiding Menger's theorem, appeared in [3].

We can use the fan from Proposition 2.1 and a very simplified argument of Theorem 2.2 (mainly the first two paragraphs) to prove Theorem 2.3. Moreover, instead of the fan of Proposition 2.1, we can use the following simpler one (using notation from the proof of Proposition 2.1): for every $i = 1, 2, \ldots, d(a)$ define:

$$(a,b)(a_i,b)P_{a_iH}, \quad \text{where} \quad P_{a_iH} = (a_i,y_1)(a_i,y_2)(a_i,y_3)\cdots(a_i,y_{l-1})(a_i,d),$$

and for every $j = 1, 2, \ldots, d(b)$ define

$$(a,b)(a,b_j)P_{G^{b_j}}, \quad \text{where} \quad P_{G^{b_j}} = (x_1,b_j)(x_2,b_j)(x_3,b_j)\cdots(x_{k-1},b_j)(c,b_j).$$

It is easy to see that this is an edge-fan of size $d(a)+d(b)$ from (a,b) to $G^d \cup {}^cH$.

Finally, we would like to stress that above approach enables us to generalize Liouville's formula for Cartesian products with more than two factors. We state this result in the following theorem.

Theorem 2.4. *Let G_i, $i = 1, 2, \ldots, n$ be graphs on at least two vertices and let $G = G_1\Box G_2\Box\cdots\Box G_n$. Then,*

$$\kappa(G) = \kappa(G_1\Box\cdots\Box G_n) = \min\left\{\frac{\kappa(G_1)}{|G_1|}|G|,\ \ldots\ ,\frac{\kappa(G_n)}{|G_n|}|G|, \delta(G_1)+\cdots+\delta(G_n)\right\}.$$

Proof. We prove given equality using induction on the number of factors n. The base case for $n = 2$ is proved in Theorem 2.2. In order to prove that equality holds for n, we consider $\kappa(G) = \kappa(G_1\Box\cdots\Box G_n)$ as the Cartesian product of two graphs $G' = G_1\Box\cdots\Box G_{n-1}$ and G_n.

Then, by the induction hypothesis,

$$\begin{aligned}\kappa(G'\Box G_n) &= \min\{\kappa(G')|G_n|,\ \kappa(G_n)|G'|,\ \delta(G')+\delta(G_n)\}\\ &= \min\left\{\kappa(G')|G_n|,\ \tfrac{\kappa(G_n)}{|G_n|}|G|,\ \delta(G_1)+\cdots+\delta(G_{n-1})+\delta(G_n)\right\}\\ &= \min\left\{\tfrac{\kappa(G_1)}{|G_1|}|G|,\ \ldots\ ,\tfrac{\kappa(G_{n-1})}{|G_{n-1}|}|G|,\ \tfrac{\kappa(G_n)}{|G_n|}|G|,\ \delta(G_1)+\cdots+\delta(G_n)\right\}\end{aligned}$$

where the last equality holds by the induction hypothesis applied on $\kappa(G') = \kappa(G_1\Box\cdots\Box G_{n-1})$ and an obvious inequality $\delta(G_1)+\cdots+\delta(G_n) < (\delta(G_1)+\cdots+\delta(G_{n-1}))|G_n|$. □

Regarding the above formula, if all G_i's are isomorphic to a graph H, then we obtain the formula

$$\kappa(H^n) = \min\left\{\kappa(H)|H|^{n-1}, n\delta(H)\right\} = n\delta(H),$$

which was observed in [3].

References

[1] W. Imrich, S. Klavžar and D. F. Rall, *Topics in Graph Theory: Graphs and Their Cartesian Product*, AK Peters, Ltd., Wellesley, MA, 2008.

[2] S. Klavžar, Recent Developments on the Structure of Cartesian Products of Graphs, *RMS-Lecture Notes Series No.* **13** (2010), 171–177.

[3] S. Klavžar and S. Špacapan, On the edge-connectivity of Cartesian product graphs, *Asian-European J. Math.* **1** (2008), 93–98.

[4] B. Liouville, Sur la connectivité des produits de graphes, *C. R. Acad. Sci. Paris Sér. A-B* **286** (1978), A363–A365.

[5] G. Sabidussi, Graphs with given group and given graph-theoretical properties, *Canad. J. Math.* **9** (1957), 515–525.

[6] S. Špacapan, Connectivity of Cartesian product of graphs, *Appl. Math. Lett.* **21** (2008), 682–685.

[7] J. -M. Xu and C. Yang, Connectivity of Cartesian product graphs, *Discrete Math.* **306** (2006), 159–165.

ARS MATHEMATICA CONTEMPORANEA

Also available at http://amc-journal.eu
ISSN 1855-3966 (printed edn.), ISSN 1855-3974 (electronic edn.)
ARS MATHEMATICA CONTEMPORANEA 7 (2014) 299–315

Minimal equivelar polytopes

Gabe Cunningham
University of Massachusetts Boston
Boston, Massachusetts, USA, 02125

Received 20 July 2012, accepted 5 January 2013, published online 10 May 2013

Abstract

Every equivelar abstract polytope of type $\{p_1, \ldots, p_{n-1}\}$ has at least $2p_1 \cdots p_{n-1}$ flags. In this paper, we study polytopes that attain this lower bound, called *tight polytopes*. Using properties of flat polytopes, we are able to give a complete local characterization of when a polytope is tight. We then show a way to construct tight polyhedra of type $\{p, q\}$ when p and q are not both odd, and a way to construct regular tight polytopes of type $\{2k_1, \ldots, 2k_{n-1}\}$.

Keywords: Abstract regular polytope, equivelar polytope, flat polytope, mixing.

Math. Subj. Class.: 51M20, 52B15, 05C25

1 Introduction

Abstract polytopes are purely combinatorial generalizations of convex polytopes, maps on surfaces, and infinite tessellations. Their study is a rich and varied field, tying together combinatorics, group theory, topology, and geometry. The most-studied polytopes are those with a high degree of symmetry, including the regular polytopes (see [9]) and the chiral polytopes (see [11, 12]). We also know a great deal about polytopes in rank 3, thanks in part to the fact that every 3-polytope can be naturally associated to a map on a surface (see [10]). In higher ranks, however, relatively little is known about the landscape of polytopes.

In order to understand the structure of polytopes in higher ranks, it would be useful to have many small examples we could study. Furthermore, finding the smallest polytope that satisfies a certain set of properties is a worthwhile and interesting endeavor in and of itself. There are many ways to interpret "smallest" in this context; here, we will work with the number of flags, which is perhaps the easiest and most natural way to quantify the size of a polytope, particularly when working with regular polytopes.

In this paper, we study the smallest *equivelar polytopes*; that is, polytopes that have a Schläfli symbol. Regular and chiral polytopes are equivelar, as are many other highly-symmetric polytopes, but there are no *a priori* bounds on how symmetric an equivelar

E-mail address: gabriel.cunningham@gmail.com (Gabe Cunningham)

polytope must be. We are able to show that every equivelar polytope with a fixed Schläfli symbol $\{p_1, \ldots, p_{n-1}\}$ has at least $2p_1 \cdots p_{n-1}$ flags (Proposition 3.3). Our goal is then to study those polytopes for which this lower bound is tight; appropriately enough, we call these *tight polytopes*. The term was first used by Marston Conder in a mini-course during the Workshop on Symmetry in Graphs, Maps and Polytopes at the Fields Institute in Toronto, Canada, in October 2011. His lecture on the smallest regular polytopes in every rank (which has now been written up in [4]) inspired the work that led to this paper.

We start by presenting background information on polytopes in Section 2. In Section 3, after proving the lower bound for the number of flags of an equivelar polytope, we investigate some simple properties of tight polytopes. Section 4 explores the connection between tightness and flatness of polytopes, and Theorem 4.4 completely characterizes tightness in terms of a local flatness property. In Section 5, we provide a method for building tight polyhedra. Finally, we present a family of regular tight polytopes in every rank in Section 6.

2 Polytopes

Our background information is mostly taken from [9, Chs. 2, 3, 4], with a few small additions.

2.1 Definition of a polytope

Let $\mathcal{P}$ be a ranked partially ordered set whose elements will be called *faces*, and let us say that two faces are *incident* if they are comparable. The faces of $\mathcal{P}$ will range in rank from -1 to n, and a face of rank j is called a *j-face*. The 0-faces, 1-faces, and $(n-1)$-faces are also called *vertices*, *edges*, and *facets*, respectively. A *flag* of $\mathcal{P}$ is a maximal chain. We say that two flags are *adjacent* if they differ in exactly one face, and that they are *j-adjacent* if they differ only in their j-face.

If F and G are faces of $\mathcal{P}$ such that $F \leq G$, then the *section* G/F consists of those faces H such that $F \leq H \leq G$. If F is a j-face and G is a k-face, then we say that the *rank* of G/F is $k - j - 1$. If removing G and F from the Hasse diagram of G/F leaves us with a connected graph, then we say that G/F is *connected*. That is, for any two faces H and H' in G/F (other than F and G themselves), there is a sequence of faces

$$H = H_0, H_1, \ldots, H_k = H'$$

such that, for each $1 \leq i \leq k$, the faces H_{i-1} and H_i are incident and $F < H_i < G$. By convention, we also define all sections of rank 1 or less to be connected.

We say that $\mathcal{P}$ is an *(abstract) polytope of rank n*, also called an *n-polytope*, if it satisfies the following four properties:

(a) There is a unique greatest face F_n of rank n and a unique least face F_{-1} of rank -1.

(b) Each flag has $n + 2$ faces.

(c) Every section is connected.

(d) (Diamond condition) Every section of rank 1 is a diamond. That is, whenever $F < G$, where F is a $(j-1)$-face and G is a $(j+1)$-face for some j, then there are exactly two j-faces H with $F < H < G$.

In ranks -1, 0, and 1, there is a unique polytope up to isomorphism. Abstract polytopes of rank 2 are also called *abstract polygons*, and for each $2 \leq p \leq \infty$, there is a unique abstract polygon with p vertices and p edges, denoted $\{p\}$.

Note that due to the diamond condition, any flag Φ has a unique j-adjacent flag (denoted Φ^j) for each $j = 0, 1, \ldots, n-1$.

If F is a j-face and G is a k-face of a polytope with $F \leq G$, then the section G/F is a $(k-j-1)$-polytope itself. We identify a face F with the section F/F_{-1} and we call the section F_n/F the *co-face at* F. The co-face at a vertex F_0 is also called a *vertex-figure* at F_0.

If $\mathcal{P}$ is an n-polytope, F is an $(i-2)$-face of $\mathcal{P}$, and G is an $(i+1)$-face of $\mathcal{P}$ such that $F < G$, then the section G/F is an abstract polygon. We say that $\mathcal{P}$ has *Schläfli symbol* $\{p_1, \ldots, p_{n-1}\}$, or that $\mathcal{P}$ is *of type* $\{p_1, \ldots, p_{n-1}\}$ if, for each $1 \leq i \leq n-1$, the section G/F is equal to $\{p_i\}$, no matter which $(i-2)$-face F and $(i+1)$-face G we choose. If $\mathcal{P}$ has a Schläfli symbol, then we say that $\mathcal{P}$ is *equivelar*.

The sections of an equivelar polytope are all equivelar polytopes themselves. In particular, if $\mathcal{P}$ is an equivelar polytope of type $\{p_1, \ldots, p_{n-1}\}$, then its facets are all equivelar polytopes of type $\{p_1, \ldots, p_{n-2}\}$, and its vertex-figures are all equivelar polytopes of type $\{p_2, \ldots, p_{n-1}\}$.

Let $\mathcal{P}$ and $\mathcal{Q}$ be two polytopes of the same rank. A surjective function $\gamma : \mathcal{P} \to \mathcal{Q}$ is called a *covering* if it preserves incidence of faces, ranks of faces, and adjacency of flags. We say that $\mathcal{P}$ *covers* $\mathcal{Q}$ if there exists a covering $\gamma : \mathcal{P} \to \mathcal{Q}$.

The *dual* of a polytope $\mathcal{P}$ is the polytope obtained by reversing the partial order. If $\mathcal{P}$ is an equivelar polytope of type $\{p_1, \ldots, p_{n-1}\}$, then the dual of $\mathcal{P}$ is an equivelar polytope of type $\{p_{n-1}, \ldots, p_1\}$.

2.2 Regularity

For polytopes $\mathcal{P}$ and $\mathcal{Q}$, an *isomorphism* from $\mathcal{P}$ to $\mathcal{Q}$ is an incidence- and rank-preserving bijection on the set of faces. An isomorphism from $\mathcal{P}$ to itself is an *automorphism* of $\mathcal{P}$, and the group of all automorphisms of $\mathcal{P}$ is denoted $\Gamma(\mathcal{P})$. We say that $\mathcal{P}$ is *regular* if the natural action of $\Gamma(\mathcal{P})$ on the flags of $\mathcal{P}$ is transitive. For convex polytopes, this definition is equivalent to any of the usual definitions of regularity.

Given a regular polytope $\mathcal{P}$, fix a *base flag* Φ. Then the automorphism group $\Gamma(\mathcal{P})$ is generated by the *abstract reflections* $\rho_0, \ldots, \rho_{n-1}$, where ρ_i maps Φ to the unique flag Φ^i that is i-adjacent to Φ. These generators satisfy $\rho_i^2 = \varepsilon$ for all i, and $(\rho_i\rho_j)^2 = \varepsilon$ for all i and j such that $|i-j| \geq 2$. Every regular polytope is equivelar, and if its Schläfli symbol is $\{p_1, \ldots, p_{n-1}\}$, then the order of each $\rho_{i-1}\rho_i$ is p_i. Note that if $\mathcal{P}$ is a regular polytope of type $\{p_1, \ldots, p_{n-1}\}$, then $\Gamma(\mathcal{P})$ is a quotient of the string Coxeter group $[p_1, \ldots, p_{n-1}]$ whose only defining relations are that $\rho_i^2 = \varepsilon$, $(\rho_{i-1}\rho_i)^{p_i} = \varepsilon$, and $(\rho_i\rho_j)^2 = \varepsilon$ whenever $|i-j| \geq 2$.

For $I \subseteq \{0, 1, \ldots, n-1\}$ and a group $\Gamma = \langle \rho_0, \ldots, \rho_{n-1} \rangle$, we define $\Gamma_I := \langle \rho_i \mid i \in I \rangle$. If $\mathcal{P}$ is a regular polytope, then its automorphism group $\Gamma := \Gamma(\mathcal{P})$ satisfies the following *intersection condition*:

$$\Gamma_I \cap \Gamma_J = \Gamma_{I \cap J} \quad \text{for } I, J \subseteq \{0, \ldots, n-1\}. \tag{2.1}$$

In general, if $\Gamma = \langle \rho_0, \ldots, \rho_{n-1} \rangle$ is a group such that each ρ_i has order 2 and such that $(\rho_i\rho_j)^2 = \varepsilon$ whenever $|i-j| \geq 2$, then we say that Γ is a *string group generated by involutions* (or *sggi*). If Γ also satisfies the intersection condition (2.1) given above, then we call Γ a *string C-group*. There is a natural way of building a regular polytope $\mathcal{P}(\Gamma)$ from a string C-group Γ such that $\Gamma(\mathcal{P}(\Gamma)) \simeq \Gamma$ and $\mathcal{P}(\Gamma(\mathcal{P})) \simeq \mathcal{P}$. In particular, the

i-faces of $\mathcal{P}(\Gamma)$ are taken to be the cosets of

$$\Gamma_i := \langle \rho_j \mid j \neq i \rangle,$$

where $\Gamma_i\varphi \leq \Gamma_j\psi$ if and only if $i \leq j$ and $\Gamma_i\varphi \cap \Gamma_j\psi \neq \emptyset$. This construction is also easily applied to any sggi (not just string C-groups), but in that case, the resulting poset is not necessarily a polytope.

2.3 Flatness

The theory of abstract polytopes accomodates certain degeneracies not present in the study of convex polytopes. For example, the face-poset of a convex polytope is a lattice (any two elements have a unique supremum and infimum), but this need not be the case with abstract polytopes. The simplest abstract polytope that is not a lattice is the digon $\{2\}$, both of whose edges are incident on both of its vertices. This type of degeneracy can be generalized as follows. If $\mathcal{P}$ is an n-polytope, and if $0 \leq k < m \leq n-1$, we say that $\mathcal{P}$ is (k,m)-*flat* if each of its k-faces is incident on every one of its m-faces. If $\mathcal{P}$ has rank n and it is $(0, n-1)$-flat, then we also simply say that it is *flat*. Note that if $0 \leq i \leq k < m \leq j \leq n-1$ and if $\mathcal{P}$ is (k,m)-flat, then it must also be (i,j)-flat. In particular, if $\mathcal{P}$ is (k,m)-flat for any $0 \leq k < m \leq n-1$, then it is also flat (*i.e.*, $(0, n-1)$-flat).

We will also need Lemma 4E3 in [9], which is stated below.

Proposition 2.1. *Let $\mathcal{P}$ be an n-polytope, and let $0 \leq k < m < i \leq n-1$. If each i-face of $\mathcal{P}$ is (k,m)-flat, then $\mathcal{P}$ is also (k,m)-flat. Similarly, if $0 \leq i < k < m \leq n-1$ and each co-i-face of $\mathcal{P}$ is $(k-i-1, m-i-1)$-flat, then $\mathcal{P}$ is (k,m)-flat.*

2.4 Mixing

The mixing construction on polytopes is analogous to the join of two maps or hypermaps [2]. Its principal use is to find a polytope that covers two or more given regular polytopes. We begin by describing the mixing operation on groups (also called the parallel product in [14]). Let $\Gamma = \langle x_1, \ldots, x_n \rangle$ and $\Gamma' = \langle x'_1, \ldots, x'_n \rangle$ be groups with n specified generators. Then the elements $z_i = (x_i, x'_i) \in \Gamma \times \Gamma'$ (for $i = 1, \ldots, n$) generate a subgroup of $\Gamma \times \Gamma'$ that we denote $\Gamma \diamond \Gamma'$ and call the *mix* of Γ and Γ' (see [9, Ch.7A]).

If $\mathcal{P}$ and $\mathcal{Q}$ are regular n-polytopes, we can mix their automorphism groups. Let $\Gamma(\mathcal{P}) = \langle \rho_0, \ldots, \rho_{n-1} \rangle$ and $\Gamma(\mathcal{Q}) = \langle \rho'_0, \ldots, \rho'_{n-1} \rangle$. Let $\alpha_i = (\rho_i, \rho'_i) \in \Gamma(\mathcal{P}) \times \Gamma(\mathcal{Q})$ for $0 \leq i \leq n-1$. Then $\Gamma(\mathcal{P}) \diamond \Gamma(\mathcal{Q}) = \langle \alpha_0, \ldots, \alpha_{n-1} \rangle$. Note that the order of any word $\alpha_{i_1} \cdots \alpha_{i_t}$ is the least common multiple of the orders of $\rho_{i_1} \cdots \rho_{i_t}$ and $\rho'_{i_1} \cdots \rho'_{i_t}$. In particular, each α_i is an involution, and $(\alpha_i\alpha_j)^2 = \varepsilon$ whenever $|i-j| \geq 2$. Therefore, $\Gamma(\mathcal{P}) \diamond \Gamma(\mathcal{Q})$ is a string group generated by involutions, and we can build a poset out of it, called the *mix of $\mathcal{P}$ and $\mathcal{Q}$* and denoted $\mathcal{P} \diamond \mathcal{Q}$. This poset will not, in general, be a polytope; indeed, it is a polytope if and only if the group $\Gamma(\mathcal{P}) \diamond \Gamma(\mathcal{Q})$ satisfies the intersection condition (2.1).

The following properties of $\mathcal{P} \diamond \mathcal{Q}$ follow immediately from the definitions:

Proposition 2.2. *Let $\mathcal{P}$ be a regular polytope of type $\{p_1, \ldots, p_{n-1}\}$, with facets isomorphic to $\mathcal{K}$ and vertex-figures isomorphic to $\mathcal{L}$. Let $\mathcal{Q}$ be a regular polytope of type $\{q_1, \ldots, q_{n-1}\}$, with facets isomorphic to $\mathcal{K}'$ and vertex-figures isomorphic to $\mathcal{L}'$. If $\mathcal{P} \diamond \mathcal{Q}$ is a polytope, then its facets are isomorphic to $\mathcal{K} \diamond \mathcal{K}'$, its vertex-figures are isomorphic to*

$\mathcal{L} \diamond \mathcal{L}'$, and it has type $\{\ell_1, \ldots, \ell_{n-1}\}$, where ℓ_i is the least common multiple of p_i and q_i for $1 \leq i \leq n-1$.

Dual to the mix is the *comix* of two groups. If Γ has presentation $\langle x_1, \ldots, x_n \mid R\rangle$ and Γ' has presentation $\langle x'_1, \ldots, x'_n \mid S\rangle$, then we define the comix of Γ and Γ', denoted $\Gamma \square \Gamma'$, to be the group with presentation

$$\langle x_1, x'_1, \ldots, x_n, x'_n \mid R, S, x_1^{-1}x'_1, \ldots, x_n^{-1}x'_n\rangle.$$

Informally speaking, we can just add the relations from Γ' to Γ, rewriting them to use x_i in place of x'_i.

The proof of the following simple proposition is essentially the same as [6, Prop. 3.3].

Proposition 2.3. *Let $\mathcal{P}$ and $\mathcal{Q}$ be finite regular n-polytopes. Then*

$$|\Gamma(\mathcal{P}) \diamond \Gamma(\mathcal{Q})| \cdot |\Gamma(\mathcal{P}) \square \Gamma(\mathcal{Q})| = |\Gamma(\mathcal{P})| \cdot |\Gamma(\mathcal{Q})|.$$

When mixing two polytopes, there is no guarantee that the result is itself a polytope. In the following simple cases, however, polytopality is guaranteed.

Proposition 2.4. *Let $\mathcal{P}$ and $\mathcal{Q}$ be regular polyhedra. Then $\mathcal{P} \diamond \mathcal{Q}$ is a regular polyhedron.*

Proof. See [7, Cor. 3.2] □

Proposition 2.5. *Let $\mathcal{P}$ be a regular n-polytope with facets isomorphic to $\mathcal{K}$. Let $\mathcal{Q}$ be a regular n-polytope with facets isomorphic to $\mathcal{K}'$. If $\mathcal{K}$ covers $\mathcal{K}'$, then $\mathcal{P} \diamond \mathcal{Q}$ is polytopal.*

Proof. The argument is essentially the same as for Lemma 3.3 in [1]. □

3 Structure of equivelar polytopes

Let $|\mathcal{P}|$ denote the number of flags of a polytope $\mathcal{P}$. We start with a couple of general remarks about the structure of equivelar polytopes.

Proposition 3.1. *Let $\mathcal{P}$ be an equivelar n-polytope of type $\{p_1, \ldots, p_{n-1}\}$, with $n \geq 2$. Then $\mathcal{P}$ has at least p_{n-1} facets and at least p_1 vertices.*

Proof. The claim is obvious when $n = 2$, since the only equivelar 2-polytopes are abstract polygons. Suppose that $n \geq 3$ and that the claim is true for all equivelar $(n-1)$-polytopes. The vertex-figures of $\mathcal{P}$ are equivelar polytopes of type $\{p_2, \ldots, p_{n-1}\}$, so by inductive hypothesis, the vertex-figures have at least p_{n-1} facets. Since each distinct facet of $\mathcal{P}$ yields a distinct facet of a vertex-figure of $\mathcal{P}$, it is clear that $\mathcal{P}$ itself has at least p_{n-1} facets. A dual argument shows that $\mathcal{P}$ also has at least p_1 vertices. □

Proposition 3.2. *Let $\mathcal{P}$ be an n-polytope. Then*

$$|\mathcal{P}| = \sum_{\text{facets } \mathcal{K} \text{ of } \mathcal{P}} |\mathcal{K}|.$$

Proof. The flags of a facet of $\mathcal{P}$ are in one-to-one correspondence with the flags of $\mathcal{P}$ containing that facet. The claim follows immediately. □

We are now able to give a lower bound on the number of flags of an equivelar polytope:

Proposition 3.3. *Let $\mathcal{P}$ be an equivelar n-polytope of type $\{p_1, \ldots, p_{n-1}\}$, with $n \geq 2$. Suppose that $\mathcal{P}$ has f facets. Then $|\mathcal{P}| \geq 2p_1 \cdots p_{n-2} f \geq 2p_1 \cdots p_{n-1}$.*

Proof. The claim is obvious when $n = 2$; in fact, in that case $|\mathcal{P}| = 2p_1$. Suppose that $n \geq 3$ and that the claim is true for all equivelar $(n-1)$-polytopes. The facets of $\mathcal{P}$ are equivelar $(n-1)$-polytopes of type $\{p_1, \ldots, p_{n-2}\}$, so by inductive hypothesis, they each have at least $2p_1 \cdots p_{n-2}$ flags. Then the first inequality follows from Proposition 3.2, and the second inequality follows from Proposition 3.1. □

Our main interest is in polytopes for which the bound in Proposition 3.3 is tight, and thus we make the following definition.

Definition 3.4. Let $\mathcal{P}$ be a finite equivelar n-polytope of type $\{p_1, \ldots, p_{n-1}\}$, with $n \geq 2$. (In particular, we suppose that each p_i is finite.) If $|\mathcal{P}| = 2p_1 \cdots p_{n-1}$, then we say that $\mathcal{P}$ is *tight*.

By Proposition 3.3, tight polytopes have the minimal number of flags for their given Schläfli symbol. Note that the dual of a tight polytope is also tight.

Every (finite) polygon is tight, since $\{p\}$ has $2p$ flags. There are also many examples in the literature of tight polyhedra, including the hemi-cube $\{4, 3\}_3$ (see [9, Sect. 4E]), the regular toroidal map $\{4, 4\}_{(2,0)}$ (see [5]), and a chiral map of type $\{6, 9\}$ (denoted $C7.1$ at [3], and appearing earlier in [15]). There are fewer notable examples in higher ranks, but the locally toroidal 4-polytope $\{\{3, 6\}_{(1,1)}, \{6, 3\}_{(1,1)}\}$ (see [13]) is one such example.

Many different (non-isomorphic) tight polytopes can share the same Schläfli symbol, even if they are regular. For example, there are three regular polytopes of type $\{4, 6\}$ with 48 flags listed at [8]. On the other hand, some Schläfli symbols are unable to support any tight polytopes at all:

Proposition 3.5. *Let $\mathcal{P}$ be an equivelar n-polytope of type $\{p_1, \ldots, p_{n-1}\}$, with $n \geq 3$. If every p_i is odd, then $\mathcal{P}$ is not tight.*

Proof. First, we note that if $n = 3$, then every edge is incident on two vertices and two facets, so $|\mathcal{P}|$ is divisible by 4. Otherwise, if $n \geq 4$, then 4 divides the number of flags in every 3-face of $\mathcal{P}$, so again $|\mathcal{P}|$ is divisible by 4. Thus, if every p_i is odd, $2p_1 \cdots p_{n-1}$ cannot equal $|\mathcal{P}|$. □

As a consequence of Proposition 3.5, though every tight polytope is minimal (*i.e.*, has the fewest flags among polytopes with the same Schläfli symbol), not every minimal polytope is tight. For example, for each n, the minimal (and only) polytope of type $\{3, \ldots, 3\}$ is the n-simplex, which has $(n+1)!$ flags instead of the $2 \cdot 3^{n-1}$ required in order to be tight.

We now examine some of the basic structure of tight polytopes.

Proposition 3.6. *Let $\mathcal{P}$ be a tight n-polytope of type $\{p_1, \ldots, p_{n-1}\}$, with $n \geq 2$. Then $\mathcal{P}$ has p_{n-1} facets and p_1 vertices.*

Proof. The first part follows from Proposition 3.3 combined with Definition 3.4, and the second part follows from a dual argument. □

Proposition 3.7. *Let $\mathcal{P}$ be a tight n-polytope of type $\{p_1, \ldots, p_{n-1}\}$, with $n \geq 3$. Then every facet and vertex-figure of $\mathcal{P}$ is tight.*

Proof. By Proposition 3.6, $\mathcal{P}$ has p_{n-1} facets; each of these is an equivelar polytope of type $\{p_1, \ldots, p_{n-2}\}$. Then Proposition 3.3 says that each of those facets has at least $2p_1 \cdots p_{n-2}$ flags. If any facet has more than that many flags, then Proposition 3.2 implies that $\mathcal{P}$ has more than $2p_1 \cdots p_{n-1}$ flags, contradicting the tightness of $\mathcal{P}$. The other part then follows by a dual argument. □

Proposition 3.8. *Let $\mathcal{P}$ be a tight polytope. Then every section of $\mathcal{P}$ of rank 2 or greater is tight.*

Proof. Let F_i and F_j be faces of $\mathcal{P}$ of rank i and j, respectively, such that $F_i < F_j$ and $j - i \geq 3$. Let

$$F_{-1} < \cdots < F_i < \cdots < F_j < \cdots < F_n$$

be a flag of $\mathcal{P}$ containing F_i and F_j. Now, Proposition 3.7 tells us that since $\mathcal{P}$ is tight, so is the section F_{n-1}/F_{-1}. Similarly, the section F_{n-2}/F_{-1} must be tight. Continuing in this manner, we can conclude that F_j/F_{-1} is tight. Now, since F_j/F_{-1} is tight, so are its vertex-figures F_j/F_0, and by repeatedly applying Proposition 3.7 again, we see that F_j/F_i is itself tight. □

Propositions 3.7 and 3.8 prove extremely useful in deducing properties of tight polytopes. Using these results, we are often able to prove that tight polytopes satisfy a certain property by using induction on the rank.

By combining Proposition 3.8 with Proposition 3.5, we can prove the following:

Proposition 3.9. *Let $\mathcal{P}$ be a tight n-polytope of type $\{p_1, \ldots, p_{n-1}\}$, with $n \geq 3$. Then no two consecutive values p_i and p_{i+1} are both odd.*

4 Flatness and tightness

In order for a polytope to be small enough to be tight, there must be a high number of incidences among a small number of faces. These incidences force the polytope to be flat:

Proposition 4.1. *Let $\mathcal{P}$ be a tight n-polytope, with $n \geq 3$. Then $\mathcal{P}$ is flat; that is, every facet is incident on every vertex.*

Proof. First, suppose that $\mathcal{P}$ is a tight 3-polytope of type $\{p_1, p_2\}$. Then the facets are p_1-gons and Proposition 3.6 tells us that there are only p_1 vertices; therefore, $\mathcal{P}$ is flat. Now, suppose that $n \geq 4$ and that the claim is true for tight $(n-1)$-polytopes. By Proposition 3.7, the facets of $\mathcal{P}$ are tight. Therefore, by inductive hypothesis, the facets are flat (that is, $(0, n-2)$-flat). Then Proposition 2.1 says that $\mathcal{P}$ is itself $(0, n-2)$-flat, from which it follows that $\mathcal{P}$ must also be $(0, n-1)$-flat. □

In fact, tight polytopes actually satisfy a much stronger property:

Proposition 4.2. *Let $\mathcal{P}$ be a tight n-polytope with $n \geq 2$. Then $\mathcal{P}$ is $(i, i+2)$-flat for each $0 \leq i \leq n-3$.*

Proof. For $n = 2$, there is nothing to prove, and by Proposition 4.1, the claim is true for $n = 3$. Suppose that $n \geq 4$ and that the claim is true for all tight $(n-1)$-polytopes. By Proposition 3.7, the facets of $\mathcal{P}$ are all tight. Therefore, by inductive hypothesis, the facets are all $(i, i+2)$-flat for $0 \leq i \leq n-4$. Then we can apply Proposition 2.1 to conclude that

$\mathcal{P}$ is itself $(i, i+2)$-flat for $0 \leq i \leq n-4$. Similarly, the vertex-figures of $\mathcal{P}$ are all tight, and by inductive hypothesis, they are all $(i, i+2)$-flat for $0 \leq i \leq n-4$ Therefore, by Proposition 2.1, $\mathcal{P}$ is $(i+1, i+3)$-flat for $0 \leq i \leq n-4$; in other words, it is $(i, i+2)$-flat for $1 \leq i \leq n-3$, and the claim follows. □

Using the following lemma, we can show that this strong flatness property fully characterizes tight polytopes.

Lemma 4.3. *Let $\mathcal{P}$ be a flat equivelar n-polytope of type $\{p_1, \ldots, p_{n-1}\}$, with $n \geq 2$. If $\mathcal{P}$ has tight facets and tight vertex-figures, then $\mathcal{P}$ is tight.*

Proof. For $n = 2$, the claim is trivial, since all equivelar polytopes of rank 2 are (abstract) polygons, which are tight. If $n \geq 3$, then the vertex-figures of $\mathcal{P}$ are polytopes of type $\{p_2, \ldots, p_{n-1}\}$. By assumption, the vertex-figures are tight, and thus they have $2p_2 \cdots p_{n-1}$ flags. The facets of $\mathcal{P}$ are polytopes of type $\{p_1, \ldots, p_{n-2}\}$, and these are also tight by assumption. Therefore, Proposition 3.6 says that each facet has p_1 vertices. Now, since $\mathcal{P}$ is flat, every facet is incident on every vertex, and thus the facets all share the same p_1 vertices. Therefore, $\mathcal{P}$ has p_1 vertices, and thus $|\mathcal{P}| = 2p_1 \cdots p_{n-1}$ by the dual version of Proposition 3.2. □

Theorem 4.4. *Let $\mathcal{P}$ be an equivelar n-polytope, with $n \geq 2$. Then $\mathcal{P}$ is tight if and only if it is $(i, i+2)$-flat for each $0 \leq i \leq n-3$.*

Proof. The claim is trivial for $n = 2$, and Proposition 4.2 settles one direction for all $n \geq 3$. Now, suppose that $n \geq 3$, that the claim is true for rank $n-1$, and that $\mathcal{P}$ is an equivelar n-polytope that is $(i, i+2)$-flat for each $0 \leq i \leq n-3$. The facets of $\mathcal{P}$ are equivelar $(n-1)$-polytopes, and since $\mathcal{P}$ is $(0, 2)$-flat, every facet of $\mathcal{P}$ must also be $(0, 2)$-flat. Similarly, for any given facet of $\mathcal{P}$ and for every $0 \leq i \leq n-4$, that facet is $(i, i+2)$-flat. Therefore, by inductive hypothesis, the facets are all tight. A similar argument shows that the vertex-figures are tight. Since $\mathcal{P}$ is $(0, 2)$-flat, it is a flat equivelar n-polytope with tight facets and vertex-figures; therefore, Lemma 4.3 says that $\mathcal{P}$ is tight. □

Corollary 4.5. *An equivelar polyhedron is tight if and only if it is flat.*

Theorem 4.4 turns the global criterion for tightness into a series of local criteria, which makes it much easier to build a tight polytope inductively.

5 Tight polyhedra

As we have seen, tight polytopes have a number of restrictive properties. We begin to wonder to what extent they exist. For example, Proposition 3.5 tells us that if p and q are both odd, then there is no tight polyhedron of type $\{p, q\}$. It turns out that the condition that p and q are not both odd is also sufficient for the existence of such polyhedra.

Theorem 5.1. *Suppose p and q are not both odd. Then there is a tight polyhedron of type $\{p, q\}$.*

Proof. By working with the dual if necessary, we can assume that p is even. In light of Corollary 4.5, it suffices to show that there is a flat equivelar polyhedron of type $\{p, q\}$. In other words, we need to construct a polyhedron such that

(i) The facets are p-gons.

(ii) The vertex-figures are q-gons.

(iii) Every facet is incident on every vertex.

(iv) Every edge is incident on two vertices and two facets.

(v) For every pair of facet and vertex, there are two edges incident to both.

We start with p vertices, labeled $v_1, \ldots, v_p$. Let $m = \lfloor \frac{q}{2} \rfloor$, and for $1 \leq i \leq p$ and $1 \leq j \leq m$, add an edge $e_{i,j}$ incident on vertices v_i and v_{i+1} (where v_{p+1} means v_1). That is, we start with a p-cycle with m-tuple edges. To finish the construction, we consider three cases.

(a) Suppose q is also even, so that $q = 2m$. For $1 \leq t \leq m$, the face f_{2t-1} will consist of the simple cycle $e_{1,t}, e_{2,t}, \ldots, e_{p,t}$, while the facet f_{2t} will consist of the simple cycle $e_{1,t}, e_{2,t+1}, e_{3,t}, \ldots, e_{p,t+1}$ (where $e_{i,m+1}$ is understood to be $e_{i,1}$). It is clear, then, that each facet is a p-gon.

(b) Suppose that q is odd, so that $q = 2m + 1$, and suppose that $p = 4s + 2$ for some s. For each $1 \leq i \leq p/2$, we add an edge d_i incident to v_i and v_{2s+1+i} (reducing the index $2s + 1 + i$ modulo p if necessary). Faces f_1 through f_{2m-1} are generated in the same way as in the previous case. Face f_{2m} consists of the edges $e_{1,m}, e_{3,m}, \ldots, e_{p-1,m}$ as well as the edges $d_1, \ldots, d_{p/2}$. Finally, facet f_{2m+1} consists of the edges $e_{2,1}, e_{4,1}, \ldots, e_{p,1}$ as well as the edges $d_1, \ldots, d_{p/2}$. Though it is clear that $f_1, \ldots, f_{2m-1}$ are all p-gons (*i.e.*, simple cycles), we need to prove the same for the faces f_{2m} and f_{2m+1}. In f_{2m}, starting from 1, we visit vertices in the order

$$1,\ 2,\ 2s+3,\ 2s+4,\ 3,\ 4,\ \ldots,\ 4s+1,\ 4s+2,\ 2s+1,\ 2s+2,\ 1;$$

therefore, we get a simple cycle. Similarly, starting from 2 in f_{2m+1}, we visit vertices in the order

$$2,\ 3,\ 2s+4,\ 2s+5,\ 4,\ 5,\ \ldots,\ 4s+2,\ 1,\ 2s+2,\ 2s+3,\ 2;$$

again, we get a simple cycle. See Figure 1 for an illustration of the three faces when $p = 6$ and $q = 3$. (In this case, we obtain the toroidal polyhedron $\{6, 3\}_{(1,1)}$; see [9, Ch. 1D].)

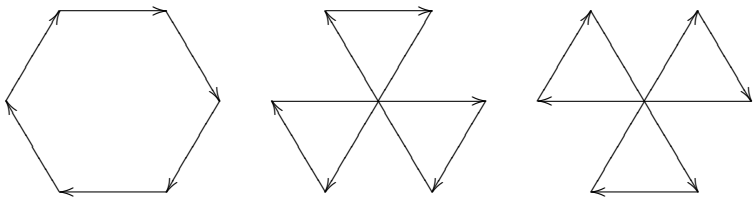

Figure 1: The three faces of a tight polyhedron of type $\{6, 3\}$

(c) Suppose again that q is odd, so that $q = 2m + 1$, but now suppose that $p = 4s$ for some s. Add an edge d_1 incident to v_1 and v_{2s+1}, and for each $2 \leq i \leq 2s$, add an

edge c_i incident to v_i and v_{4s-i+2} (reducing the index $4s-i+2$ modulo p if necessary). We construct $f_1, \ldots, f_{2m-1}$ as before. The facet f_{2m} consists of the edges $e_{1,m}, e_{3,m}, \ldots, e_{p-1,m}$ as well as d_1 and $c_2, \ldots, c_{2s}$. Similarly, the facet f_{2m+1} consists of the edges $e_{2,1}, e_{4,1}, \ldots, e_{p,1}$, as well as the edges d_1 and $c_2, \ldots, c_{2s}$. Once more, we need to show that f_{2m} and f_{2m+1} are simple cycles. In f_{2m}, we visit the vertices in the order

$$1,\ 2,\ 4s,\ 4s-1,\ 3,\ 4,\ \ldots,\ 2s-1,\ 2s,\ 2s+2,\ 2s+1,\ 1,$$

and in f_{2m+1}, we visit the vertices in the order

$$2,\ 3,\ 4s-1,\ 4s-2,\ 4,\ 5,\ \ldots,\ 2s,\ 2s+1,\ 1,\ 4s,\ 2.$$

See Figure 2 for an illustration of the three faces when $p=8$ and $q=3$.

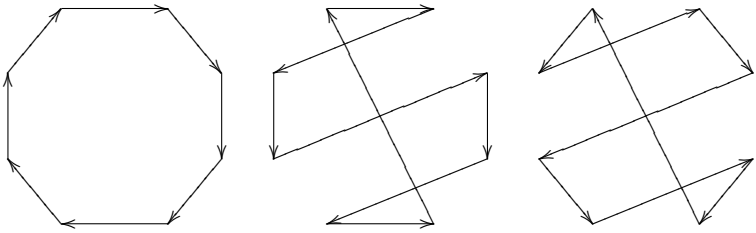

Figure 2: The three faces of a tight polyhedron of type $\{8,3\}$

Now, in every case, we have demonstrated that the faces are p-gons, and since there are only p vertices, it is clear that every facet is incident to every vertex. Furthermore, each edge is incident on exactly two vertices and two faces. Since each facet is a simple cycle, every facet/vertex pair has exactly two edges in common. It remains to be shown that the vertex-figures are q-gons. In fact, at any given vertex, the sequence $f_1, f_2, \ldots, f_q$ yields a simple cycle of faces, where consecutive faces share one of the edges at that vertex. Therefore, the vertex-figures are q-gons, completing the proof. □

The construction used here is by no means canonical; there are many tight polyhedra that do not arise in this way. For example, we can build a tight polyhedron of type $\{4,6\}$ that includes two edges between every pair of vertices (see Figure 3). In the tight polyhedron of type $\{4,6\}$ that Theorem 5.1 produces, each vertex shares three edges with each of two other vertices. These two polyhedra are clearly non-isomorphic.

Note also that when q is odd and $q \geq 5$, then the tight polyhedron of type $\{p,q\}$ that we construct is not regular. In fact, it is not even edge-transitive, since some pairs of vertices have m edges between them, while other pairs have only a single edge.

6 Regular tight polytopes

Our goal now is to find tight polytopes that are regular. As we commented earlier, the polyhedra that we construct in Theorem 5.1 often fail to be regular. Is this a defect of the construction, or do such tight regular polyhedra even exist? Consider, for example,

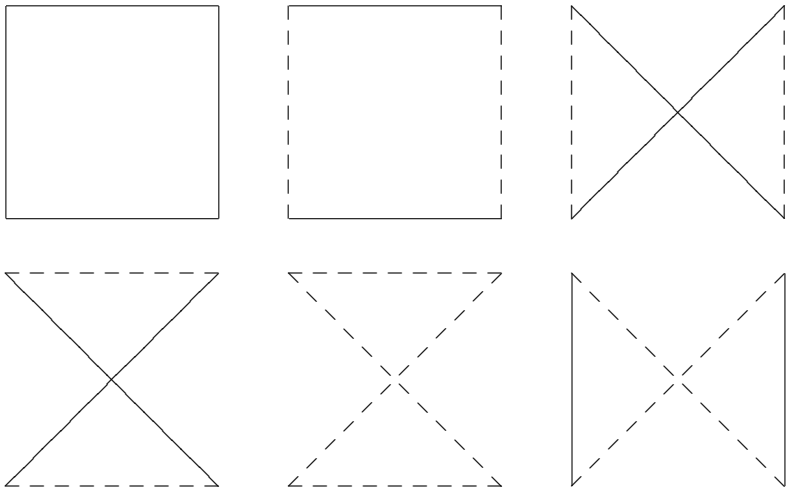

Figure 3: The six faces of a tight polyhedron of type $\{4, 6\}$

tight polyhedra of type $\{8, 5\}$ and of type $\{10, 5\}$. By checking the list of small regular polytopes at [3], we see that there are no tight regular polyhedra of type $\{8, 5\}$, but that there is a tight regular polyhedron of type $\{10, 5\}$. Other than this polyhedron and the universal polyhedron of type $\{2, 5\}$, no other tight regular polyhedra of type $\{p, 5\}$ are listed. Since the list includes all regular polytopes with up to 2000 flags, we can conclude that there are no tight regular polyhedra of type $\{p, 5\}$ when $11 \leq p \leq 200$. Similar observations for other odd values of q lead us to the following conjecture.

Conjecture 6.1. *Let q be odd and $p > 2q$. Then there are no regular tight polyhedra of type $\{p, q\}$.*

When p and q are both even, the situation is entirely different. For even p and q, there is always a regular tight polyhedron of type $\{p, q\}$. In fact, with a little more work, we can build a regular tight polytope in any rank as long as each p_i is even. We start by giving a presentation for the automorphism group. We define $\Gamma(k_1, \ldots, k_{n-1})$ to be the quotient of $[2k_1, \ldots, 2k_{n-1}]$ by the $n-2$ extra relations $(\rho_i\rho_{i+1}\rho_{i+2}\rho_{i+1})^2 = \varepsilon$, where $0 \leq i \leq n-3$. That is,

$$\begin{aligned}\Gamma(k_1, \ldots, k_{n-1}) = \langle \rho_0, \ldots, \rho_{n-1} \,|\, & \rho_0^2 = \cdots = \rho_{n-1}^2 = \varepsilon, \\ & (\rho_0\rho_1)^{2k_1} = \cdots = (\rho_{n-2}\rho_{n-1})^{2k_{n-1}} = \varepsilon, \\ & (\rho_i\rho_j)^2 = \varepsilon \text{ if } |i-j| \geq 2, \\ & (\rho_0\rho_1\rho_2\rho_1)^2 = \cdots = (\rho_{n-3}\rho_{n-2}\rho_{n-1}\rho_{n-2})^2 = \varepsilon \rangle.\end{aligned}$$

Thus, for $n = 3$, we get the presentation

$$\begin{aligned}\Gamma(k_1, k_2) = \langle \rho_0, \rho_1, \rho_2 \,|\, & \rho_0^2 = \rho_1^2 = \rho_2^2 = \varepsilon, \\ & (\rho_0\rho_1)^{2k_1} = (\rho_0\rho_2)^2 = (\rho_1\rho_2)^{2k_2} = \varepsilon, \\ & (\rho_0\rho_1\rho_2\rho_1)^2 = \varepsilon \rangle.\end{aligned}$$

We define $\mathcal{P}(k_1,\ldots,k_{n-1})$ to be the poset $\mathcal{P}(\Gamma(k_1,\ldots,k_{n-1}))$. (See [9, Ch. 2E] for the details of this construction.) Our goal will be to show that $\mathcal{P}(k_1,\ldots,k_{n-1})$ is a regular tight polytope of type $\{2k_1,\ldots,2k_{n-1}\}$.

We start by working with the case $n=3$:

Lemma 6.2. *The group $\Gamma(k_1,k_2)$ has order $8k_1k_2$.*

Proof. Let $\Gamma(k_1,k_2)=\langle\rho_0,\rho_1,\rho_2\rangle$, and let $\alpha=(\rho_1\rho_2)^2$. The relation $(\rho_0\rho_1\rho_2\rho_1)^2=\varepsilon$ implies that

$$\begin{aligned}\rho_0(\rho_1\rho_2\rho_1\rho_2)\rho_0 &= (\rho_0\rho_1\rho_2\rho_1)\rho_2\rho_0\\ &= (\rho_1\rho_2\rho_1\rho_0)\rho_2\rho_0\\ &= \rho_1\rho_2\rho_1\rho_2,\end{aligned}$$

so that $\rho_0\alpha\rho_0=\alpha$. Furthermore, $\rho_1\alpha\rho_1=\alpha^{-1}=\rho_2\alpha\rho_2$. Therefore, the cyclic subgroup N of order k_2 generated by α is normal in $\Gamma(k_1,k_2)$. Now, by adding the relation $\alpha=\varepsilon$ to the relations of $\Gamma(k_1,k_2)$, we can pass to the factor group $\Gamma(k_1,k_2)/N$. In the factor group, the relation $(\rho_0\rho_1\rho_2\rho_1)^2=\varepsilon$ is equivalent to $(\rho_0\rho_2)^2=\varepsilon$, rendering the former relation redundant. Then we can remove that relation and the redundant relation $(\rho_1\rho_2)^{2k_2}=\varepsilon$ to see that the factor group has presentation

$$\begin{aligned}\langle\rho_0,\rho_1,\rho_2\ |&\rho_0^2=\rho_1^2=\rho_2^2=\varepsilon,\\ &(\rho_0\rho_1)^{2k_1}=(\rho_0\rho_2)^2=(\rho_1\rho_2)^2=\varepsilon\rangle.\end{aligned}$$

This is the presentation for the Coxeter group $[2k_1,2]$ of order $8k_1$, and since N has order k_2, the order of $\Gamma(k_1,k_2)$ is $8k_1k_2$. □

Theorem 6.3. *The poset $\mathcal{P}(k_1,k_2)$ is a tight regular polyhedron of type $\{2k_1,2k_2\}$, and*

$$\mathcal{P}(k_1,k_2)=\mathcal{P}(k_1,1)\diamond\mathcal{P}(1,k_2)=\{2k_1,2\}\diamond\{2,2k_2\}.$$

Proof. First of all, it is clear from the presentations of their automorphism groups that $\mathcal{P}(k_1,1)=\{2k_1,2\}$ and $\mathcal{P}(1,k_2)=\{2,2k_2\}$. Let $\mathcal{P}=\{2k_1,2\}\diamond\{2,2k_2\}$. By Proposition 2.4, $\mathcal{P}$ is a regular polyhedron, and its type is $\{2k_1,2k_2\}$. Now, in $[2k_1,2]$, the generator ρ_2 is in the center, so the relation $(\rho_0\rho_1\rho_2\rho_1)^2=\varepsilon$ holds. Similarly, in $[2,2k_2]$, the generator ρ_0 is in the center, and again the relation $(\rho_0\rho_1\rho_2\rho_1)^2=\varepsilon$ holds. Therefore, this relation must hold in the mix of the two groups, which is $\Gamma(\mathcal{P})$. Then $\Gamma(\mathcal{P})$ satisfies all of the relations of $\Gamma(k_1,k_2)$, and thus it is a (not necessarily proper) natural quotient of $\Gamma(k_1,k_2)$. Since $\Gamma(k_1,k_2)$ has order $8k_1k_2$ (by Lemma 6.2), the group $\Gamma(\mathcal{P})$ has order $8k_1k_2$ or less. On the other hand, $\mathcal{P}$ is a regular polyhedron of type $\{2k_1,2k_2\}$, and so $\Gamma(\mathcal{P})$ must have order at least $8k_1k_2$. Therefore, $|\Gamma(\mathcal{P})|=8k_1k_2$, from which it follows that $\Gamma(\mathcal{P})=\Gamma(k_1,k_2)$. Therefore, $\mathcal{P}(k_1,k_2)=\mathcal{P}$, a regular tight polyhedron of type $\{2k_1,2k_2\}$. □

We note here that the polyhedron $\mathcal{P}(k_1,k_2)$ is isomorphic to the tight polyhedron $\mathcal{P}$ of type $\{2k_1,2k_2\}$ that we built in Theorem 5.1. Indeed, if we take the base flag Φ of $\mathcal{P}$ to

consist of v_1, $e_{1,1}$ and f_1, then there are automorphisms ρ_0, ρ_1, and ρ_2 that act as follows.

$$\begin{aligned}\rho_0 : v_i &\leftrightarrow v_{2k_1+3-i}\\ e_{i,j} &\leftrightarrow e_{2k_1+2-i,j}\\ &\text{Fixes all faces}\end{aligned}$$

$$\begin{aligned}\rho_1 : v_i &\leftrightarrow v_{2k_1+2-i}\\ e_{i,j} &\leftrightarrow e_{2k_1+1-i,k_2+2-j}\\ f_i &\leftrightarrow f_{2k_2+2-i}\end{aligned}$$

$$\begin{aligned}\rho_2 &: \text{Fixes all vertices}\\ e_{i,j} &\leftrightarrow \begin{cases} e_{i,k_2+2-j} & \text{if } i \text{ is odd,}\\ e_{i,k_2+3-j} & \text{if } i \text{ is even}\end{cases}\\ f_i &\leftrightarrow f_{2k_2+3-i}\end{aligned}$$

(If necessary, we reduce the index of v modulo $2k_1$, the index of f modulo $2k_2$, and the indices of e modulo $2k_1$ and k_2, respectively.) Since each ρ_i sends Φ to Φ^i, this suffices to show that $\mathcal{P}$ is regular. It is also simple to verify that $(\rho_0\rho_1\rho_2\rho_1)^2 = \varepsilon$, from which it follows that $\mathcal{P}$ is a quotient of $\mathcal{P}(k_1, k_2)$. Then since $\mathcal{P}$ and $\mathcal{P}(k_1, k_2)$ have the same number of flags, they must be isomorphic.

In order to extend the result of Theorem 6.3 to higher ranks, we start with several lemmas.

Lemma 6.4. *Let* $\Gamma(k_1, \ldots, k_{n-1}) = \langle \rho_0, \ldots, \rho_{n-1} \rangle$. *Then* $\rho_{n-1} \notin \langle \rho_0, \ldots, \rho_{n-2} \rangle$.

Proof. Let $\Gamma := \Gamma(k_1, \ldots, k_{n-1}) = \langle \rho_0, \ldots, \rho_{n-1} \rangle$. Every relator of Γ contains every generator an even number of times (possibly zero). Therefore, any relation of the form $\rho_{n-1} = w$ that holds in Γ must have at least one instance of ρ_{n-1} appearing in w. In particular, $\rho_{n-1} \notin \langle \rho_0, \ldots, \rho_{n-2} \rangle$. □

Lemma 6.5. *Let* $\Gamma(k_1, \ldots, k_{n-1}) = \langle \rho_0, \ldots, \rho_{n-1} \rangle$. *Then*

$$\langle \rho_0, \ldots, \rho_{n-2} \rangle \simeq \Gamma(k_1, \ldots, k_{n-2})$$

and

$$\langle \rho_1, \ldots, \rho_{n-1} \rangle \simeq \Gamma(k_2, \ldots, k_{n-1}).$$

Proof. It suffices to prove the first claim, since the second will then follow from a dual argument. Let $\Gamma(k_1, \ldots, k_{n-1}) = \langle \rho_0, \ldots, \rho_{n-1} \rangle$, and let $\Gamma = \langle \rho_0, \ldots, \rho_{n-2} \rangle$. It is clear that Γ is a natural quotient of $\Gamma(k_1, \ldots, k_{n-2})$, since the generators of Γ satisfy all of the relations that are satisfied by the generators of $\Gamma(k_1, \ldots, k_{n-2})$. The generators of Γ also satisfy the extra relations

$$(\rho_{n-3}\rho_{n-2}\rho_{n-1}\rho_{n-2})^2 = \varepsilon,$$
$$(\rho_{n-2}\rho_{n-1})^{2k_{n-1}} = \varepsilon,$$

and

$$(\rho_i\rho_{n-1})^2 = \varepsilon, \text{ for } 0 \le i \le n-3.$$

It remains to show that these extra relations do not cause Γ to collapse to a proper quotient of $\Gamma(k_1, \ldots, k_{n-2})$. Suppose we add the relation $\rho_{n-1} = \varepsilon$ to the relations of Γ to obtain a new group Γ'. In Γ', we can rewrite the relations above as

$$\rho_{n-3}^2 = \varepsilon,$$

$$\rho_{n-2}^{2k_{n-1}} = \varepsilon,$$

and

$$\rho_i^2 = \varepsilon \text{ for } 0 \leq i \leq n-3.$$

and these relations are all redundant with the relations that come from $\Gamma(k_1, \ldots, k_{n-2})$. Therefore, we can eliminate these relations from Γ'. Then Γ' has all of the relations from $\Gamma(k_1, \ldots, k_{n-2})$ and the single extra relation $\rho_{n-1} = \varepsilon$. Since this is the only remaining relation that contains ρ_{n-1}, and since $\Gamma' = \langle \rho_0, \ldots, \rho_{n-2} \rangle$, we can remove that relation without affecting Γ'. So we see that we can take the relations of $\Gamma(k_1, \ldots, k_{n-2})$ to be the defining relations of Γ', from which it follows that $\Gamma' \simeq \Gamma(k_1, \ldots, k_{n-2})$. Since Γ' is a natural quotient of Γ, which is a natural quotient of $\Gamma(k_1, \ldots, k_{n-2})$, we see that $\Gamma \simeq \Gamma(k_1, \ldots, k_{n-2})$ as well. □

Lemma 6.6. *Suppose that $\mathcal{P}(k_1, \ldots, k_{n-2})$ is a tight regular polytope of type $\{2k_1, \ldots, 2k_{n-2}\}$ and that $\mathcal{P}(k_2, \ldots, k_{n-2}, 1)$ is a tight regular polytope of type $\{2k_2, \ldots, 2k_{n-2}, 2\}$. Then $\mathcal{P}(k_1, \ldots, k_{n-2}, 1)$ is a tight regular polytope of type $\{2k_1, \ldots, 2k_{n-2}, 2\}$.*

Proof. Let $\Gamma(k_1, \ldots, k_{n-2}, 1) = \langle \rho_0, \ldots, \rho_{n-1} \rangle$. To prove polytopality and regularity, it suffices to show that $\Gamma(k_1, \ldots, k_{n-2}, 1)$ is a string C-group. By Lemma 6.5,

$$\langle \rho_0, \ldots, \rho_{n-2} \rangle \simeq \Gamma(k_1, \ldots, k_{n-2})$$

and

$$\langle \rho_1, \ldots, \rho_{n-1} \rangle \simeq \Gamma(k_2, \ldots, k_{n-2}, 1).$$

By assumption, both of these subgroups are string C-groups. Then [9, Prop. 2E16 (a)] says that $\Gamma(k_1, \ldots, k_{n-2}, 1)$ is a string C-group if

$$\langle \rho_0, \ldots, \rho_{n-2} \rangle \cap \langle \rho_1, \ldots, \rho_{n-1} \rangle = \langle \rho_1, \ldots, \rho_{n-2} \rangle.$$

Let v be in this intersection. Now,

$$v \in \langle \rho_1, \ldots, \rho_{n-1} \rangle \simeq \Gamma(k_2, \ldots, k_{n-2}, 1).$$

By inspecting the presentation for this group, we see that ρ_{n-1} is in the center. Therefore, we may write $v = u\rho_{n-1}^i$ with $u \in \langle \rho_1, \ldots, \rho_{n-2} \rangle$ and where i is 0 or 1. On the other hand, $v \in \langle \rho_0, \ldots, \rho_{n-2} \rangle$, and therefore

$$\rho_{n-1}^i = u^{-1}v \in \langle \rho_0, \ldots, \rho_{n-2} \rangle.$$

Since $\rho_{n-1} \notin \langle \rho_0, \ldots, \rho_{n-2} \rangle$ by Lemma 6.4, it follows that $i = 0$ and that $v = u$. Therefore, $v \in \langle \rho_1, \ldots, \rho_{n-2} \rangle$, and thus

$$\langle \rho_0, \ldots, \rho_{n-2} \rangle \cap \langle \rho_1, \ldots, \rho_{n-1} \rangle \leq \langle \rho_1, \ldots, \rho_{n-2} \rangle.$$

The other containment being obvious, we see that $\Gamma(k_1, \ldots, k_{n-2}, 1)$ is a string C-group, and therefore, $\mathcal{P}(k_1, \ldots, k_{n-2}, 1)$ is a regular polytope.

Next, we observe that

$$\begin{aligned}\Gamma(k_1, \ldots, k_{n-2}, 1) &= \langle \rho_0, \ldots, \rho_{n-1} \rangle \\ &= \langle \rho_0, \ldots, \rho_{n-2} \rangle \times \langle \rho_{n-1} \rangle,\end{aligned}$$

since ρ_{n-1} is in the center. Then since $\mathcal{P}(k_1, \ldots, k_{n-2})$ is of type $\{2k_1, \ldots, 2k_{n-2}\}$, it follows that $\mathcal{P}(k_1, \ldots, k_{n-2}, 1)$ is of type $\{2k_1, \ldots, 2k_{n-2}, 2\}$. Furthermore,

$$\begin{aligned}|\mathcal{P}(k_1, \ldots, k_{n-2}, 1)| &= 2|\mathcal{P}(k_1, \ldots, k_{n-2})| \\ &= 2 \cdot (2k_1 \cdots 2k_{n-2} \cdot 2),\end{aligned}$$

and therefore $\mathcal{P}(k_1, \ldots, k_{n-2}, 1)$ is tight. □

Lemma 6.7. *Let $k_1, \ldots, k_{n-1}$ and $k'_1, \ldots, k'_{n-1}$ be positive integers. If for each i, k'_i divides k_i, then $\Gamma(k_1, \ldots, k_{n-1})$ naturally covers $\Gamma(k'_1, \ldots, k'_{n-1})$.*

Proof. When each k'_i divides k_i, the group $\Gamma(k'_1, \ldots, k'_{n-1})$ satisfies all of the same relations as $\Gamma(k_1, \ldots, k_{n-1})$, and the result follows. □

Theorem 6.8. *The poset $\mathcal{P}(k_1, \ldots, k_{n-1})$ is a tight regular n-polytope of type $\{2k_1, \ldots, 2k_{n-1}\}$, and $\mathcal{P}(k_1, \ldots, k_{n-1}) = \mathcal{P}(k_1, \ldots, k_{n-2}, 1) \diamond \mathcal{P}(1, k_2, \ldots, k_{n-1})$.*

Proof. Theorem 6.3 shows that the claim is true for $n = 3$. Suppose that $n \geq 4$ and that the claim is true in rank $n - 1$. Let $\Gamma = \Gamma(k_1, \ldots, k_{n-2}, 1)$, $\mathcal{P} = \mathcal{P}(\Gamma)$, $\Gamma' = \Gamma(1, k_2, \ldots, k_{n-1})$, and $\mathcal{P}' = \mathcal{P}(\Gamma')$. We need to show three things:

(a) $\mathcal{P} \diamond \mathcal{P}'$ is a regular polytope of type $\{2k_1, \ldots, 2k_{n-1}\}$

(b) $|\Gamma \diamond \Gamma'| = 2^n k_1 \cdots k_{n-1}$

(c) $\Gamma(k_1, \ldots, k_{n-1}) = \Gamma \diamond \Gamma'$

By inductive hypothesis, $\mathcal{P}(k_1, \ldots, k_{n-2})$ is a tight regular polytope of type $\{2k_1, \ldots, 2k_{n-2}\}$, and $\mathcal{P}(k_2, \ldots, k_{n-2}, 1)$ is a tight regular polytope of type $\{2k_2, \ldots, 2k_{n-2}, 2\}$. Therefore, by Lemma 6.6, the poset $\mathcal{P} = \mathcal{P}(k_1, \ldots, k_{n-2}, 1)$ is a tight regular polytope of type $\{2k_1, \ldots, 2k_{n-2}, 2\}$. A dual argument shows that $\mathcal{P}'$ is a tight regular polytope of type $\{2, 2k_2, \ldots, 2k_{n-1}\}$. Now, by Lemma 6.5, the facets of $\mathcal{P}$ have group $\Gamma(k_1, \ldots, k_{n-2})$, whereas the facets of $\mathcal{P}'$ have group $\Gamma(1, k_2, \ldots, k_{n-2})$. Then Lemma 6.7 says that the group $\Gamma(k_1, \ldots, k_{n-2})$ covers $\Gamma(1, k_2, \ldots, k_{n-2})$, and thus the facets of $\mathcal{P}$ cover the facets of $\mathcal{P}'$. Then $\mathcal{P} \diamond \mathcal{P}'$ is a regular polytope, by Proposition 2.5. By Proposition 2.2, the facets of $\mathcal{P} \diamond \mathcal{P}'$ are isomorphic to $\mathcal{P}(k_1, \ldots, k_{n-2}) \diamond \mathcal{P}(1, k_2, \ldots, k_{n-2}) = \mathcal{P}(k_1, \ldots, k_{n-2})$, the vertex-figures are isomorphic to $\mathcal{P}(k_2, \ldots, k_{n-2}, 1) \diamond \mathcal{P}(k_2, \ldots, k_{n-1}) = \mathcal{P}(k_2, \ldots, k_{n-1})$, and $\mathcal{P} \diamond \mathcal{P}'$ is of type $\{2k_1, \ldots, 2k_{n-1}\}$.

Next we show that $\Gamma \diamond \Gamma'$ has the appropriate size. By Proposition 2.3,

$$|\Gamma \diamond \Gamma'| = \frac{|\Gamma| \cdot |\Gamma'|}{|\Gamma \sqcap \Gamma'|},$$

Since $\mathcal{P}$ and $\mathcal{P}'$ are tight,

$$|\Gamma| = 2^n k_1 \cdots k_{n-2}$$

and

$$|\Gamma'| = 2^n k_2 \cdots k_{n-1}.$$

Now, we obtain a presentation for $\Gamma \square \Gamma'$ by adding the relations for Γ' to those for Γ. This gives us a presentation for the group $\Gamma(1, k_2, \ldots, k_{n-2}, 1)$. Using Lemma 6.6 again, we can conclude that $\mathcal{P}(1, k_2, \ldots, k_{n-2}, 1)$ is a tight regular polytope of type $\{2, k_2, \ldots, k_{n-2}, 2\}$. Therefore,

$$\begin{aligned} |\Gamma \square \Gamma'| &= |\Gamma(1, k_2, \ldots, k_{n-2}, 1)| \\ &= 2^n k_2 \cdots k_{n-2}, \end{aligned}$$

and thus

$$\begin{aligned} |\Gamma \diamond \Gamma'| &= \frac{|\Gamma| \cdot |\Gamma'|}{|\Gamma \square \Gamma'|} \\ &= \frac{(2^n k_1 \cdots k_{n-2})(2^n k_2 \cdots k_{n-1})}{2^n k_2 \cdots k_{n-2}} \\ &= 2^n k_1 \cdots k_{n-1}. \end{aligned}$$

So $\mathcal{P} \diamond \mathcal{P}'$ is tight.

It remains to show that $\Gamma \diamond \Gamma'$ is naturally isomorphic to $\Gamma(k_1, \ldots, k_{n-1})$. It is clear from the presentation for Γ that $\Gamma(k_1, \ldots, k_{n-1})$ covers Γ and that the natural covering map is one-to-one on the subgroup $\langle \rho_0, \ldots, \rho_{n-2} \rangle$. Then since Γ is a string C-group (because $\mathcal{P}$ is a polytope), we can apply [9, Thm. 2E17] to see that the group $\Gamma(k_1, \ldots, k_{n-1})$ is also a string C-group. Therefore, $\mathcal{P}(k_1, \ldots, k_{n-1})$ is a regular polytope, and Lemma 6.5 says that its facets are $\mathcal{P}(k_1, \ldots, k_{n-2})$ and its vertex-figures are $\mathcal{P}(k_2, \ldots, k_{n-1})$. By [9, Thm. 4E5], since $\mathcal{P}(k_1, \ldots, k_{n-2})$ and $\mathcal{P}(k_2, \ldots, k_{n-1})$ are both flat, there is only a single regular polytope (up to isomorphism) with those facets and vertex-figures. Since $\mathcal{P} \diamond \mathcal{P}'$ is one such regular polytope, we see that $\mathcal{P}(k_1, \ldots, k_{n-1}) = \mathcal{P}(k_1, \ldots, k_{n-2}, 1) \diamond \mathcal{P}(1, k_2, \ldots, k_{n-1})$, as desired. □

Theorem 6.8 gives us an easy way to generate small regular polytopes in any rank, providing us with many more examples we can study. We note that it is also possible to prove the existence of a tight regular polytope of type $\{2k_1, \ldots, 2k_{n-1}\}$ in an entirely group-theoretic way; Marston Conder provides such an account as [4, Thm. 5.3] (and indeed, his regular polytopes are isomorphic to ours).

Acknowledgments

The author would like to thank Marston Conder for valuable feedback on an earlier draft of this paper. He also thanks the anonymous referees for several helpful comments.

References

[1] A. Breda D'Azevedo, G. Jones and E. Schulte, Constructions of chiral polytopes of small rank, *Canad. J. Math.* **63** (2011), 1254–1283.

[2] A. Breda D'Azevedo and Roman Nedela, Join and intersection of hypermaps, *Acta Univ. M. Belii Ser. Math.* **9** (2001), 13–28.

[3] M. Conder, Lists of all regular polytopes with up to 2000 flags, http://www.math.auckland.ac.nz/~conder.

[4] M. Conder, The smallest regular polytopes of given rank, *Adv. Math.* **236** (2013), 92–110.

[5] H. S. M. Coxeter and W. O. J. Moser, *Generators and relations for discrete groups*, fourth ed., Ergebnisse der Mathematik und ihrer Grenzgebiete (Results in Mathematics and Related Areas), vol. 14, Springer-Verlag, Berlin, 1980.

[6] G. Cunningham, Mixing chiral polytopes, *J. Alg. Comb.* **36** (2012), 263–277.

[7] G. Cunningham, Self-dual, self-petrie covers of regular polyhedra, *Symmetry* **4** (2012), 208–218.

[8] M. I. Hartley, An atlas of small regular abstract polytopes, *Periodica Mathematica Hungarica* **53** (2006), 149–156.

[9] P. McMullen and E. Schulte, *Abstract regular polytopes*, Encyclopedia of Mathematics and its Applications, vol. 92, Cambridge University Press, Cambridge, 2002.

[10] R. Nedela, *Maps hypermaps and related topics*, 2007, http://www.savbb.sk/~nedela/CMbook.pdf.

[11] D. Pellicer, Developments and open problems on chiral polytopes, *Ars Math. Contemp.* **5** (2012), 333–354.

[12] E. Schulte and A. Ivić Weiss, Chiral polytopes, *Applied geometry and discrete mathematics*, DIMACS Ser. Discrete Math. Theoret. Comput. Sci., vol. 4, Amer. Math. Soc., Providence, RI, 1991, pp. 493–516.

[13] E. Schulte and A. Ivić Weiss, Chirality and projective linear groups, *Discrete Math.* **131** (1994), 221–261.

[14] S. Wilson, Parallel products in groups and maps, *J. Algebra* **167** (1994), 539–546.

[15] S. Wilson, The smallest nontoroidal chiral maps, *J. Graph Theory* **2** (1978), 315–318.

ARS MATHEMATICA CONTEMPORANEA

Also available at http://amc-journal.eu
ISSN 1855-3966 (printed edn.), ISSN 1855-3974 (electronic edn.)
ARS MATHEMATICA CONTEMPORANEA 7 (2014) 317–336

Kronecker covers, V-construction, unit-distance graphs and isometric point-circle configurations*

Gábor Gévay
Bolyai Institute, University of Szeged, Aradi vértanúk tere 1, H-6720 Szeged, Hungary

Tomaž Pisanski
Faculty of Mathematics and Physics, University of Ljubljana
Jadranska 19, 1111 Ljubljana, Slovenia

Received 29 July 2012, accepted 17 March 2013, published online 1 June 2013

Abstract

We call a convex polytope P of dimension 3 *admissible* if it has the following two properties: (1) for each vertex of P the set of its first-neighbours is coplanar; (2) all planes determined by the first-neighbours are distinct. It is shown that the Levi graph of a point-plane configuration obtained by V-construction from an admissible polytope P is the Kronecker cover of the 1-skeleton of P. We investigate the combinatorial nature of the V-construction and use it on unit-distance graphs to construct novel isometric point-circle configurations. In particular, we present an infinite series all of whose members are subconfigurations of the renowned Clifford configurations.

Keywords: V-construction, unit-distance graph, isometric point-circle configuration, Kronecker cover, Clifford configuration, Danzer configuration, generalized cuboctahedron graph.

Math. Subj. Class.: 51A20, 52B10, 52C30, 05B30

1 Introduction

In this paper we investigate and carry over from polytopes to graphs the so-called V-construction, which was originally introduced in [16]. In this process we explain the construction in terms of the canonical double cover, also called the Kronecker cover of graphs. The reader is referred to [29] for graph coverings and to the monographs [22, 35] for the background on configurations and their Levi graphs.

*The authors acknowledge partial funding of this research via ARSS of Slovenia, grants: P1-0294 and N1-0011: GReGAS, supported in part by the European Science Foundation.

E-mail addresses: gevay@math.u-szeged.hu (Gábor Gévay), Tomaz.Pisanski@fmf.uni-lj.si (Tomaž Pisanski)

The first author used convex 3-polytopes in order to define a construction of geometric point-plane configurations in the following way [16].

Let P be a convex polytope of dimension 3 with the property that for each vertex v the set $N(v)$ of its first neighbours (i.e., vertices adjacent to v) is coplanar. In particular, this will always be true if the graph (or 1-skeleton) of the polytope P is trivalent. There are several other classes of polytopes that have this property. Furthermore, we assume that all planes obtained in this way are distinct. In particular, this condition rules out bipyramids such as the octahedron. Let us call such a polytope *admissible*.

Proposition 1.1. *Each convex 3-polytope with trivalent 1-skeleton is admissible.*

Proof. Since each vertex of a 3-polytope with trivalent 1-skeleton has exactly three first-neighbours, they are clearly coplanar. An easy argument shows that if two trivalent vertices of a 3-polytope P share the same set of first-neighbours, then the 1-skeleton of P itself cannot be trivalent. □

Suppose P is an admissible 3-polytope, and let $V(P)$ denote the set of vertices of P and $S(P)$ denote the set of planes passing through the first-neighbours of the vertices of P. Then the pair $((V(P), S(P))$ defines a geometric incidence structure of points and planes with the usual incidence. We call this procedure the *geometric V-construction*. If the 1-skeleton of P is a k-valent graph, then each point of the configuration will sit on k planes (we remark that in this case, Euler's Theorem implies $k = 3, 4$ or 5, see Section 10.1 in [20]). It immediately follows from the definition that each plane contains exactly k points. Let n be the number of vertices of P. Therefore, combinatorially, the incidence structure is an (n_k) configuration.

A natural question is what is the Levi graph of such a configuration. Recall that the *Levi graph* $L(C)$ of a configuration C is a bipartite graph whose bipartition classes consist of the points and blocks of C, respectively, and two points in $L(C)$ are adjacent if and only if the corresponding point and block in C are incident. Levi graphs are useful tools in studying configurations, because of the following property [9].

Lemma 1.2. *A configuration C is uniquely determined by its Levi graph $L(C)$.*

Another, much more difficult, question is whether we can find any conditions under which such a combinatorial configuration may be realized geometrically as a configuration of points and lines. On the other hand, it may happen that a configuration can be realized in both a point-line version in the plane, and a point-plane version in space (cf. our example at the end of Section 2). In Section 3 and 5 we also present examples of configurations for which both point-line and point-circle realizations exist.

Point-circle configurations themselves are also interesting, since, in contrast to the point-line configurations, relatively little is known about them. The most notable achievement in this respect is undoubtedly Clifford's infinite series of configurations, going back to 1871 [10, 22]. In the last two sections we present a new construction of Clifford's configurations, as well as three new infinite series of point-circle configurations.

We note that the construction introduced in [16] is more general than needed here: instead of 3-dimensional polytopes one can take d-dimensional polytopes and accordingly, instead of planes one should consider hyperplanes. Also, instead of first-neighbours it is possible to consider second-neighbours. However, we do not consider these aspects of the V-construction here.

2 Combinatorial *V*-construction

Let us generalize and carry out the V-construction on the abstract level.

To any regular graph G we may associate a combinatorial configuration. For a vertex v of G, denote by $N(v)$ the set of vertices adjacent to v. Then take the family $S(G)$ of these vertex-neighbourhoods:

$$S(G) = \{N(v) \,|\, v \in V(G)\}.$$

The triple $(V(G), S(G), \in)$ defines a combinatorial incidence structure underlying the geometric configuration of points and planes for any 3-polytope P whose 1-skeleton is G. We shall denote this structure by $N(G)$.

We note that a closely related construction occurs in the context of combinatorial geometries [31, 40].

The following general result establishes a connection between Levi graphs and Kronecker covers. It will play a central role in our constructions presented in the rest of the paper. First, we recall that a graph $\widetilde{G}$ is said to be the *Kronecker cover* (or *canonical double cover*) of the graph G if there exists a $2:1$ surjective homomorphism $f : \widetilde{G} \to G$ such that for every vertex v of $\widetilde{G}$ the set of edges incident with v is mapped bijectively onto the set of edges incident with $f(v)$ [29].

Theorem 2.1. *Let G be a graph on n vertices and let L be the Levi graph of the incidence structure $N(G)$. If no two vertices of G have the same neighbourhood, then L is the Kronecker cover of G.*

Proof. Under the assumption that no two vertices have the same set of neighbours, all sets $N(v)$, for $v \in V(G)$, are distinct. Therefore the set of vertices of L consists of V and $\{N(v)|v \in V(G)\}$. Each edge $e = uv$ from G gives rise to two edges: $uN(v)$ and $vN(u)$. Hence L is a Kronecker cover of G. If $|V(G)| \neq |\{N(v)|v \in V(G)\}|$, the argument fails. □

Some direct consequences of Theorem 2.1 for Levi graphs are as follows.

Proposition 2.2. *Let G be a graph on n vertices and let L be the Levi graph of the incidence structure $N(G)$. The graph L is connected if and only if G is connected and non-bipartite.*

Proof. If the graph G has no two vertices with a common neighborhood, the result follows from Theorem 2.1 and a well-known property of the Kronecker cover, see Proposition 1 of [29]. If this is not the case, the construction of L may be performed in two steps. First we construct the Kronecker cover H over G. We label the vertices of H in the following way. Let each vertex v of G give rise to two vertices v and v' of H in such a way that an edge uv of G gives rise to two edges uv' and $u'v$.

In the second step we identify any pair of vertices u' and v' of H if and only if $N(u) = N(v)$ in G. The resulting graph is isomorphic to L. Such an identification may occur if and only if the vertices u in v are in the same bipartition set. This means that in the Kronecker cover only vertices in the same connected component may be identified and the result follows. □

Proposition 2.3. *Let G be a k-valent graph on n vertices and let L be the Levi graph of the incidence structure $N(G)$. Then $N(G)$ is a combinatorial (n_k) point-line configuration if and only if L contains no cycle of length 4.*

Proof. In the Kronecker cover odd cycles of length r lift to cycles of length $2r$, while even cycles lift to two cycles of the same length. Hence the girth of the Kronecker cover is 4 if and only if the original graph contains a 4-cycle. Since Kronecker cover is bipartite, the alternative means girth at least 6. □

By analogy with geometric V-construction, we call a graph G *admissible* if no two of its vertices have a common neighborhood. Recall that a configuration is *combinatorially self-polar* if there exists an automorphism of order two of its Levi graph interchanging the two parts of bipartition; see for instance [35].

Theorem 2.4. *A configuration that is obtained by V-construction from an admissible graph G is combinatorially self-polar.*

Proof. By our previous discussion the Levi graph of this configuration is a Kronecker cover over G. The involution that switches at the same time the vertices in each fiber is a self-polarity. This follows from the fact that any double cover is a regular cover. □

We shall use the following result, which is an easy consequence of Proposition 1 in [29] and our Theorem 2.1.

Proposition 2.5. *Let C be a configuration obtained from an admissible graph G by V-construction. Then the Levi graph $L(C)$ is bipartite. If G is bipartite, then $L(C)$ consists of two disjoint copies of G.*

Corollary 2.6. *Applying the V-construction to the Levi graph of configuration C from Proposition 2.5 results in a configuration C' which consists of two disjoint copies of C.*

We conclude this section with the following example. Let G be the dodecahedron graph. Then $N(G)$ is a configuration (20_3). If G is embedded in $\mathbb{E}^3$ as the 1-skeleton of the regular dodecahedron, then $N(G)$ is realized as a geometric point-plane configuration (see Figure 1).

We note that the same configuration is obtained by taking the 20 vertices and the planes spanned by the 20 triangular faces of either the *small ditrigonal icosidodecahedron* or the *great ditrigonal icosidodecahedron* (these polyhedra belong to the class of the 53 non-regular non-convex uniform polyhedra [11, 25]).

On the other hand, we know that the Kronecker cover of the dodecahedron graph is isomorphic to the Levi graph of the unique triangle-free, flag-transitive (20_3) point-line configuration [5] (Figure 2) (see also Figure 1 in [4]). Thus we see that $N(G)$ can be realized geometrically as both a point-plane and a point-line configuration. As we show in the next section, a realization as a point-circle configuration may also be of interest.

3 V-construction and configurations of points and circles

In [16] it was observed that certain point-plane configurations obtained from a 3-polytope P by the V-construction could also be realized by points and circles. A simple necessary condition for this is that for each vertex v of P, the set of the first-neighbours of v forms a concyclic set, i.e. one can draw a circle through its points. Moreover, such point-circle configurations can be carried over to the plane, using stereographic projection. Here the well-known property is used that the stereographic projection is a circle-preserving map, see for instance [26] (also [10, 24]).

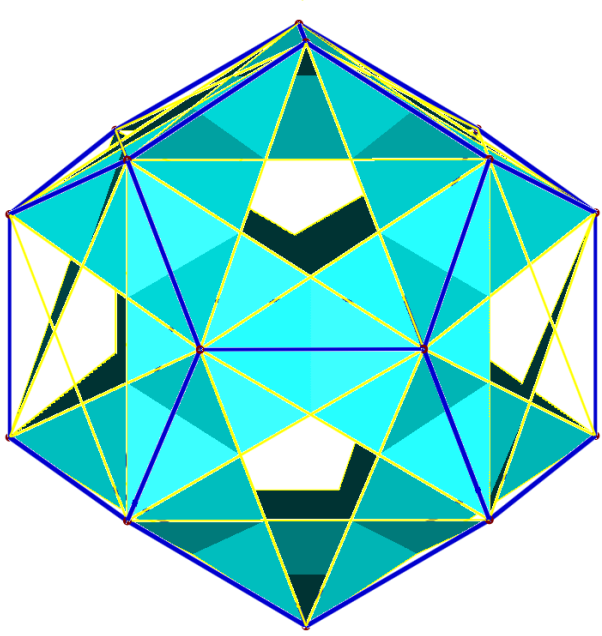

Figure 1: The (20_3) point-plane configuration obtained from the regular dodecahedron by the V-construction. Each plane is indicated by the convex hull of the three vertices spanning it.

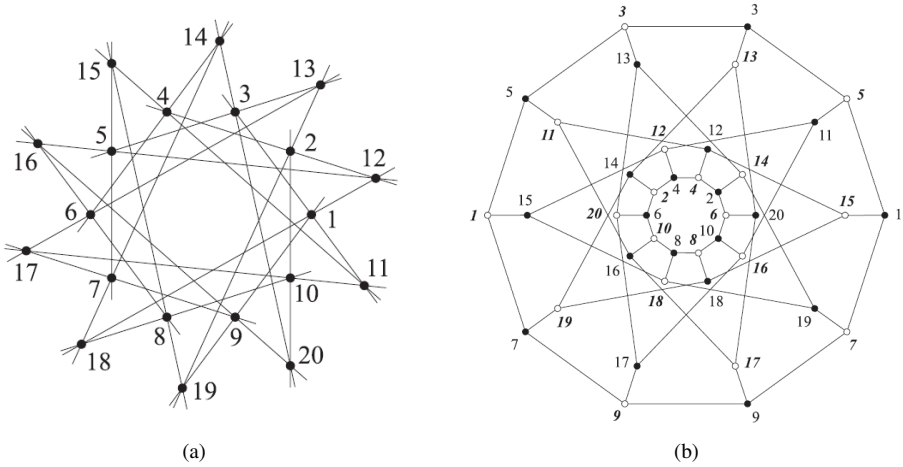

(a) (b)

Figure 2: The flag-transitive triangle-free point-line configuration (20_3) (a), and its Levi graph (b).

Lemma 3.1. *Under stereographic projection from the sphere S to the plane Σ the image of any circle on S is a circle on Σ.*

A straightforward application of this leads to the following result.

Theorem 3.2. *Any point-circle configuration on the sphere gives rise to a planar point-circle configuration.*

Here we explicitly state the result that is presented already in [16] (see Table 1 and 2 there), and follows readily from Theorem 3.2.

Corollary 3.3. *The V-construction on any Platonic or Archimedean polyhedron except for the octahedron gives rise to a planar point-circle configuration.*

An example obtained from the regular dodecahedron is depicted in Figure 3. (Note that together with this, we have three distinct geometric realizations of the same combinatorial configuration of type (20_3); cf. Figures 1 and 2.)

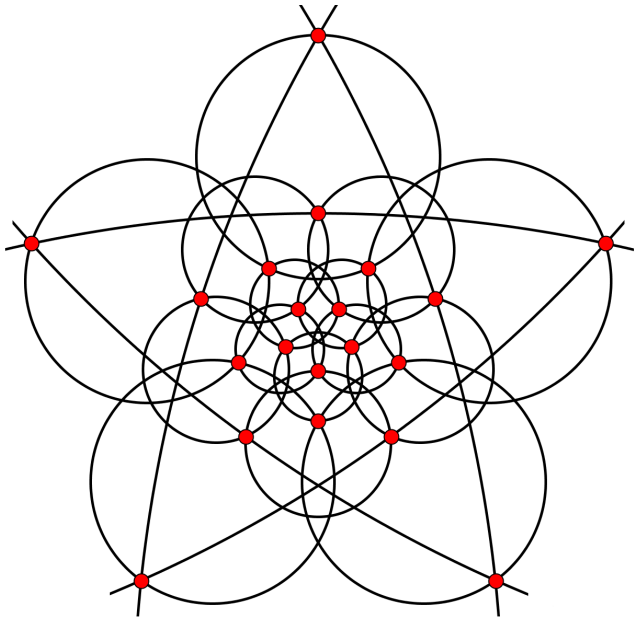

Figure 3: (20_3) point-circle configuration obtained from the regular dodecahedron by V-construction.

We remark that applying highly symmetric polytopes as a "scaffolding" for the construction of spatial point-line configurations is extensively used in [17].

The V-construction on 3-polytopes may also work in more generality. We recall the following theorem, which is a consequence of the Koebe-Andreev-Thurston circle-packing theorem (for further details, and some related problems, see [20, 37, 38, 42]).

Theorem 3.4. *Every convex 3-polytope P can be realized with all edges tangent to a sphere S; that is, there exists a combinatorially equivalent copy Q of P with all its edges tangent to S.*

This leads to the following conjecture that was essentially suggested by one of the referees.

Conjecture 3.5. *Let P be any convex 3-polytope other than a bipyramid such that its 1-skeleton is a regular graph. Then the combinatorial configuration obtained by V-construction from the graph of P can be realized as a point-circle configuration on the 2-sphere, and hence, in plane.*

In fact, the edges emanating from a vertex v of P touch the sphere S in points lying on a circle in S, and these points of contact are basically the same (combinatorially speaking) as the vertices of P adjacent to v. Of course, the circles will not meet in vertices of P. Still, it might be worth seeing if the conjecture is true.

In what follows we consider some other cases of V-construction that also give rise to planar point-circle configurations.

Proposition 3.6. *Any (n_3) configuration can be realized by points and circles in the plane.*

Proof. We may place the n points in the plane in general position, in such a way that no three lie on a line and no four lie on a circle. Obviously combinatorial lines can be realized by circles, and the combinatorial incidence is carried over to a geometric point-circle incidence. □

The (n_3) point-circle configurations have an important property that is not shared by all point-circle configurations; namely, they are movable. To see this notion, we should consider that in the simplest case the point-circle configurations are constructed in the Euclidean plane $\mathbb{E}^2$. However, by adding to $\mathbb{E}^2$ a single point at infinity, we may as well consider them as lying in the *inversive plane* [10]. Under this consideration, we say that a point-circle configuration is *rigid* if its geometric realizations form a single class under circle-preserving transformations of the inversive plane.

We note that point-circle configurations can also be considered on the extended complex plane; in this case the circle-preserving transformations are just the Möbius transformations, i.e. fractional linear transformations [24]. Incidentally, these latter play an important role in the so-called Lombardi drawings of graphs, an idea not totally unrelated to point-circle configurations and studied by D. Eppstein and his co-authors, for instance in [12].

Having defined rigidity above, we say that a point-line configuration is *movable* if is not rigid (cf. the notion of movability of point-line configurations, as defined in [22]). The following statement is a straightforward consequence of this definiton.

Proposition 3.7. *Any (n_3) point-circle configuration is movable.*

We note that movability is not a general property even for point-line configurations; for example, some classes of movable (n_4) configurations were discovered just recently [2, 3].

There is another property that distinguishes (n_3) point-circle configurations among all configurations. In general, the circles may be of different size. Let r be the number of radii used in this construction. If $r = 1$, all circles are of the same size, and the configuration is called an *isometric point-circle configuration*. It is not clear which (n_3) configurations can be realized as planar isometric point-circle configurations.

There is a large class of graphs that yields by V-construction isometric point-circle configurations in a natural way. These are the *unit-distance graphs*, i.e. graphs all of whose edges have the same length (cf. [27, 28, 43]).

Theorem 3.8. *Let G be a regular d-valent graph that is a unit-distance graph on n vertices in the plane. Then $N(G)$ is an (n_d) configuration, realizable as an isometric point-circle configuration.*

Proof. The points of the configuration are the vertices of the graph, as drawn in the plane. The unit-distance property implies that for each vertex, the set of its first-neighbours forms a concyclic set; furthermore, all these circles are of the same size. □

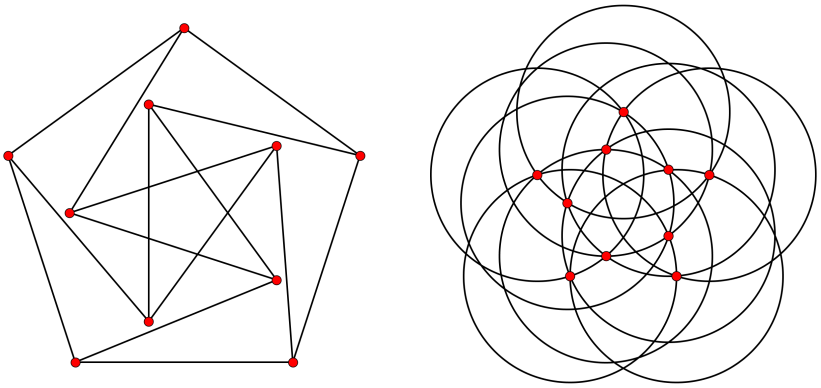

(a) (b)

Figure 4: Applying the V-construction to a unit-distance representation of the Petersen graph (a) yields an isometric point-circle realization of Desargues' configuration (b).

An interesting example is as follows. We know unit-distance representations of the Petersen graph [28, 43]; on the other hand, it is well known that the Kronecker cover of the Petersen graph is the Desargues graph [29] (which, in turn, is the Levi graph of the Desargues configuration [9]). Thus, by Theorem 2.1, the V-construction on a unit-distance representation of the Petersen graph yields an isometric point-circle realization of the Desargues configuration (see Figure 4).

We remark that the Desargues graph also has a unit-distance representation [43]. Thus one may also apply to it the V-construction, so as to obtain an isometric point-circle configuration. By our Corollary 2.6, this (20_3) configuration decomposes into two disjoint copies of the (10_3) Desargues point-circle configuration (see Figure 5, where the construction yields the two (10_3) copies in centrally symmetric position with respect to their common centre).

We mention an additional property which a point-circle configuration may or may not possess. We call a point-circle configuration $\mathcal{C}$ *lineal* if two circles meet in at most one point of $\mathcal{C}$. This property depends on the combinatorial structure of $\mathcal{C}$; in other words, $\mathcal{C}$ is lineal if and only if the underlying combinatorial configuration possesses an analogous property. In simple cases, lineality can be decided quite easily; even visual observation may suffice (provided a graphical representation is available). For example, the (20_3) configuration in Figure 3 is lineal. Clearly, so is any point-circle representation of the Desargues configuration. On the other hand, examples of Clifford's point-circle configurations, shown

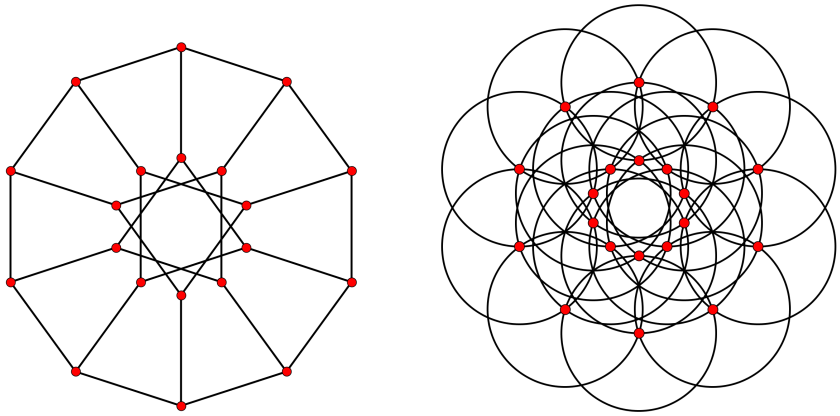

(a) (b)

Figure 5: Applying the V-construction to a unit-distance representation of the Desargues graph (a) yields a configuration consisting of two disjoint copies of another isometric realization of the point-circle Desargues configuration (b). One of the two copies can be viewed in Figure 8.

in Figures 6 and 7 in the next section, are not lineal. Here we give a criterion that can be used in some cases, like e.g. the whole series of the Clifford configurations.

Proposition 3.9. *A point-circle configuration $\mathcal{C}$ is lineal if and only if its Levi graph $L(\mathcal{C})$ contains no cycle of length 4. In particular, suppose $\mathcal{C}$ can obtained by V-construction from a graph G. Then $\mathcal{C}$ is lineal if and only if G contains no cycle of length 4.*

Proof. Observe that a cycle of length 4 in $L(\mathcal{C})$ is a complete bipartite graph $K_{2,2}$ such that one pair of its non-adjacent vertices corresponds to a pair of points (P_1, P_2) in $\mathcal{C}$, and the other pair of its non-adjacent vertices corresponds to a pair of circles meeting in (P_1, P_2). Hence the proof goes along the same lines as that of Proposition 2.3. □

4 V-construction on d-cubes and Clifford's point-circle configurations

The particular case of the cube in Corollary 3.3 can be extended to the whole class of d-cubes. Because of its interesting connections, we discuss here the general case in some detail.

We recall the infinite series of Clifford's point-circle configurations, which is associated to his renowned chain of theorems. By Coxeter [10], these theorems can be formulated as follows.

Theorem 4.1 (Clifford's chain of theorems).

(1) *Let σ_1, σ_2, σ_3, σ_4 be four circles of general position through a point S. Let S_{ij} be the second intersection of the circles σ_i and σ_j. Let σ_{ijk} denote the circle $S_{ij}S_{ik}S_{jk}$. Then the four circles σ_{234}, σ_{134}, σ_{124}, σ_{123} all pass through one point S_{1234}.*

(2) *Let σ_5 be a fifth circle through S. Then the five points S_{2345}, S_{1345}, S_{1245}, S_{1235}, S_{1234} all lie on one circle σ_{12345}.*

(3) *The six circles* σ_{23456}, σ_{13456}, σ_{12456}, σ_{12356}, σ_{12346}, σ_{12345} *all pass through one point* S_{123456}.

And so on.

We note that these circles can be considered as lying either in the (inversive) plane or on the 2-sphere. We know the Levi graph of these configurations (Coxeter [9, 10]).

Lemma 4.2. *The Levi graph of the Clifford configuration of type* (2_d^{d-1}) *is isomorphic to the* d*-cube graph.*

It turns out that our V-construction can be applied so as to obtain Clifford's configurations.

Theorem 4.3. *The* V*-construction on a* d*-cube graph gives rise to an isometric* (2_d^d) *point-circle configuration in the plane. This configuration is disconnected and composed of two copies of isometric* (2_d^{d-1}) *point-circle configurations which are isomorphic to a member of the same type of Clifford's infinite series of configurations.*

Proof. The d-cube graph is the Cartesian product of d edge graphs K_2. According to [27], it is a unit-distance graph. By Theorem 3.8, the V-construction applied on it gives rise to an isometric point-circle configuration C. Since the d-cube graph is bipartite, its Kronecker cover is composed of two disjoint isomorphic copies of the d-cube graph (by Proposition 1 in [29]). By Theorem 2.1, this Kronecker cover is the Levi graph of C. Since a configuration is uniquely determined by its Levi graph (by Lemma 1.2), it follows from Lemma 4.2 that C is in fact composed of two disjoint copies of Clifford configurations of type (2_d^{d-1}). □

Some smallest examples are depicted in Figures 6 and 7.

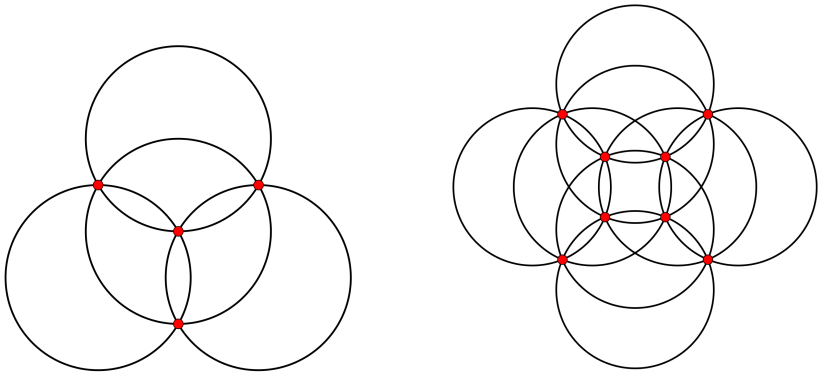

(a) (b)

Figure 6: Isometric realization of Clifford configurations: (4_3) derived from the 3-cube graph (a), and (8_4) derived from the 4-cube graph (b).

It is easy to see that the d-cube graph can be realized in the plane as a unit-distance graph in continuum many ways. In fact, take an arbitrary vertex and place it in the center of a unit circle. Its first-neighbours can be placed in different positions on the circle. Positions

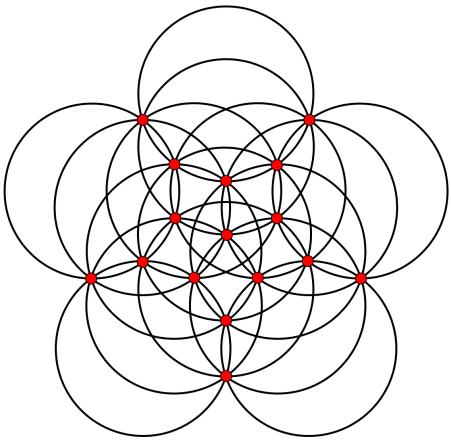

Figure 7: Isometric realization of Clifford's configuration (16_5) derived from the 5-cube graph.

of the remaining vertices are then uniquely determined by sequences of rhombuses. This immediately gives the following corollary.

Corollary 4.4. *Every Clifford configuration is realizable as a movable isometric point-circle configuration.*

Remark 4.5. Realizability of Clifford's configurations with circles of equal size is already known from [41] (see also [1]). Our approach provides an independent proof of this result.

5 Three new infinite classes of point-circle configurations

We start from the following observation. When applying the V-construction so as to obtain an isometric point-circle realization of Desargues' configuration, the underlying Petersen graph need not be represented in unit-distance form. Indeed, compare our Figures 4 and 8. (We remark that the version depicted in Figure 8b is precisely the same as one of the components of the (20_3) configuration in Figure 5b.)

Now Figure 8b suggests that this latter realization can be extended to a Clifford configuration of type (16_5). Figure 9 shows that such an extension is in fact possible (see also Figure 7). It turns out that this is a particular case of a more general relationship.

Before formulating it, recall that the *Kneser graph* $K(n,k)$ has as vertices the k-subsets of an n-element set, where two vertices are adjacent if the k-subsets are disjoint [19]. The Kneser graph $K(2n-1,n-1)$ is called an *odd graph* and is denoted by O_n. In particular, $O_3 = K(5,2)$ is isomorphic to the Petersen graph. The *bipartite Kneser graph* $H(n,k)$ has as its bipartition sets the k- and $(n-k)$-subsets of an n-element set, respectively, and the adjacency is given by containment. Although the following relationship is well-known, we give a short proof of it.

Lemma 5.1. *The bipartite Kneser graph $H(n,k)$ is the Kronecker cover of the Kneser graph $K(n,k)$.*

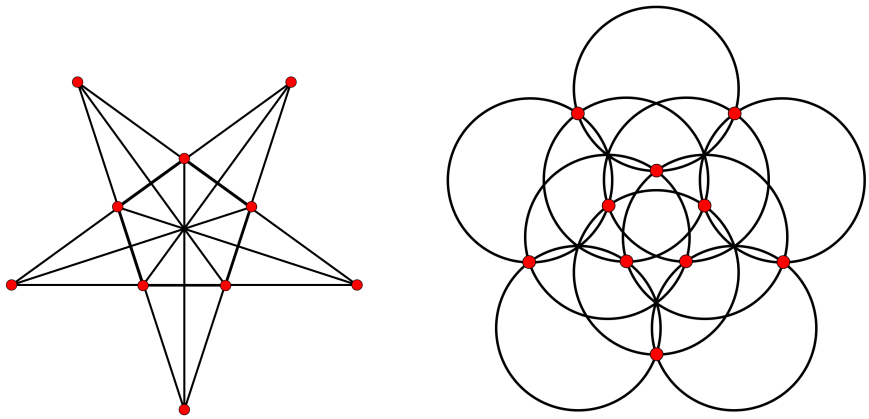

Figure 8: Isometric point-circle realization of Desargues' configuration arising from a non-unit-distance representation of the Petersen graph. (Note that this is a degenerate representation in the sense that there are edges overlapping along the sides of the inner pentagon.)

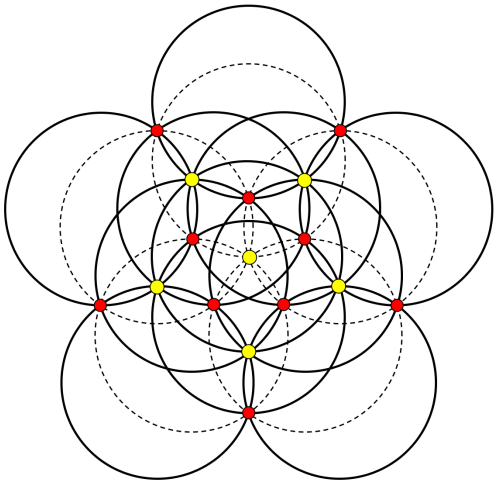

Figure 9: The Desargues point-circle configuration extended to the Clifford configuration (16_5).

Proof. Let A and B be two k-subsets and let A' and B' be their respective $(n-k)$-complements. Clearly A is adjacent to B in $K(n,k)$ if and only if A is adjacent to B' and B is adjacent to A' in $H(n,k)$, and the result follows readily. □

The bipartite Kneser graph $H(2n-1,n-1)$ is also known as the *revolving door graph*, or *middle-levels graph*; the latter name comes from the fact that it is a special

subgraph of the $(2n-1)$-cube graph Q_{2n-1} (considering Q_{2n-1} as the Hasse diagram of the corresponding Boolean lattice) [36, 39]. It is a regular graph with degree n. Note that middle-levels graph is called a *medial layer graph* in [33] and is defined for any abstract polytope of odd rank.

Theorem 5.2. *For all $n \geq 3$, there exists an isometric point-circle configuration of type*

$$\left(\binom{2n-1}{n-1}_n \right).$$

It is a subconfiguration of the Clifford configuration of type $\left(2^{2n-2}_{2n-1}\right)$. It can be obtained from the odd graph O_n by V-construction.

Proof. Let C be an incidence structure obtained from the odd graph O_n by V-construction. By Theorem 2.1, the Levi graph of C is the Kronecker cover of O_n. Lemma 5.1 implies that it is the bipartite Kneser graph $H(2n-1, n-1)$. Since this graph is a subgraph of the $(2n-1)$-cube graph Q_{2n-1}, from Lemma 1.2 follows that C is isomorphic to a subconfiguration of the Clifford configuration of type $\left(2^{2n-2}_{2n-1}\right)$. Hence it can be realized as a planar point-circle configuration. The type of this configuration follows from the definition of O_n. Furthermore, Corollary 4.4 implies that this configuration also has an isometric realization. □

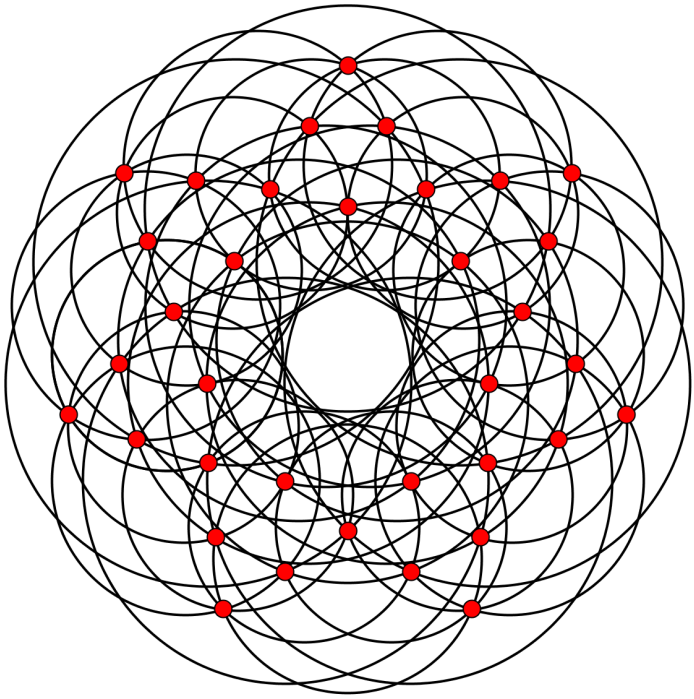

Figure 10: A point-circle realization of Danzer's (35_4) configuration.

Remark 5.3. Proposition 3.9 and Lemma 4.2 together imply that the Clifford configurations are not lineal. In contrast to this, it can be proved that their subconfigurations given by Theorem 5.2 are lineal. We leave the details to a subsequent paper.

In the particular case of $n = 4$ we have (35_4), which provides a point-circle realization of Danzer's combinatorial (35_4) configuration (see Figure 10 for a non-isometric version). On this latter, Grünbaum wrote in 2008 [21]: "It seems that any representation of Danzer's configuration is of necessity so cluttered and unhelpful for visualization that no attempt to present it has ever been made." (see also [23]).

We emphasize the geometric symmetry of this realization, which is the highest possible in the planar case; namely, D_7.

Our next new class also consists of isometric point-circle configurations.

Theorem 5.4. *For any N and any $d > 2$ there exists an isometric (n_d) point-circle configuration with $n > N$.*

Proof. Take the Cartesian product of a long odd cycle C_N and a $(d-2)$-dimensional cube graph. This is a unit-distance graph. Apply the V-construction to it. □

Finally, we construct an infinite series of non-isometric (n_4) point-circle configurations. We start from a prism P over an n-gon ($n \geq 3$) (the corresponding graph is also called a *circular ladder*). Then we take its *medial* $Me(P)$ [19, 34, 14], i.e. a new polyhedron such that its vertices are the midpoints of the original edges, and for each original vertex, the midpoints of the edges emanating from it are connected by new edges, forming a 3-cycle. In terms of solid geometry, the medial corresponds to a truncation of a right n-sided prism such that each truncating plane at a vertex is spanned by the midpoints of the edges incident with the given vertex ("deep vertex truncation", see [42]). Note that in the particular case when the prism is the cube, its medial is the Archimedean solid called a *cuboctahedron*. Accordingly, we define the *generalized cuboctahedron graph* as the 1-skeleton of $Me(P)$, and denote it by $CO(n)$. Note that this graph can equivalently be defined as the line graph of the prism graph.

Observe that $CO(n)$ is a 4-valent regular graph with $3n$ vertices. Moreover, it has a representation in the plane such that it exhibits the symmetry of a regular n-gon (thus its symmetry group is D_n); in this case its vertices lie on three concentric circles, n vertices on each. It follows that the first-neighbour sets of the vertices are concyclic, hence the V-construction can be applied. Thus we obtain the following result.

Theorem 5.5. *For any $n \geq 3$, there exists a $((3n)_4)$ point-circle configuration obtained from the generalized cuboctahedron graph $CO(n)$ by V-construction. It can be realized in the plane so that its symmetry group is the dihedral group D_n.*

An example with $n = 7$ is depicted in Figure 11. It is an open question if any member of the infinite series of these $((3n)_4)$ configurations has an isometric realization.

On the other hand, the mutual position of the points on the three orbits makes it possible to arrange the circles in several different ways, so as to obtain new, pairwise non-isomorphic $((3n)_4)$ configurations. Here we do not investigate this possibility in detail. Instead, we just present an example, also of type (21_4) (non-isomorphic with the previous one), whose original point-line version is remarkable for several reasons (see Figure 12). We only mention here that it goes back to Felix Klein, 1879 (for further details, see [23]); on the other hand, its first graphic depiction only appeared in 1990 [21, 23]. This configuration also

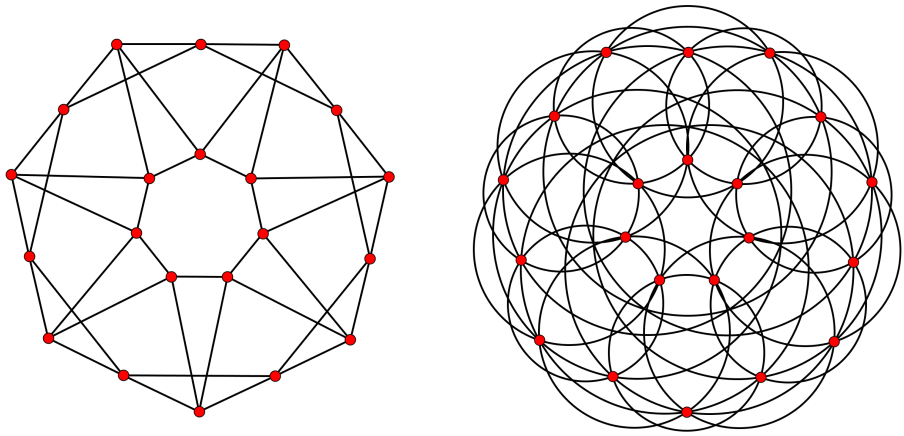

(a) (b)

Figure 11: A representation of the generalized cuboctahedron graph with D_7 symmetry (a), and a (21_4) point-circle configuration obtained from it by V-construction (b).

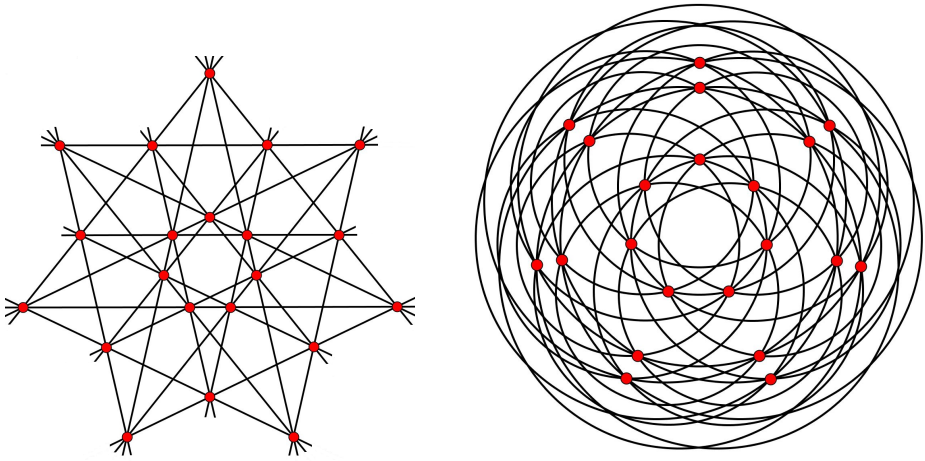

(a) (b)

Figure 12: The point-line (21_4) configuration of Grünbaum and Rigby (a), and one of its point-circle realizations with dihedral symmetry (b).

motivated the authors of [32] to present some geometric representations of a certain family of configurations that became later known as polycyclic configurations [6].

We note that several other already known families of graphs can serve as a basis for obtaining new point-circle configurations by V-construction; just to mention some of them: generalized Petersen graphs [34], I-graphs [7]. In addition, the 1-skeleton of equivelar polyhedra is also a regular graph (see e.g. [18]); hence, finding suitable planar representa-

tions among them may also be promising in this respect.

6 Some comparisons beween different realizations of configurations

Comparing point-line and point-circle configurations, several questions arise, in particular, when different kinds of geometric realization of the same combinatorial configuration is considered. First we make the following conceptual distinction. Clearly, every point-line configuration can be transformed into a point-circle configuration by some suitable inversion. However, in this case, all the circles will have a common point (the inverse image of the point at infinity). To rule out this case, we use the term *improper point-circle configuration*. Accordingly, we call a point-circle configuration *proper* if its circles are not all incident with a common point. Clearly, all our examples presented in the previous sections are proper point-circle configurations. In what follows, we shall also speak about such configurations, and mostly omit the attribute "proper".

A simple consequence of Proposition 3.6 is that by suitable displacement of the points, any planar (n_3) point-line configuration can transformed into a point-circle configuration. For an incidence number larger than 3, it is more difficult to decide the existence of a point-circle representation of a point-line configuration.

Problem 6.1. For $k \geq 4$, find an (n_k) point-line configuration which cannot be represented by a proper point-circle configuration.

The converse problem, in general, can also be quite difficult. However, here we know several examples. One of the oldest one is Miquel's $(8_3, 6_4)$ (for a simple proof why it has no point-line representation, see [35]). The infinite series of Clifford configurations also provides quite old (balanced) examples. In fact, since all the higher members contain, as a subconfiguration, the initial member of type (4_3), they cannot be represented by point-line configurations.

In the particular case of incidence number $k = 4$, we have the following lower bound (a result of Bokowski and Schewe [8]).

Theorem 6.2. *For $n \leq 17$, there are no geometric point-line configurations (n_4).*

As a consequence, consider e.g. the generalized Petersen graph $GP(n, r)$ [34]. For $n \leq 8$ it yields, by V-construction, a point-circle configuration which has no point-line representation.

In Section 3 we introduced the notion of an isometric point-circle configuration. We also distinguished point-circle configurations according as they are lineal or not. We may impose a further condition, which, together with the former two, determines a particularly nice class of configurations. We call a point-circle configuration $\mathcal{C}$ *determining* if the set of points of $\mathcal{C}$ coincides with the set of points in which more than two circles of $\mathcal{C}$ meet.

Note that while the first two conditions determine a property on more abstract level, the latter may depend on a particular representation of $\mathcal{C}$. For example, Figure 4b shows a determining representation of the Desargues configuration, while that in Figure 8b is non-determining.

Now we call $\mathcal{C}$ *perfect* if it is lineal, isometric and determining. For example, the Desargues configuration in Figure 4b is perfect.

Problem 6.3. Which configurations of points and lines can be realized as perfect point-circle configurations?

Geometric symmetry is also an interesting property which is worth investigating when different realizations of the same combinatorial configuration are compared. Are all symmetries of a point-line configuration realizable in its representation by points and circles? Of course, the converse question can also arise. Here we only mention that e.g. for the Pappus configuration not only its realization by lines can exhibit the maximal possible symmetry (D_3), but it can also be realized by circles with the same symmetry (see Figure 13).

On the other hand, it is a remarkable fact that while the Desargues configuration can be represented by points and lines with symmetry group either C_5 or D_5 (see Figures 4b and 8b, respectively), its classical point-line version can exist with neither of these symmetries. This follows from the theory developed in the paper [7] on I-graphs and the corresponding configurations. (We note that geometric realization of certain combinatorial objects with maximal symmetry is, in general, a problem which is far from trivial, see e.g. [15], and the references therein.)

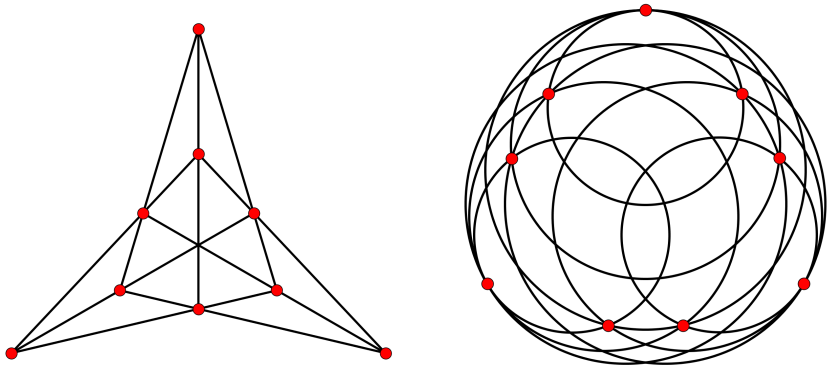

(a) (b)

Figure 13: Two different realizations of Pappus' configuration with symmetry D_3.

Considering point-circle realizations of the two oldest configurations, yet another difference occurs. Note that while Desargues' configuration has a perfect realization (shown by Figure 4b), the realization of Pappus' configuration shown by Figure 13b is not isometric (thus it is not perfect). On the other hand, when constructing an isometric representation, we find that it is no longer a determining representation (see the central triple crossing point in Figure 14b). This version is obtained from a unit-distance representation of the Pappus graph (see Figure 14a), using Corollary 2.6. Note that the symmetry reduces here to C_3 (for a representation of the Pappus graph with D_3 symmetry, see e.g. [34], Figure 21).

Acknowledgements

The authors would like to thank Marko Boben for careful reading of the manuscript, for pointing out that some circles in the (21_4) configuration on Figure 11(b) meet in two points, which is an easy proof that the configuration is not isomorphic to Klein's (21_4) configuration from [23], and for checking that Danzer's combinatorial (35_4) configuration actually admits a geometric realization and is hidden in the renowned Pascal's *Hexagrammum mys-*

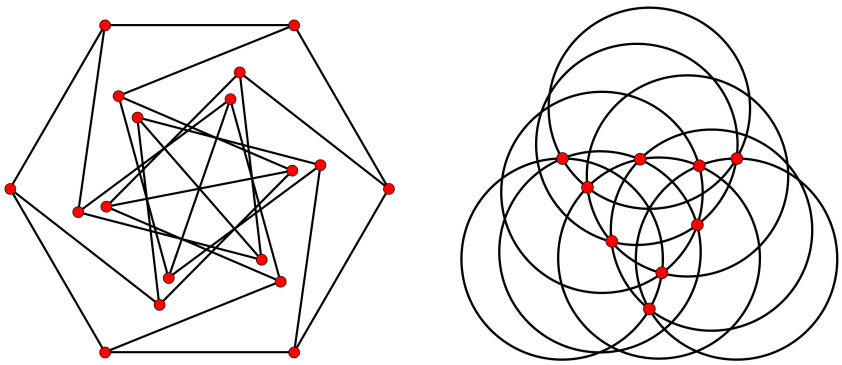

(a) (b)

Figure 14: Unit-distance representation of the Pappus graph (a), and isometric point-circle representation of the Pappus configuration derived from it (b).

ticum [30]. Last but not least we would like to thank the anonymous referee for encouraging us to pose Conjecture 3.5.

References

[1] D. W. Babbage, A chain of theorems for circles, *Bull. London Math. Soc.* **1** (1969), 343–344.

[2] L. W. Berman, Movable (n_4) configurations, *Electron. J. Combin.* **13** (2006), #R104.

[3] L. W. Berman, J. Bokowski, B. Grünbaum and T. Pisanski, Geometric "floral" configurations, *Can. Math. Bull.* **52** (2009), 327–341.

[4] A. Betten, G. Brinkmann and T. Pisanski, Counting symmetric v_3 configurations, *Discrete Applied Math.* **99** (2000), 331–338.

[5] M. Boben, B. Grünbaum, T. Pisanski and A. Žitnik, Small triangle-free configurations of points and lines, *Discrete Comput. Geom.* **35** (2006), 405–427.

[6] M. Boben and T. Pisanski, Polycyclic configurations, *European J. Combin.* **24** (2003), 431–457.

[7] M. Boben, T. Pisanski and A. Žitnik, I-graphs and the corresponding configurations, *J. Comb. Des.* **1**3 (2005) 406–424.

[8] J. Bokowski and L. Schewe, On the finite set of missing geometric configurations (n_4), *Comput. Geom.* **46** (2013) 532–540.

[9] H. S. M. Coxeter, Self-dual configurations and regular graphs, *Bull. Amer. Math. Soc.* **56** (1950), 413–455. Reprinted in: H. S. M. Coxeter, *Twelve Geometric Essays*, Southern Illinois University Press, Carbondale, 1968, 106–149.

[10] H. S. M. Coxeter, *Introduction to Geometry*, Wiley, New York, 1961.

[11] H. S. M. Coxeter, M. S. Longuet-Higgins and J. C. P. Miller, Uniform polyhedra, *Phil. Trans. Roy. Soc. London Ser. A* **246** (1954), 401–450.

[12] C. A. Duncan, D. Eppstein, M. T. Goodrich, S. G. Kobourov and M. Nöllenburg, Lombardi drawings of graphs, *J. Graph Algorithms Appl.* **16** (2012), 37–83.

[13] P. Erdős, F. Harary and W. T. Tutte, On the dimension of a graph, *Mathematika* **12** (1965), 118–122.

[14] P. Fowler and T. Pisanski, Leapfrog transformations and polyhedra of Clar type, *J. Chem. Soc. Faraday Trans.* **90** (1994), 2865–2871.

[15] G. Gévay, A class of cellulated spheres with non-polytopal symmetries, *Canad. Math. Bull.* **52** (2009), 366–379.

[16] G. Gévay, Symmetric configurations and the different levels of their symmetry, *Symmetry Cult. Sci.* **20** (2009), 309–329.

[17] G. Gévay, Constructions for large spatial point-line (n_k) configurations, *Ars Math. Contemp.* **7** (2014) 175–199.

[18] G. Gévay and J. M. Wills, On regular and equivelar Leonardo polyhedra, *Ars Math. Contemp.* **6** (2013), 1–11.

[19] C. Godsil and G. Royle, *Algebraic Graph Theory*, Springer-Verlag, New York, 2001.

[20] B. Grünbaum, *Convex Polytopes*, Graduate Texts in Mathematics, Vol. 221, Springer-Verlag, New York, 2003. (Second edition prepared by V. Kaibel, V. Klee and G. M. Ziegler).

[21] B. Grünbaum, Musings on an example of Danzer's, *European J. Combin.* **29** (2008), 1910–1918.

[22] B. Grünbaum, *Configurations of Points and Lines*, Graduate Texts in Mathematics, Vol. 103, American Mathematical Society, Providence, Rhode Island, 2009.

[23] B. Grünbaum and J. F. Rigby, The real configuration (21_4), *J. London Math. Soc.* **41** (1990), 336–346.

[24] L. Hahn, *Complex Numbers and Geometry*, The Mathematical Association of America, Washington, D. C. 1994.

[25] Z. Har'El, Uniform solution for uniform polyhedra, *Geom. Dedicata* **47** (1993), 57–110.

[26] D. Hilbert and S. Cohn-Vossen, *Geometry and Imagination*, Chelsea Publishing Company, NY 1952.

[27] B. Horvat and T. Pisanski, Products of unit distance graphs, *Discrete Math.* **310** (2010), 1783–1792.

[28] B. Horvat and T. Pisanski, Unit-distance representations of the Petersen graph in the plane, *Ars Combin.* **104** (2012), 393–415.

[29] W. Imrich and T. Pisanski, Multiple Kronecker covering graphs, *European J. Combin.* **29** (2008), 1116–1122.

[30] L. Klug, *Az általános és négy különös Pascal-hatszög configuratiója* (The Configuration of the General and Four Special Pascal Hexagons; in Hungarian), Ajtai K. Albert Könyvnyomdája, Kolozsvár, 1898. Reprinted in: L. Klug, *Die Configuration Des Pascal'schen Sechseckes Im Allgemeinen Und in Vier Speciellen Fällen (German Edition)*, Nabu Press, 2010.

[31] C. Lefèvre-Percsy, N. Percsy and D. Leemans, New geometries for finite groups and polytopes, *Bull. Belg. Math. Soc. Simon Stevin* **7** (2000), 583–610.

[32] D. Marušič and T. Pisanski, Weakly flag-transitive configurations and half-arc-transitive graphs, *European J. Combin.* **20** (1999), 559–570.

[33] B. Monson, T. Pisanski, E. Schulte and A. Ivić Weiss, Semisymmetric graphs from polytopes, *J. Combin. Theory A* **114** (2007), 421–435.

[34] T. Pisanski and M. Randić, Bridges between geometry and graph theory, in C. A. Gorini (ed.), *Geometry at Work*, MAA Notes 53, Math. Assoc. America, Washington, DC, 2000, pp. 174–194.

[35] T. Pisanski and B. Servatius, *Configurations from a Graphical Viewpoint*, Birkhäuser Advanced Texts Basler Lehrbücher Series, Birkhäuser Boston Inc., Boston, 2012.

[36] J. J. Quinn and A. T. Benjamin, Strong chromatic index of subset graphs, *J. Graph Theory* **24** (1997), 267–273.

[37] O. Schramm, How to cage an egg, *Invent. Math.* **107** (1992), 543–560.

[38] E. Schulte, Analogues of Steinitz's theorem about non-inscribable polytopes, in: K. Böröczky and G. Fejes Tóth (eds.), *Intuitive Geometry. Siófok, 1985* Colloq. Math. Soc. János Bolyai, Vol. 48, North-Holland – Math. Soc. János Bolyai, Budapest, 1987, pp. 503–516.

[39] I. Shields, B. J. Shields and C. D. Savage, An update on the middle levels problem, *Discrete Math.* **309** (2009), 5271–5277.

[40] H. Van Maldeghem, Slim and bislim geometries, in: A. Pasini (ed.) *Topics in Diagram Geometry*, Quaderni di Matematiche 12, Aracne, Roma, 2003, pp. 227–254.

[41] P. Ziegenbein, Konfigurationen in der Kreisgeometrie, *J. Reine Angew. Math.* **183** (1940), 9–24.

[42] G. M. Ziegler, Convex polytopes: extremal constructions and f-vector shapes, in: E. Miller, V. Reiner and B. Sturmfels (eds.), *Geometric Combinatorics*, IAS/Park City Math. Ser. Vol. 13, American Mathematical Society – Institute for Advanced Study, 2007, pp. 617–691.

[43] A. Žitnik, B. Horvat and T. Pisanski, All generalized Petersen graphs are unit-distance graphs *J. Korean Math. Soc.* **49** (2012), 475–491.

ARS MATHEMATICA CONTEMPORANEA

Also available at http://amc-journal.eu
ISSN 1855-3966 (printed edn.), ISSN 1855-3974 (electronic edn.)
ARS MATHEMATICA CONTEMPORANEA 7 (2014) 337–340

Unramified Brauer groups and isoclinism

Primož Moravec
Department of Mathematics, University of Ljubljana
Jadranska 21, 1000 Ljubljana, Slovenia

Received 4 October 2012, accepted 9 April 2013, published online 1 June 2013

Abstract

We show that the Bogomolov multipliers of isoclinic groups are isomorphic.

Keywords: Unramified Brauer group, Bogomolov multiplier, isoclinism.

Math. Subj. Class.: 20F12, 20F35, 13A50

1 Introduction

Let G be a finite group and V a faithful representation of G over an algebraically closed field k of characteristic zero. Suppose that the action of G upon V is generically free. A relaxed version of Noether's problem [11] asks as to whether the fixed field $k(V)^G$ is purely transcendental over k, i.e., whether the quotient space V/G is *rational*. A question related to the above mentioned is whether V/G is *stably rational*, that is, whether there exist independent variables $x_1, \ldots, x_r$ such that $k(V)^G(x_1, \ldots, x_r)$ becomes a pure transcendental extension of k. This problem has close connection with Lüroth's problem [12] and the inverse Galois problem [14, 13]. By the so-called *no-name lemma*, stable rationality of V/G does not depend upon the choice of V, but only on the group G, cf. [4, Theorem 3.3 and Corollary 3.4]. Saltman [13] found examples of groups G of order p^9 such that V/G is not stably rational over k. His main method was application of the unramified cohomology group $\mathrm{H}^2_{\mathrm{nr}}(k(V)^G, \mathbb{Q}/\mathbb{Z})$ as an obstruction. A version of this invariant had been used before by Artin and Mumford [1] who constructed unirational varieties over k that were not rational. Bogomolov [2] proved that $\mathrm{H}^2_{\mathrm{nr}}(k(V)^G, \mathbb{Q}/\mathbb{Z})$ is canonically isomorphic to

$$\mathrm{B}_0(G) = \bigcap_{\substack{A \leq G, \\ A \text{ abelian}}} \ker \mathrm{res}^G_A,$$

where $\mathrm{res}^G_A : \mathrm{H}^2(G, \mathbb{Q}/\mathbb{Z}) \to \mathrm{H}^2(A, \mathbb{Q}/\mathbb{Z})$ is the usual cohomological restriction map. Following Kunyavskiĭ [7], we say that $\mathrm{B}_0(G)$ is the *Bogomolov multiplier* of G.

E-mail address: primoz.moravec@fmf.uni-lj.si (Primož Moravec)

We recently proved [9] that $\mathrm{B}_0(G)$ is naturally isomorphic to $\mathrm{Hom}(\tilde{\mathrm{B}}_0(G), \mathbb{Q}/\mathbb{Z})$, where $\tilde{\mathrm{B}}_0(G)$ is the kernel of the commutator map $G \curlywedge G \to [G, G]$, and $G \curlywedge G$ is a quotient of the *non-abelian exterior square* of G (see Section 2 for further details). This description of $\mathrm{B}_0(G)$ is purely combinatorial, and allows for efficient computations of $\mathrm{B}_0(G)$, and a Hopf formula for $\mathrm{B}_0(G)$. We also note here that the group $\tilde{\mathrm{B}}_0(G)$ can be defined for any (possibly infinite) group G.

Recently, Hoshi, Kang, and Kunyavskiĭ [6] classified all groups of order p^5 with non-trivial Bogomolov multiplier; the question was dealt with independently in [10]. It turns out that the only examples of such groups appear within the same isoclinism family, where isoclinism is the notion defined by P. Hall in his seminal paper [5]. The following question was posed in [6]:

Question 1.1 ([6])**.** *Let G_1 and G_2 be isoclinic p-groups. Is it true that the fields $k(V)^{G_1}$ and $k(V)^{G_2}$ are stably isomorphic, or at least, that $\mathrm{B}_0(G_1)$ is isomorphic to $\mathrm{B}_0(G_2)$?*

The purpose of this note is to answer the second part of the above question in the affirmative:

Theorem 1.1. *Let G_1 and G_2 be isoclinic groups. Then $\tilde{\mathrm{B}}_0(G_1) \cong \tilde{\mathrm{B}}_0(G_2)$. In particular, if G_1 and G_2 are finite, then $\mathrm{B}_0(G_1)$ is isomorphic to $\mathrm{B}_0(G_2)$.*

The proof relies on the theory developed in [9]. We note here that we have recently become aware of a paper by Bogomolov and Böhning [3] who fully answer the above question using different techniques. We point out that our approach here is purely combinatorial and does not require cohomological machinery.

2 Proof of Theorem 1.1

We first recall the definition of $G \curlywedge G$ from [9]. For $x, y \in G$ we write ${}^x y = xyx^{-1}$ and $[x, y] = xyx^{-1}y^{-1}$. Let G be any group. We form the group $G \curlywedge G$, generated by the symbols $g \curlywedge h$, where $g, h \in G$, subject to the following relations:

$$\begin{aligned} gg' \curlywedge h &= ({}^g g' \curlywedge {}^g h)(g \curlywedge h), \\ g \curlywedge hh' &= (g \curlywedge h)({}^h g \curlywedge {}^h h'), \\ x \curlywedge y &= 1, \end{aligned}$$

for all $g, g', h, h' \in G$, and all $x, y \in G$ with $[x, y] = 1$. The group $G \curlywedge G$ is a quotient of the non-abelian exterior square $G \wedge G$ of G defined by Miller [8]. There is a surjective homomorphism $\kappa : G \curlywedge G \to [G, G]$ defined by $\kappa(x \curlywedge y) = [x, y]$ for all $x, y \in G$. Denote $\tilde{\mathrm{B}}_0(G) = \ker \kappa$. By [9] we have the following:

Theorem 2.1 ([9])**.** *Let G be a finite group. Then $\mathrm{B}_0(G)$ is naturally isomorphic to $\mathrm{Hom}(\tilde{\mathrm{B}}_0(G), \mathbb{Q}/\mathbb{Z})$, and thus $\mathrm{B}_0(G) \cong \tilde{\mathrm{B}}_0(G)$.*

Let L be a group. A function $\phi : G \times G \to L$ is called a $\tilde{\mathrm{B}}_0$-*pairing* if for all $g, g', h, h' \in G$, and for all $x, y \in G$ with $[x, y] = 1$,

$$\begin{aligned} \phi(gg', h) &= \phi({}^g g', {}^g h)\phi(g, h), \\ \phi(g, hh') &= \phi(g, h)\phi({}^h g, {}^h h'), \\ \phi(x, y) &= 1. \end{aligned}$$

Clearly a $\tilde{\mathrm{B}}_0$-pairing ϕ determines a unique homomorphism of groups $\phi^* : G \curlywedge G \to L$ such that $\phi^*(g \curlywedge h) = \phi(g,h)$ for all $g, h \in G$.

We now turn to the proof of Theorem 1.1. Let G_1 and G_2 be isoclinic groups, and denote $Z_1 = Z(G_1)$, $Z_2 = Z(G_2)$. By definition [5], there exist isomorphisms $\alpha : G_1/Z_1 \to G_2/Z_2$ and $\beta : [G_1, G_1] \to [G_2, G_2]$ such that whenever $\alpha(a_1 Z_1) = a_2 Z_2$ and $\alpha(b_1 Z_1) = b_2 Z_2$, then $\beta([a_1, b_1]) = [a_2, b_2]$ for $a_1, b_1 \in G_1$. Define a map $\phi : G_1 \times G_1 \to G_2 \curlywedge G_2$ by $\phi(a_1, b_1) = a_2 \curlywedge b_2$, where a_i, b_i are as above. To see that this is well defined, suppose that $\alpha(a_1 Z_1) = a_2 Z_2 = \bar{a_2} Z_2$ and $\alpha(b_1 Z_1) = b_2 Z_2 = \bar{b_2} Z_2$. Then we can write $\bar{a_2} = a_2 z$ and $\bar{b_2} = b_2 w$ for some $w, z \in Z_2$. By the definition of $G_2 \curlywedge G_2$ we have that $\bar{a_2} \curlywedge \bar{b_2} = a_2 z \curlywedge b_2 w = a_2 \curlywedge b_2$, hence ϕ is well defined.

Suppose that $a_1, b_1 \in G_1$ commute, and let $a_2, b_2 \in G_2$ be as above. By definition, $[a_2, b_2] = \beta([a_1, b_1]) = 1$, hence $a_2 \curlywedge b_2 = 1$. This, and the relations of $G_2 \curlywedge G_2$, ensure that ϕ is a $\tilde{\mathrm{B}}_0$-pairing. Thus ϕ induces a homomorphism $\gamma : G_1 \curlywedge G_1 \to G_2 \curlywedge G_2$ such that $\gamma(a_1 \curlywedge b_1) = a_2 \curlywedge b_2$ for all $a_1, b_1 \in G_1$. By symmetry there exists a homomorphism $\delta : G_2 \curlywedge G_2 \to G_1 \curlywedge G_1$ defined via α^{-1}. It is straightforward to see that δ is the inverse of γ, hence γ is an isomorphism.

Let $\kappa_1 : G_1 \curlywedge G_1 \to [G_1, G_1]$ and $\kappa_2 : G_2 \curlywedge G_2 \to [G_2, G_2]$ be the commutator maps. Since $\beta\kappa_1(a_1 \curlywedge b_1) = \beta([a_1, b_1]) = [a_2, b_2] = \kappa_2\gamma(a_1 \curlywedge b_1)$, we have the following commutative diagram with exact rows:

$$\begin{array}{ccccccccc} 0 & \longrightarrow & \tilde{\mathrm{B}}_0(G_1) & \longrightarrow & G_1 \curlywedge G_1 & \xrightarrow{\kappa_1} & [G_1, G_1] & \longrightarrow & 0\ . \\ & & \downarrow{\scriptstyle \tilde{\gamma}} & & \downarrow{\scriptstyle \gamma} & & \downarrow{\scriptstyle \beta} & & \\ 0 & \longrightarrow & \tilde{\mathrm{B}}_0(G_2) & \longrightarrow & G_2 \curlywedge G_2 & \xrightarrow{\kappa_2} & [G_2, G_2] & \longrightarrow & 0 \end{array}$$

Here $\tilde{\gamma}$ is the restriction of γ to $\tilde{\mathrm{B}}_0(G_1)$. Since β and γ are isomorphisms, so is $\tilde{\gamma}$. This concludes the proof.

References

[1] M. Artin and D. Mumford, Some elementary examples of unirational varieties which are not rational, *Proc. London. Math. Soc.* **25** (1972), 75–95.

[2] F. A. Bogomolov, The Brauer group of quotient spaces by linear group actions, *Izv. Akad. Nauk SSSR Ser. Mat.* **51** (1987), 485–516.

[3] F. Bogomolov and C. Böhning, Isoclinism and stable cohomology of wreath products, arXiv:1204.4747v1.

[4] J.-L. Colliot-Thélène and J.-J. Sansuc, The rationality problem for fields of invariants under linear algebraic groups (with special regards to the rationality problem), in: V. Mehta (ed.), *Proceedings of the International Colloquium on Algebraic groups and Homogeneous Spaces (Mumbai 2004)*, TIFR, Mumbai, Narosa Publishing House (2007), 113–186.

[5] P. Hall, The classification of prime-power groups, *J. Reine Angew. Math.* **182** (1940), 130–141.

[6] A. Hoshi, M. Kang and B. E. Kunyavskiĭ, Noether problem and unramified Brauer groups, ArXiv:1202.5812v1, 2012.

[7] B. E. Kunyavskiĭ, *The Bogomolov multiplier of finite simple groups*, Cohomological and geometric approaches to rationality problems, 209–217, Progr. Math., 282, Birkhäuser Boston, Inc., Boston, MA, 2010.

[8] C. Miller, The second homology of a group, *Proc. Amer. Math. Soc.* **3** (1952), 588–595.

[9] P. Moravec, Unramified groups of finite and infinite groups, *Amer. J. Math.*, to appear, arXiv:1203.3190v1.

[10] P. Moravec, Groups of order p^5 and their unramified Brauer groups, *J. Algebra*, to appear, arXiv:1203.3289v1.

[11] E. Noether, Gleichungen mit vorgeschriebener Gruppe, *Math. Ann.* **78** (1916), 221–229.

[12] I. R. Šafarevič, The Lüroth problem, *Proc. Steklov Inst. Math.* **183** (1991), 241–246.

[13] D. J. Saltman, Noether's problem over an algebraically closed field, *Invent. Math.* **77** (1984), 71–84.

[14] R. G. Swan, *Noether's problem in Galois theory*, in 'Emmy Noether in Bryn Mawr', Springer-Verlag, Berlin, 1983.

ARS MATHEMATICA CONTEMPORANEA

Also available at http://amc-journal.eu
ISSN 1855-3966 (printed edn.), ISSN 1855-3974 (electronic edn.)
ARS MATHEMATICA CONTEMPORANEA 7 (2014) 341–352

Linking Rings Structures and tetravalent semisymmetric graphs

Primož Potočnik

Faculty of Mathematics and Physics, University of Ljubljana
Jadranska 19, Ljubljana, Slovenia

IAM, University of Primorska, Muzejski trg 2, 6000 Koper, Slovenia

Stephen E. Wilson

Department of Mathematics and Statistics, Northern Arizona University
Box 5717, Flagstaff, AZ 86011, USA

Received 27 February 2012, accepted 27 October 2013, published online 7 August 2013

Abstract

In this paper, we introduce LR structures, a new and interesting form of symmetry in graphs. LR structures are motivated by the search for semisymmetric graphs of degree 4. We show that all semisymmetric graphs of girth and degree 4 can be constructed in a simple way from LR structures. We then show several ways in which LR structures can be constructed or found.

Keywords: Graph, automorphism group, symmetry, locally arc-transitive graph, semisymmetric graph, cycle structure, linking rings structure.

Math. Subj. Class.: 20B25, 05E18

1 Introduction

A regular graph Γ is *semisymmetric* provided that its symmetry group is transitive on edges but not on vertices. The search for semisymmetric graphs has an intense 40-year history, beginning with Harary and Dauber's paper [9]. This unpublished work was seen by Folkman, and motivated his paper [5], which gives the smallest such graph, on 20 vertices. The earliest known semisymmetric graph, due to Marion Gray in the 1930's, shown in early dittoed versions of Foster's Census, was rediscovered by Bouwer, described in [1] and generalized in [2]. Progress on aspects of semisymmetric graphs was made in papers published

E-mail addresses: primoz.potocnik@fmf.uni-lj.si (Primož Potočnik), stephen.wilson@nau.edu (Stephen E. Wilson)

since 1980 (see for example [4, 8, 10, 11, 12, 17, 18]). Recently, considerable attention was given to semisymmetric graphs of valence 3 [13, 14, 15], and a list of all such graphs with no more than 768 vertices was compiled in [3].

This paper continues work from [20], where the present authors began an investigation of tetravalent edge-transitive graphs, by considering those of girth at most 4. Such a graph is either *worthy* or *unworthy*, depending on whether the neighborhoods of all pairs of distinct vertices are distinct or not. Lemma 4.3 of [20] disposes of the unworthy case by showing that every unworthy tetravalent semisymmetric graph has order $4n$ for some integer n, and arises as the "subdivided double" of a dart-transitive tetravalent graph of order n. Note that the smallest semisymmetric graph, the Folkman graph on 20 vertices shown in Figure 1, is unworthy, and it can be obtained as a subdivided double of the complete graph K_5. Similarly, it was shown in [17, Theorem 5.2] that every semisymmetric graph on $4p$ vertices, for $p \geq 7$ a prime, is unworthy.

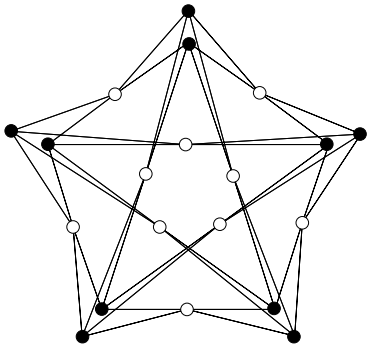

Figure 1: The Folkman graph

On the other hand, [20, Theorem 5.1(5, b)] shows that every worthy tetravalent semisymmetric graph of girth 4 and order $2n$ is isomorphic to a graph obtained, via the "partial line graph construction", from a certain kind of cycle decomposition of a vertex-transitive tetravalent graph of order n. A precise statement of this result can be found in Section 5.

The purpose of the present paper is to study worthy tetravalent semisymmetric graphs of girth 4, and the cycle decompositions from which they arise, in more detail.

2 Preliminaries

A standard notation for graphs is used throughout the paper: if Γ is a graph, then $V(\Gamma)$ is its vertex set. An edge in Γ is an unordered pair from $V(\Gamma)$ (so Γ is a *simple* graph), and the set of edges is $E(\Gamma)$. An ordered pair of adjacent vertices will be called a *dart* (or also, an *arc*). In this paper, all graphs are finite and connected. Bipartition sets in bipartite graphs are often referred to as colors, black and white, of the vertices.

A *symmetry* or *automorphism* of a graph Γ is a permutation of its vertices which preserves adjacency. The symmetries of Γ form a group, $\mathrm{Aut}(\Gamma)$, under composition. A graph is said to be vertex-, edge-, or dart-transitive if its automorphism group acts transitively on its vertices, edges, or darts, respectively. Dart-transitive graphs are also called *symmetric* or *arc-transitive*.

A graph Γ is *semisymmetric* provided that it is connected, regular, and $\mathrm{Aut}(\Gamma)$ is transitive on edges but not on vertices. It follows easily (see [5] for example) that such a graph Γ is bipartite, and that $\mathrm{Aut}(\Gamma)$ is transitive on each of the two color classes of vertices.

If for every vertex v of a regular graph Γ, the stabilizer $\mathrm{Aut}(\Gamma)_v$ acts transitively on the neighbors of v, then Γ is said to be *locally dart-transitive*. It is well known that a locally dart-transitive graph is edge-transitive (recall that all the graphs are assumed to be connected), and that it is either dart-transitive or semisymmetric (depending on whether $\mathrm{Aut}(\Gamma)$ is transitive on the vertices or not).

3 Cycle decompositions

Let Λ be a (connected) regular tetravalent graph and $\mathcal{C}$ a partition of $E(\Lambda)$ into cycles (that is, sets of edges which induce in Λ connected subgraphs of valence 2). We shall call such a pair $(\Lambda, \mathcal{C})$ a *cycle decomposition*. For the rest of this section, let $(\Lambda, \mathcal{C})$ denote a cycle decomposition.

Two edges of Λ will be called *opposite at vertex* v, if they are both incident with v and belong to the same element of $\mathcal{C}$. The *partial line graph* of a cycle decomposition $(\Lambda, \mathcal{C})$ is the graph $\mathbb{P}(\Lambda, \mathcal{C})$ whose vertices are edges of Λ, and two edges of Λ are adjacent in $\mathbb{P}(\Lambda, \mathcal{C})$ whenever they share a vertex in Λ and are not opposite at that vertex.

The left hand side of Figure 2 shows a tetravalent graph Λ and a cycle decomposition $\mathcal{C}$ with cycles indicated by a-a, b-b, etc; and the right hand side of Figure 2 shows the partial line graph of $(\Lambda, \mathcal{C})$.

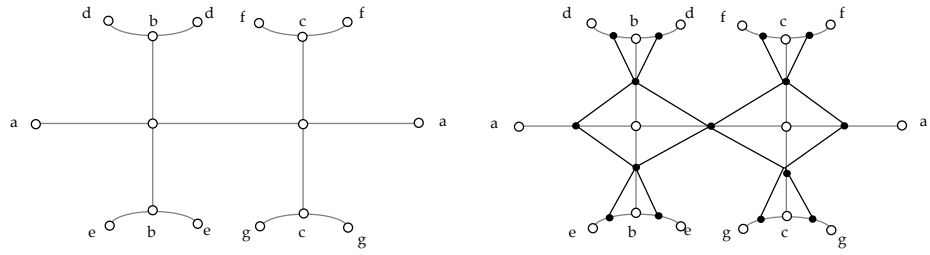

Figure 2: A cycle decomposition and its partial line graph

An *isomorphism* between two cycle decompositions $(\Lambda_1, \mathcal{C}_1)$ and $(\Lambda_2, \mathcal{C}_2)$ is an isomorphism f of Λ_1 onto Λ_2 for which $f(\mathcal{C}_1) = \mathcal{C}_2$. An automorphism is an isomorphism from a cycle decomposition to itself. The group of automorphisms of $(\Lambda, \mathcal{C})$ will be denoted by $\mathrm{Aut}(\Lambda, \mathcal{C})$.

A cycle decomposition $(\Lambda, \mathcal{C})$ is said to be *flexible* provided that for every vertex v and each edge e containing v, there is a symmetry in $\mathrm{Aut}(\Lambda, \mathcal{C})$ which fixes pointwise the cycle $D \in \mathcal{C}$ containing e and interchanges the other two neighbors of v. The edges joining v to those neighbors are in some other cycle C of $\mathcal{C}$, and the symmetry is called a *C-swapper at v*.

A cycle decomposition $(\Lambda, \mathcal{C})$ is called *bipartite* if $\mathcal{C}$ can be partitioned into two subsets $\mathcal{G}$ and $\mathcal{R}$ so that each vertex of Λ meets one cycle from $\mathcal{G}$ and one from $\mathcal{R}$. Especially in constructions, we will refer to the edges of the cycles in $\mathcal{G}$ and those in $\mathcal{R}$ as *green* and *red*,

respectively. The largest subgroup of $\mathrm{Aut}(\Lambda, \mathcal{C})$ preserving each of the sets $\mathcal{G}$ and $\mathcal{R}$ will be denoted by $\mathrm{Aut}^+(\Lambda, \mathcal{C})$, and we will think of it as the color-preserving group of $(\Lambda, \mathcal{C})$.

Note that in a bipartite cycle decomposition, an element of $\mathrm{Aut}(\Lambda, \mathcal{C})$ either preserves each of the sets $\mathcal{G}$ and $\mathcal{R}$ setwise, and is thus contained in $\mathrm{Aut}^+(\Lambda, \mathcal{C})$, or interchanges the sets $\mathcal{G}$ and $\mathcal{R}$. (In particular, in a bipartite flexible structure, swappers belong to $\mathrm{Aut}^+(\Lambda, \mathcal{C})$.) This shows that the index of $\mathrm{Aut}^+(\Lambda, \mathcal{C})$ in $\mathrm{Aut}(\Lambda, \mathcal{C})$ is at most 2. If this index is 2, then we say that $(\Lambda, \mathcal{C})$ is *self-dual*. Thus $(\Lambda, \mathcal{C})$ is self-dual if and only if there is $\sigma \in \mathrm{Aut}(\Lambda, \mathcal{C})$ such that $\mathcal{G}\sigma = \mathcal{R}$ and $\mathcal{R}\sigma = \mathcal{G}$.

We can now define the central notion of this paper:

4 LR Structures

Definition 4.1. A cycle decomposition $(\Lambda, \mathcal{C})$ is called a *linking ring structure* (or briefly, an *LR structure*) provided that it is bipartite, flexible and that $\mathrm{Aut}^+(\Lambda, \mathcal{C})$ acts transtively on $V(\Lambda)$.

If $(\Lambda, \mathcal{C})$ is an LR structure, then it follows from the definition that $G = \mathrm{Aut}^+(\Lambda, \mathcal{C})$ acts transitively on red darts, as well as on green darts, in such a way that the permutation group $G_v^{\Lambda(v)}$, induced by the vertex-stabiliser G_v on the neighbourhood $\Lambda(v)$, is intransitive and is in fact permutation isomorphic to the permutation group $\langle (1,2), (3,4) \rangle \leq S_4$ (we shall call the permutation group $\langle (1,2), (3,4) \rangle$ the *intransitive Klein* 4*-group*). Conversely, if a connected tetravalent graph Λ admits a vertex- but not edge-transitive group of automorphisms G such that $G_v^{\Lambda(v)}$ is permutation isomorphic to the intransitive Klein 4-group, then the two edge-orbits of G form the sets $\mathcal{G}$ and $\mathcal{R}$ of an LR structure $(\Lambda, \mathcal{C})$ for which $\mathrm{Aut}^+(\Lambda, \mathcal{C})$ contains G. This shows that, in the group-theoretical language, an LR structure could be equivalently defined as a transitive permutation group G admitting two self-paired orbitals A_1 and A_2 of degree 2 such that $G_v^{\Lambda(v)}$ is permutation isomorphic to the intransitive Klein 4-group.

Since $\mathrm{Aut}^+(\Lambda, \mathcal{C})$ acts transitively on $\mathcal{G}$ and on $\mathcal{R}$, it follows that all cycles in $\mathcal{G}$ must have the same length, say p, and all cycles in $\mathcal{R}$ must be of the same length q. We then say that the LR structure $(\Lambda, \mathcal{C})$ is of *type* $\{p, q\}$. For a self-dual structure, of course, $p = q$.

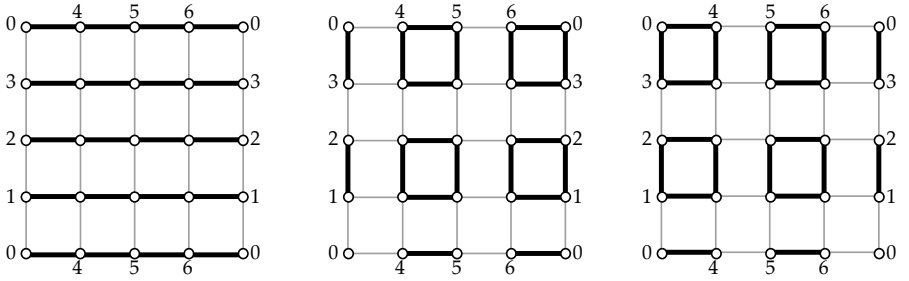

Figure 3: Three LR structures on the 4-dimensional cube Q_4, presented as a toroidal map $\{4, 4\}_{4,0}$. The labels indicate the identifications of vertices and edges.

Note that a tetravalent graph can admit more than one LR structure. For example, the 4-dimensional cube Q_4 (see Figure 3) has three distinct bi-colorings of edges, each of which

makes it into a self-dual LR structure of type $\{4,4\}$. The three structures are isomorphic.

This leads us to pose the following open question:

Question 1: Does there exist a graph admitting non-isomorphic LR structures?

5 Suitable LR Structures

Let us now describe the relationship between LR structures and tetravalent edge-transitive graphs. If $(\Lambda,\mathcal{C})$ is a cycle decomposition, then a cycle C in Λ is said to be *alternating* if no two consecutive edges of C belong to the same element of $\mathcal{C}$. In [20], a cycle decomposition $(\Lambda,\mathcal{C})$ was called *smooth*, provided that Λ contained no alternating 4-cycles, and no 3-cycles except possibly those contained in $\mathcal{C}$. Note that the latter condition on 3-cycles is automatically satisfied for an LR structure: if $(\Lambda,\mathcal{C})$ is an LR structure, and if bcd is a triangle in Λ, but not in $\mathcal{C}$, then two of the three edges are the same color; say bc and cd are red, while bd is green. Then a swapper at b which fixes the red cycle containing bcd would interchange the two green neighbors at b. But one of these is d, which is left fixed by this symmetry. This is a contradiction, and so no such triangle can exist.

Definition 5.1. An LR structure which is not self-dual and contains no alternating 4-cycles is called *suitable*.

It is not difficult to see that a cycle decomposition $(\Lambda,\mathcal{C})$ is a suitable LR structure if and only if it satisfies the conditions stated in [20, Theorem 5.1(5, b)]. This theorem, combined with Lemma 6.3, which will be proved in the following section, implies the following correspondence, which explains the relevance of LR structures to the study of tetravalent edge-transitive graphs.

Theorem 5.2. *The partial line graph construction $\mathbb{P}$ induces a bijective correspondence between the set of LR structures and the set of worthy bipartite locally dart-transitive tetravalent graphs of girth 4. If $(\Lambda,\mathcal{C})$ is an LR structure, then $\mathbb{P}(\Lambda,\mathcal{C})$ is semisymmetric if and only if $(\Lambda,\mathcal{C})$ is suitable; and is arc-transitive otherwise. If $(\Lambda,\mathcal{C})$ contains an alternating 4-cycles, then $\mathbb{P}(\Lambda,\mathcal{C})$ is a skeleton of an arc-transitive map of type $\{4,4\}$ on the torus.*

Remark. If a graph Λ has a cycle decomposition $\mathcal{C}$ for which $(\Lambda,\mathcal{C})$ is a suitable LR structure, it is conceivable that it might allow a different cycle decomposition $\mathcal{C}'$ for which $(\Lambda,\mathcal{C}')$ is an LR structure. We know of no such example, and we conjecture that none exist. Proving that the conjecture holds would allow us to simplify our notation, and talk about an *LR graph* Λ. We will discuss this conjecture further in our final section.

Every new LR structure gives a new edge-transitive graph, and so we are interested in finding and creating LR structures. The aim of this paper is to provide constructions of LR structures (and thus of bipartite tetravalent edge-transitive graphs), which show how varied the LR structures can be.

6 Basic constructions

We begin our investigation of LR structures by presenting some basic contructions.

6.1 LR Structures on the wreath graphs

The wreath graph $W(n,2)$ is defined to be the graph on $2n$ vertices u_i, v_i, for $i \in \mathbb{Z}_n$, with all edges from vertices of subscript i to those of subscript $i+1$. Alternatively, $W(n,2)$

can be defined as the lexicographic product of the cycle C_n with the edgeless graph on two vertices.

Construction 6.1. If n is even, let Λ be the wreath graph $W(n,2)$ and let $\mathcal{C}$ be the set of 4-cycles of $W(n,2)$ of the form $[u_i, u_{i+1}, v_i, v_{i+1}]$. Color such a 4-cycle red if i is even and green if i is odd. Then $(\Lambda, \mathcal{C})$ is clearly a self-dual LR-structure of type $\{4,4\}$.

The partial line graphs of the LR-structures on the wreath graphs defined above are thus arc-transitive tetravalent graphs, which may also be obtained as 2-fold covers over the wreath graphs. These graphs have appeared in the literature before, for example in [6, 7].

6.2 Toroidal LR Structures

Consider the LR structure on the cube Q_4 depicted in the left-hand side of Figure 3. This structure can be generalized to other maps on the torus:

Definition 6.2. Let $\mathcal{M}$ be a map of type $\{4,4\}$ on the torus. Then $\mathcal{M}$ arises as a quotient $\{4,4\}_T$ of the tessellation $\{4,4\}$ by a group T of translations. Color edges of the tessellation belonging to one parallel class green, the other edges red. Since translations preserve these colors, we can consider the edges of $\mathcal{M}$ colored in the same way. If the group T is normalized by horizontal and vertical reflections, we will say that T is *reflective*. In this case, then those reflections act on $\mathcal{M}$ as well, giving the structure its swappers. In any map of type $\{4,4\}$ on the torus, the group of translations is transitive on vertices, and so if T is reflective, the resulting graph $\{4,4\}_T$ is an LR structure, and we will call it a *toroidal* LR structure.

Note that if $(\Lambda, \mathcal{C})$ is a toroidal LR structure, then $\mathbb{P}(\Lambda, \mathcal{C})$ is a bipartite edge-transitive skeleton of a map of type $\{4,4\}$ on the torus.

Remark: The possibilities for the group T of translations satisfying the requirement that T is normalized by all horizontal and vertical reflections are exactly these two:

(I) T is generated by $(b,0)$ and $(0,c)$ for some b and c both at least 3. The resulting graph has bc vertices and is of type $\{b,c\}$. We will call this structure $\{4,4\}_{[b,c]}$.

(II) T is generated by (b,c) and $(b,-c)$ for some b and c both at least 2. The resulting graph has $2bc$ vertices and is of type $\{2b,2c\}$. We will call this structure $\{4,4\}_{<b,c>}$.

These two types are shown in Figure 4; on the left is $\{4,4\}_{[4,3]}$, and on the right is $\{4,4\}_{<3,2>}$.

Observe that every toroidal LR structure, as defined above, has alternating 4-cycles. Surprisingly, the converse holds as well.

Lemma 6.3. *An LR structure which has an alternating 4-cycle is toroidal and arises as in Definition 6.2.*

Proof. Suppose that a,b,c,d is an alternating 4-cycle in which $\{a,b\}$ and $\{c,d\}$ are the green edges, $\{b,c\}$ and $\{d,a\}$ the red. Then a green swapper at a fixes a and d but not b, and so sends $abcd$ to a different alternating 4-cycle containing the red edge $\{d,a\}$. Thus every red edge belongs to at least two alternating 4-cycles, and similarly, so does every green. Now if any edge belongs to more than two alternating 4-cycles, it is not hard to show that the structure must be the toroidal structure for the map $\{4,4\}_{2,2}$ (its underlying

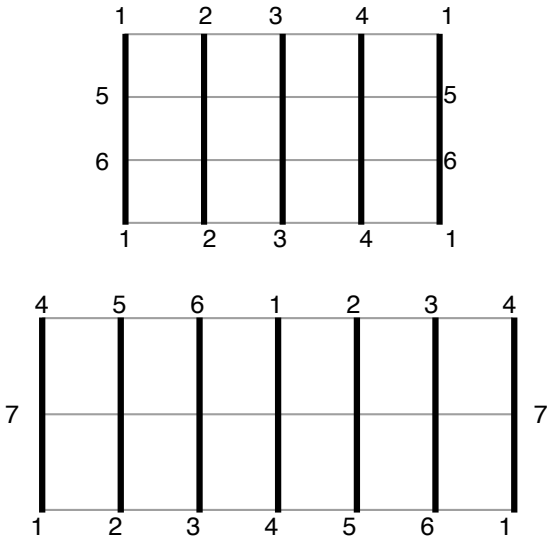

Figure 4: Two kinds of toroidal LR structures

graph is $K_{4,4}$). If not, then every edge belongs to exactly two alternating 4-cycles. Using these cycles as faces constructs a map on a surface. The map has quadrangular faces, and four meet at every vertex and so the Euler characteristic of the surface is 0. The surface is thus the torus or the Klein bottle. The results of the paper [21] show that no map on the Klein bottle can have swappers except for some whose skeleton is not a simple graph, and therefore the map and structure must be toroidal. □

This lemma, combined with [20, Theorem 5.1(5, b)], proves Theorem 5.2

6.3 Barrels

In this section, we introduce our first families of suitable LR structures. The *barrels* $Br(k, n; r)$ and the *mutant barrels* $MBr(k, n; r)$ are, of all known LR structures, the simplest to describe, the easiest to visualize and the most common to occur.

The structure $Br(k, n; r)$ is defined for k even, $k \geq 4$, $n \geq 5$, and $r^2 = \pm 1 \bmod n$ but not $r = \pm 1 \bmod n$. It has vertices $\mathbb{Z}_k \times \mathbb{Z}_n$, with (i, j) red-adjacent to $(i \pm 1, j)$ and green-adjacent to $(i, j \pm r^i)$. We may and usually do assume that $0 \leq r < \frac{n}{2}$.

We should mention that the underlying graphs of the LR structures $Br(k, n; r)$ have appeared in different contexts under different names before, most recently in [16], where the class of $\mathcal{Y}$ graphs include the graph $Br(k, n; r)$ as $\mathcal{Y}(k, n, r, 0)$.

Figure 5 shows part of such a graph having $n = 5$ and $r = 2$, with red edges shown thin, green edges shown bold.

$Br(k, n; r)$, has color-preserving symmetries $(i, j) \mapsto (i, j+1)$ and $(i, j) \mapsto (i+1, rj)$, which show it to be vertex transitive. In the stabilizer of $(0, 0)$ are symmetries $(i, j) \mapsto (-i, j)$ and $(i, j) \mapsto (i, -j)$ which act as swappers there. Thus, $Br(k, n; r)$ is an LR

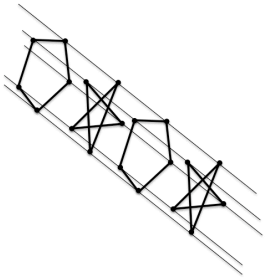

Figure 5: part of $Br(k, 5; 2)$

structure.

A related graph is $MBr(k, n; r)$, which is defined if both k and n are even, $k \geq 2$, $n \geq 6$, and $r^2 = \pm 1 \bmod n$ but not $r = \pm 1 \bmod n$. It has vertices $\mathbb{Z}_k \times \mathbb{Z}_n$, with (i, j) red-adjacent to $(i + 1, j)$ for $0 \leq i < k - 1$, $(k - 1, j)$ red-adjacent to $(0, j + n/2)$ and (i, j) green-adjacent to $(i, j \pm r^i)$ for all i.

$MBr(k, n; r)$ has symmetries that are swappers with definitions similar to those for $Br(k, n; r)$. Thus, every member of these two families is an LR structure.

For most parameters k, n and r, the LR structures $Br(k, n; r)$ and $MBr(k, n; r)$ are suitable. Each one has kn vertices and is of type $\{k, n\}$, $\{2k, n\}$, respectively.

We are now ready to determine which barrels give rise to suitable LR-structures.

Theorem 6.4. *Each of the LR structures $Br(k, n; r), MBr(k, n; r)$ has kn vertices and is of type $\{k, n\}$, $\{2k, n\}$, respectively.*

The LR structures $Br(k, n; r)$ are suitable for all admissible parameters: $k \geq 4$ even, $n \geq 5$, and $2 \leq r < \frac{n}{2}$, $r^2 \equiv \pm 1 \pmod n$.

The LR structure $MBr(k, n; r)$ is suitable for all admissible parameters: $k \geq 4$ even, $n \geq 6$ even, $2 \leq r < \frac{n}{2}$, $r^2 \equiv \pm 1 \pmod n$, with the exceptions of $MBr(k, 2k; k - 1)$ for k even, $k \geq 4$, which is self-dual; and $MBr(2, n; \frac{n}{2} \pm 1)$, which has alternating 4-cycles.

Proof. The claim about the type of $Br(k, n; r)$ and $MBr(k, n; r)$ follows immediately from the definition of the two structures. It is also clear that no member of either family has an alternating 4-cycle, except in the case of $MBr(2, n; \frac{n}{2} \pm 1)$; here, an alternating 4-cycle is $(0, 0) \sim (0, 1) \sim (1, 1 + \frac{n}{2}) \sim (1, 1 + \frac{n}{2} + r) = (1, 0) \sim (0, 0)$.

Number the red cycles $1, 2, \ldots$ in the order in which they appear around a fixed green cycle, and do the same for green cycles. In $Br(k, n; r)$, every green cycle appears once around each red cycle and vice versa; in $MBr(k, n; r)$, every green cycle appears twice around each red cycle and vice versa. Then in every red cycle, the green cycles appear in the same order, $1, 2, \ldots$, while around alternating green cycles, they appear in the orders $1, 2, 3 \ldots$ and $1, 1 + r, 1 + 2r, \ldots$. In most cases, these are different orders, and so no symmetry can switch red with green. The only way that these can be the same order is if:

(1) each number appears twice, so the graph is the underlying graph of a mutant barrel LR structure,

(2) the cycles have the same length, so that $n = 2k$,

(3) $r + 1 \equiv 2 \bmod k$, so that $r = k + 1$

It remains to show that $MBr(k, 2k; k-1)$ is indeed self-dual. To do that, we observe that it is isomorphic to the following LR structure: vertices are elements of $\mathbb{Z}_k \times \mathbb{Z}_k \times \mathbb{Z}_2$; red edges are of the form:

- $(i, j, d) \sim (i + 1, j, d), \quad 0 \leq i < k - 1$
- $(k - 1, j, d) \sim (0, j, d + 1)$,

while green edges are of the form:

- $(i, j, d) \sim (i, j + 1, d + i), \quad 0 \leq j < k - 1$
- $(i, k - 1, d) \sim (i, 0, d + 1 + i)$,

The function $\varphi : (i, j, r) \mapsto (i, j + rk)$ is an isomorphism from this structure to the structure $MBr(k, 2k; k-1)$. In this form, it is easy to check that $(i, j, r) \mapsto (j, i, r + ij)$ is a color-reversing symmetry of the structure. Thus, $MBr(k, 2k; k-1)$ is self-dual and so not suitable. □

We conclude this section by mentioning that the smallest suitable barrel $Br(4, 5; 2)$ gives rise to the the semisymmetric graph $\mathbb{P}(Br(4, 5; 2))$, which has 40 vertices, 80 edges, and the automorphism group of which has order 80. This appears to be the smallest automorphism group of any semisymmetric graph. There is a second semisymmetric graph of the same size whose group also has size 80. This graph is $\mathbb{P}(MBr(2, 10; 3))$.

7 Quotients and covers

Quotients and covers of graphs have become a standard tool in studying vertex-transitive graphs, and can be used almost without any change in the setting of LR structures as well. Here we only briefly summarize the basic ideas of the covering techniques.

Let Λ be a graph, and let $\mathcal{B}$ be a partition of the vertex-set $V(\Lambda)$. Then the *quotient graph* $\Lambda_{\mathcal{B}}$ is the graph with $\mathcal{B}$ as its vertex-set and with two elements $B_1, B_2 \in \mathcal{B}$ adjacent in $\Lambda_{\mathcal{B}}$ whenever there is an edge in Λ between some $v_1 \in B_1$ and some $v_2 \in B_2$. If the partition $\mathcal{B}$ is invariant under some $G \leq \mathrm{Aut}(\Lambda)$, then G acts in a natural way on $\Lambda_{\mathcal{B}}$ by automorphisms. If there are no edges within the elements of $\mathcal{B}$ and if the graph induced by two adjacent elements of $\mathcal{B}$ is a perfect matching, then Λ is called a *cover* of $\Lambda_{\mathcal{B}}$.

An important special case of quotients and covers arises in the following setting. Let G be a vertex-transitive group of automorphisms of a connected graph Λ, and let N be a normal subgroup of G acting semiregularly on $V(\Lambda)$ (i.e. $N_v = 1$ for every $v \in V(\Lambda)$). Then the orbits of N form a G-invariant partition of $V(\Lambda)$. The corresponding quotient graph is then called a *G-normal quotient* of Λ by N and denoted by Λ_N. If in addition Λ is a cover of Λ_N, then it is called a *regular cover*. In this case, the action of G on Λ_N induces a faithful vertex-transitive action of G/N on Λ_N, and we say that $G \leq \mathrm{Aut}(\Lambda)$ is a *lift* of $G/N \leq \mathrm{Aut}(\Lambda_N)$.

All these notions extend naturally to LR structures. In particular, if $G \leq \mathrm{Aut}(\Lambda, \mathcal{C})$ and $\mathcal{B}$ is a G-invariant partition of $V(\Lambda)$ such that Λ is a cover of $\Lambda_{\mathcal{B}}$, then one can define an LR structure $(\Lambda_{\mathcal{B}}, \mathcal{C}_{\mathcal{B}})$ in an obvious way. For example, take any of the three LR structures on Q_4 depicted in Figure 3, and let $\mathcal{B}$ be a partition of $V(Q_4)$ into pairs of antipodal

vertices in Q_4. The corresponding quotient graph $(Q_4)_{\mathcal{B}}$ is isomorphic to $K_{4,4}$, and Q_4 is a cover of the quotient. In fact, letting N be the group generated by the automorphism of Q_4 interchanging the pairs of antipodal vertices, we see that $(Q_4)_{\mathcal{B}} = (Q_4)_N$ is a normal quotient of Q_4. Clearly, $\mathcal{B}$ is invariant under $\mathrm{Aut}(Q_4)$, and so the three (isomorphic) LR structures on Q_4 induce three isomorphic LR structures on $K_{4,4}$.

7.1 Loose and antipodal attachments

Consider two cycles, C_1 and C_2, of an LR structure $(\Lambda, \mathcal{C})$, one green and one red, which intersect in a common vertex v. If v is the only vertex in their intersection, then the vertex-transitivity of the automorphism group implies that any two intersecting cycles meet in exactly one vertex. Following the language of [19], we will say in this case that the LR structure is *loosely attached*.

On the other hand, if there is another vertex u in the intersectection of C_1 and C_2, then the existence of swappers at v implies that u is the vertex which is antipodal to v on C_1 and C_2 (in particular, C_1 and C_2 are of even length). If this is the case, then by vertex-transitivity, any two intersecting cycles intesect in exactly two vertices, located antipodally on the intersecting cycles. LR structures of this type will be called *antipodally attached.*

Of course, if $(\Lambda, \mathcal{C})$ is an antipodally attached LR structure, then the permutation swapping the two vertices in each antipodal pair is a central involution in $\mathrm{Aut}(\Lambda, \mathcal{C})$, and thus generates a normal subgroup $N \leq \mathrm{Aut}(\Lambda, \mathcal{C})$. Unless the type of $(\Lambda, \mathcal{C})$ is $\{4, q\}$ or $\{p, 4\}$, identifying pairs of antipodal vertices projects $(\Lambda, \mathcal{C})$ onto a loosely attached LR structure $(\Lambda_N, \mathcal{C}_N)$ and the projection is a regular covering projection.

We already have examples of both kinds of attachments and the corresponding projections. Each toroidal LR structure $\{4, 4\}_{<b,c>}$ is antipodally attached, and the projection sends it onto $\{4, 4\}_{[b,c]}$ (if b and c are both at least 3). Each $MBr(2k, 2n; r)$ is antipodally attached, and the projection sends it onto $Br(k, n; r)$ (if k and n are both at least 3).

If $(\Lambda, \mathcal{C})$ is an antipodally attached LR structure of type $\{4, 4\}$, then it is easy to see that Λ is a wreath graph with $\mathcal{C}$ the decomposition presented in Construction 6.1.

Antipodally attached LR structures of type $\{4, q\}$ for some $q > 4$ will be studied in a future paper, where we show that such a structure arises from a certain cycle decomposition, called a "cycle structure", in a smaller tetravalent dart-transitive graph, thus allowing a reduction to smaller graphs.

The above discussion is summarized in the following theorem.

Theorem 7.1. *Let $(\Lambda, \mathcal{C})$ be an antipodally attached LR structure of type $\{p, q\}$. If $p = q = 4$, then $(\Lambda, \mathcal{C})$ is the type $\{4, 4\}$ LR structure on a wreath graph $W(n, 2)$ described in Construction 6.1. If $p, q \geq 6$, then $(\Lambda, \mathcal{C})$ arises as a 2-fold cover of a loosely attached LR-structure.*

Question 2: For which loosely attached LR structures does an antipodally attached cover exist?

Question 3: How is such a cover constructed?

Question 4: If $(\Lambda, \mathcal{C})$ is suitable and antipodally attached, when is the factor structure suitable?

8 The Big question

In Section 5, we conjectured that a suitable LR structure is unique on its graph. We believe that a stronger conjecture holds:

Conjecture 8.1. *If* $(\Lambda, \mathcal{C})$ *is an LR structure for which* $\mathrm{Aut}^+(\Lambda, \mathcal{C})$ *is a proper subgroup of* $\mathrm{Aut}(\Lambda)$*, then it is self-dual.*

Certainly, if $\mathrm{Aut}^+(\Lambda, \mathcal{C})$ is a proper subgroup of $\mathrm{Aut}(\Lambda, \mathcal{C})$, then $(\Lambda, \mathcal{C})$ is self-dual. So we may suppose that $\mathrm{Aut}(\Lambda)$ contains some σ which sends some red edges to red edges and some red edges to green edges. The conjecture would imply that $(\Lambda, \mathcal{C})$ is self-dual. While that conjecture is still open, we can and will prove that such an LR structure must be of a self-dual type.

Theorem 8.2. *If* $(\Lambda, \mathcal{C})$ *is an LR structure of type* $\{p, q\}$ *and* $\mathrm{Aut}(\Lambda)$ *contains some* σ *which does not preserve* $\mathcal{C}$*, then* $p = q$*.*

Proof. We will actually prove that under the hypothesis, some symmetry must send some red cycle to a green cycle. Suppose not. Let m be maximal such that some σ in $\mathrm{Aut}(\Lambda)$ sends some m consecutive edges of a red cycle to green edges. Then m must be less than both p and q. Suppose that $u_0, u_1, \ldots, u_{m-1}, u_m, u_{m+1}, \ldots$ are consecutive vertices on some red cycle, $v_0, v_1, \ldots, v_{m-1}, v_m, v_{m+1}, \ldots$ are consecutive vertices on some green cycle, and that for $i = 0, 1, 2 \ldots, m, u_i\sigma = v_i$. Suppose that a, b are the green neighbors of u_m, that c, d are the red neighbors of v_m. Finally, let μ be a green swapper at u_m and τ be a red swapper at v_m, as shown in Figure 6.

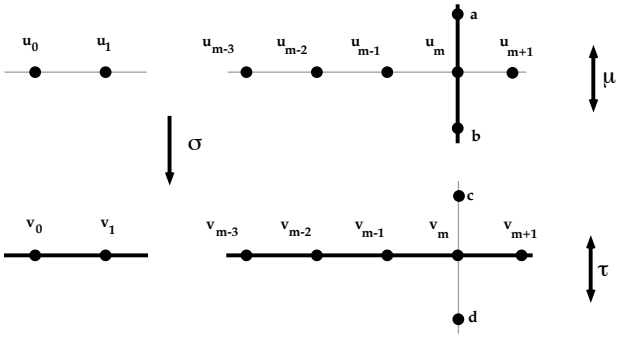

Figure 6: A color-mixing symmetry σ

Because m is maximal, we know that $u_{m+1}\sigma \neq v_{m+1}$. Assume, without loss of generality, that $u_{m+1}\sigma = c, a\sigma = v_{m+1}, b\sigma = d$. Consider $\sigma' = \sigma\tau\sigma^{-1}\mu\sigma$. Then for $i = 0, 1, 2, \ldots, m, \mu$ fixes u_i and τ fixes v_i and so $u_i\sigma' = v_i$. And $u_{m+1}\sigma' = u_{m+1}\sigma\tau\sigma^{-1}\mu\sigma = c\tau\sigma^{-1}\mu\sigma = d\sigma^{-1}\mu\sigma = b\mu\sigma = a\sigma = v_{m+1}$, contradicting the maximality of m. Thus $p = q$. □

The techniques of this proof will extend to prove the existence of a symmetry which sends one red cycle and all of its green neighbors to a green cycle and all of its red neighbors, but we cannot see how to push the technique any farther.

In future papers, we will show both algebraic and combinatorial constructions for LR structures.

References

[1] I. Z. Bouwer, An edge but not vertex transitive cubic graph, *Bull. Can. Math. Soc.* **11** (1968), 533–535.

[2] I. Z. Bouwer, On edge but not vertex transitive regular graphs, *J. Combin. Theory, Ser. B* **12** (1972), 32–40.

[3] M. D. E. Conder, A. Malnič, D. Marušič, and P. Potočnik, A census of semisymmetric cubic graphs on up to 768 vertices, *J. Algebraic Combin.* **23** (2006), 255–294.

[4] S. F. Du, F. R. Wang, and L. Zhang, An infinite family of semisymmetric graphs constructed from affine geometries, *European J. Combin.* **24** (2003), 897–902.

[5] J. Folkman, Regular line-symmetric graphs, *J. Combin. Theory* **3** (1967), 215–232.

[6] A. Gardiner and C. Praeger, On 4-valent symmetric graphs, *European J. Combin.* **15** (1994), 375–381.

[7] A. Gardiner and C. Praeger, A characterization of certain families of 4-valent symmetric graphs, *European J. Combin.* **15** (1994), 383–397.

[8] D. Goldschmidt, Automorphisms of trivalent graphs, *Ann. Math.* **111** (1980), 377–406.

[9] F. Harary and E. Dauber, Line-symmetric but not point-symmetric graphs, unpublished and apparently irrecoverable.

[10] M. E. Iofinova and A. A. Ivanov, Biprimitive cubic graphs, Investigations in Algebraic Theory of Combinatorial Objects, (Proceedings of the seminar, Institute for System Studies, Moscow, 1985) Kluwer Academic Publishers, London, 1994, 459–472.

[11] A. V. Ivanov, On edge but not vertex transitive regular graphs, *Ann. Discrete Math.* **34** (1987), 273–286.

[12] F. Lazebnik and R. Viglione, An infinite series of regular edge- but not vertex-transitive graphs, *J. Graph Theory* **41** (2002), 249–258.

[13] Z. Lu and M.Y. Xu, Cubic semisymmetric graphs constructed from Cayley graphs of degree 4, *Graph Theory Notes N. Y.* **44** (2003), 44–51.

[14] A. Malnič, D. Marušič, and C.Q. Wang, Cubic edge-transitive graphs of order $2p^3$, *Discrete Math.* **274** (2004), 187–198.

[15] A. Malnič, D. Marušič, P. Potočnik, and C.Q. Wang, An infinite family of cubic edge- but not vertex-transitive graphs, *Discrete Math.* **280** (2004), 133–148.

[16] D. Marušič and P. Šparl, On Quartic Half-arc-transitive Metacirculants, *J. Alg. Combin.* **28** (2008), 365–395.

[17] D. Marušič and P. Potočnik, Semisymmetry of generalized Folkman graphs, *European J. Combin.* **22** (2001), 333–349.

[18] D. Marušič and P. Potočnik, Bridging semisymmetric and half-arc-transitive actions on graphs, *European J. Combin.* **23** (2002), 719–732. *J. Graph Theory*, (2000).

[19] D. Marušič and C. Praeger, Tetravalent Graphs Admitting Half-Transitive Group Actions: Alternating Cycles, *J. Comb. Theory, Ser. B* **75** (1995), 188-205.

[20] P. Potočnik and S. Wilson, Tetravalent edge-transitive graphs of girth at most 4, *J. Comb. Theory, Ser. B* **97** (2007), 217–236.

[21] S. Wilson, Uniform maps on the Klein bottle, *J. for Geom. and Graphics* **10** (2006), 161–171.

ARS MATHEMATICA CONTEMPORANEA

Also available at http://amc-journal.eu
ISSN 1855-3966 (printed edn.), ISSN 1855-3974 (electronic edn.)
ARS MATHEMATICA CONTEMPORANEA 7 (2014) 353–359

A simple method of computing the catch time

Nancy E. Clarke *
Department of Mathematics and Statistics, Acadia University
Wolfville, NS, Canada B4P 2R6

Stephen Finbow *
Department of Mathematics, Statistics and Computer Science
St. Francis Xavier University
P.O. Box 5000, Antigonish, NS, Canada B2G 5W3

Gary MacGillivray *
Department of Mathematics and Statistics, University of Victoria
P.O. Box 3060 STN CSC, Victoria, BC, Canada V8W 3R4

Received 17 February 2012, accepted 9 May 2013, published online 6 September 2013

Abstract

We describe a simple method for computing the maximum length of the game cop and robber, assuming optimal play for both sides.

Keywords: Pursuit game, Cops and Robber, catch time.

Math. Subj. Class.: 05C57, 91A43

1 Introduction

The perfect information pursuit game "Cop and Robber" was introduced independently by Quilliot [13] in 1978, and Nowakowski and Winkler in 1983 [12]. It is played on a graph by two sides called *the cop* and *the robber*. The cop begins the game by choosing a vertex to occupy. The robber then chooses a vertex and the two sides move alternately, with the cop moving first. A move for the cop consists of either traversing an edge to a neighbouring vertex, or passing on his turn and remaining at the same vertex. A move for the robber is defined analogously. The cop wins if he *catches* the robber by occupying the same vertex as the robber after a finite number of moves. Otherwise the robber wins. The graphs on

*Research supported by NSERC.
E-mail addresses: nancy.clarke@acadiau.ca (Nancy E. Clarke), sfinbow@stfx.ca (Stephen Finbow), gmacgill@math.uvic.ca (Gary MacGillivray)

which the cop has a winning strategy are called *cop-win*, or *dismantlable*. The book by Bonato and Nowakowski [3] is a wonderful introduction to this game and its variants.

Let G be a cop-win graph. We define the *catch time of* G, first introduced in [2], denoted $catchtime(G)$, to be the minimum number of cop moves needed to be guaranteed to catch the robber, where the minimum is taken over all possible strategies on the assumption of optimal play by both sides. Passes count as moves. A variety of results imply ways to compute $catchtime(G)$, and discover the associated optimal strategies, in cubic time using some auxiliary structure [1, 8, 11, 12]. In this paper we describe a method for determining the catch time using only local information about neighbourhoods. It leads to a simple algorithm which is easy to carry out with pencil and paper if a drawing of the graph is available, and which can be implemented to run in cubic time.

2 Cop-win orderings and an associated strategy

There are at least three different characterizations of finite cop-win graphs [8, 12, 13] (also see [7, 10, 11]). The one that is of primary interest here is due to Nowakowski and Winkler, and Quilliot, independently.

Theorem 2.1. [12, 13] *Let G be a finite graph. Then G is cop-win if and only if there exists an enumeration $v_1, v_2, \ldots, v_n$ of the vertices of G such that for $i = 1, 2, \ldots, n-1$ there exists $j_i > i$ such that $(N[v_i] \cap \{v_i, v_{i+1}, \ldots, v_n\}) \subseteq N[v_{j_i}]$.*

The notation $N[x]$ that appears in the above theorem and elsewhere denotes the *closed neighbourhood of* x, defined to be the set containing x and all vertices adjacent to x.

The enumeration of the vertices of G in Theorem 2.1 has come to be known as a *cop-win ordering* or *dismantling ordering* of G. A vertex $x \in V(G)$ is called a *corner* if there exists $y \in V(G) - \{x\}$ such that $N[y] \supseteq N[x]$, or if $V(G) = \{x\}$. When such a vertex y exists, we say that it *covers* x. Cop-win orderings are constructed by iteratively deleting corners from the graph (also, see [5, 6]). We will make use of the following propositions which are key to the proof of Theorem 2.1 and the associated strategy. In Section 4 we will show how our results can be viewed as a generalization of this theorem. The methods of proof we use are essentially those of Nowakowski and Winkler, and Clarke [7, 9, 10, 12].

Proposition 2.2. [12, 13] *Let x be a corner of the graph G. Then G is cop-win if and only if $G - x$ is cop-win.*

By *optimal play* we mean that the cop seeks to catch the robber as quickly as possible, and the robber seeks to evade capture for as long as possible. Various aspects of optimal play are considered by Boyer *et al.* [4]. They show that in some cases of optimal play it is necessary for the cop to revisit a vertex, and in some cases it is necessary for the distance between the cop and robber to increase at some time.

Proposition 2.3. [12, 13] *If G is cop-win then, assuming optimal play, just before the robber's last move, the robber is on a corner of G and the cop is on a vertex that covers it. The game ends on the cop's next move.*

We now give a description of the cop's strategy that arises from the proof of Theorem 2.1. The following is applied recursively for $i = 1, 2, \ldots, n-1$. The vertex v_i is a corner of G_i, the subgraph of G induced by $\{v_i, v_{i+1}, \ldots, v_n\}$. (Note that $G_1 = G$.) While the robber plays the game on G_i, the cop plays as if it were on $G_{i+1} = G_i - v_i$, that is, if

the robber moves to v_i the cop plays his winning strategy for G_{i+1} as if the robber were on a particular vertex y that covers v_i. By Proposition 2.2, the cop has a winning strategy on G_{i+1}. Thus, at some point either the cop and robber occupy the same vertex, or the cop is on y and the robber is on v_i. In the former case the game on G_i is also over, and in the latter case it is over after one more cop move. It can be proved by induction that this strategy leads to the bound $catchtime(G) \leq |V| - 1$. Essentially the same argument is used to prove Theorem 3.3. The strategy can be formulated using retractions [7, 10]. We do the same for our results in Section 4.

3 Finding the catch time

Cop-win orderings are constructed by deleting corners from the graph one at a time. The key to the method described below for finding the catch time is deleting many corners simultaneously. Since it is possible for every vertex of a graph (cop-win or not) to be a corner – informally, for any graph G replace each vertex by a copy of K_2 and add all possible edges between copies of K_2 that replaced adjacent vertices of G – it is necessary to have a means of selecting which subset of the corners to delete.

Let G be a graph. Define an equivalence relation Θ_G on V by $(u, w) \in \Theta_G$ if and only if $N[u] = N[w]$. Note that the subgraph of G induced by each equivalence class is complete, and either there are no edges joining vertices in different equivalence classes, or all possible edges joining them are present. Let $G \,/\, \Theta_G$ be the graph whose vertices are the equivalence classes $\{[x] : x \in V\}$ of Θ_G, with $[x]$ adjacent to $[y]$, where $y \notin [x]$, if and only if $xy \in E(G)$ (that is, every vertex in $[x]$ is adjacent to every vertex in $[y]$). Equivalently, $G \,/\, \Theta_G$ is the subgraph of G induced by selecting one vertex from each equivalence class of Θ_G. By construction, no two vertices of $G \,/\, \Theta_G$ have the same neighbourhood. Thus, if $[y]$ covers $[x]$ in $G \,/\, \Theta_G$, the neighbourhood of $[y]$ properly contains the neighbourhood of $[x]$. Hence, if G is not complete, every vertex x belonging to a corner of $G \,/\, \Theta_G$ is covered in G by a vertex y such that $N_G[y] \supset N_G[x]$. In particular, for every such x there exists such a y for which $[y]$ is not a corner of $G \,/\, \Theta_G$. The main purpose of introducing the equivalence relation Θ_G is to assure that "twins", that is, vertices with identical neighbourhoods, are treated in exactly the same way.

Proposition 3.1. *Let G be a graph which is not complete and $X \subseteq V$ be the set of vertices belonging to corners of $G \,/\, \Theta_G$. Then G is cop-win if and only of $G - X$ is cop-win.*

Proof. Let $X = \{x_1, x_2, \ldots, x_k\}$. Since G is not complete, X is a proper subset of V. Since each vertex in X is covered by a vertex in the non-empty set in $V - X$, we have, by Proposition 2.2, that G is cop-win if and only if $G - x_1$ is cop-win if and only if $G - \{x_1, x_2\}$ is cop-win, and so on until, finally, if and only if $G - X$ is cop-win. □

Let G be a cop-win graph. By Proposition 3.1 we can define an ordered partition $X_1, X_2, \ldots, X_k$ of V by setting $G_i = G - \cup_{t=1}^{i-1} X_t$ (so that $G_1 = G$), and X_i to be the set of corners of $G_i \,/\, \Theta_{G_i}$. Note that the subgraph of G induced by the *top layer* X_k is necessarily a complete graph. We call $X_1, X_2, \ldots, X_k$ the *cop-win partition of* G and, for $i = 1, 2, \ldots, k$ call the set X_i the i-th layer. Note that $X_i, X_{i+1}, \ldots, X_k$ is the cop-win partition of G_i.

Proposition 3.2. *A graph is cop-win if and only if it has a cop-win partition.*

Proof. By the discussion above we need only show that a graph with a cop-win partition is cop-win. Suppose that $X_1, X_2, \ldots, X_k$ of G is a cop-win partition of G. The enumeration of $V(G)$ constructed by first listing the vertices in X_1 (in any order), then those in X_2, and so on until, finally, the vertices in X_k are listed is a cop-win ordering. The result now follows from Theorem 2.1. □

Suppose that G has a cop-win partition $X_1, X_2, \ldots, X_k$, where $k > 1$. If some vertex of X_k is adjacent to all vertices of X_{k-1}, then all vertices of X_k must be adjacent to all vertices of X_{k-1}: since the subgraph induced by X_k is complete, any vertex of X_k with a non-neighbour in X_{k-1} would belong to a corner in $G_{k-1} \,/\, \Theta_{G_{k-1}}$. Further, if $X_k = \{x_k\}$ then x_k is adjacent to every vertex of X_{k-1} as, in G_{k-1}, any such vertex must be covered by a vertex in X_k.

Theorem 3.3. *Let G have a cop-win partition $X_1, X_2, \ldots, X_k$. Then $catchtime(G) = k-1$ if every vertex of X_k is adjacent to every vertex of X_{k-1}, or G has only one vertex. Otherwise, $catchtime(G) = k$.*

Proof. We first show by induction on k that the robber can be caught in at most the given number of cop moves. If $k = 1$, then G is complete and $catchtime(G) = 0$ when G has one vertex and $catchtime(G) = 1$ otherwise. Suppose $k = 2$. If every vertex in X_2 is adjacent to every vertex of X_1, then an optimal play game will end in one cop move. Otherwise, every vertex in X_2 has a non-neighbour in X_1. The cop begins by choosing a vertex $x_2 \in X_2$. No matter which vertex non-adjacent to x_2 the robber chooses, by definition of X_1 and since the subgraph induced by X_2 is complete, the cop can move to a vertex of X_2 that covers the robber position. The game ends in one more cop move, as required.

Suppose that the statement holds for all cop-win graphs in which the cop-win partition has $k-1$ layers. Let G be a cop-win graph for which the cop-win partition has k layers. By Proposition 3.1, the graph $G_2 = G - X_1$ is cop-win and has a cop-win partition with $k-1$ layers. As before, while the robber plays the game on G, the cop plays the game as if it were on G_2. If the robber is in X_1 then by definition of X_1 he has a *shadow* (a particular vertex that covers his position) in G_2. By the induction hypothesis and assuming optimal play, after at most $catchtime(G_2) - 1$ cop moves, the robber or his shadow is on a vertex $x_2 \in X_2$ and the cop is on a vertex y of G_2 that covers it (the robber could actually be located in X_1 which is covered by x_2). The robber can evade capture for at most two more cop moves. On the next cop move the cop catches the robber's shadow (or possibly the robber) on some vertex z of G_2. Suppose he has only caught the shadow. Then the robber is on a vertex $x_1 \in X_1$ which is covered by z. No matter to which vertex the robber moves, the cop now has a move to the same vertex, so the game ends on the next cop move.

The proof that there is an optimal play game requiring the given number of moves is also by induction on k. The statement is easy to see when $k = 1$. Suppose it holds for all cop-win graphs in which the cop-win partition has $k-1$ layers. Let G be a cop-win graph for which the cop-win partition has k layers. By the induction hypothesis and assuming optimal play, there is a game on G_2 that requires $catchtime(G_2)$ moves. Since there is never an advantage to the cop in using a vertex in X_1 – a cover in G_2 could be used instead – in order to make the game on G last as long as possible, the robber first plays his optimal game on G_2. By Proposition 2.3, just before the robber's last move in this game, the robber is on a vertex $x_2 \in X_2$ and the cop is on a vertex y that covers it (in G_2). By definition of

X_2, in the game on G, the robber has a move to a vertex in $x_1 \in X_1$ which is not adjacent to y. Since x_1 is a corner of G, the cop has a move to a vertex that covers x_1. (A cover of x_1 is adjacent to all neighbours of x_1, hence is adjacent to x_2. Since y covers x_2, it is adjacent to all neighbours of x_2, including the vertex that covers x_1.) The game therefore lasts one move longer than before. This completes the proof. □

Theorem 3.3 implies a straightforward algorithm for computing the catch time. Given a graph G with n vertices, the first step is to find the quotient graph, $G \,/\, \Theta_G$. If G is represented by an adjacency matrix, A, then viewing each row as characteristic vector of the corresponding vertex, two vertices belong to the same equivalence class if the corresponding rows are identical. The equivalence classes, and consequently $G \,/\, \Theta_G$ (choose one vertex from each equivalence class) can be found in $O(n^2)$ time. The corners of $G \,/\, \Theta_G$ are also easy to find from the rows of A in time $O(n^2)$. Hence the first set, X_1, in a cop-win partition can be determined in quadratic time. After marking the vertices in X_1 as deleted, the process is repeated with $G - X_1$ and so on, until the cop-win partition $X_1, X_2, \ldots, X_k$ is determined. Since $k \leq n$, this process takes time $O(n^3)$. The last step is to test whether every vertex of X_k is adjacent in G to every vertex in X_{k-1}, which takes time $O(n^2)$, and then apply the theorem. Hence the catch time can be determined in cubic time.

We conclude this section by noting that, by definition of the catch time of the cop-win graph G, for any initial position chosen by the cop there is an initial position available to the robber such that optimal play by both sides results in a game of length at least $catchtime(G)$. Further, there exists at least one initial position available to the cop (for example, any one in the "top" layer of the cop-win partition, plus possibly some others) such that optimal play by both sides results in a game of length exactly $catchtime(G)$.

4 Retractions and a description of the strategy

The purpose of this section is to illustrate how our results can be seen as a generalization of Theorem 2.1, and to present the cop's strategy implied by Theorem 3.3 in the language of retractions (see [7, 10]), thus perhaps making the implied recursion more transparent.

We first describe an alternate approach that could have been used instead of proceeding directly to the cop-win partition as in Section 3. An advantage of using this point of view is that the connection with Theorem 2.1 is immediate.

By a *cop-win layering* of a graph G we mean an ordered partition $X_1, X_2, \ldots, X_\ell$ of $V(G)$ such that for $i = 1, 2, \ldots, \ell - 1$ the set X_i is a set of corners of $G_i = G - \cup_{t=1}^{i-1} X_t$ each of which has a cover in G_{i+1}. Each set X_i is called a *layer*.

A cop-win ordering $v_1, v_2, \ldots, v_n$ gives a cop-win layering by setting $X_i = \{v_i\}$, $1 \leq i \leq n$. Conversely, a cop-win layering $X_1, X_2, \ldots, X_k$ of G gives a cop-win ordering in the same way as described before. The following statements hold using essentially the same proofs as before.

Theorem 4.1. *A graph G is cop-win if and only if it admits a cop-win layering.*

Theorem 4.2. *If G has a cop-win layering $X_1, X_2, \ldots, X_k$, then $catchtime(G) \leq k-1$ if every vertex of X_k is adjacent to every vertex of X_{k-1}, or G has only one vertex. Otherwise, $catchtime(G) \leq k$.*

Let $\mathcal{L} = X_1, X_2, \ldots, X_k$ be a cop-win layering of G. Define $\mu_G(\mathcal{L}) = k - 1$ if every vertex of X_k is adjacent to every vertex of X_{k-1} or if G has only one vertex, and $\mu_G(\mathcal{L}) = k$ otherwise.

Theorem 4.3. *The maximum length of the cop and robber game on the cop-win graph G equals $\min_{\mathcal{L}} \mu_G(\mathcal{L})$, where the minimum is over all cop-win layerings of G.*

Given a cop-win ordering $v_1, v_2, \ldots, v_n$ of G, Theorem 4.2 can be used to improve the upper bound of $n-1$ cop moves in the associated strategy. Define a cop-win layering by letting X_1 be a maximum size set of consecutive vertices $X_1 = \{v_1, v_2, \ldots, v_{i_1}\}$ such that each vertex in X_1 has a cover in $V(G) - X_1$. Now delete the vertices in X_1 and define X_2 in the same way using the graph $G_2 = G - X_1$. Continue in this way until, finally, a cop-win layering $\mathcal{L} = X_1, X_2, \ldots, X_\ell$ is defined. Then $catchtime(G) \leq \mu_G(\mathcal{L})$.

For the purposes of what follows, it is convenient to regard the graphs under consideration as being reflexive, that is, having a loop at each vertex. A pass corresponds to moving along the loop from a vertex to itself.

Let G be a graph and H be a fixed subgraph of G. A *retraction of G to H* is a homomorphism of G to H that maps H identically to itself. Formally, it is a function $f : V(G) \to V(H)$ such that $f(h) = h$ for all vertices h of H, and if $xy \in E(G)$ then $f(x)f(y) \in E(H)$. If there exists a retraction of G to H, then H is called a *retract* of G.

Theorem 4.4. [12, 14] *Any retract of a cop-win graph is cop-win.*

Retractions provide a convenient way of describing the cop's strategy arising from Theorem 2.1 [7, 10] (also see [9]). The same method can be used to describe the strategy arising from Theorem 4.2. Suppose that G has at least two vertices and let $\mathcal{L} = X_1, X_2, \ldots, X_\ell$ be a cop-win layering of the vertices of G. For $i = 1, 2, \ldots, \ell - 1$ there is a retraction f_i of the graph $G_i = G - \cup_{t=1}^{i-1} X_t$ to G_{i+1} that maps each vertex in X_i to a vertex in G_{i+1} that covers it. (If there is more than one candidate for this vertex, it does not matter which one is chosen.) When G is a complete graph with at least two vertices, or every vertex in X_ℓ is non-adjacent to some vertex in $X_{\ell-1}$ there is also a retraction f_ℓ of the (complete) subgraph induced by X_ℓ to any one of its vertices. On his j-th move, the cop plays on $G_{\ell-j+1} = f_{\ell-j} \circ \cdots \circ f_2 \circ f_1(G) = G - \cup_{t=1}^{\ell-j} X_t$. We allow $j = 0$ when $|X_\ell| > 1$ and every vertex in X_ℓ has a non-neighbour in $X_{\ell-1}$. No matter where the robber is located in G, his *shadow* (i.e. image under the mapping $f_{\ell-j} \circ \cdots \circ f_2 \circ f_1$) is located on one of the vertices of this graph. Since the cop is "on" the robber's shadow after making his move when $j = 1$, and the retractions allow him to stay on it in each subsequent move, the cop is guaranteed to catch the robber after at most $\mu_G(\mathcal{L})$ moves.

References

[1] A. Berarducci and B. Intriglia, On the cop number of a graph, *Advances in Applied Math.* **14** (1993), 389–403.

[2] A. Bonato, P. A. Golovach, G. Hahn and J. Kratochvíl, The Capture Time of a Graph, *Discrete Math.* **309** (2009), 5588–5595.

[3] A. Bonato and R. J. Nowakowski, *The game of Cops and Robbers on Graphs*, AMS Student Mathematical Library, AMS, Providence, RI, 2011.

[4] M. Boyer, S. El Harti, A. El Ouarari, R. Ganian, T. Gavenčiak, G. Hahn, C. Moldenauer, I. Rutter, B. Thériault, M. Vatshelle, Cops-and-robbers: remarks and problems, manuscript, 2011.

[5] V. Chepoi, Bridged graphs are cop-win graphs: an algorithmic proof, *J. Combin. Theory Ser. B* **69** (1997), 97–100.

[6] V. Chepoi, On Distance-preserving and Domination Elimination Orderings, *SIAM J. Discrete Math.* **11** (1998), 414–436.

[7] N. E. Clarke, *Constrained Cops and Robber*, Ph.D. Thesis, Dalhousie University, 2002.

[8] N. E. Clarke and G. MacGillivray, Characterizations of k-copwin graphs, *Discrete Math.* **312** (2012), 1421–1425.

[9] N. E. Clarke and R. J. Nowakowski, Cops, Robber and Photo Radar, *Ars Combinatoria* **56** (2000), 97–103.

[10] N. E. Clarke and R. J. Nowakowski, Cops, Robber, and Traps, *Utilitas Mathematica* **60** (2001), 91–98.

[11] G. Hahn and G. MacGillivray, An algorithmic characterisation of k-copwin graphs and digraphs, *Discrete Math.* **306**, 2492–2497.

[12] R. J. Nowakowski and P. Winkler, Vertex to Vertex Pursuit in a Graph, *Discrete Math.* **43** (1983), 23–29.

[13] A. Quilliot, *Jeux de Points Fixes sur les graphes*, Thèse de 3ème cycle, Université de Paris VI, 1978, 131–145.

[14] A. Quilliot, *Problèmes de jeux, de point Fixe, de connectivité et de represésentation sur des graphes, des ensembles ordonnés et des hypergraphes*, Thèse d'Etat, Université de Paris VI, 1983.

ARS MATHEMATICA CONTEMPORANEA

Also available at http://amc-journal.eu
ISSN 1855-3966 (printed edn.), ISSN 1855-3974 (electronic edn.)
ARS MATHEMATICA CONTEMPORANEA 7 (2014) 361–377

Systematic celestial 4-configurations

Angela Berardinelli
Department of Mathematics, University of North Texas, Denton, Texas, USA

Leah Wrenn Berman
Department of Mathematics & Statistics, University of Alaska Fairbanks, Fairbanks, Alaska, USA

Received 26 June 2012, accepted 20 June 2013, published online 15 November 2013

Abstract

Celestial 4-configurations are a class of highly symmetric geometric configurations of points and lines in the plane in which 4 points lie on each line and 4 lines pass through each point (that is, they are (n_4) configurations). The set of isometries of the plane that map a configuration to itself (that is, the *symmetries* of the configuration) partition the points into orbits, called the *symmetry classes of points*, and likewise the symmetries of the configuration partition the lines into orbits as well, forming the set of symmetry classes of lines. Celestial 4-configurations have the property that two lines from each of two symmetry classes of lines pass through each point, and two points from each of two symmetry classes of points lie on each line; a celestial 4-configuration with k symmetry classes is called k-celestial. Celestial configurations may be classified as being *trivial*, *systematic*, or *sporadic*. Previously, three non-trivial classes of 3-celestial 4-configurations were known. This paper presents a number of new systematic families of celestial 4-configurations, including 16 new 3-celestial families, four 4-celestial families, and three classes of h-celestial configurations for infinitely many values of h, although it does not provide a complete classification.

Keywords: Configurations, incidence geometry.

Math. Subj. Class.: 52C30, 51E30

E-mail addresses: AngelaBerardinelli@my.unt.edu (Angela Berardinelli), lwberman@alaska.edu (Leah Wrenn Berman)

1 Introduction

A *4-configuration* is a collection of points and straight lines, typically in the Euclidean or projective plane, so that each point has four lines passing through it and each line has four points lying on it; such configurations are often referred to as (n_4) configurations, when the number n of points and lines of the configuration is to be emphasized. If the configuration has non-trivial geometric symmetry, that is, if there exists a nontrivial isometry of the plane that maps the configuration to itself, then we say the configuration is *symmetric*, and the points and lines of the configuration may be partitioned into *symmetry classes* of points and of lines (i.e., the maximal orbit of a point under the symmetry group forms the symmetry class of that point, and similarly in the construction of the symmetry classes of lines). This usage of the word "symmetric" follows Grünbaum [14, p. 16] in reserving the word "symmetric" to refer to geometric properties of configurations. In other places in the literature (e.g. [7]), the word symmetric has been used to refer to (n_k) configurations, which are 'symmetric' in the numbers of points and lines; again following Grünbaum, we shall call such configurations *balanced*, and reserve the use of 'symmetric' to emphasize geometric symmetry properties. If the number n of points and lines is relevant, we refer to an (n_k) configuration.

A 4-configuration is *celestial* if it has two points from each of two symmetry classes lying on each line and two lines from each of two symmetry classes of lines passing through each point; if there are h total symmetry classes of points and lines, we refer to an h-celestial 4-configuration. Figure 1a shows an example of a 3-celestial 4-configuration with 21 points and lines: each point has two lines from each of two symmetry classes (indicated by color) passing through it, and each line has two points from each of two symmetry classes of points (again indicated by color) lying on it. Note that not all symmetric 4-configurations are celestial, however; Figure 1b shows a (20_4) configuration with three symmetry classes of points and lines, with the property that one symmetry class of lines (shown in green) is incident with points from all three symmetry classes of points.

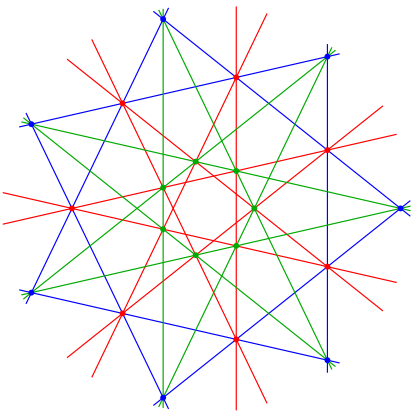

(a) A (21_4) 3-celestial 4-configuration.

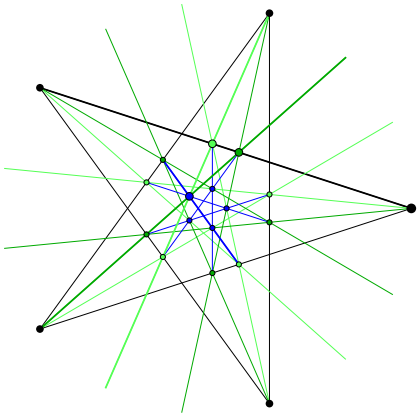

(b) A non-celestial (20_4) 3-astral 4-configuration, first shown in [13].

Figure 1: Examples of symmetric 4-configurations.

There has been a fair amount of investigation of 4-configurations in the past 20 years,

beginning with Grünbaum and Rigby's 1990 discovery of an intelligible way of presenting a (21_4) configuration [15]; this is the configuration shown in Figure 1a, which is the celestial 4-configuration with the fewest number of points and lines. In 2003, Marko Boben and Tomaž Pisanski introduced a class of highly symmetric configurations that they called *polycyclic configurations* which had rotational symmetry [8]. Celestial 4-configurations formed an important class of examples discussed in that paper.

Initial investigation into the classification of symmetric 4-configurations initially focused on *astral* configurations [1, 11] which have two symmetry classes of points and lines, two lines from each of two symmetry classes passing through each point, and two points from each of two symmetry classes lying on each line; that is, they are 2-celestial configurations. General celestial 4-configurations continued to be investigated as well [12], and a number of axioms were developed associating to each celestial configuration a configuration symbol (usually, several equivalent symbols). Given a potential configuration symbol, it is straightforward to determine if it corresponds to a configuration by verifying whether the axioms are satisfied. For this reason, celestial 4-configurations form the most well-understood class of 4-configurations and serve as building blocks for several other classes of configurations; for examples, see [2, 3, 4, 5, 6] (in some of those references, celestial configurations are referred to as *k-astral* configurations). However, despite their utility and the fact that there are concrete rules governing their existence, there has been very little work done in *classifying* h-celestial 4-configurations for $h > 2$.

The most comprehensive description of celestial configurations occurs in Branko Grünbaum's recent monograph *Configurations of Points and Lines* [14]. In Section 1.5 of that reference, Grünbaum defines h-*astral* configurations to be configurations which have h symmetry classes of points and h symmetry classes of lines. We follow this usage. Unfortunately, in Sections 3.5 – 3.9 of the same reference, he refers to what we are calling *celestial* 4-configurations as "k-astral" configurations, and all of his discussion of k-astral configurations in those sections refers to celestial configurations only. However, there are very nice classes of 4-configurations that are k-astral (they have k symmetry classes of points and lines) but not k-celestial; for example, see Figure 1b, in which one of the symmetry classes of lines is incident with points from three different symmetry classes of points (rather than points from only two symmetry classes of points). In this article, we use the term k-*astral* to refer to a configuration with k symmetry classes of points and lines, whether celestial or not, and the term k-*celestial* to refer to a k-astral 4-configuration with the added property that every line contains two points from each of two symmetry classes and every point has two lines from each of two symmetry classes passing through it.

Following [14], celestial configurations are divided into three broad classes (discussed in more detail below): (1) trivial configurations; (2) systematic configurations, of which there are three known classes, and (3) sporadic configurations, which are non-trivial and (provably) non-systematic.

In this paper, we present a number of new families of systematic celestial 4-configurations. This answers affirmatively the following open question from Grünbaum [14, Section 3.7]: "Do there exist any other systematic families [of 4-celestial configurations] besides the ones listed above?" and also the open exercise 8, "Find some systematic families for [4-celestial] configurations other than the ones that arise from an h-celestial configuration with $h < k$ by insertion of matched pairs".

2 Celestial configurations

The theory of celestial configurations has been developed over the past 20 years. The first known published pictures of celestial configurations appeared in [15] and as examples in a paper by Marušič and Pisanski [17], as well as in the paper on polycyclic configurations by Boben and Pisanski [8]; the configurations as a class were introduced by Grünbaum in unpublished course notes for a course on configurations [9]. The particular case of 2-celestial 4-configurations, also simply known as *astral* 4-configurations (in general, an (n_q) configuration is *astral* if it has $\lfloor \frac{q+1}{2} \rfloor$ symmetry classes of points and lines, so a 4-configuration is astral if it has 2 symmetry classes of points and lines), was considered in [1, 2, 8, 10, 11]; these configurations were completely classified in [1], with a more intelligible proof provided in [14, Section 3.6].

The most complete treatment of celestial 4-configurations, using the current terminology and approach, appears in Grünbaum's recent monograph on configurations, *Configurations of points and lines* [14, Section 3.5–3.8]. We follow his treatment in the following presentation (although, again, all his discussion in those sections refers to celestial configurations as k-astral configurations).

Every h-celestial (n_4) configuration may be represented by a *configuration symbol*

$$m\#(s_1, t_1; s_2, t_2; \ldots; s_h, t_h),$$

where h is the number of symmetry classes of points, n is the total number of points in the configuration, $m = \frac{n}{h}$ is the number of points in each symmetry class, and the s_i and t_i give the instructions for constructing the configuration geometrically.

Given points P and Q and lines ℓ_1 and ℓ_2, denote the line containing P and Q as $P \vee Q$ and the point of intersection of lines ℓ_1 and ℓ_2 as $\ell_1 \wedge \ell_2$. If $w_0, w_1, \ldots, w_{m-1}$ form the vertices of a regular convex m-gon, labelled cyclically, then a *line of span s with respect to the w_i* is any line of the form $w_i \vee w_{i+s}$, and given the set of all lines $L_i = w_i \vee w_{i+s}$ of span s with respect to w_i, the *t-th intersection of the span s lines* is the set of points $L_i \wedge L_{i-t}$.

Given a configuration symbol $m\#(s_1, t_1; s_2, t_2; \ldots; s_h, t_h)$, which is known to correspond to a configuration, that is, given a *valid* configuration symbol, the corresponding configuration may be constructed as follows.

1. Construct the vertices of a regular convex m-gon and label them cyclically as

   $$(v_0)_0, (v_0)_1, \ldots, (v_0)_{m-1},$$

   and collectively as v_0. (Typically, $(v_0)_i = \left(\cos\left(\frac{2\pi i}{m}\right), \sin\left(\frac{2\pi i}{m}\right)\right)$ so that the points v_0 lie on the unit circle.)

2. Construct all lines of span s_1 with respect to the v_0 and label them collectively as L_0; in particular, $(L_0)_i = (v_0)_i \vee (v_0)_{i+s_1}$.

3. Construct a second set of points v_1 as the t_1-st intersection of the span s_1 lines L_0; that is, $(v_1)_i = (L_0)_i \wedge (L_0)_{i-t_1}$.

4. In general, lines L_{j-1} are lines of span s_j with respect to the points v_{j-1}, so that $(L_{j-1})_i = (v_{j-1})_i \vee (v_{j-1})_{i+s_j}$, and points v_j are the t_j-th intersection of the lines L_{j-1}, so that $(v_j)_i = (L_{j-1})_i \wedge (L_{j-1})_{i-t_j}$.

For the configuration symbol corresponds to a valid configuration, the points with label v_h (that is, the t_h-th intersections of the lines L_h) must correspond, as a set, to the points with label v_0, so that the construction closes up. That is, for the construction to be valid, the points v_h constructed at the last step should have the same radius as the points v_0, they should have the same "angle"—the angle between point $(v_h)_0$ and $(v_0)_0$ should be an even multiple of $\frac{\pi}{m}$, and all sets of points and lines generated by the algorithm should be distinct. In addition, we want to avoid "extra incidences", where lines constructed in a certain step accidentally pass through points constructed several steps back.

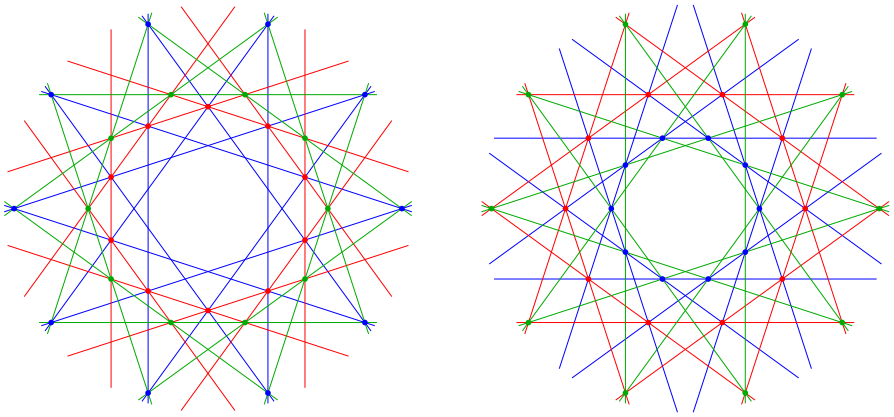

(a) symbol $10\#(4,3;1,2;1,3)$ (b) symbol $10\#\{1,3;1,3;4,2\}$

Figure 2: Two different 3-celestial 4-configurations. In each case, the points v_0 and lines L_0 are blue, the points v_1 and lines L_1 are red, and the points v_2 and lines L_2 are green.

Consequently, a configuration symbol $m\#(s_1,t_1;\ldots;s_h,t_h)$ with *sequence* $(s_1,t_1;\ldots;s_h,t_h)$ is *valid* if it satisfies the following four axioms:

(A1) (Even condition) The quantity $\frac{1}{2}\sum_{i=1}^{h}(s_i-t_i)$ is an integer.

This condition ensures that after following the configuration construction steps, the angle of the last set of points constructed coincides with the angles of the original set of points (rather than being offset by a factor of $\frac{\pi}{m}$).

(A2) (Order condition) No adjacent symbols in the sequence, taken cyclically, are equal: that is, $s_i \neq t_i \neq s_{i+1}$ for $i = 1,\ldots,h-1$ and $s_h \neq t_h \neq s_1$.

This condition ensures that all symmetry classes of lines and points constructed are distinct.

(A3) (Cosine condition) $\prod_{i=1}^{h}\cos\left(\frac{s_i\pi}{m}\right) = \prod_{i=1}^{h}\cos\left(\frac{t_i\pi}{m}\right)$

This condition ensures that the radius of the last set of points constructed is equal to the radius of the original set of points.

Thus, satisfying (A1) and (A3) ensures that the points v_0 and the points v_h coincide as sets.

(A4) (Substring condition) No subsequence $s_p, t_p; \ldots; s_q$ or $t_p; s_{p+1}, \ldots; s_q, t_q$ may be completed to a sequence $s_p, t_p; \ldots; s_q, a$ or $a, t_p; s_{p+1}, \ldots; s_q, t_q$ which satisfies the previous rules (i.e., corresponds to a valid smaller configuration).

This is a technical condition to prohibit lines or points having extra, unwanted incidences.

Given a valid configuration symbol, any sequence formed with entries taken alternately without replacement from the set $S = \{s_1, s_2, \ldots, s_h\}$ and the set $T = \{t_1, \ldots, t_h\}$, or vice versa, will satisfy axioms (A1) and (A3); if they are ordered so as to satisfy axioms (A2) and (A4), then the new configuration symbol will also be valid. For example, the configuration shown in Figure 2a, with symbol $10\#(4, 3; 1, 2; 1, 3)$ has sets $S = \{4, 1, 1\}$ and $T = \{3, 2, 3\}$. If we construct the configuration symbol $10\#\{1, 3; 1, 3; 4, 2\}$, which satisfies axioms (A1) – (A4), the corresponding configuration also exists; see Figure 2b.

A *valid configuration cohort* refers to any symbol

$$m\#S; T$$

where the multisets S and T satisfy axioms (A1) and (A3), for which there *exists* a sequence with entries alternately from S and T satisfying axioms (A2) and (A4). (Note that we explictly allow S and T to have repeated elements, but the order of the elements in the sets S and T is irrelevant.) If $|S| = |T| = h$, we may occasionally refer to an h-cohort; in this case, corresponding configurations are h-celestial. Given a cohort, every sequence with entries taken alternately from S and T, or from T and then from S, which satisfies (A2) and (A4) will correspond to a valid configuration symbol. Thus, in trying to classify celestial configurations, it is easier to classify configuration cohorts.

2.1 Classification of cohorts

If $S = T$, then the corresponding cohort is necessarily valid. Configuration cohorts of the form $m\#S; S$ are called *trivial*. Some cohort sets fall into an infinite family. For example, the 2-celestial cohorts have been completely classified: there is one infinite family $6q\#\{3q - p, p\}; \{2q, 3q - 2p\}$. A cohort which is a member of an infinite family is called *systematic*. Cohorts which are provably neither systematic nor trivial are called *sporadic*; for example, there are 15 sporadic 2-celestial cohorts [1],[14, Section 3.6]. Configurations whose corresponding cohorts are trivial/systematic/sporadic are also called trivial/systematic/sporadic.

Definition 2.1. An $(h + j)$-cohort symbol

$$m\#\{s_1, s_2, ..., s_h, a_1, a_2, ..., a_j\}; \{t_1, t_2, ..., t_h, a_1, a_2, ..., a_j\}$$

is *reducible* if and only if

$$m\#\{s_1, s_2, ..., s_h\}; \{t_1, t_2, ..., t_h\}$$

is a valid h-cohort symbol.

A cohort which is not reducible is called *primitive*.

2.2 Determining valid cohorts

In order to classify cohorts, it is useful to be able to generate, for a given h and m, a list of all valid h-cohorts $m\#S;T$.

Theorem 2.2. *Given cohort symbol*

$$m\#\{s_1,\ldots,s_h\};\{t_1,\ldots,t_h\}$$

with $h \geq 2$, the symbol violates (A2) (that is, every possible configuration sequence has at least two adjacent entries that are equal) if and only if there exists $a \in S \cap T$ that appears at least h times in the list $(s_1, s_2, \ldots, s_h, t_1, t_2, \ldots, t_h)$.

Proof. [$\Longleftarrow$] Let $a \in S \cap T$ be an element repeated x times in the sequence

$$(s_1, s_2, \ldots, s_h, t_1, t_2, ..., t_h),$$

and assume $x \geq h$. Let X count the number of times a appears in S. To form a valid configuration symbol, it must be possible to construct a configuration sequence $(s_1, t_1; s_2, t_2; \ldots; s_h, t_h)$, relabelling the subscripts as necessary, so that no two adjacent elements are equal (with s_1 and t_h considered to be adjacent). We may place all of the elements of S into the sequence (in the appropriate slots) first. Then all positions adjacent to one of the as that have been placed from S cannot be filled with one of the $(x - X)$ as from T. The placement that eliminates the fewest possible positions for the as in T is to place all the as from S adjacent to each other in this way: $(a, t_1; a, t_2; ...; a, t_X; s_{X+1}, t_{X+1}; ...; s_h, t_h)$, so that there are $h-(X+1)$ slots in which as from T could be placed (since there are $(X+1)$ slots t_i which are blocked by the as). However, there are $(x-X) \geq (h-X) > (h-X-1)$ as which need to be placed, a contradiction.

[$\Longrightarrow$] Assume every element in $S \cap T$ appears fewer than h times in the sequence

$$(s_1, s_2, \ldots, s_h, t_1, t_2, \ldots, t_h),$$

and let a be the element in $S \cap T$ which appears the most times in that sequence.

Case 1: $S \cap T = \emptyset$. Then

$$\{s_1, t_1; s_2, t_2; \ldots; s_h, t_h\}$$

is a valid configuration sequence.

Case 2: $S \cap T \neq \emptyset$. Then there exists $a \in S \cap T$ which appears $x < h$ times in the list $(s_1, s_2, ..., s_h, t_1, t_2, ..., t_h)$. Suppose a appears X times in S. Then

$$\{a, t_1; a, t_2; \ldots; a, t_X; s_{X+1}, a; s_{X+2}, a; \ldots; s_x, a; s_{x+1}, t_{x+1}; \ldots; s_h, t_h\}$$

is a valid configuration sequence. □

Corollary 2.3. *If $S \cap T = \{a\}$, then $m\#\{s_1, s_2, \ldots, s_h, a\}; \{t_1, t_2, \ldots, t_h, a\}$ is reducible to $m\#\{s_1, s_2, \ldots, s_h\}; \{t_1, t_2, \ldots, t_h\}$.*

Corollary 2.4. *If $m\#S;T$ is a $(h+1)$-cohort and $\{a, b\} \subseteq S \cap T$ in which one of a or b appears at least h times in the list $(s_1, s_2, \ldots, s_h, s_{h+1}, t_1, t_2, ..., t_h, t_{h+1})$ then $m\#S;T$ is* not *reducible.*

Proof. Suppose a appears at least once, and b appears at least h times. Attempt to reduce $m\#S;T$ by removing one of the pairs of a's. The resulting cohort is not valid, by Theorem 2.2. □

2.3 2-celestial configurations

2-celestial configurations have been completely classified (see [1] and [14, Section 3.6]). There is one infinite cohort:

$$6q\#\{3q-p,p\};\{2q,3q-2p\}$$

and 15 sporadic cohorts, shown in Table 1, plus disconnected multiples.

Table 1: Sporadic 2-celestial cohorts

$30\#\{7,1\};\{6,4\}$	$30\#\{11,1\};\{10,6\}$
$30\#\{12,2\};\{11,7\}$	$30\#\{13,7\};\{12,10\}$
$30\#\{14,6\};\{13,11\}$	$30\#\{8,2\};\{6,6\}$
$30\#\{12,6\};\{10,10\}$	$30\#\{13,1\};\{12,8\}$
$30\#\{14,4\};\{12,12\}$	
$42\#\{13,1\};\{12,6\}$	$42\#\{19,5\};\{18,12\}$
$42\#\{18,6\};\{17,11\}$	
$60\#\{22,2\},\{21,9\}$	$60\#\{27,3\},\{26,14\}$
$60\#\{25,5\},\{24,12\}$	

In determining the list of all valid h-cohorts for a given h, the challenging axiom to verify is clearly (A3), since determining when products of sines or cosines are rational, or more generally, of solving trigonometric diophantine equations, is extremely challenging. The proof of the complete classification of 2-celestial configurations presented in [14], which is considerably less complex than that presented in [1], used results of Gerald Myerson [18] which determined all rational products of three and four sines of rational angles, and, more importantly for the current problem, determined all rational solutions to

$$\sin(\pi x_1)\sin(\pi x_2)=\sin(\pi x_3)\sin(\pi x_4)$$

which may be converted into the corresponding product of cosines using a simple trigonometric identity.

3 New systematic families

A fairly recent article by Miklós Laczkovich [16] apparently provides results on solutions to

$$\sin(\pi p_1)\sin(\pi p_2)\sin(\pi p_3)=\sin(\pi q_1)\sin(\pi q_2)\sin(q_3),$$

but its results are somewhat inexplicit and inaccessible for our current purposes.

For the remainder of this article, we will present known systematic families of h-celestial configurations—mostly for $h=3,4$—which have been found primarily by ad hoc methods of analyzing lists of valid cohorts. For $h=3,4$ data were found by an exhaustive computer search using *Mathematica*. Essentially, for each m, we ran a simple incrementing loop on the discrete parameters

$$1\le t_3\le t_2\le t_1\le s_3\le s_2\le s_1\le\frac{m}{2}$$

which for each choice of discrete parameters checked whether it is trivial and whether it satisfies (A1), (A2) (using Theorem 2.2), and (A3); the expensive part of this process is checking the cosine condition. We collected all symbols that pass these tests. Then, using Corollaries 2.3 and 2.4 and the fact that all 2-celestial configurations are known, we eliminated reducible configurations. Finally, in the case of 3-cohorts, we removed already-classified configurations. This left us with reasonably clean, sorted lists of all unclassified configurations for a given m. The generating Mathematica notebook and raw data are available at `https://sites.google.com/a/alaska.edu/lwberman/`, as well as lists of celestial configurations that are still unclassified. Production of the data was the main content of one of the author's [AB] Summer Fellows project at Ursinus College in 2009. We have generated data for 3-configurations for all $m \leq 120$ and for 4-configurations for $m \leq 64$.

Traditionally, in the discussion of symbols for cohorts and configurations, the parameters s_i and t_i are chosen to be less than $m/2$. However, in the description of infinite families of cohorts, it is often helpful to allow the parameters to take on larger values; we consider the geometry of the configuration construction to determine the appropriate way to reduce the symbol.

Suppose a regular m-gon has all diagonals of span s. Then a diagonal of span s and of span $-s = m - s \bmod m$ correspond to the same line. Reflecting over a diameter gives a different diagonal, but of the same span. We define the *standard form* of a symbol element s to be a number s' with $1 \leq s' < \frac{m}{2}$ computed by doing the following:

1. First, take the absolute value of s
2. Then, reduce s modulo m.
3. If $s \geq \frac{m}{2}$, replace s with $m - s$; otherwise, s is already between 1 and $\frac{m}{2}$.

In the presentations of the infinite families, the spans in question are not, typically, given in standard form, although the list of valid cohorts is generated in standard form (that is, we restrict the values of s_i and t_i to be positive and less than $\frac{m}{2}$).

4 3-celestial families

A number of years ago, one of the authors [LWB] found the following systematic cohorts of 3-celestial configurations (which were unpublished until their discussion in [14, Section 3.7]):

- $2q\#\{q-p, p, q-2r\}; \{q-r, r, q-2p\}$
- $3q\#\{q+p, q-p, p\}; \{q, q, 3p\}$
- $10q\#\{5q-p, 2p, p\}; \{5q-4p, 4q, 2q\}$

At the time, these families appeared to be exhaustive for 3-celestial configurations $m\#S, T$ where m was not divisible by 6, and there was a conjecture that there were no other cohorts for such m. Very little was known about classification of 3-celestial configurations when m *was* divisible by 6: one systematic family for $m = 6q$ was listed in [14, Section 3.7], but this family, $m\#\{3q-p, r, p\}; \{3q-2p, 2q, r\}$, is reducible to the known family of 2-celestial configurations.

Subsequent computer experiments have revealed the existence of six 3-celestial cohorts for $m = 70$. These have not yet been explained. In addition, there is a single unclassified cohort for $m = 105$. These are listed in Table 2. Both 70 and 105 are divisible by 35, which raises the unexpected possibility that there is an infinite family for m divisible by 35, but no such family is known. (It is not unreasonable that an infinite family of the form $m = 35q$ would not have any entries for $q = 1$; for example, the infinite family of 2-celestial configurations does not have any entries for $q = 1$, since there are no configurations with $m = 6$.)

Table 2: Unclassified cohorts for $m = 70$ and $m = 105$.

$$m = 70$$
$$\{24, 14, 4\}; \{20, 19, 9\}$$
$$\{28, 12, 2\}; \{27, 13, 10\}$$
$$\{29, 10, 1\}; \{26, 16, 14\}$$
$$\{30, 17, 3\}; \{28, 22, 8\}$$
$$\{33, 23, 20\}; \{32, 28, 18\}$$
$$\{34, 14, 6\}; \{31, 30, 11\}$$
$$m = 105$$
$$\{45, 30, 15\}; \{42, 35, 21\}$$

However, a number of new systematic families of 3-celestial cohorts have been found in the case when m is divisible by 6, discussed in Section 5.1, below.

5 3-celestial cohorts when m is divisible by 6

5.1 $m = 6q$

For m divisible by 6, the following families are known.

Family 1: $6q\#\{2q, q-p, 3p\}; \{2q-p, q+2p, p\}$, $p = 1, \ldots, 2q-1$

Family 2: $6q\#\{3q-p, 2p, p\}; \{2q, 2q, 3q-4p\}$, $p = 1, .., q-1$

Family 3: $6q\#\{2q+p, q-2p, p\}; \{2q, q+p, 3p\}$, $p = 1, \ldots, 2q-1$

Family 4: $6q\#\{3q-3p, 2p, p\}; \{3q-4p, q+p, q-p\}$, $p = 1, 2, \ldots, 3q-1$

Family 5: $6q\#\{q+2p, q-2p, p\}; \{q+p, q-p, 3p\}$, $p = 1, \ldots, 3q-1$

Family 6: $6q\#\{3q-p, 6p, p\}; \{3q-4p, 2q+2p, 2q-2p\}$, $p = 1, \ldots, \lfloor \frac{3q}{2} \rfloor$

Family 7: $6q\#\{2p, 3p, 3q-3p\}; \{3q-4p, q-2p, q+2p\}$, $p = 1, \ldots, \lfloor \frac{3q}{2} \rfloor - 1$

Family 8: $6q\#\{3q-2p, q-2p, q+2p\}; \{2q, 3q-3p, 3p\}$, $p = 1, \ldots, \lfloor \frac{3q}{2} \rfloor$

Family 9: $6q\#\{3q-3p, 6p, 3p\}; \{q+4p, 3q-4p, q-4p\}$, $p = 1, \ldots, \lfloor \frac{q}{2} \rfloor$

Verification of the validity of these families proceeds by verifying the cosine condition, using standard trigonometric identities: the identity $\cos(a)\cos(b) = \frac{1}{2}(\cos(a+b)+\cos(a-$

$b)$) is especially useful. For example, to see that Family 1 works, note that in the cosine condition, if $\phi = \frac{\pi}{6q}$,

$$\begin{aligned}
\text{LHS} &= \cos(2q\phi)\cos((q-p)\phi)\cos(3p\phi) \\
&= \cos\left(\frac{\pi}{3}\right)\cos((q-p)\phi)\cos(3p\phi) \\
&= \frac{1}{2}\cos((q-p)\phi)\cos(3p\phi) \\
&= \frac{1}{4}\left(\cos((q-p+3p)\phi) + \cos(((q-p)-3p)\phi)\right) \\
&= \frac{1}{4}\cos((q+2p)\phi) + \frac{1}{4}\cos((q-4p)\phi).
\end{aligned}$$

On the other hand,

$$\begin{aligned}
\text{RHS} &= \cos((2q-p)\phi)\cos((q+2p)\phi)\cos(p\phi) \\
&= [\cos((2q-p)\phi)\cos(p\phi)]\cos((q+2p)\phi) \\
&= \frac{1}{2}\left(\cos((2q-p+p)\phi) + \cos((2q-p-p)\phi)\right)\cos((q+2p)\phi) \\
&= \frac{1}{2}\left(\cos\left(\frac{2q\pi}{6q}\right) + \cos((2q-2p)\phi)\right)\cos((q+2p)\phi) \\
&= \frac{1}{2}\left(\frac{1}{2} + \cos((2q-2p)\phi)\right)\cos((q+2p)\phi) \\
&= \frac{1}{4}\cos((q+2p)\phi) + \frac{1}{2}\cos((2q-2p)\phi)\cos((q+2p)\phi) \\
&= \frac{1}{4}\cos((q+2p)\phi) + \frac{1}{4}\left(\cos\left(\frac{3q\pi}{6q}\right) + \cos((q-4p)\phi)\right) \\
&= \frac{1}{4}\cos((q+2p)\phi) + 0 + \frac{1}{4}\cos((q-4p)\phi),
\end{aligned}$$

so the cosine condition is satisfied. In practice, it is easier to let a computer algebra system verify the cosine condition.

Consider all $m \leq 120$ which are divisible by 6 but not 12, that is,

$$m = 18, 30, 42, 54, 66, 78, 90, 102, 114.$$

For $m = 18, 54, 78, 102, 114$ these nine families completely exhaust the experimentally derived configurations. For $m = 30, 42, 90$ we expected that there would be additional configurations, because these are values of m which yielded sporadic 2-celestial configurations, and this expectation was fulfilled.

Surprisingly, there is a collection of cohorts for $m = 66$, given in Table 3, in addition to the cohorts have already been identified as $2q$, $3q$ and $6q$ cohorts, which do not seem to be part of a systematic infinite family. However, they do satisfy the following family description:

$$66\#\{24p, 12p, 6p\}; \{11+6p, 11+3p, 2\cdot 11-3p\}, \quad p = 1, \ldots, 10$$

and

$$66\#\{24p, 12p, 6p\}; \{11+6p, 2\cdot 11, 11-6p\}, \quad p = 1, \ldots, 5$$

Table 3: The unexpected 3-celestial cohorts for $m = 66$.

$m = 66$	
$\{24, 12, 6\}; \{19, 17, 14\}$	$\{30, 12, 6\}; \{29, 19, 4\}$
$\{24, 12, 6\}; \{22, 17, 5\}$	$\{30, 18, 6\}; \{29, 20, 13\}$
$\{24, 18, 12\}; \{23, 17, 16\}$	$\{30, 18, 6\}; \{29, 22, 7\}$
$\{24, 18, 12\}; \{23, 22, 1\}$	$\{31, 7, 2\}; \{30, 18, 6\}$
$\{25, 8, 5\}; \{24, 12, 6\}$	$\{31, 22, 13\}; \{30, 24, 18\}$
$\{28, 5, 1\}; \{24, 18, 12\}$	$\{31, 23, 10\}; \{30, 24, 18\}$
$\{30, 12, 6\}; \{25, 22, 19\}$	$\{32, 13, 1\}; \{30, 24, 18\}$
$\{30, 12, 6\}; \{26, 25, 7\}$	

These cohorts, along with the $2q$, $3q$ and $6q$ cohorts, exhaust the data for $m = 66$ but they do not appear to obviously generalize to an additional $6q$ family.

5.2 $m = 12q$

For 3-celestial configurations with m divisible by 12, in addition to the $6q$ families discussed in the previous section, there are three known $12q$ families:

- $12q\#\{5q, 3p, q\}; \{4q + p, 4q - p, p\}$, $p = 1, \ldots, 2q - 1$
- $12q\#\{5q, q, 6q - 4p\}; \{6q - p, 2p, p\}$, $p = 1, \ldots, 3q - 1$
- $12q\#\{5q, 6q - 4p, q\}; \{6q - 2p, 3q + p, 3q - p\}$, $p = 1, \ldots, q - 1$

The $2q, 3q, 6q$ and $12q$ families completely exhaust the known data for all $m \leq 120$ except for the following cases.

- $m = 66, 70, 105$: conjectured sporadic cohorts (the 66 family is "classified" but does not appear to generalize)
- $m = 30, 60, 90, 120$: there are four known $30q$ families (see below), but there are more systematic families yet to be found.
- $m = 42, 84$: almost certainly there are systematic families, but none have been found yet.

5.3 $m = 30, 42, 60$

These are very complicated. Note that for 2-celestial configurations, sporadic configurations exist precisely when $m = 30, 42, 60$. Thus additional families, and probably additional sporadic cases, are to be expected for these values.

Known familes for m divisible by 30 are the following.

- $30q\#\{15q - p, 10q, p\}; \{15q - 2p, 12q, 6q\}$
- $30q\#\{15q - p, 12q, p\}; \{15q - 2p, 13q, 7q\}$
- $30q\#\{15q - p, 6q, p\}; \{15q - 2p, 11q, q\}$
- $30q\#\{12q, 6q, 3p\}; \{10q + p, 10q - p, p\}$

These are not exhaustive.

6 4-celestial families

The situation with 4-celestial configurations is considerably less well-understood than the 3-celestial configurations. A few infinite families have been discovered, for m divisible by 2, 3, 6, 10, but the data suggest that the complete story is not yet known.

In particular, unlike the case of 2-celestial and 3-celestial configurations, there are a few known 4-celestial configurations for prime m. A single cohort exists for $m = 17$, and there are two cohorts for $m = 61$. These are listed in Table 4.

Table 4: Known 4-celestial cohorts for prime m.

$$\begin{array}{l} m = 17 \\ \quad \{8, 4, 2, 1\}; \{7, 6, 5, 3\} \\ m = 61 \\ \quad \{28, 24, 8, 1\}; \{26, 21, 19, 17\} \\ \quad \{29, 25, 24, 8\}; \{28, 27, 21, 18\} \end{array}$$

Like the case for 3-celestial configurations, we discovered some systematic families of 4-celestial configurations; these families have two parameters in addition to q.

- $2q\#\{q-p, p, 2p, q-4r\}; \{q-r, r, 2r, q-4p\}$
- $3q\#\{q+p, q-p, p, 3r\}; \{q+r, q-r, r, 3p\}$
- $6q\#\{p, q+2p, q+2r, 2q-p\}; \{3p, q-r, q-p, 2q+r\}$
- $10q\#\{p, 5q-p, r, 5q-r\}; \{2q, 4q, 5q-2r, 5q-2p\}$

However, these are far from exhaustive.

7 Other families

7.1 The general case where $m = 2q$

We found a single family of systematic 2^{k+1}-celestial configurations for even m:

$$2q\#\{q-p, p, 2p, 4p, \ldots, 2^{k-1}p, q-2^k r\}; \{q-r, r, 2r, 4r, \ldots, 2^{k-1}r, q-2^k p\} \quad (7.1)$$

Note that the previously-known 3-celestial family with m divisible by 2, mentioned in Section 4, is the case $k = 1$ of this family, and the 4-celestial case where $k = 2$ is mentioned in Section 6.

We require the following lemma, whose proof is a straightforward induction on k; the base case is the trigonometric identity

$$\sin(2\theta) = 2\sin(\theta)\cos(\theta)$$

in the case where $\theta = \frac{r\pi}{m}$.

Lemma 7.1. *If k, r, m are positive integers, then*

$$\sin\left(\frac{2^k r\pi}{m}\right) = 2^k \sin\left(\frac{r\pi}{m}\right)\cos\left(\frac{2^0 r\pi}{m}\right)\cos\left(\frac{2^1 r\pi}{m}\right)\cdots\cos\left(\frac{2^{k-1} r\pi}{m}\right).$$

To see that the family in (7.1) works, it suffices to show that the cosine condition is satisfied. Note that

$$\cos\left(\frac{(q-p)\pi}{m}\right) = \sin\left(\frac{p\pi}{2q}\right)$$

and

$$\cos\left(\frac{(q-2^k r)\pi}{2q}\right) = \sin\left(\frac{(2^k r)\pi}{m}\right).$$

Interpreting the left-hand cohort as a product of cosines and simpifying, we see that

$$\begin{aligned} LHS &= \cos\left(\frac{(q-p)\pi}{m}\right)\left[\cos\left(\frac{(p)\pi}{m}\right)\cos\left(\frac{(2p)\pi}{m}\right)\cos\left(\frac{(4p)\pi}{m}\right)\cdots \right. \\ &\qquad \left. \cos\left(\frac{(2^{k-1}p)\pi}{m}\right)\right]\cos\left(\frac{(q-2^k r)\pi}{m}\right) \\ &= \sin\left(\frac{(p)\pi}{m}\right)\left[\prod_{i=0}^{k-1}\cos\left(\frac{(2^i p)\pi}{m}\right)\right]\sin\left(\frac{(2^k r)\pi}{m}\right) \\ &= \frac{1}{2^{k-1}}\sin\left(\frac{2^k p\pi}{m}\right)\sin\left(\frac{(2^k r)\pi}{m}\right) \quad \text{(applying Lemma 7.1)} \end{aligned}$$

Since the left-hand and right-hand cohorts are symmetric in p and r, the right-hand cohort also simplifies to

$$\frac{1}{2^{k-1}}\sin\left(\frac{(2^k r)\pi}{m}\right)\sin\left(\frac{(2^k p)\pi}{m}\right)$$

so the entire cohort satisfies (A3), the cosine condition.

7.2 The general case where $m = 10q$

Case 1: $4 \mid h$. There is an infinite family of $4j$-celestial 4-configurations when $m = 10q$ and $h = 4j$, of the form

$$\begin{aligned} 10q\#\{&p_1, \ldots, p_{2j}, 5q-p_1, \ldots, 5q-p_{2j}\}; \\ &\{\underbrace{2q, \ldots, 2q}_{j}, \underbrace{4q, \ldots, 4q}_{j}, 5q-2p_1, \ldots, 5q-2p_{2j}\}. \end{aligned} \tag{7.2}$$

The 4-celestial family mentioned in Section 6 is the case $j = 1$.

To see that this family satisfies the cosine condition, let $\phi = \frac{\pi}{10q}$ and note that in the left-hand side, for each i, the pair

$$\begin{aligned} \cos((5q-p_i)\phi)\cos(p_i\phi) &= \frac{1}{2}\left(\cos\left(\frac{5q\pi}{10q}\right) + \cos((5q-2p_i)\phi)\right) \\ &= \frac{1}{2}\cos((5q-2p_i)\phi), \end{aligned}$$

so the entire left-hand side of the cosine condition becomes

$$\left(\frac{1}{2}\right)^{2j} \prod_{i=1}^{2j} \cos((5q - 2p_i)\phi) = \frac{1}{4^j} \prod_{i=1}^{2j} \cos((5q - 2p_i)\phi).$$

On the other hand, note that in the right-hand side, we have $\prod_{i=1}^{2j} \cos((5q - 2p_i)\phi)$ already. Finally, note that each of the j pairs

$$\begin{aligned}
\cos\left(\frac{2q\pi}{10q}\right)\cos\left(\frac{4q\pi}{10q}\right) &= \frac{1}{2}\left[\cos\left(\frac{6q\pi}{10q}\right) + \cos\left(\frac{4q\pi}{10q}\right)\right] \\
&= \frac{1}{2}\left[\cos\left(\frac{3\pi}{5}\right) + \cos\left(\frac{\pi}{5}\right)\right] \\
&= \frac{1}{2}\left(\frac{1}{4}(1-\sqrt{5}) + \frac{1}{4}(1+\sqrt{5})\right) \\
&= \frac{1}{2}\left(\frac{1}{4} + \frac{1}{4}\right) \\
&= \frac{1}{4}.
\end{aligned}$$

Thus, the entire right-hand side equals $\frac{1}{4^j}\prod_{i=1}^{2j} \cos((5q - 2p_i)\phi)$, so the cosine condition is satisfied.

Case 2: $3 \mid h$**.** A similar infinite family exists when $m = 10q$ and $3 \mid h$: if $h = 3j$, then

$$10q\#\{p_1, 2p_1, 5q - 2p_1, \ldots, p_j, 2p_j, 5q - 2p_j\}, \\ \{2q, 4q, 5q - 4p_1, \ldots, 2q, 4q, 5q - 4p_j\} \quad (7.3)$$

is a $3j$-celestial infinite family. Again, the 3-celestial family discussed in Section 4 is the case $j = 1$.

The proof is similar to the previous family. Each right-hand triple $\{2q, 4q, 5q - 4p_i\}$ becomes a multiplicand $\frac{1}{4}\cos((5q-4p_i)\phi)$ in the cosine condition. On the other side, each left-hand triple $\{5q - p, p, 2p\}$ becomes

$$\begin{aligned}
[\cos((5q - p)\phi)\cos(p\phi)]\cos(2p\phi) &= \frac{1}{2}\left[\cos\left(\frac{5q\pi}{10q}\right) + \cos((5q - 2p)\phi)\right]\cos(2p\phi) \\
&= \frac{1}{2}\cos((5q - 2p)\phi)\cos(2p\phi) \\
&= \frac{1}{2}\left(\frac{1}{2}\left(\cos\left(\frac{5q\pi}{10q}\right) + \cos((5q - 4p)\phi)\right)\right) \\
&= \frac{1}{4}\cos((5q - 4p)\phi).
\end{aligned}$$

so the cosine condition is satisfied using any number of appropriate triples in the cohorts.

8 Open questions for the classification of celestial 4-configurations

Despite these classification results, there is clearly a lot about celestial configurations that is poorly understood.

Question 8.1. Are the 3-celestial cohorts for $m = 70$, $m = 105$ sporadic, or are they members of an infinite family?

Question 8.2. Identify more systematic families of 3-celestial configurations for m divisible by $30, 42, 60$. Are there systematic families for $m = 90$, $m = 120$ that are not multiples of smaller families? (Compare the situation for $m = 6q$ and $m = 12q$; there are families for $m = 12q$ that are different from the smaller $6q$ families.)

Question 8.3. What's going on with the "sporadic family" of 3-celestial cohorts found for $m = 66$? Does it generalize?

Question 8.4. In [16], M. Laczkovich discussed methods for identifying all rational solutions

$$\sin(\pi p_1)\sin(\pi p_2)\sin(\pi p_3) = \sin(\pi q_1)\sin(\pi q_2)\sin(\pi q_3).$$

If all solutions to this equation were known, then, using techniques similar to the classification of 2-celestial configurations, it should be possible to classify all 3-celestial configurations. However, Laczkovich's results are not presented in an obviously accessible way for this purpose. How can his results be used to classify 3-celestial configurations, or at least to identify new families?

For $m \leq 120$, there are no 3-celestial configurations for prime m. However, there is one 4-celestial cohort with $m = 17$, and there are two 4-celestial cohorts for $m = 61$.

Question 8.5. Are there any 3-celestial configurations for prime m or prime powers m? Are there other 4-celestial configurations for prime m? prime powers?

Question 8.6. Identify new systematic families of 4-celestial configurations, especially for m divisible by 6.

Question 8.7. Given a known family, is there a general technique to apply "cosine trickery" to produce a different family that has related parameters? That is, from a single infinite family, are there a number of "combinatorially related" infinite families that can be produced?

Question 8.8. For $h = 3$ and $h = 4$, systematic families for $m = 2q, 3q$ and $10q$ have been identified. Two of these ($m = 2q$ and $m = 10q$) correspond to infinite families for infinitely many h. Is there a corresponding infinite family of h-celestial configurations for $m = 3q$? Are there infinite families of h-celestial configurations for $m = 2q$ when h is not a power of 2? Are there more infinite families when $m = 10q$?

9 Data

Raw data is available at

`https://sites.google.com/a/alaska.edu/lwberman/`.

It was produced using *Mathematica*.

Acknowledgements

The authors thank the Ursinus College Summer Fellows Program for funding the initial part of this project.

References

[1] L. W. Berman, A characterization of astral (n_4) configurations, *Discrete Comput. Geom.* **26** (2001), 603–612.

[2] L. W. Berman, Even astral configurations, *Electron. J. Combin.* **11** (2004), Research Paper 37, 23 pp. (electronic).

[3] L. W. Berman, Movable (n_4) configurations, *Electron. J. Combin.* **13** (2006), Research Paper 104, 30 pp. (electronic).

[4] L. W. Berman, Some results on odd astral configurations, *Electron. J. Combin.* **13** (2006), Research Paper 27, 31 pp. (electronic).

[5] L. W. Berman and N. A. Burtt, A new construction for symmetric $(4, 6)$-configurations, *Ars Math. Contemp.* **3** (2010), 165–175.

[6] L. W. Berman and B. Grünbaum, Deletion constructions of symmetric 4-configurations. Part I, *Contrib. Discrete Math.* **5** (2010), 18–33.

[7] A. Betten, G. Brinkmann and T. Pisanski, Counting symmetric configurations v_3, in: *Proceedings of the 5th Twente Workshop on Graphs and Combinatorial Optimization (Enschede, 1997)*, volume 99, 2000 pp. 331–338, doi:10.1016/S0166-218X(99)00143-2.

[8] M. Boben and T. Pisanski, Polycyclic configurations, *European J. Combin.* **24** (2003), 431–457, doi:10.1016/S0195-6698(03)00031-3.

[9] B. Grünbaum, Configurations, 1991, unpublished course notes.

[10] B. Grünbaum, Astral (n_k) configurations, *Geombinatorics* **3** (1993), 32–37.

[11] B. Grünbaum, Astral (n_4) configurations, *Geombinatorics* **9** (2000), 127–134.

[12] B. Grünbaum, Configurations of points and lines, in: *The Coxeter legacy*, Amer. Math. Soc., Providence, RI, pp. 179–225, 2006.

[13] B. Grünbaum, Musings on an example of Danzer's, *European J. Combin.* **29** (2008), 1910–1918, doi:10.1016/j.ejc.2008.01.004.

[14] B. Grünbaum, *Configurations of points and lines*, volume 103 of *Graduate Studies in Mathematics*, American Mathematical Society, Providence, RI, 2009.

[15] B. Grünbaum and J. F. Rigby, The real configuration (21_4), *J. London Math. Soc. (2)* **41** (1990), 336–346, doi:10.1112/jlms/s2-41.2.336.

[16] M. Laczkovich, Configurations with rational angles and trigonometric Diophantine equations, in: *Discrete and computational geometry*, Springer, Berlin, volume 25 of *Algorithms Combin.*, pp. 571–595, 2003.

[17] D. Marušič and T. Pisanski, Weakly flag-transitive configurations and half-arc-transitive graphs, *European J. Combin.* **20** (1999), 559–570, doi:10.1006/eujc.1999.0302.

[18] G. Myerson, Rational products of sines of rational angles, *Aequationes Math.* **45** (1993), 70–82, doi:10.1007/BF01844426.

ARS MATHEMATICA CONTEMPORANEA

Also available at http://amc-journal.eu
ISSN 1855-3966 (printed edn.), ISSN 1855-3974 (electronic edn.)
ARS MATHEMATICA CONTEMPORANEA 7 (2014) 379–403

Embeddings of graphs of fixed treewidth and bounded degree*

Jonathan L. Gross

Columbia University, Department of Computer Science NY 10027 USA, New York, USA

Received 23 August 2012, accepted 28 August 2013, published online 5 December 2013

Abstract

Let $\mathcal{F}$ be any family of graphs of fixed treewidth and bounded degree. We construct a quadratic-time algorithm for calculating the genus distribution of the graphs in $\mathcal{F}$. Within a post-order traversal of the decomposition tree, the algorithm involves a full-powered upgrading of *production rules* and *root-popping*. This algorithm for calculating genus distributions in quadratic time complements an algorithm of Kawarabayashi, Mohar, and Reed for calculating the minimum genus of a graph of bounded treewidth in linear time.

Keywords: Genus distribution, partial genus distribution, treewidth, tree decomposition.

Math. Subj. Class.: 05C10

1 Introduction

For $i = 0, 1, 2, \ldots$, let $g_i(G)$ be the number of topologically distinct cellular embeddings of the graph G in the orientable surface S_i of genus i. The ***genus distribution*** of the graph G is the sequence of numbers

$$g_i(G) : i = 0, 1, \ldots$$

The smallest and largest numbers i such that $g_i(G)$ is positive are called the ***minimum genus*** and the ***maximum genus***, respectively, of the graph G. It is easily proved and well-known that there are cellular embeddings of a graph G in every surface whose genus lies between the minimum and the maximum. The set of numbers between (and including) the minimum and maximum genus is called the ***genus range*** of G.

*This paper was presented at the AMS Meeting of January, 2012 in Boston, MA.

E-mail address: gross@cs.columbia.edu (Jonathan L. Gross)

The main objective of this paper is to derive a quadratic-time algorithm to calculate the entire genus distribution for any family of simple graphs with fixed treewidth and bounded degree. Since the second barycentric subdivision of a general graph is a simple graph with the same genus distribution as the general graph to which it is homeomorphic, it follows that this can be extended to general graphs by subdividing edges.

This paper also introduces a general form of partial genus distribution for arbitrarily large degree and for arbitrary root-subgraphs, i.e., beyond vertices and edges, a relativized form of partial genus distribution modulo a fixed rotation system for its root subgraph, and a general form of production rules for iterative reassembly of a given graph from one or more small subgraphs.

Basic results on genus distribution

Five fundamental papers [10, 7, 18, 15, 20] of the present author and his co-authors Khan and Poshni have established methods for calculating the genus distribution of a graph that is constructed by various kinds of amalgamation of two graphs of known genus distribution. These papers also establish ways to calculate the genus distributions of chains and cycles of copies of graphs of known genus distribution. The methods developed in these papers include *recombinant strands, partitioned genus distributions, and production rules*.

More recently, combining these calculation methods with the algorithmic techniques of *post-order traversal* and *root-popping* has facilitated the calculation of genus distributions for 3-regular outerplanar graphs [8], for 4-regular outerplanar graphs [19], and for 3-regular Halin graphs [9]. Combining these same calculation methods with edge-addition [16] has led to the genus distribution of mesh graphs of the form $P_3 \times P_n$.

Connections of treewidth to embedding problem

Since the introduction of the concept of *treewidth* by Robertson and Seymour, bounding the treewidth has been widely used to obtain polynomial-time algorithms for problems that are otherwise NP-hard. In particular, deciding whether an arbitrarily selected graph can be embedded in a given surface is NP-complete [25]; however, for any class of graphs of bounded treewidth, Kawarabayashi, Mohar, and Reed [14] have derived a linear-time algorithm for calculating the minimum genus.

Although outerplanar graphs have treewidth 2, and although Halin graphs and $P_3 \times P_n$ meshes have treewidth 3 (see [3]), treewidth plays no explicit role in the calculation of genus distributions in any of the papers just mentioned. Indeed, the five fundamental papers on graph amalgamations cited above include applications to graphs of arbitrarily high treewidth and arbitrarily high degree. Nonetheless, the pastings in those papers occur in localities of the amalgamand graphs in which the treewidth and degree are bounded.

In the present paper, various key ideas from the earlier papers are abstracted, generalized, and combined with treewidth to yield a quadratic-time algorithm for the genus distribution of the graphs in any family of graphs of bounded degree and bounded treewidth. It will be apparent that as treewidth and degree increase, the multiplicative constant of the

quadratic term grows rapidly. Accordingly, one anticipates continued interest in the derivation of special methods for calculating the genus distributions of graph families of special interest.

TERMINOLOGY

In what follows, a ***graph*** is taken to be connected and simple, unless something else can be inferred from the immediate context. We use V_G and E_G to denote the vertex set and edge set of a graph G.

The embeddings are in oriented surfaces. Terminology used here is predominantly consistent with [13] and [1]. See also [17] and [28]. We abbreviate "face-boundary walk" as ***fb-walk***.

DEF. In this paper, a ***subgraph-rooted*** graph is a triple (G, H, u), where H is a subgraph of G and $u \in V_H$. The third parameter u is called the ***pivot***. Sometimes, the form (G, H) with no pivot is used. If $H \cong K_1$ or $H \cong K_2$, then the graph is ***vertex-rooted*** or ***edge-rooted***, respectively. When the context clarifies the meaning, the graph may simply be called ***rooted***.

Remark 1.1. Pivot vertices are used here to change the root subgraph as a sequence of graphs is formed in the process of reassembly of a given graph. In [8], we achieved a change of root with what we called "root-splitting". In [9], a change of root was accomplished by "pie-merges".

OUTLINE OF THIS PAPER

Section 2 of this paper describes treewidth from a perspective that is relevant to its use in the algorithm. Section 3 describes how a decomposition tree is used to analyze a graph into *fragments* to be amalgamated. Section 4 introduces a highly general way of partitioning the genus distribution of a graph; it shows that the number of cells of the partition depends only on the treewidth and the maximum degree, and not on the number of vertices of that graph. Section 5 shows that the number of ways to amalgamate a given pair of embeddings of graphs G and G' depends only on the degrees of the vertices of the subgraph of amalgamation. Section 6 describes production rules, as they occur in the algorithm. Section 7 describes and analyzes the genus distribution algorithm. Section 8 offers some conclusions about the algorithm and opportunities for future research.

This paper is largely self-contained, except for some details of the well-established methods of constructing productions (which is quite necessary for the algorithm), as in [10] and [18]. Prior experience with calculating genus distributions of graph amalgamations, especially as in [8] and [9], is likely to be quite helpful.

2 Treewidth

The usual definition of *treewidth* is based on the concept of *tree decomposition*. These are both due to Robertson and Seymour [21]. An excellent exposition is given by [3]. For applications of treewidth to topological graph theory, see [17].

DEF. Let $G = (V, E)$ be a graph, and T a tree with nodes 1, 2, ..., s. Let $\mathcal{X} = \{X_i \mid 1 \leq i \leq s\}$ be a family of subsets of V (associated with the respective nodes 1, 2, ..., s) whose union is V such that

- the induced graph on the set of images in T of each vertex of V is a subtree of T;
- for every edge uv in the graph G, there is a node i in the tree T such that both u and v are members of X_i.

Then the pair $(\mathcal{X}, T)$ is a ***tree decomposition*** of G, and the tree T is called a ***decomposition tree*** for G.

TERMINOLOGY. For the sake of clarity, we will refer to "vertices" and "edges" in the graph G and to "nodes" and "lines" in the tree T.

ABUSE OF NOTATION. Throughout this paper, we refer to the sets X_i of a decomposition tree as "nodes".

DEF. The ***width*** of a tree decomposition $(\mathcal{X}, T)$ equals

$$max\left\{|X_i| \;\middle|\; 1 \leq i \leq |V_T|\right\} - 1$$

DEF. The ***treewidth*** of a graph G is the smallest k such that G has a tree decomposition of width k.

Proposition 2.1. *A connected graph has treewidth 1 if and only if it is a tree.* □

Proposition 2.2 ([27])**.** *A connected graph has treewidth 2 if and only if it contains a cycle and does not contain a K_4-minor.* □

Proposition 2.3. *Every graph of treewidth 2 is planar.*
Proof. A non-planar graph has either K_5 or $K_{3,3}$ as a minor. Both these Kuratowski graphs have K_4 as a minor. By Proposition 2.2, a graph with a K_4-minor cannot have treewidth 2. □

TREEWIDTH CHARACTERIZATION WITH k-TREES

An alternative characterization of treewidth, in terms of k-trees (see, for instance, [4]), is the starting point of our present approach to genus distributions:

DEF. A ***k-tree*** is defined recursively:

- The complete graph K_{k+1} is a k-tree.
- If G is a k-tree and C is a k-clique in G, then the graph obtained by joining a new vertex to the vertices of C is a k-tree.

Proposition 2.4. *The **treewidth** of a graph G is the least number k such that G is a subgraph of a k-tree.*

Proof. The proof is a direct consequence of the definitions. □

FULL DECOMPOSITION TREES

DEF. A ***full decomposition tree of width*** k for a graph G is a decomposition tree T in which

- every node has $k+1$ vertices, and
- every pair of adjacent nodes intersects in k vertices.

We observe that each line of a full decomposition tree corresponds to the k vertices shared by the two nodes whose adjacency is represented by that line.

Proposition 2.5. *Let T be a full decomposition tree of treewidth k for an n-vertex graph G. Then $|V_T| = n - k$.*

Proof. Each node of the decomposition tree T contains $k+1$ vertices of G. Each line of T corresponds to k vertices of G. Since V_G is the union of the nodes of T, it follows that

$$\begin{aligned} n = |V_G| &= |V_T|(k+1) - |E_T|k \\ &= |V_T|(k+1) - (|V_T|-1)k \\ &= |V_T| + k \\ \therefore |V_T| &= n - k \end{aligned}$$

□

Running Example – Part 1. Figure 2.1 shows an 8-vertex graph of treewidth 2 and a full decomposition tree of width 2. We observe that the number of nodes of the full decomposition tree is $8 - 2 = 6$.

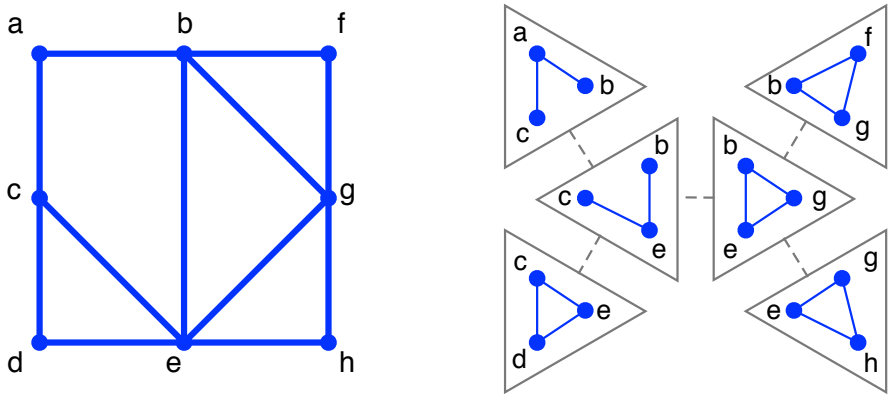

Figure 2.1: A graph, and a full decomposition tree of width 2, represented as a subgraph of a 2-tree.

The figure on the left is the graph itself. Each gray triangle on the right represents a 3-clique of the 2-tree. Each dashed gray line represents an adjacency of two 3-cliques in the 2-tree. Each node of the full decomposition tree is the set of vertices lying within one

of the gray triangles. The edges drawn within the gray triangles are a reminder of the adjacencies in the graph itself. In §3, the subgraphs shown within the gray triangles are called *node-fragments*.

Theorem 2.6. *Let G be a graph of treewidth k. Then G has a full decomposition tree of width k.*

Proof. Let T be a decomposition tree of width k for a graph G of treewidth k. If the vertex set from G in one of two adjacent nodes of T is contained in the other, then contract the line of T that joins those two nodes, and eliminate the smaller node. We observe that this operation does not change the width of the resulting tree. Iterate this operation until the resulting decomposition tree for G has the following property:

> (P_1) For every node $X_i \in V_T$ and for each of its neighboring nodes X_j, there is a vertex in X_i that does not lie in the node X_j.

For simplicity, we assume that the initial tree T already has property P_1. Since the maximum size of a node of T is $k+1$, and since no two adjacent nodes are identical, it follows that the intersection of any pair of adjacent nodes contains at most k vertices.

If some node X_i of tree T contains fewer than $k+1$ vertices, then choose a vertex from any neighboring node and insert a copy of it into node X_i. If the node X_i now contains every vertex in that neighbor, then contract the line of T that joins those two nodes. Iterate until every node of the resulting tree has $k+1$ vertices of G. By construction, this tree has property P_1. We may now assume that the initial tree T also has this property:

> (P_2) Every node $X_i \in V(T)$ has $k+1$ vertices of G.

Remark 2.7. It would be possible to design an algorithm for genus distribution that does not require the given decomposition tree to be converted into a full decomposition tree T. The reason we perform this conversion here is to simplify subsequent discussion, for instance, of the use of *partial genus distributions* in §4.

Now suppose that X_i and X_j are adjacent nodes of T such that

$$\begin{aligned} X_i &= \{v_1, \ldots, v_m, u_{m+1}, \ldots, u_{k+1}\} \\ X_j &= \{v_1, \ldots, v_m, w_{m+1}, \ldots, w_{k+1}\} \quad \text{and} \\ X_i \cap X_j &= \{v_1, \ldots, v_m\} \quad \text{where } m < k. \end{aligned}$$

Then replace the line (X_i, X_j) in T by the node path

$$\begin{aligned} X_i &= \{v_1, \ldots, v_m, u_{m+1}, \ldots, u_{k+1}\} \\ X_i^{(1)} &= \{v_1, \ldots, v_m, w_{m+1}, u_{m+2}, \ldots, u_{k+1}\} \\ X_i^{(2)} &= \{v_1, \ldots, v_m, w_{m+1}, w_{m+2}, u_{m+3}, \ldots, u_{k+1}\} \\ &\cdots \\ X_i^{(k-m)} &= \{v_1, \ldots, v_m, w_{m+1}, \ldots, w_k, u_{k+1}\} \\ X_j &= \{v_1, \ldots, v_m, w_{m+1}, \ldots, w_{k+1}\} \end{aligned}$$

The resulting tree is a full decomposition tree for G of width k. □

Corollary 2.8. *For any fixed treewidth k, there is an algorithm to construct a full decomposition tree for a given graph G of treewidth k in linear time in $|V_G|$.*

Proof. A linear-time algorithm to construct a decomposition tree T of width k for the graph G is given by [2]. Since the number of edges of such a tree is linear in $|V_G|$, it follows that a full decomposition tree for G of width k can be constructed from T within linear time. □

Corollary 2.9. *Let G be a graph of treewidth k, and let T be a full decomposition tree for G. Then there is a k-tree T^k with the following property:*

Each node of T is a $(k+1)$-clique of the k-tree T^k.

Proof. This is implied by the definition of a full decomposition tree. □

The genus distribution of a graph G is to be derived from the partial genus distributions of the induced graphs (in G) on the vertices in the respective nodes of the tree T, by iterative amalgamation. Various key ideas for deriving the genus distribution of a graph G by iterative amalgamation of a set of subgraphs of G are developed in [6], [7], [8], [9], [10], [15], [18], [19], and [20].

3 Fragments and Amalgamations

The algorithm to calculate the genus distribution of a graph G with bounded treewidth and bounded degree reassembles the graph G by iteratively amalgamating induced subgraphs on the nodes of a full decomposition tree for G.

DEF. A ***node-fragment of a graph*** G with respect to a decomposition tree T is the induced subgraph in G on the set of vertices of G that lie within a single node of T. For a leaf-node of T, the corresponding node-fragment may be called a ***leaf-fragment***.

DEF. Let (G, H, u) and (G', H', u') be an ordered pair of disjoint subgraph-rooted graphs, and let $\eta : H - u \to H' - u'$ be a graph isomorphism. ***Graph amalgamation*** is the operation that forms a new graph $G *_\eta G'$ from $G \cup G'$ by merging the subgraphs $H - u$ and $H' - u'$ as prescribed by η. In this paper, the subgraph H' becomes the new root subgraph, and a new pivot is chosen according to the post-order of the decomposition tree. This is illustrated in Part (2) of the Running Example.

NOTATIONAL CONVENTION. We denote the vertices and edges of the subgraph $H *_\eta H'$ of the amalgamated graph $G *_\eta G'$ by the same names as in the subgraph H of graph G, the first amalgamand. The vertices and edges that are contributed by only one amalgamand retain the names used in that amalgamand.

DEF. A ***fragment of a graph*** G with respect to a decomposition tree T for G is either a node-fragment or a ***compound fragment***, by which we mean the result of amalgamating any two fragments across the induced subgraphs of the vertices that lie in both of two adjacent nodes of the tree T. Every amalgamation in the reassembly of G from its fragments corresponds to a line of the decomposition tree T.

Given a graph G and a full decomposition tree T of width k, with T envisioned as drawn in the plane, it is clear that G can be reassembled by iteratively amalgamating fragments on pairs of vertices.

- We fix an arbitrary leaf-node of the tree T as a root of T, and we determine a post-order traversal of T based at that root-node.
- We observe that during a post-order traversal, every line of T is traversed twice. We amalgamate across a line whenever the second traversal of that line occurs.
- Each fragment of the graph G is a rooted subgraph of G. In any fragment F, the root subgraph is the induced graph in G on the node of T in which the fragment F meets the fragment to which it will be amalgamated. In a non-leaf-fragment, the root-subgraph is to be chosen according to the post-order of T.

LABELING FRAGMENTS AND SELECTING ROOTS OF FRAGMENTS

In order to discuss the process of iterative amalgamation, it is helpful to have some rules for assigning labels to fragments.

DEF. The ***label of a fragment*** F for a graph G with a full decomposition tree T of width k is of the form $G[x_1, \ldots, x_q; r_1, \ldots, r_k; r_{k+1}]$, where the vertex set of the fragment F is

$$\{x_1, \ldots, x_q, r_1, \ldots, r_k, r_{k+1}\}$$

- The vertices $r_1, \ldots, r_k, r_{k+1}$ are from whatever node of the fragment F will be pasted to another fragment in the next amalgamation involving F that occurs in the post-order.
- The root-subgraph of fragment F is the induced subgraph on vertices $r_1, \ldots, r_k$, r_{k+1}.
- Vertex r_{k+1} is the pivot.
- The vertices $x_1, \ldots, x_q$ are the remaining vertices of fragment F.

DEF. In the course of reassembly of a graph from its node-fragments by iterative amalgamation, for each fragment F, whether a node-fragment or a compound fragment, its ***partner fragment*** F' is the fragment to which F is amalgamated during the reassembly. Similarly, each node-fragment M has a ***partner node-fragment*** M'.

Running Example – Part 2. The root subgraph of a node-fragment is the node-fragment itself. In each node-fragment of Figure 3.1, the two vertices with bold labels are the first two to be pasted to another node. The third vertex in the node is the initial pivot. These are determined by the post-order traversal. We have taken the node $G[; c, e; d]$ at the lower left of the tree as the root-node of the decomposition tree and used a counter-clockwise traversal.

Here is the reassembly sequence for the graph of Figure 3.1.

1. The first node-fragment is $F_0 = G[; e, g; h]$.

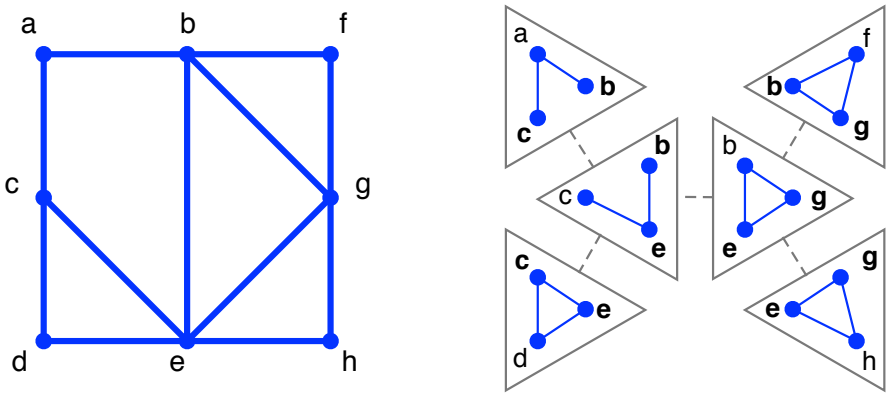

Figure 3.1: Roots of a decomposition 2-tree for a graph G.

2. The node-fragment (at the center-right) adjacent to F_0 is labeled $G[;e,g;b]$. When node-fragments $F_0 = G[;e,g;h]$ and its partner $F_0' = G[;e,g;b]$ are amalgamated, the resulting fragment is
$$F_1 = G[h;b,g;e]$$

3. When fragment $F_1 = G[h;b,g;e]$ is amalgamated with node-fragment $F_1' = G[;b,g;f]$, the resulting fragment is
$$F_2 = G[f,h;b,e;g]$$

4. When fragment $F_2 = G[f,h;b,e;g]$ is amalgamated with node-fragment $F_2' = G[;b,e;c]$, the resulting fragment is
$$F_3 = G[f,g,h;b,c;e]$$

5. When fragment $F_3 = G[f,g,h;b,c;e]$ is amalgamated with node-fragment $F_3' = G[;b,c;a]$, the resulting fragment is
$$F_4 = G[a,f,g,h;c,e;b]$$

6. When fragment $F_4 = G[a,f,g,h;e,c;b]$ is amalgamated with node-fragment $F_4' = G[;e,c;d]$, the resulting fragment is
$$F_5 = G[a,b,f,g,h;c,e;d] = G$$

We observe the following properties of each of the amalgamation in the sequence:

- The pivot of each of the amalgamand fragments F_i and F_i' is not a vertex of the other amalgamand fragment.
- The root-subgraph of the amalgamated fragment F_{i+1} is the root-subgraph of one of the amalgamand fragments F_i and F_i'. More precisely, it is whichever of the two root-subgraphs will be used whenever F_{i+1} is amalgamated to F_{i+1}'.

- The pivot of the amalgamated fragment F_{i+1} is the unique vertex in the root-subgraph that will *not* be merged with another vertex in the next amalgamation step involving fragment F_{i+1}.

Remark 3.1. Although the partner fragments F'_i were all node-fragments in this example, this would not be the case with a more complicated decomposition tree.

4 Partitioning the Genus Distribution

Partitioning the embeddings of a rooted graph has proven to be a highly useful technique in calculating genus distributions. A surface-by-surface inventory of the cells of the partition is called a *partitioned genus distribution*. The criteria for partitioning has been the incidence of fb-walks on the roots.

In the simplest case, we have a graph (G, v) rooted at a single 2-valent vertex v. We can then partition the genus distribution sequence $\{g_i(G) : i = 0, 1, \ldots\}$ into two ***partial genus distribution sequences***

$$d_i(G, v) : i = 0, 1, \ldots \qquad \text{and} \qquad s_i(G, v) : i = 0, 1, \ldots$$

where

- $d_i(G, v)$ is the number of embeddings of G in which two distinct fb-walks are incident on the root-vertex v; and
- $s_i(G, v)$ is the number of embeddings of G in which a single fb-walk is twice incident on the root-vertex v.

The prototypical approach to calculating these distributions is to construct simultaneous recursions for d_i and s_i and to obtain g_i by adding their solutions.

In the next smallest case, that of two 2-valent roots u and v, there are ten different partial genus distributions. For instance, in [10] and [7], we have defined

- $dd'_i(G, u, v)$ as the number of embeddings of G in S_i in which there are two different fb-walks incident on u, one of which is also incident on v, and another fb-walk incident on v that is not incident on u.
- $sd'_i(G, u, v)$ as the number of embeddings of G in S_i in which one fb-walk is twice incident on u and also incident on v, and another fb-walk is incident on v and not on u.

When there are multiple roots and/or a root-subgraph, the number of partial genus distributions sequences grows rapidly with the total number of root-vertices or of vertices in the root-subgraph. We can partition the genus distribution of a graph G into as many partial genus distributions as needed, the sum of which is the genus distribution sequence $\{g_i(G) : i = 0, 1, \ldots\}$.

In the general case now under consideration, the genus distribution of a subgraph-rooted graph (G, H, u) is partitioned here according to the cyclic sequence of incidences of fb-walks on the vertices of the root-subgraph H and on the pivot u. This section provides the details, an example, and an upper bound on the number of restricted sequences in the

partition corresponding to a graph of treewidth k and maximum degree Δ. This upper bound depends only on the treewidth and maximum degree of a graph, and not on its number of vertices.

DEF. A ***gapped word*** on the root-vertices $r_1, \ldots, r_k, r_{k+1}$ of a rooted graph (G, H, r_{k+1}) is a word on the alphabet $\{r_1, \ldots, r_k, r_{k+1}, \bullet\}$ that contains no two consecutive occurrences of the bullet $\bullet$, which is called a ***gap***. Each gapped word represents the cyclic order in which the various root-vertices occur in an fb-walk of an embedding. When two root-vertices r_i and r_j are separated by a gap symbol, it means that the subwalk of the corresponding fb-walk between r_i and r_j contains one or more non-root-vertices. When two root-vertices r_i and r_j are adjacent, it means that there is an edge $r_i r_j$ traversed by the fb-walk.

Two gapped words are equivalent if one is a cyclic permutation of the other. The principal representative of each equivalence class of gapped words is the one that is lexicographically first. We regard the bullet as lexicographically last, i.e., after all the root-vertices.

DEF. A multi-set of principal gapped words (written as a tuple) is called a ***root-phrase*** if

- each root-vertex occurs in the union of the gapped words as many times as its valence in G;
- the principal gapped words are in the order of non-increasing size, with lexicographic order used for tie-breaking.

Each root-phrase represents a cell of the partition of the embeddings of (G, H, u). Moreover, each root-phrase may be subscripted by an integer that represents the genus of a surface.

These two examples illustrate how a root-phrase is used in our generalization of partial genus distributions. (With larger root-subgraphs, some components of a root-phrase may have integer coefficients.)

Example 4.1. For non-adjacent roots u and v, $dd'_i(G, u, v)$ is represented by the root-phrase $(u\bullet v\bullet,\ u\bullet, v\bullet)_i$.

Example 4.2. For non-adjacent roots u and v, $sd'_i(G, u, v)$ is represented by the root-phrase $(u\bullet u\bullet v\bullet,\ v\bullet)_i$.

DEF. The ***partitioned genus distribution*** of (G, H, u) is a linear combination of the subscripted root-phrases, in which the coefficient of each subscripted root-phrase is the number of oriented embeddings of G corresponding to that root-phrase, in the surface whose genus equals the particular subscript.

DEF. We use the abbreviation ***pgd*** for partitioned genus distribution.

DEF. We observe that the restriction of the pgd of (G, H, u) to a single root-phrase, taken over all subscripts in the genus range, is the inventory of embeddings within a single partition cell, i.e., the cell corresponding to the given root-phrase. This inventory is called a ***partial genus distribution*** of (G, H, u). The word ***partial***, when used here as a noun, is a synonym for root-phrase. In this sense, we may say that the pgd is a linear combination of the subscripted partials.

Running Example – Part 3. The node-fragment $G[;e,g;h]$ has the following pgd:

$$(egh, ehg)_0 \tag{4.1}$$

The only embedding of that fragment has two (oriented) fb-walks, egh and ehg. Since all the vertices in the only two fb-walks are root-vertices, and since the root-vertices are mutually adjacent, there are no gaps in the gapped words of the only root-phrase. Similarly the node-fragment $G[;e,g;b]$ has the following pgd:

$$(beg, bge)_0 \tag{4.2}$$

The compound fragment $G[h;b,g;e]$ has the pgd

$$(be\bullet g, bge, eg\bullet)_0 + (bg \bullet e, beg, e\bullet g)_0 + (beg\bullet ebge\bullet g)_1 + (be\bullet gebg\bullet eg)_1 \tag{4.3}$$

To see this most easily, one draws the four embeddings and traces the fb-walks in each embedding.

NOTATION. We use $p(n)$ to denote the number of partitions of a positive integer n. We recall the asymptotic formula of Hardy and Ramanujan:

$$p(n) \sim \frac{1}{4n\sqrt{3}}\, e^{\pi\sqrt{\frac{2n}{3}}} \qquad \text{as } n \longrightarrow \infty$$

We use the number of partitions toward an upper bound on the number of partials of a rooted graph.

NOTATION. We denote the ***degree of a vertex*** v of a graph Y by $\delta_Y(v)$. If Y is a subgraph of a graph X, this convention distinguishes the degree of vertex v in the subgraph Y from its degree in X.

Theorem 4.3. *Let $\mathcal{F}$ be a family of graphs of treewidth k and maximum degree Δ, each of which is rooted on an isomorphic copy of a fixed graph H, in which $V_H = \{r_1, \ldots, r_k\}$. Then the number of partials associated with amalgamating two arbitrary members of $\mathcal{F}$ across root-subgraph H is at most*

$$\frac{[k\Delta]!}{(\Delta!)^k} \cdot p(k\Delta) \cdot 2^{k\Delta}$$

That is, it has an upper bound that is independent of the number of vertices of the graphs being amalgamated.

Proof. Here we regard a root-phrase as a "raw" character string in the alphabet $V_H = \{r_1, \ldots, r_k\}$, into which gaps and commas are eventually inserted. The length of a raw character string for a graph G is $\sum_{i=1}^{k} \delta_G(r_i)$. (We need to use δ_G rather than δ_H because we are concerned with the degree of each vertex of H within the graph G, not just within H.) Thus, the cardinality of the set of raw character strings is

$$\frac{[\sum_{i=1}^{k} \delta_G(r_i)]!}{\prod_{i=1}^{k} \delta_G(r_i)!} \;\leq\; \frac{[k\Delta]!}{(\Delta!)^k}$$

We may insert the commas into each raw character string so that the number of characters between two successive commas is non-increasing, as one reads the string from beginning to end. The cardinality of the set of comma-enriched raw character strings so obtained is at most $p(k\Delta)$. The number of ways to insert from 0 to $k\Delta$ gaps into such a comma-enriched character string so that

- no two gaps are adjacent,
- no gap occurs immediately after a comma, and
- no gap occurs at the beginning of the first word

is at most $2^{k\Delta}$. We have pre-normalized the root-phrases so that no gap occurs at the beginning of a word and so that the gapped words are in the order of non-increasing length. Thus, every normalized gapped word is a member of the set of such gap-enriched, comma-enriched character strings. This establishes the upper bound of the theorem. □

When we are reassembling a graph G of treewidth k and maximum degree Δ from the node-fragments of a full decomposition tree, the k-vertex root-subgraph across which two fragments are amalgamated varies by one vertex at a time, as we traverse the decomposition tree. The isomorphism type of the root-subgraph across which we merge fragments may vary from one amalgamation to the next. Thus, rather than only with the partials associated with a fixed root-subgraph H, we need to be concerned with the set of all partials for root-subgraphs with a given number of vertices.

Theorem 4.4. *Let G be a graph of treewidth k and maximum degree Δ. Then the number of partials required when reassembling G from the node-fragments of a full decomposition tree of width k is at most*

$$\frac{[(k+1)\Delta]!}{(\Delta!)^{k+1}} \cdot p((k+1)\Delta) \cdot 2^{(k+1)\Delta}$$

That is, the number of partials has an upper bound that is independent of the number of vertices of the graph G.

Proof. As illustrated in Part 3 of the Running Example, we need to consider partials on $k+1$ symbols. The isomorphism type of the k-vertex subgraph of amalgamation may change from amalgamation to amalgamation, and we provide for this by permitting the locations of the gaps to vary in the root-phrases. Since at most one gap occurs between two letters of the alphabet, the number of ways to insert the gaps is at most $2^{(k+1)\Delta}$. □

NOTATION. For a subgraph-rooted graph (G, H), we denote the corresponding set of partials by $\mathcal{P}_H$.

5 Embeddings of the Amalgamated Graph

DEF. Let ρ and σ be rotation systems for graphs X and Y, respectively, such that Y is a subgraph of X. We say that they are ***consistent at a vertex*** v of Y if the rotation σ at v is the restriction of the rotation ρ at v. If at every vertex of V_Y, the rotation σ is the restriction

of the rotation ρ, then ρ and σ are ***consistent rotation systems***. Moreover, the embeddings corresponding to rotations systems ρ and σ are then called ***consistent embeddings***.

Given rotation systems ρ and σ for the rooted graphs (G, H) and (G', H') and an isomorphism $\eta : H \to H'$, such that the restriction of σ to $\eta(H)$ agrees with the restriction of σ to H', we seek to count or give an upper bound for the number of embeddings of the amalgamated graph $(G *_\eta G', H *_\eta H')$ that are consistent with ρ and σ. The balance of this section is directed toward that objective. We consider the configuration at each vertex of the subgraph H.

A list of citations of early studies of restricted rotation systems is given by [24].

Isolated vertices in the subgraph H

The following proposition is to be used when there is a vertex of the root-subgraph H that has no neighbors in H.

Proposition 5.1. *Let (G, H) and (G', H') be subgraph-rooted graphs and $\eta : H \to H'$ an isomorphism. Let ρ and σ be rotation systems for G and G' such that $\sigma = \eta \circ \rho \circ \eta^{-1}$. Let v be an isolated vertex of the root-subgraph H, that is, with $\delta_H(v) = 0$. Then the number of rotations at v of $(G *_\eta G', H *_\eta H')$ that are consistent with ρ and σ is*

$$\delta_G(v) \binom{\delta_G(v) + \delta_{G'}(v) - 1}{\delta_G(v)} \tag{5.1}$$

Proof. A rotation at vertex v in $(G *_\eta G', H *_\eta H')$ is a cyclic ordering of the edges of $(G *_\eta G', H *_\eta H')$ that are incident at v. We regard the edges of E_G incident on vertex v as partitioning a cycle into $\delta_G(v)$ compartments into which edges of $E_{G'}$ incident at v are to be inserted. Once one of these $\delta_G(v)$ compartments is selected as the location of some arbitrarily selected "first" edge of $E_{G'}$, there are $\delta_G(v) + 1$ compartments into which the remaining $\delta_{G'}(v) - 1$ edges can be inserted. Since the order of these remaining edges is fixed, we may regard each of them as a zero, and partition them with $\delta_G(v)$ ones. Therefore, the number of ways to insert these $\delta_{G'}(v) - 1$ edges equals the number of binary strings of length $\delta_G(v) + \delta_{G'}(v) - 1$ with $\delta_G(v)$ ones. □

Example 5.2. In [10], we amalgamate two vertex-rooted graphs (G, v) and (G', v') at 2-valent roots. Thus, $\delta_G(v) = \delta_{G'}(v) = 2$, and $\delta_H(v) = 0$. The number of rotations in the amalgamated graph that are consistent with a pair of rotations, one from G and one from G', is

$$\delta_G(v) \binom{\delta_G(v) + \delta_{G'}(v) - 1}{\delta_G(v)} = 2\binom{2+2-1}{2} = 2\binom{3}{2} = 6$$

Vertices of positive degree in the subgraph H

The case in which a vertex v of the root-subgraph H has positive degree requires sufficiently complicated notation, that it is useful to precede the general analysis by a definition, a lemma, and an example.

DEF. Let α and β be linear orderings of disjoint sets $S = \{x_1, \ldots, x_p\}$ and $T = \{y_1, \ldots, y_q\}$, respectively. We say that a linear ordering γ of the set $S \cup T$ is an ***interleaving of the orderings*** α and β if the restrictions of γ to S and T are identical to α and β, respectively.

Lemma 5.3. *The number of ways to interleave two sequences of respective lengths p and q is*

$$\binom{p+q}{q}$$

Proof. There is an obvious bijection from the set of interleavings to the set of binary strings of length $p + q$ with q ones. □

Example 5.4. We depict in Figure 5.1 an amalgamation $G * G'$ in which the vertex v of the root-subgraph H has degree 2 in H, degree 7 in G, and degree 5 in G'. The rotations at vertex v are

$$\begin{aligned} \rho \cap \sigma \text{ in } H: &\quad e_1, e_2 \\ \rho \text{ in } G: &\quad c_1^1, c_2^1, c_3^1, e_1,\ c_1^2, c_2^2, e_2 \\ \sigma \text{ in } G': &\quad d_1^1, d_2^1, e_1,\ d_1^2, e_2 \end{aligned}$$

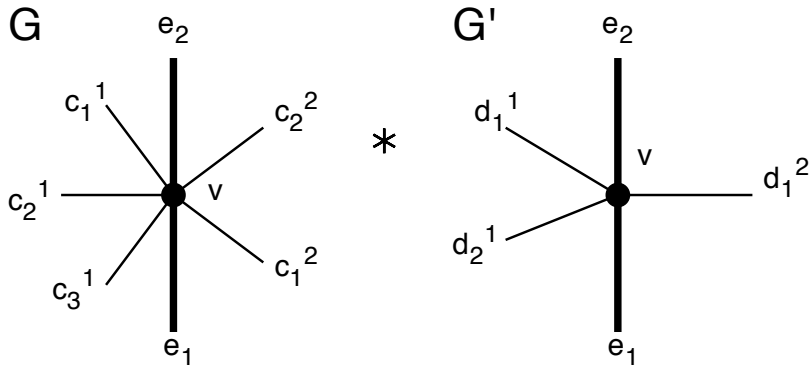

Figure 5.1: A vertex v of degree 2 in the (darkened) subgraph H, degree 7 in G, and degree 5 in G'.

The vertex v has degree 10 in the amalgamated graph $G * G'$. A rotation at v in $G * G'$ is consistent with the rotations ρ and σ if and only if the edge-sets $\{c_1^1, c_2^1, c_3^1\}$ and $\{d_1^1, d_2^1\}$ are interleaved between e_2 and e_1 and the edge-sets $\{c_1^2, c_2^2\}$ and $\{d_1^2\}$ are interleaved between e_1 and e_2. By Lemma 5.3, the number of rotations at v in $G * G'$ that are consistent with the rotations ρ and σ is

$$\binom{5}{2}\binom{3}{1}$$

Proposition 5.5. *Let (G, H) and (G', H') be subgraph-rooted graphs and $\eta : H \to H'$ an isomorphism. Let ρ and σ be rotation systems for G and G' such that $\sigma = \eta \circ \rho \circ \eta^{-1}$. Let v be a vertex of H with degree $\delta_H(v) > 0$ and the following rotations:*

$$\begin{aligned}(\rho \cap \sigma)|_v \text{ in } H: &\quad e_1, e_2, \ldots, e_{\delta_H(v)}\\ \rho|_v \text{ in } G: &\quad c_1^1, c_2^1, \ldots, c_{\delta_1}^1, e_1,\ c_1^2, c_2^2, \ldots, c_{\delta_2}^2, e_2,\ \ldots, e_{\delta_H(v)}\\ \sigma|_v \text{ in } G': &\quad d_1^1, d_2^1, \ldots, d_{\delta'_1}^1, e_1,\ d_1^2, d_2^2, \ldots, d_{\delta'_2}^2, e_2,\ \ldots, e_{\delta_H(v)}\end{aligned}$$

Then the number of rotations at v in $(G *_\eta G', H *_\eta H')$ that are consistent with ρ and σ is

$$\prod_{i=1}^{\delta_H(v)} \binom{\delta_i + \delta'_i}{\delta_i} \tag{5.2}$$

Proof. A rotation $\tau|_v$ at v in $(G *_\eta G', H *_\eta H')$ is consistent with the rotations $\rho|_v$ and $\sigma|_v$ if and only if it has the following property:

> In the rotation $\tau|_v$, between two consecutive edges e_{i-1} and $e_i \in E_H$ (and between $e_{\delta_H(v)}$ and e_1) in the rotation $\rho \cap \sigma$, the edge sequences $c_1^i, c_2^i, \ldots, c_{\delta_i}^i$ and $d_1^i, d_2^i, \ldots, d_{\delta'_i}^i$ are interleaved.

By Lemma 5.3, the conclusion follows. □

Counting consistent rotation systems

We have now arrived at the goal of this section.

Theorem 5.6. *Let (G, H) and (G', H') be subgraph-rooted graphs and $\eta : H \to H'$ an isomorphism. Let ρ and σ be rotation systems for G and G' such that $\sigma = \eta \circ \rho \circ \eta^{-1}$. For each vertex $v \in V_H$, we have the rotation*

$$(\rho \cap \sigma)|_v \text{ in } H: e_1^v, e_2^v, \ldots, e_{\delta_H(v)}^v$$

according to the following parameter values:

- *$\delta_H(v)$ is the degree of v in H.*
- *If $\delta_H(v) \neq 0$, then for $j = 1, \ldots, \delta_H(v)$, let δ_j and δ'_j be the numbers of edges of E_G and $E_{G'}$, respectively, that lie between the edges e_{j-1} and e_j in the rotation $\rho|_v$ and in the rotation $\sigma|_v$, respectively (where $j-1$ is taken to be n if $j = 1$).*

Then the number of rotation systems for $(G *_\eta G', H *_\eta H')$ that are consistent with ρ and σ is

$$\prod_{\substack{v \in V_H \\ \delta_H(v)=0}} \delta_G(v) \binom{\delta_G(v) + \delta_{G'}(v) - 1}{\delta_G(v)} \cdot \prod_{\substack{v \in V_H \\ \delta_H(v)>0}} \prod_{i=1}^{\delta_H(v)} \binom{\delta_i(v) + \delta'_i(v)}{\delta_i(v)} \tag{5.3}$$

Proof. This follows from Proposition 5.1 and Proposition 5.5. □

Theorem 5.7. *Let $\mathcal{F}$ be a family of graphs of treewidth k and maximum degree Δ, each of which is rooted on an isomorphic copy of a spanning subgraph of K_{k+1}. Let (G, H), $(G', H') \in \mathcal{F}$, and let $\eta : H \to H'$ be an isomorphism. Let ρ and σ be rotation systems for G and G' such that $\sigma = \eta \circ \rho \circ \eta^{-1}$. Then the number of rotation systems for $(G *_\eta G', H *_\eta H')$ that are consistent with both ρ and σ is at most*

$$\left[\Delta\binom{2\Delta - 1}{\Delta}\right]^{k+1} \tag{5.4}$$

That is, it has an upper bound that is independent of the number of vertices of the graph G.

Proof. This theorem is a corollary of Theorem 5.6. □

SPECIAL CASE: AMALGAMATING ACROSS AN EDGE

The simplest case of amalgamating graphs (G, H) and (G', H') across isomorphic root-subgraphs with edges is the case in which the root-subgraphs are isomorphic to K_2. The subcase in which both endpoints of both root-edges are 2-valent was developed in [18].

Corollary 5.8. *Let ρ and σ be rotation systems for the rooted graphs (G, vw) and $(G', v'w')$, where the pasting matches vertices v and w with vertices v' and w', respectively. Then the number of embeddings of $(G *_\eta G', vw)$ that are consistent with ρ and σ is*

$$\binom{deg_G v + deg_{G'} v' - 2}{deg_G v - 1}\binom{deg_G w + deg_{G'} w' - 2}{deg_G w - 1} \tag{5.5}$$

Proof. Every embedding of $(G *_\eta G', vw)$ that is consistent with ρ and σ has its rotations completely determined by ρ and σ, except at the image of the vertices v and v' and at the image of the vertices w and w'. Figure 5.2 illustrates the situation. The names v and w for vertices in $G *_\eta G'$ adhere to the notational convention introduced in §3.

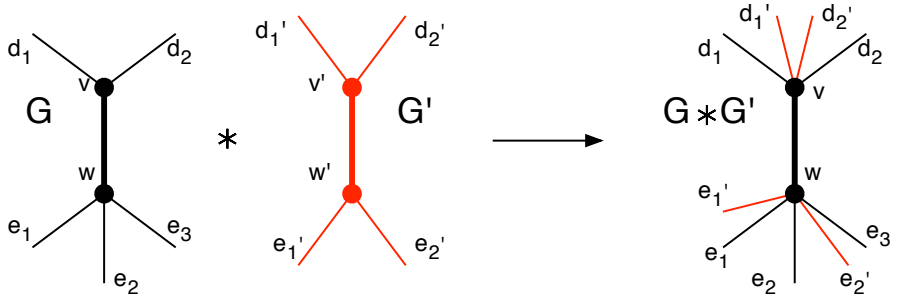

Figure 5.2: Amalgating two graphs on an edge.

Formula (5.5) follows from application of Theorem 5.6. □

Remark 5.9. In Corollary 5.8, the notation vw for the root-edge of the graph $G *_\eta G'$ is consistent with the notational convention given in §3 for naming the root-vertices and root-edges of $G *_\eta G'$.

6 Production Rules for Graph Amalgamations

DEF. A ***production*** for a graph operation is a rule that prescribes the effect on the genus distribution of applying that operation to its operands. That is, based on the partials of the operands and the genera of their respective embedding surfaces, it says how many embeddings the resulting graph has of each genus and of each type of partial. The operands and the operation appear at the tail of a right-arrow and are called the ***antecedent of the production***. The consequential information appears at the head of the right-arrow and is called the ***consequent of the production***.

Running Example – Part 4. A single production suffices to calculate the partial genus distribution (4.3) of the compound fragment $G[h; b, g; e]$ from partial genus distributions (4.1) and (4.2), for the node-fragments $G[; e, g; h]$ and $G[; e, g; b]$, respectively:

$$(egh, ehg)_i * (egb, ebg)_j \quad \longrightarrow_{[eg;\ eh,gh;\ eb,gb]} \begin{array}{l} (be\bullet g, bge, eg\bullet)_{i+j} + (bg\bullet e, beg, e\bullet g)_{i+j} \\ +(beg\bullet ebge\bullet g)_{i+j+1} + (be\bullet gebg\bullet eg)_{i+j+1} \end{array}$$

Remark 6.1. We observe that this production is asymmetric. That is, it converts the pivot vertex h of the earlier node-fragment in the post-order into a bullet.

This particular form of production is designed for reassembling a graph from a full decomposition tree by iterative amalgamation of fragments. In each case, all of the vertices of each of the two amalgamand-fragments lie in a single node within that fragment. For treewidth k, the two nodes intersect in k vertices. We observe that the subscript

$$[eg;\ eh, gh;\ eb, gb]$$

of the arrow operator contains three lists of edges.

1. The first list is the set of edges that lie in the root-subgraphs of both amalgamand fragments.
2. The second list contains the other edges that join vertices within the presenting node of the first amalgamand fragment.
3. The third list contains the other edges that join vertices within the presenting node of the second amalgamand fragment.

The antecedent of each production is a root-phrase with an integer variable as subscript, followed by an asterisk denoting amalgamation, and then another root-phrase with another integer variable as subscript. The consequent of each production is a sum of root-phrases, each of which has as its subscript a formula giving the genus of the surface of the amalgamated graph that corresponds to the two operand embeddings.

The coefficient of each such subscripted partial indicates in how many ways an fb-walk corresponding to that partial can be created by amalgamating two operand embeddings that correspond to the two partials in the antecedent. The sum of the coefficients is subject to the upper bound of Formula 5.3.

If the two root-phrases in the antecedent are inconsistent on the root-subgraph (which can occur for treewidth four or more), then the consequent is empty. We use the two

partials in the antecedent and the first list of edges in the subscript of the arrow operator to construct rotation systems for the set of embeddings of the amalgamated graph that are consistent with those two partials. Figure 6.1 illustrates the situation for Running Example – Part 4. For each of these rotation systems, we use the Heffter-Edmonds face-tracing algorithm to calculate the number of faces in the consequent embeddings relative to the sum of the numbers in the antecedent embeddings, after which we use the Euler polyhedral equate to calculate the corresponding increment or decrement in genus. The time required depends only on the root-subgraphs, not on the numbers of vertices in the amalgamands.

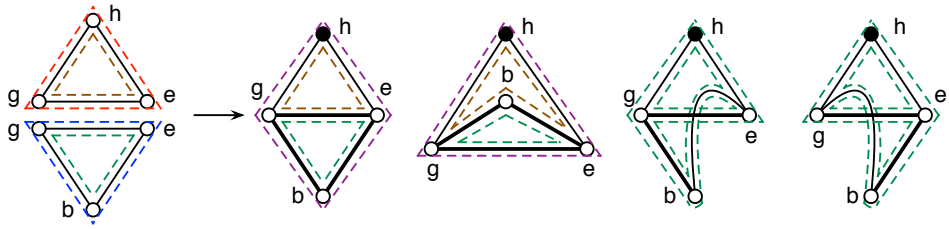

Figure 6.1: Deriving a production.

Theorem 6.2. *Let $\mathcal{G}$ be a family of subgraph-rooted graphs of treewidth at most k and maximum degree at most Δ, where k and Δ are fixed positive integers. Let $(G, H), (G', H') \in \mathcal{G}$, and let $\eta : H \to H'$ be an isomorphism. Then the number of productions required to calculate the pgd of $(G *_\eta G', H)$ from the pgd's of (G, H) and (G', H') is at most*

$$\left(\frac{[(k+1)\Delta]!}{(\Delta!)^{k+1}} \cdot p((k+1)\Delta) \cdot 2^{(k+1)\Delta} \right)^2$$

That is, the number of productions has an upper bound that is independent of the numbers of vertices of the graphs G and G'.

Proof. One needs a production for each ordered pair of partials used, and no more. Thus, the number of productions needed is at most the square of the number of partials determined by Theorem 4.4. □

Recurrences and closed forms

Productions were used in [10], and then in [7], [18], and [15] to derive systems of simultaneous recurrence relations for pgds. Using generating functions on the simultaneous recurrences, one can sometimes derive closed forms, as in [5].

7 Genus Distribution Algorithm

A skeletal version of the algorithm for calculating the genus distribution of the graphs in a family $\mathcal{G}$ of graphs of treewidth k and maximum degree at most $\Delta_{\mathcal{G}}$ is straightforward and intuitive.

Algorithm 7.1 (Genus Distribution Algorithm)**.**
Input: an n-vertex graph G of treewidth k and maximum degree Δ
Output: a pgd and the genus distribution for G.

Comment: INITIALIZE

1. Calculate a full decomposition tree T of width k for G.
2. Determine a post-order for decomposition-tree T, with the lines $\ell_1, \ell_2, \ldots, \ell_{n-k-1}$ in the post-order, so that the j^{th} amalgamation is across line ℓ_j.
3. For $j = 1, \ldots, n-k-1$,
   (a) Construct the subgraph-rooted node-fragment (M_j, M_j, u_j) as the induced graph on the j^{th} node of T in the post-order.
   (b) Identify the partner (M'_j, M'_j, u'_j), and construct the isomorphism $\eta_j : M_j - \{u_i\} \to M'_j - \{u'_i\}$
   Comment: "Partner" is defined in §3.
   (c) Calculate the pgd of the node-fragment (M_j, M_j, u_j).
4. Let $(F_1, H_1, u_1) = (M_1, M_1, u_1)$, and let (F'_1, H'_1, u'_1) be its partner, i.e., let $(F'_1, H'_1, u'_1) = (M'_1, M'_1, u'_1)$

Comment: MAIN LOOP REASSEMBLES G

5. For each line ℓ_j of the decomposition tree
   (a) Amalgamate the two fragments (F_j, H_j, u_j) and (F'_j, H'_j, u'_j) via the isomorphism η_j to produce the fragment F_{j+1}.
   (b) Let H_{j+1} be whichever of M_j or M'_j is the latter node-fragment in the post-order. Let the pivot u_{j+1} be whichever vertex of the root-subgraph H_{j+1} will not be pasted in the next amalgamation that involves the fragment F_{j+1}.
   (c) Use productions to calculate the pgd of $(F_{j+1}, H_{j+1}, u_{j+1})$ from the pgd's of (F_j, H_j, u_j) and (F'_j, H'_j, u'_j).

   Comment: CALCULATE g_i's BY SUMMING.
   N.B. We recall from §4 that for a subgraph-rooted graph (G, H), we denote the corresponding set of partials by $\mathcal{P}_H$.
6. For $i = 0, \ldots, \lfloor \beta(G)/2 \rfloor$, calculate $g_i(G)$ by the formula

$$g_i(G) \;=\; \sum_{\pi \in \mathcal{P}_{H_{n-k}}} \pi_i(G)$$

BREADTH OF THE GENUS RANGE

Analysis of Algorithm 7.1 uses the concept of *breadth of the genus range*.

DEF. The ***breadth of the genus range*** of a graph G is given by the equation

$$\gamma_B(G) \;=\; \gamma_{\max}(G) \;-\; \gamma_{\min}(G) \;+\; 1$$

Thus, $\gamma_B(G)$ is equal to the number of values of the index i such that $g_i(G) \geq 1$.

Proposition 7.1. *The breadth of the genus range of any graph G is at most $(2|E_G|+3)/6$.*

Proof.
$$\begin{aligned}\gamma_B(G) &= \gamma_{\max}(G) - \gamma_{\min}(G) + 1 \\ &\leq \frac{\beta(G)}{2} - \gamma_{\min}(G) + 1 \\ &\leq \frac{|E_G| - |V_G| + 1}{2} - \frac{|E_G| - 3|V_G| + 6}{6} + 1 \\ &= \frac{2|E_G| + 3}{6}\end{aligned}$$
□

Corollary 7.2. *Let $\mathcal{G}$ be a family of simple graphs of maximum degree at most $\Delta_{\mathcal{G}}$. Then the breadth of the genus range of any n-vertex graph G in $\mathcal{G}$ is at most $(n\Delta_{\mathcal{G}} + 3)/6$.*

Proof. Since $2|E_G| \leq n\Delta_{\mathcal{G}}$, by Euler's theorem on degree sum, this follows immediately from Proposition 7.1. □

Analysis of the algorithm

As established by [26], assigning an upper bound to the degree of a graph does not reduce the computational complexity of the minimum genus problem. Thus, bounding the treewidth is essential to the computational complexity of our algorithm.

Proposition 7.3. *Let $\mathcal{G}$ be a family of subgraph-rooted graphs, each of treewidth at most k and of maximum degree at most Δ, where k and Δ are fixed positive integers. Let $(G, H, u), (G', H', u') \in \mathcal{G}$ and let $\eta : H - \{u\} \to H' - \{u'\}$ be an isomorphism. Then the time required to calculate the pgd of $(G *_\eta G', H, u)$ from the pgd's of (G, H, u) and (G', H', u') is in $O(|V_G| \cdot |V_{G'}|)$.*

Proof. The time depends predominantly on the number of applications of productions, which depends, in turn, only on the product of the numbers of partials in the respective pgd's of G and G' with non-zero subscripted coefficients. The number of non-zero subscripted coefficients of the partials depends on the breadths of their genus ranges. This theorem now follows from Corollary 7.2 and Theorem 4.4. □

Theorem 7.4. *Let $\mathcal{G}$ be a family of graphs of treewidth at most k and maximum degree at most Δ, where k and Δ are fixed positive integers. Then the time needed to calculate the genus distribution of an n-vertex graph $G \in \mathcal{F}$, starting from a full decomposition tree T for G, is in $O(n^2)$.*

Proof. We proceed step by step.

Step 1. A full decomposition tree T for the graph G can be calculated in time proportional to $|V_T|$, which is in $O(n)$, by Corollary 2.8.

Step 2. The post-order of the decomposition tree T can be calculated in time proportional to $|V_T|$, which is in $O(n)$.

Substep 3a. The time needed to construct each of the node-fragments $M_1, \ldots, M_{n-k}$ from the given graph G is in $O(k^2)$, since each node of the decomposition tree T has $k+1$ vertices. The time for this substep is in $O(1)$.

Substep 3b. Each partner can be located by a post-order traversal. Each isomorphism η_j is an artifact of the tree decomposition. The time for this substep is in $O(1)$.

Substep 3c. There is a fixed upper bound of $(k!)^{k+1}$ for the number of embeddings of M_j, since M_j is a subgraph of the complete graph K_{k+1}. The time needed to determine the appropriate subscripted partial for each embedding of a node-fragment, by using the Heffter-Edmonds algorithm, is in $O(k\Delta_{M_j})$, that is, linear in the number of edges of the node-fragment, and constant, accordingly, with respect to $|V_G|$.

Step 3 total. Since there are $n-k$ node-fragments, by Proposition 2.5, it follows that the total time needed for Step 3 is in $O(n)$.

Step 4. This initializing step takes $O(1)$-time.

Substep 5a. The time needed to calculate a representation of the amalgamated graph F_{j+1} from representations of the amalgamands is proportional to $|E_{F_j}|+|E_{F'_j}|$, which is linear in $|V_{F_j}|+|V_{F'_j}|$, because the degree of the graph G is bounded. This substep takes $O(|V_{F_j}|+|V_{F'_j}|)$-time.

Substep 5b. This substep is achieved by referring to the post-order traversal of tree T.

Substep 5c. The number of productions is constant, by Theorem 6.2. The numbers of subscripted partials with non-zero coefficient in the pgd's of the amalgamand fragments are proportional to $\gamma_B(F_j)$ and $\gamma_B(F'_j)$, respectively. By Corollary 7.2, $\gamma_B(F_j)$ and $\gamma_B(F'_j)$ are proportional to $|V_{F_j}|$ and $|V_{F'_j}|$, respectively. By Proposition 7.3, the time for this substep is $O(|V_{F_j}| \cdot |V_{F'_j}|)$, subject to the assumption that multiplication of integers takes constant time.

Step 5 total. Let $\mathcal{S}$ denote the sequence of pairs of fragments that occurs in the reassembly of G from the node-fragments corresponding to the decomposition tree T. The time for each iteration of the body of the loop in Step 4 is dominated by the time needed for Substep 5c. Thus, the total time needed to calculate the pgd of G is at most

$$\sum_{(F,F')\in\mathcal{S}} c|V_F| \cdot |V_{F'}| \;=\; c \sum_{(F,F')\in\mathcal{S}} |V_F| \cdot |V_{F'}|$$

We further suppose that the number of vertices in the node-fragment F_i is n_i, for $i = 1, \ldots, n-k$, and we observe that in the total reassembly no two node-fragments occur twice as subgraphs of fragments that are amalgamated. It follows that

$$\begin{aligned} \sum_{(F,F')\in\mathcal{S}} |V_F| \cdot |V_{F'}| &= \sum_{i=1}^{n-k}\sum_{j=1}^{n-k} n_i n_j \;-\; \sum_{i=1}^{n-k} n_i^2 \\ &< (n_1 + n_2 + \cdots + n_{n-k})^2 \\ &= n^2 \end{aligned}$$

Step 6. Of course, each term $g_i(G)$ in the genus distribution for G is obtained from the pgd by summing all the coefficients of subscripted partials with subscript i. The time needed for

such a calculation of each $g_i(G)$ is proportional to the number of different partials, which is bounded by a constant. Thus, the time needed to calculate the genus distribution from the pgd is proportional to the size of the genus range, and thus, in $O(n)$. □

8 Conclusions

Stahl [22, 23] has called a family of graphs H-***linear*** if its members can be derived by iterative amalgamation of copies of a graph H, and he has introduced a form of production matrices whose elements are univariate polynomials, in which the degree of a term corresponds to an increment of genus as an additional copy of the graph H is amalgamated to a growing linear chain. The treewidth of the graphs in an H-linear family is the tree width of the graph H. Although the size of such matrices can be very large, corresponding to the number of partial genus distributions associated with a given maximum degree, it is of fixed size. Accordingly, the time-complexity needed to take a power of such a production matrix depends only on the time needed to multiply two polynomials of linearly increasing degree.

Practical algorithms for the genus distributions and partitioned genus distributions of the graphs in various interesting linear families of graphs, implicit in [23, 10, 15, 18, 11, 12], fall within the quadratic time-complexity upper limit given by Theorem 7.4. Moreover, quadratic-time calculation of genus distributions is implicit in [7, 19] for graph families, including circular ladders and Möbius ladders, that are not H-linear, but which could be characterized as *ring-like*. Beyond that, there is a practical quadratic-time algorithm for the cubic Halin graphs [9], which are a non-linear family.

We observe that in a genus distribution calculation by our algorithm, the partials and productions can be generated dynamically as needed, rather than in advance. This suggests the feasibility of implementing such an algorithm for graphs of reasonably small treewidth and maximum degree, since the number of productions needed might be far smaller than the total number possible for that treewidth and degree.

The exposition here illustrates once again how bounding the treewidth can be used to reduce otherwise NP-hard calculations regarding embeddings to polynomial time. Here we have also bounded the degree. This immediately suggests this general problem:

Research Problem 1. Determine whether the genus distribution of the graphs of bounded treewidth can be calculated in polynomial-time, if the degree is not bounded.

Of course, rather than being content with an algorithm with such a vast proliferation of partials and productions, one hopes for closed formulas or tractable recursions for interesting classes of graphs. A related line of investigation would involve bounding the treewidth and prescribing the minimum genus (which effectively bounds the average degree). The following two problems may be approachable.

Research Problem 2. Algorithms for calculating the genus distributions of 3-regular and 4-regular outerplanar graphs are given by [8] and [19], respectively. Calculate the genus distributions of arbitrary outerplanar graphs.

Research Problem 3. A ***Halin graph*** is obtained from a plane tree with at least four vertices and no vertices of degree two, by drawing a cycle through the leaves. An algorithm for the genus distribution of any 3-regular Halin graph is given by [9]. Calculate the genus distributions of arbitrary Halin graphs.

Research Problem 4. A remaining problem of self-evident theoretical interest is determination of a lower bound on the time needed to calculate the genus distribution of a graph of fixed treewidth and bounded maximum degree.

ACKNOWLEDGEMENT

The author wishes to thank Imran Khan and Mehvish Poshni for their many valuable comments on the early drafts of this paper. The author also wishes to thank an anonymous referee for various helpful suggestions.

References

[1] L. W. Beineke, R. J. Wilson, J. L. Gross and T. W. Tucker, Editors, *Topics in Topological Graph Theory*, Cambridge Univ. Press, 2009.

[2] H. L. Bodlaender, A linear-time algorithm for finding tree-decompositions of small treewidth, *SIAM J. Comput.* **25** (1996), 1305–1317.

[3] H. L. Bodlaender, A partial k-arboretum of graphs with bounded treewidth, *Theoretical Comp. Sci.* **209** (1998), 1–45.

[4] R. B. Borie, R. G. Parker and C. A. Tovey, Recursively constructed graphs, §2.4 (pp. 101–122) of *Handbook of Graph Theory*, second edition, eds. J. L. Gross, J. Yellen and P. Zhang, CRC Press (imprint of Taylor and Francis), 2014.

[5] M. L. Furst, J. L. Gross and R. Statman, Genus distribution for two classes of graphs, *J. Combin. Theory (B)* **46** (1989), 22–36.

[6] J. L. Gross, Genus distribution of graphs under surgery: adding edges and splitting vertices, *New York J. Math.* **16** (2010), 161–178.

[7] J. L. Gross, Genus distribution of graph amalgamations: Self-pasting at root-vertices, *Australasian J. Combin.* **49** (2011), 19–38.

[8] J. L. Gross, Genus distributions of cubic outerplanar graphs, *J. of Graph Algorithms and Applications* **15** (2011), 295–316.

[9] J. L. Gross, Embeddings of cubic Halin graphs: a surface-by-surface inventory, *Ars Math. Contemp.* **6** (2013), 37–56.

[10] J. L. Gross, I. F. Khan and M. I. Poshni, Genus distribution of graph amalgamations: Pasting at root-vertices, *Ars Combin.* **94** (2010), 33–53.

[11] J. L. Gross, I. F. Khan and M. I. Poshni, Genus distribution for iterated claws, preprint 2013, 20pp.

[12] J.L. Gross, T. Mansour, T.W. Tucker and D.G.L. Wang, Log-concavity of combinations of sequences and applications to genus distributions, draft manuscript, 2013.

[13] J. L. Gross and T. W. Tucker, *Topological Graph Theory*, Dover, 2001; (original edn. Wiley, 1987).

[14] K. Kawarabayashi, B. Mohar and B. Reed, A simpler linear time algorithm for embedding graphs into an arbitrary surface and the genus of graphs of bounded tree-width, *Proc. 49th Ann. Symp. on Foundations of Computer Science (FOCS'08)* IEEE (2008), 771–780.

[15] I. F. Khan, M. I. Poshni and J. L. Gross, Genus distribution of graph amalgamations at roots of higher degree, *Ars Math. Contemp.* **3** (2010), 121–138.

[16] I. F. Khan, M. I. Poshni and J. L. Gross, Genus distribution of $P_3 \square P_n$, *Discrete Math.* **312** (2012), 2863–2871.

[17] B. Mohar and C. Thomassen, *Graphs on Surfaces*, Johns Hopkins University Press, 2001.

[18] M. I. Poshni, I. F. Khan and J. L. Gross, Genus distribution of edge-amalgamations, *Ars Math. Contemporanea* **3** (2010), 69–86.

[19] M. I. Poshni, I. F. Khan and J. L. Gross, Genus distribution of 4-regular outerplanar graphs, *Electronic J. Combin.* **18** (2011) #P212, 25pp.

[20] M. I. Poshni, I. F. Khan and J. L. Gross, Genus distribution of graphs under self-edge-amalgamations, *Ars Math. Contemporanea* **5** (2012), 127–148.

[21] N. Robertson and P. D. Seymour, Graph minors. II, Algorithmic aspects of tree-width, *J. Algorithms* **7** (1986), 309–322.

[22] S. Stahl, Permutation-partition pairs. III. Embedding distributions of linear families of graphs, *J. Combin. Theory, Ser. B* **52** (1991), 191–218.

[23] S. Stahl, On the zeros of some genus polynomials, *Canad. J. Math.* **49** (1997), 617–640.

[24] J. Širáň and M. Škoviera, Relative embeddings of graphs on closed surfaces, *Math. Nachr.* **136** (1988), 275–284.

[25] C. Thomassen, The graph genus problem is NP-complete, *J. Algorithms* **10** (1989), 568–576.

[26] C. Thomassen, The genus problem for cubic graphs, *J. Combin. Theory (B)* **69** (1997), 52–58.

[27] J. A. Wald and C. J. Colbourn, Steiner trees, partial 2-trees, and minimum IFI networks, *Networks* **13** (1983), 159–167.

[28] A. T. White, *Graphs of Groups on Surfaces*, North-Holland, 2001.

ARS MATHEMATICA CONTEMPORANEA

Also available at http://amc-journal.eu
ISSN 1855-3966 (printed edn.), ISSN 1855-3974 (electronic edn.)
ARS MATHEMATICA CONTEMPORANEA 7 (2014) 405–421

Fullerene patches II

Jack E. Graver
Department of Mathematics, Syracuse University, Syracuse, NY 13244 USA

Christina Graves , Stephen J. Graves
Department of Mathematics, The University of Texas at Tyler, Tyler, TX 75799, USA

Received 3 October 2012, accepted 12 June 2013, published online 11 December 2013

Abstract

In this paper, we show that fullerene patches with nice boundaries containing between 1 and 5 pentagons fall into several equivalence classes; furthermore, any two fullerene patches in the same class can be transformed into the same minimal configuration using combinatorial alterations.

Keywords: Fullerenes, fullerene patches, pseudoconvex patches.

Math. Subj. Class.: 05C10, 05C75, 92E10

1 Introduction

A plane graph with all faces hexagonal except one external face, with all vertices on the boundary of the outside face having valence 2 or 3, and with all other vertices (called *internal vertices*) having valence 3 is called a *graphene patch*. One way to construct a graphene patch is to take a closed simple (non-self-intersecting) curve in Λ, the hexagonal tessellation of the plane, and replace all vertices, edges and faces outside the curve by a single outside face. It is clear that a graphene patch constructed in this way is uniquely determined (up to an isomorphism of plane graphs) by its *boundary code*; that is, the sequence of valences of boundary vertices in cyclic order. A boundary code can be written starting at any vertex and proceeding in either a clockwise or counterclockwise direction. Hence, a given boundary code is actually a representative of the equivalence class of codes under cyclic permutations and inversions.

E-mail address: jegraver@syr.edu (Jack E. Graver), cgraves@uttyler.edu (Christina Graves), sgraves@uttyler.edu (Stephen J. Graves)

However, not every graphene patch may be constructed in this way. Specifically, the boundary of a graphene patch may yield a self-intersecting curve when projected onto Λ. In this case, the patch may not be uniquely determined by its boundary code. In [9], Guo, Hansen, and Zheng described two nonisomorphic graphene patches with the same boundary code. We say that the boundary code of a graphene patch is *ambiguous* if there are two or more nonisomorphic graphene patches with the same boundary code. It is implicit in [4] that ambiguity for graphene patches is topological in the following sense: Consider two nonisomorphic graphene patches with the same boundary code and use the boundary code to trace the boundary as a self-intersecting circuit in Λ. We may think of this self-intersecting circuit as a local homeomorphism f of the unit circle into the plane. Then each patch gives an extension of f to a local homeomorphism into the entire disk. That these graphene patches are nonisomorphic corresponds to the fact that the extensions are not homotopic.

In this paper we investigate patches with ambiguous boundaries that include some pentagonal faces. In particular we will be interested in patches on a *fullerene:* a trivalent plane graph with only hexagonal and pentagonal faces. For the patches we consider, we show that the ambiguities are combinatoral rather than topological.

Definition 1.1. A *fullerene patch* or, in this paper, simply a *patch* is a plane graph with all faces hexagonal or pentagonal except for one external face of a different degree (not 5 or 6), with all vertices on the boundary of the external face having valence 2 or 3, and with all remaining *internal* vertices having valence 3. We again use the term *boundary code* to describe the sequence of valences of 2's and 3's in cyclic order on the boundary.

We will adopt the notation from [7] and let a patch be denoted as $\Pi = (V, E, F, B)$ where V and E are the vertex and edge sets, F is the set of faces *excluding* the external face, and B is the boundary of the external face. One method of constructing a patch is to take a simple closed curve on a fullerene, and consider the subgraph created by deleting all vertices and edges on the "outside" of the curve. However, the uniqueness property of similarly-constructed graphene patches does not hold for fullerene patches constructed in this way. In fact, very frequently nonisomorphic patches will have identical boundary codes. Even graphene patches formed from closed simple curves on fullerenes are not known to have unambiguous boundary.

Definition 1.2. Two patches with the same boundary code are *similar*. For any patch Π the collection of patches similar to Π is called its *similarity class* and is denoted by $\mathcal{S}(\Pi)$; the class is *trivial* when all patches in $\mathcal{S}(\Pi)$ are isomorphic.

In this paper we consider patches containing between 1 and 5 pentagons with "nice boundaries." We show that the similarity classes of these patches are of eight basic types and that for patches in the same similarity class there exists a sequence of combinatorial alterations that transforms one patch to another.

2 Linear patches

Let $\Pi = (V, E, F, B)$ be a patch. For any internal face $f \in F$, let $B(f)$ denote its boundary; so either $B(f) \cap B$ is empty or consists of one or more paths. These paths are the paths on the boundary B joining consecutive degree-3 vertices.

Definition 2.1. The paths of $B(f) \cap B$ over all f are called the *segments* of the boundary. If $B(f) \cap B$ consists of only one segment, then $|B(f) \cap B|$ is the length of the path. A segment of length i will be called an *i-segment*, and the number of i-segments in B will be denoted by s_i.

Definition 2.2. *Linear* patches are patches with $s_1 = 0$ consisting of strings of hexagons capped off at each end with a hexagon or a pentagon – see Figure 1.

In [7] it was shown that the similarity class of a linear patch with at most one pentagonal end is trivial. On the other hand, the similarity class of any linear patch with two pentagonal ends includes some additional nonlinear patches and is nontrivial, as is illustrated in Figure 3.

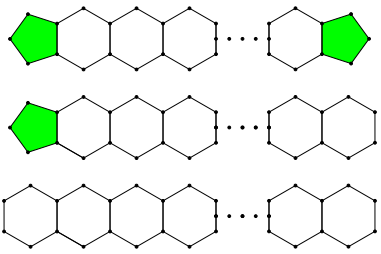

Figure 1: Linear patches.

Lemma 2.3. *Let $\Pi = (V, E, F, B)$ be a patch with $s_1 = 0$.*

1. *If Π admits a face f such that $B(f) \cap B$ consists of more than one segment, then Π is a linear patch.*
2. *If Π admits a pentagonal face f such that $|B(f) \cap B| = 4$, then Π is a linear patch.*
3. *If Π admits a hexagonal face f such that $|B(f) \cap B| = 5$, then Π is a linear patch.*

Proof. These results clearly hold for all patches with one or two faces. Let $\Pi = (V, E, F, B)$ be a patch with $s_1 = 0$ and $n > 2$ faces, and assume that these results hold for all such patches with fewer than n faces.

First assume that Π admits a face f such that $B(f) \cap B$ consists of more than one segment. Since $s_1 = 0$, each boundary segment has length at least 2. Thus f is a hexagon, each boundary segment of $B(f) \cap B$ has length 2, and f shares one edge with a face g and the antipodal edge with a face h. Deleting f leaves two subpatches, Π_g and Π_h, where

$|B(g)\cap B(\Pi_g)|\geq 5$ and $|B(h)\cap B(\Pi_h)|\geq 5$. So Π_g and Π_h are both linear by induction, and hence Π is linear.

Assume next that Π admits a pentagonal face f such that $|B(f)\cap B|=4$ or a hexagonal face f such that $|B(f)\cap B|=5$. Then f shares an edge with exactly one other face, g. Since Π has more than 2 faces, g has more than one boundary segment and we are back in the first case. □

It is convenient to treat linear patches and non-linear patches separately.

Lemma 2.4. *If $\Pi=(V,E,F,B)$ is a non-linear patch with $s_1=0$, then*

1. *for $f\in F$, $B(f)\cap B$ is empty or a single segment;*
2. *for $f\in F$, $|B(f)\cap B|=4$ implies f is a hexagon;*
3. *$s_5=0$;*
4. *$p(\Pi)=6-s_3-2s_4$, where $p(\Pi)$ is the number of pentagons contained in the patch Π.*

Proof. The first three conditions follow at once from Lemma 2.3. The fourth condition is a special case of the following direct consequence of Euler's formula, proved in [7]: $p(\Pi)=6+s_1-s_3-2s_4-3s_5$. □

It is an obvious consequence of this fourth condition that a non-linear patch with $s_1=0$ may contain at most six pentagonal faces. If Π is such a patch with six pentagonal faces, $s_3=s_4=s_5=0$. Hence its boundary consists of m segments of length 2, for some m. Adding a layer of hexagons around this boundary yields another patch with an identical boundary and m more faces; this is the F expansion defined in [10]. Therefore all non-linear patches with $s_1=0$ and six pentagonal faces have ambiguous boundary code, and in fact the similarity class of each is infinite. Thus we restrict our attention to non-linear patches with $s_1=0$ and with one to five pentagonal faces. Following [3]:

Definition 2.5. A *pseudoconvex patch* is a non-linear patch with $s_1=0$ containing one to five pentagonal faces.

3 Pseudoconvex patches

Pesudoconvex patches were discussed in detail in [8], and we use the same terminology here.

Definition 3.1. A *side* of a pseudoconvex patch is the section of the boundary (including the faces) between a consecutive pair of degree 2 vertices. The *length* of a side is one less than the number of faces on the side. Three consecutive degree 2 vertices on the boundary correspond to a side of length zero containing just one face.

For a pseudoconvex patch or a linear patch Π, we introduce several parameters and more notation:

1. $\ell(\Pi)$ denotes the sum of the lengths of every side;

2. $s = s(\Pi)$ denotes the number of sides of Π;
3. The cyclic sequence $[\ell_1, \ldots, \ell_s]$ denotes the side lengths of Π listed in cyclic order around the patch and is called the *side parameters* of the patch.
4. The similarity class $\mathcal{S}(\Pi)$ will also be denoted by $\mathcal{S}_{[\ell_1,\ldots,\ell_s]}$ when Π has side parameters $[\ell_1, \ldots, \ell_s]$.

The following lemma summarizes a few results proven in [8].

Lemma 3.2. *Let $\Pi = (V, E, F, B)$ be a pseudoconvex patch with side parameters $[\ell_1, \ldots, \ell_s]$. Then*

1. $s = s(\Pi) = 6 - p(\Pi)$.
2. *There are no consecutive 0's in $[\ell_1, \ldots, \ell_s]$.*
3. *If ℓ_s and ℓ_2 are both nonzero and all faces on the ℓ_1 side are hexagons (including both terminal 3-faces when $\ell_1 > 0$), deleting all of the faces on the ℓ_1 side of Π results in $\Pi' = (V', E', F', B')$ which is either a linear patch or another pseudoconvex patch. The side parameters of Π' are*
   (a) $[\ell_1 + 1, \ell_2 - 1, \ell_3, \ldots, \ell_{s-1}, \ell_s - 1]$, *when $s > 2$;*
   (b) $[\ell_1 + 1, \ell_2 - 2]$, *when $s = 2$;*
   (c) $[\ell_1 - 1]$, *when $s = 1$*

4 Combinatorial ambiguities

Definition 4.1. By a *hexpath* joining two pentagonal faces we mean either a linear patch with pentagonal terminal faces or two linear patches with one pentagonal terminal face and one hexagonal terminal face sharing the hexagonal terminal face and making an angle of 120 degrees. See Figures 3 and 4. The Coxeter coordinates (n) of a straight hexpath is the length of the corresponding straight path in the dual; the Coxeter coordinates (n, k) of a two leg hexpath are the lengths of the corresponding straight paths in the dual. We often refer to them as either (n)-*hexpaths* or (n, k)-*hexpaths*. The notation $(n, 0)$-hexpath, $(0, n)$-hexpath and (n)-hexpath will be used interchangeably.

Lemma 4.2. *Let Π be a pseudoconvex patch containing at least two pentagons and let Π' be a subpatch of Π containing at least one pentagon but not every pentagon. Then there exists a hexpath from a pentagon in Π' to a pentagon not in Π'.*

Proof. Let Π and Π' be as stated. Consider the facial distances between every pentagon in Π' to every pentagon not in Π'. Let f be a pentagon in Π' and g be a pentagonal face not in Π' so that the distance between f and g is the minimum over all such pairs. Consider a shortest polygonal path of faces in Π joining f to g. By the choice of f and g, all of the faces on this polygonal path are hexagons; it remains to show that this path is indeed a hexpath. Since all interior faces in the corresponding dual path are triangular, no shortest path can make a sharp, 60° turn (see [1] in Figure 2); otherwise, the hexagon h at the turn may simply be deleted from the path resulting in a shorter path.

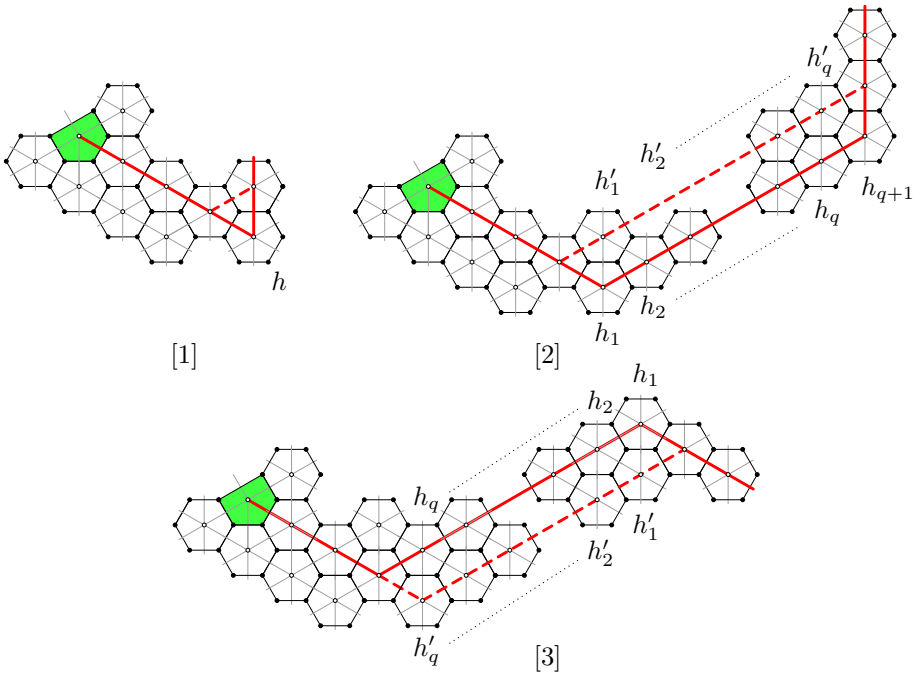

Figure 2: Pictoral proof of existence of hexpath from Lemma 4.2.

Next suppose that the shortest dual path joining f and g makes consecutive left turns (see [2] in Figure 2). Let $h_1, \ldots, h_{q+1}$ denote the faces on the segment between the turns including both faces at the turns. Note that the edge in common with h_1 and face labeled h'_1 would be a boundary segment of length 1 if h'_1 did not belong to the patch. Hence, h'_1 belongs to the patch. Also, h'_1 must be a hexagon, otherwise we contradict the way f and g were chosen. Now the same argument can be applied to h'_2 and so it too belongs to the patch. Inductively, $h'_1, \ldots, h'_q$ are all hexagons belonging to the patch. Replacing $h_1, \ldots, h_{q+1}$ by $h'_1, \ldots, h'_q$ results in a shorter dual path joining f and g and a contradiction. By the same argument there cannot be two consecutive right turns.

Finally, we choose from among all shortest dual paths joining f and g the one with the longest straight segment before a first left turn. (If the first turn is a right turn, we will interpret this as starting off with a segment of length 0 followed by a left turn.) We wish to prove that this particular shortest dual path has just two straight segments. Suppose there is a right turn after the first left turn. Starting with the face at the right turn, we label the faces back to but not including the face at the left turn $h_1, \ldots, h_q$ (see [3] in Figure 2). Employing the argument just used above, we see that the faces labeled $h'_1, \ldots, h'_q$ must be hexagons belonging to the patch. Replacing $h_1, \ldots, h_q$ by $h'_1, \ldots, h'_q$ then results in an f, g-path of the same length but with a longer initial straight segment contradicting our choice of this path. □

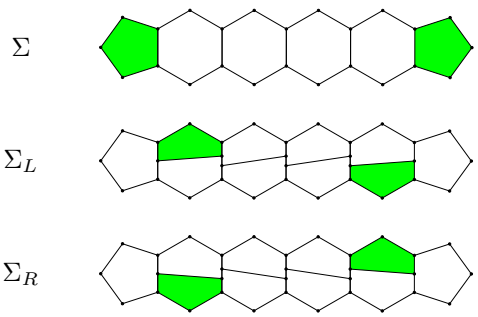

Figure 3: A (5)-hexpath, Σ, and the similar patchs Σ_L and Σ_R, each representing an α step.

Endo and Kroto [5] provided a method of constructing a patch similar to a linear patch. Let Σ be an (n)-hexpath joining a pair of pentagonal faces, where $n > 1$. Then the similar patch is formed by inserting one new vertex on each edge of Σ separating a pentagon from its adjacent hexagon, and two new vertices on each edge of Σ separating two adjacent hexagons. Edges may then be added in two different ways, as demonstrated in Figure 3, resulting in the similar patch Σ'_L containing a $(1, n-2)$- hexpath or the similar patch Σ'_R containing a $(n-2, 1)$-hexpath. If Π is a pseudoconvex patch containing such a hexpath Σ, replacing Σ by Σ_L or Σ_R results in a pseudoconvex patch Π' that is similar to Π and contains $n-1$ more faces. Replacing Π by Π' is called an α *step*; if this replacement is made in a larger patch, then the choice of Σ_L versus Σ_R may result in non-isomorphic patches.

The Endo-Kroto construction can be generalized to any (n, k)-hexpath joining a pair of pentagonal faces with $nk > 1$. Let Σ be such a hexpath. Then a similar patch is formed by inserting one new vertex on each edge of Σ separating a pentagon from its adjacent hexagon, and two new vertices on each edge of Σ separating two adjacent hexagons and adding edges, as demonstrated in Figure 4, is a similar patch containing an $(n-1, k-1)$-hexpath joining a pair of pentagonal faces. We denote this new patch by Σ'. Note that in this case, the edges may be added in just one way. If Π is a pseudoconvex patch containing such a hexpath Σ, replacing Σ by Σ' results in a pseudoconvex patch Π' that is similar to Π and contains $n+k-1$ more faces. Replacing Π by Π' is called an β *step.*

It is clear that any patch obtained from Π by a sequence of α and β steps will be similar to Π. We also note that when a $(1, n-2)$-hexpath, an $(n-2, 1)$-hexpath or an $(n-1, k-1)$-hexpath is bordered by a sufficient set of hexagons, we may reverse these constructions. We call this reverse constructions α^{-1} and β^{-1} steps.

Since each α or β step produces another patch in the same similarity class with more faces, the sequence of similar patches constructed by a sequence of α and β steps must all be distinct. As we will soon verify, the number of patches in the similarity class of a pseudoconvex patch is finite. Therefore starting with any pseudoconvex patch, any sequence of α and β steps must terminate in a similar pseudoconvex patch for which no α or β step is possible.

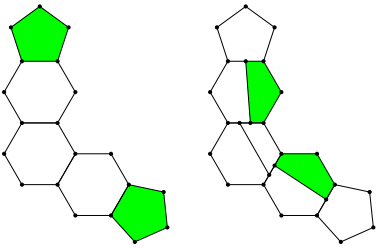

Figure 4: A $(2,2)$-hexpath Σ, and the similar patch Σ' containing a $(1,1)$-hexpath.

Cone	Tip
Λ_1	a pentagonal face
$\Lambda_{2(a)}$	a quadrilateral face
$\Lambda_{3(a)}$	a triangular face
$\Lambda_{3(b)}$	a "half-edge"
$\Lambda_{4(a)}$	a valence 2 face
$\Lambda_{4(b)}$	a pendant vertex
Λ_5	a loop

Table 1: Geometric Cone Tips.

Definition 4.3. A patch Π in the similarity class $\mathcal{S}$ is called a *terminal patch* if no α or β step is possible in Π. The smallest linear or pseudoconvex subpatch of a terminal patch containing all of the pentagonal faces is a *minimal configuration.*

Terminal patches and minimal configurations are closely related to nanocones and the tips of nanocones. We will need several results that were proven in the context of nanocones.

Definition 4.4. A nanocone or *cone* is an infinite trivalent plane graph with hexagonal faces and one to five pentagonal faces. Adopting the terminology from [3], two cones are *equivalent* if each has a finite subgraph so that when the subgraphs are deleted the remaining graphs are isomorphic.

This is an equivalence relation among cones forming eight equivalence classes. These classes are described by Klein and Balaban in [11]. A proof that these are indeed the only possibilities is given in [3]. That paper, in turn, relies in part on a result of Balke in [1]. Using the terminology from [3], we summarize this classification and consolidate the results from these three papers that are relevant to this paper. The classification of cones is based on the classification of the nontrivial rotations in the symmetry group of Λ, the regular hexagonal tessellation; the list of these rotations is given below.

Proposition 4.5. *The nontrivial rotations in the symmetry group of* Λ *are:*

1. *rotations by* 60° *about the centers of faces;*

2. *rotations by* 120°

   (a) *about the centers of faces or*

   (b) *about vertices;*

3. *rotations by* 180°

   (a) *about centers of faces or*

   (b) *about centers of edges;*

4. *rotations by* 240°

   (a) *about the centers of faces or*

   (b) *about vertices;*

5. *rotation by* 300° *about centers of faces.*

If x is the center of one of the above rotations by $k \times 60^\circ$, we may excise a $k \times 60^\circ$ wedge at x and identify the edges to get a *geometric cone,* which we will denote by Λ_k or $\Lambda_{k(a)}$ or $\Lambda_{k(b)}$. A geometric cone is an infinite graph that has, with exactly one exception at the cone tip, only hexagonal faces and only vertices of degree 3. The exceptions at the tip of these geometric cones are pictured in Figure 5 and listed in Table 1.

Now each of these geometric cone tips can be replaced by a tight configuration of pentagonal faces resulting in a unique cone, called the *representative cone*, for each of the eight equivalence classes; the smallest pseudoconvex patch containing the configuration of pentagonal faces is called the *cone tip*. These eight cone tips are also pictured in Figure 5 and are denoted by Ω_i as shown in the figure.

Given a pseudoconvex patch Π with side parameters $(\ell_1, \ldots, \ell_s)$ we may reverse the process discussed in Lemma 3.2: instead of deleting all of the faces of a side we may add a row of hexagons to a side. Adding a row of hexagons to each side in turn results in a patch with all side parameters increased by 1; call this patch Π_1. Repeatedly adding rings of hexagons produces an infinite sequence of nested graphs $\Pi_0 = \Pi$, Π_1, $\Pi_2, \ldots$, and the union of these patches is a trivalent graph with all hexagonal faces except exactly s $(1 \leq s \leq 5)$ pentagonal faces - that is, a cone. Hence each linear or pseudoconvex patch may also be thought of as a patch in a uniquely determined cone.

The focus of [3] is the collection of pseudoconvex patches in which all side lengths are equal, *symmetric patches*, or in which $\ell_1 = \ell_2 - 1 = \cdots = \ell_s - 1$, *near-symmetric patches*. These patches are called *cone patches* in [3] when they include a pentagon as a bounding face and correspond to our cone tips. Also, in [3], the appropriate cone tip for a given cone patch is determined by whether the patch is symmetric or near-symmetric.

By repeatedly adding hexagons to the sides of a pseudoconvex patch, we may embed each pseudoconvex patch in a symmetric or near-symmetric patch. To see this we consider the pseudoconvex patches based on the value of s.

Lemma 4.6. *Every pseudoconvex patch* Π *is a subpatch of a symmetric or near-symmetric patch, and there is a unique cone containing* Π.

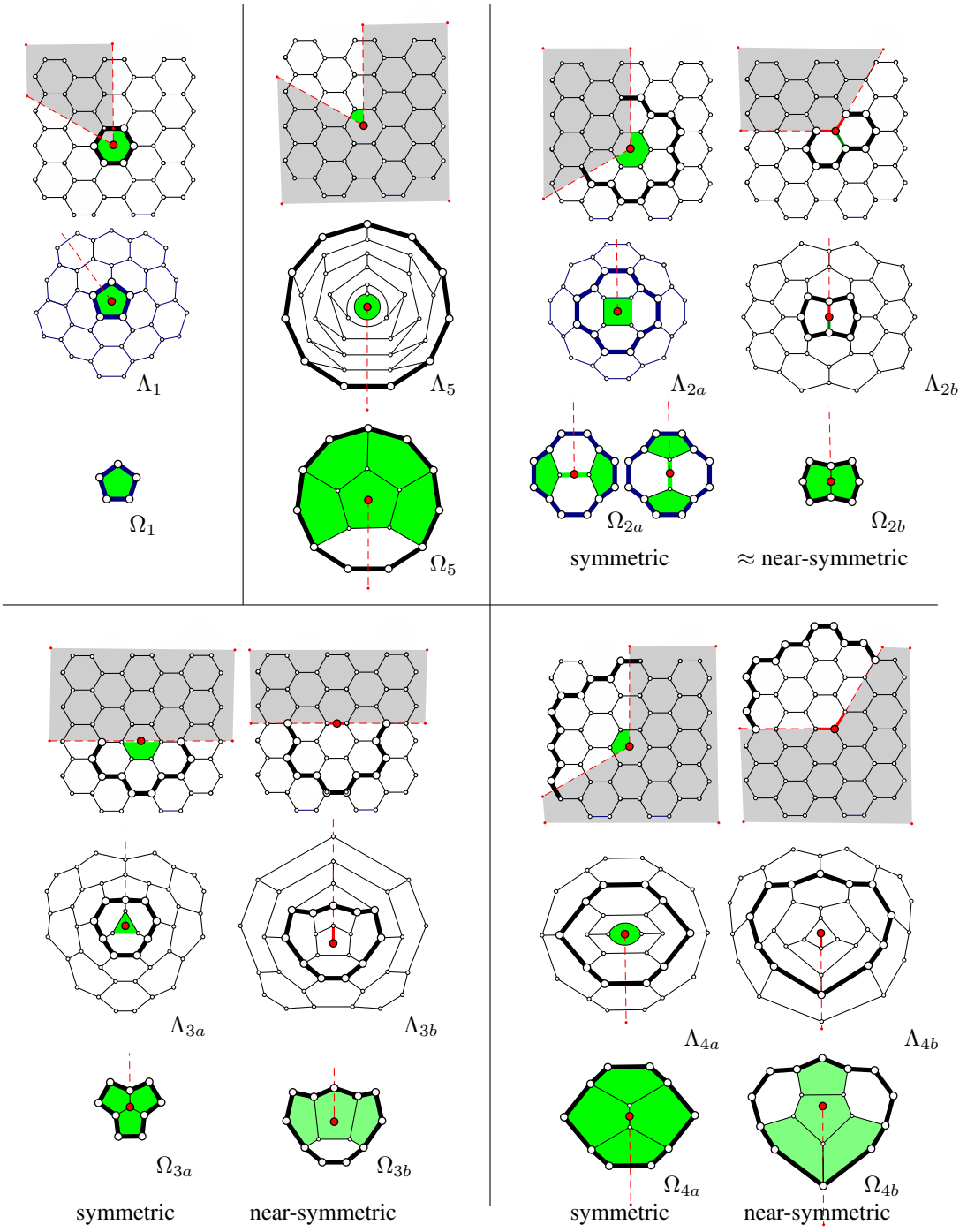

Figure 5: Cone Tips.

Proof. Let Π be a pseudoconvex patch. If $s = 1$, Π is a symmetric patch containing 5 pentagons. It follows from [3] that the unique cone containing Π has the cone tip Ω_5. If $s = 2$, let Π have side lengths $[\ell_1, \ell_2]$ with $\ell_1 \leq \ell_2$. We may add a row of hexagons to the side of length ℓ_2 to get a pseudoconvex patch with side length $\ell_1' = \ell_1 + 2$ and $\ell_2' = \ell_2 - 1$. If $\ell_1' < \ell_2' - 1$, we may repeat the process and we may continue to do so until we reach a cone patch Π^* with side lengths $\ell_1^* = \ell_2^* - 1$, $\ell_1^* = \ell_2^*$ or $\ell_1^* = \ell_2^* + 1$. We also note that $\ell_2' - \ell_1' = \ell_2 - \ell_1 - 3$ and therefore $|\ell_2^* - \ell_1^*| \equiv |\ell_2 - \ell_1| \bmod 3$. We conclude that when $\ell_1 \equiv \ell_2 \bmod 3$ the extension to a cone patch is symmetric and by [3] is the unique cone tip Ω_{4a}; otherwise the extension to a cone patch is near-symmetric and is the unique cone tip Ω_{4b}.

When $s = 3$, let Π have side lengths $[\ell_1, \ell_2, \ell_3]$; we again repeatedly add a row of hexagons to the longest side which will result in a cone patch Π^* with side lengths $\ell_1^* = \ell_2^* - 1 = \ell_3^* - 1$ or $\ell_1^* = \ell_2^* = \ell_3^*$ after suitable reordering. In this case, we note that the process of adding a row of hexagons changes the parity of each length. Hence, if the side lengths of Π are all even or all odd, the resulting cone patch Π^* will have equal side lengths and by [3] the unique cone containing Π has the cone tip Ω_{3a}; if the side lengths of Π do not all have the same parity, the unique cone containing Π has the cone tip Ω_{3b}.

Finally, consider $s = 4$, with Π having side lengths $[\ell_1, \ell_2, \ell_3, \ell_4]$. If $\ell_2 \neq \ell_4$, we may repeatedly add hexagons to the larger of these two sides side until $\ell_2' = \ell_4'$. Then, we may add hexagons to the side corresponding to larger of ℓ_1' and ℓ_3' and repeat this until we have a pseudoconvex patch Π'' with $\ell_1'' = \ell_3''$ and $\ell_2'' = \ell_4''$. If the lengths are not all equal, (without loss of generality) we assume that $\ell_1'' > \ell_2''$. Now alternately adding hexagons to the ℓ_1'' and ℓ_3'' sides will result in a cone patch Π^* with side lengths $\ell_1^* = \ell_2^* = \ell_3^* = \ell_4^*$ or (reordering if needed, $\ell_1^* = \ell_2^* - 1 = \ell_3^* - 1 = \ell_4^* - 1$. Noting that $(\ell_1^* + \ell_3^*) \equiv (\ell_2^* + \ell_4^*) \bmod 3$ if and only if $(\ell_1 + \ell_3) \equiv (\ell_2 + \ell_4) \bmod 3$, we conclude from [3] that the unique cone containing Π has the cone tip Ω_{2a} when $(\ell_1 + \ell_3) \equiv (\ell_2 + \ell_4) \bmod 3$ and the cone tip Ω_{2b} otherwise. □

Two observations: first, the cone tip Ω_{2a} is the Stone-Wales patch from [12]. A 90° rotation of the Stone-Wales patch is boundary preserving; that is, in a larger patch the Stone-Wales patch can be replaced by its rotation. However, this rotation may result in a non-isomorphic larger patch. Secondly, each pseudoconvex patch in a similarity class can be embedded in a fixed cone patch. Since the number of faces in a cone patch is bounded by a function of its side lengths, the number of faces in a patch in a given similarity class is bounded. In the next lemma, we summarize our results along with some of those from [1],[2], [3] and [11].

Definition 4.7. A pseudoconvex patch containing one of the cone tips Ω_1, Ω_{2a} (in either orientation), Ω_{2b}, Ω_{3a}, Ω_{3b}, Ω_{4a}, Ω_{4b} or Ω_5 is called a *cone tip patch.*

Lemma 4.8. *Let $\mathcal{S}$ be a non-empty similarity class of pseudoconvex patches. Then $\mathcal{S}$ is finite and, with the exception of case (2) below, contains one unique cone tip patch.*

1. *If $\mathcal{S} = \mathcal{S}_{[\ell_1,\ell_2,\ell_3,\ell_4,\ell_5]}$, then $\mathcal{S}$ contains the cone tip patches with configuration Ω_1 at the tip.*

2. *If $\mathcal{S} = \mathcal{S}_{[\ell_1,\ell_2,\ell_3,\ell_4]}$, where $(\ell_1+\ell_3) \equiv (\ell_2+\ell_4)$ mod 3, then $\mathcal{S}$ contains two cone tip patches with configuration Ω_{2a} (one in each orientation) at the tip or one cone tip patch with configuration Ω_{2a} when the patch admits a symmetry agreeing with the Stone-Wales transformation at the tip.*
3. *If $\mathcal{S} = \mathcal{S}_{[\ell_1,\ell_2,\ell_3,\ell_4]}$, where $(\ell_1+\ell_3) \not\equiv (\ell_2+\ell_4)$ mod 3, then the cone tip patch in $\mathcal{S}$ has configuration Ω_{2b} at the tip.*
4. *If $\mathcal{S} = \mathcal{S}_{[\ell_1,\ell_2,\ell_3]}$, where ℓ_1, ℓ_2 and ℓ_3 have the same parity, then the cone tip patch in $\mathcal{S}$ has configuration Ω_{3a} at the tip.*
5. *If $\mathcal{S} = \mathcal{S}_{[\ell_1,\ell_2,\ell_3]}$, where ℓ_1, ℓ_2 and ℓ_3 do not have the same parity, then the cone tip patch in $\mathcal{S}$ has configuration Ω_{3b} at the tip.*
6. *If $\mathcal{S} = \mathcal{S}_{[\ell_1,\ell_2]}$, where $\ell_1 \equiv \ell_2$ mod 3, then the cone tip patch in $\mathcal{S}$ has configuration Ω_{4a} at the tip.*
7. *If $\mathcal{S} = \mathcal{S}_{[\ell_1,\ell_2]}$, where $\ell_1 \not\equiv \ell_2$ mod 3, then the cone tip patch in $\mathcal{S}$ has configuration Ω_{4b} at the tip.*
8. *If $\mathcal{S} = \mathcal{S}_{[\ell_1]}$, then the cone tip patch in $\mathcal{S}$ has configuration Ω_5 at the tip.*

The method by which the cone tip patch in $\mathcal{S}_{[\ell_1,\ldots,\ell_s]}$ is constructed is described in [3]. In Figure 5, we have illustrated this or a similar construction for all of the cone tips except Ω_5; the region of Λ included here is not large enough to include the path. Note that in the cases that s equals 4 or 5, the triangle may actually cross the path and the identification cannot be made. This simply means that no pseudoconvex patch exists with those side lengths. For all other values of s the geometric cone can be constructed; but, in some cases, the singularity may be so close to the boundary that the tip can't be inserted and again $\mathcal{S}_{[\ell_1,\ldots,\ell_s]}$ will be empty.

We now turn to minimal configurations. By definition, these linear or pseudoconvex patches contain no pair of pentagons that are joined by an (n)-hexpath for $n > 1$ or an (n,k)-hexpath for $nk > 1$ and they admit no pseudoconvex subpatch containing all of the pentagonal faces. The cone tips Ω_{2a} (in either orientation), Ω_{2b}, Ω_{3a}, Ω_{3b}, Ω_{4a}, Ω_{4b} or Ω_5 are clearly minimal. There is one other configuration that is clearly minimal: three pentagons sharing alternate edges with a central hexagon, the left-hand configuration in Figure 8 which we denote by Ω_3.

Lemma 4.9. *The only minimal configurations are the cone tips and Ω_3.*

Proof. We see at once that Ω_{2b} is the only minimal configuration that is linear. Let Ω be a minimal configuration other than Ω_{2b}. Since Ω is pseudoconvex, any side of length 0 must be a hexagonal face that can be deleted to get a smaller pseudoconvex patch containing all of the pentagonal faces. Hence all of the side lengths are positive and all boundary segments have lengths 2 and 3. It will be convenient to call the faces with boundary segments of length 3 *corner faces*. If all of the faces on a side, including both corners, are hexagons, they may all be deleted resulting in a smaller pseudoconvex patch containing all of the pentagonal faces. Hence, each side of Ω contains a pentagonal face. There are two basic

cases to consider: there is just one pentagon on the boundary or there are at least two pentagons on the boundary.

Suppose first that Ω has more than one pentagonal face on its sides and list them in counterclockwise order $f_1, \ldots, f_m$. Since no side is devoid of pentagons, any two consecutive pentagonal faces are joined by an (n)-hexpath or an (n, m)-hexpath on the boundary. Hence f_i is joined to f_{i+1} by a (1)-hexpath or a $(1,1)$-hexpath, for $i = 1, \ldots, m-1$, and f_m is joined to f_1 by a (1)-hexpath or a $(1,1)$-hexpath. We note that, if f_i is joined to f_{i+1} by a $(1,1)$-hexpath, the intervening hexagonal face must be a corner. We also note that the number of corners is equal to the number of sides.

By formula (1) from Lemma 3.2, the number of pentagons on the sides (the number of hexpaths) plus the number of sides (the number of $(1,1)$-hexpaths) is six or less. We conclude that the number of (1)-hexpaths plus twice the number of $(1,1)$-hexpaths on the boundary is six or less while the total number of hexpaths is less than six. Hence the possibilities for the sequences of Coxeter coordinates for the hexpaths joining consecutive pentagons around the boundary are:

1. $\{(1), (1)\}$;
2. $\{(1), (1,1)\}$;
3. $\{(1,1), (1,1)\}$;
4. $\{(1), (1), (1)\}$;
5. $\{(1), (1), (1,1)\}$;
6. $\{(1), (1,1), (1,1)\}$;
7. $\{(1,1), (1,1), (1,1)\}$;
8. $\{(1), (1), (1), (1)\}$;
9. $\{(1),(1), (1), (1,1)\}$;
10. $\{(1), (1), (1,1), (1,1)\}$;
11. $\{(1), (1,1), (1), (1,1)\}$;
12. $\{(1), (1), (1), (1), (1)\}$;
13. $\{(1), (1),(1), (1), (1,1)\}$.

The number of (1) hexpaths plus 2 times the number of $(1,1)$ hexpaths is the number of faces on the boundary. If this number is less than 5 (cases 1 to 5 and 8) then every face is on the boundary. Case (1) with only 2 bounding faces is Ω_{2b}. Case (2) can only be two pentagons and a hexagon sharing a common vertex; this is not a minimal configuration but contains Ω_{2b}. Case (3) with 2 pentagonal faces alternating with two hexagonal corners is Ω_{2a}; Case (4) can only be Ω_{3a} and Case (5) can only be Ω_{3b}. Case (6) has five faces in its boundary hence the interior is a single pentagon and the patch is Ω_{4b}. Case (7) has six faces in its boundary; hence the interior is a single hexagon bounded by pentagons on alternate edges: Ω_3. The boundary in Case (8) consists of 4 pentagons giving Ω_{4a}.

In case Case (9), we have 4 pentagons and 1 hexagon on the boundary; hence, they bound a pentagon giving Ω_5. Cases (10) and (11) have boundaries consisting of 4 pentagons

and 2 hexagons all incident with a common interior hexagon. In these cases there is always a pair of pentagons joined by a (2) hexpath through the central hexagon; hence, these are not minimal configurations. Case (12) is excluded since it has 5 pentagons around a central pentagon, giving 6 pentagons. Finally Case (13) has 5 pentagons and one hexagon around a hexagon and, like cases (10) and (11), admits a pair of pentagons joined by a (2)-hexpath through the central hexagon and thus is not minimal.

Now we must confront the case where there is only one pentagon f on the boundary. Since f must be incident with every other face, Ω has 1 or 2 sides; if it has 2 sides f must meet both sides and hence must be a corner. In either case if f is a corner, its removal leaves a pseudoconvex patch Π with 3 or 4 pentagons but all hexagons on its boundary. If Π admits two pentagons joined by a (n)-hexpath with $n > 1$ or an (n, m)-hexpath with $mn > 1$, then Ω is not minimal. Hence, Π contains a pseudoconvex patch Π' consisting of one of Ω_{3a}, Ω_{3b}, Ω_3, Ω_{4a} or Ω_{4b} surrounded by a ring of hexagons. Using Lemma 4.2, it is straight forward but somewhat tedious to verify that, in each case, f is joined to some pentagon in Π' by a (n, m)-hexpath where $mn > 1$.

All that remains to consider is the case where Ω has one side and only one pentagonal, non-corner face f on that side. In this case the interior of Ω contains a copy Ω_{4a} or Ω_{4b}. As above it is straight forward but somewhat tedious to eliminate the possibility that f is not adjacent to a face of this core. Assume then that f shares an edge with a face of Ω_{4a} or Ω_{4b}. Again, one easily checks that none of these possibilities is minimal. □

One last task before we can state and prove the main result of our paper is to introduce two infinite families of exceptional similarity classes, $\mathcal{S}_{[1,1,n,n]}$, $n > 1$, (Figure 6) and $\mathcal{S}_{[0,2,n,n+1]}$, $n > 2$, (Figure 7), and one additional exceptional similarity class $\mathcal{S}_{[2,2,2]}$ (Figure 8). Each of these similarity classes contain exactly two pseudoconvex patches neither of which can be transformed into the other by a sequence of $\alpha, \beta, \alpha^{-1}$ and β^{-1} steps. Specifically the arrangements of the pentagons precludes applying α or β and there are not sufficient bounding hexagons to apply α^{-1} or β^{-1}. The patches in Figure 8 have asymmetric boundaries and the symmetries of the patches in Figure 6 do not match the Stone-Wales transformation at the tip.

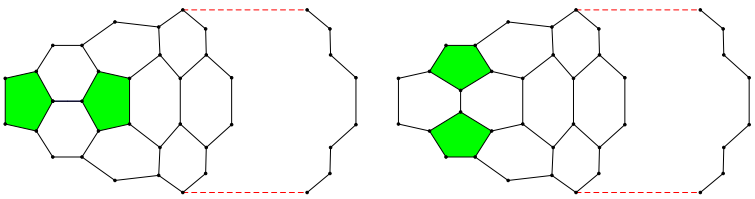

Figure 6: The only two patches in $\mathcal{S}_{[1,1,n,n]}$, $n > 1$.

Theorem 4.10. *Let $\mathcal{S}$ be a nonempty similarity class of pseudoconvex patches different from $\mathcal{S}_{[2,2,2]}$, $\mathcal{S}_{[1,1,n,n]}$, and $\mathcal{S}_{[0,2,n,n+1]}$, and let Π and Π' be two pseudoconvex patches in $\mathcal{S}$. Then there is a sequences of α, β, α^{-1} and β^{-1} steps that transform Π into Π'.*

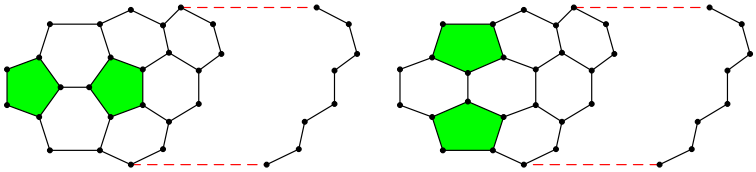

Figure 7: The only two patches in $\mathcal{S}_{[0,2,n,n+1]}$, $n > 2$.

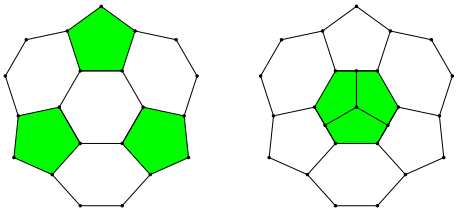

Figure 8: The only two patches in $\mathcal{S}_{[2,2,2]}$. The patch on the left is Ω_3.

Proof. Let Π and Π' be two pseudoconvex patches in $\mathcal{S}$. Then by Lemma 4.9, there is a sequence of α and β steps taking Π to a cone tip patch or a patch containing Ω_3 in $\mathcal{S}$ and a sequence of α and β steps taking Π' to a cone tip patch or a patch containing Ω_3 in $\mathcal{S}$. If both sequences of steps end in the same patch, concatenating one sequence with the reverse of the other is the sequence we seek. By Lemma 4.8 the only cases in which the terminal patches could be different are: $\mathcal{S}$ equals $\mathcal{S}_{[\ell_1,\ell_2,\ell_3]}$ where ℓ_1, ℓ_2 and ℓ_3 have the same parity and $S_{[\ell_1,\ell_2,\ell_3,\ell_4]}$ where $(\ell_1 + \ell_3) \equiv (\ell_2 + \ell_4) \bmod 3$. In these cases, there are two distinct possibilities for the terminal patch. All that remains to show that, for the similarity classes in these cases but different from the excluded case, there is a short sequence of α, β, α^{-1} and β^{-1} steps that takes one of the terminal patches into the other. These steps are illustrated in Figures 9 and 10. In both cases, the necessity of avoiding the excluded patches forces additional hexagonal faces providing sufficient room to transform one patch into the other. □

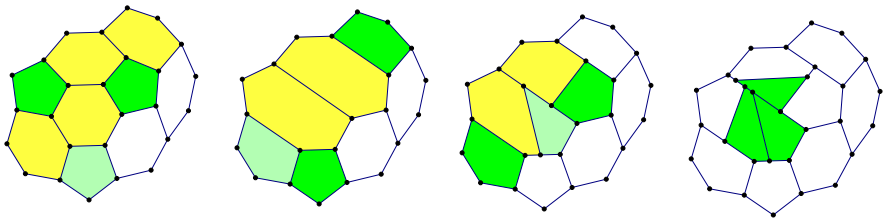

Figure 9: A patch Π with exactly three pentagons containing the exceptional case and at least two more faces.

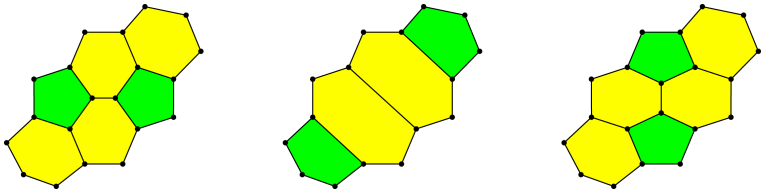

Figure 10: A patch Π with two pentagons in configuration Ω_{2b} and the transformation to the rotated configuration Ω_{2b}. Only the shaded hexagons are necessary for the transformations; the others are "spectator" faces.

Using the terminology from [3], we have the following corollaries for cones.

Corollary 4.11. *If Θ and Φ are two equivalent cones then there is a sequences of α, β, α^{-1} and β^{-1} steps that transform Θ into Φ.*

Corollary 4.12. *With the exception of the patches with side parameters $[1,1,1,1]$ or $[2,2,2]$, any symmetric or near-symmetric patch in a cone may be transformed into any other symmetric or near-symmetric patch with the same boundary by a sequence of α's, β's, α^{-1}'s, and β^{-1}'s.*

References

[1] L. Balke, Classification of disordered tilings, *Annals of Combinatorics* **1** (1997), 297–311.

[2] J. Bornhoft, G. Brinkmann and J. Greinus, Pentagon-hexagon-patches with short boundaries, *European Journal of Combinatorics* **24** (2003), 517–529.

[3] G. Brinkmann and N. V. Cleemput, Classification and generation of nanocones, *Discrete Applied Mathematics* **159** (2011), 1528–1539.

[4] G. Cargo and J. E. Graver, When does a curve bound a distorted disk?, *SIAM J. Discrete Math* **25** (2011), 280–305.

[5] M. Endo and H. W. Kroto, Formation of carbon nanofibers, *J. Phys. Chem.* **96** (1992), 6941–6944.

[6] J. E. Graver, The (m,k)-patch boundary code problem, *MATCH* **48** (2003), 189–196.

[7] J.E. Graver and C. Graves, Fullerene Patches I, *Ars Mathematica Contemporanea* **3** (2010) 104–120.

[8] C. Graves and J. McLoud-Mann, Side lengths of pseudoconvex fullerene patches, *Ars Mathematica Contemporanea* **5** (2012) 291–302.

[9] X. Guo, P. Hansen and M. Zheng, Boundary uniqueness of fusenes, *Discrete Applied Mathematics* **118** (2002), 209–222.

[10] M. Hasheminezhad, H. Fleischner and B. D. McKay, A universal set of growth operations for fullerenes, *Chem. Phys. Lett.* **464** (2008), 118–121

[11] D. J. Klein and A. T. Balaban, The eight classes of positive-curvature graphic nanocones, *J. Chemical Information and Modeling* **46** (2006), 307–320.

[12] A. J. Stone and D. J. Wales, Theoretical studies of icosahedral C_{60} and some related species, *Chem. Phys. Lett.* **128** (1986), 501–503.

ARS MATHEMATICA CONTEMPORANEA

Also available at http://amc-journal.eu
ISSN 1855-3966 (printed edn.), ISSN 1855-3974 (electronic edn.)
ARS MATHEMATICA CONTEMPORANEA 7 (2014) 423–440

Genus distributions of iterated 3-wheels and 3-prisms

Mehvish I. Poshni , Imran F. Khan
PUCIT, University of the Punjab, Lahore 54000, Pakistan

Jonathan L. Gross
Department of Computer Science, Columbia University, New York, NY 10027, USA.

Received 19 September 2012, accepted 22 October 2013, published online 26 December 2013

Abstract

The *iterated 3-prism* Pr_3^n is the cartesian product $C_3 \square P_n$ of a 3-cycle and an n-vertex path. At each end of the iterated 3-prism, there is a 3-cycle whose vertices are 3-valent in $C_3 \square P_n$. The *iterated 3-wheel* W_3^n is obtained by contracting one of these 3-cycles in $C_3 \square P_{n+1}$ to a single vertex. Using *rooted-graphs*, we derive simultaneous recursions for the *partitioned genus distributions* of W_3^n and a formula for the genus distribution of the graphs Pr_3^n. A seemingly straightforward way to construct either the sequence of iterated prisms Pr_3^n or the sequence of iterated wheels W_3^n, would be by iterative amalgamation of a copy of $C_3 \square K_2$, such that a copy of C_3 contained in it is matched to the "newest" copy of C_3 in the growing graph. Calculating genus distributions for the sequences would then involve an excessively large set of simultaneous recurrences. To avoid this, we propose a method of iterative surgery, under which the same vertex is considered a root-vertex in all graphs of the sequence, and in which the successive calculations of genus distributions require only four simultaneous recurrences. We also prove that the genus distribution of Pr_3^n not only dominates the genus distribution of W_3^{n-1}, but is also dominated by the genus distribution of W_3^n.

Keywords: genus distribution, rooted-graph, production, partitioned genus distribution, 3-prism, 3-wheel.

Math. Subj. Class.: 05C10

E-mail address: mehvish.irfan@pucit.edu.pk (Mehvish I. Poshni), imran.farid@pucit.edu.pk (Imran F. Khan)gross@cs.columbia.edu (Jonathan L. Gross)

1 Introduction

In this paper, the *rooted-graphs method* is used for computing genus distributions of the iterated 3-prism Pr_3^n, i.e., the cartesian product $C_3 \square P_n$ of the 3-cycle C_3 and the path graph P_n. This is made possible by reducing the problem of computing genus distributions of Pr_3^n to the problem of computing genus distributions of the iterated 3-wheel W_3^{n-1} obtained by contracting one of two cubic 3-cycles in Pr_3^n, for $n \geq 2$, to a single vertex. Figure 1.1 shows the iterated 3-prisms Pr_3^{n+1} and the iterated 3-wheels W_3^n for $n = 1, 2,$ and 3.

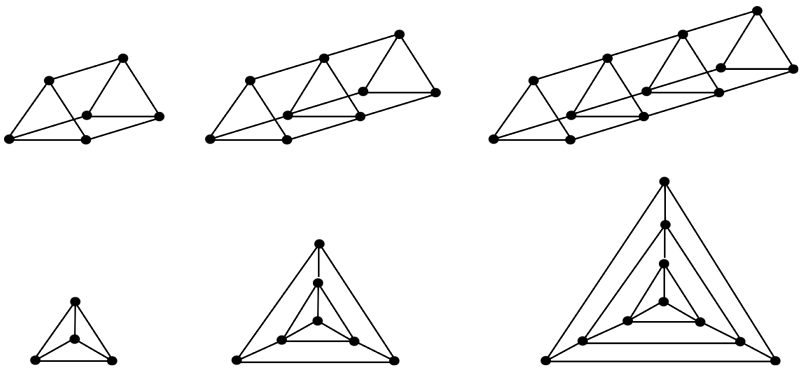

Figure 1.1: Iterated 3-prisms Pr_3^{n+1} and iterated 3-wheels W_3^n for $n = 1, 2, 3$.

The motivation for obtaining genus distributions of iterated 3-prisms via genus distributions of iterated 3-wheels stems from the observation that subdividing the edges incident with a particular vertex of the iterated 3-wheel and adding an edge between the subdivision vertices yields the iterated 3-prism, as shown in Figure 1.2.

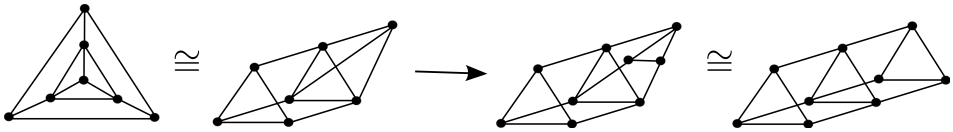

Figure 1.2: Obtaining the iterated 3-prism Pr_3^3 from the iterated 3-wheel W_3^2.

Familiarity with fundamentals in topological graph theory is assumed (see [7] or [22]). Graphs are assumed to be connected and graph embeddings are assumed to be 2-cellular. The ***genus distribution*** of a graph is the sequence of the number of its 2-cellular embeddings in each orientable surface. It may be written as a sequence g_0, g_1, g_2, $\cdots$ or as a polynomial $g_0 + g_1x^1 + g_2x^2 + \cdots$. A closed walk along the boundary of a face is known as a ***face-boundary walk***. We abbreviate a face-boundary walk as ***fb-walk***. An open sub-walk of an fb-walk is known as a ***strand*** and a minimal open sub-walk of an fb-walk that starts and ends at a vertex v, with no intermediate occurrences of v, is called a ***v-strand***.

A ***single-vertex-rooted graph***, or more simply a ***single-rooted graph***, is a graph in which any vertex is designated a root-vertex. The notation (G, v) is used to signify that the vertex v serves as the root-vertex of the graph G. Analogously, a ***double-rooted graph*** is a graph with any two vertices designated as roots. The *rooted-graphs method* has also been

used with edges and sub-graphs serving as roots. In this paper, however, we assume that any reference to a root is a reference to a root-vertex.

The problem of computing genus distributions was first introduced in [5]. Since then genus distributions have been computed for various families of graphs using different techniques (see, for example, [15], [16], [9], [1], [10], [17], [12], [18], [11], [2], [20], [19], [21], and [3]). More recently, techniques for finding *partitioned genus distribution* of *rooted-graphs* have been developed in [6], [4], [13], [8] and [14] for calculating genus distributions of large classes of graphs. In contradistinction to all previous results, where each graph operation results in one or more new root-vertices in the resulting graph, this paper has the novel feature that the same root-vertex is retained as a root for each graph W_3^n, for successive values of n.

In §2, we introduce some machinery for obtaining recurrences for *partitioned genus distribution* of the graph W_3^n in terms of the *partials* of W_3^{n-1}. In §3, a formula for the genus distribution of Pr_3^n is derived in terms of the partitioned genus distribution of W_3^{n-1}. It is also shown that genus distribution of Pr_3^n dominates the genus distribution of W_3^{n-1} and is dominated by the genus distribution of W_3^n.

2 Genus distributions of iterated 3-wheels

2.1 Rim-insertion

Let (W_3^n, v) be a rooted-graph with root-vertex v. The graph (W_3^{n+1}, v) can be obtained from (W_3^n, v) by performing the following graph operations:

(i) each of the three edges incident on v is subdivided.

(ii) the subdivision vertices are made pairwise adjacent by adding three new edges.

The vertex v is retained as the root-vertex for W_3^{n+1}. Thus, W_3^{n+1} has three more vertices and six more edges than the graph W_3^n. This is illustrated in Figure 2.1. We refer to this operation as ***rim-insertion***.

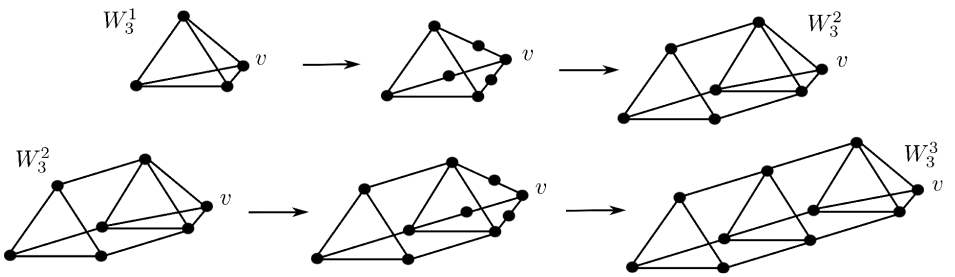

Figure 2.1: Applying rim-insertion to W_3^n iteratively, for $n = 1$ and 2.

2.2 Partials and partitioned genus distribution

In any given embedding ι of the graph (W_3^n, v), the trivalent root-vertex v occurs exactly thrice in the fb-walks of the regions of the embedding, giving rise to three v-strands. Based

on how the three v-strands stand in relation to each other, the vertex v may occur once or twice or thrice in the same fb-walk. As illustrated in Figure 2.2, the embeddings of (W_3^n, v) on the surface S_i can be classified into the following four types:

- Type a: root-vertex v occurs in three distinct fb-walks.
- Type b: root-vertex v occurs twice in one fb-walk and once in another fb-walk.
- Types c' and c'': root-vertex v occurs thrice in the same fb-walk. The two ways in which this can happen are shown in Figure 2.2.

These four types are referred to as ***partial-types***. The number of embeddings of the graph W_3^n of partial-types a, b, c', and c'' on the surface S_i are known as ***partials*** and are denoted by a_i, b_i, c'_i and c''_i, respectively.

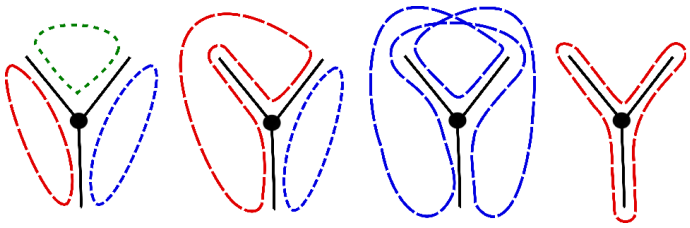

Figure 2.2: Partial-types a, b, c' and c'' from left to right.

The ***partitioned genus distribution*** of the graph W_3^n is the set of sequences of its partials for each orientable surface. Clearly, summing the partials for each orientable surface would yield the genus distribution of the graph. Like the genus distribution sequence, the partitioned genus distribution sequence may also be written as a polynomial.

Example 2.1. *The partitioned genus distribution of the 3-wheel* W_3^1 *is* $2a_0 + 12b_1 + 2c'_1$ *which implies that its genus distribution is* $2 + 14x$.

2.3 Productions for the rim-insertion operation

It is evident that for each embedding ι_w of the graph W_3^n, the rim-insertion operation induces $(3!)^3 = 216$ embeddings of W_3^{n+1} whose rotation systems are consistent with the rotation system of ι_w. By handling all 216 possibilities collectively with the rim-insertion operation, rather than, say, by inserting the edges of a new rim one at a time, we are able to keep the number of simultaneous recursions (see Corollary 2.4) down to four. This simplifies the calculation of partitioned genus distributions for W_3^n, as demonstrated in §2.4.

A ***production for rim-insertion*** classifies the 216 embeddings of W_3^{n+1}, produced as a consequence of applying rim-insertion to an embedding of W_3^n, into their respective partial-types. The productions for each of the four partial-types are given in Theorem 2.3. A production is symbolically written as:

$$x_i[W_3^n] \longrightarrow \sum_{\substack{y \text{ ranges over all} \\ \text{sub-partial types} \\ \text{with } \Delta \in \{0,1,2\}}} \alpha_{y_{i+\Delta}} y_{i+\Delta}[W_3^{n+1}]$$

Each such production can be construed as signifying that any embedding of W_3^n of partial-type x and genus i, as a result of rim-insertion, produces exactly $\alpha_{y_{i+\Delta}}$ embeddings of W_3^{n+1} having partial-type y and genus $i+\Delta$. For each such production, the sum of all coefficients $\alpha_{y_{i+\Delta}}$ on the right-hand-side is 216.

We refer to the left-hand-side of a production as the ***antecedent*** and the right-hand-side of a production as the ***consequent***.

Remark 2.2. If instead of the rim-insertion operation, the edges of a new rim are added one at a time, the rim-insertion operation breaks into three stages. The first stage consists of joining two of the three subdivision vertices, inserted on the edges incident on the root, resulting in a 4-fold increase in the number of embeddings. The second stage consists of a subsequent 6-fold increase in the number of embeddings from joining a trivalent vertex to a bivalent vertex, and the third stage consists of a further 9-fold increase from joining two trivalent vertices. Such a breakdown of the rim-insertion operation into three distinct operations has the disadvantage that a different definition of production has to be used for each of these three operations, leading to three sets of productions and three sets of simultaneous recursions corresponding to these sets of productions. It would require a considerable amount of effort to reduce the three sets of simultaneous recursions to the single set of simultaneous recursions of Corollary 2.4.

Theorem 2.3 gives the complete set of productions for rim-insertion with the graphs W_3^n and W_3^{n+1} omitted from the antecedent and consequent, respectively, for greater readability.

Theorem 2.3. *When an embedding of the single-rooted graph (W_3^n, v) undergoes rim-insertion it produces embeddings of the resultant graph (W_3^{n+1}, v) whose partial-types and genera are specified by the following productions:*

$$a_i \longrightarrow a_i + 42a_{i+1} + 15b_{i+1} + 117b_{i+2} + 30c'_{i+2} + 11c''_{i+2} \tag{2.1}$$

$$b_i \longrightarrow 6a_i + 54a_{i+1} + 72b_{i+1} + 54c'_{i+2} + 6c'_{i+1} + 24c''_{i+2} \tag{2.2}$$

$$c'_i \longrightarrow 30a_i + 15b_i + 117b_{i+1} + c'_i + 42c'_{i+1} + 11c''_{i+1} \tag{2.3}$$

$$c''_i \longrightarrow 27a_i + 162b_{i+1} + 27c'_{i+1} \tag{2.4}$$

Proof. Subdividing the edges incident on the root-vertex of W_3^n does not change the partial-type of the resultant graph embedding. All fb-walks other than the ones containing the root-vertex remain unchanged. The fb-walks incident on the root-vertex are changed only by the introduction of occurrences of the subdivision vertices. Similarly, the edge-ends of the three new edges (added as part of the rim-insertion) are inserted into faces incident on the root-vertex. Consequently, only the fb-walks incident on the root-vertex undergo any change.

Each fb-walk incident on the root-vertex can be viewed as being constituted from strands passing over the root and over one or more subdivision vertices. The addition of the three new edges in effect breaks an fb-walk into strands which recombine with each other and with traversals of the new edges to generate new fb-walks, as shown in Figure 2.3 for partial-type a. Figure 2.3 does not account exhaustively for all 216 embeddings and is meant only as an illustration of the point in fact. The embedding types produced in the cases shown are of types a, b, c', and c'' from left to right, respectively. Notice, that in the first case the three fb-walks incident on the root break into strands that recombine to

produce three additional faces. Since there are three additional vertices, six more edges and three more faces, it follows by the Euler-polyhedral equation that the genus of the resulting graph embedding is identical to the genus of the original graph embedding prior to rim-insertion. In the remaining three cases shown, there is one less face resulting in a graph embedding with a genus increment of two. This accounts for the four terms a_i, b_{i+2}, c'_{i+2}, and c''_{i+2} in the consequent of Production (2.1). Derivations of the remaining contributions to the consequent are similar, and the number of drawings needed, if one proceeds by hand, can be reduced by consideration of symmetries.

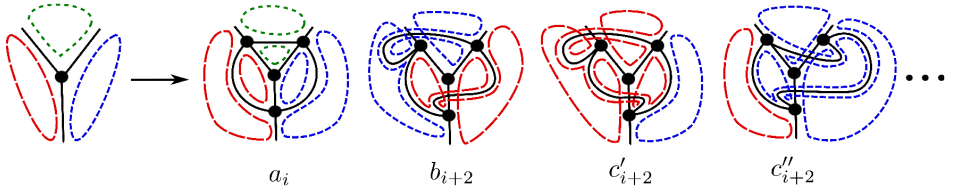

Figure 2.3: Changes in fb-walks for partial-type a.

The proof for Productions (2.1)−(2.4) consists of running the above-mentioned algorithm based on Heffter-Edmonds face-tracing for each partial-type. In doing this manually, symmetries are useful for expediting the derivations. Figure 2.4 illustrates one such scenario. The empty box covering one of the subdivision vertices represents an unknown rotation. For the remaining two vertices, fixing the rotation at one and varying it in all six ways on the other breaks the fb-walks into the four strands distinguished by the color and graphic indicated in the legend to the left of the figure.

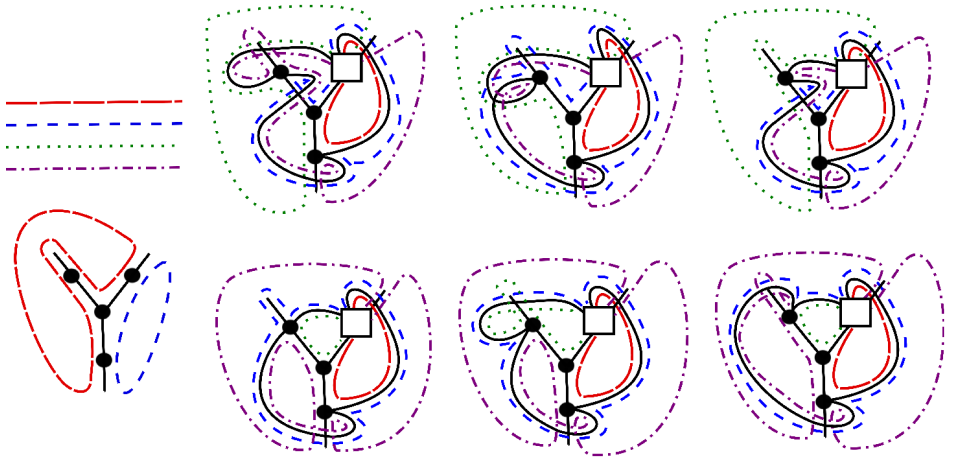

Figure 2.4: Similar embedding types produced from symmetries.

In the upper half of the figure, the placement of the strands is such that for each way of choosing the unknown rotation, represented by the empty box, the same type of embedding will be produced for all three models. Similar is the case for the three models shown at the bottom. Such symmetries can simplify the derivation of the Productions (2.1)−(2.4).

To organize the efforts for deriving the 216 partial-types in the consequent of the productions, we consider the derivation of Production (2.4). We regard the rotations at the vertices v_1, v_2 and v_3 in the inserted rim of the embedding model of Figure 2.5 as the canonical set of rotations.

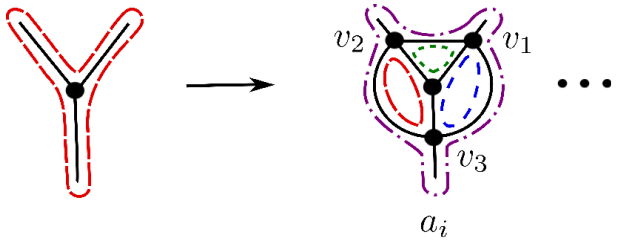

Figure 2.5: Set of canonical rotations at vertices v_1, v_2 and v_3 in the rim.

Then the remaining partial-types in the consequent of Production (2.4) can be obtained according to three principles:

(i) Two of the three rotations at v_1, v_2, v_3 are fixed as in the canonical set. Varying the rotation at the third vertex in five ways gives 5 embeddings: 2 of type a_i and 3 of type b_{i+1}. By symmetry, there are three ways to choose such a vertex. This yields a total of 15 $(= 3 \times 5)$ embeddings: 6 $(= 3 \times 2)$ of type a_i and 9 $(= 3 \times 3)$ of type b_{i+1}.

(ii) Fix the rotation on v_1 as in the canonical set. There are 25 ways of varying the non-canonical rotations at the vertices v_2 and v_3. There are five ways of fixing a non-canonical rotation at v_2 giving rise to five cases:

  (a) For three of these five cases, the five non-canonical rotations at v_3 produce 5 embeddings of type b_{i+1} giving a total of 15 $(= 3 \times 5)$ embeddings of type b_{i+1}.

  (b) For the remaining two of the five cases, the five non-canonical rotations at v_3 produce 2 embeddings of type a_i and 3 of type b_{i+1} giving a total of 4 $(= 2 \times 2)$ embeddings of type a_i and 6 $(= 2 \times 3)$ embeddings of type b_{i+1}.

  (c) This accounts for the 25 embeddings: 4 of type a_i and 21 $(= 15 + 6)$ of type b_{i+1}.

  By symmetry, the same is true if the canonical rotation is retained on vertex v_2 or v_3 instead of v_1. This gives a total of 75 embeddings: 12 $(= 3 \times 4)$ of type a_i and 63 $(= 3 \times 21)$ of type b_{i+1}.

(iii) If none of the rotations at the vertices in the rim is a canonical rotation, then there are a total of 125 embeddings. There are twenty five ways of fixing the non-canonical rotations at v_2 and v_3.

  (a) For four of these twenty five cases, varying the non-canonical rotations at v_1 produces 2 embeddings of types a_i and 3 of type b_{i+1} giving a total of 8 $(= 4 \times 2)$ embeddings of type a_i and 12 $(= 4 \times 3)$ embeddings of type b_{i+1}.

(b) For nine of the twenty five cases, varying the non-canonical rotations at v_1 produces 2 embeddings of type b_{i+1} and 3 embeddings of type c'_{i+1} giving a total of 18 $(= 9 \times 2)$ embeddings of type b_{i+1} and 27 $(= 9 \times 3)$ embeddings of type c'_{i+1}.

(c) In the remaining twelve of the twenty five cases, varying the non-canonical rotations at v_1 produces 5 embeddings of type b_{i+1} for a total of 60 $(= 12 \times 5)$ embeddings of type b_{i+1}.

(d) This gives a total of 125 embeddings: 8 of type a_i, 90 $(= 12 + 18 + 60)$ of type b_{i+1} and 27 of type c'_{i+1}.

In summary the following types of embeddings are accounted for:

- One embedding of type a_i for the canonical set of rotations in Figure 2.5.
- From principle (i) 6 embeddings of type a_i and 9 embeddings of type b_{i+1}.
- From principle (ii) 12 embeddings of type a_i and 63 embeddings of type b_{i+1}.
- From principle (iii) 8 embeddings of type a_i, 90 embeddings of type b_{i+1} and 27 embeddings of type c'_{i+1}.

The sum of the number of embeddings for each partial-type obtained above accounts for the consequent of Production (2.4). The proofs for the remaining productions can be organized along similar lines. For brevity, detailed proofs of the given productions are omitted. □

Corollary 2.4. *Given the partitioned genus distribution of single-rooted graph (W_3^n, v), the partitioned genus distribution of the graph (W_3^{n+1}, v) is specified by the following recurrences that express the partials of W_3^{n+1} as a sum of partials of W_3^n:*

NB: The partials on the right-hand-sides are for the graph W_3^n.

$$a_i[W_3^{n+1}] = a_i + 42a_{i-1} + 6b_i + 54b_{i-1} + 30c'_i + 27c''_i \tag{2.5}$$

$$b_i[W_3^{n+1}] = 15a_{i-1} + 117a_{i-2} + 72b_{i-1} + 15c'_i + 117c'_{i-1} + 162c''_{i-1} \tag{2.6}$$

$$c'_i[W_3^{n+1}] = 30a_{i-2} + 54b_{i-2} + 6b_{i-1} + c'_i + 42c'_{i-1} + 27c''_{i-1} \tag{2.7}$$

$$c''_i[W_3^{n+1}] = 11a_{i-2} + 24b_{i-2} + 11c'_{i-1} \tag{2.8}$$

Proof. The terms $a_i[W_3^{n+1}] + 42a_{i+1}[W_3^{n+1}]$ in the consequent of Production (2.1) contribute to the terms $a_i[W_3^n] + 42a_{i-1}[W_3^n]$ in Equation (2.5). Similarly, the terms $6a_i[W_3^{n+1}] + 54a_{i+1}[W_3^{n+1}]$ in the consequent of Production (2.2) contribute to all the terms in Equation (2.5) containing partial-type b, and finally the terms $30a_i[W_3^{n+1}]$ and $27a_i[W_3^{n+1}]$ in the consequents of Productions (2.3) and (2.4), respectively, contribute to the terms in Equation (2.5) containing partial-types c' and c'', respectively.

Recurrences (2.6)−(2.8) can also be obtained by transposing the productions in a similar manner. □

The reader may observe the similarity between Equations (2.5) and (2.7). In fact, as the following result shows $a_{i-1}[W_3^n] = c'_i[W_3^n]$. Corollaries 2.2 and 2.7 are given for the interested reader and will not be used later.

Corollary 2.5. *The partial* $a_i[W_3^n] = c'_{i+1}[W_3^n]$ *for all values of* i *and* n.

Proof. By the Heffter-Edmonds face-tracing algorithm, the partitioned genus distribution of the graph W_3^1 is $2a_0 + 12b_1 + 2c'_1$. The result is clearly true for the base case. Assume that the proposition is true for W_3^k for all values of i and some $k \geq 1$. Then, by inductive hypothesis, Equation (2.5) becomes

$$\begin{aligned}
a_i[W_3^{k+1}] &= c'_{i+1}[W_3^k] + 42c'_i[W_3^k] + 6b_i[W_3^k] + 54b_{i-1}[W_3^k] + 30c'_i[W_3^k] \\
&\quad + 27c''_i[W_3^k] \\
&\Longrightarrow \\
a_{i-1}[W_3^{k+1}] &= c'_i[W_3^k] + 42c'_{i-1}[W_3^k] + 6b_{i-1}[W_3^k] + 54b_{i-2}[W_3^k] + 30c'_{i-1}[W_3^k] \\
&\quad + 27c''_{i-1}[W_3^k] \\
&= c'_i[W_3^k] + 42c'_{i-1}[W_3^k] + 6b_{i-1}[W_3^k] + 54b_{i-2}[W_3^k] + 30a_{i-2}[W_3^k] \\
&\quad + 27c''_{i-1}[W_3^k] \qquad \text{(by inductive hypothesis)} \\
&= c'_i[W_3^{k+1}]
\end{aligned}$$

□

Remark 2.6. Corollary 2.7 below shows that the genus distribution sequence of an iterated 3-wheel is dominated by the genus distribution sequence of the successive member of the family of iterated 3-wheels. All iteratively defined graph families do not necessarily exhibit this characteristic. For instance, the edge-amalgamated open chains containing one, two and three copies of $K_{3,3}$, respectively, have rising minimum genus [13].

Corollary 2.7. *The genus distribution sequence of* W_3^n *is dominated by the genus distribution sequence of* W_3^{n+1}

Proof. By re-arranging the terms, Equation (2.5) may be re-written as

$$\begin{aligned}
a_i[W_3^{n+1}] &= a_i[W_3^n] + b_i[W_3^n] + c'_i[W_3^n] + c''_i[W_3^n] + \big(42a_{i-1}[W_3^n] + 5b_i[W_3^n] \\
&\quad + 54b_{i-1}[W_3^n] + 29c'_i[W_3^n] + 26c''_i[W_3^n]\big) \\
&= g_i[W_3^n] + \big(42a_{i-1}[W_3^n] + 5b_i[W_3^n] + 54b_{i-1}[W_3^n] + 29c'_i[W_3^n] \\
&\quad + 26c''_i[W_3^n]\big)
\end{aligned}$$

It follows that $g_i[W_3^{n+1}] \geq g_i[W_3^n]$, for all $i \geq 0$. □

2.4 Genus distributions of W_3^2, W_3^3, W_3^4, and W_3^5

By using the Heffter-Edmonds face-tracing algorithm the partitioned genus distribution of W_3^1 is

$$a_0[W_3^1] = 2 \qquad b_1[W_3^1] = 12 \qquad c'_1[W_3^1] = 2$$

Substituting these values into the recurrences given in Corollary 2.4, we get the partitioned genus distribution of W_3^2 as follows:

$$
\begin{aligned}
a_0[W_3^2] &= a_0 = 2\\
b_0[W_3^2] &= 0\\
c_0'[W_3^2] &= 0\\
c_0''[W_3^2] &= 0
\end{aligned}
$$

$$
\begin{aligned}
a_1[W_3^2] &= a_1 + 42a_0 + 6b_1 + 54b_0 + 30c_1' + 27c_1''\\
&= 0 + 42 \times 2 + 6 \times 12 + 0 + 30 \times 2 + 0 = 216\\
b_1[W_3^2] &= 15a_0 + 15c_1' = 15 \times 2 + 15 \times 2 = 60\\
c_1'[W_3^2] &= c_1' = 2\\
c_1''[W_3^2] &= 0
\end{aligned}
$$

$$
\begin{aligned}
a_2[W_3^2] &= 54b_1 = 54 \times 12 = 648\\
b_2[W_3^2] &= 117a_0 + 72b_1 + 117c_1' = 117 \times 2 + 72 \times 12 + 117 \times 2 = 1332\\
c_2'[W_3^2] &= 30a_0 + 6b_1 + 42c_1' = 30 \times 2 + 6 \times 12 + 42 \times 2 = 216\\
c_2''[W_3^2] &= 11a_0 + 11c_1' = 11 \times 2 + 11 \times 2 = 44
\end{aligned}
$$

$$
\begin{aligned}
a_3[W_3^2] &= 0\\
b_3[W_3^2] &= 0\\
c_3'[W_3^2] &= 54b_1 = 54 \times 12 = 648\\
c_3''[W_3^2] &= 24b_1 = 24 \times 12 = 288
\end{aligned}
$$

The partitioned genus distribution of W_3^2 and the genus distribution obtained from it is listed in Table 2.1.

Table 2.1: Genus distribution of W_3^2.

i	a_i	b_i	c_i'	c_i''	g_i
0	2	0	0	0	2
1	216	60	2	0	278
2	648	1332	216	44	2240
3	0	0	648	288	936

For partitioned genus distribution of W_3^3, we again use Corollary 2.4 and substitute the values of partials of W_3^2 from Table 2.1 as follows:

$$
\begin{aligned}
a_0[W_3^3] &= a_0 = 2\\
b_0[W_3^3] &= 0\\
c_0'[W_3^3] &= 0\\
c_0''[W_3^3] &= 0
\end{aligned}
$$

$$
\begin{aligned}
a_1[W_3^3] &= a_1 + 42a_0 + 6b_1 + 30c_1' = 216 + 42 \times 2 + 6 \times 60 + 30 \times 2 = 720\\
b_1[W_3^3] &= 15a_0 + 15c_1' = 15 \times 2 + 15 \times 2 = 60\\
c_1'[W_3^3] &= c_1' = 2\\
c_1''[W_3^3] &= 0
\end{aligned}
$$

$$
\begin{aligned}
a_2[W_3^3] &= a_2 + 42a_1 + 6b_2 + 54b_1 + 30c_2' + 27c_2''\\
&= 648 + 42 \times 216 + 6 \times 1332 + 54 \times 60 + 30 \times 216 + 27 \times 44 = 28620\\
b_2[W_3^3] &= 15a_1 + 117a_0 + 72b_1 + 15c_2' + 117c_1'\\
&= 15 \times 216 + 117 \times 2 + 72 \times 60 + 15 \times 216 + 117 \times 2 = 11268\\
c_2'[W_3^3] &= 30a_0 + 6b_1 + c_2' + 42c_1' = 30 \times 2 + 6 \times 60 + 216 + 42 \times 2 = 720\\
c_2''[W_3^3] &= 11a_0 + 11c_1' = 11 \times 2 + 11 \times 2 = 44
\end{aligned}
$$

$$
\begin{aligned}
a_3[W_3^3] &= 42a_2 + 54b_2 + 30c_3' + 27c_3''\\
&= 42 \times 648 + 54 \times 1332 + 30 \times 648 + 27 \times 288 = 126360\\
b_3[W_3^3] &= 15a_2 + 117a_1 + 72b_2 + 15c_3' + 117c_2' + 162c_2''\\
&= 15 \times 648 + 117 \times 216 + 72 \times 1332 + 15 \times 648 + 117 \times 216 + 162 \times 44\\
&= 173016\\
c_3'[W_3^3] &= 30a_1 + 54b_1 + 6b_2 + c_3' + 42c_2' + 27c_2''\\
&= 30 \times 216 + 54 \times 60 + 6 \times 1332 + 648 + 42 \times 216 + 27 \times 44 = 28620\\
c_3''[W_3^3] &= 11a_1 + 24b_1 + 11c_2' = 11 \times 216 + 24 \times 60 + 11 \times 216 = 6192
\end{aligned}
$$

$$
\begin{aligned}
a_4[W_3^3] &= 0\\
b_4[W_3^3] &= 117a_2 + 117c_3' + 162c_3'' = 117 \times 648 + 117 \times 648 + 162 \times 288 = 198288\\
c_4'[W_3^3] &= 30a_2 + 54b_2 + 42c_3' + 27c_3''\\
&= 30 \times 648 + 54 \times 1332 + 42 \times 648 + 27 \times 288 = 126360\\
c_4''[W_3^3] &= 11a_2 + 24b_2 + 11c_3' = 11 \times 648 + 24 \times 1332 + 11 \times 648 = 46224
\end{aligned}
$$

The partitioned genus distribution and the genus distribution of W_3^3 is given in Table 2.2.

Table 2.2: Genus distribution of W_3^3.

i	a_i	b_i	c_i'	c_i''	g_i
0	2	0	0	0	2
1	720	60	2	0	782
2	28620	11268	720	44	40652
3	126360	173016	28620	6192	334188
4	0	198288	126360	46224	370872

Similar computations can be made for larger values of n. See Tables 2.3−2.4 for genus distributions of W_3^4 and W_3^5.

Table 2.3: Genus distribution of W_3^4.

i	a_i	b_i	c_i'	c_i''	g_i
0	2	0	0	0	2
1	1224	60	2	0	1286
2	152496	26388	1224	44	180152
3	4000752	1845504	152496	17280	6016032
4	20878560	23948136	4000752	900072	49727520
5	10707552	51333264	20878560	6932304	89851680
6	0	0	10707552	4758912	15466464

Table 2.4: Genus distribution of W_3^5.

i	a_i	b_i	c_i'	c_i''	g_i
0	2	0	0	0	2
1	1728	60	2	0	1790
2	403380	41508	1728	44	446660
3	27945000	6768360	403380	28368	35145108
4	576580680	291382272	27945000	3988224	899896176
5	3302335008	3432610224	576580680	132308640	7443834552
6	3671430624	10025837856	3302335008	1034083584	18033687072
7	0	3276510912	3671430624	1467564480	8415506016

3 Genus distributions of iterated 3-prisms

Subdivision of any two edges incident on the root-vertex v of (W_3^{n-1}, v), and adding an edge between the subdivision vertices produces the graph (Pr_3^n, v). For the rest of this section, we use the term ***edge-addition*** to refer to this particular operation. Each embedding ι_w of (W_3^{n-1}, v) induces four embeddings of (Pr_3^n, v) under edge-addition. The partial-types of the four embeddings of Pr_3^n produced are determined by the partial-type of the embedding ι_w.

3.1 Productions for edge-addition

Akin to productions for rim-insertion, one can also define productions for other graph operations. In what follows, we derive productions for the edge-addition operation:

Theorem 3.1. *When an embedding of the single-rooted graph (W_3^{n-1}, v) of partial-type a, c' or c'' undergoes the edge-addition operation to produce (Pr_3^n, v), the types of embeddings of Pr_3^n produced are specified by the following productions:*

$$a_i[W_3^{n-1}] \longrightarrow a_i[Pr_3^n] + 3b_{i+1}[Pr_3^n] \tag{3.1}$$

$$c_i'[W_3^{n-1}] \longrightarrow 3b_i[Pr_3^n] + c_i'[Pr_3^n] \tag{3.2}$$

$$c_i''[W_3^{n-1}] \longrightarrow 4b_i[Pr_3^n] \tag{3.3}$$

Proof. In any given embedding of W_3^{n-1} of type a, subdividing the edges incident on the root-vertex ensures that each pair of subdivision vertices occurs in exactly one of the fb-walks incident on the root-vertex. Because of this symmetry, for any choice of subdivision vertices adding an edge between them results in the same type of embeddings. As illustrated in Figure 3.1, the partial-types and genera of the embeddings produced as a result are specified by Production (3.1).

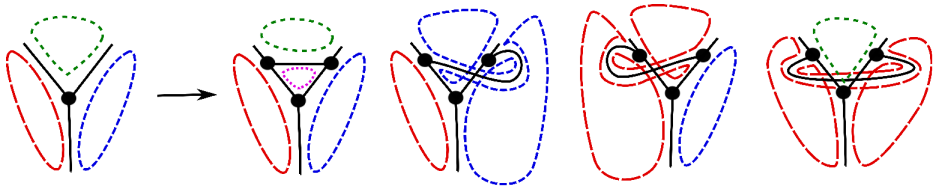

Figure 3.1: Production (3.1).

A similar argument can be made for the productions for types c' and c''. These are visualized in Figure 3.2 and Figure 3.3, respectively. □

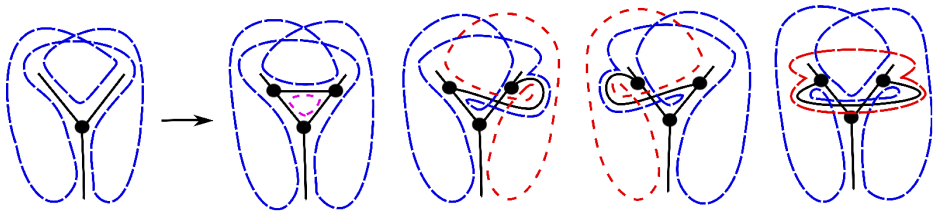

Figure 3.2: Production (3.2).

Figure 3.3: Production (3.3).

Theorem 3.2. *When an embedding of the single-rooted graph (W_3^{n-1}, v) of partial-type b undergoes the edge-addition operation to produce (Pr_3^n, v), the types of embeddings of Pr_3^n produced are specified by only one of the following two productions:*

$$b_i[W_3^{n-1}] \longrightarrow 2a_i[Pr_3^n] + 2c'_{i+1}[Pr_3^n] \tag{3.4}$$

$$b_i[W_3^{n-1}] \longrightarrow a_i[Pr_3^n] + b_i[Pr_3^n] + 2c''_{i+1}[Pr_3^n] \tag{3.5}$$

Proof. Let ι be a type b embedding. The left-hand-side of Figure 3.4 illustrates how subdividing the three edges incident on the root-vertex produces the subdivision vertices v_1,

v_2 and v_3 such that the fb-walks incident on the root-vertex are $(v_1 * v_2 * v_2 * v_3 *)$ and $(v_3 * v_1 *)$, where $*$ represents zero or more occurrences of vertices other than the subdivision vertices. Figure 3.4 illustrates the case when an edge-addition takes place between v_1 and v_2. By symmetry, this is also true for the case when an edge is added between v_2 and v_3. Both cases correspond to Production (3.4).

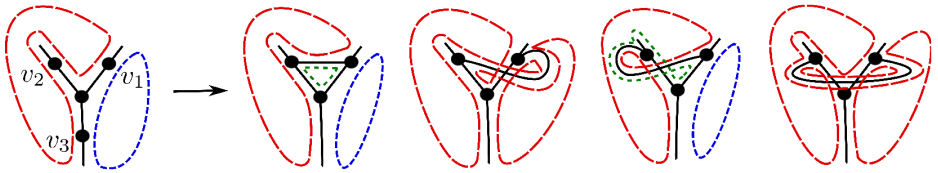

Figure 3.4: Production (3.4).

Production (3.5) specifies the scenario when an edge is added between v_1 and v_3, as shown in Figure 3.5. □

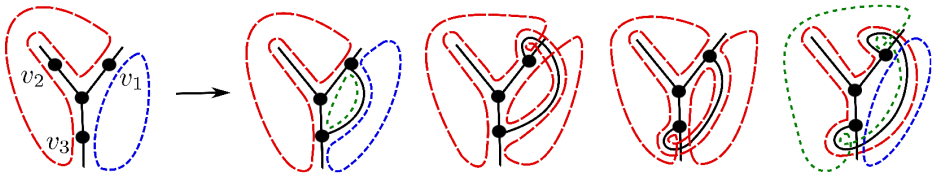

Figure 3.5: Production (3.5).

Corollary 3.3. *Let t_i represent an embedding of Pr_3^n of genus i and any partial-type. When an embedding of the single-rooted graph (W_3^{n-1}, v) undergoes the edge-addition operation, the genera of the embeddings of Pr_3^n produced are specified as follows:*

$$a_i[W_3^{n-1}] \longrightarrow t_i[Pr_3^n] + 3t_{i+1}[Pr_3^n] \tag{3.6}$$

$$b_i[W_3^{n-1}] \longrightarrow 2t_i[Pr_3^n] + 2t_{i+1}[Pr_3^n] \tag{3.7}$$

$$c_i'[W_3^{n-1}] \longrightarrow 3t_i[Pr_3^n] + t_i[Pr_3^n] \tag{3.8}$$

$$c_i''[W_3^{n-1}] \longrightarrow 4t_i[Pr_3^n] \tag{3.9}$$

Proof. Productions (3.6), (3.8) and (3.9) follow directly from Theorem 3.1. Production (3.7) follows from Theorem 3.2, as an embedding of W_3^{n-1} of partial-type b and genus i in all cases produces two embeddings of Pr_3^n of genus i and two of genus $i+1$. □

Corollary 3.4. *Given the partitioned genus distribution of single-rooted graph (W_3^{n-1}, v), the genus distribution of the graph Pr_3^n is specified by the following formula:*

$$\begin{aligned} g_i[Pr_3^n] \; &= a_i[W_3^{n-1}] + 3a_{i-1}[W_3^{n-1}] + 2b_i[W_3^{n-1}] + 2b_{i-1}[W_3^{n-1}] \\ &\quad + 4c_i'[W_3^{n-1}] + 4c_i''[W_3^{n-1}] \end{aligned} \tag{3.10}$$

Proof. This follows by transposing the productions in Corollary 3.3. □

Remark 3.5. It may be observed that the genus distribution sequence of Pr_3^n also dominates the genus distribution sequence of W_3^{n-1}.

3.2 Genus distributions of small iterated 3-prisms

The genus distribution of Pr_3^n can be computed by substituting the values of the partitioned genus distribution of W_3^{n-1} into Equation (3.10), for $n \geq 2$. We show this for $n = 3$ and $n = 4$ by substituting values from Tables 2.1 and 2.2 into Equation (3.10) as follows:

Genus distribution of Pr_3^3

$$\begin{aligned} g_0[Pr_3^3] &= a_0[W_3^2] + 2b_0[W_3^2] + 4c_0'[W_3^2] + 4c_0''[W_3^2] \\ &= 2 + 2 \times 0 + 4 \times 0 + 4 \times 0 \ = \ 2 \end{aligned}$$

$$\begin{aligned} g_1[Pr_3^3] &= a_1[W_3^2] + 3a_0[W_3^2] + 2b_1[W_3^2] + 2b_0[W_3^2] + 4c_1'[W_3^2] + 4c_1''[W_3^2] \\ &= 216 + 3 \times 2 + 2 \times 60 + 2 \times 0 + 4 \times 2 + 4 \times 0 \ = \ 350 \end{aligned}$$

$$\begin{aligned} g_2[Pr_3^3] &= a_2[W_3^2] + 3a_1[W_3^2] + 2b_2[W_3^2] + 2b_1[W_3^2] + 4c_2'[W_3^2] + 4c_2''[W_3^2] \\ &= 648 + 3 \times 216 + 2 \times 1332 + 2 \times 60 + 4 \times 216 + 4 \times 44 \ = \ 5120 \end{aligned}$$

$$\begin{aligned} g_3[Pr_3^3] &= a_3[W_3^2] + 3a_2[W_3^2] + 2b_3[W_3^2] + 2b_2[W_3^2] + 4c_3'[W_3^2] + 4c_3''[W_3^2] \\ &= 0 + 3 \times 648 + 2 \times 0 + 2 \times 1332 + 4 \times 648 + 4 \times 288 \ = \ 8352 \end{aligned}$$

Genus distribution of Pr_3^4

$$\begin{aligned} g_0[Pr_3^4] &= a_0[W_3^3] + 2b_0[W_3^3] + 4c_0'[W_3^3] + 4c_0''[W_3^3] \\ &= 2 + 2 \times 0 + 4 \times 0 + 4 \times 0 \ = \ 2 \end{aligned}$$

$$\begin{aligned} g_1[Pr_3^4] &= a_1[W_3^3] + 3a_0[W_3^3] + 2b_1[W_3^3] + 2b_0[W_3^3] + 4c_1'[W_3^3] + 4c_1''[W_3^3] \\ &= 720 + 3 \times 2 + 2 \times 60 + 2 \times 0 + 4 \times 2 + 4 \times 0 \ = \ 854 \end{aligned}$$

$$\begin{aligned} g_2[Pr_3^4] &= a_2[W_3^3] + 3a_1[W_3^3] + 2b_2[W_3^3] + 2b_1[W_3^3] + 4c_2'[W_3^3] + 4c_2''[W_3^3] \\ &= 28620 + 3 \times 720 + 2 \times 11268 + 2 \times 60 + 4 \times 720 + 4 \times 44 \ = \ 56492 \end{aligned}$$

$$\begin{aligned} g_3[Pr_3^4] &= a_3[W_3^3] + 3a_2[W_3^3] + 2b_3[W_3^3] + 2b_2[W_3^3] + 4c_3'[W_3^3] + 4c_3''[W_3^3] \\ &= 126360 + 3 \times 28620 + 2 \times 173016 + 2 \times 11268 + 4 \times 28620 + 4 \times 6192 \\ &= 720036 \end{aligned}$$

$$\begin{aligned} g_4[Pr_3^4] &= a_4[W_3^3] + 3a_3[W_3^3] + 2b_4[W_3^3] + 2b_3[W_3^3] + 4c_4'[W_3^3] + 4c_4''[W_3^3] \\ &= 0 + 3 \times 126360 + 2 \times 198288 + 2 \times 173016 + 4 \times 126360 + 4 \times 46224 \\ &= 1812024 \end{aligned}$$

$$\begin{aligned} g_5[Pr_3^4] &= a_5[W_3^3] + 3a_4[W_3^3] + 2b_5[W_3^3] + 2b_4[W_3^3] + 4c_5'[W_3^3] + 4c_5''[W_3^3] \\ &= 0 + 3 \times 0 + 2 \times 0 + 2 \times 198288 + 4 \times 0 + 4 \times 0 \ = \ 396576 \end{aligned}$$

In a similar manner, genus distributions of Pr_3^n can be computed for larger values of n. We show genus distributions of Pr_3^n for some small values of n in Table 3.1

Table 3.1: Genus distributions of Pr_3^n, for $n = 5, 6, 7$, and 8.

g_i	Pr_3^5	Pr_3^6	Pr_3^7	Pr_3^8
g_0	2	2	2	2
g_1	1358	1862	2366	2870
g_2	214136	498788	910448	1449116
g_3	8881128	44501868	137348784	319427892
g_4	104071392	1384449840	8434131048	32260431816
g_5	335149488	15315619320	215271967896	1516697746416
g_6	196655040	57841006176	2282687116992	33465180312144
g_7	0	58174969824	9638974212192	343447934792400
g_8	0	0	13727729155968	1575240986550240
g_9	0	0	4218604167168	2866735730052288
g_{10}	0	0	0	1571115983393664

As noted in Remark 3.5, genus distribution of the iterated 3-prism Pr_3^n always dominates genus distribution of the iterated 3-wheel W_3^{n-1}, where Pr_3^n is obtained by adding an edge to a homeomorphic copy of W_3^{n-1}. A shift in perspective would be to view the iterated 3-wheel W_3^n as having been obtained from Pr_3^n by adding a 3-valent vertex to it. A natural question here would be to ask how the genus distributions of W_3^n and Pr_3^n compare. From Tables 2.1−2.4 and Table 3.1, it can be observed that genus distribution of W_3^n dominates the genus distribution of Pr_3^n, for small values of n. In fact, this is true in general as the following theorem shows:

Theorem 3.6. *Genus distribution of W_3^n dominates the genus distribution of Pr_3^n.*

Proof. Let v_1, v_2, v_3 be the three vertices in Pr_3^n to which a new vertex is joined, in order to obtain W_3^n. There are 8 possible sets of rotations at these three vertices. For each such set of rotations, examining the strands of fb-walks incident at v_1, v_2, and v_3 leads to the conclusion that every embedding of Pr_3^n contains a face in which all three vertices appear. Thus, for every embedding of Pr_3^n, it is possible to obtain an embedding of W_3^n on the same surface, by placing the new vertex in that face. It follows that for each surface, there are at-least as many embeddings of W_3^n as there are for Pr_3^n. □

4 Conclusions

Unlike previous results using the rooted-graphs method, this paper uses a single unchanging root-vertex for computing genus distributions for each member of the family of iterated 3-wheels W_3^n and of the family of iterated 3-prisms Pr_3^n. This paper also establishes that the sequence of genus distribution of W_3^n dominates the sequence of genus distribution of Pr_3^n, which in turn dominates the sequence of genus distribution of W_3^{n-1}.

A general direction for future work is to programatically examine the possibilities for manipulating root-vertices for computing genus distributions. The approach and algorithm used in this paper seem in principle to be extendible to Pr_m^n, for any fixed m, with a cor-

responding increase in the size of the productions and partials, with definitions of partials based on integer partitions analogous to the way they have been defined in [8].

Some questions raised by this paper are as follows:

1. In keeping with the strong unimodality conjecture, genus distributions of iterated 3-wheels W_3^n and 3-prisms Pr_3^n, that were computed for small values of n, were found to be log concave. Can the recurrences for the partials be analyzed for affirming the log concavity of genus distributions for these families?

2. It can also be observed from Tables 2.1−2.4 that for some small iterated 3-wheels the mode of the genus distribution is either the maximum genus or one less than the maximum genus. For larger n, the mode seems to migrate backwards. Our empirical evidence suggests that for large n, the ratio of the maximum genus of W_3^n to the mode of its genus distribution is approximately 1.185. Can this be proven using the recurrences for the partials of iterated 3-wheels?

3. The distribution of each partial is observed to be log concave for the iterated 3-wheel W_3^n, for small values of n (See Tables 2.1−2.4 for $n = 2, 3, 4,$ and 5). Does this hold true in general?

4. In case of W_3^{n-1} and Pr_3^n, it is clear that the domination of genus distribution of Pr_3^n is an outcome of the fact that it is obtained from W_3^{n-1} by an edge-addition between vertices adjacent to the 3-valent root vertex of W_3^{n-1}. This means that for any embedding of W_3^{n-1}, there is a way to embed this edge in a way that subdivides a face. For the same reason, it is also clear that if we were to take an arbitrary graph G with a 3-valent vertex, then subdividing any two edges incident on the 3-valent vertex and adding an edge between the subdivision vertices, results in graph whose genus distribution dominates the genus distribution of G. The result does not generalize to graphs with edges that do not share a 3-valent endpoint. For instance, a dipole D_4 has 6 planar embeddings, but subdividing two edges and adding an edge between the subdivision vertices produces a graph with 4 planar embeddings. Similarly, the result does not generalize to the case where the edges being subdivided do not share a common endpoint, for instance, it is possible to subdivide two edges of the planar circular ladder CL_3 and add an edge between the subdivision vertices so as to produce a homeomorphic copy of $K_{3,3}$ in the resultant graph. It would be interesting to have general results that characterize the operations that, when applied to a graph, produce graphs whose genus distributions dominate that of the original graph.

References

[1] J. Chen, J. L. Gross and R. G. Rieper, Overlap matrices and total imbedding distributions, *Discrete Math.* **128** (1994), 73–94.

[2] Y. C. Chen, Y. P. Liu and T. Wang, The total embedding distributions of cacti and necklaces, *Acta Math. Sinica — English Series* **22** (2006), 1583–1590.

[3] Y. Chen, T. Mansour and Q. Zou, Embedding distributions of generalized fan graphs, *Acta Math. Sinica — English Series* **22** (2006), 1583–1590. Canad. Math. Bull. (2011) Online 31, August.

[4] J. L. Gross, Genus distribution of graph amalgamations: Self-pasting at root-vertices, *Australas. J. Combin.* **49** (2011), 19–38.

[5] J. L. Gross and M. L. Furst, Hierarchy for imbedding-distribution invariants of a graph, *J. Graph Theory* **11** (1987), 205–220.

[6] J. L. Gross, I. F. Khan and M. I. Poshni, Genus distribution of graph amalgamations: Pasting at root-vertices, *Ars Combin.* **94** (2010), 33–53.

[7] J. L. Gross and T. W. Tucker, *Topological Graph Theory*, Dover, 2001; (original edn. Wiley, 1987).

[8] I. F. Khan, M. I. Poshni and J. L. Gross, Genus distribution of graph amalgamations: Pasting when one root has arbitrary degree, *Ars Math. Contemp.* **3** (2010), 121–138.

[9] J. H. Kwak and J. Lee, Genus polynomials of dipoles, *Kyungpook Math. J.* **33** (1993), 115–125.

[10] J. H. Kwak and J. Lee, Enumeration of graph embeddings, *Discrete Math.* **135** (1994), 129–151.

[11] J. H. Kwak and S. H. Shim, Total embedding distributions for bouquets of circles, *Discrete Math.* **248** (2002), 93–108.

[12] B. P. Mull, Enumerating the orientable 2-cell imbeddings of complete bipartite graphs, *J. Graph Theory* **30** (1999), 77–90.

[13] M. I. Poshni, I. F. Khan and J. L. Gross, Genus distributions of graphs under edge-amalgamations, *Ars Math. Contemp.* **3** (2010), 69–86.

[14] M. I. Poshni, I. F. Khan and J. L. Gross, Genus distributions of graphs under self-edge-amalgamations, *Ars Math. Contemp.* **5** (2012), 127–148.

[15] S. Stahl, Region distributions of graph embeddings and Stirling numbers, *Discrete Math.* **82** (1990), 57–78.

[16] S. Stahl, Permutation-partition pairs III: Embedding distributions of linear families of graphs, *J. Combin. Theory (B)* **52** (1991), 191–218.

[17] S. Stahl, On the zeroes of some genus polynomials, *Canad. J. Math.* **49** (1997), 617–640.

[18] E. H. Tesar, Genus distribution of Ringel ladders, *Discrete Math.* **216** (2000) 235–252.

[19] T. I. Visentin and S. W. Wieler, On the genus distribution of (p, q, n)-dipoles, *Electronic J. Combin.* **14** (2007), Art. No. R12.

[20] L. X. Wan and Y. P. Liu, Orientable embedding distributions by genus for certain types of graphs, *Ars Combin.* **79** (2006), 97–105.

[21] L. X. Wan and Y. P. Liu, Orientable embedding genus distribution for certain types of graphs, *J. Combin. Theory (B)* **47** (2008), 19–32.

[22] A. T. White, *Graphs of Groups on Surfaces*, North-Holland, 2001.

ARS MATHEMATICA CONTEMPORANEA

Also available at http://amc-journal.eu
ISSN 1855-3966 (printed edn.), ISSN 1855-3974 (electronic edn.)
ARS MATHEMATICA CONTEMPORANEA 7 (2014) 441–452

Average distance, radius and remoteness of a graph*

Baoyindureng Wu †
College of Mathematics and System Science, Xinjiang University
Urumqi 830046, P.R. China

Wanping Zhang
Foundation department, Karamay Vocational and Technical College
Karamay 833600, P.R. China

Received 28 February 2012, accepted 25 August 2013, published online 26 December 2013

Abstract

Let $G = (V, E)$ be a connected graph on n vertices. Denote by $\bar{l}(G)$ the average distance between all pairs of vertices in G. The *remoteness* $\rho(G)$ of a connected graph G is the maximum average distance from a vertex of G to all others. The aim of this paper is to show that two conjectures in [5] concerned with average distance, radius and remoteness of a graph are true.

Keywords: Distance, radius, eccentricity, proximity, remoteness.

Math. Subj. Class.: 05C12, 05C35

1 Introduction

All graphs considered in this paper are finite and simple. For notation and terminology not defined here, we refer to West [21]. Let $G = (V, E)$ be a finite simple graph with vertex set V and edge set E, $|V|$ and $|E|$ are its order and size, respectively. The distance between vertices u and v is denoted by $d(u, v)$, is the length of a shortest path connecting u and v. The average distance between all pairs of vertices in G is denoted by $\bar{l}(G)$. That is $\bar{l}(G) = \frac{1}{\binom{n}{2}} \sum_{u,v \in V(G)} d(u, v)$, where the summation run over all unordered pairs of vertices. The *eccentricity* $e_G(v)$ of a vertex v in G is the largest distance from v to another vertex of G, i.e. $\max\{d(v, w)|\ w \in V(G)\}$. The *diameter* of G is the maximum eccentricity in G,

*This research was supported by NSFC (No. 11161046).

†Corresponding author.
E-mail addresses: baoyinwu@gmail.com (Baoyindureng Wu), zwp19980126@163.com (Wanping Zhang)

denoted by $diam(G)$. Similarly, the *radius* of G is the minimum eccentricity in G, denoted by $rad(G)$; and the *average eccentricity* of G is denoted by $ecc(G)$. In other words,

$$rad(G) = \min_{v\in V} e_G(v), \quad diam(G) = \max_{v\in V} e_G(v) \text{ and } ecc(G) = \frac{1}{n}\sum_{v\in V} e_G(v).$$

For a connected graph G of order n, $\sigma_G(u)$ denotes the average distance from u to all other vertices of G, that is $\sigma_G(u) = \frac{1}{n-1}\sum_{v\in V(G)} d(u,v)$. The *proximity* $\pi(G)$ of a connected graph G is the minimum average distance from a vertex of G to all others. Similarly, the *remoteness* $\rho(G)$ of a connected graph G is the maximum average distance from a vertex of G to all others. They were recently introduced in [2, 3], that is

$$\pi(G) = \min_{v\in V} \sigma_G(v) \text{ and } \rho(G) = \max_{v\in V} \sigma_G(v).$$

The sum of distances from a vertex of G to all others is known as its transmission. Proximity and remoteness can also be seen as the minimum and maximum normalized transmission in a graph. Indeed, by their definitions

$$\pi(G) \le rad(G) \le ecc(G) \le diam(G) \text{ and } \pi(G) \le \bar{l}(G) \le \rho(G) \le diam(G).$$

There are a number of results which are devoted to the relation between average distance and other graph parameters (see [6-15, 22]). A vertex $u \in V(G)$ with the minimum eccentricity is called a $center$ of G. It is well-known that every tree has either exactly one center or two, adjacent centers. The center of graphs have been extensively studied in the literature (see [16]). Some more results on the radius of graphs can be found in [18, 17].

A Soltés or a path-complete graph is the graph obtained from a clique and a path by adding at least one edge between an endpoint of the path and the clique. The Soltés graphs are known to maximize the average distance $\bar{l}$ when the number of vertices and of edges are fixed [20].

In [4] Aouchiche and Hansen established the Nordhaus-Gaddum-type theorem for $\pi(G)$ and $\rho(G)$. In [5] the same authors gave the upper bounds on $rad(G) - \pi(G)$, $diam(G) - \pi(G)$ and $\rho(G) - \pi(G)$, and proposed five related conjectures, two of which are the following.

Conjecture A. (Conjecture 5, [5]) Among all connected graphs G on $n \ge 3$ vertices with average distance $\bar{l}$ and remoteness ρ, the Soltés graphs with diameter $\lfloor \frac{n+1}{2} \rfloor$ maximize $\rho - \bar{l}$.

Conjecture B. (Conjecture 1, [5]) Let G be a connected graph on $n \ge 3$ vertices with remoteness ρ and radius r. Then connected graph G on $n \ge 3$ vertices,

$$\rho - r \ge \begin{cases} \frac{n^2}{4n-4} - \frac{n}{2}, & \text{if } n \text{ is even,} \\ \frac{3-n}{4}, & \text{if } n \text{ is odd.} \end{cases}$$

The inequality is best possible as shown by the cycle C_n if n is even and of the graph composed by the cycle C_n together with two crossed edges on four successive vertices of the cycle.

The aim of this note is to confirm the validity of the above conjectures.

Conjecture 2 in [5] is solved in [19], and Conjecture 4 in [5] is solved in [1]. Up to now, Conjecture 3 in [5] still remains open.

2 Proof of Conjecture A

For convenience, we use some additional definition and notations. Let G be a connected graph. A vertex $u \in V(G)$ is called a *peripheral* vertex if $\sigma(u) = \rho(G)$. For a vertex $u \in V(G)$, let $V_i(u) = \{v \in V(G) |\ d(u,v) = i\}$ and $n_i(u) = |V_i(u)|$ for each $i \in \{1, \ldots, d\}$, where $d = e_G(u)$. In what follows, $V_i(u)$ is simply denoted by V_i for a peripheral vertex u of G.

Lemma 2.1. *Let G be a connected graph of order $n \geq 3$. Let u be a peripheral vertex of G and let $d = e_G(u)$. Let G' be the graph obtained from G by joining each pair of all nonadjacent vertices x, y of G, where $x, y \in V_j \cup V_{j+1}$ for some $j \in \{1, \ldots, d-1\}$. We have*

$$\rho(G') - \bar{l}(G') \geq \rho(G) - \bar{l}(G),$$

with equality if and only if $G' = G$.

Proof. It is clear that for any $x \in V(G)$, $d_{G'}(u,x) = d_G(u,x)$ and $d_{G'}(v,w) \leq d_G(v,w)$ for any $v, w \in V(G)$. It follows that $\sigma_{G'}(u) = \sigma_G(u)$ and $\sigma_{G'}(v) \leq \sigma_G(v)$ for any $v \in V(G')$. Combining this with the assumption that u is a peripheral vertex of G, it follows that u is also a peripheral vertex of G'. Thus $\rho(G') = \sigma_{G'}(u) = \sigma_G(u) = \rho(G)$. Moreover, it is obvious that $\bar{l}(G') \leq \bar{l}(G)$, with equality if and only if $G' = G$. So, $\rho(G') - \bar{l}(G') \geq \rho(G) - \bar{l}(G)$, with equality if and only if $G' = G$. □

Lemma 2.2. *Let G be a connected graph of order $n \geq 3$. Let u be a peripheral vertex of G and $e_G(v) = d$. Assume that $G[V_j \cup V_{j+1}]$ is a clique for each $j \in \{0, \ldots, d-1\}$. Let G' be the graph with $V(G') = V(G)$ and $E(G') = E(G) \cup \{xy : x \in V_{d-2}, y \in V_d\}$. If $d > \lfloor \frac{n+1}{2} \rfloor$, then*

$$\rho(G') - \bar{l}(G') \leq \rho(G) - \bar{l}(G),$$

with equality if and only if n is even and $d = \frac{n}{2} + 1$.

Proof. Note that

$$\sigma_{G'}(x) = \begin{cases} \sigma_G(x) - \frac{1}{n-1} n_d, & \text{if } x \in \bigcup_{j=1}^{d-2} V_j \cup \{u\} \\ \sigma_G(x), & \text{if } x \in V_{d-1} \\ \sigma_G(x) - \frac{1}{n-1}(n - n_{d-1} - n_d), & \text{if } x \in V_d\,. \end{cases}$$

Since u is a peripheral vertex of G, $\sigma_{G'}(u) \geq \sigma_{G'}(x)$ for any $x \in \bigcup_{j=1}^{d-2} V_j$. Moreover, since $d > \lfloor \frac{n+1}{2} \rfloor$, $n_{d-1} + n_d \leq \frac{n}{2}$, with equality if and only if n is even and $d = \frac{n}{2} + 1$.

Thus $n - n_{d-1} - n_d \geq \frac{n}{2}$. Again by the assumption that u is a peripheral vertex of G, $\sigma_{G'}(u) \geq \sigma_{G'}(x)$ for any $x \in V_d$. Also, for any $y \in V_{d-1}$, $\sigma_{G'}(y) = \sigma_{G'}(x)$ for any $x \in V_d$. Thus $\sigma_{G'}(u) > \sigma_{G'}(y)$. It means that u is a peripheral vertex of G', and $\rho(G') = \sigma_{G'}(u)$. So, $\rho(G) - \rho(G') = \sigma_{G'}(u) - \sigma_G(u) = \frac{1}{n-1} n_d$. On the other hand, one can see that

$$\bar{l}(G) - \bar{l}(G') = \frac{1}{\binom{n}{2}} \big[(n - n_{d-1} - n_d) n_d\big] = \frac{2}{(n-1)n} \big[(n - n_{d-1} - n_d) n_d\big] \geq \frac{1}{n-1} n_d.$$

It follows that

$$\bar{l}(G) - \bar{l}(G') \geq \rho(G) - \rho(G'),$$

with equality if n is even and $d = \frac{n}{2} + 1$. □

Lemma 2.3. *Let G be a connected graph of order $n \geq 3$. Let u be a peripheral vertex of G and $e_G(v) = d$. Assume that $G[V_j \cup V_{j+1}]$ is a clique for each $j \in \{0, \ldots, d-1\}$. Let i be the smallest integer in $\{1, \ldots, d\}$ such that $n_i(u) \geq 2$. Let $V_{i-1}(u) = \{u_{i-1}\}$ and v a vertex in $V_i(u)$. Denote by G' the graph with $V(G') = V(G)$ and $E(G') = E(G) \setminus (\{u_{i-1}y : \ y \in V_i \setminus \{v\}\} \cup A)$, where $A = \{vx : \ x \in V_{i+1}\}$ if $i \leq d-1$, and $A = \emptyset$ otherwise. If $d < \lfloor \frac{n+1}{2} \rfloor$, then*

$$\rho(G') - \bar{l}(G') > \rho(G) - \bar{l}(G).$$

Proof. One can see that if $i \leq d-1$, then

$$\sigma_{G'}(x) - \sigma_G(x) = \begin{cases} \frac{1}{n-1}(n-i-1), & \text{if } x \in \bigcup_{j=1}^{i-1} V_j \cup \{v, u\} \\ \frac{1}{n-1} i, & \text{if } x \in V_i \setminus \{v\} \\ \frac{1}{n-1}(i+1), & \text{if } x \in \bigcup_{j=i+1}^{d} V_j, \end{cases}$$

if $i = d$, then

$$\sigma_{G'}(x) - \sigma_G(x) = \begin{cases} \frac{1}{n-1}(n-d-1), & \text{if } x \in \bigcup_{j=1}^{d-1} V_j \cup \{v, u\} \\ \frac{1}{n-1} d, & \text{if } x \in V_d \setminus \{v\} \end{cases}$$

If $i \leq d-1$, then by $d \leq \lfloor \frac{n+1}{2} \rfloor - 1$, we have $i+1 \leq \lfloor \frac{n+1}{2} \rfloor - 1$ and $n-i-1 > i+1$. Moreover, since u is a peripheral vertex of G, u is also a peripheral vertex of G'. If $i = d$, then it is trivial to see that u is a peripheral vertex of G'. So, $\rho(G') - \rho(G) = \sigma_{G'}(u) - \sigma_G(u) = \frac{1}{n-1}\big(n-i-1\big)$.

On the other hand, if $i \leq d-1$, then

$$\begin{aligned} \bar{l}(G') - \bar{l}(G) &= \frac{1}{\binom{n}{2}}\big[\big(i+1\big)\big(n_{i+1} + n_{i+2} + \cdots + n_d\big) + i\big(n_i - 1\big)\big] \\ &= \frac{1}{\binom{n}{2}}\big[\big(i+1\big)\big(n-i-n_i\big) + i\big(n_i - 1\big)\big] \\ &= \frac{2}{(n-1)n}\big[\big(i+1\big)n - i^2 - 2i - n_i\big]. \end{aligned}$$

Define a function: $f(i) = (n-i-1) - \frac{2}{n}[(i+1)n - i^2 - 2i - n_i]$. By an easy calculation, one has $f(i) = n - 3(i+1) + \frac{2}{n}(i^2 + 2i + n_i)$ and thus $f'(i) = -3 + \frac{2}{n}(2i+2)$. Since $i \leq d-1$, by $d < \lfloor \frac{n+1}{2} \rfloor$, we have $f'(i) < 0$. Thus $f(i)$ is a decreasing function on $[0, \lfloor \frac{n+1}{2} \rfloor - 2]$, and achieves its minimum value at $\lfloor \frac{n+1}{2} \rfloor - 2$. One can check that

$$f(\lfloor \frac{n+1}{2} \rfloor - 2) > 0.$$

Therefore $f(i) > 0$, and thus $\rho(G') - \rho(G) > \bar{l}(G') - \bar{l}(G)$, the result follows.

If $i = d$, then $\rho(G') - \rho(G) = \frac{1}{n-1}\big(n-d-1\big)$, and

$$\bar{l}(G') - \bar{l}(G) = \frac{2d(n_d - 1)}{(n-1)n} = \frac{2d(n-d-1)}{(n-1)n}.$$

Since $d \leq \lfloor \frac{n+1}{2} \rfloor - 1$,

$$\frac{\rho(G') - \rho(G)}{\bar{l}(G') - \bar{l}(G)} = \frac{n}{2d} > 1.$$

□

Lemma 2.4. *Let G be a connected graph of order $n \geq 3$. Let u be a peripheral vertex of G and $e_G(v) = d$. Assume that $G[V_j \cup V_{j+1}]$ is a clique for each $j \in \{0, \ldots, d-1\}$ and that $n_i(u) \geq 2$ for some $i \in \{1, \ldots, d-1\}$. Further, assume that i is the minimum subject to the above condition. Let v be a vertex in $V_i(u)$ and $V_{i-1} = \{u_{i-1}\}$. Let G' be the graph with $V(G') = V(G)$ and $E(G') = E(G) \cup A \setminus \{vu_{i-1}\}$, where $A = \{vy : \ y \in V_{i+2}\}$ if $i \leq d-2$, and $A = \emptyset$ otherwise. If $d = \lfloor \frac{n+1}{2} \rfloor$, then*

$$\rho(G') - \bar{l}(G') > \rho(G) - \bar{l}(G).$$

Proof. Note that if $i \leq d-2$, then

$$\sigma_{G'}(x) - \sigma_G(x) = \begin{cases} \frac{1}{n-1}, & \text{if } x \in \bigcup_{j=1}^{i-1} V_j \ \cup \{u\} \\ 0, & \text{if } x \in V_i \cup V_{i+1} \\ -\frac{1}{n-1}, & \text{if } x \in \bigcup_{j=i+2}^{d} V_j \ , \end{cases}$$

if $i = d-1$, then

$$\sigma_{G'}(x) - \sigma_G(x) = \begin{cases} \frac{1}{n-1}, & \text{if } x \in \bigcup_{j=1}^{d-2} V_j \ \cup \{u\} \\ 0, & \text{if } x \in V_{d-1} \cup V_d \ . \end{cases}$$

Thus $\rho(G') = \sigma_{G'}(u) = \sigma_G(u) + \frac{1}{n-1} = \rho(G) + \frac{1}{n-1}$. On the other hand, since $i \leq d-1 = \lfloor \frac{n-1}{2} \rfloor < \frac{n}{2}$, we have

$$\begin{aligned} \bar{l}(G') - \bar{l}(G) &= \frac{1}{\binom{n}{2}} \big[i - \big(n_{i+2} + n_{i+3} + \cdots + n_d \big) \big] \\ &= \frac{2}{(n-1)n} \big(n_i + n_{i+1} + 2i - n \big) \\ &\leq \frac{2}{(n-1)n} i \\ &< \frac{1}{n-1}. \end{aligned}$$

The results follows. □

The statement of Conjecture A is refined as follows.

Theorem 2.5. *Among all connected graphs G on $n \geq 3$ vertices with average distance $\bar{l}$ and remoteness ρ, the maximum value of $\rho - \bar{l}$ is attained by the Soltés graphs with diameter d, where*

$$\begin{cases} d = \frac{n+1}{2}, & \text{if } n \text{ is odd} \\ d \in \{\frac{n}{2}, \frac{n}{2}+1\} & \text{if } n \text{ is even} \ . \end{cases}$$

Proof. It is immediate from Lemmas 2.1-2.4.

□

In the remaining sections, we prove Conjecture B.

3 Some preparations

Let G be a connected graph. Recall that for a vertex $u \in V(G)$, let $V_i(u) = \{v \in V(G) | \ d(u,v) = i\}$ and $n_i(u) = |V_i(u)|$ for each $i \in \{1, \ldots, d\}$, where $d = diam(G)$.

Lemma 3.1. *Let G be connected graph with order n and radius $r \geq 2$. If u is a center of G, then $n_i(u) \geq 2$ for all $i \in \{1, \ldots, r-1\}$.*

Proof. By contradiction, suppose that $n_i(u) = 1$ for some $1 \leq i \leq r-1$ and let $V_i(u) = \{w\}$. Let P be a shortest path connecting u and w in G, v be the neighbor of u on P. For a vertex $x \in V(G) \setminus \{v\}$,

$$d(v,x) \begin{cases} = d(u,x) - 1, & \text{if } d(u,x) \geq i \\ \leq d(u,x) + 1, & \text{if } d(u,x) < i \, . \end{cases}$$

It follows that $ecc(v) = r - 1$, a contradiction. □

Corollary 3.2. *If G is a connected graph with order n and radius r, then $r \leq \frac{n}{2}$.*

Proof. Let u be a center of G. By Lemma 3.1, $n_i(u) \geq 2$ for all $i \in \{1, \ldots, r-1\}$. So, $n \geq 1 + \sum_{i=1}^{r} n_i(u) \geq 2r$, the result then follows. □

For a graph G, $p(G)$ denotes the maximum cardinality of a subset of vertices that induce a path in G.

Theorem 3.3. *(Erdős, Saks, Sós [18]) For any connected graph G, $p(G) \geq 2rad(G) - 1$.*

Corollary 3.4. *Let G be a connected graph of order $n \geq 3$. For an even n, $rad(G) = \frac{n}{2}$ if and only if $G \cong P_n$ or $G \cong C_n$.*

Proof. The sufficiency is obvious. Next we prove its necessity. By Theorem 3.3, $p(G) \geq n-1$. Let $P = v_1 \ldots v_{n-1}$ be an induced path of G, and let v_n be the remaining vertex of G. We consider the vertex $v_{\frac{n}{2}}$. Since $d(v_{\frac{n}{2}}, v_i) < \frac{n}{2}$ for each $i \neq \frac{n}{2}$, and $rad(G) = \frac{n}{2}$, we have $d(v_{\frac{n}{2}}, v_n) = \frac{n}{2}$. So, $v_n v_i \notin E(G)$ for each $2 \leq i \leq n-2$, and thus $N(v_n) \subseteq \{v_1, v_n\}$. It implies that $G \in \{P_n, C_n\}$. □

For an odd integer $n \geq 5$, we define some special graphs of order n with $rad(G) = \frac{n-1}{2}$: $C_{n-1}(1)$ is the graph obtained from C_{n-1} by adding a new vertex which joins two adjacent vertices of C_{n-1}; $C_{n-1}(2)$ is the graph obtained from C_{n-1} by adding a new vertex which joins two vertices with distance two on C_{n-1}; $C_{n-1}(3)$ is the graph obtained from C_{n-1} by adding a new vertex which joins three consecutive vertices of C_{n-1}. One can see that $p(C_n) = p(C_{n-1}(1)) = n-1$ and $p(C_{n-1})(2)) = p(C_{n-1}(3)) = n-2$.

The construction of the following graphs are illustrated in Figure 1. For an $i \in \{1, \ldots, n-1\}$, $P_{n-1}(i-1, i, i+1)$ is the graph obtained from P_{n-1} by adding a new vertex which is adjacent to the vertices v_{i-1}, v_i, v_{i+1}; $P_{n-1}(i-1, i+1)$ is the graph obtained from P_{n-1} by adding a new vertex which is adjacent to the vertices v_{i-1}, v_{i+1}; $P_{n-1}(i, i+1)$ is the graph obtained from P_{n-1} by adding a new vertex which is adjacent to the vertices v_i, v_{i+1}; For $j \in \{2, \ldots, n-2\}$, $P_{n-1}(j)$ is the graph obtained from P_{n-1} by adding a new vertex which adjacent to v_j, where $i-1, i+1$ are taken modulo $n-1$.

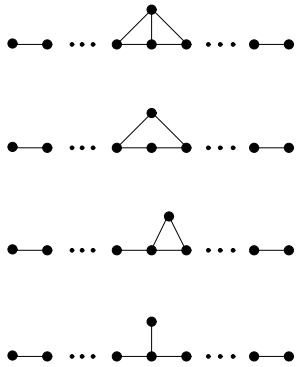

Figure 1. Graphs with an odd order n, $rad(G) = \frac{n-1}{2}$ and $p(G) = n - 1$

Note that $P_{n-1}(n-1, n, n+1) = P_{n-1}(n-1, 1, 2) \cong C_n(1)$ and $P_{n-1}(n-1, n) \cong C_n$. It is easy to see that $p(P_{n-1}(i-1, i, i+1)) = p(P_{n-1}(i-1, i+1)) = p(P_{n-1}(i, i+1)) = n - 1$ for each $i \in \{1, \ldots, n-1\}$, and $p(P_{n-1}(j)) = n - 1$ for each $j \in \{2, \ldots, n-2\}$.

The result of Lemma 3.5 is straightforward. But its proof is somewhat tedious and will be given in Section 4.

Lemma 3.5. *Let G be a connected graph of order $n \geq 5$. If n is odd and $rad(G) = \frac{n-1}{2}$, then*

(1) $p(G) = n$ if and only if $G \cong P_n$

(2) $p(G) = n-1$ if and only if $G \in \{P_{n-1}(i-1, i, i+1), P_{n-1}(i-1, i+1), P_{n-1}(i, i+1) : i \in \{1, \ldots, n-1\}\}$, or $G \cong P_{n-1}(j)$ for some $j \in \{2, \ldots, n-2\}$.

(3) $p(G) = n - 2$ if and only if $G \in \{C_{n-1}(2), C_{n-1}(3)\}$.

Corollary 3.6. *Let G be a connected graph of order $n \geq 5$. If n is odd and $rad(G) = \frac{n-1}{2}$, then $\rho(G) \geq \frac{n+1}{4}$, with equality if and only if*

$$G \in \{C_n, C_n(1), C_n(2), C_n(3)\}.$$

Proof. By Lemma 3.5, we consider the following cases. If $G \cong P_n$, then

$$\rho(G) = \frac{1}{n-1} \sum_{i=1}^{n-1} i = \frac{n}{2} > \frac{n+1}{4}.$$

Assume that either $G \cong P_{n-1}(1, 2)$ or $G \in \{P_{n-1}(i-1, i, i+1), P_{n-1}(i-1, i+1), P_{n-1}(i, i+1), P_{n-1}(i) : i \in \{2, \ldots, n-2\}$. Let $P = v_1 \ldots v_{n-1}$ be the induced path of G, and v_n be the new vertex, added to P in the construction of G. Since $n \geq 5$,

$$\rho(G) \geq \rho(v_1) > \frac{1}{n-1} \sum_{i=1}^{n-2} i = \frac{n-2}{2} \geq \frac{n+1}{4}.$$

We saw that $P_{n-1}(n-1, 1) \cong C_n$, $P_{n-1}(n-1, n, n+1) \cong C_n(1) \cong P_{n-1}(n-1, 1, 2)$. It is easy to check that $\rho(G) = \frac{n+1}{4}$ for $G \in \{C_n, C_n(1), C_n(2), C_n(3)\}$ and $\rho(P_{n-1}(2, n-1)) = \rho(P_{n-1}(n-2, 1)) > \frac{n+1}{4}$. □

Now we are ready to prove Conjecture B.

Theorem 3.7. *Let G be a connected graph on $n \geq 3$ vertices with remoteness ρ and radius r. Then*

$$\rho - r \geq \begin{cases} \frac{n^2}{4n-4} - \frac{n}{2}, & \text{if } n \text{ is even,} \\ \frac{3-n}{4}, & \text{if } n \text{ is odd,} \end{cases}$$

with equality if and only if

$$\begin{cases} G \cong C_n, & \text{if } n \text{ is even,} \\ G \in \{C_n, C_{n-1}(1), C_{n-1}(2), C_{n-1}(3)\}, & \text{if } n \text{ is odd .} \end{cases}$$

Proof. If $n = 3$, then $G \cong P_3$ or $G \cong K_3$. Since $\rho(P_3) = \frac{3}{2}$, $\rho(K_3) = 1$, and $rad(P_3) = rad(K_3) = 1$,

$$\rho - r \geq 0,$$

the result holds. Next we assume that $n \geq 5$, and consider $r - \rho$, instead of $\rho - r$. Let u be a center of G, and $n_i = n_i(u)$ for each $i \in \{1, \ldots, r\}$.

Define a function $f(r) = r - \frac{1}{n-1}(n - 2r + r^2)$. By Corollary 3.2, since $r \leq \frac{n}{2}$, $f'(r) = 1 - \frac{1}{n-1}(2r - 2) > 0$. Thus $f(r)$ is a strictly increasing function on the interval $[1, \frac{n}{2}]$, and achieves its maximum value $\frac{n}{2} - \frac{n^2}{4n-4}$ at $r = \frac{n}{2}$.

Case 1. n is even

By Lemma 3.1, $n_i \geq 2$ for each $i \in \{1, \ldots, r-1\}$. Therefore,

$$\begin{aligned} r - \rho &\leq r - \frac{1}{n-1} \sum_{i=1}^{r} i n_i \\ &\leq r - \frac{1}{n-1} \Big((n - 2r + 2) + \sum_{i=2}^{r-1} 2i + r \Big) \\ &= r - \frac{1}{n-1}(n - 2r + r^2) \\ &\leq \frac{n}{2} - \frac{n^2}{4n-4}. \end{aligned}$$

By Corollary 3.4, it is easy to check that $r - \rho = \frac{n}{2} - \frac{n^2}{4n-4}$ if and only if $G \cong C_n$.

Case 2. n is odd

By the similar argument as in Case 1, we have

$$r - \rho \leq r - \frac{1}{n-1}(n - 2r + r^2) = f(r).$$

Since $f(r)$ is a strictly increasing function on the interval $[1, \frac{n-1}{2}]$, if $r \leq \frac{n-1}{2} - 1$, then

for $n \geq 5$,

$$\begin{aligned} f(\frac{n-1}{2}-1) &= (\frac{n-1}{2}-1)-\frac{1}{n-1}(3+(\frac{n-1}{2}-1)^2) \\ &= \frac{n-1}{4}-\frac{2n-6}{n-1} \\ &< \frac{n-3}{4}. \end{aligned}$$

So, it remains to consider the case when $r = \frac{n-1}{2}$. By Corollary 3.6, since $\rho(G) \geq \frac{n+1}{4}$,

$$r-\rho \leq \frac{n-1}{2}-\frac{n+1}{4} \leq \frac{n-3}{4},$$

with equality if and only if $G \in \{C_n, C_n(1), C_n(2), C_n(3)\}$. □

4 Proof of Lemma 3.5

(1) is trivial.

The sufficiency of (2) is obvious by the construction of those graphs. To show the necessity of (2), let $P = v_1 \dots v_{n-1}$ be an induced path of G and v_n be the remaining vertex of G.

Claim 1. If v_n has two neighbors $v_i, v_j \in N(v_n)$ with $i, j \in \{1, \dots, n-1\}$, then $|i-j| \leq 2$ or $|i-j| \geq n-3 = (n-1)-2$.

Proof of Claim 1. If $n = 5$, the cliam holds trivially. Next we show the claim by contradiction for $n \geq 7$. Suppose that there exist two vertices $v_i, v_j \in N(v_n)$ with $i, j \in \{1, \dots, n-1\}$ such that $3 \leq |i-j| \leq n-4 = (n-1)-3$. Without loss of generality, let $i < j$.

Case 1. $i \geq \frac{n-1}{2}$ or $j \leq \frac{n+1}{2}$

By the symmetry, we just consider the case when $i \geq \frac{n-1}{2}$. Note that

$$d_P(v_{\frac{n-1}{2}}, v_k) < \frac{n-1}{2}$$

for each $k \in \{1, \dots, n-2\}$, $d_P(v_{\frac{n-1}{2}}, v_{n-1}) = \frac{n-1}{2}$, and

$$d_G(v_{\frac{n-1}{2}}, v_n) \leq d_G(v_{\frac{n-1}{2}}, v_i) + 1.$$

Since $3 \leq |i-j| \leq n-4 = (n-1)-3$, we have $d_G(v_{\frac{n-1}{2}}, v_i) \leq \frac{n-1}{2} - 3$, and $d_G(v_{\frac{n-1}{2}}, v_n) \leq \frac{n-1}{2} - 2$. Furthermore

$$d_G(v_{\frac{n-1}{2}}, v_{n-1}) \leq d_P(v_{\frac{n-1}{2}}, v_i) + 2 + d_P(v_j, v_{n-1}) < \frac{n-1}{2}.$$

This proves that $ecc(v_{\frac{n-1}{2}}) < \frac{n-1}{2}$, which contradicts $rad(G) = \frac{n-1}{2}$.

Case 2. $i < \frac{n-1}{2} < \frac{n+1}{2} < j$

We show that $ecc(v_n) < \frac{n-1}{2}$. Let C be the cycle obtained from the segment of P between v_j and v_j adding the vertex v_n and joining it to v_i and v_j. It is clear that the length of C is at most $n-2$. So, for any vertex v on C, $d(v_n, v) \leq \frac{|C|}{2} < \frac{n-1}{2}$. To prove $d(v_n, w) < \frac{n-1}{2}$, it suffices to show that $\max\{d(v_n, v_1), d(v_n, v_{n-1})\} < \frac{n-1}{2}$. This holds, because

$$d_G(v_n, v_1) \leq d_P(v_{\frac{n-1}{2}}, v_1) < \frac{n-1}{2}, \quad d_G(v_n, v_{n-1}) \leq d_P(v_{\frac{n-1}{2}}, v_{n-1}) < \frac{n-1}{2}.$$

So, $ecc(v_n) < \frac{n-1}{2}$, which contradicts $rad(G) = \frac{n-1}{2}$. □

By Claim 1 and $p(G) = n-1$, one has $d(v_n) \leq 3$. Furthermore, if $d(v_n) = 3$, then $N(v_n) = \{v_{i-1}, v_i, v_{i+1}\}$ for some $i \in \{1, \ldots, n-1\}$, and thus $G \cong P_{n-1}(i-1, i, i+1)$. Also, if $d(v_n) = 2$, then $1 \leq |i-j| \leq 2$, and thus $G \in \{P_{n-1}(i, i+1), P_{n-1}(i-1, i+1)\}$ for some $i \in \{1, \ldots, n-1\}$. If $d(v_n) = 1$, then by $p(G) = n-1$, $G \cong P_{n-1}(j)$ for some $j \in \{2, \ldots, n-2\}$. This completes the proof of (2).

The sufficiency of (3) is trivial. Next we show its necessity. By Theorem 2.3, let $P = v_1 \ldots v_{n-2}$ be an induced path of G, and v_{n-1}, v_n the remaining two vertices of G.

Claim 2. Either $N(v_{n-1}) \setminus \{v_n\} = \{v_1, v_{n-2}\}$ or $N(v_n) \setminus \{v_{n-1}\} = \{v_1, v_{n-2}\}$.

Proof of Claim 2. By contradiction, suppose that Claim 2 is not true. If there exist $i, j \in \{2, \ldots, n-3\}$ such that $v_i \in N(v_{n-1})$ and $v_j \in N(v_n)$, $d(v_{\frac{n-1}{2}}, v_k) \leq \frac{n-1}{2} - 1$ for $k \in \{n-1, n\}$. Together this with $d(v_{\frac{n-1}{2}}, v_k) \leq \frac{n-1}{2} - 1$ for $k \in \{1, \ldots, n-2\}$, we have $ecc(v_{\frac{n-1}{2}}) \leq \frac{n-1}{2} - 1$, a contradiction. Hence,

$$either\ N(v_{n-1}) \setminus \{v_n\} \subseteq \{v_1, v_{n-2}\}\ or\ N(v_n) \setminus \{v_{n-1}\} \subseteq \{v_1, v_{n-2}\}.$$

Without loss of generality, assume that $N(v_{n-1}) \setminus \{v_n\} \subseteq \{v_1, v_{n-2}\}$. Since $N(v_{n-1}) \setminus \{v_n\} \neq \{v_1, v_{n-2}\}$ and $p(G) = n-2$, we have $N(v_{n-1}) \setminus \{v_n\} = \emptyset$. Moreover, since G is connected, we conclude that

$$N(v_{n-1}) = \{v_n\}\ and\ N(v_n) \setminus \{v_{n-1}, v_1, v_{n-2}\} \neq \emptyset.$$

If there exists $i \in \{3, \ldots, n-4\}$ such that $v_i \in N(v_n) \setminus \{v_{n-1}, v_1, v_{n-2}\}$, then it follows $d(v_{\frac{n-1}{2}}, v_n) \leq \frac{n-1}{2} - 2$ and thereby $d(v_{\frac{n-1}{2}}, v_{n-1}) \leq \frac{n-1}{2} - 1$. So, $ecc(v_{\frac{n-1}{2}}) < \frac{n-1}{2}$, which contradicts $rad(G) = \frac{n-1}{2}$. This means that

$$N(v_n) \setminus \{v_{n-1}, v_1, v_{n-2}\} \subseteq \{v_2, v_{n-3}\}.$$

Since $N(v_n) \setminus \{v_{n-1}, v_1, v_{n-2}\} \neq \emptyset$, let $v_2 \in N(v_n)$, without loss of generality. If $n = 5$, then by $p(G) = 3$, $v_1, v_3 \in N(v_5)$, and thus $e(v_5) = 1$, a contradiction. For $n \geq 7$, since $p(G) = n-2$, $v_{n-3} \in N(v_n)$ or $v_{n-2} \in N(v_n)$. In both cases, one can see that $ecc(v_n) \leq \max\{\frac{n-3}{2}, 2\} < \frac{n-1}{2}$. This proves Claim 2. □

By Claim 2, let $N(v_{n-1}) \setminus \{v_n\} = \{v_1, v_{n-2}\}$. Since $P = v_1 \ldots v_{n-2}$ is an induced path, $G[\{v_1, \ldots, v_{n-1}\}] \cong C_{n-1}$.

Claim 3. If v_n has two neighbors $v_i, v_j \in N(v_n)$ with $i, j \in \{1, \ldots, n-1\}$, then $|i-j| \leq 2$ or $|i-j| \geq n-3 = (n-1)-2$.

Proof of Claim 3. By contradiction, suppose that v_n has two neighbors $v_i, v_j \in N(v_n)$ with $i, j \in \{1, \ldots, n-1\}$ and $3 \leq |i-j| \leq n-4$. One can see that, for any vertex v_k, $d(v_n, v_k) \leq \max\{\frac{|i-j|+1}{2}, \frac{n-1-|i-j|+1}{2}\} \leq \frac{n-3}{2} < \frac{n-1}{2}$, it means that $ecc(v_n) < \frac{n-1}{2}$, a contradiction. □

By Claim 3 and $p(G) = n-2$, one has $d(v_n) \leq 3$. Furthermore, if $d(v_n) = 3$, then $N(v_n) = \{v_{i-1}, v_i, v_{i+1}\}$ for some $i \in \{1, \ldots, n-1\}$, and thus $G \cong C_{n-1}(3)$. Also, if $d(v_n) = 2$, then $|i-j| = 2$, and thus $G \cong C_{n-1}(2)$. This completes the proof of the necessity of (3).

Acknowledgement

The authors are grateful to the referees for their valuable comments.

References

[1] X. An, B. Wu, Average distance and proximity of a graph, in preparation.

[2] M. Aouchiche, *Comparaison Automatisée d'Invariants en Théorie des Graphs*, Ph.D. Thesis, École Polytechnique de Montréal, 2006.

[3] M. Aouchiche, G. Caporossi and P. Hansen, Variable neighborhood search for extremal graphs. 20. automated comparison of graph invariants, *MATCH Commun. Math. Comput. Chem.* **58** (2007), 365–384.

[4] M. Aouchiche and P. Hansen, Nordhaus-Gaddum relations for proximity and remoteness in graphs, *Comput. Math. Appl.* **59** (2010), 2827–2835.

[5] M. Aouchiche and P. Hansen, Proximity and remoteness in graphs: results and conjectures, *Networks* **58** (2011), 95–102.

[6] R. A. Beezer, J. E. Riegsecker, B. A. Smith, Using minimum degree to bound average distance, *Discrete Math.* **226** (2001), 365–371.

[7] F. Buckley and F. Harary, *Distance in Graphs*, Addison-Wesley, Reading, MA, 1990.

[8] F. G. Chung, The average distance and the independence number, *J. Graph Theory* **12** (1988), 229–235.

[9] P. Dankelmann, Average distance and the independence number, *Discrete Appl. Math.* **51** (1994), 73-83.

[10] P. Dankelmann, Average distance and the domination number, *Discrete Appl. Math.* **80** (1997), 21–35.

[11] P. Dankelmann, Average distance and generalized packing in graphs, *Discrete Math.* **310** (2010), 2334–2344.

[12] P. Dankelmann and R. Entringer, Average distance, minimum degree, and spanning trees, *J. Graph Theory* **33** (2000), 1–13.

[13] P. Dankelmann, S. Mukwembi and H. C. Swart, Average distance and edge-connectivity I, *SIAM J. Discrete Math.* **22** (2008), 92–101.

[14] P. Dankelmann, S. Mukwembi and H. C. Swart, Average distance and edge-Connectivity II, *SIAM J. Discrete Math.* **21** (2008), 1035–1052.

[15] E. DeLaVina and B. Waller, Spanning trees with many leaves and average distance, *Elec. J. Combin.* **15** (2008), R33.

[16] R. C. Entringer, D. E. Jackson and D. A. Snyder, Distance in graphs, *Czech. Math. J.* **26** (1976), 283–296.

[17] P. Erdős, J. Pach, R. Pollack and Z. Tuza, Radius, diameter, and minimum degree, *J. Combin. Theory Ser. B* **47** (1989), 73–79.

[18] P. Erdős, M. Saks and V. T. Sós, Maximum induced trees in graphs, *J. Combin. Theory Ser. B* **41** (1986), 61–79.

[19] B. Ma, B. Wu and W. Zhang, Proximity and average eccentricity of a graph, *Infor. Process. Lett.* **112** (2012), 392–395

[20] L. Soltés, Trnansmission in graphs: a bound and vertex removing, *Math. Slovaca* **41** (1991), 11–16.

[21] D. B. West, Introduction to Graph Theory, second Ed., Prentice Hall, Upper Saddle River, NJ, 2001.

[22] B. Wu, G. Liu, X. An, G. Yan and X. Liu, A conjecture on average distance and diameter of a graph, *Discrete Math. Alog. Appl.* **3** (2011), 337–342.

ARS MATHEMATICA CONTEMPORANEA

Also available at http://amc-journal.eu
ISSN 1855-3966 (printed edn.), ISSN 1855-3974 (electronic edn.)
ARS MATHEMATICA CONTEMPORANEA 7 (2014) 453–459

Commuting graphs and extremal centralizers*

Gregor Dolinar
Faculty of Electrical Engineering, University of Ljubljana
Tržaška cesta 25, SI-1000 Ljubljana, Slovenia

Alexander Guterman †
Faculty of Algebra, Department of Mathematics and Mechanics, Moscow State University
GSP-1, 119991 Moscow, Russia

Bojan Kuzma
University of Primorska, Glagoljaška 8, SI-6000 Koper, Slovenia, and
IMFM, Jadranska 19, SI-1000 Ljubljana, Slovenia

Polona Oblak ‡
Faculty of Computer and Information Science, University of Ljubljana
Tržaška cesta 25, SI-1000 Ljubljana, Slovenia

Received 29 September 2012, accepted 13 June 2013, published online 27 December 2013

Abstract

We determine the conditions for matrix centralizers which can guarantee the connectedness of the commuting graph for the full matrix algebra $M_n(\mathbb{F})$ over an arbitrary field $\mathbb{F}$. It is known that if $\mathbb{F}$ is an algebraically closed field and $n \geq 3$, then the diameter of the commuting graph of $M_n(\mathbb{F})$ is always equal to four. We construct a concrete example showing that if $\mathbb{F}$ is not algebraically closed, then the commuting graph of $M_n(\mathbb{F})$ can be connected with the diameter at least five.

Keywords: Commuting graph, matrix ring, centralizer.

Math. Subj. Class.: 05C40, 15A27, 15A04

*The work is partially supported by the joint Slovene–Russian grant BI-RU/10-11-010.
†The work is partially supported by RFBR grant 11-01-00794-a.
‡Corresponding author
E-mail addresses: gregor.dolinar@fe.uni-lj.si (Gregor Dolinar), guterman@list.ru (Alexander Guterman), bojan.kuzma@famnit.upr.si (Bojan Kuzma), polona.oblak@fri.uni-lj.si (Polona Oblak)

1 Introduction

Let $n \geq 2$ and let $M_n(\mathbb{F})$ be a ring of all $n \times n$ matrices over a field $\mathbb{F}$. The *commuting graph* $\Gamma(M_n(\mathbb{F}))$ of $M_n(\mathbb{F})$ is a simple graph with the vertex set consisting of all non-scalar matrices from $M_n(\mathbb{F})$, and two vertices form an edge if the corresponding matrices are distinct and commute.

Recently, connections between various algebraic structures and their commuting graphs were investigated, see, e.g. [1, 3, 4, 5, 8, 9, 10, 12, 15]. For example, Mohammadian [15] recently proved that a ring is isomorphic to $M_2(\mathbb{F})$, with $\mathbb{F}$ finite, if and only if the commuting graph of the ring under consideration is isomorphic to $\Gamma(M_2(\mathbb{F}))$. Akbari, Ghandehari, Hadian and Mohammadian conjectured in [3] that this is also true for $M_n(\mathbb{F})$, where $n \geq 2$.

The connectedness and diameter of the commuting graph of a matrix ring $M_n(\mathbb{F})$ have been also studied extensively. If $\mathbb{F}$ is an algebraically closed field and $n \geq 3$, Akbari, Mohammadian, Radjavi, and Raja [4, Corollary 7] proved that the diameter of $\Gamma(M_n(\mathbb{F}))$ is always equal to four. For fields which are not algebraically closed the situation is completely different, e.g. if $\mathbb{F}$ is the field of rational numbers, then the commuting graph is never connected (see [2, Remark 8]). A necessary and sufficient condition for which $\Gamma(M_n(\mathbb{F}))$ is connected was given in [2, Theorem 6]. Namely, it was proven that $\Gamma(M_n(\mathbb{F}))$ is connected if and only if every field extension of $\mathbb{F}$ of degree n contains at least one proper intermediate field. In the case when commuting graph of $M_n(\mathbb{F})$ is connected, its diameter is known to be at most six and it is conjectured that it is at most five, see [4, Theorem 17] and [4, Conjecture 18]. In the present paper, we show that $\Gamma(M_9(\mathbb{Z}_2))$ is connected and has the diameter at least 5, where $\mathbb{Z}_m$ is the ring of integers modulo m. We also characterize connected commuting graphs in the language of centralizers. Observe that this characterization is different from [2, Theorem 6], where the language of field extension was used.

Definition 1.1. For a matrix $A \in M_n(\mathbb{F})$, the *centralizer* of A, denoted by $\mathcal{C}(A)$, is the set of all matrices in $M_n(\mathbb{F})$ commuting with A.

Let us remark that the set of non-scalar matrices in $\mathcal{C}(A)$ coincides with the closed neighborhood of vertex $A \in \Gamma(M_n(\mathbb{F}))$.

Centralizer induces a natural equivalence relation on $M_n(\mathbb{F})$:

Definition 1.2. Matrices A and B are *$\mathcal{C}$-equivalent* (abbreviated $A \sim B$) if $\mathcal{C}(A) = \mathcal{C}(B)$.

Definition 1.3. A matrix A is *$\mathcal{C}$-minimal* if for every $X \in M_n(\mathbb{F})$ with $\mathcal{C}(A) \supseteq \mathcal{C}(X)$ it follows that $A \sim X$.

Definition 1.4. A non-scalar matrix A is *$\mathcal{C}$-maximal* if for every non-scalar $X \in M_n(\mathbb{F})$ with $\mathcal{C}(A) \subseteq \mathcal{C}(X)$ it follows that $A \sim X$.

Let us remark that $\mathcal{C}$-minimal and $\mathcal{C}$-maximal matrices in $M_n(\mathbb{F})$ were already classified, see Šemrl [16] and recent paper [7] by the authors. Also, $\mathcal{C}$-minimal and $\mathcal{C}$-maximal matrices were used as a main tool by Dolinar, Kuzma, and Oblak [8] to investigate distances between vertices in the commuting graph $\Gamma(M_n(\mathbb{F}))$ and they will be used to prove the results of this paper as well.

We use the following notations. By E_{ij} we denote the matrices with 1 on (i, j)-th position and 0 elsewhere. By 0_k and I_k we denote the $k \times k$ zero matrix and the $k \times k$

identity matrix, respectively. When it is clear from the context, we omit the subscript. For a given scalar $\lambda \in \mathbb{F}$, define $J_k(\lambda) = \lambda I + \sum_{i=1}^{k-1} E_{i(i+1)}$ to be an elementary upper-triangular Jordan matrix. We denote $J_k = J_k(0)$. A matrix $A \in M_n(\mathbb{F})$ is an *idempotent* if $A^2 = A$, it is a *nilpotent* if there exists an integer $k \geq 1$ such that $A^k = 0$. Non-zero matrix A with $A^2 = 0$ is called a *square-zero matrix*. For a monic polynomial $m \in \mathbb{F}[x]$ we let $C(m) = \sum_{i=1}^{n-1} E_{(i+1)i} - \sum_{i=1}^{n} m_{i-1}E_{in} \in M_n(\mathbb{F})$ be a companion matrix of m, where $m(x) = m_0 + m_1x + \cdots + m_{n-1}x^{n-1} + x^n$. Given a matrix A, let $\mathbb{F}[A] = \{p(A) |\ p \in \mathbb{F}[x]\}$ be the unital algebra generated by A.

2 Connectedness of commuting graphs

In this section we provide a characterization of matrices for which $\Gamma(M_n(\mathbb{F}))$ is connected in the language of extremal centralizers. We need the following result on $\mathcal{C}$-maximal matrices from our recent paper [7].

Proposition 2.1. [7, Theorem 3.2] *Let $\mathbb{F}$ be an arbitrary field. The following statements are equivalent for a non-scalar matrix $A \in M_n(\mathbb{F})$.*

(i) A is $\mathcal{C}$-maximal.

(ii) A belongs to one of the following three classes:

(a) A is $\mathcal{C}$-equivalent to an idempotent,

(b) A is $\mathcal{C}$-equivalent to a square-zero matrix,

(c) A is similar to $C \oplus \cdots \oplus C$, where C is a companion matrix of an irreducible polynomial, such that there is no proper intermediate field between $\mathbb{F}$ and $\mathbb{F}[C]$.

Theorem 2.2. *Let $n \geq 2$ and let $\mathbb{F}$ be an arbitrary field. A commuting graph $\Gamma(M_n(\mathbb{F}))$ is not connected if and only if there exists a matrix in $M_n(\mathbb{F})$ which is simultaneously $\mathcal{C}$-minimal and $\mathcal{C}$-maximal.*

Proof. First, let $n = 2$. Then, $\Gamma(M_2(\mathbb{F}))$ is never connected because every non-scalar matrix in $\mathcal{C}(E_{11})$ is diagonal, hence $\mathcal{C}$-equivalent to E_{11} and thus E_{11} and E_{12} are not connected in $\Gamma(M_2(\mathbb{F}))$ (see also Akbari and Raja [5, Remark 8]). Moreover, E_{11} is always a $\mathcal{C}$-minimal and $\mathcal{C}$-maximal matrix, so the theorem is true in the case $n = 2$ for every field $\mathbb{F}$.

Second, let $n \geq 3$. We will prove each direction of the equivalence in the theorem separately.

(i). Suppose A is a $\mathcal{C}$-minimal and $\mathcal{C}$-maximal matrix. According to Proposition 2.1 we have to consider three cases separately.

Case 1. Let A be $\mathcal{C}$-equivalent to an idempotent. Then we may assume that $A = I_r \oplus 0_{n-r}$ for some $r \in \{2, \ldots, n-1\}$. Thus $\mathcal{C}(A) = M_r(\mathbb{F}) \oplus M_{n-r}(\mathbb{F})$. Recall that $J_r \in M_r(\mathbb{F})$ is a nilpotent upper-triangular Jordan cell, so $\mathcal{C}(I_r + J_r) = \{\alpha_0 I_r + \alpha_1 J_r + \cdots + \alpha_{r-1}J^{r-1} |\ \alpha_i \in \mathbb{F}\} = \mathbb{F}[J_r]$. It easily follows that

$$\mathcal{C}((I_r + J_r) \oplus 0_{n-r}) = \mathbb{F}[J_r] \oplus M_{n-r}(\mathbb{F}).$$

Hence $\mathcal{C}((I_r + J_r) \oplus 0_{n-r}) \subsetneq \mathcal{C}(A)$, so A is not $\mathcal{C}$-minimal, a contradiction.

Case 2. Let A be $\mathcal{C}$-equivalent to a non-scalar square-zero matrix. Then we may assume $A = \begin{pmatrix} 0_r & 0 & I_r \\ 0 & 0_{n-2r} & 0 \\ 0 & 0 & 0_r \end{pmatrix} = J_n^{n-r}$ for some integer r, $1 \leq r \leq \frac{n}{2}$. However, $\mathcal{C}(J_n) \subsetneq \mathcal{C}(A)$, hence A is not $\mathcal{C}$-minimal, a contradiction.

Case 3. Let $A = C \oplus \cdots \oplus C$, where C is a companion matrix of some irreducible monic polynomial $m \in \mathbb{F}[x]$, such that there is no proper intermediate field between $\mathbb{F}$ and $\mathbb{F}[C]$. We will prove that actually $A = C$.

Suppose $\mathbb{F}$ is an infinite field. Then A being $\mathcal{C}$-minimal implies that A is non-derogatory (see [7, Lemma 2.7]). Therefore $A = C$, i.e. A contains only one summand. Hence $\mathbb{F}[C]$ is a field extension of $\mathbb{F}$ of degree n. Recall that C is a companion matrix of an irreducible polynomial, such that there is no proper intermediate field between $\mathbb{F}$ and $\mathbb{F}[C]$ thus it follows by [2, Theorem 6] that $\Gamma(M_n(\mathbb{F}))$ is not connected.

Suppose $\mathbb{F} = GF(p^k)$ is a finite field and suppose that $A = C \oplus \cdots \oplus C$ contains more than one summand. Since $\mathbb{F}[C]$ is a field extension of $\mathbb{F}$ with degree $d = \deg m$, it is isomorphic to $\mathbb{K} = GF(p^{kd})$. Let $\gamma_C \in \mathbb{K}$ correspond to matrix C under this isomorphism. Since A contains more than one summand, d is a proper divisor of n. So, $\mathbb{K} = GF(p^{kd})$ is a proper intermediate field between $\mathbb{F}$ and $GF(p^{kn})$. It is known that the multiplicative group of $GF(p^{kn})$ is cyclic, so let $\xi \in GF(p^{kn})$ be its generator. Then $\mathbb{F}[\xi] = GF(p^{kn})$ and minimal polynomial $f \in \mathbb{F}[x]$ for ξ is irreducible over $\mathbb{F}$ of degree n. For matrix $X = C(f) \in M_n(\mathbb{F})$, $\mathbb{F}[X]$ is a field isomorphic to $GF(p^{kn})$. Since $GF(p^{kd}) \subseteq GF(p^{kn})$, some polynomial in X is isomorphic to $\gamma_C \in GF(p^{kd})$, and hence also to C. Consequently, by Skolem-Noether theorem, $p(X)$ is similar to a matrix $A = C \oplus \cdots \oplus C$ for some $p \in \mathbb{F}[x]$. By applying a suitable similarity to X we can assume that $p(X) = A$, hence $\mathcal{C}(X) \subseteq \mathcal{C}(A)$. Since A is $\mathcal{C}$-minimal, $\mathcal{C}(X) = \mathcal{C}(A)$, so X is a polynomial in A by the centralizer Theorem (see [13, p. 113, Corollary 1] and also [17, p. 106, Theorem 2]). Therefore the rational form of X (see [11, Chapter 3] for details) has at least as many cells as the rational form of A. A contradiction to the fact that X is similar to $C(f)$. It follows that $A = C$ and we conclude as in the infinite case that $\Gamma(M_n(\mathbb{F}))$ is not connected.

(ii). Suppose the commuting graph $\Gamma(M_n(\mathbb{F}))$ is not connected. By [4, Theorem 11] any two non-scalar idempotents are connected and thus there exists a non-scalar matrix A which is not connected to any non-scalar idempotent. We may assume that A is already in its rational form. Then A consists of a single cell because otherwise a matrix $A_1 \oplus A_2$ would be connected to an idempotent $I \oplus 0$. Hence $A = C(m^\alpha)$ for some irreducible polynomial m and positive integer α. If $\alpha \geq 2$, then A would be connected to a non-scalar square-zero matrix $B = m(A)^{\alpha-1}$. It is easy to see that B commutes with a rank-one matrix which further commutes with an idempotent, a contradiction. So, $\alpha = 1$ and thus A is non-derogatory, hence $\mathcal{C}$-minimal as it was proved in [7, Theorem 2.6]. If $A = C(m)$ is not $\mathcal{C}$-maximal, then there exists a proper intermediate field $\mathbb{K}$ between $\mathbb{F}$ and $\mathbb{F}[A]$ by Proposition 2.1. We can assume $\mathbb{K} = \mathbb{F}[X]$ is a simple extension for some $X \in \mathbb{F}[A]$. The minimal polynomial of X has smaller degree than the minimal polynomial of A, otherwise $\mathbb{F}[X] = \mathbb{F}[A]$. Hence the rational form of X contains more than one cell and therefore X, and thus also A is connected to a non-scalar idempotent, a contradiction. □

3 Commuting graph with diameter greater than four

Recall that the diameter of a commuting graph $\Gamma(M_n(\mathbb{F}))$, where $\mathbb{F}$ is algebraically closed and $n \geq 3$, is equal to four [4]. Below we provide an example showing that if $\mathbb{F}$ is not algebraically closed, then the diameter of $\Gamma(M_n(\mathbb{F}))$ can be indeed greater than 4.

Theorem 3.1. *The graph $\Gamma(M_9(\mathbb{Z}_2))$ is connected with diameter at least 5.*

Proof. Note that $\mathbb{Z}_2$ permits only one field extension of degree $n = 9$, the Galois field $GF(2^9)$ which contains $GF(2^3)$ as the only proper intermediate field. So, by [2, Theorem 6] the commuting graph of $M_9(\mathbb{Z}_2)$ is connected. To see that its diameter is at least 5, consider a polynomial $m(\lambda) = \lambda^9 + \lambda^8 + \lambda^4 + \lambda^2 + 1 \in \mathbb{Z}_2[\lambda]$. It is easy to see that this polynomial is irreducible. Let $\widehat{A} = C(m) \in M_9(\mathbb{Z}_2)$ be its companion matrix. Since $\widehat{A}$ has a cyclic vector, $\mathcal{C}(\widehat{A}) = \mathbb{Z}_2[\widehat{A}]$ by a well known Frobenius result on dimension of centralizer (see for example [2, Corollary 1]), and this is a field extension of $\mathbb{Z}_2$ [14, Theorem 4.14, p. 472] of index $n = 9$. Actually, $\mathcal{C}(\widehat{A})$ is isomorphic to $GF(2^9)$ by the uniqueness of field extensions for finite fields. In the sequel we identify these two fields.

Since the field extension $\mathbb{Z}_2 \subset GF(2^9)$ contains only $GF(2^3)$ as a proper intermediate field, we see that each $X \in \mathcal{C}(\widehat{A}) \setminus GF(2^3)$ satisfies $\mathbb{Z}_2[X] = \mathbb{Z}_2[\widehat{A}] = \mathcal{C}(\widehat{A})$ and in particular X and $\widehat{A}$ are polynomials in each other so they are $\mathcal{C}$-equivalent. Moreover, each non-scalar $\widehat{Y} \in GF(2^3)$ satisfies $\mathbb{Z}_2[\widehat{Y}] = GF(2^3)$, because no proper intermediate fields exist between $\mathbb{Z}_2$ and its overfield $GF(2^3)$, and in particular, $\mathcal{C}(\widehat{Y}_1) = \mathcal{C}(\widehat{Y}_2)$ for any two non-scalar $\widehat{Y}_1, \widehat{Y}_2 \in GF(2^3) \subset GF(2^9) = \mathcal{C}(\widehat{A})$.

There exists a polynomial p so that $\widehat{Y} = p(\widehat{A}) \in GF(2^3) \setminus \{0, 1\}$. As the field $GF(2^3)$ contains no idempotents other than 0 and 1 we see that the rational canonical form of $\widehat{Y}$ consists only of cells which correspond to some powers of the same irreducible polynomial. Likewise, the field contains no non-zero nilpotents, so each cell of $\widehat{Y}$ corresponds to the same irreducible polynomial. Moreover, $GF(2^3)$ has no subfields other than $\mathbb{Z}_2$, so $\mathbb{Z}_2[\widehat{Y}] = GF(2^3)$ and hence the minimal polynomial of $\widehat{Y} \in GF(2^3)$ has degree $[GF(2^3) : \mathbb{Z}_2] = 3$. This polynomial is relatively prime to its derivative, so in a splitting field, $\widehat{Y}$ has three distinct eigenvalues. It easily follows that $\widehat{Y}$ is similar to a matrix $C \oplus C \oplus C$, with C being a 3×3 companion matrix of some irreducible polynomial of degree 3. Let S_1 be an invertible matrix such that $\widehat{Y} = S_1^{-1}(C \oplus C \oplus C)S_1$ and define

$$A = S_1 \widehat{A} S_1^{-1}.$$

Clearly, $p(A) = S_1 \widehat{Y} S_1^{-1} = C \oplus C \oplus C$ and it follows that

$$\mathcal{C}(p(A)) = \begin{bmatrix} \mathbb{Z}_2[C] & \mathbb{Z}_2[C] & \mathbb{Z}_2[C] \\ \mathbb{Z}_2[C] & \mathbb{Z}_2[C] & \mathbb{Z}_2[C] \\ \mathbb{Z}_2[C] & \mathbb{Z}_2[C] & \mathbb{Z}_2[C] \end{bmatrix}. \tag{3.1}$$

Since $\mathbb{Z}_2[\widehat{Y}] = GF(2^3)$ we obtain $\mathbb{Z}_2[C] = GF(2^3)$.

Consider a 3×3 block matrix

$$N = \begin{bmatrix} E_{13} & 0 & 0 \\ 0 & 0 & E_{13} \\ E_{32} & 0 & 0 \end{bmatrix}, \quad E_{13}, E_{13}, E_{32} \in M_3(\mathbb{Z}_2).$$

It is immediate that $N^3 = 0$, so $I + N$ is invertible. Define

$$B = (I + N)A(I + N)^{-1}.$$

We will show that $d(A, B) \geq 5$.

Suppose there exists a path $A — V — Z — W — B$ of length 4. Note that $V \in GF(2^3) \subset \mathcal{C}(A)$. Otherwise, if $V \in \mathcal{C}(A) \setminus GF(2^3)$, then $\mathcal{C}(V) = \mathcal{C}(A)$ and such V has exactly the same neighbours as A. Since $B = (I + N)A(I + N)^{-1}$, it follows $W = (I + N)U(I + N)^{-1}$ for some $U \in GF(2^3) \subset \mathcal{C}(A) = (I + N)^{-1}\mathcal{C}(B)(I + N)$. Recall that any two non-scalar elements in $GF(2^3)$ have the same centralizer. So in particular we might take $U = V = p(A) = C \oplus C \oplus C$ where polynomial p was defined before. For any $Z \in \mathcal{C}(V) \cap \mathcal{C}((I + N)V(I + N)^{-1})$ we have

$$Z = (I + N)\widehat{Z}(I + N)^{-1}, \qquad Z, \widehat{Z} \in \mathcal{C}(V)$$

and hence, by postmultiplying with $(I + N)$ and rearranging,

$$Z - \widehat{Z} = N\widehat{Z} - ZN. \tag{3.2}$$

Let us write $Z = \left[Z_{ij}\right]_{1\leq i,j\leq 3}$ and $\widehat{Z} = \left[\widehat{Z}_{ij}\right]_{1\leq i,j\leq 3}$ as 3×3 block matrices and by (3.1) we have that $Z_{ij}, \widehat{Z}_{ij} \in \mathbb{Z}_2[C] = GF(2^3) \subseteq M_3(\mathbb{Z}_2)$, hence each of them is either zero or invertible. Then (3.2) implies

$$\left[Z_{ij} - \widehat{Z}_{ij}\right]_{ij} = \begin{bmatrix} -Z_{11}E_{13} - Z_{13}E_{32} + E_{13}\widehat{Z}_{11} & E_{13}\widehat{Z}_{12} & E_{13}\widehat{Z}_{13} - Z_{12}E_{13} \\ -Z_{21}E_{13} - Z_{23}E_{32} + E_{13}\widehat{Z}_{31} & E_{13}\widehat{Z}_{32} & E_{13}\widehat{Z}_{33} - Z_{22}E_{13} \\ -Z_{31}E_{13} - Z_{33}E_{32} + E_{32}\widehat{Z}_{11} & E_{32}\widehat{Z}_{12} & E_{32}\widehat{Z}_{13} - Z_{32}E_{13} \end{bmatrix}.$$

Observe that each block on the left side belongs to $\mathbb{Z}_2[C] = GF(2^3) \subseteq M_3(\mathbb{Z}_2)$, and so is either zero or invertible. On the other hand, on the right side, each block in the last two columns has rank at most two. We deduce that the last two columns on both sides are zero. In particular, comparing the second columns we see that $\widehat{Z}_{12} = Z_{12} = 0$ and $\widehat{Z}_{32} = 0$, so $Z_{22} = \widehat{Z}_{22}$, and $Z_{32} = \widehat{Z}_{32} = 0$. Putting this in the above equation and simplifying, the last column gives $\widehat{Z}_{13} = 0$, so $Z_{13} = \widehat{Z}_{13} = 0$, $Z_{23} = \widehat{Z}_{23}$, and $Z_{33} = \widehat{Z}_{33}$. Also, comparing the $(2, 3)$ positions, we obtain

$$0 = Z_{23} - \widehat{Z}_{23} = E_{13}\widehat{Z}_{33} - \widehat{Z}_{22}E_{13} = e_1(\widehat{Z}_{33}^{\mathrm{T}}e_3)^{\mathrm{T}} - \widehat{Z}_{22}e_1e_3^{\mathrm{T}}.$$

Moreover, $\widehat{Z}_{33}^{\mathrm{T}}e_3 = \lambda e_3$ and $\widehat{Z}_{22}e_1 = \lambda e_1$, $\lambda \in \mathbb{Z}_2$. Since $\widehat{Z}_{33}, \widehat{Z}_{22} \in \mathbb{Z}_2[C]$ and every vector is cyclic for C we see that $\widehat{Z}_{33} = \widehat{Z}_{22} = \lambda I_3$. The matrix equation therefore simplifies to

$$\begin{bmatrix} Z_{11} - \widehat{Z}_{11} & 0 & 0 \\ Z_{21} - \widehat{Z}_{21} & 0 & 0 \\ Z_{31} - \widehat{Z}_{31} & 0 & 0 \end{bmatrix} = \begin{bmatrix} -Z_{11}E_{13} + E_{13}\widehat{Z}_{11} & 0 & 0 \\ -Z_{21}E_{13} - \widehat{Z}_{23}E_{32} + E_{13}\widehat{Z}_{31} & 0 & 0 \\ -Z_{31}E_{13} - \lambda E_{32} + E_{32}\widehat{Z}_{11} & 0 & 0 \end{bmatrix}.$$

Comparing the position $(1, 1)$ gives by similar arguments as above that $\widehat{Z}_{11} = Z_{11} = \mu I_3$. Inserting this into the equation we see after rearrangement that the rank of the block at position $(3, 1)$ is equal to $\mathrm{rk}((\mu - \lambda)E_{32} - Z_{31}E_{13}) \leq 2$, which forces the two blocks at

position $(3,1)$ to be zero, i.e. $Z_{31} - \widehat{Z}_{31} = 0 = (\mu - \lambda)E_{32} - Z_{31}E_{13} = (\mu - \lambda)e_3e_2^{\mathrm{T}} - Z_{31}e_1e_3^{\mathrm{T}}$. We immediately get $Z_{31} = \widehat{Z}_{31} = 0 = (\mu - \lambda)$. Therefore, $Z_{11} = Z_{22} = Z_{33} = \lambda I_3$. Finally, comparing the $(2,1)$ positions gives

$$Z_{21} - \widehat{Z}_{21} = -Z_{21}E_{13} - \widehat{Z}_{23}E_{32},$$

and arguing as above, $Z_{21} = \widehat{Z}_{21} = 0$. Hence, Z is a scalar matrix. So, $\mathcal{C}(V) \cap \mathcal{C}(W)$ contains only scalar matrices, which gives that $d(A,B) \geq 5$. □

References

[1] A. Abdollahi, Commuting graphs of full matrix rings over finite fields, *Linear Algebra Appl.* **428** (2008), 2947–2954.

[2] S. Akbari, H. Bidkhori and A. Mohammadian, Commuting graphs of matrix algebras, *Commun. Algebra* **36** (2008), 4020–4031.

[3] S. Akbari, M. Ghandehari, M. Hadian and A. Mohammadian, On commuting graphs of semisimple rings, *Linear Algebra Appl.* **390** (2004), 345–355.

[4] S. Akbari, A. Mohammadian, H. Radjavi and P. Raja, On the diameters of commuting graphs, *Linear Algebra Appl.* **418** (2006), 161–176.

[5] S. Akbari and P. Raja, Commuting graphs of some subsets in simple rings, *Linear Algebra Appl.* **416** (2006), 1038–1047.

[6] R. Bhatia and P. Rosenthal, How and why to solve the operator equation $AX - XB = Y$, *Bull. London Math. Soc.* **29** (1997), 1–21.

[7] G. Dolinar, A. Guterman, B. Kuzma and P. Oblak, Extremal matrix centralizers, *Linear Algebra Appl.* **438** (2013), 2904–2910.

[8] G. Dolinar, B. Kuzma and P. Oblak, On maximal distances in a commuting graph, *Electron. J. Linear Algebra* **23** (2012), 243–256.

[9] D. Dolžan and P. Oblak, Commuting graph of matrices over semirings, *Linear Algebra Appl.* **435** (2011), 1657–1665.

[10] M. Giudici and A. Pope, The diameters of commuting graphs of linear groups and matrix rings over the integers modulo m, *Australasian Journal of Combinatorics* **48** (2010), 221–230.

[11] R. A. Horn, C. R. Johnson, *Matrix Analysis*, Cambridge UP, 1991.

[12] A. Iranmanesh and A. Jafarzadeh, On the commuting graph associated with the symmetric and alternating groups, *J. Alg. Appl.* **7** (2008), 129–146.

[13] N. Jacobson, *Lectures in abstract algebra Volume II: Linear algebra*, Graduate Texts in Mathematics 31, Springer-Verlag, New York-Berlin, 1953.

[14] K. D. Joshi, *Foundations of discrete mathematics*. New age international publishers, Bangalore, 1989.

[15] A. Mohammadian, On commuting graphs of finite matrix rings, *Commun. Algebra* **38** (2010), 988–994.

[16] P. Šemrl, Non-linear commutativity preserving maps, *Acta Sci. Math. (Szeged)* **71** (2005), 781–819.

[17] J. H. M. Wedderburn, *Lectures on Matrices*, American Mathematical Society Colloquium Publications, Volume XVII, 1934.

ARS MATHEMATICA CONTEMPORANEA

Also available at http://amc-journal.eu
ISSN 1855-3966 (printed edn.), ISSN 1855-3974 (electronic edn.)
ARS MATHEMATICA CONTEMPORANEA 7 (2014) 461–477

Triangle randomization for social network data anonymization*

Ljiljana Brankovic
University of Newcastle, Callaghan NSW 2308, Australia

Nacho López
Universitat de Lleida, C.Jaume II, 69, E-25001 Lleida, Spain

Mirka Miller
University of Newcastle, Callaghan NSW 2308, Australia
University of West Bohemia, Pilsen, Czech Republic
King's College London, The Strand, United Kingdom

Francesc Sebé
Universitat de Lleida, C.Jaume II, 69, E-25001 Lleida, Spain

Received 25 July 2011, accepted 29 August 2012, published online 27 June 2014

Abstract

In order to protect privacy of social network participants, network graph data should be anonymised prior to its release. Most proposals in the literature aim to achieve k-anonymity under specific assumptions about the background information available to the attacker. Our method is based on randomizing the location of the triangles in the graph. We show that this simple method preserves the main structural parameters of the graph to a high extent, while providing a high re-identification confusion.

Keywords: Anonymity, privacy, social network.

Math. Subj. Class.: 68R10

*This paper is a part of Bled'11 Special Issue.

This work was partly supported by: the Spanish Ministry of Economy and Competitiveness through project TIN2010-18978; RGC CEF grant G0189479, The University of Newcastle; and by a Marie Curie International Incoming Fellowship within the 7th European Community Framework Programme.

E-mail addresses: Ljiljana.Brankovic@newcastle.edu.au (Ljiljana Brankovic), nlopez@matematica.udl.cat (Nacho López), mirka.miller@newcastle.edu.au (Mirka Miller), fsebe@matematica.udl.cat (Francesc Sebé)

1 Introduction

A social network comprises a set of participants and the relations among them. Such a network is naturally modelled by a graph structure, where each participant in the network is assigned to a vertex and relations are represented by edges connecting pairs of vertices.

Analysis of social network graph data [15, 17], and evolution [9] is a source of valuable information for numerous research areas, including sociology, psychology, economics and epidemiology, to mention but a few. The results of such research have shed light on wide range of problems, from the dynamics of happiness [5], obesity [4] and smoking [12] to crime investigation [6]. Notwithstanding the benefits that such studies offer in various areas of life, they also introduce threats to individuals' privacy. Social networks contain sensitive personal data whose publication or exchange would compromise their members' privacy. As an example, consider a graph in which nodes are e-mail addresses and the edges represent 'message exchange' relations. The list of people a person communicates with is an example of very sensitive data. In order to alleviate privacy risks, it is generally accepted that access to social network data for scientific research requires a pre-processing phase to reduce the opportunities for inferring information about individuals. This should be done in such a way so as to maintain a high quality of the transformed data so that the analysis can be performed with acceptable accuracy.

Privacy in social networks considers two basic aspects:

- *Vertex anonymity:* It should not be possible to infer the identity of vertices in the published anonymized network.
- *Edge anonymity:* Given two social network participants, it should not be possible to infer whether an edge exists between their corresponding vertices, *i.e.*, whether they are related.

Naive anonymization provided by the removal of individuals' identifiers has been proven insufficient since background knowledge such as the vertex degree or the neighborhood subgraph of some participants often permits the identification of many of the vertices. Therefore, additional privacy measures must be applied. These measures can be classified into:

- *Generalization based techniques:* Nodes and edges are first clustered and then collapsed into supervertices and superedges [2, 8].
- *Perturbation based techniques:* The original social network is modified by adding and/or removing vertices and/or edges [3, 10, 19, 20, 21].

Privacy of any anonymization technique depends on the previous knowledge the attacker is assumed to have. In [10] the attacker is assumed to know the degrees of all the vertices in the network, and thus the original network is modified by edge additions and/or deletions until the degree sequence is k-anonymous [14]. A similar approach is given in [21], which provides k-anonymity even when the attacker has prior knowledge about the neighborhood subgraph of target vertices.

Recently, *information-theoretic models* have been proposed, which seek to achieve robustness against any background structural knowledge of the attacker. The k-Symmetry [19] and k-Automorphism [20] models aim to protect against "identity disclosure" (vertex anonymity) by adding vertices and edges until, for each vertex of the

graph, there exist at least $k-1$ other vertices that are structurally equivalent to it. The k-Isomorphism [3] model also considers edge privacy and generates an anonymous graph that consists of k disjoint isomorphic subgraphs. Such models impose hard structural requirements on anonymized graphs that require extensive modifications to the original graph. From the computational point of view, implementing these security models depends on the capability to cope with some known NP-hard problems on graphs.

In [16], n-confusion is proposed as a privacy model that generalizes k-anonymity. This model requires that the set of nodes from the released graph that can correspond to any given identity has a size larger or equal to n. In this paper, the privacy is analyzed from that point of view.

1.1 Our approach

Information-theoretic models achieving k-anonymity against any structural knowlege [3, 19, 20] are hard to put into practice and require extensive perturbation of the original graph. We claim adequate privacy can be achieved by means of simpler random noise techniques.

Structural background knowledge may be of diverse nature. We focus our attention on two specific parameters: vertex degree and the number of triangles passing through a given vertex. In [19] it is shown that their combined knowledge provides a high re-identification power in a trivially anonymized graph. Both parameters are implicit parts of other structural properties. For instance, knowledge of the neighbourhood subgraph of a vertex implies knowing its degree and all triangles passing through the vertex. Any anonymization procedure that perturbs both parameters also impairs re-identification methods based on more complex structural knowledge implicitly involving the parameters. An additional important aspect is that both parameters are easy to measure so that they can be part of computationally efficient anonymization techniques.

We propose a method that first removes the triangles of the graph (by deleting at least one edge of each triangle) and next randomly adds edges to the resulting graph so as to create approximately as many triangles as there were in the original graph. This triangle randomization process makes the information about triangles passing through a vertex less reliable for matching purposes, while it also perturbs the degree of the vertices in the graph. At the same time, the global structure of the graph remains very similar to the original one. It is easy to see that this procedure preserves the connected components since removing one edge from a triangle can never disconnect the graph and new edges are only added between vertices that are connected by a path of length 2. Experimental results show that other graph structure parameters are preserved to a high extent.

1.2 Main contributions

In this paper we propose a novel perturbation technique for preserving privacy in social networks, based on randomization of the locations of triangles in the graph. Our technique (1) is simple and can be efficiently implemented on large graphs; (2) provides high level of privacy, as supported by our experiments; (3) provides a high degree of data utility, as supported by experimental evidence.

The organisation of the paper is as follows. In the next section we present the anonymization algorithm and give bounds on the number of triangles in the perturbed graph. In Section 3 we analyse the privacy of our technique by providing the bounds for the degree and a number of triangles passing through each vertex of the perturbed

graph, and using these bounds to measure degree-triangle anonymity. Section 4 presents our experimental results on real and synthetic data sets, both in terms of utility and privacy. In Section 5 we give some concluding remarks and directions for future research.

2 Anonymization procedure

We model a social network as an undirected graph $G = (V, E)$, where V and E are the sets of vertices and edges, respectively. If $u, v, w \in V$ and $uv, vw, wu \in E$, then (u, v, w) is said to be a triangle of G.

Our proposal is a perturbation-based technique consisting of two rounds, where anonymization is achieved by means of edge removal and addition. Its description is given in Algorithm 1.

Input: Original graph $G = (V, E)$
Output: Masked graph G
1 $T = NumTriangles(G)$;
2 **while** $NumTriangles(G) > 0$ **do**
3 $(v_i, v_j, v_k) = TakeTriangleAtRandom(G)$;
4 $b = TakeAtRandomFrom(\{0, 1, 2\})$;
5 **if** *b=0* **then**
6 $RemoveEdge(G, (v_j, v_k))$
7 **else if** *b=1* **then**
8 $RemoveEdge(G, (v_i, v_k))$
9 **else**
10 $RemoveEdge(G, (v_i, v_j))$
11 **end**
12 **end**
13 **while** $NumTriangles(G) < T$ **do**
14 $(v_i, v_j) = TakeEdgeAtRandom(G)$;
15 $b = TakeAtRandomFrom(\{0, 1\})$;
16 **if** *b=0* **then**
17 $v_k = TakeNeighborAtRandom(G, v_i)$;
18 **if** $v_k \neq v_j$ **and** $(v_k, v_j) \notin E$ **then**
19 $AddEdge(G, (v_k, v_j))$
20 **end**
21 **else**
22 $v_k = TakeNeighborAtRandom(G, v_j)$;
23 **if** $v_k \neq v_i$ **and** $(v_k, v_i) \notin E$ **then**
24 $AddEdge(G, (v_k, v_i))$
25 **end**
26 **end**
27 **end**
28 **return** (G)

Algorithm 1: Triangle randomization algorithm

The first round (steps 1-12) is a procedure that randomly selects a triangle of G, then randomly selects one of its edges and removes it; this is repeated until there are no more triangles left. Note that the removal of a single edge may cause the deletion of several triangles. The second round (steps 13-27) adds edges that create one or more triangles

each.

Note that the number of triangles after the algorithm has finished, T', may not equal the original number T. Since Algorithm 1 terminates when the addition of a single edge gives a graph with the total number of triangles $T' \geq T$, it is very likely that this results in $T' \approx T$. This fact introduces some additional uncertainty that further obstructs possible matching attempts.

We next provide a bound on the number of triangles T' in the perturbed graph G'.

Proposition 2.1. *Let G be a graph that has been perturbed into G' using Algorithm 1, and let $T \geq 1$ and T' be the number of triangles in G and G', respectively. Then $T' < T + \Delta' - 1$, where Δ' is the maximum degree in G'.*

Proof. Let $G' = (V', E')$ and $G'' = (V'', E'')$, $V'' = V'$ and $E'' = E' \setminus \{uv\}$, where uv is the very last edge added by the Algorithm 1 (informally, G'' is the graph obtained by Algorithm 1 just before the very last edge, say uv, is added), and let T'' be the number of triangles in G''. Then $T' = T'' + T^{uv}$, where T^{uv} is the number triangles created by addition of the edge uv. Then we have $T^{uv} = |N''(u) \cap N''(v)| \leq |N''(u)| < \Delta'$, where $N''(u)$ is the neighbourhood of u in G''. Since $T'' \leq T - 1$ we have $T' < T + \Delta' - 1$. □

The previous proposition states that T' is at most $T + \Delta' - 2$. From the proof, this extremal situation is given when $T'' = T - 1$ and $T^{uv} = |N''(u) \cap N''(v)| = |N''(u)| = \Delta' - 1$. We pose the following open problem.

Problem 2.2. Is there a family of graphs G with arbitrarily large values of T that can be perturbed to graphs G' such that $T' = T + \Delta' - 2$?

3 Data privacy

In this section, we analyse the privacy of our proposal assuming that the attacker's background knowledge comprises the degree and the number of triangles passing through some vertices. The objective of the proposed method is to disrupt any attempt to obtain knowledge about the identity of the nodes in the published anonymized network. So as to evaluate the extent to which this objective is achieved, we need some methods for measuring it. These are the privacy metrics.

3.1 Degree-triangle variation

Let us consider a vertex $u \in G$, and let us denote its degree, that is, the number of vertices adjacent to u, as d_u. The number of triangles passing through u is denoted by t_u. For each vertex u, we consider the pair (d_u, t_u).

When Algorithm 1 is applied to a particular graph G, given a vertex u, its *degree-triangles* pair (d_u, t_u) is transformed to another pair (d'_u, t'_u). Next proposition defines the *destiny region* of a pair (d_u, t_u), that is, the subset of $\mathbb{Z} \times \mathbb{Z}$ where the pair (d'_u, t'_u) may take its value.

Proposition 3.1. *Let G be a graph that has been perturbed into G' using Algorithm 1. Let (d_u, t_u) be the degree-triangles pair of u in G where $d_u \geq 1$, and let (d'_u, t'_u) be the corresponding pair in G'. Denoting by T and T' the number of triangles of G and G',*

respectively, the following inequalities hold:

$$\max\{1, d_u - t_u\} \leq d'_u \leq d_u + T \ ;$$

$$\max\{0, d'_u - d_u\} \leq t'_u \leq \min\left\{T', \frac{d'_u(d'_u-1)}{2}\right\}.$$

Proof. In the first round of Algorithm 1, edges of triangles are randomly removed until no triangles are left in G. For each edge removed from a triangle, the degree of its vertices is decreased by at most one. Hence, at the end of the first round, (d_u, t_u) is transformed to $(x, 0)$, where x is an integer that ranges between $\max\{1, d_u - t_u\}$ and d_u (the edge adjacent to a vertex of degree one will not be removed since it cannot be part of any triangle). Since the degree of a vertex cannot decrease during the second round, we obtain $\max\{1, d_u - t_u\} \leq d'_u$.

After that, the second round of Algorithm 1 adds edges that create triangles. Each edge addition to the graph increases the degree of a vertex by at most one. Since the second round iterates at most T times, we get the degree of u cannot be more than $d_u + T$. At the end, the number of triangles passing through a vertex may be at most T'. Taking into account that a vertex of degree d cannot be part of more than $\frac{d(d-1)}{2}$ triangles, we get $t'_u \leq \min\left\{T', \frac{d'_u(d'_u-1)}{2}\right\}$.

A vertex u with $d'_u > d_u$ implies that its degree has increased during the triangle addition phase. In this phase, each time u receives a new edge, the number of triangles passing through it also increases by at least one. This implies that $d'_u - d_u \leq t'_u$. Since t'_u cannot take a negative value, we obtain $\max\{0, d'_u - d_u\} \leq t'_u$.

□

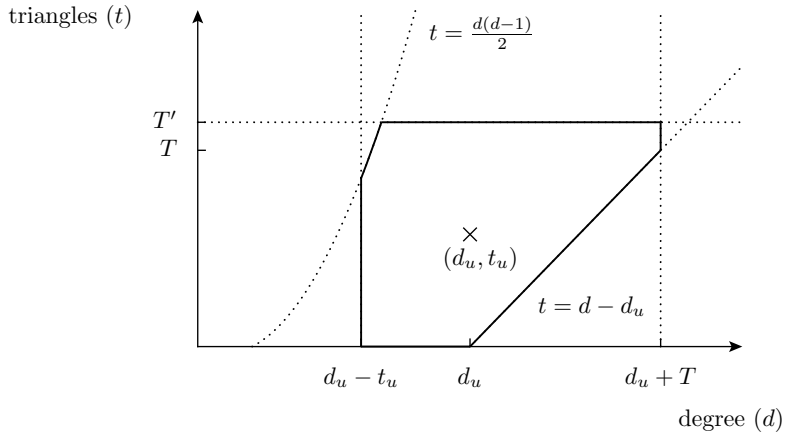

Figure 1: Destiny region D_u of (d_u, t_u) whose bounds are given in Proposition 3.1.

There are some special cases where the destiny region of a vertex can be better estimated. For instance, Algorithm 1 does not perturb isolated vertices ($d_u = 0$) nor connected components with just two vertices. Such simple structures are very common in social network graphs, and classical k-anonymity is directly provided on them when

such isomorphic structures appear k times. In general, given a pair (d_u, t_u) from a graph containing T triangles, we can compute the bounds of its destiny region D_u. The size of this region depends on T and T'. Our experiments have shown that in practice $T \approx T'$ so that its size is $O(T^2)$. The shape of D_u is illustrated in Figure 1.

Not every point in D_u corresponds to a vertex u with (d_u, t_u), as illustrated by the following example.

Example:

Let $G = (V, E)$ be a graph with $V = \{a, b, c, d, e\}$ and $E = \{ab, ae, bc, be, cd, de\}$ (see Figure 2). G contains one triangle (a, b, e). Regarding vertex a, we have $(d_a, t_a) = (2, 1)$.

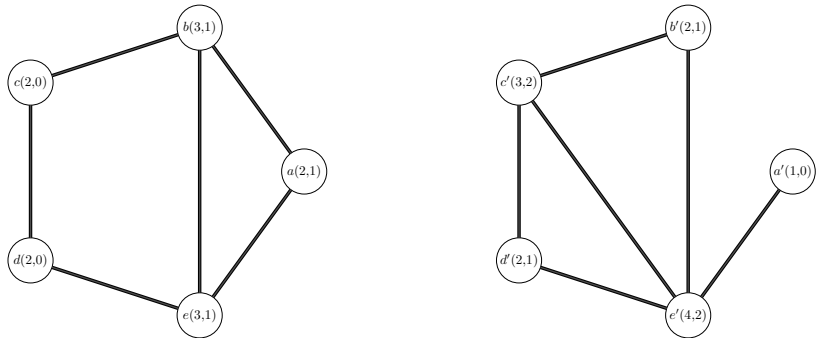

Figure 2: Graph G (left) and its anonymized graph G' (right) generated by Algorithm 1. In this case $T = 1$ and $T' = 2$. Numbers in brackets indicate the degree-triangles pairs.

From Proposition 3.1 we have $D_a = \{(1, 0), (2, 0), (2, 1), (3, 1), (3, 2)\}$. Algorithm 1 will first eliminate the triangle by randomly removing one of its edges. It will result in $(d_a, t_a) = (1, 0)$ with probability $\frac{2}{3}$ (either ab or ae are removed) and $(d_a, t_a) = (2, 0)$ (edge be is removed) with probability $\frac{1}{3}$. Next, one edge will be added so as to create a new triangle. It can be seen that at the end (d_a, t_a) becomes $(2, 1)$ with probability $\frac{2}{5}$; $(1, 0)$ with probability $\frac{1}{3}$; and $(3, 1)$ or $(2, 0)$ with probability $\frac{2}{15}$. Moreover, T' may become 2 in some cases (this is the case in G'), but the tuple $(3, 2) \in D_a$ is not possible for vertex a starting from its original value $(2, 1)$.

3.2 Measuring degree-triangle confusion

Let us consider an adversary whose goal is to re-identify a vertex u in an anonymized graph G' assuming her knowledge on u is given by the pair (d_u, t_u), that is, the adversary knows the number of relationships of u and the number of 'three party friends' that u belongs to.

Confusion is provided as long as the adversary has some level of uncertainty about the vertices of G' that may correspond to u. The set of candidate vertices is given by the set of vertices in G' that belong to the destiny region of u, namely D_u. The adversary does not know the value of T (number of triangles in the original graph G), but a good estimate is given by $T \approx T'$. If just one vertex of G' falls in D_u, then u will be re-identified resulting in the corresponding privacy compromise. The desirable situation is that in which the destiny

region contains a large number of vertices, thus ensuring a high level of confusion. Let us define

$$\mathcal{M}_{G,G'}(u) = |\{v \in V \mid (d'_v, t'_v) \in D_u\}|,$$

as a local measure of confusion on u once G' has been released. Although not all vertices in D_u have the same probability of corresponding to u (as shown in the previous example), identifying u is not an easy task for an adversary with a limited knowledge of the original graph G. Hence, we propose the following confusion measure.

Definition 3.2 (Degree-triangle confusion)**.** Let $G = (V, E)$ and $G' = (V, E')$ be two graphs with a common set of vertices V. We say that (G, G') is a k-degree-triangle confusing pair of graphs if $\mathcal{M}_{G,G'}(u) \geq k$ for every $u \in V$. That is, every vertex in G has at least k matching candidate vertices in G'.

Note that the largest k satisfying $\mathcal{M}_{G,G'}(u) \geq k$ for each $u \in V$ corresponds to $\min_{u \in V}\{\mathcal{M}_{G,G'}(u)\}$. In the example of Figure 2, $\mathcal{M}_{G,G'}(b) = 4$ since vertices $\{b', c', d', e'\}$ fall in the destiny region of b (see Figure 3). For the rest of the vertices, we have $\mathcal{M}_{G,G'}(a) = 4$, $\mathcal{M}_{G,G'}(c) = \mathcal{M}_{G,G'}(d) = 3$ and $\mathcal{M}_{G,G'}(e) = 4$. Hence, (G, G') is 3-degree-triangle confusing.

Since $k = \min_{u \in V}\{\mathcal{M}_{G,G'}(u)\}$, it usually happens that the destiny region of most vertices contains more than k vertices. In order to provide more information about degree-triangle confusion, we will also analyze the median and the maximum values in $\{\mathcal{M}_{G,G'}(u) \mid u \in V\}$. The median value will provide the number of matching candidates for a "typical" vertex, meanwhile the maximum one corresponds to the worst case for an attacker.

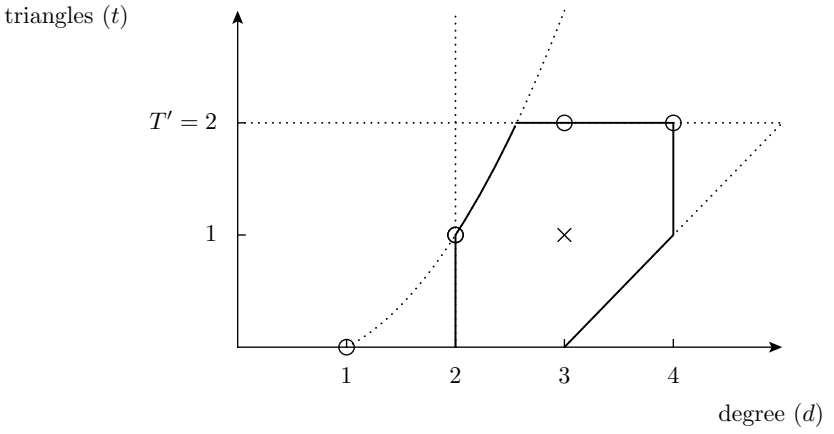

Figure 3: Destiny region of vertex b. Vertices of G' are represented by little circles (tuple $(2, 1)$ appears twice since it corresponds to vertices b' and d'). Vertex a', $(1, 0)$, is out of D_b.

4 Experimental results

The proposed anonymization procedure has been implemented in Python[1] using the Networkx[2] v1.7 graph library and tested over real and synthetic social network data.

4.1 Graph data sets

The following real data sets and synthetic graph generators have been employed in our experiments:

- The *Coauthors* graph is generated from bibliographic data available at the collection of Computer Science Bibliographies[3], where each author is assigned a vertex and edges are built from co-authorship relations. In our experiments, a graph with 11510 vertices and 11135 edges has been built. Data sets constructed in the same way have been previously used in [10, 20].
- The *Condmat* graph represents the collaboration network of scientists posting preprints on the condensed matter archive at `www.arxiv.org`. This version is based on preprints posted between January 1, 1995 and June 30, 2003. This graph is composed of 31163 vertices and 120029 edges. It has been used by several authors as a test-bed for community-finding algorithms for large networks (see, for example,[13]).
- The *Holme-Kim model* produces scale-free synthetic graphs in which the probability $P(k)$ that a vertex interacts with k other vertices follows a power law distribution, that is, $P(k) \sim C{\cdot}k^{-\gamma}$. Many real world graphs have a power law degree distribution with $2 \leq \gamma \leq 4$, as noted in [1]. The graphs generated by this model have $\gamma \approx 2.9$ which is considered a good approximation to many real world graphs. This model extends the well known *Barabasi-Albert* model (see [1]) including an extra step referred to as *triangle formation step*. In the *Barabasi-Albert* model, an empty graph with m vertices is first generated. After that, the construction algorithm iterates by adding a degree m vertex v at each step. Each edge of v is attached to an existing vertex with a probability proportional to its degree (this is the *preferential attachment (PA) step*). The Holme-Kim model incorporates an additional phase: for each edge between v and w added in the PA step, add one more edge from v to a randomly chosen neighbor of w with a given probability p. As a consequence, Holme-Kim graphs range between low-clustered graphs for $p = 0$ (Barabasi-Albert graphs) and highly-clustered ones for $p = 1$ (see [7]).
- The *Watts-Strogatz model* was inspired by the small-world phenomenon which is based on the notion that every person in the world is connected to anyone else through a chain of six mutual acquaintances at most (also known as "six degrees of separation"). Starting from a ring lattice on n vertices, where vertices have degree k, this model takes each edge and rewires it with probability p. This model interpolates between regularity ($p = 0$) and total disorder ($p = 1$). For $0 < p < 1$ we obtain highly clustered graphs having a small diameter, as it happens in many real world graphs (see [18]).

[1] `http://python.org`
[2] `http://networkx.lanl.gov`
[3] `http://liinwww.ira.uka.de/bibliography`

4.2 Graph utility measures

The method proposed in this paper introduces some changes to a graph prior to its release. In order to quantify the extent to which the original graph has been modified, we compute some statistical network measures and see how they are affected as a result of masking. These are the utility metrics.

The following utility measures have been considered:

- Number of links (*size*),
- Number of triangles,
- Average clustering coefficient,
- Average shortest path length (*Av. SPL*),
- Minimum, median and maximum vertex degree.

The (local) clustering coefficient c_u of a vertex u measures how close the neighbors of u are to being a clique, that is, $c_u = \frac{2t_u}{d_u(d_u-1)}$ when $d_u \geq 2$, and $c_u = 0$ otherwise. Given an order n graph $G = (V, E)$, the average clustering coefficient is,

$$\frac{1}{n} \sum_{u \in V} c_u.$$

Besides, the average shortest path length is,

$$\frac{1}{n(n-1)} \sum_{u,v \in V} \text{dist}(u, v),$$

where $\text{dist}(u, v)$ is the distance (length of a shortest path) between u and v. The other parameters are self-explanatory.

4.3 Experiments on real data sets

Algorithm 1 has been run ten times over the *Coauthors* and *Condmat* graphs. The median computation time has been 2.03 and 4.19 minutes, respectively.

Utility measures

Utility measures of the original graphs and their anonymized versions are shown in Table 1. As can be seen, the metrics of a graph and its perturbed versions exhibit a high correlation. After masking, the size is slightly increased while the median number of triangles is preserved although in some experiments it resulted in a slightly larger value (no more than four additional triangles were created in all the experiments). Degree parameters are well preserved in both graphs too. The average clustering and average SPL have been the most affected parameters in the *Condmat* graph. Figure 4 shows the distribution of (d_u, t_u) pairs for both graphs. Focusing our attention on the *Condmat* graph, it can be seen that vertices with high degree have less trianges after anonymization. As a consequence, the Av. clustering is reduced.

	Coauthors		*Condmat*	
	Original	Anonymized (median)	Original	Anonymized (median)
Size	11135	12040	120029	179244
Triangles	6395	6395	232994	232994
Av. Clustering	0.4591	0.4206	0.6488	0.47217
Av. SPL	3.3543	3.207	5.2995	4.2047
Min. Degree	0	0	0	0
Median Degree	2	2	25	27.5
Max. Degree	73	74	202	211

Table 1: Metrics of *Coauthors* and *Condmat* graphs before and after anonymization.

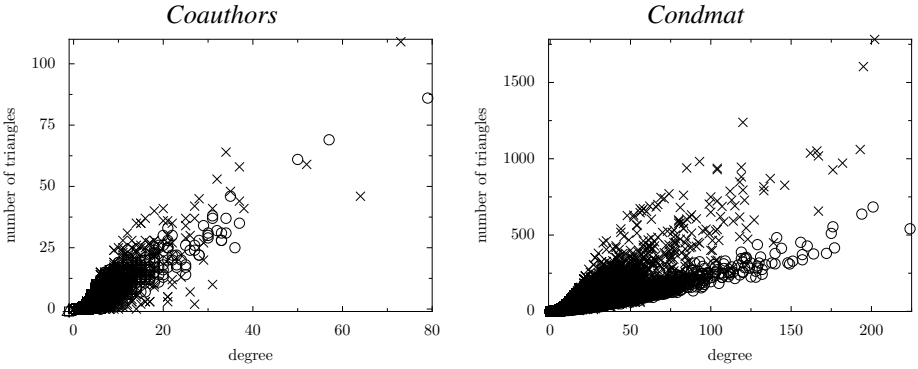

Figure 4: Degree-triangles distribution for *coauthors* and *condmat* graphs before (symbol $\times$) and after (symbol $\circ$) anonymization.

Degree-triangle privacy

The value of $\mathcal{M}_{G,G'}(u)$ has been measured individually for every vertex u after each experiment.

The *Coauthors* graph has 11510 vertices: 2574 of them are isolated vertices and 1982 are located in connected components with two vertices. These vertices are not affected by Algorithm 1 but they are indistinguishable in terms of re-identification. The remaining 6954 vertices are masked by Algorithm 1. Table 2 summarizes the results. As can be seen, the minimum value for $\mathcal{M}_{G,G'}(u)$ is 20, that is, (G, G') is a 20-degree-triangle confusing pair of graphs. Nevertheless, a 'typical' vertex has an elevated amount of vertices (6947) in its destiny region (more than 60% of vertices).

The *Condmat* graph contains 703 isolated vertices and 830 vertices belonging to connected components with two vertices. The remaining 29630 vertices have been masked by Algorithm 1. The destiny region of a 'typical' vertex contains 29630 vertices (95.1% of vertices). The smallest destiny region for any node includes 7198 vertices, that is, 24.3% of vertices (see Table 2). In this example, the degree-triangle confusion parameter is $k = 703$ which comes from isolated vertices.

	Values in $\{\mathcal{M}_{G,G'}(u) \mid u \in V\}$					
vertices u such that (d_u, t_u) satisfies	*Coauthors* (11510 vertices)			*Condmat* (31163 vertices)		
	Min.	Med.	Max.	Min.	Med.	Max.
$d_u = 0$	2574	2574	2574	703	703	703
$d_u = 1$	1982	1982	1982	830	830	830
$d_u > 1$ or $t_u > 1$	20	6947	6954	7198	29630	29630

Table 2: Minimum, median and maximum values of $\{\mathcal{M}_{G,G'}(u) \mid u \in V\}$ for *Coauthors* and *Condmat* graphs. The degree-triangle confusion measure for each graph is the minimum value in the table.

4.4 Experiments over synthetic graphs

Experiments on synthetic graphs have been performed over graphs with 10^5 vertices. For each model, we have generated ten random graphs with parameter p taking the following values: $0, 0.2, 0.4, 0.6, 0.8, 1$. Regarding Watts-Strogatz graphs, they have been generated from cubic graphs so that the resulting graphs have a minimum degree equal to three, except for $p = 0$, where the resulting graph is regular of degree 6. In all the cases, the generator provided by the Networkx library has been employed. Each graph from the test set has been masked ten times and the utility and privacy metrics have been computed (average values are analyzed).

Utility measures

The computation time of Algorithm 1 on both models is depicted in the left graphic of Figure 5. It can be seen that the computation time is strongly correlated with the number of triangles of the graph (right graphic of Figure 5). For a Watts-Strogatz (WS) graph of order 10^5 containing 300000 triangles, Algorithm 1 takes a little bit more than 11 hours. When $p = 0.5$, both models generate graphs with a close number of triangles (50000) and a similar computation time (around 4 hours) is required for both models. The number of triangles in the anonymized graphs almost equals the amount of triangles of the original ones, as it can be seen from the overlapping lines in the right graphic of Figure 5. More specifically, the maximum difference of $T' - T$ has been 6, which is a negligible quantity for graphs containing 300000 triangles.

The number of edges of the generated Watts-Strogatz (WS) graphs has been $3 \cdot 10^5$ in all the cases. The amount of edges after anonymization has been increased in all the cases, except for $p = 0$, where the anonymized graph contains 299591 edges (a 0.001% difference). The maximum difference appears for $p = 0.2$, where the corresponding anonymized graph has 322052 edges. Nevertheless, the maximum difference is about 7.35% of edges. Regarding Holme-Kim (HK) graphs, their size is close to $2 \cdot 10^5$. The HK anonymized graphs contain more edges than the corresponding value for the original ones, but again the maximum relative difference (for $p = 0.6$) is 2.07% (See Figure 6).

Degree parameters variation appears in Figure 7. It can be seen that the maximum difference of WS graphs appears for $p = 0.2$, where the maximum degree has been doubled (from 12 to 24), the median degree increases from 5.5 to 7.5 and the minimum degree

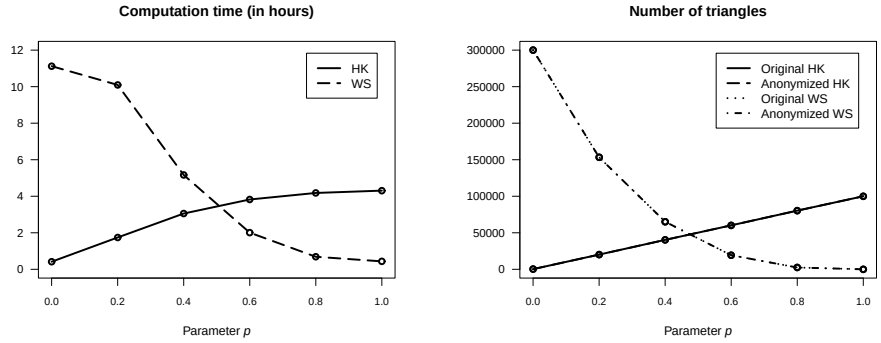

Figure 5: Computation time (left) and number of triangles for Watts-Strogatz (WS) and Holme-Kim (HK) graphs with 10^5 vertices, as a function of parameter p, before and after anonymization (right).

decreases from 3 to 1. Regarding HK graphs, degree parameters have been less affected.

The clustering coefficients in both models have been preserved to a high extent (see Figure 8). In WS graphs, the difference tends to zero as $p \to 1$. Besides, we observe the reverse behaviour in the HK model where the maximum difference appears at $p = 1$ where anonymized HK graphs are less clustered.

Degree-Triangle privacy

The minimum, median and maximum values of the degree-triangle confusion measure have been computed in both models. The results are shown in Figure 9 and Table 3. For Holme-Kim graphs, the privacy has been compromised for $p = 0, 0.4$ and 0.6, where $\min\{\mathcal{M}_{G,G'}(u) \mid u \in V\} = 1$, that is, there is at least one re-identifiable vertex in these cases. Holme-Kim graphs have a few vertices with high degree containing a small number of triangles. These vertices are difficult to mask, specially when the number of triangles T of the whole graph is also low. Masking data sets with outliers is known to be a thorny issue [11]. Prior to releasing a masked graph containing such nodes, some additional measures such as removing them or adding some additional noise should be taken. Nevertheless, a 'typical' (median) vertex contains an acceptable number of vertices in its destiny region, as Table 3 shows.

Regarding the Watts-Strogatz graphs, we have $\min\{\mathcal{M}_{G,G'}(u) \mid u \in V\} = 1$ just for $p = 1$. WS graphs have a low number of triangles (only 20 in our experiment) for $p = 1$. As a consequence, Algorithm 1 produces an insignificant modification to WS graphs so that vertices with a high degree are probably not affected and become easily re-identificable in the masked graph. Nevertheless, a 'typical' vertex contains a high number of vertices into its destiny region (7276), as Table 3 and the dashed line in left graphic of Figure 9 shows. As could be expected, these examples show the presented algorithm is not adequate for graphs having a reduced amount of triangles.

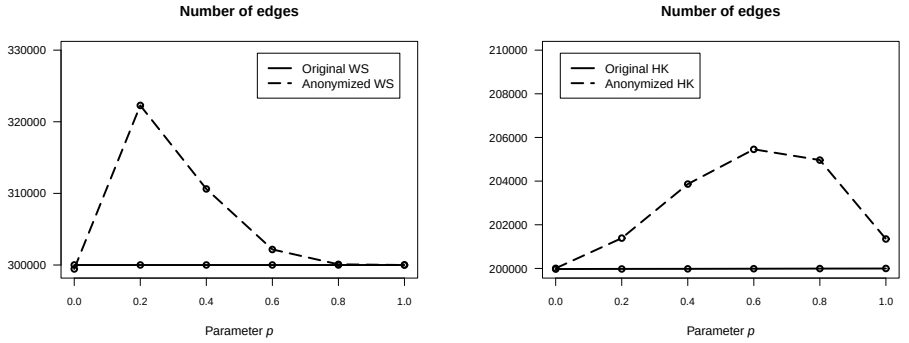

Figure 6: Number of edges for Watts-Strogatz (WS) (left) and Holme-Kim (HK) (right) graphs with 10^5 vertices, as a function of parameter p, before and after anonymization.

	Values in $\{\mathcal{M}_{G,G'}(u) \mid u \in V\}$					
Parameter p	Watts-Strogatz			Holme-Kim		
	Min.	Med.	Max.	Min.	Med.	Max.
0	10^5	10^5	10^5	1	13	70087
0.2	12368	90486	10^5	2	320	91885
0.4	271	59702	99990	1	968	95642
0.6	43	36453	98897	1	2278	99163
0.8	6	19392	87726	23	6489	99906
1.0	1	7276	44654	86101	99999	10^5

Table 3: Minimum, median and maximum values in $\{\mathcal{M}_{G,G'}(u) \mid u \in V\}$ for *Watts-Strogatz* (WS) and *Holme-Kim* (HK) graphs.

5 Conclusion and future work

In this paper a new anonymization method for social network graph data has been presented. The method is composed of two differentiated phases. The first phase iterates by randomly removing one edge of a randomly selected triangle in the graph until no triangles are left. In the second phase, the removed triangles are randomly reallocated in the graph. Due to its simplicity and low cost of the required operations, the method can be efficiently implemented in an algorithm whose running time grows linearly with the amount of triangles.

Empirical experiments have shown the method provides a high privacy level. Regarding data quality, experiments have shown structural parameters are better preserved in graphs with a larger homogeneity among vertices.

Some open issues that will be addressed in future research are:

- Quantify the probability distribution of the degree-triangles pair in the destiny region.
- Find techniques to increase structural parameters preservation in non-homogeneous graphs.

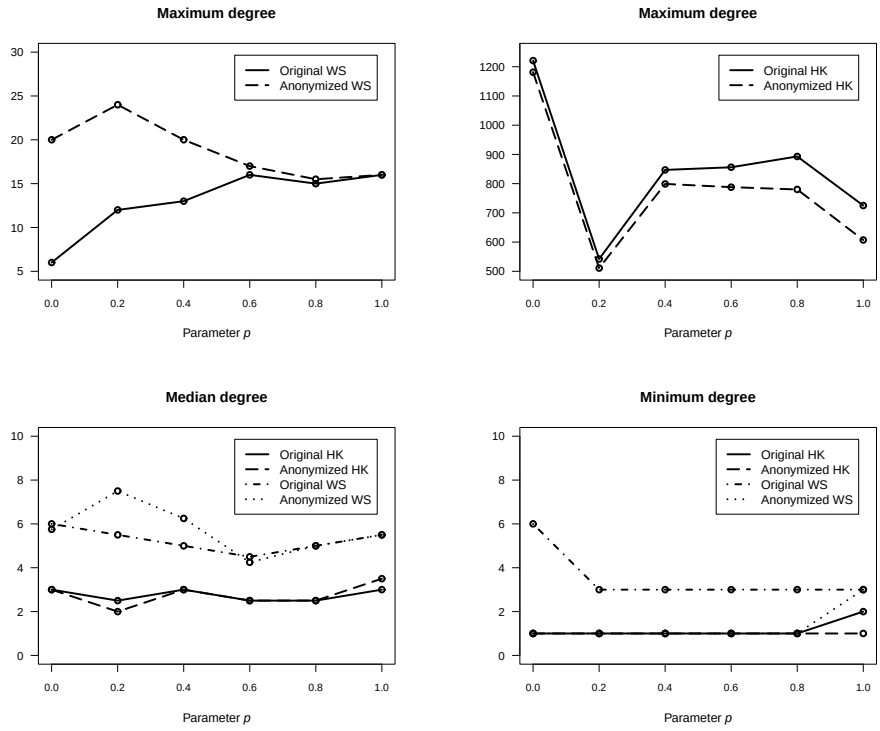

Figure 7: Maximum, median and minimum degree for Watts-Strogatz (WS) and Holme-Kim (HK) graphs with 10^5 vertices, as a function of parameter p, before and after anonymization.

Acknowledgements

The authors thank the referees for their constructive and helpful comments, which led to several improvements to the manuscript.

References

[1] A. Barabási and R. Albert, Emergence of scaling in random networks, *Science* **286** (1999) 509–512.

[2] A. Campan and T. M. Truta, A clustering approach for data and structural anonymity in social networks, *Proc. of PinKDD'08*, 2008.

[3] J. Cheng, A.W-C. Fu and J. Liu, K-Isomorphism: privacy preserving network publication against structural attacks, *Proc. of SIGMOD'10*, 2010.

[4] N. A. Christakis and J. H. Fowler, The spread of obesity in a large social network over 32 Years, *The New England Journal of Medicine*, **357**, (2007), 370–379.

[5] J. H. Fowler and N. A. Christakis, Dynamic spread of happiness in a large social network: longitudinal analysis over 20 years in the Framingham Heart Study, *British Medical Journal*, **337**, No. a2338, (2008), 1-9.

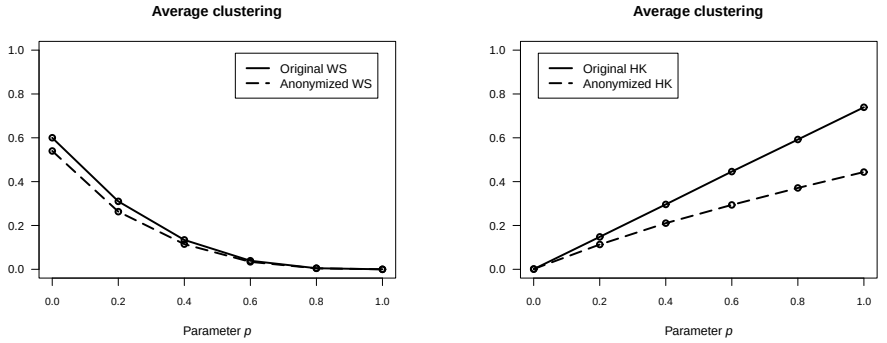

Figure 8: Average clustering for Watts-Strogatz (WS) and Holme-Kim (HK) graphs with 10^5 vertices, as a function of parameter p, before and after anonymization.

[6] M. Godwin, Maurice victim target networks as solvability factors in serial murder, *Social Behavior and Personality: an international journal*, **26**, No. 1, (1998) , 7583.

[7] P. Holme and B. J. Kim, Growing scale-free networks with tunable clustering, *Physical Review E.*, **65**, (2002)

[8] M. Hay, G. Miklau, D. Jensen, D. Towsley and P. Weis, Resisting structural re-identification in anonymized social networks, *Proc. of VLDB'08*, 2008.

[9] R. Kumar, J. Novak and A. Tomkins, Structure and evolution of online social networks, *Proc. of KDD'06*, 2006.

[10] K. Liu and E. Terzi, Towards identity anonymization on graphs, *Proc. of SIGMOD'08*, 2008.

[11] J.M. Mateo-Sanz, F. Sebé and J. Domingo-Ferrer, Outlier protection in continuous microdata masking, Proc. of PSD'04, Lecture Notes in Computer Science, **3050**, 2004, 201–215.

[12] L. Mercken, T. A. B. Snijders, C. Steglich, E. Vertiainen and H. De Vries, Smoking-based selection and influence in gender-segregated friendship networks: a social network analysis of adolescent smoking, *Addiction*, **105**, Issue 7, (2010), 12801289.

[13] M. E. J. Newman, The structure of scientific collaboration networks, *Proc. Natl. Acad. Sci. USA 98*, (2001), 404–409

[14] P. Samarati and L. Sweeney, Protecting privacy when disclosing information: k-anonymity and its enforcement through generalization and supression, Tech. rep., SRI Intl. Tech. Rep., 1998.

[15] J. Scott, *Social Network Analysis Handbook* (2nd ed.), Sage Publications Ltd., 2000.

[16] K. Stokes and V. Torra, n-Confusion: a generalization of k-anonymity, Proc. of 5th Intl. Workshop on Privacy and Anonymity in the Information Society, 2012.

[17] S. Wasserman and K. Faust, *Social Network Analysis: Methods and applications (Structural Analysis in the Social Sciences)*. Cambridge University Press, 1994.

[18] D. J. Watts and S. H. Strogatz, Collective dynamics of 'small-world' networks, *Nature*, **393** (1998), 440–442.

[19] W. Wu, Y. Xiao, W. Wang, Z. He and Z. Wang, K-Symmetry model for identity anonymization in social networks, *Proc. of EDBT'2010*, 2010.

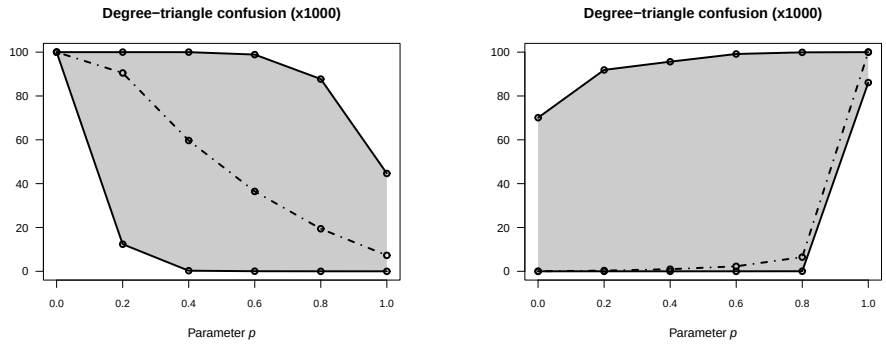

Figure 9: Degree-triangle confusion measure for Watts-Strogatz (left) and Holme-Kim (right) graphs with 10^5 vertices, as a function of parameter p. The dashed line indicates the value of $\mathcal{M}_{G,G'}(u)$ for a typical vertex, while the borders of the dark region are the maximum and the minimum values of the confusion measure $\mathcal{M}_{G,G'}(u)$.

[20] L. Zou, L. Chen and M. T. Öszu, K-Automorphism: a general framework for privacy preserving network publication, *Proc. of VLDB'09*, 2009.

[21] B. Zhou and J. Pei, Preserving privacy in social networks against neighborhood attacks, *Proc. of ICDE'08*, 2008, 506–515.

ARS MATHEMATICA CONTEMPORANEA

Also available at http://amc-journal.eu
ISSN 1855-3966 (printed edn.), ISSN 1855-3974 (electronic edn.)
ARS MATHEMATICA CONTEMPORANEA 7 (2014) 479–485

A manifold associated to a topological (n_k) configuration*

Jürgen Bokowski
Technische Universität Darmstadt, Germany

Ricardo Strausz
Universidad National Autónoma de México, México, D.F., México

Received 13 October 2011, accepted 17 December 2013, published online 11 July 2014

Abstract

In the study of topological (n_k) configurations in the projective plane we have n pseudo-lines and n points. Precisely k of these points are incident with each pseudo-line and, vice versa, precisely k pseudo-lines are incident with each point. We describe a non-orientable 2-manifold associated in a natural way to a topological (n_k) configuration in the projective plane. Apart from being interesting in its own right, this manifold defines an equivalence class within topological configurations. It can be used to distinguish topological (n_k) configurations.

Keywords: Point-line configuration, pseudo-line, 2-manifold.

Math. Subj. Class.: 51E20, 52C30, 05B30

1 Introduction

This article concerns point-line configurations in the sense of B. Grünbaum's research monograph, [8]. We recommend the reader to have a look at this book and we assume the reader to know pseudo-line arrangements in the projective plane as rank 3 oriented matroids, compare [1], or [2].

We define a *topological* (n_k) *configuration* in the projective plane as a pair of n pseudo-lines and n points in the projective plane such that the point-line incidence graph is k-regular.

*This paper is a part of Bled'11 Special Issue.

E-mail addresses: juergen@bokowski.de (Jürgen Bokowski), strausz@matem.unam.mx (Ricardo Strausz)

The study of these topological configurations can help to solve problems for geometric configurations, i.e., when all pseudo-lines are straight lines. When we consider pseudo-lines and points only as abstract elements, we have *a combinatorial* (n_k) *configuration*. When starting with a combinatorial configuration, we can first try to find all corresponding topological ones, a corresponding investigation was done in [9].

Whenever a class of topological (n_k) configurations is given, we provide in this paper a concept to subdivide this class into natural subclasses. We use for that an associated 2-manifold.

2 Manifold associated to a topological configuration

When two pseudo-line arrangements are given, it is in general not an easy task to tell of whether they are isomorphic. We say that the pseudo-line arrangements are isomorphic up to a relabeling of its elements when there exists a relabeling of the pseudo-lines and a topological transformation of the projective plane that maps the first set of pseudo-lines onto the possibly relabeled second set of pseudo-lines. This notion defines equality of oriented matroids (in rank 3) up to relabeling its elements.

We can also say that two given topological (n_k) configurations are isomorphic up to relabeling, when their oriented matroids are equal up to relabeling its elements and when the point-line incidences remain the same.

However, for a given combinatorial configuration there are in general many topological configurations. It is useful to subdivide them into natural classes. This is what we suggest.

We associate a 2-manifold to each topological (n_k) configuration. When the 2-manifold differs for two topological (n_k) configurations, the configurations are not isomorphic up to relabeling, When the 2-manifolds coincide, we have a natural common property of the configurations.

The n pseudo-lines of a topological (n_k) configuration form a rank 3 oriented matroid or a pseudo-line arrangement in the projective plane.

We pick for such a topological (n_k) configuration with n pseudo-lines in the projective plane an additional pseudo-line as the *pseudo-line at infinity*. This allows us to orient all given pseudo-lines of the topological (n_k) configuration. These orientations induce a cyclic order for each set of k points lying on a particular pseudo-line of the configuration. We call an oriented pair (P_i, P_{i+1}) of adjacent points in such a cyclic sequence of points $(P_1, \ldots, P_k)$ on a pseudo-line l of the configuration a *segment* $s_i(l)$.

A segment $s_i(l)$ can also be considered to be that part of the pseudo-line l that connects the corresponding defining points (P_i, P_{i+1}) and that contains no additional point of the configuration. We distinguish for such a segment $s_i(l)$, $i \in \{1, \ldots, k\}$, its two sides, the *right side* ${s_i}^+(l)$ with respect to the orientation of the pseudo-line l and the *left side* $s_i^-(l)$ with respect to its orientation. We speak of the two *signed segments* of a segment. When we follow a signed segment across the pseudo-line at infinity, the right side and the left side interchanges, i.e., $s_k^+(l) = (P_k, P_1)^+$ and $s_1^-(l) = (P_1, P_2)^-$ form a connected path. We say that $s_i^+(l)$ points to the right of the oriented pseudo line l between P_1 and P_k and up to

the pseudo-line at infinity. In the remaining part of l $s_k^+(l)$ points to the left.

When we go around a point p of the configuration, we have $2 \cdot k$ adjacent pairs of signed segments. The signed segments of such a pair both point to the same adjacent region, and they both are joined via the *midpoint* p. We call these $2 \cdot k$ pairs of signed segments *angles* at p. We glue angles with the same signed segment along their equal signed segments. When we do this repeatedly, we obtain a polygon of signed segments: *a closed path*.

Definition 2.1. *Configuration manifold* of a topological (n_k) configuration. We define a manifold given by a topological (n_k) configuration by taking as its 2-cells all closed paths that we obtain from the above construction. The manifold property is clear. Each 2-cell has at least three edges (signed segments) and each signed edge is incident with precisely one additional signed edge.

In Figure 1 we see as an example, a geometric (12_3) configuration. All pairs of segments between adjacent points of the configuration are drawn. When we follow the sequences of connected line segments, we can count the path lengths of them.

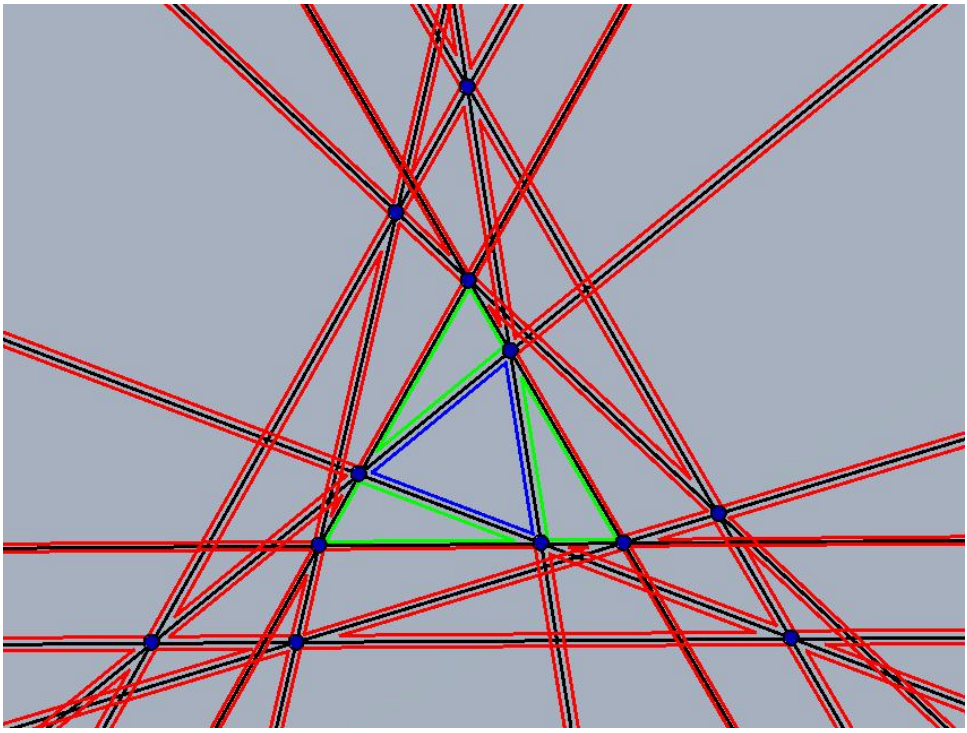

Figure 1: Configuration manifold of a (12_3) configuration

3 Mutation class of a topological configuration

For a combinatorial configuration we often have many topological realizations. Already in the (17_4) case, the unique combinatorial configuration that admits a topological configuration, compare [8], Figure 3.2.2, or [3], Proposition 3, has not a unique topological realization. We have several topological solutions that can be changed via mutations of the pseudo-line arrangement without changing the combinatorial configuration. A mutation is sometimes also referred to as a Reidemeister move. We have depicted this example in Figure 2. On the line at infinity there are two points, not points of the configuration, at which precisely three pseudo-lines meet. We can change the topological configuration locally such that one pseudo-line of these three pseudo-lines is not incident with the meet of the other two. Locally meens that we have no other pseudo-line intersecting the triangle formed by the three pseudo-lines. We can get two different oriented triangles bounded by the corresponding 3 pseudo-lines at those points without changing the combinatorial configuration. A change of the orientation of such a triangle is called a mutation.

The oriented matroid does change this way, however, these changes are not considered to change a lot the topological configuration.

We define a graph in which the points are pseudo-line arrangements with a given number of elements and edges occur between pairs of pseudo-line arrangments when they differ just by one orientation of such a triangle of three pseudo-lines and when there is no pseudo-line intersecting this triangle. This graph is known as the mutation graph for uniform oriented matroids.

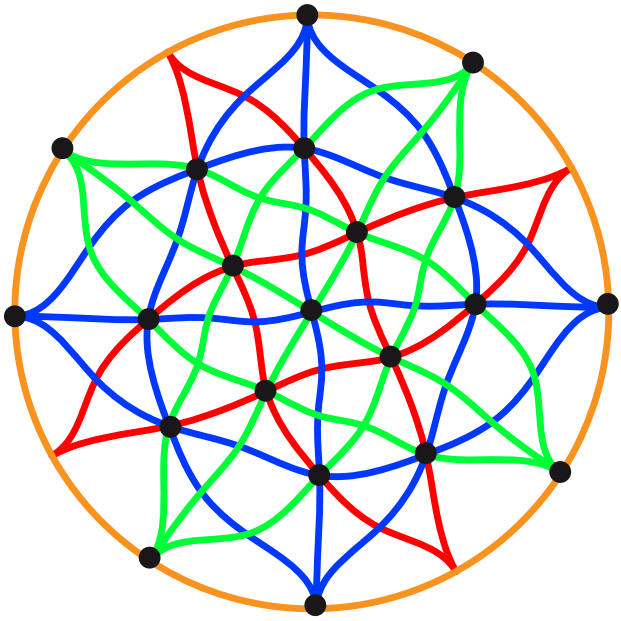

Figure 2: Topological (17_4) configuration

Definition 3.1. *Mutation class* of a topological configuration. We call such a mutation of the topological configuration that keep the combinatorial configuration invariant an *ad-*

missible mutation, and we speak about the connected component of the mutation graph of topological realizations generated via admissible mutations and call it the *mutation class* of a topological configuration.

4 Cycle length vector of the associated manifold

Definition 4.1. *Cycle length vector.* We calculate all cycle lengths of a configuration manifold, we sort these lengths in increasing order to obtain what we call the *cycle length vector* of the configuration.

From the definition it is clear that the cycle length vector does not change when we relabel the pseudo-lines, it is invariant under relabeling the configuration.

For example, the three (geometric) (9_3) configurations $(9_3)_1$, $(9_3)_2$, and $(9_3)_3$, compare [8], Figure 2.2.1, have different cycle length vectors $(6, 6, 14, 14, 14)$, $(3, 3, 3, 3, 3, 3, 3, 3, 33)$, and $(3, 3, 3, 14, 14, 14)$, respectively. When we have another geometric version of one of these drawings, we can tell via the cycle length vector which version we have. We have depicted the second case in Figure 3. The cycles of length 3 are easily seen. The reader can verify that there is only one additional final cycle of length 33.

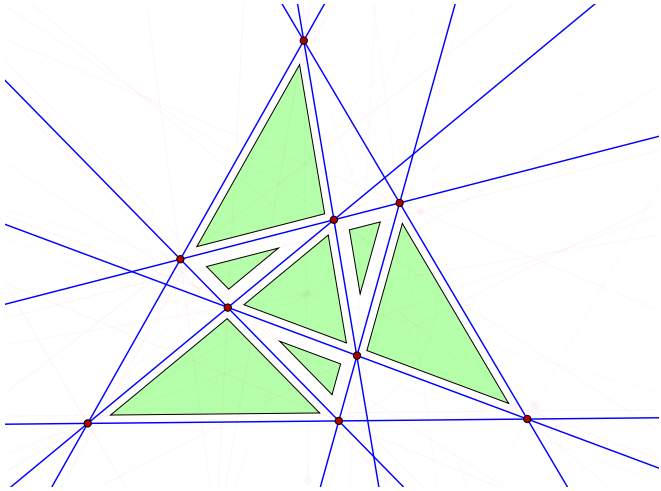

Figure 3: Geometric $(9_3)_2$ configuration

The cycle length vector provides us with a short invariant of a topological configuration. It has turned out that it can e.g. distinguish all different 17 mutation classes of (18_4) configurations. We present all these 17 cycle length vectors in Table 1, listed in the order in which the examples were presented in [7]. The last vector in Table 1 is the cycle length vector of the additional topological configuration that was found recently when all mutation classes of topological (18_4) configurations were generated, see [4]. In Figure 4 you see the new topological example, on the right, together with the former known combinatorially isomorphic Case 5.

[3,3,8,8,8,8,8,13,13,13,13,13,33], [3,3,3,3,3,3,8,8,8,18,28,28,28], [3,3,8,18,18,45,49], [3,3,3,3,44,44,44], [3,3,8,8,10,13,13,13,13,29,31], [5,5,8,8,8,8,8,8,8,8,8,31,31], [3,3,3,8,28,45,54], [3,3,12,13,13,13,13,13,13,48], [8,13,13,13,13,13,18,19,34], [8,13,13,13,13,13,13,18,40], [3,3,12,13,13,13,13,34,40], [3,8,13,13,13,13,18,29,34], [3,5,8,8,8,8,8,13,13,13,57], [3,3,8,8,8,8,13,13,18,29,33], [3,8,8,8,13,13,13,13,13,13,13,13,13], [3,3,3,3,3,3,18,18,18,18,18,18,18], [3,3,3,13,24,98].

Table 1: All possible cycle length vectors for topological (18_4) configurations.

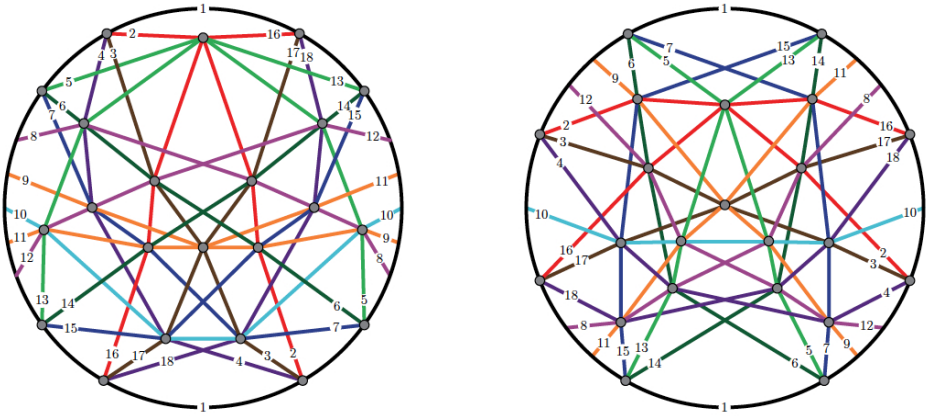

Figure 4: Two topological (18_4) configurations with an isomorphic combinatorial configuration

5 Properties of the configuration manifold

Before we write the next theorem with properties of configuration manifolds, we wish to mention [6], i.e., another paper with a link between pseudo-line arrangements and topological graph theory.

Theorem 5.1. *Properties of configuration manifolds.*

1. *Configuration manifolds are non-orientable 2-manifolds.*
2. *The configuration manifold of a topological configuration determines its combinatorial configuration.*
3. *The configuration manifold of a topological configuration is an invariant of its mutation class.*

Proof. Ad 1: Since we work in the non-orientable projective plane, we can go along the Möbius strip of any closed pseudo-line of the arrangement. This Möbius strip is a part of the configuration manifold. So the configuration manifold is non-orientable.

Ad 2: In the definition of the configuration manifold we have the information of all circular sequences of points along each pseudo-line. We only have to follow all straight ahead paths along the edges. This is the information of the combinatorial configuration.

Ad 3: The definition of a mutation class tells us that the configuration manifold does not change when an admissible mutation changes the topological configuration. The construction of the manifold simply ignores those intersections of pseudo-lines that do not occur at points of the configuration. □

Remarks: 1. A combinatorial configuration which admits topological configurations can have different configuration manifolds. This property was already shown via Figure 4.

2. The cycle length vector can be used to distinguish all 17 connected admissible mutation graph components in the (18_4) case. The list of cycle length vectors in Table 1 together with the result of the generation algorithm of topological configurations, presented in [4], provides us with this property.

Our cycle length vector of a configuration manifold has already been tested as an invariant in the classification of [5] that was based on [4] . An algorithm was used for generating all topological (n_k) configurations in the projective plane for given n and given k without determining first all corresponding abstract (n_k) configurations.

The (18_4) case (JAVA code of V. Pilaud with one hour CPU-time) had mainly the character of confirming the satisfiability result of Lars Schewe, [9], however, the case of Figure 4 appeared as a surprising additional aspect. The behavior of the (19_4) case (JAVA code with 16 days of CPU-time) was completely different. Here we had to sort the output of nearly 70,000 mutation classes of topological (19_4) configurations, i.e., topological configurations up to mutation equivalence. For this investigation additional techniques are useful and the presented invariant here was only one intermediate step within this investigation. A detailed report about this (19_4) case can be found in [5].

References

[1] A. Björner, M. Las Vergnas, B. Sturmfels, N. White and G. Ziegler, Oriented Matroids, *Encyclopedia of Mathematics and its Applications*, vol. 46, Cambridge University Press, Cambridge, 1999.

[2] J. Bokowski, *Computational Oriented Matroids*, Cambridge University Press, Cambridge, 2006.

[3] J. Bokowski, B. Grünbaum and Lars Schewe, Topological configurations (n_4) exist for all $n \geq 17$, *Eur. J. Comb.* **30** (2009), 1778–1785.

[4] J. Bokowski and V. Pilaud, Enumerating topological (n_k)-configurations, *Computational Geometry: Theory and Applications* **47** (2014), 175–186, special issue for the 23rd Canadian Conference on Computational Geometry, available via arXiv.

[5] J. Bokowski and V. Pilaud, On topological and geometric (19_4)-configurations, 13p., 2013 submitted, available via arXiv.

[6] J. Bokowski and T. Pisanski, Oriented matroids and complete graph embeddings, *Journal of Combinatorial Theory Series A* **114** (2007), 1–19.

[7] J. Bokowski and L. Schewe, On the finite set of missing geometric configurations (n_4), *Computational Geometry: Theory and Applications* **46** (2013), 532–540.

[8] B. Grünbaum, *Configurations of Points and Lines*, Graduate Studies in Mathematics, vol. 103, American Mathematical Society, Providence, RI, 2009.

[9] Lars Schewe, *Satisfiability Problems in Discrete Geometry*, PhD thesis, Shaker, Technische Universität Darmstadt, 2007.

ARS MATHEMATICA CONTEMPORANEA

Also available at http://amc-journal.eu
ISSN 1855-3966 (printed edn.), ISSN 1855-3974 (electronic edn.)
ARS MATHEMATICA CONTEMPORANEA 7 (2014) 487–497

Fast recognition of direct and strong products*

Richard H. Hammack
Department of Mathematics and Applied Mathematics,
Virginia Commonwealth University,
Richmond, Virginia, USA

Wilfried Imrich
Department Mathematics and Information Technology,
Montanuniversität Leoben,
A-8700 Leoben, Austria

Received 9 April 2012, accepted 17 May 2014, published online 24 September 2014

Abstract

This note describes fast algorithms for computing the prime factors of connected, nonbipartite graphs with respect to the direct product, and of connected graphs with respect to the strong product. The complexities are $O(m \min(n^2, \Delta^3))$ for the direct product, and $O(m\, a(G)\Delta)$ for the strong, where n is the order of the graph G to be factored, m its size, $a(G)$ its arboricity, and Δ its maximum degree. That is, the complexities are linear in m for fixed Δ.

Keywords: Graph products, algorithms.

Math. Subj. Class.: 05C85, 05C75, 05C12

1 Introduction

The Cartesian, direct, and strong products of graphs are the only nontrivial, associative products defined on the Cartesian products of the vertex sets having the property that the projections onto the factors are weak homomorphisms [4]. These products enjoy many interesting algebraic properties, such as unique prime factorization. Connected graphs have unique prime factor decompositions with respect to the Cartesian and the strong product in the class Γ of simple graphs [9, 10, 1, 7], and connected nonbipartite graphs have unique prime factor decompositions with respect to the direct product in the class Γ_0 of graphs where loops but not multiple edges are allowed [7].

*This paper is a part of Bled'11 Special Issue.

E-mail addresses: rhammack@vcu.edu (Richard H. Hammack), imrich@unileoben.ac.at (Wilfried Imrich)

In the case of the Cartesian product the prime factors can be computed in linear time, that is, in $O(m)$ time, where m is the size of the graph; see [6].

For the other two products the situation is different. For the strong product the paper [2] by Feigenbaum and Schäffer was the first that presented a polynomial algorithm for the unique factorization of connected graphs. This was then extended to the factorization of nonbipartite connected graphs with respect to the direct product by Imrich [5]. In both papers the main aim was to show that the factorization was possible in polynomial time, hence neither of [2, 5] contains an estimate of the complexity of the algorithm presented there. A rough estimate shows that it is $O(n^{4.5})$ in [2] and $O(n^5)$ in [5], where n is the order of the graph.

Both algorithms depend on the factorization of auxiliary graphs with respect to the Cartesian product. The auxiliary graphs are called *Cartesian skeletons* and are defined algorithmically in [2, 5]. The algorithmic definition makes it difficult to work with them.

Later, non-algorithmic definitions were given [3], along with efficient algorithms that compute them. However, it was not known whether it was possible to find the prime factors with respect to the direct and the strong products within the same time complexities needed for computing the skeletons.

The present paper shows that this is indeed the case. We prove that connected, nonbipartite graphs can be factored over the direct product in $O(m \min(n^2, \Delta^3))$ time, and that the prime factors of connected graphs with respect to the strong product can be found in $O(m\, a(G)\Delta)$ time, where n is the order, m the size, Δ the maximum degree, and $a(G)$ the arboricity of the graph G that is to be factored. (The *arboricity* $a(G)$ of a graph G is the minimum number of forests into which $E(G)$ can be partitioned. It is easily seen that $a(G) \leq \Delta$.)

Although both algorithms that are presented here have complexities close to $O(n^4)$ in the worst case, which just slightly better than that of the algorithms of Feigenbaum and Schäffer [2] (for the strong product) and of Imrich [5] (for the direct product), their main advantage is that their complexities for graphs with known bounds on the maximum degree or the arboricity (in the case of the strong product) and can be explicitly stated.

In particular, we wish to point out that, for fixed Δ and growing m, we have $m \leq n\Delta$, hence n also grows, and Δ^3 must eventually become smaller than n^2. Also note that $a(G)\Delta \leq \Delta^2$. Hence the complexities grow linearly in m for fixed Δ. Algorithms with such complexities are called *quasilinear*.

On the way, in Section 2.1, we also prove new bounds on the number of prime factors of a graph with respect to the strong and the direct product.

2 Definitions

We consider finite graphs G which may have loops but not multiple edges, and denote the class of these graphs by Γ_0, while $\Gamma \subset \Gamma_0$ is the class of graphs without loops. An edge joining g to g' is denoted gg'. The open neighborhood of a vertex g is denoted $N(g)$, or $N_G(g)$ when it is necessary to indicate the graph under discussion. The closed neighborhood of g is $N[g] = N(g) \cup \{g\}$. Again, we often write this as $N_G[g]$.

Given graphs H and K, the Cartesian product $H \,\square\, K$, the direct product $H \times K$ and the strong product $H \boxtimes K$, are defined on the Cartesian product $V(H) \times V(K)$ of the

vertex sets of the factors and have the following edge sets:

$$\begin{aligned} E(H \,\square\, K) &= \{(h,k)(h',k') \mid hh' \in E(H), k = k', \text{ or } h = h', kk' \in E(K)\}, \\ E(H \times K) &= \{(h,k)(h',k') \mid hh' \in E(H) \text{ and } kk' \in E(K)\}, \\ E(H \boxtimes K) &= E(H \,\square\, K) \cup E(H \times K). \end{aligned}$$

(Examples are shown in Figure 1.) All three products are commutative and associative. Also, the complete graph K_1 on one vertex is a unit for $\square$ and $\boxtimes$, as $K_1 \,\square\, H \cong H$ and $K_1 \boxtimes H \cong H$ for all graphs H. The graph K_1^* consisting of a single vertex with a loop satisfies $K_1^* \times H \cong H$, and is the unit for $\times$.

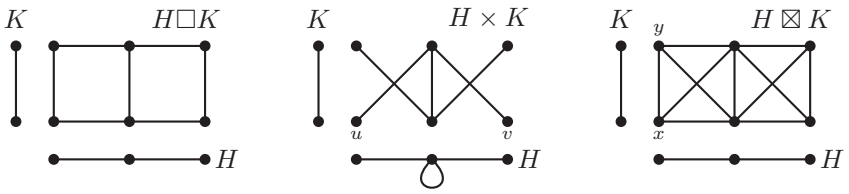

Figure 1: The three standard graph products

Let $a = (a_1, a_2, \ldots, a_k)$ be a vertex of a product $G = G_1 * G_2 * \cdots * G_k$, where $*$ designates any of the symbols $\square$, $\times$, or $\boxtimes$. Then the *G_i-layer* G_i^a of G_i through a is defined as the subgraph of G induced by the set of vertices

$$\{(a_1, a_2, \ldots, a_{i-1}, x_i, a_{i+1} \ldots, a_k) \mid x_i \in V(G_i)\}.$$

For the Cartesian and the strong product, the G_i-layers are isomorphic to G_i. For the direct product, $G_i^a \cong G_i$ if all a_j have a loop in G_j for $j \neq i$. Otherwise G_i^a has no edges.

We call the mapping $a \mapsto a_i$ a *projection*. For a subgraph H of G, it restricts to a mapping $p_i : H \to G_i$. For the direct product this is a homomorphism; for the other two products it is a weak homomorphism[1].

If $X \subseteq V(G)$, the subgraph of G induced on X is denoted $\langle X \rangle$, or $\langle X \rangle_G$ if there is a risk of ambiguity. As a consequence of the definitions, if $X_i \subseteq V(G_i)$ for $1 \leq i \leq k$, then

$$\langle X_1 \times X_2 \times \cdots \times X_k \rangle_{G_1 \,\square\, G_2 \,\square \cdots \square\, G_k} = \langle X_1 \rangle_{G_1} \,\square\, \langle X_2 \rangle_{G_2} \,\square \cdots \square\, \langle X_k \rangle_{G_k}, \quad (2.1)$$

where the $\times$ indicates the Cartesian product of sets.

A nontrivial graph is called *prime* with respect to a particular product if whenever it is represented as a product of two factors, one of the factors is the unit for the product. As already mentioned, connected graphs have unique prime factor decompositions with respect to the Cartesian and the strong product in Γ, and connected nonbipartite graphs have unique prime factor decompositions with respect to the direct product in Γ_0.

There are two significant equivalence relations R and S on the vertex set of a graph. To motivate this, note that Cartesian products possess a certain degree of rigidity; any automorphism of $H \,\square\, K$ is induced by automorphisms of H and K (or their transposition

[1]Recall that a homomorphims is an edge-preserving map, whereas a weak homomorphims either preserve edges or maps them into single vertices.

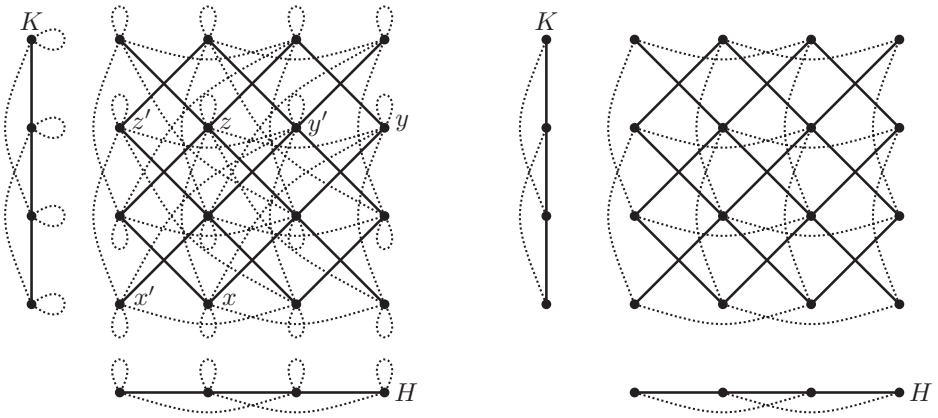

Figure 2: Left: Graphs $H, K, H \times K$ (solid) and H^s, K^s, $(H \times K)^s$ (dotted). Right: Graphs $H, K, H \times K$ (solid) and Cartesian skeletons $S(H), S(K), S(H \times K)$ (dotted).

if they are isomorphic). This is not so with the direct and strong products. For example, in Figure 1 the vertices u and v of $H \times K$ can be transposed. The same is true for x and y in $H \boxtimes K$. It is easy to see the reason for this. In the case of the direct product, the interchange is possible because $N(u) = N(v)$; it is possible for the strong product because $N[x] = N[y]$. We declare that two vertices x, y are in *relation R* if $N(x) = N(y)$, and they are in *relation S* if $N[x] = N[y]$. Notice that both R and S are equivalence relations.

We say a graph is *R-thin* if every R-equivalence class consists of a single vertex; it is *S-thin* if every S-equivalence class has a single vertex. In discussions of prime factoring over the direct product, it is helpful (at least initially) to assume that all graphs are R-thin. For the strong product, we assume S-thinness.

Another important concept is the Boolean square. The *Boolean square* G^s of a graph G has vertex set $V(G^s) = V(G)$ and edges $E(G^s) = \{xy \mid N_G(x) \cap N_G(y) \neq \emptyset\}$. The left side of Figure 2 shows graphs H, K and $H \times K$ (bold) and their Boolean squares (dotted). It is easy to confirm that

$$(G_1 \times G_2)^s = G_1^s \times G_2^s,$$

and this is indeed reflected in the figure. Furthermore, letting $\mathcal{N}G$ denote the graph G after removal of all loops, we have

$$\mathcal{N}((G_1 \times G_2)^s) = \mathcal{N}G_1^s \boxtimes \mathcal{N}G_2^s. \tag{2.2}$$

The most important concept in this paper is a certain subgraph of G^s called the Cartesian skeleton. It is obtained from G^s by removal of the so-called dispensable edges.

We call an edge xy of G^s *dispensable* if $x = y$ or if there exists some $z \in V(G)$ for which both of the following statements hold.

1. $N_G(x) \cap N_G(y) \subset N_G(x) \cap N_G(z)$ or $N_G(x) \subset N_G(z) \subset N_G(y)$,
2. $N_G(y) \cap N_G(x) \subset N_G(y) \cap N_G(z)$ or $N_G(y) \subset N_G(z) \subset N_G(x)$.

In Figure 2 (left) the edge xy is dispensable because $N_G(x) \cap N_G(y) \subset N_G(x) \cap N_G(z)$ and $N_G(y) \cap N_G(x) \subset N_G(y) \cap N_G(z)$. Also, $x'y'$ is dispensable, as $N_G(x') \subset N_G(z') \subset N_G(y')$ and $N_G(y') \cap N_G(x') \subset N_G(y') \cap N_G(z')$.

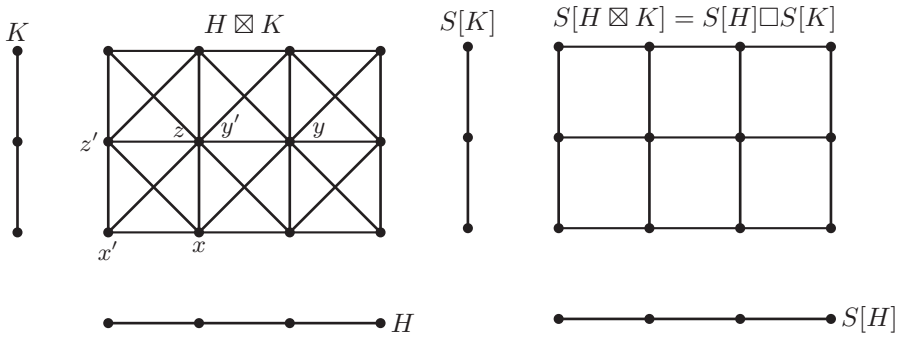

Figure 3: Left: Graphs $H, K, H \boxtimes K$; Right: Closed Cartesian skeletons $S[H], S[K]$, $S[H \boxtimes K]$.

The *Cartesian skeleton* of a graph G is the graph $S(G)$ obtained from G^s by removing all dispensable edges. For example, the dotted lines in Figure 2 (right) are the Cartesian skeletons of H, K and $H \times K$. This figure illuminates a general principle that was proved in [3]: If the product $H \times K$ is R-thin and has no isolated vertices, then

$$S(H \times K) = S(H) \,\square\, S(K). \tag{2.3}$$

For the strong product a similar construction, the *closed Cartesian skeleton* $S[G]$, is useful. It is a subgraph of G obtained by removing all dispensable edges of G, where an edge xy of G is dispensable if for some $z \in V(G)$ both of the following conditions hold:

1 (strong). $N_G[x] \cap N_G[y] \subset N_G[x] \cap N_G[z]$ or $N_G[x] \subset N_G[z] \subset N_G[y]$,
2 (strong). $N_G[y] \cap N_G[x] \subset N_G[y] \cap N_G[z]$ or $N_G[y] \subset N_G[z] \subset N_G[x]$.

Figure 3 shows graphs H, K and $H \boxtimes K$ on the left and their closed Cartesian skeletons $S[H], S[K]$ and $S[H \boxtimes K]$ on the right. Notice the edge xy (for example) is dispensable, because $N_G[x] \cap N_G[y] \subset N_G[x] \cap N_G[z]$ and $N_G[y] \cap N_G[x] \subset N_G[y] \cap N_G[z]$. Also, $x'y'$ is dispensable, as $N_G[x'] \subset N_G[z'] \subset N_G[y']$ and $N_G[y'] \cap N_G[x'] \subset N_G[y'] \cap N_G[z']$.

If $H \boxtimes K$ is S-thin, then, similarly to Equation (2.3), we have

$$S[H \boxtimes K] = S[H] \,\square\, S[K], \tag{2.4}$$

as noted in reference [3], in which it is also shown that the Cartesian skeletons of connected nonbipartite graphs are connected. Moreover, the condition of nonbipartiteness can be dropped in the case of the closed Cartesian skeleton: $S[G]$ is connected if G is.

Note that Equations (2.3) and (2.4) express equality of graphs, not just isomorphism. That is, e.g., graphs $S(H \times K)$ and $S(H) \,\square\, S(K)$ have identical vertex sets and edge sets.

The article [3] also presents algorithms and complexity analysis for computing $S(G)$ and $S[G]$. The skeleton $S(G)$ can be computed in $\min\{O(mn^2), O(m\Delta^3)\}$ time. Its space complexity is determined by the size of the output and is thus between $O(n)$ and $O(n^2)$.

On the other hand, the closed Cartesian skeleton $S[G]$ can be computed in $O(m\, a(G)\Delta)$ time, where $a(G)$ is the *arboricity* of G, that is, the minimum number of forests into which

the $E(G)$ can be partitioned. One can show that $\delta/2 < a(G) \leq \Delta$, where δ is the minimum degree of G.[2]

2.1 Bounds on the number of factors

We will need bounds on the number of prime factors of graphs relative to different products.

A simple computation shows that a product of k nontrivial graphs has at least 2^k vertices. In other words, a graph on n vertices can have at most $\log_2 n$ factors with respect to any product. However, note that the strong product of k copies of K_2 is K_{2^k}, and that every vertex has degree $2^k - 1$. Thus any vertex of a strong product of k nontrivial connected factors has degree at least $2^k - 1$.

For the Cartesian product it is well known that a connected graph has at most δ factors.

Lemma 2.1. *Suppose a graph G has n vertices and minimum degree δ. Then:*

1. *G has at most $\log_2 n$ factors with respect to the Cartesian, direct, or strong product.*
2. *If G is connected, it has at most δ factors with respect to the Cartesian product.*
3. *If G is connected, it has at most $\log_2(\delta+1)$ factors with respect to the strong product.*

Proof. We have already addressed the first two statements. If G is connected, then so are all of its strong product factors. If G has k factors, then $\delta \geq 2^k - 1$, so $\log_2(\delta+1) \geq k$. □

For the direct product we have the following corollary.

Corollary 2.2. *A connected, nonbipartite graph has at most $\log_2(\delta\Delta + 1)$ factors with respect to the direct product.*

Proof. Let $G = G_1 \times G_2 \times \cdots \times G_k$. Then $G^s = G_1^s \times G_2^s \times \cdots \times G_k^s$, so any bound on the number of factors of G^s also bounds the number of factors of G. Equation (2.2) implies

$$\mathcal{N}G^s = \mathcal{N}G_1^s \boxtimes \mathcal{N}G_2^s \boxtimes \cdots \boxtimes \mathcal{N}G_k^s\,.$$

Hence k is also bounded by the number of factors of $\mathcal{N}G^s$ over the strong product. As $\log_2(\delta_{\mathcal{N}G^s} + 1) \geq k$, the assertion will follow as soon as we establish $\delta_G\Delta_G \geq \delta_{\mathcal{N}G^s}$.

Indeed, for any vertex x of $\mathcal{N}G^s$ the definition of G^s yields $\deg_G(x)\Delta_G \geq \deg_{\mathcal{N}G^s}(x)$. If x has minimum degree in G, this is $\delta_G\Delta_G \geq \deg_{\mathcal{N}G^s}(x)$; thus $\delta_G\Delta_G \geq \delta_{\mathcal{N}G^s}$. □

3 Thin graphs and the direct product

Suppose we want to compute the prime factorization $G = G_1 \times G_2 \times \cdots \times G_k$ of an R-thin, connected, nonbipartite graph G. The compatibility of the Cartesian skeleton with the direct product as expressed in Equation (2.3) implies

$$S(G) = S(G_1) \,\square\, S(G_2) \,\square\, \cdots \,\square\, S(G_k). \tag{3.1}$$

Because $S(G)$ is connected, there is a Cartesian prime factorization

$$S(G) = \mathop{\square}_{i\in I} H_i \tag{3.2}$$

[2]These relations are not hard to show. The right side is routine. For the left side one invokes a theorem of Nash-Williams [8], see [4, Exercise 20.2] and the hint thereto.

that is unique up to the order and isomorphisms of the factors. By [4, p. 296], this equals the presentation in (3.1) or a refinement of it. Thus the number of Cartesian factors of $S(G)$ can be larger than the number of direct factors of G. Since we can compute $S(G)$ and its prime factorization over $\Box$, our task is to find a partition $J_1, J_2, \ldots, J_k$ of I such that

$$S(G_i) = \bigsquare_{j \in J_i} H_j$$

for all $i, 1 \le i \le k$.

Section 24.3 of [4] shows that each J_i is a minimal subset of I for which the H_{J_i}-layers of $H_{J_i} \,\Box\, H_{I\setminus J_i}$ (where $H_{J_i} = \bigsquare_{j\in J_i} H_j$ and $H_{I\setminus J_i} = \bigsquare_{j\in I\setminus J_i} H_j$) correspond to the layers of a factor of G with respect to the direct product. In other words, each J_i is a minimal subset of I for which $G = p_{J_i}(G) \times p_{I\setminus J_i}(G)$, where p_{J_i} is the projection of $V(G) = V(S(G))$ onto $V(H_{J_i})$, and $p_{J_i}(G)$ is the smallest graph for which this projection is a homomorphism. (The graph $p_{I\setminus J_i}(G)$ is defined similarly.)

It is also shown there that the complexity of checking whether a subset $J \subseteq I$ induces a factoring $G = p_J(G) \times p_{I\setminus J}(G)$ is $O(m\,|I|)$. As I has $2^{|I|}$ subsets, the complexity of checking them all is $O\big(m\,2^{|I|}|I|\big)$.

Now, the Cartesian skeleton $S(G)$ has the same number of vertices as G. By Lemma 2.1, we infer that $|I| \le \log_2 n$. Hence the prime factors of G with respect to the direct product can be computed from the Cartesian skeleton in $O(m2^{\log_2 n}\log_2 n) = O(mn\log n)$ time.

Recall that the Cartesian skeleton can be computed in $\min\{O(mn^2), O(m\Delta^3)\}$ time. Clearly $O(mn\log n) \le O(mn^2)$, so if $n\log_2 n \le \Delta^3$, then the prime factorization of G over the direct product (from $S(G)$) does not cost more than the computation of $S(G)$. But, if $\Delta^3 < n\log_2 n$, then the computation of the Cartesian skeleton is cheaper than the computation of the prime factorization as presented above.

If we could somehow reduce the number of subsets of I that must be investigated, then we might be able to retain the time complexity $O(m\Delta^3)$ for the prime factorization of G even when $\Delta^3 < n\log_2 n$. This is indeed possible.

But before stating it in the next proposition, we first recall an elemental fact about vertex neighborhoods in direct products, namely if $G = G_1 \times G_2 \times \cdots \times G_k$, then

$$N_G((a_1, a_2, \ldots, a_k)) = N_{G_1}(a_1) \times N_{G_2}(a_2) \times \cdots \times N_{G_k}(a_k), \tag{3.3}$$

where $\times$ is the Cartesian product of sets. Taking induced subgraphs, this becomes

$$\langle N_G((a_1, a_2, \ldots, a_k))\rangle_G = \langle N_{G_1}(a_1)\rangle_{G_1} \times \langle N_{G_2}(a_2)\rangle_{G_2} \times \cdots \times \langle N_{G_k}(a_k)\rangle_{G_k}, \tag{3.4}$$

where $\times$ is the direct product of graphs. A subgraph of a product that is a product of subgraphs of the factors is called a *box* relative to the product. The above equation implies that the subgraph induced on any open neighborhood of a graph is a box relative to any direct product factorization of the graph.

Proposition 3.1. *If G is a connected, nonbipartite R-thin graph of order n and size m, then its direct product prime factorization can be found in $\min\{O(mn^2), O(m\Delta^3)\}$ time.*

Proof. By the above arguments it suffices to treat the case $\Delta^3 < n^2$; see also [4, p. 296].

Let us have a closer look at the Cartesian skeleton of a graph G with prime factorization $G_1 \times G_2 \times \cdots \times G_k$. By our previous discussion we have:

$$\begin{aligned} G &= G_1 \times G_2 \times \cdots \times G_k, && (3.5)\\ S(G) &= S(G_1) \,\square\, S(G_2) \,\square\, \cdots \,\square\, S(G_k), && (3.6)\\ G^s &= G_1^s \times G_2^s \times \cdots \times G_k^s. && (3.7) \end{aligned}$$

Furthermore, given $a \in V(G)$, the layers G_i^a, $S(G_i)^a$ and $(G_i^s)^a$ have the same vertex sets. Moreover, the layers $(G_i^s)^a$ are all isomorphic to G_i^s. Given $v \in V(G^s)$, Equation (3.4) applied to (3.7) gives

$$\langle N_{G^s}(v)\rangle_{G^s} = \bigtimes_{i=1}^{k} \langle N_{G_i^s}(v_i)\rangle_{G_i^s}. \tag{3.8}$$

Notice that all $\langle N_{G_i^s}(v_i)\rangle_{G_i^s}$ are connected, but that they need not be prime (with respect to the direct product), and that the G_i^s may not be R-thin.

Equation (3.3) applied to (3.7) gives $N_{G^s}(v) = N_{G_1^s}(v_1) \times N_{G_2^s}(v_2) \times \cdots \times N_{G_k^s}(v_k)$. Consider the subgraph of $S(G) = S(G_1) \,\square\, S(G_2) \,\square\, \cdots \,\square\, S(G_k)$ induced on this vertex set. Using Equation (2.1), we get

$$\langle N_{G^s}(v)\rangle_{S(G)} = \bigsquare_{i=1}^{k} \langle N_{G_i^s}(v_i)\rangle_{S(G_i)}. \tag{3.9}$$

Call this box $S(G)(v)$.

Comparing Equations (3.9) and (3.6), we see that $S(G)(v)$ contains all edges of $S(G_i)^v$ that are incident with v for any i. Thus, the connected component of $S(G)(v)$ through v contains edges from all $S(G_i)$. Clearly it is a box, and we denote it by B. By Equation (3.9) we have

$$\begin{array}{ccccccccc} S(G) & = & S(G_1) & \square & S(G_2) & \square & \cdots & \square & S(G_k) \\ \cup\!| & & \cup\!| & & \cup\!| & & & & \cup\!| \\ B & = & B_1 & \square & B_2 & \square & \cdots & \square & B_k\,. \end{array} \tag{3.10}$$

Observe that the number of vertices of $S(G)(v)$ is the same as the number of vertices of $N_{G^s}(v)$, which is at most Δ^2, a bound for the maximum degree of G^s. But then the number of Cartesian factors of $S(G)(v)$ is at most $2\log_2 \Delta$, and this also bounds the number of Cartesian factors of B. Thus the factoring of B in Equation (3.10) has a refinement $B = B_1' \,\square\, B_2' \,\square\, \cdots \,\square\, B_\ell'$, where $\ell \le 2\log_2 \Delta$, and each B_s' is a prime factor of some B_i. (Recall that – as mentioned in the introduction – computing the prime factorization of $S(G)$ is linear in m, and hence this is also the case for B.)

From (3.10), we see that each Cartesian prime factor B_s' of B is a prime factor of some B_i, and hence i is the only index $1 \le i \le k$ for which $S(G_i)$ has prime factors H_j with $E({B_s'}^v) \cap E(H_j^v) \neq \varnothing$. Form a new partition $J_1', J_2', \ldots, J_\ell'$ of I, where J_s' consists of indices $j \in I$ for which $E({B_s'}^v) \cap E(H_j^v) \neq \varnothing$. This new partition need not be unique, for an $E(H_j^v)$ may meet layers of several prime factors of B. To be definite, we define the J_s' inductively by first declaring $J_s' = \{j \in I \mid E({B_1'}^v) \cap E(H_j^v) \neq \emptyset\}$ and thereafter $J_s' = \{j \in I - \bigcup_{\lambda=1}^{s-1} J'_\lambda \mid E({B_s'}^v) \cap E(H_j^v) \neq \emptyset\}$.

Letting the ℓ graphs

$$H_s' = \bigsquare_{j \in J_s'} H_j$$

play the role of the H_i we thus see that we can find the prime factors of G from $S(G)$ in

$$O(m2^{2\log\Delta}2\log\Delta) = O(m\Delta^2\log\Delta) = O(m\Delta^3)$$

time, which is the same time complexity as that for computing $S(G)$ if $\Delta^3 \leq n^2$. □

4 Thin graphs and the strong product

Let G be a connected S-thin graph. It is uniquely factorable into prime graphs with respect to the strong product, say as

$$G = G_1 \boxtimes G_2 \boxtimes \cdots \boxtimes G_k\,.$$

By [3], the strong Cartesian skeleton of G is the Cartesian product of the strong Cartesian skeletons of the G_i, in symbols,

$$S[G] = S[G_1] \,\square\, S[G_2] \,\square\, \cdots \,\square\, S[G_k]\,. \tag{4.1}$$

Similarly to the case of the direct product, there is a unique prime factorization

$$S[G] = \bigsquare_{i\in I} H_i.$$

It is equal to the the presentation in Equation (4.1) or to a refinement of it. Again our task is to find a partition $J_1, J_2, \ldots, J_k$ of I such that

$$S[G_i] = \bigsquare_{j\in J_i} H_j$$

for all $i, 1 \leq i \leq k$. As before we have to check all minimal subsets J_i of I. We have to ensure that the H_{J_i}-layers of $H_{J_i} \,\square\, H_{I\setminus J_i}$ (where $H_{J_i} = \bigsquare_{j\in J_i} H_j$ and $H_{I\setminus J_i} = \bigsquare_{j\in I\setminus J_i} H_j$) correspond to the layers of a factor of G with respect to the strong product. (Again, see Section 24.3 of [4].)

Here too the complexity of doing this is $O(m2^{\log_2|I|}\log_2|I|)$. Since the bound $\log_2 n$ for $|I|$ yields the bound $O(mn\log n)$, which will usually be larger than $O(m\,a(G)\Delta)$, we follow a similar approach as before.

Before beginning, we note that in the case of the strong product, Formulas (3.3) and (3.4) play out as follows. If $G = G_1 \boxtimes G_2 \boxtimes \cdots \boxtimes G_k$, then

$$N_G[(a_1, a_2, \ldots, a_k)] = N_{G_1}[a_1] \times N_{G_2}[a_2] \times \cdots \times N_{G_k}[a_k], \tag{4.2}$$

where $\times$ is the Cartesian product of sets.

Proposition 4.1. *Let G be a connected S-thin graph of order n and size m. Then its prime factors with respect to the strong product can be computed in $O(m\,a(G)\Delta)$ time.*

Proof. The proof parallels that of Proposition 3.1. Choose a vertex v of minimal degree in G and consider its closed neighborhood

$$N_G[v] = N_{G_1}[v_1] \times N_{G_2}[v_2] \times \cdots \times N_{G_k}[v_k].$$

By Equation (2.1), the subgraph of $S[G] = S[G_1] \,\square\, S[G_2] \,\square\, \cdots \,\square\, S[G_k]$ induced on this vertex set is the box

$$\langle N_G[v]\rangle_{S[G]} = \langle N_{G_1}[v_1]\rangle_{S[G_1]} \,\square\, \langle N_{G_2}[v_2]\rangle_{S[G_2]} \,\square\, \cdots \,\square\, \langle N_{G_k}[v_k]\rangle_{S[G_k]}.$$

As before, let B be the component of this box containing v. Then B is a box with no more than $\delta + 1$ vertices, and it factors as

$$\begin{array}{ccccccccc} S[G] & = & S[G_1] & \square & S[G_2] & \square & \cdots & \square & S[G_k] \\ \cup\!| & & \cup\!| & & \cup\!| & & & & \cup\!| \\ B & = & B_1 & \square & B_2 & \square & \cdots & \square & B_k\,. \end{array} \tag{4.3}$$

This factoring of B has a refinement $B = B'_1 \,\square\, B'_2 \,\square \cdots \square\, B'_\ell$, where $\ell \le \log_2(\delta + 1)$, and each B'_s is a prime factor of some B_i. As in the proof of Proposition 3.1, we can form a new partition $J'_1, J'_2, \ldots, J'_\ell$ of I, where J'_s consists of indices $j \in I$ for which $E(B'^v_s) \cap E(H^v_j) \neq \varnothing$. Arguing as before, we see that we can find the prime factors of G from $S[G]$ in

$$O\big(m 2^{\log \delta} \log(\delta + 1)\big) = O(m\,\delta \log \delta)$$

time. From $\delta < 2a(G)$ we infer that $O(m\,\delta \log \delta) = O(m\,a(G)\Delta)$. The observation that the prime factors of B can be computed in $O(\delta\Delta)$ time completes the proof. □

We wish to point out that we have no guarantee that $N_G[v]$ is thin, which excludes it from our present factorization methods.

5 Factoring graphs that are not thin

Up to here we have factored only thin graphs. The reason is that we made strong use of properties of the Cartesian skeleton that do not hold if the graphs are not thin. In order to factor a graph G that is not thin we first compute the quotient graphs G/R or G/S. These are formed from G by contracting all R-classes (respectively all S-classes) of G to single vertices. The resulting graphs are thin, and factored by the methods just described. (See Section 8.2 of [4, 24.4].) Notice that one can compute G/R, respectively G/S, in $O(m)$ time.

Once G/R, respectively G/S, has been factored, the question is whether this leads to factorization of G. While every factorization of G induces a factorization of G/R, respectively G/S, this is not true in the other direction. For example, consider the graph G consisting of a triangle C_3 on the vertices $v_0v_1v_2$ and two pendant edges v_0a and v_0b. It is not R-thin, because the vertices a and b have the same neighborhoods. As G has 5 vertices, it is prime. Contracting the R-class $\{a, b\}$ to a single vertex, we obtain the thin graph G/R, which is a triangle with one pendant edge. It is easily seen that this graph is the direct product of two copies of an edge with a loop. Similar examples are possible for the strong product.

Hence, we observe that G may have fewer prime factors than G/R, respectively G/S. We now use [4, 24.4] to compute them. First the direct product.

By [4, 24.4], connected, nonbipartite graphs G of size m and order n can be factored with respect to the direct product in $O(m2^k k)$ time, where k is a bound on the number of direct factors of G. With the general bound $k \le \log_2 n$ this yields the bound $O(mn^2)$ for the factorization of G.

If $\Delta^3 < n^2$ we use the bound $k \le \log_2(\delta\Delta)$ from Corollary 2.2. It yields the estimate

$$m2^k k \le m2^{\log_2(\delta\Delta)} \log_2(\delta\Delta) \le m\delta\Delta(\log_2 \delta + \log_2 \Delta) \le 2m\Delta^3\,.$$

Theorem 5.1. *The prime factors (over the direct product) of a connected, nonbipartite graph of size m, order n, and maximum degree Δ can be found in $O(m \min(n^2, \Delta^3))$ time.*

For the strong product we have the same complexity $O(m2^k k)$, but here k is the number of strong factors of G. Using the bound $\log_2(\delta+1)$ for k we thus obtain the following.

$$O(m2^k k) = O\big(m2^{\log_2(\delta+1)}\log_2(\delta+1)\big) = O\big(m(\delta+1)\delta\big) = O(m\,a(G)\Delta)\,.$$

Theorem 5.2. *The prime factors (over the strong product) of a connected graph of size m, arboricity $a(G)$, and maximum degree Δ can be computed in $O(m\,a(G)\Delta)$ time.*

Acknowledgement We thank the two reviewers for thorough and thoughtful reports.

References

[1] W. Dörfler and W. Imrich, Über das starke Produkt von endlichen Graphen, *Österreich. Akad. Wiss. Math.-Natur. Kl. S.-B. II,* **178** (1970), 247–262.

[2] J. Feigenbaum and A. A. Schäffer, Finding prime factors of strong direct product graphs in polynomial time, *Discrete Math.,* **109** (1992), 77–102.

[3] R. Hammack and W. Imrich, On Cartesian skeletons of graphs, *Ars Math. Contemp.*, **2** (2009), 191–205.

[4] R. Hammack, W. Imrich, and S. Klavžar, *Handbook of Product Graphs, Second Edition*, Series: Discrete Mathematis and its Applications, CRC Press, 2011.

[5] W. Imrich, Factoring cardinal product graphs in polynomial time, *Discrete Math.,* **192** (1998), 119–144.

[6] W. Imrich and I. Peterin, Recognizing Cartesian products in linear time. *Discrete Math.,* **307** (3-5) (2007), 472–483.

[7] R. McKenzie, Cardinal multiplication of structures with a reflexive relation, *Fund. Math.,* **70** (1971), 59–101.

[8] C. St. J. A. Nash-Williams, Decomposition of finite graphs into forests, *Journal of the London Mathematical Society* **39** (1964), 12.

[9] G. Sabidussi, Graph multiplication, *Math Z.,* **72** (1960), 446–457.

[10] V. G. Vizing, The Cartesian product of graphs (Russian), *Vyčisl. Sistemy*, **9** (1963), 30–43.

ARS MATHEMATICA CONTEMPORANEA

Also available at http://amc-journal.eu
ISSN 1855-3966 (printed edn.), ISSN 1855-3974 (electronic edn.)
ARS MATHEMATICA CONTEMPORANEA 7 (2014) 499–518

On the automorphism groups of almost all circulant graphs and digraphs*

Soumya Bhoumik
Department of Mathematics, Fort Hays State University
Hays, KS 67601, USA

Edward Dobson †
Department of Mathematics and Statisitics, Mississippi State University
Mississippi State, MS 39762 USA
and
UP IAM, University of Primorska
Muzejeski trg 2, 6000 Koper, Slovenia

Joy Morris
Department of Mathematics and Computer Science, University of Lethbridge
Lethbridge, AB T1K 3M4 Canada

Received 4 March 2012, accepted 18 June 2013, published online 6 October 2014

Abstract

We attempt to determine the structure of the automorphism group of a generic circulant graph. We first show that almost all circulant graphs have automorphism groups as small as possible. The second author has conjectured that almost all of the remaining circulant (di)graphs (those whose automorphism group is not as small as possible) are normal circulant (di)graphs. We show this conjecture is not true in general, but is true if we consider only those circulant (di)graphs whose order is in a "large" subset of integers. We note that all non-normal circulant (di)graphs can be classified into two natural classes (generalized wreath products, and deleted wreath type), and show that neither of these classes contains almost every non-normal circulant digraph.

Keywords: Circulant graph, automorphism group, Cayley graph, DRR, GRR.

Math. Subj. Class.: 05C25, 05E18

*This paper is a part of Bled'11 Special Issue.

†Project sponsored by the National Security Agency under Grant Number H98230-11-1-0179

E-mail addresses: s_bhoumik@fhsu.edu (Soumya Bhoumik), dobson@math.msstate.edu (Edward Dobson), joy.morris@uleth.ca (Joy Morris)

1 Introduction

We must begin by introducing Cayley (di)graphs and circulant (di)graphs.

Definition 1.1. Let G be a group and $S \subset G$ such that $1_G \notin S$. Define a digraph $\Gamma = \Gamma(G, S)$ by $V(\Gamma) = G$ and $E(\Gamma) = \{(u, v) : v^{-1}u \in S\}$. Such a digraph is a **Cayley digraph of G with connection set S**. A Cayley graph of G is defined analogously though we insist that $S = S^{-1} = \{s^{-1} : s \in S\}$. If $G = \mathbb{Z}_n$, then a Cayley (di)graph of G is a **circulant (di)graph of order n.**

It is straightforward to verify that for $g \in G$, the map $g_L : G \to G$ by $g_L(x) = gx$ is an automorphism of Γ. Thus $G_L = \{g_L : g \in G\}$, the left regular representation of G, is a subgroup of the automorphism group of Γ, $\mathrm{Aut}(\Gamma)$.

Determining the full automorphism group of a Cayley (di)graph is one of the most fundamental questions one can ask about a Cayley (di)graph. While it is usually quite difficult to determine the automorphism group of a Cayley (di)graph, characterizing almost all Cayley graphs of a group G, based on the structure of G, has been of consistent interest in the last few decades. Babai, Godsil, Imrich, and Lovász (see [2, Conjecture 2.1]) conjectured that almost all Cayley graphs of any group G that is not generalized dicyclic or abelian with exponent greater than 2 are GRRs (graphs that have automorphism group G_L). A similar conjecture (with no exceptions) was made for digraphs being DRRs (digraphs that have automorphism group G_L) by Babai and Godsil [2]. Babai and Godsil [2, Theorem 2.2] proved these two conjectures for nilpotent (and nonabelian in the case of undirected graphs) groups of odd order.

Definition 1.2 (Xu [15])**.** A **normal** Cayley (di)graph of the group G is a Cayley (di)graph $\Gamma = \Gamma(G, S)$ such that $G_L \lhd \mathrm{Aut}(\Gamma)$.

Xu also conjectured [15, Conjecture 1] that almost every Cayley (di)graph is normal. The precise formulation of Xu's conjecture is:

Conjecture 1.3 (Conjecture 1, [15])**.** *For any positive integer n, we let $\mathcal{F}_n$ denote the class of all groups of order n, and let*

$$f(n) = \min_{G \in \mathcal{F}_n} \frac{\#\text{ of normal Cayley digraphs of } G}{\#\text{ of Cayley digraphs of } G}.$$

Then $\lim_{n\to\infty} f(n) = 1$.

In 2010, the second author showed that almost all Cayley graphs of an abelian group G of odd prime-power order are normal [4].

Before proceeding farther, we specify what we will mean in this paper when we say something about "almost all" graphs in a particular family:

Definition 1.4. Let $F_2 \subseteq F_1$ be two families of circulant (di)graphs, and $F_i(n)$ $(i = 1, 2)$ be the graphs of order $n \in \mathbb{N}$ in F_i. Then by **almost all** circulant (di)graphs in F_1 are in F_2, we mean that

$$\lim_{n\in\mathbb{N}, n\to\infty} \frac{|F_2(n)|}{|F_1(n)|} = 1.$$

If in the above we replace $\mathbb{N}$ by some set I of infinitely many integers, we say that "almost all" circulant (di)graphs in F_1 **of order n, where $n \in I$**, are in F_2.

Our object in this paper is to determine as far as we can what the automorphism group of a generic circulant (di)graph should look like, by recursively classifying (or attempting to classify) the automorphism groups of almost all circulant (di)graphs that do not fall within a previous step's classification.

The following maps will be used in a number of places in this paper:

Definition 1.5. Let $\iota_G : G \to G$ be defined by $\iota_G(g) = g^{-1}$ for every $g \in G$. If $G \cong \mathbb{Z}_n$, we use ι_n instead of $\iota_{\mathbb{Z}_n}$.

Let $\rho : \mathbb{Z}_n \to \mathbb{Z}_n$ by $\rho(i) = i + 1 \pmod n$. Thus $\langle \rho \rangle = (\mathbb{Z}_n)_L$.

Notice that if G is abelian then ι_G is an automorphism of every Cayley graph $\Gamma(G, S)$ since $S = S^{-1}$. Thus it is not possible for a Cayley graph on an abelian group G to be a GRR unless $G = \mathbb{Z}_2^k$, $k \geq 1$, while Imrich [7, Theorem] has shown that $\mathbb{Z}_2^k$ has a GRR if and only if $k \neq 2, 3, 4$. Nowitz showed [11] during the classification of GRRs that a Cayley graph on a generalized dicyclic group cannot be a GRR.

Definition 1.6. We say that a Cayley (di)graph $\Gamma = \Gamma(G, S)$ has automorphism group **as small as possible** if one of the following holds:

- Γ is a GRR or a DRR; or
- G is either abelian or generalized dicyclic, and $|\mathrm{Aut}(\Gamma)| = 2|G|$.

When $G = \mathbb{Z}_n$, we let $\mathrm{Small}(n)$ denote the set of all circulant graphs whose automorphism group is as small as possible, and $\mathrm{Small} = \cup_{n \in \mathbb{N}} \mathrm{Small}(n)$.

When G is abelian and $\mathrm{Aut}(\Gamma(G, S))$ is as small as possible, we have that $\mathrm{Aut}(\Gamma(G, S)) = \langle G_L, \iota_G \rangle$. Clearly ι_n normalizes $(\mathbb{Z}_n)_L$, so every member of Small will be a normal circulant graph. The first theorem in this paper, Theorem 3.2, shows that almost all circulant graphs are in Small, and thus are normal. This represents some progress towards the proof of Xu's conjecture, and is the first step in our determination of the structure of the automorphism group of a generic circulant graph. It is a natural extension of the work of Babai and Godsil, mentioned above [2, Theorem 2.2].

From there, we proceed to consider classifying the automorphism groups of circulant (di)graphs that are not DRRs. In [4, Conjecture 4.1], the second author conjectured that almost every Cayley (di)graph whose automorphism group is not as small as possible is a normal Cayley (di)graph. We show that this conjecture fails for circulant digraphs of order n, where $n \equiv 2 \pmod 4$ has a fixed number of distinct prime factors (Theorem 3.5), and point out some "gaps" in the proof of [4, Theorem 3.5], which lead to additional counterexamples to [4, Conjecture 4.1] for graphs in the case where $n = p$ or p^2 and p is a **safe prime**, i.e. $p = 2q + 1$ where q is prime, or when n is a power of 3 (Theorem 3.6). Finally, we prove that the conjecture holds for digraphs of order n where n is odd and not divisible by 9 (Theorem 3.7) and for graphs of order n, where n is odd, not a safe prime or the square of a safe prime and not divisible by 9 (Theorem 3.8).

In Section 4, we focus on non-normal circulant (di)graphs. A variety of authors (see [5, 6, 8, 9]) have shown that non-normal Cayley (di)graphs are either generalized wreath products (see Definition 2.5) or have the same automorphism group as a deleted wreath product (see Definition 2.14). We show in general, neither of these classes dominate.

In the next section, we will focus on background results and terminology, as well as developing the counting tools needed in Sections 3 and 4.

2 Preliminaries and tools

We start by stating basic definitions, and then proceed to known results in the literature that we will need. We will finish with results that will be the main tools throughout the rest of the paper.

Definition 2.1. Let G be a transitive permutation group with block system $\mathcal{B}$. By $G/\mathcal{B}$, we mean the subgroup of $S_{\mathcal{B}}$ induced by the action of G on $\mathcal{B}$, and by $\mathrm{fix}_G(\mathcal{B})$ the kernel of this action. Thus $G/\mathcal{B} = \{g/\mathcal{B} : g \in G\}$ where $g/\mathcal{B}(B_1) = B_2$ if and only if $g(B_1) = B_2$, $B_1, B_2 \in \mathcal{B}$, and $\mathrm{fix}_G(\mathcal{B}) = \{g \in G : g(B) = B \text{ for all } B \in \mathcal{B}\}$.

Let G be a transitive permutation group, $\mathcal{B}$ a block system of G, and $\langle\rho\rangle \leq G$. Since $\langle\rho\rangle$ is transitive and abelian, it is regular [13, Proposition 4.4], and so there is a subgroup of $\langle\rho\rangle$ (namely $\mathrm{fix}_{\langle\rho\rangle}(\mathcal{B})$) whose orbits are precisely the blocks of $\mathcal{B}$. It is therefore not difficult to show that $\mathcal{B}$ consists of the cosets of some (cyclic) subgroup of $\mathbb{Z}_n$.

A **vertex-transitive (di)graph** is a (di)graph whose automorphism group acts transitively on the vertices of the (di)graph.

Definition 2.2. The **wreath (or lexicographic) product** of Γ_1 and Γ_2, denoted $\Gamma_1 \wr \Gamma_2$, is the digraph such that $V(\Gamma_1 \wr \Gamma_2) = V(\Gamma_1) \times V(\Gamma_2)$ and edge set

$$\{((x,x'),(y,y')) : xy \in E(\Gamma_1), x', y' \in V(\Gamma_2) \text{ or } x = y \text{ and } x'y' \in E(\Gamma_2)\}.$$

We remark that the wreath product of a circulant digraph of order m and a circulant digraph of order n is circulant. Note that what we have just defined as $\Gamma_1 \wr \Gamma_2$ is sometimes defined as $\Gamma_2 \wr \Gamma_1$, particularly in the work of Praeger, Li, and others from the University of Western Australia.

Definition 2.3. Let Ω be a set and $G \leq S_\Omega$ be transitive. Let G act on $\Omega \times \Omega$ by $g(\omega_1, \omega_2) = (g(\omega_1), g(\omega_2))$ for every $g \in G$ and $\omega_1, \omega_2 \in \Omega$. We define the **2-closure of G**, denoted $G^{(2)}$, to be the largest subgroup of S_Ω whose orbits on $\Omega \times \Omega$ are the same as G's. Let $\mathcal{O}_1, \ldots, \mathcal{O}_r$ be the orbits of G acting on $\Omega \times \Omega$. Define digraphs $\Gamma_1, \ldots, \Gamma_r$ by $V(\Gamma_i) = \Omega$ and $E(\Gamma_i) = \mathcal{O}_i$. Each Γ_i, $1 \leq i \leq r$, is an **orbital digraph of G**, and it is straightforward to show that $G^{(2)} = \cap_{i=1}^{r} \mathrm{Aut}(\Gamma_i)$. A **generalized orbital digraph of** G is an arc-disjoint union of orbital digraphs of G. We say G is **2-closed** if $G^{(2)} = G$.

Clearly the automorphism group of a graph or digraph is 2-closed.

The following theorem appears in [10] and is a translation of results that were proven in [6, 8, 9] using Schur rings, into group theoretic language. We have re-worded part (1) slightly to clarify the meaning. In the special case of circulant digraphs of square-free order n, an equivalent result was proven independently in [5].

Theorem 2.4. *Let $G \leq S_n$ contain $\langle\rho\rangle$. Then one of the following statements holds:*

1. *There exist $G_1, \ldots, G_r$ such that $G^{(2)} = G_1 \times \ldots \times G_r$, and for each G_i, either $G_i \cong S_{n_i}$, or G_i contains a normal regular cyclic group of order n_i. Furthermore, $r \geq 1$, $\gcd(n_i, n_j) = 1$ for $i \neq j$, and $n = n_1 n_2 \cdots n_r$.*
2. *G has a normal subgroup M whose orbits form the block system $\mathcal{B}$ of G such that each connected generalized orbital digraph contains a subdigraph Γ which is an orbital digraph of G and has the form $\Gamma = (\Gamma/\mathcal{B}) \wr \bar{K}_b$, where $b = |M \cap \langle\rho\rangle|$.*

Definition 2.5. A circulant digraph $\Gamma(\mathbb{Z}_n, S)$ is said to be a **(K, H)-generalized wreath circulant digraph** (or just a **generalized wreath circulant digraph**) if there exist groups H, K with $1 < K \leq H \leq \mathbb{Z}_n$ such that $S \setminus H$ is a union of cosets of K.

The name generalized wreath is chosen for these digraphs as if $K = H$, then Γ is in fact a wreath product. We now wish to investigate the relationship between generalized wreath circulant digraphs and the preceding result. We shall have need of the following lemma.

Lemma 2.6. *Let Γ be a disconnected generalized orbital digraph of a transitive group G. Then the components of Γ form a block system $\mathcal{B}$ of G.*

Proof. As the blocks of $G^{(2)}$ are identical to the blocks of G [12, Theorem 4.11] ([12] is contained in the more accessible [14]), we need to show that the set of components $\mathcal{B}$ of Γ is a block system of $G^{(2)}$. This is almost immediate as $G^{(2)} = \cap_{i=1}^{r} \mathrm{Aut}(\Gamma_i)$, where $\Gamma_1, \cdots, \Gamma_r$ are all of the orbital digraphs of G. Assume that $\Gamma = \cup_{i=1}^{s} \Gamma_i$, for some $s \leq r$. Then $\cap_{i=1}^{s} \mathrm{Aut}(\Gamma_i) \leq \mathrm{Aut}(\Gamma)$, so that $\mathcal{B}$ is a block system of $\cap_{i=1}^{s} \mathrm{Aut}(\Gamma_i)$. Also, $G \leq G^{(2)} = \cap_{i=1}^{r} \mathrm{Aut}(\Gamma_i) \leq \cap_{i=1}^{s} \mathrm{Aut}(\Gamma_i)$. Thus $\mathcal{B}$ is a block system of $G^{(2)}$ as $\mathcal{B}$ is a block system of $\cap_{i=1}^{s} \mathrm{Aut}(\Gamma_i)$. □

We will require the following partial order on block systems.

Definition 2.7. We say that $\mathcal{B} \preceq \mathcal{C}$ if for every $B \in \mathcal{B}$ there exists $C \in \mathcal{C}$ with $B \subseteq C$. That is, each block of $\mathcal{C}$ is a union of blocks of $\mathcal{B}$. For $g \in \mathrm{Stab}_G(C)$, $C \in \mathcal{C}$, we denote by $g|_C$ the permutation defined by $g|_C(x) = g(x)$ if $x \in C$ and $g|_C(x) = x$ otherwise. For $H \leq \mathrm{Stab}_G(C)$, we write $H|_C = \{g|_C : C \in \mathcal{C}\}$.

Our main tool in examining generalized wreath circulants will be the following result.

Lemma 2.8. *Let G be 2-closed with a normal subgroup M and a regular subgroup $\langle \rho \rangle$. Let $\mathcal{B}$ be the block system of G formed by the orbits of M, and suppose that each connected generalized orbital digraph contains a subdigraph Γ which is an orbital digraph of G and has the form $\Gamma = (\Gamma/\mathcal{B}) \wr \bar{K}_b$, where $b = |M \cap \langle \rho \rangle|$. Then there exists a block system $\mathcal{C} \succeq \mathcal{B}$ of G such that $\mathrm{fix}_{G^{(2)}}(\mathcal{B})|_C \leq G^{(2)}$ for every $C \in \mathcal{C}$.*

Proof. Observe that we may choose $M = \mathrm{fix}_G(\mathcal{B})$, in which case $|M \cap \langle \rho \rangle| = |B|$, where $B \in \mathcal{B}$, so that b is the size of a block of $\mathcal{B}$. First suppose that if $B, B' \in \mathcal{B}$, $B \neq B'$, then any orbital digraph Γ' that contains some edge of the form $x\vec{y}$ with $x \in B$, $y \in B'$ has every edge of the form $x\vec{y}$, with $x \in B$, $y \in B'$. It is then easy to see that every orbital digraph Γ of G can be written as a wreath product $\Gamma' = \Gamma_1 \wr \Gamma_2$, where Γ_1 is a circulant digraph of order n/b and Γ_2 is a circulant digraph of order b. Then $G/\mathcal{B} \wr \mathrm{fix}_G(\mathcal{B})|_B \leq \mathrm{Aut}(\Gamma')$ for every orbital digraph Γ', and so $G/\mathcal{B} \wr (\mathrm{fix}_G(\mathcal{B})|_B) \leq G^{(2)}$. Then result then follows with $\mathcal{C} = \mathcal{B}$. (Note that G is 2-closed, so $G^{(2)} = G$.)

Denote the orbital digraph that contains the edge $x\vec{y}$ by Γ_{xy}. We may now assume that there exists some $B, B' \in \mathcal{B}$, $B \neq B'$, and $x \in B$, $y \in B'$ such that Γ_{xy} does not have every edge of the form $x'\vec{y}'$, with $x' \in B$ and $y' \in B'$. Note then that no $\Gamma_{x'y'}$ with $x' \in B$ and $y' \in B'$ has every directed edge from B to B'. Let $\mathcal{X}$ be the set of all Γ_{xy} such that if $x \in B_1 \in \mathcal{B}$ and $y \in B_2 \in \mathcal{B}$, $B_1 \neq B_2$, then Γ_{xy} does not have every edge from B_1 to B_2. Let $\hat{\Gamma}$ be the generalized orbital digraph whose edges consist of all edges from every orbital digraph in $\mathcal{X}$, as well as every directed edge contained within a block of $\mathcal{B}$. Then no

orbital digraph that is a subgraph of $\hat{\Gamma}$ can be written as a connected wreath product $\Gamma' \wr \bar{K}_b$ for some Γ', and so by hypothesis, $\hat{\Gamma}$ must be disconnected.

By Lemma 2.6, the components of $\hat{\Gamma}$ form a block system $\mathcal{C} \succeq \mathcal{B}$ of G. (To see that $\mathcal{C} \succeq \mathcal{B}$, note that $\hat{\Gamma}$ contains every edge from B to B', so B is in a connected component of $\hat{\Gamma}$. Since G is transitive, $\mathcal{C} \succeq \mathcal{B}$.) Let $\Gamma_1, \Gamma_2, \ldots, \Gamma_r$ be the orbital digraphs of G, and assume that $\cup_{i=1}^{s} \Gamma_i = \hat{\Gamma}$. If $1 \leq i \leq s$, then $(G^{(2)}/\mathcal{C}) \wr (\mathrm{fix}_{G^{(2)}}(\mathcal{C})|_C) \leq \mathrm{Aut}(\Gamma_i)$; this is because $G^{(2)} \leq \mathrm{Aut}(\Gamma_i)$, Γ_i is disconnected, and each component is contained in a block of $\mathcal{C}$. Thus $\mathrm{fix}_{G^{(2)}}(\mathcal{B})|_C \leq \mathrm{Aut}(\Gamma_i)$ for every $1 \leq i \leq s$. If $s+1 \leq i \leq r$, then if $B, B' \in \mathcal{B}$, $B \neq B'$ and $\vec{xy} \in E(\Gamma_i)$ for some $x \in B$, $y \in B'$, then $\vec{xy} \in E(\Gamma_i)$ for every $x \in B$ and $y \in B'$. Also observe that as the subgraph of $\hat{\Gamma}$ induced by B is K_b, the subgraph of Γ_i induced by G is $\bar{K}_b$. We conclude that $\Gamma_i = \Gamma_i/\mathcal{B} \wr \bar{K}_b$, and so $\mathrm{Aut}(\Gamma_i/\mathcal{B}) \wr S_b \leq \mathrm{Aut}(\Gamma_i)$. Then $\mathrm{fix}_{G^{(2)}}(\mathcal{B})|_B \leq \mathrm{Aut}(\Gamma_i)$ for every $B \in \mathcal{B}$. As $\mathcal{B} \preceq \mathcal{C}$, $\mathrm{fix}_{G^{(2)}}(\mathcal{B})|_C \leq \mathrm{Aut}(\Gamma_i)$ for every $1 \leq i \leq r$ and as $G^{(2)} = \cap_{i=1}^{r} \mathrm{Aut}(\Gamma_i)$, $\mathrm{fix}_{G^{(2)}}(\mathcal{B})|_C \leq G^{(2)}$ for every $C \in \mathcal{C}$. □

Lemma 2.9. *Let Γ be a circulant digraph of order n. Then Γ is a (K, H)-generalized wreath circulant digraph if and only if there exists $G \leq \mathrm{Aut}(\Gamma)$ such that G contains a regular cyclic subgroup, and $\mathrm{fix}_{G^{(2)}}(\mathcal{B})|_C \leq G^{(2)}$ for every $C \in \mathcal{C}$, where $\mathcal{B} \preceq \mathcal{C}$ are formed by the orbits of K and H, respectively.*

Proof. Suppose first that $G \leq \mathrm{Aut}(\Gamma)$ with $\rho \in G$, and there exist block systems $\mathcal{B} \preceq \mathcal{C}$ of G such that $\mathrm{fix}_{G^{(2)}}(\mathcal{B})|_C \leq G^{(2)} \leq \mathrm{Aut}(\Gamma)$ for every $C \in \mathcal{C}$. Since $\rho \in G$, the action of $\mathrm{fix}_{G^{(2)}}(\mathcal{B})|_C$ is transitive on every $B \subseteq C$, so between any two blocks $B_1, B_2 \in \mathcal{B}$ that are not contained in a block of $\mathcal{C}$, we have that there is either every edge from B_1 to B_2 or no edges from B_1 to B_2. Let $\mathcal{B}$ be formed by the orbits of $K \leq \langle \rho \rangle$. Then for every edge $\vec{xy}$ whose endpoints are not both contained within a block of $\mathcal{C}$, $(y - x) + K \subset S$. Let $\mathcal{C}$ be formed by the orbits of $H \leq \langle \rho \rangle$. Then $S \setminus H$ is a union of cosets of K as required.

Conversely, suppose that Γ is a (K, H)-generalized wreath circulant digraph. Then $\rho^m|_C \in \mathrm{Aut}(\Gamma)$ for every $C \in \mathcal{C}$, where $m = [\mathbb{Z}_n : K]$. Let $G \leq \mathrm{Aut}(\Gamma)$ be the maximal subgroup of $\mathrm{Aut}(\Gamma)$ that admits both $\mathcal{B}$ and $\mathcal{C}$ as block systems; clearly $\rho \in G$. Also, since $G^{(2)}$ has the same block systems as G and $G^{(2)} \leq \mathrm{Aut}(\Gamma)$, $G^{(2)} = G$. Now, if $g \in \mathrm{fix}_G(\mathcal{B})$, then $g|_C \in \mathrm{Aut}(\Gamma)$ as well. But this implies that $g|_C \in G$. □

Combining Lemma 2.8 and Lemma 2.9, and recalling that the full automorphism group of a (di)graph is always 2-closed, we have the following result.

Corollary 2.10. *Let Γ be a circulant digraph whose automorphism group $G = \mathrm{Aut}(\Gamma)$ satisfies Theorem 2.4(2). Then Γ is a generalized wreath circulant digraph.*

We now wish to count the number of generalized wreath circulant digraphs.

Lemma 2.11. *The total number of generalized wreath circulant digraphs of order n is at most*

$$\sum_{p|n} 2^{n/p-1} \Bigg(\sum_{q|(n/p)} 2^{(n-n/p)/q} \Bigg),$$

where p and q are prime.

Proof. Let Γ be a (K, H)-generalized wreath circulant digraph of order n. By Lemma 2.9, there exists $G \leq \mathrm{Aut}(\Gamma)$ that admits $\mathcal{B}$ and $\mathcal{C}$ such that $\rho \in G$, and $\mathrm{fix}_{G^{(2)}}(\mathcal{B})|_C \leq \mathrm{Aut}(\Gamma)$

for every $C \in \mathcal{C}$, where $\mathcal{B}$ is formed by the orbits of K and $\mathcal{C}$ is formed by the orbits of H. Let $\mathcal{B}$ consist of m blocks of size k. Then $\rho^m|_C \in \mathrm{Aut}(\Gamma)$ for every $C \in \mathcal{C}$. Choose $q|k$ to be prime, and let $G' \leq \mathrm{Aut}(\Gamma)$ be the largest subgroup of $\mathrm{Aut}(\Gamma)$ that admits a block system $\mathcal{D}$ consisting of n/q blocks of size q. Note then that $\rho^{n/q}|_C \in G'$ for every $C \in \mathcal{C}$. Let p be a prime divisor of the number of blocks of $\mathcal{C}$, and $\mathcal{E}$ the block system of $\langle\rho\rangle$ consisting of p blocks of size n/p. Then $\mathcal{C} \preceq \mathcal{E}$ and $\rho^{n/q}|_E \in G'$ for every $E \in \mathcal{E}$. Thus every (K, H)-generalized wreath circulant digraph is a (L_q, M_p)-generalized wreath circulant digraph, where L_q has prime order q where q divides $|K|$ and M_p has order n/p where p divides $n/|H|$. Note that there is a unique subgroup of $\mathbb{Z}_n$ of prime order q for each $q|n$, and that M_p is also the unique subgroup of $\mathbb{Z}_n$ of order n/p.

As $|L_q| = q$, we use the definition of an (L_q, M_p)-generalized wreath circulant digraph to conclude that $S \setminus M_p$ is a union of some subset of the $(n - n/p)/q$ cosets of L_q that are not in M_p. Thus there are $2^{(n-n/p)/q}$ possible choices for the elements of S not in M_p. As there are at most $2^{n/p-1}$ choices for the elements of S contained in M_p, there are at most $2^{n/p-1} \cdot 2^{(n-n/p)/q} = 2^{n/p+n/q-n/(pq)-1}$ choices for S. Summing over every possible choice of q and then p, we see that the number of generalized wreath digraphs is bounded above by

$$\sum_{p|n} 2^{n/p-1} \Bigg(\sum_{q|(n/p)} 2^{(n-n/p)/q} \Bigg).$$

□

We will denote the set of all circulant digraphs of order n whose automorphism groups are of generalized wreath type by $\mathrm{GW}(n)$. The corresponding set of all circulant graphs will be denoted by $\mathrm{GWG}(n)$. Note that no term in the previous summation given in Lemma 2.11 is larger than $2^{n/p+n/q-n/(pq)-1}$, where q is the smallest prime divisor of n and p is the smallest prime divisor of n/q. As the number of prime divisors of n is at most $\log_2 n$, we have the following result.

Corollary 2.12. *Let q be the smallest prime dividing n, and p the smallest prime prime dividing n/q. Then*

$$|\mathrm{GW}(n)| \leq (\log_2^2 n) 2^{n/p+n/q-n/pq-1}.$$

Using the fact that there are at most two elements that are self-inverse in $\mathbb{Z}_n$ (namely 0 and $n/2$ if n is even, and $0 \notin S$), and at most one coset of $\mathbb{Z}_n/L_q$ that is self-inverse and not in M_p (as $\mathbb{Z}_n/L_q$ is cyclic), and the fact that $(p + q - 1)/pq \leq 3/4$, a similar argument shows that:

Corollary 2.13. *Let q be the smallest prime dividing n, and p the smallest prime prime dividing n/q. Then*

$$|\mathrm{GWG}(n)| \leq (\log_2^2 n) 2^{n(p+q-1)/(2pq)+1/2} \leq (\log_2^2 n) 2^{3n/8+1/2}.$$

We now consider circulant (di)graphs Γ for which $\mathrm{Aut}(\Gamma)$ satisfies Theorem 2.4 (1), and use the notation of that result. If no $G_i \cong S_{n_i}$ with $n_i \geq 4$, then $\mathrm{Aut}(\Gamma)$ contains a normal regular cyclic group and Γ is a normal circulant digraph. Otherwise, we have the following definition.

Definition 2.14. A circulant (di)graph $\Gamma(\mathbb{Z}_n, S)$ is of **deleted wreath type** if there exists some $m > 1$ such that:

- $m \mid n$;
- $\gcd(m, n/m) = 1$; and
- if $H = \langle n/m \rangle$ is the unique subgroup of order m in G, then $S \cap H \in \{\emptyset, H \setminus \{0\}\}$, and for every $g \in \langle m \rangle \setminus \{0\}$, $S \cap (g+H) \in \{\emptyset, \{g\}, (g+H) \setminus \{g\}, g+H\}$. (Notice that because $\gcd(m, n/m) = 1$, the group $\langle m \rangle$ contains precisely one representative of each coset of H in G.)

A circulant digraph is said to be of **strictly deleted wreath type** if it is of deleted wreath type and is not a generalized wreath circulant.

There are deleted wreath type circulants which are not of strictly deleted wreath type. For an example of this, consider a circulant digraph on pqm vertices where $m \geq 4$ and p, q and m are relatively prime, whose connection set is $S = (\langle pq \rangle \setminus \{0\}) \cup (m + \langle mq \rangle)$. This digraph is an (H, K)-generalized wreath circulant for $H = \langle q \rangle$ and $K = \langle mq \rangle$. It is also of deleted wreath type with $H = \langle pq \rangle$, since $S \cap H = H \setminus \{0\}$, while for $g \in \langle m \rangle \setminus \{0\}$, we have $S \cap (g + H) = \{g\}$ if $g \in m + \langle mq \rangle$ and $S \cap (g + H) = \emptyset$ otherwise.

Definition 2.15. For a positive integer m, and a digraph Γ, we denote by $m\Gamma$ the digraph consisting of m vertex-disjoint copies of Γ. The digraph $\Gamma \wr \bar{K}_m - m\Gamma$ is a **deleted wreath product**. Thus this digraph is the digraph whose vertex set is the vertex set of $\Gamma \wr \bar{K}_m$ and whose edge set is the edge set of $\Gamma \wr \bar{K}_m$ with the edges of $m\Gamma$ removed.

The name deleted wreath type is chosen as these digraphs have automorphism groups that are isomorphic to the automorphism groups of deleted wreath products.

Lemma 2.16. *Let $\Gamma = \Gamma(\mathbb{Z}_n, S)$, and let $m \geq 4$ be a divisor of n such that $\gcd(m, n/m) = 1$. Then Γ is of deleted wreath type with m being the divisor of n that satisfies the conditions of that definition, if and only if $\mathrm{Aut}(\Gamma)$ contains a subgroup isomorphic to $H \times S_m$ with the canonical action, for some 2-closed group H with $\mathbb{Z}_{n/m} \leq H \leq S_{n/m}$.*

Proof. In this proof for a given m satisfying $n = km$ and $\gcd(m, k) = 1$, it will be convenient to consider $\mathbb{Z}_n = \mathbb{Z}_k \times \mathbb{Z}_m$ in the obvious fashion. For $i \in \mathbb{Z}_k$, set $B_i = \{(i, j) : j \in \mathbb{Z}_m\}$.

First, suppose Γ is of deleted wreath type with $m \geq 4$ being the divisor of n that satisfies the conditions of that definition, and $n = mk$. Using $\mathbb{Z}_n = \mathbb{Z}_k \times \mathbb{Z}_m$, we see that for every $i \in \mathbb{Z}_k \setminus \{0\}$, we have $S \cap B_i \in \{\emptyset, \{(i, 0)\}, B_i \setminus \{(i, 0)\}, B_i\}$. Also, $S \cap B_0 \in \{\emptyset, B_0 \setminus \{(0, 0)\}\}$. Let $\mathcal{B} = \{B_i : i \in \mathbb{Z}_k\}$ and let $G \leq \mathrm{Aut}(\Gamma)$ be maximal such that G admits $\mathcal{B}$ as a block system. Let $H \leq S_k$ be the projection of G onto the first coordinate. Since $\mathbb{Z}_k \times \mathbb{Z}_m \cong \langle \rho \rangle \leq G$, clearly $\mathbb{Z}_k \leq H$.

We claim that $H \times S_m \leq \mathrm{Aut}(\Gamma)$. Let $((i_1, j_1), (i_2, j_2)) \in E(\Gamma)$, and $(h, g) \in H \times S_m$. Suppose first that $i_1 = i_2$. We have $S \cap B_0 \in \{\emptyset, B_0 \setminus \{(0, 0)\}\}$, and $i_1 = i_2$ forces $S \cap B_0 \neq \emptyset$. Hence $\Gamma[B_i]$ is complete, so clearly $((h(i_1), g(j_1)), (h(i_2), g(j_2))) \in E(\Gamma)$, as $h(i_2) = h(i_1)$. Now suppose $i_1 \neq i_2$. So $h(i_1) \neq h(i_2)$. Let $i = i_2 - i_1$ and let $i' = h(i_2) - h(i_1)$, with $1 \leq i, i' \leq k - 1$. By the definition of H, there is some $g \in G$ that takes B_{i_1} to $B_{h(i_1)}$ and B_{i_2} to $B_{h(i_2)}$. Hence the number of arcs in Γ from B_{i_1} to B_{i_2}, which is $|S \cap B_i|$, must be the same as the number of arcs from $B_{h(i_1)}$ to $B_{h(i_2)}$, which is $|S \cap B_{i'}|$. Since $1 \leq i, i' \leq k - 1$ and $(i_1, j_1), (i_2, j_2) \in E(\Gamma)$, $|S \cap B_i| = |S \cap B_{i'}|$ must be $1, m - 1$ or m. Since $m \geq 4 > 2$, the integers $1, m - 1$ and m are all distinct, so $S \cap B_i$ and $S \cap B_{i'}$ are uniquely determined by their cardinality. If $|S \cap B_i| = 1$, then

$S \cap B_i = \{(i,0)\}$ and $j_2 = j_1$. Hence $g(j_1) = g(j_2)$, and since $S \cap B_{i'} = \{(i',0)\}$, the arc $((h(i_1), g(j_1)), (h(i_2), g(j_2)))$ is in Γ. Similarly, if the cardinality is $m-1$, then $S \cap B_i = \{B_i \setminus \{(i,0)\}\}$ so $j_2 \neq j_1$. Hence $g(j_1) \neq g(j_2)$, and since $S \cap B_{i'} = \{B_{i'} \setminus \{(i',0)\}\}$, the arc $((h(i_1), g(j_1)), (h(i_2), g(j_2)))$ is in Γ. Finally, if the cardinality is m, then $S \cap B_i = B_i$, and $S \cap B_{i'} = B_{i'}$, so the arc $((h(i_1), g(j_1)), (h(i_2), g(j_2)))$ is in Γ. Thus $H \times S_m \leq \mathrm{Aut}(\Gamma)$.

By [12, Theorem 4.11], we have that $(H \times S_m)^{(2)}$ admits $\mathcal{B}$ as $H \times S_m \leq \mathrm{Aut}(\Gamma)$ does. Finally, by [3, Theorem 5.1], $\mathrm{Aut}(\Gamma) \geq (H \times S_m)^{(2)} \geq H^{(2)} \times S_m$. As H is the projection of G onto the first coordinate, we conclude that $H^{(2)} = H$ and H is 2-closed.

Conversely, assume that $\mathrm{Aut}(\Gamma)$ contains a subgroup isomorphic to $H \times S_m$ with the canonical action, for some 2-closed group H with $\mathbb{Z}_{n/m} \leq H \leq S_{n/m}$. Clearly $\mathrm{Stab}_{1\times S_m}(0,0)$ is transitive on $B_i \setminus \{(i,0)\}$, and so the orbits of $\mathrm{Stab}_{1\times S_m}(0,0)$ on B_i are $\{(i,0)\}$ and $B_i \setminus \{(i,0)\}$. Also $1 \times S_m \leq H \times S_m \leq \mathrm{Aut}(\Gamma)$ implies $\mathrm{Stab}_{1\times S_m}(0,0) \leq \mathrm{Stab}_{H\times S_m}(0,0) \leq \mathrm{Stab}_{\mathrm{Aut}(\Gamma)}(0,0)$. Thus each $S \cap B_i$ is a union of some (possibly none) of these two orbits. Hence the only possibilities for each $S \cap B_i$ are $\emptyset, \{(i,0)\}, B_i \setminus \{(i,0)\}$ and B_i if $1 \leq i \leq k-1$; and since $0 \notin S$, $S \cap B_0$ is either $\emptyset$ or $B_0 \setminus \{(0,0)\}$. □

We remark that the above lemma shows that a deleted wreath product type circulant digraph is not a normal circulant digraph when $m \geq 4$.

The following result is an easy consequence of Lemma 2.16 together with the fact that the 2-closure of a direct product is the direct product of the 2-closures of the factors [3, Theorem 5.1].

Corollary 2.17. *A non-normal circulant (di)graph whose automorphism group satisfies the conclusion of Theorem 2.4(1) is of deleted wreath type with* $m \geq 4$.

Corollary 2.18. *There are at most* $2^{n/m+1}$ *graphs* Γ *and at most* $2^{2n/m}$ *digraphs* Γ *that contain* $K \times S_m$ *for any choice of* K *that is 2-closed and has* $\mathbb{Z}_{n/m} \leq K \leq S_{n/m}$, *where* $m \geq 4$. *Equivalently, there are at most* $2^{2n/m}$ *digraphs of deleted wreath type, and at most* $2^{n/m+1}$ *graphs of deleted wreath type, for any fixed* $m \geq 4$ *with* $m \mid n$ *and* $\gcd(m, n/m) = 1$.

Proof. A consequence of Lemma 2.16 is that there are $2 \cdot 4^{n/m-1} < 4^{n/m} = 2^{2n/m}$ digraphs Γ of order n such that $K \times S_m \leq \mathrm{Aut}(\Gamma)$ for $m \geq 4$. Note that a digraph Γ with $\mathrm{Aut}(\Gamma) = K \times S_m$, $m \geq 3$, is a graph if and only if K contains the map $\iota_{n/m}$. Then $\iota_{n/m}(g + H) = (-g) + H$ where $H = \langle n/m \rangle$, and so if n/m is odd, there are at most $4^{n/(2m)} = 2^{n/m}$ graphs Γ that contain $K \times S_m$ for any choice of K that is 2-closed and has $\mathbb{Z}_{n/m} \leq K \leq S_{n/m}$. Even if n/m is even, only one nontrivial coset of $\langle n/m \rangle$ is fixed by $\iota_{n/m}$, so there are at most $2 \cdot 4 \cdot 4^{(n/m-2)/2} = 2^{n/m+1}$ graphs Γ that contain $K \times S_m$ for any choice of K that is 2-closed and has $\mathbb{Z}_{n/m} \leq K \leq S_{n/m}$. □

3 Normal circulants

In this section our main focus is on determining whether or not almost all circulants that do not have automorphism groups as small as possible are normal circulants, as conjectured by the second author [4, Conjecture 1]. We begin by showing that almost every circulant graph of order n has automorphism group as small as possible. We remark that Babai and Godsil [2, Theorem 5.3] have shown this to be true for Cayley graphs on abelian groups of order n, where $n \equiv 3 \pmod 4$.

We require some additional notation that will be used through the remainder of this paper.

Definition 3.1. Let $\mathrm{ACG}(n)$ be the set of all circulant graphs of order n.

Throughout this paper $\mathbb{Z}_n^*$ denotes the group of units (invertible elements) of $\mathbb{Z}_n$. For $a \in \mathbb{Z}_n^*$, we define $\bar{a} : \mathbb{Z}_n \to \mathbb{Z}_n$ by $\bar{a}(i) = ai$. As previously defined, if $a = -1$ then we denote $\bar{a}$ by ι_n. Finally, by $|g|$ we denote the order of any element g in any group G.

Theorem 3.2. *For almost every circulant graph* Γ, $\mathrm{Aut}(\Gamma)$ *is as small as possible. More precisely,*

$$\lim_{n\to\infty} \frac{|\mathrm{Small}(n)|}{|\mathrm{ACG}(n)|} = 1.$$

Proof. We first count the number of circulant graphs of order n not in $\mathrm{Small}(n)$. By Corollary 2.13, there are at most $\log_2^2 n \cdot 2^{3n/8+1/2}$ generalized wreath circulant graphs of order n.

Now assume $\Gamma \notin \mathrm{GWG}(n) \cup \mathrm{Small}(n)$. By Corollary 2.10, $\mathrm{Aut}(\Gamma)$ satisfies Theorem 2.4(1). Either $\mathrm{Aut}(\Gamma)$ normalizes $\langle\rho\rangle$ or $G_i = S_{n_i}$ for some $n_i \geq 4$ (using the notation of Theorem 2.4(1)). We will find an automorphism α of $\mathbb{Z}_n$ such that $\alpha \in \mathrm{Aut}(\Gamma) \setminus \langle\iota_n\rangle$. Obviously, if $\langle\rho\rangle \triangleleft \mathrm{Aut}(\Gamma)$, then since $\Gamma \notin \mathrm{Small}(n)$, such an α exists. If $G_i = S_{n_i}$ and $n_i \geq 4$, then G_i contains a nontrivial automorphism $\bar{b}$ of $\mathbb{Z}_{n_i}$. Regard $\mathbb{Z}_n$ as $\mathbb{Z}_{n/n_i} \times \mathbb{Z}_{n_i}$ in the usual way. If $n_i \geq 7$ then we may choose $b \neq \pm 1$, and $\alpha = \overline{(1, b)}$. We may assume n is arbitrarily large, so if $4 \leq n_i < 7$ we may assume $n/n_i \geq 3$, and let $\alpha = \overline{(-1, 1)}$. Thus there exists $\alpha \in \mathrm{Aut}(\mathbb{Z}_n) \cap \mathrm{Aut}(\Gamma)$ but not in $\langle\iota_n\rangle$.

Now observe that ι_n has at most two fixed points, and so has at most $(n-2)/2 + 2$ orbits. Let $\alpha \in \mathrm{Aut}(\mathbb{Z}_n)$ be such that $\alpha \notin \langle\iota_n\rangle$. Observe that we may divide the orbits of $\langle\iota_n, \alpha\rangle$ into three types: singleton orbits, orbits of length 2, and orbits of length greater than 2. As $\langle\iota_n\rangle$ has at most 2 singleton orbits, $\langle\iota_n, \alpha\rangle$ has at most two singleton orbits, namely 0 and $n/2$. If $x \neq 0, n/2$, then x is contained in an orbit of $\langle\iota_n\rangle$ of length 2. If such an x is contained in an orbit of $\langle\iota_n, \alpha\rangle$ of length 2, then setting $\alpha = \bar{a}$, $a \in \mathbb{Z}_n^*$, we have that $\{x, -x\} = \{ax, -ax\}$, in which case either $x = ax$ and x is a fixed point of α, or $x = -ax$ and x is a fixed point of $\iota_n\alpha$. If $x = ax$ set $\beta = \alpha$ and if $x = -ax$, set $\beta = \iota_n\alpha$. Then $\langle\iota_n, \alpha\rangle = \langle\iota_n, \beta\rangle$, and x is a fixed point of β. It is easy to see that the set of fixed points of β, say $H(\beta)$, forms a subgroup of $\mathbb{Z}_n$, and so $|H(\beta)| \leq n/2$. Thus $\langle\iota_n, \alpha\rangle$ has at at most $(n/2-1)/2$ orbits of length two, and so at most $(n/2-1)/2+2$ orbits of length one or two. Every remaining orbit of $\langle\iota_n, \alpha\rangle$ is a union of orbits of $\langle\iota_n\rangle$ of size 2, and so every remaining orbit of $\langle\iota_n, \alpha\rangle$ has length at least 4. Clearly, the number of orbits of $\langle\iota_n, \alpha\rangle$ is maximized if it has 2 orbits of length 1, $(n/2-1)/2$ orbits of length 2, and the remainder have length greater than 2. In this case, there will be at most $(n/2-1)/4 = n/8 - 1/4$ orbits of length greater than 2. We conclude that there are at most $3n/8 + 5/4$ orbits of $\langle\iota_n, \alpha\rangle$, and as S must be a union of orbits of $\langle\iota_n, \alpha\rangle$ not including $\{0\}$, there are at most $2^{3n/8+1/4}$ such circulant graphs for each $\alpha \in \mathrm{Aut}(\mathbb{Z}_n)$, $\alpha \notin \langle\iota_n\rangle$. As there are at most n (actually $\varphi(n)$ of course) automorphisms of $\mathbb{Z}_n$, there are at most $n \cdot 2^{3n/8+1/4}$ circulant graphs that contain an automorphism of $\mathbb{Z}_n$ other than ι_n.

We have shown that there are at most $n \cdot 2^{3n/8+1/4} + \log_2^2 n \cdot 2^{3n/8+1/2} < \sqrt{2}(n + \log_2^2 n)2^{3n/8}$ circulant graphs of order n that are not in $\mathrm{Small}(n)$. As there are $2^{(n-2)/2+1} = 2^{n/2}$ circulant graphs of order n if n is even and $2^{(n-1)/2}$ circulant graphs

of order n if n is odd,

$$\lim_{n\to\infty} \frac{|\mathrm{Small}(n)|}{|\mathrm{ACG}(n)|} \geq 1 - \lim_{n\to\infty} \frac{\sqrt{2}(n+\log_2^2 n)2^{3n/8}}{2^{(n-1)/2}} = 1.$$

□

The above theorem clearly shows that almost all circulant graphs are normal. In 2010, the second author made the following conjecture for Cayley (di)graphs (not necessarily circulant) whose automorphism group is not as small as possible [4, Conjecture 1].

Conjecture 3.3. *Almost every Cayley (di)graph whose automorphism group is not as small as possible is a normal Cayley (di)graph.*

It is difficult to determine the automorphism group of a (di)graph, so the main way to obtain examples of vertex-transitive graphs is to construct them. An obvious construction is that of a Cayley (di)graph, and the conjecture of Imrich, Lovász, Babai, and Godsil says that when performing this construction, additional automorphisms are almost never obtained. The obvious way of constructing a Cayley (di)graph of G that does not have automorphism group as small as possible is to choose an automorphism α of G and make the connection set a union of orbits of α. The above conjecture in some sense says that this construction almost never yields additional automorphisms other than the ones given by the construction.

Throughout the remainder of this paper, all circulant digraphs of order n whose automorphism groups are of deleted wreath, and strictly deleted wreath types will be denoted by $\mathrm{DW}(n)$, and $\mathrm{SDW}(n)$ respectively. The corresponding set of all graphs whose automorphism groups are of deleted wreath type will be denoted by $\mathrm{DWG}(n)$. If we wish to consider a subset of one of these sets with a restriction on m, we indicate this in a subscript, as for example $\mathrm{DW}(n)_{m\geq 4}$. Also, the sets of all digraphs that are circulants, DRR circulants, normal circulants, and non-normal circulants of order n will be denoted as $\mathrm{ACD}(n), \mathrm{DRR}(n), \mathrm{Nor}(n)$ and $\mathrm{NonNor}(n)$, respectively. The corresponding sets of all graphs that are circulants, normal circulants, and nonnormal circulants, will be denoted by $\mathrm{ACG}(n)$, $\mathrm{NorG}(n)$, and $\mathrm{NonNorG}(n)$, respectively.

The following lemma will prove useful in determining how many circulant (di)graphs are not normal.

Lemma 3.4. *If a circulant digraph Γ of composite order n that is a (K, H)-generalized wreath circulant digraph is normal, then $4 \mid n$.*

Proof. Without loss of generality we may assume that K is of prime order p. Let $\mathcal{B}$ be the block system of $\langle\rho\rangle$ formed by the orbits of $\langle\rho^m\rangle$, where $|H| = n/m$. Then $\rho^{n/p}|_B \in \mathrm{Aut}(\Gamma)$ for every $B \in \mathcal{B}$. Set $G = \langle\rho, \rho^{n/p}|_B : B \in \mathcal{B}\rangle$, and let $\mathcal{C}$ be the block system of G formed by the orbits of $\langle\rho^{n/p}\rangle$, so that $\mathrm{fix}_G(\mathcal{C}) = \langle\rho^{n/p}|_B : B \in \mathcal{B}\rangle$, and has order $p^{n/m}$. Then $\mathcal{C}$ is also a block system of $N(n)$, where $N(n) = \{x \to ax + b : a \in \mathbb{Z}_n^*, b \in \mathbb{Z}_n\}$. Let $n = p_1^{a_1}p_2^{a_2}\cdots p_r^{a_r}$ be the prime power decomposition of n. As $N(n) = \Pi_{i=1}^r N(p_i^{a_i})$, we see that a Sylow p-subgroup of $\mathrm{fix}_{N(n)}(\mathcal{C})$ is a Sylow p-subgroup of $1_{S_{n/p^a}} \times N(p^a)$, where $p = p_j$ and $a = a_j$ for some j. Let $\mathcal{E}$ be the block system of $N(p^a)$ consisting of blocks of size p. Then a Sylow p-subgroup of $\mathrm{fix}_{N(p^a)}(\mathcal{E})$ has order at most p^2 as a Sylow p-subgroup of $N(p^a)$ is metacyclic. If $\Gamma \in \mathrm{Nor}(n)$, then $\langle\rho\rangle \triangleleft G$ since $G \leq \mathrm{Aut}(\Gamma)$, so $G \leq N(n)$. This implies that a Sylow p-subgroup of $\mathrm{fix}_G(\mathcal{C})$ has order at most p^2, and

so $p^{n/m} \leq p^2$. Since $H > 1$ we have $n > m$, so this forces $n = 2m$, and $\mathcal{B}$ consists of 2 blocks. Finally, let $\delta = \rho^{n/p}|_B$, where $B \in \mathcal{B}$ with $0 \in B$. If $\Gamma \in \mathrm{Nor}(n)$, then $\gamma = \rho^{-1}\delta^{-1}\rho\delta \in \langle\rho\rangle$, and straightforward computations will show that $\gamma(i) = i + n/p$ if i is even, while $\gamma(i) = i - n/p$ if i is odd. As $\gamma \in \langle\rho\rangle$, we must have that $n/p \equiv -n/p \pmod n$, and so $2n/p \equiv 0 \pmod n$. This then implies that $p = 2$ and so $4|n$ as required. □

We first show that Conjecture 3.3 is false for circulant digraphs of order n, where $n \equiv 2 \pmod 4$ has a fixed number of distinct prime factors.

Theorem 3.5. *Let $n = 2p_1^{e_1}p_2^{e_2}\cdots p_r^{e_r}$, where the p_i are distinct odd primes and r is fixed. Then*

$$\lim_{n\to\infty, r \text{ fixed}} \frac{|\mathrm{NonNor}(n)|}{|\mathrm{Nor}(n)\backslash\mathrm{DRR}(n)|} \geq \frac{1}{2(2^r-1)}.$$

Proof. By Lemma 3.4, we have that $|\mathrm{NonNor}(n)| \geq |\mathrm{GW}(n)|$. We claim that $|\mathrm{GW}(n)| \geq 2^{n/2+n/(2p)-1}$, where $1 \neq p$ is the smallest divisor of $n/2$. To see this, we construct this number of distinct generalized wreath circulant digraphs of order n, as follows: $\mathcal{B}$ will be the block system formed by the orbits (cosets) of $\langle n/2\rangle$, and $\mathcal{C}$ the block system formed by the orbits (cosets) of $\langle p\rangle$. Since there are n/p elements in each block of $\mathcal{C}$, there are $2^{n/p-1}$ choices for $S \cap C_0$, where C_0 is the block of $\mathcal{C}$ that contains 0. Since there are $n/2 - n/(2p)$ orbits (cosets) of $\langle n/2\rangle$ that are not in C_0, there are $2^{n/2-n/(2p)}$ choices for $S - C_0$ that create a generalized circulant digraph with this choice of $\mathcal{B}$ and $\mathcal{C}$. These $2^{n/p+n/2-n/(2p)-1} = 2^{n/2+n/(2p)-1}$ generalized circulant digraphs are all distinct (though not necessarily nonisomorphic), so $|\mathrm{GW}(n)| \geq 2^{n/2+n/(2p)-1}$ as claimed.

Let $S(n)$ be the set of all circulant digraphs of order n whose automorphism group contains a nontrivial automorphism of $\mathbb{Z}_n$. Clearly then $|S(n)| \geq |\mathrm{Nor}(n)\backslash\mathrm{DRR}(n)|$. We now seek an upper bound on $|S(n)|$. Observe that for any circulant digraph Γ, if there exists an nontrivial automorphism $\alpha \in \mathrm{Aut}(\Gamma) \cap \mathrm{Aut}(\mathbb{Z}_n)$, then we may choose such an α of prime order.

Let $1 \neq a \in \mathbb{Z}_n^*$ have prime order ℓ. We first consider the case that $\bar{a}$ has a fixed point $i \neq 0$. Then $ai \equiv i \pmod n$, so $(a-1)i \equiv 0 \pmod n$. Since $a \neq 1$, we must have $\gcd(i, n) = m > 1$, which clearly implies $i \in \langle m\rangle$. Since $a \in \mathbb{Z}_n^*$, $a = sn/m + 1$ for some $0 < s < m$ must be a unit, i.e., $\gcd(n, sn/m + 1) = 1$. Note that $m > 2$, since if $m = 2$ then $s = 1$, but $\gcd(n, n/2 + 1) \geq 2$ since $n/2$ is odd. Now, $\bar{a}$ fixes n/m points $\{0, m, \cdots, (n/m-1)m\}$, and since $|\bar{a}| = \ell$ is prime, every non-singleton orbit of $\bar{a}$ has length ℓ. So $\bar{a}$ has $n(1-1/m)/\ell$ orbits of length ℓ, and $n/m + n/\ell - n/(m\ell)$ orbits in total. We will separate the cases $\ell = 2$ and $\ell = 3$ to make the proof easier. If $\ell = 2$ then $1/m + 1/\ell - 1/(m\ell) = 1/2 + 1/(2m) \leq (p+1)/(2p)$ since $m \geq p$ (p is still the smallest nontrivial divisor of $n/2$), so if $|\bar{a}| = 2$, then α has at most $(p+1)n/(2p)$ orbits. If $\ell = 3$ then $1/m + 1/\ell - 1/(m\ell) = 1/3 + 2/(3m) \leq (p+2)/(3p)$ since $m \geq p$, so if $|\bar{a}| = 3$, then $\bar{a}$ has at most $(p+2)n/(3p)$ orbits. Finally, if $\ell \geq 5$ then $1/m + 1/\ell - 1/(m\ell) \leq (m+4)/(5m) \leq 7/15$ since $m \geq 3$, so if $|\bar{a}| \geq 5$ then $\bar{a}$ has at most $7n/15$ orbits.

Finally, notice that if $\bar{a}$ fixes only 0, it will have 1 fixed point and $n-1$ points that are not fixed. If $|\bar{a}| = 2$ then its orbits are all of length 1 or 2, and since $n-1$ is odd, it cannot be partitioned into orbits of length 2. So an element of order 2 must have some fixed point other than 0. Hence if $\bar{a}$ fixes only 0, it must have order at least 3, so each non-singleton

orbit must have length at least 3. Hence $\bar{a}$ has at most $\lfloor (n-1)/3 \rfloor < n/3$ orbits other than $\{0\}$.

We now split the set of all elements of $\mathbb{Z}_n^*$ that have prime order into disjoint subsets: U (consisting of all elements of order 2 that have fixed points); V (consisting of all elements of order 3 that have fixed points); W (consisting of all elements of order 5 or greater that have fixed points) and X (consisting of all elements that have no fixed points other than 0). Notice that $\mathbb{Z}_n^* = \mathbb{Z}_{p_1^{e_1}}^* \times \ldots \times \mathbb{Z}_{p_r^{e_r}}^*$ and each $\mathbb{Z}_{p_i^{e_i}}^*$ is cyclic, so contains a unique element of order 2. Any element of order 2 in $\mathbb{Z}_n^*$ must be a product of elements of order 1 or 2 from the $\mathbb{Z}_{p_i}^*$, at least one of which must have order 2. So there are $2^r - 1$ elements of order 2 in $\mathbb{Z}_n^*$. Also, there are at most n elements of any other order in $\mathbb{Z}_n^*$. Thus,

$$\begin{aligned} |S(n)| &\leq \sum_{\bar{a}\in U} 2^{(p+1)n/(2p)} + \sum_{\bar{a}\in V} 2^{(p+2)n/(3p)} + \sum_{\bar{a}\in W} 2^{7n/15} + \sum_{\bar{a}\in X} 2^{n/3} \\ &\leq (2^r - 1)2^{(p+1)n/(2p)} + n(2^{(p+2)n/(3p)} + 2^{7n/15} + 2^{n/3}). \end{aligned}$$

Now,

$$\lim_{n\to\infty, r \text{ fixed}} \frac{|\mathrm{NonNor}(n)|}{|\mathrm{Nor}(n)\backslash \mathrm{DRR}(n)|} \geq \lim_{n\to\infty, r \text{ fixed}} \frac{2^{n/2+n/(2p)-1}}{|S(n)|} = \frac{1}{2(2^r-1)}.$$

□

A **safe prime** is a prime number $p = 2q + 1$, where q is also prime.

We now show that it is not true that almost all circulant graphs of order p or p^2, where p is a safe prime, or of order 3^k, are normal. This shows that [4, Theorem 3.5] is not correct. We provide a correct statement of [4, Theorem 3.5] as well as point out explicitly where "gaps" occur in the proof. As a consequence, much of the following result is essentially the same as the proof of [4, Theorem 3.5]. The entire argument is included for completeness.

Theorem 3.6. *Let $X = \{p, p^2 : p \text{ is a safe prime}\} \cup \{3^k : k \in \mathbb{N}\}$, T the set of all powers of odd primes, and $R = T \setminus X$. Then*

$$\lim_{n\in R, n\to\infty} \frac{|\mathrm{NonNorG}(n)|}{|\mathrm{ACG}(n) \setminus \mathrm{Small}(n)|} = 0.$$

Additionally, if $n \in X$, then more than one fifth of all elements of $\mathrm{ACG}(n) \setminus \mathrm{Small}(n)$ *are in* $\mathrm{NonNorG}(n)$.

Proof. Let $n = p^k \in T$, where p is an odd prime, $\Gamma = \Gamma(\mathbb{Z}_n, S)$.

First suppose that $k = 1$. The statement about X is vacuously true for $p = 3$ and easy to verify for $p = 5$, so we assume $p > 5$. If $p = 2q + 1$ is a safe prime, then $\mathbb{Z}_p^*$ is cyclic of order $2q \geq 6$, so every element of $\mathbb{Z}_p^*$ has order 2, q, or $2q$. Since $\iota_p \in \mathrm{Aut}(\Gamma)$, if $\Gamma \notin \mathrm{Small}(p)$ is normal then $\bar{a} \in \mathrm{Aut}(\Gamma)$ for $a \in \mathbb{Z}_p^*$ of order q or $2q$. Since $q > 2$, the orbit of length q that contains 1 in $\mathbb{Z}_p^*$ does not contain -1, so the orbits of $\langle \alpha, \iota_p \rangle$ have length 1 (the orbit of 0) and $2q = p - 1$ (everything else). So $\Gamma = K_p$ or $\bar{K}_p$ and $\mathrm{Aut}(\Gamma) = S_p$ contradicting Γ being normal. Hence $\mathrm{ACG}(p) \setminus \mathrm{Small}(p) \subseteq \mathrm{NonNorG}(p)$. (The proof of [4, Theorem 3.5] overlooks this case.)

Now if p is not a safe prime, then we can write $(p-1)/2 = rs$ where $1 < r \leq s < (p-1)/2$. As $\mathbb{Z}_p^*$ is cyclic of order $p - 1$, there is $a \in \mathbb{Z}_p^*$ with $|a| = 2r$. Then $\bar{a}$ has $s + 1$ orbits

(the cosets of $\langle a\rangle$ in $\mathbb{Z}_p^*$, together with 0). Since $|a|$ is even, $-1 \in \langle a\rangle$. If S is a union of these orbits, Γ is a graph, and since $|a| > 2$, $\Gamma \notin \mathrm{Small}(p)$. Hence $|\mathrm{ACG}(p) \setminus \mathrm{Small}(p)| \geq 2^s \geq 2^{\sqrt{(p-1)/2}}$. Meanwhile, if $\mathrm{Aut}(\Gamma) \not< \mathrm{AGL}(1,p)$ then $\mathrm{Aut}(\Gamma) = S_p$ by [1], and $\Gamma = K_p$ or $\bar{K}_p$. So $|\mathrm{NonNor}(p)| = 2$ and clearly $2/(2^{\sqrt{(p-1)/2}}) \to 0$ as $p \to \infty$.

Now let $k \geq 2$. Through the rest of this proof, let $a = p^{k-1} + 1$. We show that $\bar{a} \in \mathrm{Aut}(\Gamma)$ if and only if $\Gamma \in \mathrm{NonNor}(n)$. Using the binomial theorem, it is easy to see that $|\bar{a}| = p$. Furthermore, $\bar{a}$ fixes every element of $\langle p\rangle$, and fixes setwise every coset of $\langle p^{k-1}\rangle$. Since $|\bar{a}| = p$ and $\bar{a}$ does not fix any element of any coset of $\langle p^{k-1}\rangle$ that is not in $\langle p\rangle$, the orbits of $\bar{a}$ on each coset of $\langle p^{k-1}\rangle$ that is not in $\langle p\rangle$ have length p. Thus if $\bar{a} \in \mathrm{Aut}(\Gamma)$, then Γ is a $(\langle p^{k-1}\rangle, \langle p\rangle)$-generalized wreath circulant digraph, and in fact by Lemma 3.4, $\Gamma \in \mathrm{NonNor}(n)$. Conversely, if $\Gamma \in \mathrm{NonNor}(n)$, then by Theorem 2.4, $\mathrm{Aut}(\Gamma)$ either falls into category (1) with a single factor in the direct product (since $n = p^k$ does not permit coprime factors) and since $\Gamma \in \mathrm{NonNor}(n)$, Γ is complete (or empty), or category (2) so by Corollary 2.10, $\Gamma \in \mathrm{GW}(n)$. Since $K_n, \bar{K}_n \in \mathrm{GW}(n)$, $\Gamma \in \mathrm{GW}(n)$. It is straightforward to verify using the definition of a generalized wreath circulant, that $\bar{a} \in \mathrm{Aut}(\Gamma)$.

Now suppose $p = 3$. We have $\mathbb{Z}_{3^k}^*$ is cyclic of order $2 \cdot 3^{k-1}$. For $\Gamma \in \mathrm{Nor}(3^k) \setminus \mathrm{Small}(3^k)$, there exists $-1 \neq b \in \mathbb{Z}_{3^k}^*$ with $\bar{b} \in \mathrm{Aut}(\Gamma)$. If $|b|$ is divisible by 3, then since $\mathbb{Z}_{3^k}^*$ is cyclic and a generates the unique subgroup of order 3, we have $\bar{a} \in \langle \bar{b}\rangle$, so $\bar{a} \in \mathrm{Aut}(\Gamma)$. Hence $\Gamma \in \mathrm{NonNor}(3^k)$. But the only divisor of $2 \cdot 3^{k-1}$ not divisible by 3 is 2, and so $b = -1$. This shows that if $\Gamma \in \mathrm{NorG}(3^k)$ then $\Gamma \in \mathrm{Small}(3^k)$. Thus $\mathrm{ACG}(3^k) \setminus \mathrm{Small}(3^k) \subseteq \mathrm{NonNorG}(3^k)$.

Now we calculate $|\mathrm{NonNorG}(n)|$. As noted above, if $\Gamma \in \mathrm{NonNorG}(n)$ then $\bar{a} \in \mathrm{Aut}(\Gamma)$, and the orbits of $\bar{a}$ all have length 1 or length p. Now since multiplication is commutative, ι_{p^k} permutes the orbits of $\langle \bar{a}\rangle$, and since $|\bar{a}| = p$ is odd, $\iota_{p^k} \notin \langle \bar{a}\rangle$, so ι_{p^k} will exchange pairs of orbits of $\langle \bar{a}\rangle$, except the orbit $\{0\}$. Consequently, $\langle \bar{a}, \iota_{p^k}\rangle$ will have one orbit of length 1 ($\{0\}$); $(p^{k-1}-1)/2$ orbits of length 2 (whose union is $\langle p\rangle \setminus \{0\}$); and $(p^k - p^{k-1})/(2p)$ orbits of length $2p$ (everything else). So $\langle \bar{a}, \iota_{p^k}\rangle$ has exactly $p^{k-1} - (1 + p^{k-2})/2$ orbits other than $\{0\}$. Since we have shown that $\Gamma \in \mathrm{NonNor}(p^k)$ if and only if $\langle \bar{a}, \iota_{p^k}\rangle \leq \mathrm{Aut}(\Gamma)$, $|\mathrm{NonNor}(p^k)| = 2^{p^{k-1} - (1+p^{k-2})/2}$.

Now we find a lower bound for $|\mathrm{ACG}(n) \setminus \mathrm{Small}(n)|$ when $n \in R$ and $k > 2$. Since p is an odd prime, $\mathbb{Z}_{p^k}^*$ is cyclic of order $(p-1)p^{k-1}$. Let $b \in \mathbb{Z}_{p^k}^*$ have order $p-1$. Note that $\iota_{p^k} \in \langle \bar{b}\rangle$ since b has even order, and $\bar{b} \neq \iota_{p^k}$ since $p > 3$ (the proof of [4, Theorem 3.5] overlooks the fact that $\bar{b} = \iota_{p^k}$ when $p = 3$). Clearly, $\bar{b}$ fixes 0, and since the order of $\bar{b}$ is $p-1$, every other orbit of $\bar{b}$ has length at most $p-1$, so $\bar{b}$ has at least $(p^k-1)/(p-1)$ orbits other than $\{0\}$. Thus there are at least $2^{(p^k-1)/(p-1)}$ circulant graphs of order p^k whose automorphism group contains $\bar{b}$, and $|\mathrm{ACG}(p^k) \setminus \mathrm{Small}(p^k)| \geq 2^{1+(p^k-1)/(p-1)}$, $p > 3$. Note that as $k \geq 2$, $(p^k-1)/(p-1) \neq 1$. Then

$$\begin{aligned}\lim_{p^k\to\infty} \frac{|\mathrm{NonNorG}(p^k)|}{|\mathrm{ACG}(p^k) \setminus \mathrm{Small}(p^k)|} &\leq \lim_{p^k\to\infty} \frac{2^{p^{k-1}-(1+p^{k-2})/2}}{2^{(p^k-1)/(p-1)}} \\ &= \lim_{p^k\to\infty} \frac{1}{2^{(3p^{k-2}+1)/2+\sum_{i=0}^{k-3} p^i}}.\end{aligned}$$

Thus as $k \geq 3$, the result follows. (The proof of [4, Theorem 3.5] concludes the above limit is 1 in all cases – hence the gap in that theorem when $k = 2$.)

For the remainder of the proof we suppose that $k = 2$ and $p > 3$. Substituting $k = 2$ into our formula for $|\mathrm{NonNorG}(n)|$, we conclude that $|\mathrm{NonNorG}(p^2)| = 2^{p-1}$.

If $p = 2q + 1$ is a safe prime, q prime, then $\langle \bar{a} \rangle$ is the unique subgroup of order p in $\mathbb{Z}^*_{p^2}$, so any subgroup of $\mathbb{Z}^*_{p^2}$ that contains -1 but does not contain $a = p + 1$, must have even order not a multiple of p. Since $\mathbb{Z}^*_{p^2}$ is cyclic of order $p(p-1) = 2pq$, the group C of order $2q$ is the only such subgroup. Then if $\Gamma \in \mathrm{Nor}(p^2) \setminus \mathrm{Small}(p^2)$, then $\mathrm{Aut}(\Gamma) = C \cdot (\mathbb{Z}_{p^2})_L$. Now, C fixes 0 and since C has order $2q$ and is cyclic, the other orbits of C all have length precisely $2q$ (it is not hard to show that the only elements of $\mathbb{Z}^*_{p^2}$ that fix anything but 0 are 1 and the elements of order p; this forces the orbit lengths of C to be the order of C), so there are $(p^2 - 1)/2q = 1 + p$ orbits of C other than $\{0\}$, and hence fewer than 2^{1+p} graphs in $\mathrm{Nor}(p^2)$ are not in $\mathrm{Small}(p^2)$ (the "fewer than" is due to the fact that some of these graphs are not normal, for example K_{p^2}). Hence $\mathrm{NonNor}(p^2)/(\mathrm{ACG}(p^2) \setminus \mathrm{Small}(p^2)) \geq 2^{p-1}/(2^{p-1} + 2^{p+1}) = 1/5$.

Suppose now that p is not a safe prime. Then there exists $b \in \mathbb{Z}^*_{p^2}$ of order $p - 1$. Since p is not a safe prime, there exists $1 < r \leq s < (p-1)/2$ such that $rs = (p-1)/2$. As every non-singleton orbit of $\langle \bar{b} \rangle$ has length $p - 1$ (as shown for the orbits of C in the preceding paragraph), every nonsingleton orbit of $\langle \bar{b}^s \rangle$ has length $(p-1)/s$. Then $\bar{b}^s$ has $s(p+1)$ orbits not including $\{0\}$ and since $|b^s| = 2r > 2$, $\bar{b}^s \neq \iota_{p^2}$. We conclude that there are at least $2^{s(p+1)}$ graphs of order p^2 in $\mathrm{ACG}(p^2) \setminus \mathrm{Small}(p^2)$. As there are 2^{p-1} non-normal circulant graphs of order p^2 and $s \geq \sqrt{(p-1)/2}$,

$$\lim_{p^2 \to \infty} \frac{|\mathrm{NonNorG}(p^2)|}{|\mathrm{ACG}(p^2) \setminus \mathrm{Small}(p^2)|} \leq \lim_{p \to \infty} \frac{2^{p-1}}{2^{s(p+1)}} = 0.$$

□

We now verify that Conjecture 3.3 does hold for circulant digraphs of order n, and also for circulant graphs of order n, for large families of integers. Note that, using Corollaries 2.10 and 2.17, we have for any n, $|\mathrm{NonNor}(n)| \leq |\mathrm{DW}(n)_{m \geq 4}| + |\mathrm{GW}(n)|$.

Theorem 3.7. *Let n be any odd integer such that $9 \nmid n$. Then almost all circulant digraphs of order n that are not DRRs are normal circulant digraphs.*

Proof. A lower bound for $|\mathrm{ACD}(n) \setminus \mathrm{DRR}(n)|$ is the number of circulant graphs of order n, which is $2^{(n-1)/2}$. We first find an upper bound for $|\mathrm{DW}(n)_{m \geq 4}|$. As n is odd, we have $2n/m \leq 2n/5$. Also, n is an upper bound on the number of nontrivial divisors of n. By Corollary 2.18, $|\mathrm{DW}(n)_{m \geq 4}| \leq \sum_{m|n, m \geq 4} 2^{2n/m} \leq n \cdot 2^{2n/5}$.

By Corollary 2.12, we have $|\mathrm{GW}(n)| \leq \log_2^2 n \cdot 2^{n/p + n/q - n/(pq) - 1}$, where q is the smallest prime divisor of n and p is the smallest prime divisor of n/q. Since n is odd we have $q \geq 3$, and since $9 \nmid n$ we have $p \geq 5$. If $q \geq 5$ then $1/p + 1/q - 1/(pq) < 1/p + 1/q \leq 2/5$, while if $q = 3$ then $1/p + 1/q - 1/(pq) = 2/(3p) + 1/3 \leq 7/15$, so we always have $1/p + 1/q - 1/(pq) \leq 7/15$. Note that if $9|n$ then $p = q = 3$, and this inequality is not true. Then

$$\lim_{n \to \infty} \frac{|\mathrm{NonNor}(n)|}{|\mathrm{ACD}(n) \setminus \mathrm{DRR}(n)|} \leq \lim_{n \to \infty} \frac{n \cdot 2^{2n/5} + \log_2^2 n \cdot 2^{7n/15}}{2^{(n-1)/2}} = 0.$$

□

Theorem 3.8. *Let n be any odd integer such that $9 \nmid n$, and n is not a safe prime or the square of a safe prime. Then almost all circulant graphs of order n that do not have automorphism group as small as possible are normal circulant graphs.*

Proof. We need to show that

$$\lim_{n\to\infty, n\notin T} \frac{|\mathrm{NonNorG}(n)|}{|\mathrm{ACG}(n) \setminus \mathrm{Small}(n)|} = 0,$$

where $T = \{p, p^2 : p \text{ is a safe prime}\} \cup \{n : 9 \mid n\} \cup \{n : 2 \mid n\}$. This is true if n is a prime power by Theorem 3.6, so we assume there is a proper divisor m of n such that $\gcd(m, n/m) = 1$. We also assume that $n/m > m$, and regard $\mathbb{Z}_n$ as $\mathbb{Z}_{n/m} \times \mathbb{Z}_m$ in the natural way.

We begin by finding a lower bound for $|\mathrm{ACG}(n) \setminus \mathrm{Small}(n)|$. Let $\Gamma \in \mathrm{ACG}(n)$ such that $\bar{a} \in \mathrm{Aut}(\Gamma)$ where $a = (1, -1)$. Obviously $\bar{a} \notin \langle \rho, \iota_n \rangle$, so $\Gamma \notin \mathrm{Small}(n)$. Straightforward computations will show that the orbits of $\langle \bar{a}, \iota_n \rangle \leq \mathrm{Aut}(\Gamma)$ are the sets $\{(0,0)\}$, $\{(i,0),(-i,0)\}$, $\{(0,j),(0,-j)\}$, and $\{(i,j),(-i,j),(i,-j),(-i,-j)\}$, where $i \in \mathbb{Z}_{n/m} \setminus \{0\}$ and $j \in \mathbb{Z}_m \setminus \{0\}$. We conclude that $\langle \bar{a}, \iota_n \rangle$ has

$$1 + \frac{n/m - 1}{2} + \frac{m-1}{2} + \frac{n - n/m - m + 1}{4} = \frac{n + n/m + m + 1}{4} > \frac{n}{4}$$

orbits. Hence $|\mathrm{ACG}(n) \setminus \mathrm{Small}(n)| \geq 2^{n/4}$. Recall (by Corollaries 2.10 and 2.17) $|\mathrm{NonNorG}(n)| \leq |\mathrm{DWG}(n)_{m\geq 4}| + |\mathrm{GWG}(n)|$. By Corollary 2.18, we have that $|\mathrm{DWG}(n)_{m\geq 4}| \leq \sum_{m|n, m\geq 4} 2^{n/m+1}$. Since n is odd, m is odd, so $m \geq 5$, so $n/m \leq n/5$, and $\sum_{m|n,m\geq 4} 2^{n/m+1} \leq n2^{n/5+1}$. By Corollary 2.13, we have that $|\mathrm{GWG}(n)| \leq (\log_2^2 n) 2^{n(p+q-1)/(2pq)+1/2}$, where p is the smallest divisor of n and q is the smallest divisor of n/p. As in the proof of Theorem 3.7, it is straightforward to show that since n is odd and not divisible by 9, $(p+q-1)/(pq) \leq 7/15$. Hence

$$\begin{aligned} \lim_{n\to\infty, n\notin S} \frac{|\mathrm{NonNorG}(n)|}{|\mathrm{ACG}(n) \setminus \mathrm{Small}(n)|} &\leq \lim_{n\to\infty, n\notin S} \frac{n2^{n/5+1} + (\log_2^2 n) 2^{7n/30+1/2}}{2^{n/4}} \\ &= 0. \end{aligned}$$

□

4 Non-normal circulants

By Theorem 2.4, a circulant (di)graph that is not normal is generalized wreath or deleted wreath type. For each of these classes, we will now consider whether or not almost all non-normal circulant (di)graphs lie within this class. The short answer is "No" and is given by the following result.

Theorem 4.1. *Let Γ be a circulant digraph of order pq, where p and q are primes and $p, q \geq 5$. Then*

1. *if $q \neq p$ then*

$$\frac{|\mathrm{GW}(pq)|}{|\mathrm{SDW}(pq)|} = \frac{2^{p+q-1} - 2}{2^{2p-1} + 2^{2q-1} - 2^p - 2^q - 2},$$

2. *if p is fixed, then* $\lim_{q\to\infty} |\mathrm{GW}(pq)|/|\mathrm{SDW}(pq)| = 0$,
3. *if $q = p + c$ for some constant $c \geq 2$, then*

$$\lim_{p\to\infty} \frac{|\mathrm{GW}(pq)|}{|\mathrm{SDW}(pq)|} = \frac{2^c}{(1 + 2^{2c})},$$

4. *if $q = p$ then all non-normal circulants are generalized wreath products.*

Proof. Note that for $\Gamma \in \mathrm{SDW}(pq)$ we have $m \in \{p, q\}$ so $m \geq 5$ and $\Gamma \in \mathrm{NonNor}(n)$.

(1): We require exact counts of $|\mathrm{GW}(pq)|$ and of $|\mathrm{SDW}(pq)|$. First, when $n = pq$ a generalized wreath product will actually be a wreath product. For a wreath product digraph with p blocks of size q, there are $q - 1$ possible elements of $S \cap \langle p\rangle$, and $p - 1$ choices for the cosets of $\langle p\rangle$ to be in S. Hence there are 2^{p+q-2} wreath product circulant digraphs with p blocks of size q. Similarly, there are 2^{q+p-2} wreath product circulant digraphs with q blocks of size p. The only digraphs that have both of these properties are K_{pq} and its complement, each of which has been counted twice, so $|\mathrm{GW}(pq)| = 2 \cdot 2^{p+q-2} - 2 = 2^{p+q-1} - 2$.

Now we count strictly deleted wreath products. As mentioned in the first sentence of the proof of Corollary 2.18, there are precisely $2 \cdot 4^{p-1}$ digraphs whose automorphism group contains $K \times S_q$, and $2 \cdot 4^{q-1}$ digraphs whose automorphism group contains $K' \times S_p$. Of the first set, $2 \cdot 2^{p-1}$ are wreath products (those in which $S \cap (rq + \langle p\rangle)$ is chosen from $\{\emptyset, rq + \langle p\rangle\}$, for every $1 \leq r \leq p - 1$). Similarly, of the second set, $2 \cdot 2^{q-1}$ are wreath products (those in which $S \cap (rp + \langle q\rangle)$ is chosen from $\{\emptyset, rp + \langle q\rangle\}$, for every $1 \leq r \leq q - 1$). Finally, notice that if a digraph is counted in both the first and second sets then its automorphism group must contain $S_q \times S_p$. Consequently, the number of elements in $S \cap (rp + \langle q\rangle)$ is constant over r, as is the number of elements in $S \cap (rq + \langle p\rangle)$. Since we have already eliminated wreath products from our count, the first number must be 1 or $p - 1$, and the second must be 1 or $q - 1$. Furthermore, if the first number is 1 then we have $p \in S$ but $p + q \notin S$, so the second cannot be $q - 1$ (and the same holds if we exchange p and q), so there are only 2 choices for such digraphs: that in which all of the values are 1, which is $K_p \Box K_q$ (where $\Box$ denotes the cartesian product), and its complement, in which all of the values are $p - 1$ or $q - 1$. Summing up, we see that $|\mathrm{SDW}(pq)| = 2 \cdot 4^{p-1} + 2 \cdot 4^{q-1} - 2 \cdot 2^{p-1} - 2 \cdot 2^{q-1} - 2$. The result follows.

(2): This follows from (1) by letting q tend to infinity.

(3): Substituting $q = p + c$ into (1) and letting p tend to infinity, we have

$$\lim_{p\to\infty} \frac{|\mathrm{GW}(pq)|}{|\mathrm{SDW}(pq)|} = \lim_{p\to\infty} \frac{2^{c-1} - 2^{1-2p}}{2^{-1} + 2^{2c-1} - 2^{-p} - 2^{c-p} - 2^{1-2p}}.$$

Deleting the terms that tend to zero, we are left with

$$\lim_{p\to\infty} \frac{2^{c-1}}{2^{-1} + 2^{2c-1}} = \frac{2^c}{1 + 2^{2c}},$$

as claimed.

(4): By Theorem 2.4, if $\Gamma \in \mathrm{NonNor}(p^2)$, then $\mathrm{Aut}(\Gamma)$ must either fall into category (1) or category (2). If it falls into category (1) then, since $n = p^2$ and the n_i are coprime, there can only be a single factor in the direct product, and since $\Gamma \in \mathrm{NonNor}(n)$, the factor must be S_{p^2}, so $\Gamma \in \{K_{p^2}, \bar{K}_{p^2}\} \subseteq \mathrm{GW}(p^2)$. If it falls into category (2) then by Corollary 2.10, $\Gamma \in \mathrm{GW}(p^2)$. □

Notice that if we choose a constant $c \geq 2$ and define $T_c = \{pq : q = p+c\}$ where p and q are prime, then as a consequence of Theorem 4.1(3), since $0 < 2^c/(1+2^{2c}) < \infty$, neither generalized wreath circulant digraphs nor strictly deleted circulant digraphs dominates in T_c. The recent breakthrough by Zhang [16] shows that the union of the first 70 million T_cs is infinite, and therefore that at least one of these sets is infinite. Essentially, we have shown that if $n = pq$ is a product of two primes, then generalized wreath products dominate amongst circulant digraphs of order n if $p = q$ (in fact there are no others); neither family dominates if p and q are "close" to each other, and strictly deleted wreath products dominate if one prime is much larger than the other.

We now give two infinite sets N_1 and N_2 of integers, each integer in both sets being divisible by three distinct primes. In N_1, almost all non-normal circulant digraphs are of strictly deleted wreath type (and N_1 includes all of the square-free integers that are not divisible by 2 or 3). Meanwhile in N_2, almost all non-normal circulant digraphs are generalized wreath circulant digraphs.

Theorem 4.2. *Let* $N_1 = \{n \in \mathbb{N} |\ n$ *is the product of at least three primes and* $q^2 \nmid n$ *where* $q \geq 5$ *is the smallest prime divisor of* $n\}$. *Then,*

$$\lim_{n \in N_1, n \to \infty} \frac{|\mathrm{SDW}(n)|}{|\mathrm{NonNor}(n)|} = 1$$

Proof. By Corollaries 2.10 and 2.17, $\mathrm{NonNor}(n) \subseteq \mathrm{GW}(n) \cup \mathrm{SDW}(n)_{m \geq 4}$, and by the definition of $\mathrm{SDW}(n)$, these sets are disjoint. Since $q \geq 5$ we also have $m \geq 5$ for any proper divisor m of n, so $\mathrm{SDW}(n) = \mathrm{SDW}(n)_{m \geq 4}$. Hence $|\mathrm{NonNor}(n)| = |\mathrm{GW}(n)| + |\mathrm{SDW}(n)|$. We show that $\lim_{n \to \infty} \frac{|\mathrm{GW}(n)|}{|\mathrm{NonNor}(n)|} = 0$, which implies the result.

The first sentence of the proof of Corollary 2.18 notes that for a proper divisor m of n, the number of digraphs Γ with $H \times S_m \leq \mathrm{Aut}(\Gamma)$ for some 2-closed group $H \leq S_{n/m}$ is precisely $2 \cdot 4^{n/m-1}$. The maximum number of times that a specific circulant digraph Γ can be counted in $\sum_{m|n} 2 \cdot 4^{n/m-1}$, is the number of divisors of n, $d(n) \leq n$. Thus $|\mathrm{DW}(n)| \geq \sum_{m|n} 2 \cdot 4^{n/m-1}/n$, and so by Lemma 2.16, $|\mathrm{NonNor}(n)| \geq \sum_{m|n} 2 \cdot 4^{n/m-1}/n$. By Corollary 2.12, we have that $|\mathrm{GW}(n)| \leq (\log_2^2 n) 2^{n/p+n/q-n/(pq)-1}$, where q is the smallest prime divisor of n and p is the smallest prime divisor of n/q. Then

$$\begin{aligned}
\lim_{n \to \infty} \frac{|\mathrm{GW}(n)|}{|\mathrm{NonNor}(n)|} &\leq \lim_{n \to \infty} \frac{(\log_2^2 n) 2^{n/p+n/q-n/(pq)-1}}{\sum_{m|n} 2 \cdot 4^{n/m-1}/n} \\
&< \lim_{n \to \infty} \frac{(\log_2^2 n) 2^{n/(q+2)+n/q}}{4 \cdot 4^{n/q-1}/n} \\
&= \lim_{n \to \infty} \frac{n \log_2^2 n}{2^{2n/(q(q+2))}}.
\end{aligned}$$

Since $q(q+2) < n^{2/3}$ as q is the smallest prime factor of n, $q^2 \nmid n$, and n has at least 3 prime factors, we have $n/(q(q+2)) > n^{1/3}$, so $\lim_{n \to \infty} \frac{|\mathrm{GW}(n)|}{|\mathrm{NonNor}(n)|} = 0$. □

Theorem 4.3. *For any natural number* n, *let* p_n *be the smallest prime divisor of* n, *and* q_n *the smallest prime divisor of* n *such that* $q_n \neq p_n$ *and* $q_n^2 \nmid n$. *Let* $N_2 = \{n \in \mathbb{N} : p_n \geq$

$5, p_n^2 \mid n$, n has at least 3 distinct prime divisors, and $q_n > 2p_n\}$. *Then*

$$\lim_{n\in N_2, n\to\infty} \frac{|\mathrm{GW}(n)|}{|\mathrm{NonNor}(n)|} = 1.$$

Proof. Let $p = p_n$. First notice that there are $2^{p-1+n/p-1}$ circulant digraphs that are wreath products $\Gamma_1 \wr \Gamma_2$ where Γ_1 has order n/p and Γ_2 has order p: 2^{p-1} choices for $S \cap \langle n/p\rangle$ and $2^{n/p-1}$ choices for which cosets of $\langle n/p\rangle$ are in S. All of these digraphs are distinct, so since by Lemma 3.4 these are all non-normal, we have $|\mathrm{NonNor}(n)| \geq 2^{p+n/p-2}$.

By Corollary 2.18, for a proper divisor $m \geq p_n > 4$ of n, the number of digraphs of deleted wreath type is at most $4^{n/m}$. Thus

$$|\mathrm{DW}(n)| \leq \sum_{m|n,\gcd(m,n/m=1)} 4^{n/m}.$$

Let $\prod_{i=1}^{t} p_i^{a_i}$ be the prime decomposition of n, and let $p_k^{a_k} = \min_{1\leq i\leq t}\{p_i^{a_i}\}$. Clearly $4^{n/(p_k^{a_k})}$ is the largest term in this sum, and there are at most $d(n)$ (the number of divisors of n) terms in this sum. Thus $|\mathrm{DW}(n)| \leq d(n)\cdot 4^{n/(p_k^{a_k})}$.

Observe that if $a_k \geq 2$, then $p_k^{a_k} \geq 5p > 2p$ since $p \geq 5$ is the smallest divisor of n. Also, if $a_k = 1$, then by hypothesis $p_k \geq q_n > 2p$. Hence $p_k^{a_k} - 2p \geq 1$ since both are integers. Now,

$$\begin{aligned}
\lim_{n\to\infty} \frac{|\mathrm{DW}(n)|}{|\mathrm{NonNor}(n)|} &\leq \lim_{n\to\infty} \frac{d(n)\cdot 4^{n/(p_k{}^{a_k})}}{2^{p+n/p-2}} \\
&< \lim_{n\to\infty} \frac{4n}{2^{p+n\cdot(p_k^{a_k}-2p)/(pp_k^{a_k})}} \\
&\leq \lim_{n\to\infty} \frac{4n}{2^{p+n/(pp_k^{a_k})}}.
\end{aligned}$$

Since n has at least 3 distinct prime divisors, there is some j such that $p_j \neq p, p_k$. Now $p_j^{a_j} > p_k^{a_k}$ by our choice of k, and $p_j^{a_j} \geq p_j > p$, so since $n/(pp_k^{a_k}) \geq p_j^{a_j}$, we have $(n/(pp_k^{a_k}))^2 \geq pp_k^{a_k}$. Hence $pp_k^{a_k} \leq n^{2/3}$, so $n/(pp_k^{a_k}) \geq n^{1/3}$. So the above limit is at most

$$\lim_{n\to\infty} \frac{4n}{2^{p+n^{1/3}}} = 0.$$

□

Acknowledgement: The authors are indebted to the anonymous referees whose suggestions improved the clarity of the proofs as well as the exposition in this manuscript.

References

[1] B. Alspach, Point-symmetric graphs and digraphs of prime order and transitive permutation groups of prime degree, *J. Combinatorial Theory Ser. B* **15** (1973), 12–17.

[2] L. Babai and C. D. Godsil, On the automorphism groups of almost all Cayley graphs, *European J. Combin.* **3** (1982), 9–15.

[3] P. J. Cameron, Michael Giudici, Gareth A. Jones, William M. Kantor, Mikhail H. Klin, Dragan Marušič and Lewis A. Nowitz, Transitive permutation groups without semiregular subgroups, *J. London Math. Soc.* **66** (2002), 325–333.

[4] E. Dobson, Asymptotic automorphism groups of Cayley digraphs and graphs of abelian groups of prime-power order, *Ars Math. Contemp.* **3** (2010), 200–213.

[5] E. Dobson and J. Morris, On automorphism groups of circulant digraphs of square-free order, *Discrete Math.* **299** (2005), 79–98.

[6] S. A. Evdokimov and I. N. Ponomarenko, Characterization of cyclotomic schemes and normal Schur rings over a cyclic group, *Algebra i Analiz* **14** (2002), 11–55.

[7] W. Imrich, Graphs with transitive abelian automorphism group, in *Combinatorial theory and its applications*, Coll. Math. Soc. János Bolyai 4, Balatonfüred, Hungary (1969), 651-656.

[8] K. H. Leung and S. H. Man, On Schur rings over cyclic groups. II, *J. Algebra* **183** (1996), 273–285.

[9] K. H. Leung and S. H. Man, On Schur rings over cyclic groups, *Israel J. Math.* **106** (1998), 251–267.

[10] C. H. Li, Permutation groups with a cyclic regular subgroup and arc transitive circulants, *J. Algebraic Combin.* **21** (2005), 131–136.

[11] L. A. Nowitz, On the non-existence of graphs with transitive generalized dicyclic groups, *J. Combinatorial Theory* **4** (1968), 49–51.

[12] H. Wielandt, *Permutation groups through invariant relations and invariant functions*, lectures given at The Ohio State University, Columbus, Ohio, 1969.

[13] H. Wielandt, *Finite permutation groups*, Translated from the German by R. Bercov, Academic Press, New York, 1964.

[14] H. Wielandt, *Mathematische Werke/Mathematical works. Vol. 1*, Walter de Gruyter & Co., Berlin, 1994, Group theory, With essays on some of Wielandt's works by G. Betsch, B. Hartley, I. M. Isaacs, O. H. Kegel and P. M. Neumann, Edited and with a preface by Bertram Huppert and Hans Schneider.

[15] M.-Y. Xu, Automorphism groups and isomorphisms of Cayley digraphs, *Discrete Math.* **182** (1998), 309–319, Graph theory (Lake Bled, 1995).

[16] Y. Zhang, Bounded gaps between primes, *Annals of Math.* **179** (2014), 1121–1174.

ARS MATHEMATICA CONTEMPORANEA

Also available at http://amc-journal.eu
ISSN 1855-3966 (printed edn.), ISSN 1855-3974 (electronic edn.)
ARS MATHEMATICA CONTEMPORANEA 7 (2014) 519–536

Chamfering operation on k-orbit maps*

María del Río Francos

Institute of Mathematics Physics and Mechanics,
University of Ljubljana, Slovenia,
Jadranska 19, Ljubljana 1000, Slovenia

Received 20 September 2013, accepted 25 September 2014, published online 6 October 2014

Abstract

A map, as a 2-cell embedding of a graph on a closed surface, is called a k-orbit map if the group of automorphisms (or symmetries) of the map partitions its set of flags into k orbits. Orbanić, Pellicer and Weiss studied the effects of operations as medial and truncation on k-orbit maps. In this paper we study the possible symmetry types of maps that result from other maps after applying the chamfering operation and we give the number of possible flag-orbits that has the chamfering map of a k-orbit map, even if we repeat this operation t times.

Keywords: Map, flag graph, symmetry type graph, chamfering operation.

Math. Subj. Class.: 52B15, 05C10, 57M15, 51M20, 52B10

1 Introduction

Topologically, a *map* $\mathcal{M}$ is a cellular embedding of a connected graph on a closed surface, with no boundary. While combinatorially, we define a map by an edge coloured cubic graph $\mathcal{G}_{\mathcal{M}}$, to which we refer as the *flag graph* of the map $\mathcal{M}$, as Lins and Vince (1982-83) define it in [18] and [25], respectively. The vertex set of $\mathcal{G}_{\mathcal{M}}$ is the set of flags of the map, and the edges define the connectivity between pairs of flags. Flags are a very important tool in describing combinatorially the structure of a map. They have been used not only for maps but also for hypermaps [9, 23], maps on the surfaces with boundary [1], abstract polytopes [22] or maniplexes [28].

A map $\mathcal{M}$ is called a k-orbit map if its group of automorphisms, or symmetries, partitions the set of flags into exactly k orbits. The most symmetric maps are well known as *regular* (or *reflexible*) maps, those for which its automorphism group acts transitively on their set of flags, i.e. they have exactly one flag-orbit. Other highly symmetric type of maps

*This paper is a part of Bled'11 Special Issue.

E-mail address: maria.delrio@fmf.uni-lj.si (María del Río Francos)

are the so called *chiral* maps, which flags are partitioned into two orbits in such way that any two adjacent flags belong to different orbits, [12, 13, 22]. In other words, the flag graph of a chiral map is a bipartite graph and each part is an orbit.

In [19] the question of possible symmetry types of maps resulting from other maps after applying various operations was raised. In particular, the medial and truncation operations on k-orbit maps were considered, for $k \leq 4$. In this paper we use the chamfering operation on k-orbit maps and determine, in terms of k, the number of possible flag-orbits that has the chamfering map of a k-orbit map. Table 1 depicts all possible cases.

The operation of *chamfering* an object is related to the idea of beveling ("to file down") the edges of a solid object. Given a map $\mathcal{M}$, the chamfering operation replaces the edges of $\mathcal{M}$ with hexagonal faces while keeping the faces of $\mathcal{M}$. This operation divides each flag of the map $\mathcal{M}$ into four different flags in the chamfering map. This operation is also used on the study of fullerenes (see [6]), for instance, which also leads to chemical applications as in [17]. Theorem 5.3 summarizes all the results presented in this paper.

To solve our problem, we define another graph to which we refer as the *symmetry type graph* of a map, this is, the quotient graph of the flag graph of a map under the action of its automorphism group. A strategy of how to generate symmetry type graphs is shown in [2]. Dress and Huson (1987) refer to such graphs as the Delaney-Dress symbol, [7]. Dress and Brinkmann (1996), as well as Balaban and Pisanski (2012), give applications to mathematical chemistry in [8] and [1], respectively.

In [20], Orbanić, Pellicer, Pisanski and Tucker (2011), show the 14 symmetry type graphs of edge-transitive maps. Later, in [4] and [5], the complete list of possible symmetry type graphs with at most 6 vertices is determined. In particular, in [4] are described some properties of the symmetry type graphs, and also, the advantages of symmetry type graphs were applied to completely solve the problem of symmetry types of medial maps. While, in [5] is given an extension of the results in [19] of all possible symmetry type graphs of a map and its truncated map might have, for up to 7 and 9 vertices.

The paper is organized in the following way. In Section 2, we formally define a map and its flag graph. In Section 3, we define the symmetry type graph of a k-orbit map and give some of its properties, also studied in [4]. In Section 4, we define the chamfering map and find some conditions for the original map as for its chamfering map in manner to determine whether the chamfering map of a k-orbit map has $4k$ flag-orbits or not. Finally, we conclude with Theorems 5.1 and 5.3 where we obtain the number of flag-orbits that the chamfering map has if we repeat this operation t times on the same map.

2 Maps

A *map* $\mathcal{M}$ is defined as a cellular embedding of a connected graph on a surface. Let $\mathcal{BS}$ be the barycentric subdivision of $\mathcal{M}$ and let Φ be a triangle in $\mathcal{BS}$. Label the vertices of Φ by Φ_0, Φ_1 and Φ_2 according to whether they represent a vertex, an edge or a face (mutually incident) in the map $\mathcal{M}$. Note that every triangle of $\mathcal{BS}$ is adjacent to other three triangles, see Figure 1. If two triangles Φ and Ψ of $\mathcal{BS}$ are adjacent by the edge with vertices Φ_j and Φ_k, with $j, k \in \{0, 1, 2\}$ and $j \neq k$, then we say that Φ and Ψ are i-adjacent, for $i \in \{0, 1, 2\}$ and $i \neq j, k$. In this case we shall denote Ψ by Φ^i (likewise Φ by Ψ^i) and note that for every triangle Φ and $i \in \{0, 1, 2\}$, $(\Phi^i)^i = \Phi$.

Combinatorially, a map can be seen as a set $\mathcal{F}(\mathcal{M})$ of *flags*, and the relation between pairs of elements in $\mathcal{F}(\mathcal{M})$ in the following way. To each flag in $\mathcal{F}(\mathcal{M})$, we assign a

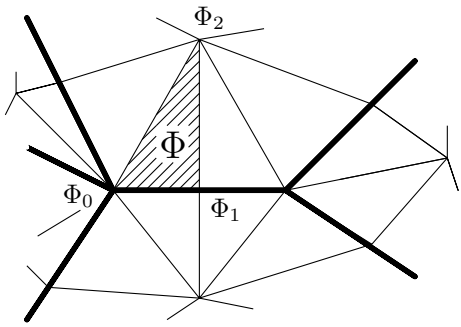

Figure 1: Barycentric subdivision of $\mathcal{M}$ and the flag $\Phi = (\Phi_0, \Phi_1, \Phi_2) \in \mathcal{F}(\mathcal{M})$.

triangle Φ in $\mathcal{BS}$ described by the ordered triple (Φ_0, Φ_1, Φ_2), represented by the vertices of Φ in $\mathcal{BS}$, and denote by Φ^i the corresponding i-adjacent flag of Φ in $\mathcal{M}$, with $i \in \{0, 1, 2\}$. Note that as it happens for the degenerated cases: as a map with a single vertex and edge but two faces, or a map with two vertices, one edge and a face; two adjacent flags can be represented by the same triple, however they are assigned to different triangles. We shall say that a map $\mathcal{M}$ is a non-degenerated map if the triples (Φ_0, Φ_1, Φ_2) are in one to one correspondence to the flags of $\mathcal{M}$.

Let s_0, s_1 and s_2 be the three permutations in the symmetric group $Sym(\mathcal{F}(\mathcal{M}))$ such that, for every flag Φ,

$$\Phi^{s_i} = \Phi \cdot s_i = \Phi^i,$$

with $i = 0, 1, 2$. Note that s_0, s_1, s_2 and $s_0 s_2$ are fixed point free involutions. Furthermore, by the connectivity of the map the action of the subgroup of $Sym(\mathcal{F}(\mathcal{M}))$ generated by these three distinguished involutions, denoted by $\mathrm{Mon}(\mathcal{M}) := \langle s_0, s_1, s_2 \rangle$, is transitive on the set of flags $\mathcal{F}(\mathcal{M})$. The group $\mathrm{Mon}(\mathcal{M})$ is known as the *monodromy (or connection) group* of the map $\mathcal{M}$, [10].

An *automorphism* of the map $\mathcal{M}$ is a bijection between vertices, edges and faces preserving their adjacency on the map. Thus, an automorphism of $\mathcal{M}$ induces a permutation of the flags in $\mathcal{F}(\mathcal{M})$ such that its action commutes with the elements of $\mathrm{Mon}(\mathcal{M})$. In other words, for every automorphism α of $\mathcal{M}$, every flag $\Phi \in \mathcal{F}(\mathcal{M})$ and every $i \in \{0, 1, 2\}$ it follows that

$$\Phi^{s_i}\alpha = (\Phi\alpha)^{s_i},$$

[14]. The connectivity of the map implies that the only automorphism that fixes a flag is the identity one. That is, the action of the automorphism group $\mathrm{Aut}(\mathcal{M})$ over the set $\mathcal{F}(\mathcal{M})$ is semi-regular, and hence divides $\mathcal{F}(\mathcal{M})$ into k orbits of the same size; in such case $\mathcal{M}$ is called a k-orbit map. If the action of $\mathrm{Aut}(\mathcal{M})$ over the set $\mathcal{F}(\mathcal{M})$ is transitive we say that the map is *regular* (or *reflexible*). The 2-orbit maps were widely studied and classified (in different contexts) in [9] and [15]. The most studied and understood type of 2-orbit maps is the *chiral* one, which has two orbits on its flags where any two adjacent flags belong to different orbits.

2.1 Flag graph

Given a map $\mathcal{M}$, we can construct a graph $\mathcal{G}_\mathcal{M}$ in the following way. The set of flags $\mathcal{F}(\mathcal{M})$ of the map $\mathcal{M}$ corresponds to the vertex set of the graph $\mathcal{G}_\mathcal{M}$, and two vertices Φ and Ψ in $V(\mathcal{G}_\mathcal{M})$ are adjacent by an edge of colour $i = 0, 1, 2$ if and only if the corresponding flags are i-adjacent in $\mathcal{M}$ (see Figure 2). We shall refer to the graph $\mathcal{G}_\mathcal{M}$ as the *flag graph* of the map $\mathcal{M}$.

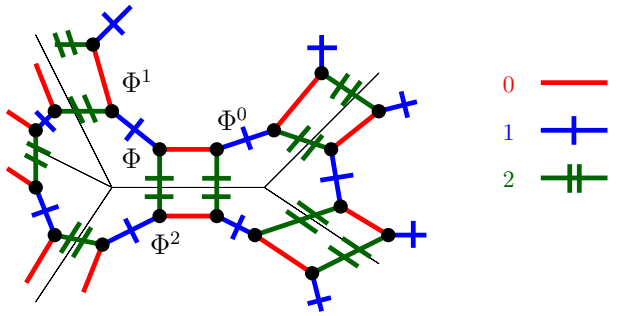

Figure 2: Local representation of the flag graph $\mathcal{G}_\mathcal{M}$ of a map $\mathcal{M}$.

Observe that the distinguished generators s_0, s_1 and s_2 of the monodromy group $\mathrm{Mon}(\mathcal{M})$ of the map $\mathcal{M}$ label the coloured edges of its flag graph $\mathcal{G}_\mathcal{M}$ in a natural way. Hence, for each flag $\Phi \in \mathcal{F}(\mathcal{M})$, a word $w = s_{i_0} s_{i_1} \cdots s_{i_n} \in \mathrm{Mon}(\mathcal{M})$ describes a path along the edges in $\mathcal{G}_\mathcal{M}$, coloured by $i_0, i_1, \ldots, i_n$, starting at the vertex Φ and ending at the vertex Φ^w, with

$$\Phi^w = (\Phi^{i_0}) \cdot s_{i_1} \cdots s_{i_n} =: \Phi^{i_0, i_1, \ldots, i_n}.$$

Since in general the action of $\mathrm{Mon}(\mathcal{M})$ is not semi-regular on $\mathcal{F}(\mathcal{M})$, this implies that one can have differently "coloured" walks in $\mathcal{G}_\mathcal{M}$ going from Φ to another flag Ψ that induce different words of $\mathrm{Mon}(\mathcal{M})$ that act on the flag Φ in the same way.

Note that in $\mathcal{G}_\mathcal{M}$ the edges of a given colour form a perfect matching (an independent set of edges containing all the vertices of the graph), and the union of two sets of edges of different colour is a subgraph whose components are even cycles; such subgraph is known as a *2-factor* of $\mathcal{G}_\mathcal{M}$. In particular, note that since $(s_0 s_2)^2 = 1$ and $s_0 s_2$ is fixed-point free, the cycles with edges of alternating colours 0 and 2 are all of length four.

Note that the connected components of the 2-factor of colours 0 and 2 in $\mathcal{G}_\mathcal{M}$, define the set of edges of $\mathcal{M}$. In other words, the edges of $\mathcal{M}$ can be identified with the orbits of $\mathcal{F}(\mathcal{M})$ under the action of the subgroup generated by the involutions s_0 and s_2; that is, $E(\mathcal{M}) = \{\Phi^{\langle s_0, s_2 \rangle} \mid \Phi \in \mathcal{F}(\mathcal{M})\}$. Similarly, we find that the vertices and faces of $\mathcal{M}$ are identified with the respective orbits of the subgroups $\langle s_1, s_2 \rangle$ and $\langle s_0, s_1 \rangle$ on $\mathcal{F}(\mathcal{M})$. That is, $V(\mathcal{M}) = \{\Phi^{\langle s_1, s_2 \rangle} \mid \Phi \in \mathcal{F}(\mathcal{M})\}$ and $F(\mathcal{M}) = \{\Phi^{\langle s_0, s_1 \rangle} \mid \Phi \in \mathcal{F}(\mathcal{M})\}$. Thus, the group $\langle s_0, s_1, s_2 \rangle$ acts transitively on the sets of vertices, edges and faces of $\mathcal{M}$.

The automorphism group $\mathrm{Aut}(\mathcal{M})$ of $\mathcal{M}$ induces a bijection between the flags of $\mathcal{M}$ preserving their adjacencies, and an edge-coloured preserving automorphism of the graph $\mathcal{G}_\mathcal{M}$ is a bijection between the vertices of $\mathcal{G}_\mathcal{M}$, preserving the adjacencies on the elements of $\mathcal{F}(\mathcal{M})$. Consequently, $\mathrm{Aut}(\mathcal{M})$ is isomorphic to the edge-coloured preserving automorphism group of the flag graph $\mathcal{G}_\mathcal{M}$.

Recall that $\mathrm{Aut}(\mathcal{M})$ partitions the set $\mathcal{F}(\mathcal{M})$ into k orbits of the same size. Let $\mathrm{Orb}(\mathcal{M}) := \{\mathcal{O}_\Phi | \Phi \in \mathcal{F}(\mathcal{M})\}$ be the set of all flag-orbits of $\mathcal{M}$. By the connectivity of $\mathcal{G}_\mathcal{M}$ we have the following lemma.

Lemma 2.1. *Let $\mathcal{O}_1, \mathcal{O}_2 \in \mathrm{Orb}(\mathcal{M})$, $\Phi \in \mathcal{F}(\mathcal{M})$, and $w \in \mathrm{Mon}(\mathcal{M})$. If $\Phi \in \mathcal{O}_1$ and $\Phi^w \in \mathcal{O}_2$, then $\Psi \in \mathcal{O}_1$ if and only if $\Psi^w \in \mathcal{O}_2$, for any $\Psi \in \mathcal{F}(\mathcal{M})$.*

3 Symmetry type graph of a map

We define a graph $T(\mathcal{M})$ (fairly, a pre-graph as in [24]), that we call the *symmetry type graph* of $\mathcal{M}$, as the quotient of the flag graph $\mathcal{G}_\mathcal{M}$, under the action of the automorphism group $\mathrm{Aut}(\mathcal{M})$ of the map. Hence, the vertices of $T(\mathcal{M})$ correspond to the elements in $\mathrm{Orb}(\mathcal{M})$, where two vertices $\mathcal{O}_\Phi, \mathcal{O}_\Psi \in \mathrm{Orb}(\mathcal{M})$ are adjacent by an edge of colour $i = 0, 1, 2$ if and only if there are flags $\Phi' \in \mathcal{O}_\Phi$ and $\Psi' \in \mathcal{O}_\Psi$ that are i-adjacent in $\mathcal{G}_\mathcal{M}$ (if the two i-adjacent flags Φ' and Ψ' belong to the same flag-orbit, then the edge of colour i is projected into a semi-edge in $T(\mathcal{M})$). By Lemma 2.1 the symmetry type graph $T(\mathcal{M})$ is a 3-valent (pre-)graph of chromatic index 3.

It can be seen that the action of $\mathrm{Mon}(\mathcal{M})$ on the set $\mathrm{Orb}(\mathcal{M})$ is defined as $\mathcal{O}_\Phi \cdot w = \mathcal{O}_{\Phi^w}$, for any $w \in \mathrm{Mon}(\mathcal{M})$ and $\Phi \in \mathcal{F}(\mathcal{M})$. This action is transitive, as is the action of $\mathrm{Mon}(\mathcal{M})$ on $\mathcal{F}(\mathcal{M})$. Since $\mathcal{G}_\mathcal{M}$ is a connected graph, then its corresponding symmetry type graph $T(\mathcal{M})$ is connected as well.

The symmetry type graph of regular maps is a graph with a single vertex and three semi-edges of colours 0, 1 and 2. Moreover, the symmetry type graph of chiral maps is a graph with two vertices and three parallel edges coloured by 0 ,1 and 2, connecting both vertices. In fact, chiral maps are commonly said to be of symmetry type 2.

The number of symmetry types of k-orbit maps is bounded by the number of connected cubic graphs with k vertices, properly three edge-coloured, where the colours 0 and 2 are as in the Figure 3. The reader can refer to [4] and [5] for all possible symmetry type graphs with at most 6 vertices.

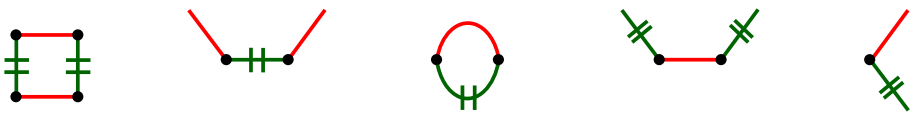

Figure 3: Possible quotients of 0-2 coloured 4-cycles of $\mathcal{G}_\mathcal{M}$.

4 Chamfering map

The chamfering map $\mathrm{Cham}(\mathcal{M})$ of any (non-degenerated) map $\mathcal{M}$ is produced, as its name says: by chamfering the edges in $\mathcal{M}$. More precisely, the edges of a map $\mathcal{M}$ are replaced by hexagonal faces, surrounding the faces of $\mathcal{M}$, in $\mathrm{Cham}(\mathcal{M})$ (see Figure 4). Hence, the set of faces of $\mathrm{Cham}(\mathcal{M})$ is in correspondence with the set of faces $F(\mathcal{M})$ and the set of edges $E(\mathcal{M})$ of $\mathcal{M}$. That is, the set of faces of $\mathrm{Cham}(\mathcal{M})$ is

$$F(\mathrm{Cham}(\mathcal{M})) = F(\mathcal{M}) \cup E(\mathcal{M}).$$

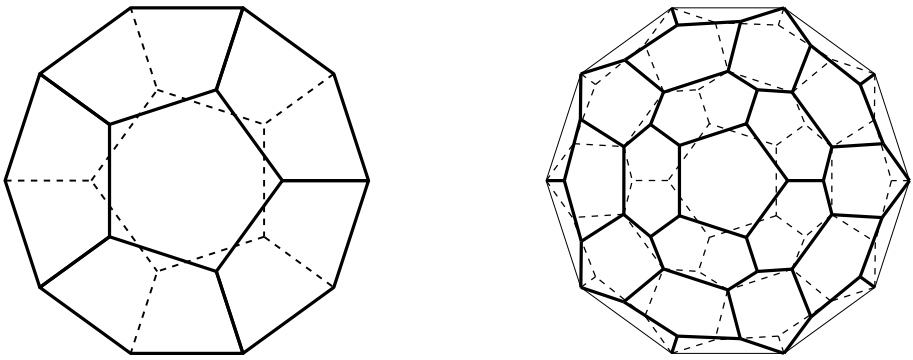

Figure 4: Dodecahedron (left) and the chamfering of the dodecahedron (right).

It is straightforward to see that the map $\mathrm{Cham}(\mathcal{M})$ has two types of edges: those between hexagonal faces and those between a face Φ_2 in $F(\mathcal{M})$ and its adjacent hexagonal faces (corresponding to the incident edges on the face Φ_2 in $\mathcal{M}$). This is, the set of edges of $\mathrm{Cham}(\mathcal{M})$ is

$$E(\mathrm{Cham}(\mathcal{M})) = \{\{\Phi_0, \{\Phi_0, \Phi_2\}\} | \Phi \in \mathcal{F}(\mathcal{M})\} \cup \{\{\Phi_1, \Phi_2\} | \Phi \in \mathcal{F}(\mathcal{M})\}.$$

In fact, $\mathrm{Cham}(\mathcal{M})$ has exactly $4|E(\mathcal{M})|$ edges. Finally, the set of vertices of $\mathcal{M}$ is a proper subset of the vertices of $\mathrm{Cham}(\mathcal{M})$, and the remaining $2|E(\mathcal{M})|$ vertices in $V(\mathrm{Cham}(\mathcal{M})) \setminus V(\mathcal{M})$ (each of these vertices are adjacent to exactly one vertex in $V(\mathcal{M})$), all have degree 3. Thus, the set of vertices of $\mathrm{Cham}(\mathcal{M})$ is

$$V(\mathrm{Cham}(\mathcal{M})) = V(\mathcal{M}) \cup \{\{\Phi_0, \Phi_2\} | \Phi \in \mathcal{F}(\mathcal{M})\}.$$

For an alternative definition of chamfering we refer the reader to [6].

Observe that the map on the left (dodecahedron) in Figure 4 is regular, while the map on the right is a 4-orbit map with symmetry type 4_{D_p} (Figure 5). There is a single orbit of

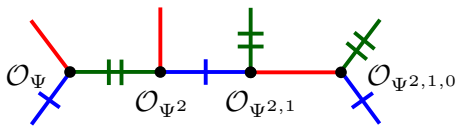

Figure 5: Symmetry type graph 4_{D_p}.

flags, $\mathcal{O}_\Psi$, on a pentagon and three different flags on a hexagon. Note that by chamfering a non-degenerated map $\mathcal{M}$, every flag $\Phi := (\Phi_0, \Phi_1, \Phi_2)$ in $\mathcal{F}(\mathcal{M})$ is divided into four flags of $\mathrm{Cham}(\mathcal{M})$, as is depicted in Figure 6, and the corresponding four flags to $\Phi \in \mathcal{F}(\mathcal{M})$ in $\mathrm{Cham}(\mathcal{M})$ can be written as

$$(\Phi, 0) := (\Phi_0, \{\Phi_0, \{\Phi_0, \Phi_2\}\}, \Phi_1), \qquad (\Phi, 1) := (\{\Phi_0, \Phi_2\}, \{\Phi_0, \{\Phi_0, \Phi_2\}\}, \Phi_1),$$
$$(\Phi, 2) := (\{\Phi_0, \Phi_2\}, \{\Phi_1, \Phi_2\}, \Phi_1), \qquad (\Phi, 3) := (\{\Phi_0, \Phi_2\}, \{\Phi_1, \Phi_2\}, \Phi_2).$$

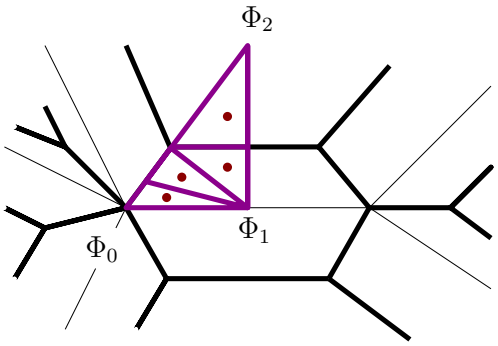

Figure 6: The four respective flags of $\mathcal{F}(Cham(\mathcal{M}))$ to the flag $\Phi = \{\Phi_0, \Phi_1, \Phi_2\} \in \mathcal{F}(\mathcal{M})$.

It is then straightforward to see that the adjacencies of the flags of $\mathrm{Cham}(\mathcal{M})$ are closely related to those of the flags of $\mathcal{M}$. In fact, we have that,

$$\begin{array}{lll}
(\Phi,0)^0 = (\Phi,1), & (\Phi,0)^1 = (\Phi^{s_2},0), & (\Phi,0)^2 = (\Phi^{s_1},0),\\
(\Phi,1)^0 = (\Phi,0), & (\Phi,1)^1 = (\Phi,2), & (\Phi,1)^2 = (\Phi^{s_1},1),\\
(\Phi,2)^0 = (\Phi^{s_0},2), & (\Phi,2)^1 = (\Phi,1), & (\Phi,2)^2 = (\Phi,3),\\
(\Phi,3)^0 = (\Phi^{s_0},3), & (\Phi,3)^1 = (\Phi^{s_1},3), & (\Phi,3)^2 = (\Phi,2).
\end{array}$$

Thus, we define the algorithm in Figure 7 to construct the flag graph of $\mathrm{Cham}(\mathcal{M})$ out of $\mathcal{G}_{\mathcal{M}}$.

Proposition 4.1. *The flag graph $\mathcal{G}_{\mathrm{Cham}(\mathcal{M})}$, of the chamfering map $\mathrm{Cham}(\mathcal{M})$ of any map $\mathcal{M}$, can be quotient into a graph as the symmetry type graph 4_{D_p}.*

Proof. Let $\mathcal{A}_i = \{(\Phi, i) | \Phi \in \mathcal{F}(\mathcal{M})\}$ be the subset of $\mathcal{F}(\mathrm{Cham}(\mathcal{M}))$ containing all flags of $\mathrm{Cham}(\mathcal{M})$ of the form (Φ, i), with $i = 0, 1, 2, 3$. Then, $\mathcal{F}(\mathrm{Cham}(\mathcal{M})) = \mathcal{A}_0 \cup \mathcal{A}_1 \cup \mathcal{A}_2 \cup \mathcal{A}_3$ and $\mathcal{A}_i \cap \mathcal{A}_j = \emptyset$ whenever $i \neq j$. Hence, $(\mathcal{A}_0, \mathcal{A}_1, \mathcal{A}_2, \mathcal{A}_3)$ is a partition of the set of flags $\mathcal{F}(\mathrm{Cham}(\mathcal{M}))$. Based on Figure 7, it is straightforward to see that the quotient of $\mathcal{G}_{\mathrm{Cham}(\mathcal{M})}$ over such partition, is isomorphic to the symmetry type graph of a map with symmetry type 4_{D_p} (see Figure 5). □

Note that for any flags $\Upsilon \in \mathcal{A}_3$, $\Upsilon^2 \in \mathcal{A}_2$, $\Upsilon^{2,1} \in \mathcal{A}_1$ and $\Upsilon^{2,1,0} \in \mathcal{A}_0$, we can define a flag $\Phi_\Upsilon \in \mathcal{F}(\mathcal{M})$, by assembling these four flags in $\mathrm{Cham}(\mathcal{M})$. Observe that an automorphism $\bar{\alpha} \in \mathrm{Aut}(\mathrm{Cham}(\mathcal{M}))$ that sends a flag $\Upsilon' \in \mathcal{A}_i$ to another flag also contained in $\mathcal{A}_i$, with $i = 0, 1, 2, 3$, is induced by an automorphism $\alpha \in \mathrm{Aut}(\mathcal{M})$ that sends $\Phi_{\Upsilon'}$ to the assembled flag $\Phi_{\Upsilon'\bar{\alpha}}$ in $\mathcal{M}$. Say this in other way, for each automorphism $\alpha \in \mathrm{Aut}(\mathcal{M})$, there is an automorphism $\bar{\alpha} \in \mathrm{Aut}(\mathrm{Cham}(\mathcal{M}))$ such that $(\Phi, i)\bar{\alpha} = (\Phi\alpha, i)$, with $\Phi \in \mathcal{F}(\mathcal{M})$ and $i = 0, 1, 2, 3$. Then, it follows that

$$|\mathrm{Orb}(\mathrm{Cham}(\mathcal{M}))| \leq 4|\mathrm{Orb}(\mathcal{M})|.$$

Motivated by Proposition 4.3 of [19], we are interested in studying the number of possible flag-orbits of the chamfering map $\mathrm{Cham}(\mathcal{M})$.

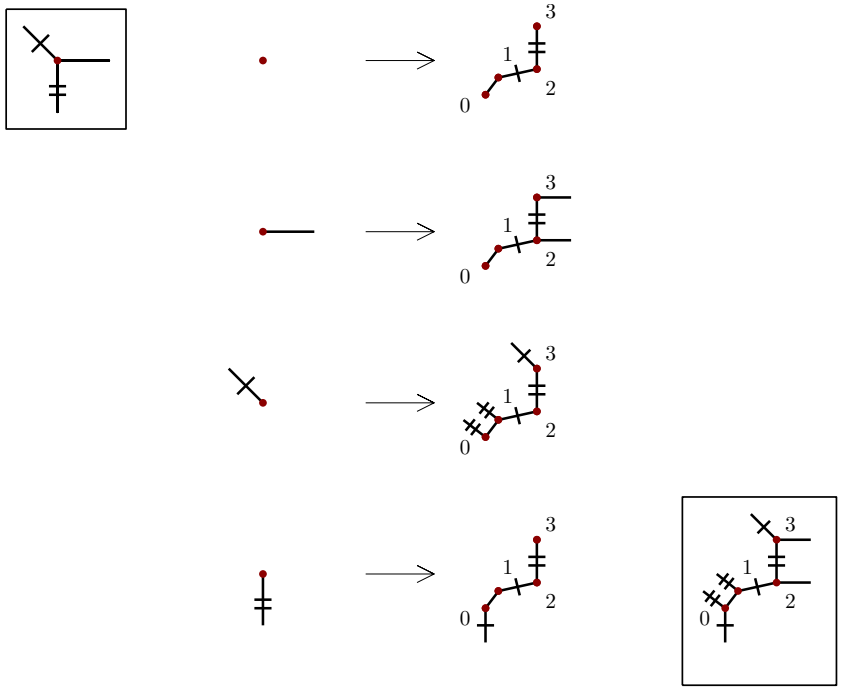

Figure 7: Local representation of a flag in $\mathcal{G}_{\mathcal{M}}$, in the left. The image under the chamfering operation, locally obtained, in the right.

Certainly, the chamfering map $\mathrm{Cham}(\mathcal{M})$, of a k-orbit map $\mathcal{M}$, has $4k$ orbits on the set of flags $\mathcal{F}(\mathrm{Cham}(\mathcal{M}))$, if for any $\Phi, \Psi \in \mathcal{F}(\mathcal{M})$ there is no flag of the form (Φ, i) in the same orbit as a flag of the form (Ψ, j), with $i, j \in \{0,1,2,3\}$ and $i \neq j$. In fact, if the chamfering map $\mathrm{Cham}(\mathcal{M})$ of a k-orbit map $\mathcal{M}$ is a $4k$-orbit map then, the algorithm presented in Figure 7 works as an algorithm on the vertices of $T(\mathcal{M})$ to obtain the symmetry type graph $T(\mathrm{Cham}(\mathcal{M}))$ with $4k$ vertices, of the chamfering map of $\mathcal{M}$.

We denote by r_0, r_1 and r_2 the distinguished generators of $\mathrm{Mon}(\mathrm{Cham}(\mathcal{M}))$. Observe that, in particular, $(\Phi^{s_0}, 3) = (\Phi, 3) \cdot r_0$, $(\Phi^{s_1}, 3) = (\Phi, 3) \cdot r_1$, and $(\Phi^{s_2}, 3) = (\Phi, 3) \cdot r_2 r_1 r_0 r_1 r_0 r_1 r_2$, for any $\Phi \in \mathcal{F}(\mathcal{M})$. This is, the action of the subgroup

$$D = \langle r_0, r_1, r_2 r_1 r_0 r_1 r_0 r_1 r_2 \rangle \leq \mathrm{Mon}(\mathrm{Cham}(\mathcal{M}))$$

over the subset of flags $\mathcal{F}(\mathcal{M}) \times \{3\}$ in $\mathrm{Cham}(\mathcal{M})$ is isomorphic to the action of the monodromy group $\mathrm{Mon}(\mathcal{M})$ over the set $\mathcal{F}(\mathcal{M})$, inducing the following action isomorphism.

$$(f, g) : (\mathcal{F}(\mathcal{M}), \langle s_0, s_1, s_2 \rangle) \to (\mathcal{F}(\mathcal{M}) \times \{3\}, \langle r_0, r_1, r_2 r_1 r_0 r_1 r_0 r_1 r_2 \rangle),$$

where $f : \Phi \mapsto (\Phi, 3)$ is a bijective function, and $g : (s_0, s_1, s_2) \mapsto (r_0, r_1, r_2 r_1 r_0 r_1 r_0 r_1 r_2)$ is a group isomorphism, as that defined in [14]. Then, the action of D is transitive on the set of flags $\mathcal{F}(\mathcal{M}) \times \{3\}$. Moreover, the action of D on $\mathcal{F}(\mathrm{Cham}(\mathcal{M}))$ fixes the set $\mathcal{A}_3$ and permutes the sets $\mathcal{A}_0$, $\mathcal{A}_1$ and $\mathcal{A}_2$. Further on, because

$$(\Phi, 3) \cdot r_2 = (\Phi, 2), \ (\Phi, 3) \cdot r_2 r_1 = (\Phi, 1) \ \text{ and } \ (\Phi, 3) \cdot r_2 r_1 r_0 = (\Phi, 0),$$

conjugating D by the elements r_2, $r_2 r_1$ and $r_2 r_1 r_0$ in $\mathrm{Mon}(\mathrm{Cham}(\mathcal{M}))$, we obtain three different subgroups of $\mathrm{Mon}(\mathrm{Cham}(\mathcal{M}))$, that act transitively on the set of flags $\mathcal{F}(\mathcal{M}) \times \{2\}$, $\mathcal{F}(\mathcal{M}) \times \{1\}$ and $\mathcal{F}(\mathcal{M}) \times \{0\}$, respectively. Therefore, we say that the conjugate subgroup $D^{a_i} \leq \mathrm{Mon}(\mathrm{Cham}(\mathcal{M}))$ fixes the set $\mathcal{A}_i$, for each $i = 0, 1, 2, 3$, and permutes the sets $\mathcal{A}_{j_1}$, $\mathcal{A}_{j_2}$ and $\mathcal{A}_{j_3}$, with $j_1, j_2, j_3 \in \{0,1,2,3\} \setminus \{i\}$, where $a_0 = r_2 r_1 r_0$, $a_1 = r_2 r_1$, $a_2 = r_2$, and $a_3 = id$

With the following lemma we see that the chamfering map of a k-orbit map $\mathcal{M}$, not necessarily has $4k$ flag-orbits. By an *equivelar* map with Schläfli type $\{6, 3\}$ we mean a map that all its faces are 6-gons, and all its vertices have degree 3.

Lemma 4.2. *Let* $\mathrm{Cham}(\mathcal{M})$ *be the chamfering map of a map* $\mathcal{M}$. *If there is an automorphism* $\alpha \in \mathrm{Aut}(\mathrm{Cham}(\mathcal{M}))$ *such that* $(\Phi, i)\alpha = (\Psi, j)$ *for some* $\Phi, \Psi \in \mathcal{F}(\mathcal{M})$ *and* $i \neq j$, *with* $i, j \in \{0,1,2,3\}$. *Then,* $\mathcal{M}$ *is an equivelar map with Schläfli type* $\{6, 3\}$.

Proof. Consider the partition $(\mathcal{A}_0, \mathcal{A}_1, \mathcal{A}_2, \mathcal{A}_3)$ of the set $\mathcal{F}(\mathrm{Cham}(\mathcal{M}))$, where $\mathcal{A}_i = \{(\Phi, i) | \Phi \in \mathcal{F}(\mathcal{M})\}$, $i = 0, 1, 2, 3$, and recall that if we assemble the flags $\Upsilon \in \mathcal{A}_3$, $\Upsilon^2 \in \mathcal{A}_2$, $\Upsilon^{2,1} \in \mathcal{A}_1$ and $\Upsilon^{2,1,0} \in \mathcal{A}_0$, we can define a flag $\Phi_\Upsilon \in \mathcal{F}(\mathcal{M})$.

Suppose that there is an automorphism $\alpha \in \mathrm{Aut}(\mathrm{Cham}(\mathcal{M}))$ such that $(\Phi, i)\alpha = (\Psi, j)$ for some $\Phi, \Psi \in \mathcal{F}(\mathcal{M})$ and $i \neq j$, with $i, j \in \{0,1,2,3\}$. We shall verify the image, under α, of the assembled flags $(\Phi, 0), (\Phi, 1), (\Phi, 2), (\Phi, 3)$, corresponding to $\Phi \in \mathcal{F}(\mathcal{M})$, in terms of the adjacent flags of (Ψ, j). Note that $\Phi_0 \in (\Phi, 0)$ and $\Phi_2 \in (\Phi, 3)$, but they are neither in $(\Phi, 1)$ nor in $(\Phi, 2)$. Then, we have the following cases.

0) For $i = 0$.

- If $(\Phi,0)\alpha = (\Psi,1)$, then $\Phi_0\alpha = \{\Psi_0,\Psi_2\}$ and $\Phi_2\alpha = (\Psi^{2,1})_1$, since $(\Phi,0)\alpha = (\Psi,1) := (\{\Psi_0,\Psi_2\},\{\Psi_0\{\Psi_0,\Psi_2\}\},\Psi_1)$ and $(\Phi,3)\alpha = (\Phi,0)^{0,1,2}\alpha = ((\Phi,0)\alpha)^{0,1,2} = (\Psi,1)^{0,1,2} = (\Psi^{2,1},0) := (\Psi_0,\{\Psi_0,\{\Psi_0,(\Psi^2)_2\}\},(\Psi^{2,1})_1)$.
- If $(\Phi,0)\alpha = (\Psi,2)$, then $\Phi_0\alpha = \{\Psi_0,\Psi_2\}$ and $\Phi_2\alpha = (\Psi^{0,1})_1$, since $(\Phi,0)\alpha = (\Psi,2) := (\{\Psi_0,\Psi_2\},\{\Psi_1,\Psi_2\},\Psi_1)$ and $(\Phi,3)\alpha = (\Phi,0)^{0,1,2}\alpha = ((\Phi,0)\alpha)^{0,1,2} = (\Psi,2)^{0,1,2} = (\Psi^{0,1},1) := (\{(\Psi^0)_0,\Psi_2\},\{(\Psi^0)_0,\{(\Psi^0)_0,\Psi_2\}\},(\Psi^{0,1})_1)$.
- If $(\Phi,0)\alpha = (\Psi,3)$, then $\Phi_0\alpha = \{\Psi_0,\Psi_2\}$ and $\Phi_2\alpha = (\Psi^{0,1})_1$, since $(\Phi,0)\alpha = (\Psi,3) := (\{\Psi_0,\Psi_2\},\{\Psi_1,\Psi_2\},\Psi_2)$ and $(\Phi,3)\alpha = (\Phi,0)^{0,1,2}\alpha = ((\Phi,0)\alpha)^{0,1,2} = (\Psi,3)^{0,1,2} = (\Psi^{0,1},2) := (\{(\Psi^0)_0,\Psi_2\},\{(\Psi^{0,1})_1,\Psi_2\},(\Psi^{0,1})_1)$.

Similarly, we follow the same analysis in the next cases.

1) For $i=1$.

- If $(\Phi,1)\alpha = (\Psi,0)$, then $\Phi_0\alpha = \{\Psi_0,\Psi_2\}$ and $\Phi_2\alpha = (\Psi^{2,1})_1$.
- If $(\Phi,1)\alpha = (\Psi,2)$, then $\Phi_0\alpha = \{(\Psi^0)_0,\Psi_2\}$ and $\Phi_2\alpha = (\Psi^1)_1$.
- If $(\Phi,1)\alpha = (\Psi,3)$, then $\Phi_0\alpha = \{(\Psi^0)_0,\Psi_2\}$ and $\Phi_2\alpha = (\Psi^1)_1$.

2) For $i=2$.

- If $(\Phi,2)\alpha = (\Psi,0)$, then $\Phi_0\alpha = \{\Psi_0,(\Psi^2)_2\}$ and $\Phi_2\alpha = (\Psi^1)_1$.
- If $(\Phi,2)\alpha = (\Psi,1)$, then $\Phi_0\alpha = \{(\Psi^0)_0,\Psi_2\}$ and $\Phi_2\alpha = (\Psi^1)_1$.
- If $(\Phi,2)\alpha = (\Psi,3)$, then $\Phi_0\alpha = \{(\Psi^{1,0})_0,\Psi_2\}$ and $\Phi_2\alpha = \Psi_1$.

3) For $i=3$.

- If $(\Phi,3)\alpha = (\Psi,0)$, then $\Phi_0\alpha = \{\Psi_0,(\Psi^{1,2})_2\}$ and $\Phi_2\alpha = \Psi_1$.
- If $(\Phi,3)\alpha = (\Psi,1)$, then $\Phi_0\alpha = \{(\Psi^{1,2})_0,(\Psi^{1,2})_2\}$ and $\Phi_2\alpha = \Psi_1$.
- If $(\Phi,3)\alpha = (\Psi,2)$, then $\Phi_0\alpha = \{(\Psi^{1,2})_0,\Psi_2\}$ and $\Phi_2\alpha = (\Psi^{0,1})_1$.

Observe from the cases above, that all the vertices $\{\Psi_0,\Psi_2\}$, $\{(\Psi^0)_0,\Psi_2\}$, $\{\Psi_0,(\Psi^2)_2\}$, $\{(\Psi^{1,0})_0,\Psi_2\}$, $\{\Psi_0,(\Psi^{1,2})_2\}$, $\{(\Psi^{1,2})_0,(\Psi^{1,2})_2\}$ and $\{(\Psi^{1,2})_0,\Psi_2\}$ are vertices with degree 3 in $\mathrm{Cham}(\mathcal{M})$. So as all the faces $(\Psi^{2,1})_1$, $(\Psi^{0,1})_1$, $(\Psi^1)_1$ and Ψ_1, correspond to 6-gons in $\mathrm{Cham}(\mathcal{M})$. Thus, the vertex Φ_0 has degree 3 and the face Φ_2 is a 6-gon in $\mathcal{M}$, with $\Phi\in\mathcal{F}(\mathcal{M})$. Furthermore, let $\Phi^w=\Delta\in\mathcal{F}(\mathcal{M})$, with $w\in\mathrm{Mon}(\mathcal{M})$. Then we have that

$$(\Delta,i)\alpha = (\Phi^w,i)\alpha = (\Phi,i)^{\bar{w}}\alpha = ((\Phi,i)\alpha)^{\bar{w}} = (\Psi,j)^{\bar{w}},$$

with $\bar{w}\in\mathrm{Mon}(\mathrm{Cham}(\mathcal{M}))$. Recall that the conjugated subgroup D^{a_i} of $\mathrm{Mon}(\mathrm{Cham}(\mathcal{M}))$ fixes the set $\mathcal{A}_i$ and permutes the sets $\mathcal{A}_{j_1}$, $\mathcal{A}_{j_2}$ and $\mathcal{A}_{j_3}$, with $j_1,j_2,j_3\in\{0,1,2,3\}\setminus\{i\}$, where $a_0=r_2r_1r_0$, $a_1=r_2r_1$, $a_2=r_2$, and $a_3=id$. Since $(\Delta,i)=(\Phi,i)^{\bar{w}}$, it follows that $\bar{w}\in D^{a_i}$, and henceforth $(\Delta,i)\alpha=(\Psi,j)^{\bar{w}}\in\mathcal{A}_{j_k}$, with $j,j_k\in\{0,1,2,3\}\setminus\{i\}$.

Thus, we follow with a similar analysis as the previous one for $(\Delta,i)\alpha=(\Psi,j)^{\bar{w}}$, and we conclude that the vertex Δ_0 has degree 3 and the face Δ_2 is a 6-gon in $\mathcal{M}$. This latter

was for arbitrary $\Delta \in \mathcal{F}(\mathcal{M})$ and $w \in \mathrm{Mon}(\mathcal{M})$. Therefore, we have that each vertex in $V(\mathcal{M})$ has degree 3 and every face $F(\mathcal{M})$ is a 6-gon. Consequently, the map $\mathcal{M}$ is an equivelar map with Schäfli type $\{6,3\}$. □

By the Euler characteristic of a map, the surface of an equivelar map with Schläfli type $\{6,3\}$ is either the torus or Klein bottle. In the following subsection we find the number of flag-orbits of the chamfering of an equivelar map of type $\{6,3\}$.

4.1 Chamfering of equivelar maps of type $\{6,3\}$

In [16] Hubard, Orbanić, Pellicer and Weiss studied the symmetry types of equivelar maps in the torus, described as $\{6,3\}_{v_1,v_2}$, where v_1 and v_2 are two linearly independent vectors. In [27] Wilson shows that there are two kinds of maps of type $\{6,3\}$ in the Klein bottle, and denotes them by $\{6,3\}_{|m,n|}$ and $\{6,3\}_{\backslash m,n\backslash}$ respectively, where the two glide reflections of these maps are on axes that are at distance a multiple of n and have length a multiple of m.

Regarding equivelar toroidal maps of type $\{6,3\}$, from Theorem 8 in [16], we obtain the following proposition.

Proposition 4.3. *Equivelar toroids with Schläfli type $\{6,3\}$ are either regular, chiral, or have symmetry type 3^{02} or 6_{H_p}.*

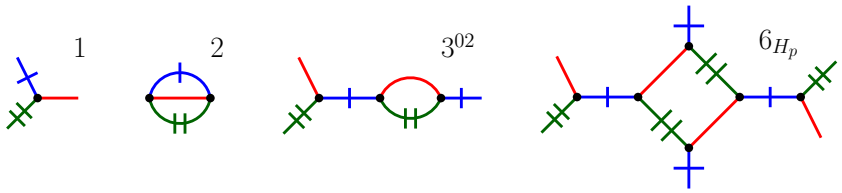

Figure 8: Symmetry type graphs of regular, chiral, 3^{02} and 6_{H_p} maps.

An equivelar toroidal map of type $\{6,3\}$ is described as $\{6,3\}_{v_1,v_2}$, where the linearly independent vectors v_1 and v_2 are a linear combination of the basis $\{\sqrt{3}e_1, \frac{\sqrt{3}}{2}e_1 + \frac{3}{2}e_2\}$, with the origin in the centre of an hexagon in the $\{6,3\}$-tessellation of the plane.

In Figures 9–12 examples of equivelar toroids and their corresponding chamfering maps are depicted. Note that by chamfering a toroidal map $\mathcal{M} := \{6,3\}_{v_1,v_2}$ we replace the edges of $\mathcal{M}$ by the corresponding hexagonal faces in $\mathrm{Cham}(\mathcal{M})$. Thus, the centres of adjacent faces of $\mathrm{Cham}(\mathcal{M})$ are at half distance than in the centres of adjacent hexagons of $\mathcal{M}$. This implies that the chamfering map $\mathrm{Cham}(\mathcal{M})$ is the equivelar toroidal map $\{6,3\}_{2v_1,2v_2}$. Thus, we have the following lemma.

Lemma 4.4. *Let $\mathcal{M}$ be an equivelar toroidal map of type $\{6,3\}$. Then the symmetry type graph $T(\mathrm{Cham}(\mathcal{M}))$ is isomorphic to $T(\mathcal{M})$.*

As what it concerns to equivelar maps of type $\{6,3\}$ in the Klein bottle. Following [27], the two kinds of maps of type $\{6,3\}$ in the Klein bottle are denoted by $\{6,3\}_{|m,n|}$ and $\{6,3\}_{\backslash m,n\backslash}$ respectively, where m and n are measured in
respect to the centres of the hexagons. The map in the Klein bottle, described as $\{6,3\}_{|m,n|}$,

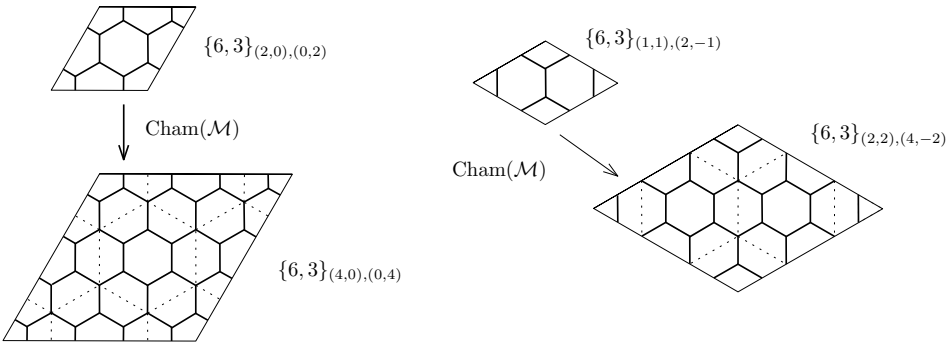

Figure 9: Chamfering of regular toroids of type $\{6,3\}$.

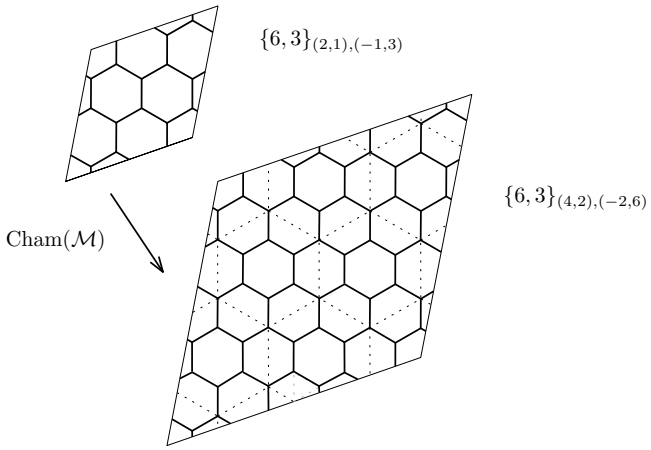

Figure 10: Chamfering of chiral toroids of type $\{6,3\}$.

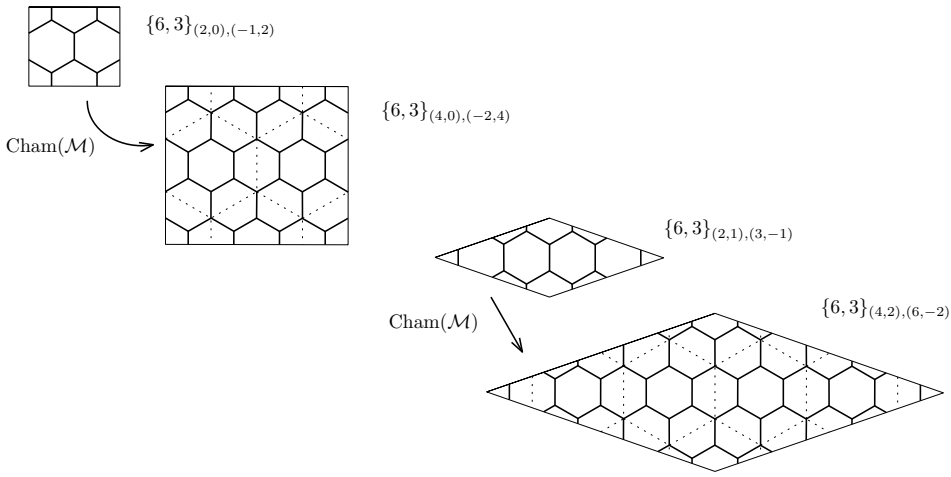

Figure 11: Chamfering of 3-orbit toroids of type $\{6,3\}$.

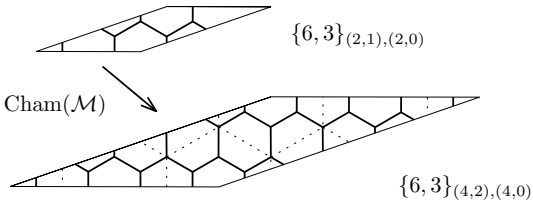

Figure 12: Chamfering of 3-orbit toroids of type $\{6,3\}$.

results by using two glide reflections of length $\frac{m}{2}$ on axes of type (a) or (b), as in Figure 13, that are $n\frac{\sqrt{3}}{2}$ apart. And, the map in the Klein bottle, described as $\{6,3\}_{\backslash m,n\backslash}$, results by using two glide reflections of length $m\frac{\sqrt{3}}{2}$ on axes of type (c) or (d) as in Figure 13, that are $\frac{n}{2}$ apart. In both cases, the generating glide reflections are symmetries of the regular hexagonal tessellation of the plane. Since the glide reflection axes (a), (b), (c) and (d) are either

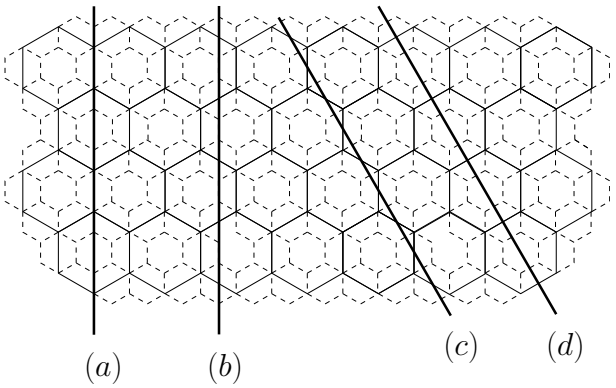

Figure 13: Possible glide reflection axes in $\{6,3\}$.

parallel to the edges of the hexagons or cross the edges in their midpoint, by chamfering an equivelar map $\mathcal{M}$ in the Klein bottle, of type either $\{6,3\}_{|m,n|}$ or $\{6,3\}_{\backslash m,n\backslash}$, the distance between both glide reflection axes and their length are the half than for those in $\mathcal{M}$. This is, in $\mathrm{Cham}(\mathcal{M})$, the values of m and n are the half as those for $\mathcal{M}$. Therefore, the chamfering map $\mathrm{Cham}(\mathcal{M})$ is an equivelar map in the Klein bottle described as $\{6,3\}_{|2m,2n|}$, or as $\{6,3\}_{\backslash 2m,2n\backslash}$, with glide reflection axes of type (a) or (d), respectively.

Hence, we obtain the following lemma.

Lemma 4.5. *If $\mathcal{M}$ is the toroidal map $\{6,3\}_{v_1,v_2}$ or a map in the Klein bottle of type either $\{6,3\}_{|m,n|}$, or $\{6,3\}_{\backslash m,n\backslash}$, then $\mathrm{Cham}(\mathcal{M})$ is a map on the same surface of type $\{6,3\}_{2v_1,2v_2}$, $\{6,3\}_{|2m,2n|}$, or $\{6,3\}_{\backslash 2m,2n\backslash}$, respectively.*

Following [27] we can see that maps $\{6,3\}_{|m,n|}$ and $\{6,3\}_{\backslash m,n\backslash}$ have $3mn$ edges and thereby $12mn$ flags. Moreover, the automorphism group of these maps have $4m$ elements. Thus, the maps $\{6,3\}_{|m,n|}$ and $\{6,3\}_{\backslash m,n\backslash}$ are $3n$-orbit maps. Hence, $\mathrm{Cham}(\{6,3\}_{|m,n|}) = \{6,3\}_{|2m,2n|}$ and $\mathrm{Cham}(\{6,3\}_{\backslash m,n\backslash}) = \{6,3\}_{\backslash 2m,2n\backslash}$ have $48mn$ flags and their respective automorphism group have $8m$ elements. Therefore, $\{6,3\}_{|2m,2n|}$ and $\{6,3\}_{\backslash 2m,2n\backslash}$ are $6n$-orbit maps. In Figures 14 and 15 are depicted examples of maps of type $\{6,3\}_{|m,1|}$ and $\{6,3\}_{\backslash m,1\backslash}$, with m even and odd, and its chamfering maps. Note that both maps of type $\{6,3\}_{|m,1|}$ and $\{6,3\}_{\backslash m,1\backslash}$ have symmetry type 3^{02}, while their chamfering maps $\{6,3\}_{|2m,2|}$ and $\{6,3\}_{\backslash 2m,2\backslash}$ have symmetry type 6_{H_p}.

Corollary 4.6. *If $\mathcal{M}$ is a k-orbit toroidal equivelar map of Schläfli type $\{6,3\}$, then $\mathrm{Cham}(\mathcal{M})$ is a k-orbit map, with $k = 1,2,3,6$. If $\mathcal{M}$ is a k-orbit equivelar map of Schläfli type $\{6,3\}$ in the Klein bottle, then $3|k$ and $\mathrm{Cham}(\mathcal{M})$ is a $2k$-orbit map.*

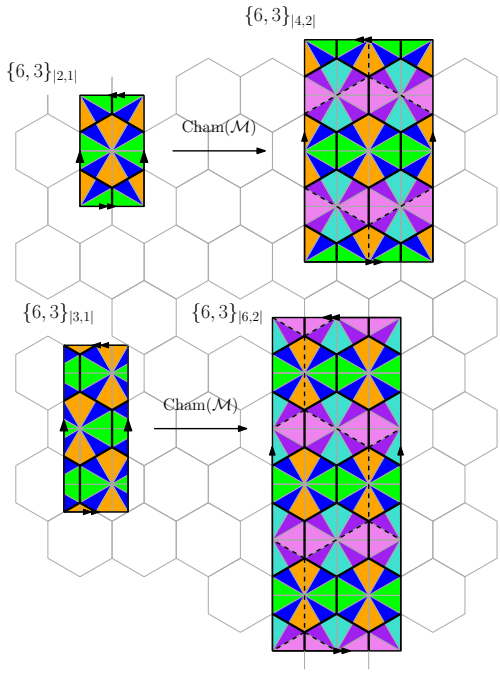

Figure 14: Chamfering of a 3-orbit map of type $\{6,3\}_{|m,1|}$ in the Klein bottle.

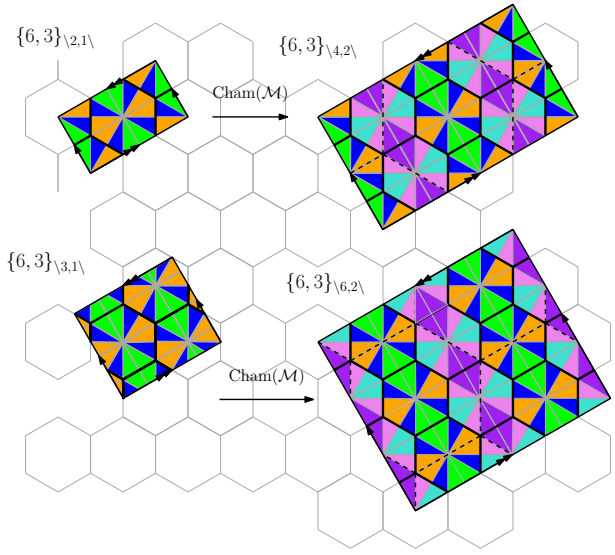

Figure 15: Chamfering of a 3-orbit map of type $\{6,3\}_{\backslash m,1\backslash}$ in the Klein bottle.

5 Conclusion

Putting our results together we see that lemma 4.2 implies that if $\mathcal{M}$ is a k-orbit map such that $\mathrm{Cham}(\mathcal{M})$ is not a $4k$-orbit map, then it is of type $\{6,3\}$. Hence, Corollary 4.6 implies the following theorem.

Theorem 5.1. *Let $\mathcal{M}$ be a k-orbit map. Then, $\mathrm{Cham}(\mathcal{M})$ has either k, $2k$ or $4k$ flag-orbits.*

We denote as $T(\mathrm{Cham}(T'))$ the chamfering symmetry type graph with $4k$ vertices that results from applying the algorithm in Figure 7 to the symmetry type graph T' of a k-orbit map. (See for instance Figures 16). As a consequence of the above discussion we have the following corollary.

Corollary 5.2. *Let $\mathcal{M}$ be a k-orbit map with symmetry type either 1, 2, 3^{02} or 6_{H_p}, and $\mathrm{Cham}(\mathcal{M})$ its chamfering map. Then the following holds.*

(1) If $\mathcal{M}$ is a regular map, then $\mathrm{Cham}(\mathcal{M})$ is either regular of type $\{6,3\}$ (and hence toroidal), or has symmetry type 4_{D_p}.

(2) If $\mathcal{M}$ is a chiral map, then $\mathrm{Cham}(\mathcal{M})$ is either chiral of type $\{6,3\}$ (and hence toroidal), or has symmetry type graph $T(\mathrm{Cham}(2))$ with 8 vertices. (See Figure 16.)

(3) If $\mathcal{M}$ has symmetry type 3^{02}, then $\mathrm{Cham}(\mathcal{M})$ is either a toroidal map of type $\{6,3\}$ with symmetry type graph 3^{02}, or $\mathrm{Cham}(\mathcal{M})$ is a 6-orbit map in the Klein bottle and has symmetry type graph 6_{H_p}, or it has symmetry type graph $T(\mathrm{Cham}(3^{02}))$ with 12 vertices. (See Figure 16.)

(4) If $\mathcal{M}$ has symmetry type 6_{H_p}, then $\mathrm{Cham}(\mathcal{M})$ is either a toroidal map of type $\{6,3\}$ and has symmetry type graph 6_{H_p}, or $\mathrm{Cham}(\mathcal{M})$ is a 12-orbit map in the Klein bottle, or it has symmetry type graph $T(\mathrm{Cham}(6_{H_p}))$ with 24 vertices. (See Figure 16.)

In [6] A. Deza, M. Deza and V. Grishukhin denote by $\mathrm{Cham}_t(\mathcal{M})$ the t-times chamfering of $\mathcal{M}$. It is straightforward to see that $\mathrm{Cham}_t(\mathcal{M})$ of a k-orbit equivelar map $\mathcal{M}$ on the torus is a k-orbit map described as $\{6,3\}_{2^t v_1, 2^t v_2}$. Similarly, $\mathrm{Cham}_t(\mathcal{M})$ of a k-orbit equivelar map $\mathcal{M}$ on the Klein bottle is a $2k$-orbit map denoted either $\{6,3\}_{|2^t m, 2^t n|}$ or $\{6,3\}_{\backslash 2^t m, 2^t n \backslash}$.

Finally, based on the results obtained in the previous section, we conclude with the following theorem.

Theorem 5.3. *Let $\mathcal{M}$ be a k-orbit map and $\mathrm{Cham}_t(\mathcal{M})$ the t-times chamfering map of $\mathcal{M}$ having s flag-orbits. Then at least one of the following holds.*

1. *$s = 4^t k, 2^t k$ or k.*
2. *If $s \neq 4^t k$, then $\chi(\mathcal{M}) = 0$ ($\mathcal{M}$ is on the torus or on the Klein bottle) and $\mathcal{M}$ is of type $\{6,3\}$.*
3. *If $\mathcal{M}$ is on the torus of type $\{6,3\}$ then $s = k$ and $k = 1, 2, 3, 4$.*
4. *If $\mathcal{M}$ is on the Klein bottle of type $\{6,3\}$ then $s = 2^t k$ and $3|k$.*

Furthermore, joining the results obtained for the medial and truncation operations on k-orbit maps, in [19], that motivated the work done for this paper, with the results in obtained for the chamfering operation on k-orbit maps, we obtain the following table.

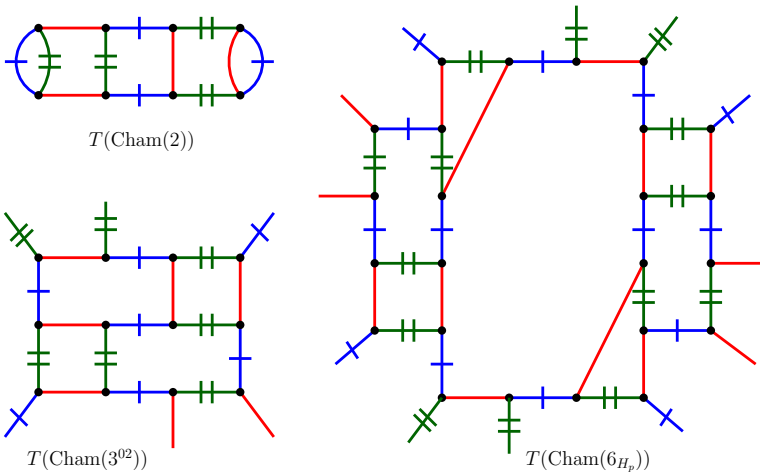

Figure 16: Symmetry type graphs of $\mathrm{Cham}(\mathcal{M})$, with $\mathcal{M}$ of type 2, 3^{02} and 6_{H_p}.

$\mathcal{M}'$	$\mathrm{Me}(\mathcal{M})$	$\mathrm{Tr}(\mathcal{M})$	$\mathrm{Cham}(\mathcal{M})$		
$\lvert\mathrm{Orb}(\mathcal{M}')\rvert$	$2k$ or k	$3k$, $\frac{3k}{2}$ or k	$4k$,	$2k$ $k\vert 3$	or k $k = 1, 2, 3, 6$

Table 1: Possible number of possible flag-orbits of a map $\mathcal{M}'$ with regard to $k = \lvert\mathrm{Orb}(\mathcal{M})\rvert$, where $\mathcal{M}'$ is the medial, truncation or chamfering map of $\mathcal{M}$.

Acknowledgments

The author would like to thank Isabel Hubard and Tomaž Pisanski for many valuable discussions, as well as their support and orientation for the completion of this work. I further acknowledge the partial support from the Slovenian Research Agency (ARRS) for the scholarship granted for my PhD. Part of this work was done during my visit to the Instituto de Matemáticas of the Universidad Nacional Autónoma e México that was supported by PAPIIT-UNAM, grant IN106811.

References

[1] A. T. Balaban and T. Pisanski, Flag graphs and their applications in mathematical chemistry for benzenoids *J. Math. Chem.* **50 (4)** (2012), 893–903.

[2] B. Brinkmann, N. Van Cleemput and T. Pisanski, Generation of various classes of trivalent graphs. *Theor. Comp. Sci.* **502 (2)** (2013), 16–29.

[3] G. Cunningham, M. de Río-Francos, I. Hubard and M. Toledo, *Symmetry type graphs of polytopes and maniplexes,* submitted.

[4] M. del Río-Francos I. Hubard, A. Orbanić and T. Pisanski, Medial symmetry type graphs. *Electronic J. of Comb.* **20 (3)** (2013), P29.

[5] M. del Río-Francos, *Truncation symmetry type graphs,* submitted.

[6] A. Deza, M. Deza and V. P. Grishukhim, Fullerenes and coordination polyhedra versus half-cube embeddings *Disc. Math.* **192** (1998), 41-80.

[7] A.W.M. Dress and D. Huson, On Tilings of the Plane. *Geom. Dedicata,* **24** (1987), 295–310.

[8] A. Dress and G. Brinkmann, Phantasmagorical Fulleroids. *MATCH Commun. Math. Comput. Chem.,* **33** (1996), 87–100.

[9] R. Duarte, *2-Restrictedly-regular hypermaps of small genus*. PhD thesis, University of Aveiro, Aveiro, Portugal, 2007.

[10] J. L. Gross and T. W. Tucker, *Topological Graph Theory*. Wiley Interscience Series in Discrete Mathematics and Optimization, 1987.

[11] M. I. Hartley, All polytopes are quotients, and isomorphic polytopes are quotients by conjugate subgroups. *Disc. Comput. Geom.* **21 (2)** (1999), 289-298.

[12] M. I. Hartley, I. Hubard and D. Leemans, Two atlases of abstract chiral polytopes for small groups. *Ars Math. Contemp.* **5** (2012), 371–382.

[13] I. Hubard and A. I. Weiss, Self-duality of chiral polytopes. *J. Combin. Theory Ser. A* **111 (1)** (2005), 128–136.

[14] I. Hubard, A. Orbanić and A. I. Weiss, Monodromy groups and self-invariance. *Canad. J. Math.,* **61 (6)** (2009), 1300–1324.

[15] I. Hubard, Two-orbit polyhedra from groups. *European J. Combin.,* **31 (3)** (2010), 943–960.

[16] I. Hubard, A. Orbanić, D. Pellicer and A. I. Weiss, Symmetries of equivelar 4-toroids. *Disc. Comp. Geom.***48 (4)** (2012), 1110–1136.

[17] R. B. King and M. V. Diudea,The chirality of icosahedral fullerenes: a comparison of tripling (leapfrog), quadrupling (chamfering), and septupling (capra) transformations. *J. Math. Chem.* **39 (314)** (2006), 597-604.

[18] S. Lins, Graph-Encoded Maps. *J. Comb. Theory, Ser. B* **32 (2)** (1982), 171–181

[19] A. Orbanić, D. Pellicer and A. I. Weiss, Map operation and k-orbit maps. *J. Combin. Theory, Ser. A* **117 (4)** (2009), 411–429.

[20] A. Orbanić, D. Pellicer, T. Pisanski and T. W. Tucker, Edge-transitive maps of low genus. *Ars Math. Contemp.* **4 (2)** (2011), 385–402.

[21] D. Pellicer and A. I. Weiss, Uniform maps on surfaces of non-negative Euler characteristic *Symmetry Cult. Sci.,Symmetry: Culture and Science,Symmetrion,internacional,* 2011.

[22] D. Pellicer, Developments and open problem on chiral polytopes, *Ars Math. Contemp.* **5** (2012), 333–354.

[23] D. Pinto,Duality of hypermaps with symmetric or alternating monodromy group, *Ars Math. Contemp.* **5** (2012), 259–354.

[24] T. Pisanski, A classification of cubic bicirculants. *Disc. Math.* **307 (3–5)** (2007), 567–578.

[25] A. Vince, Combinatorial Maps *J. Combin. Theory, Ser. B* **34** (1983), 1-21.

[26] S. E. Wilson, Operators over regular maps. *Pacific J. Math.,* **81 (2)** (1979), 559–568.

[27] S. E. Wilson, Uniform maps on the Klein bottle. *J. Geom. Graph.* **10 (2)** (2006), 161171.

[28] S. E. Wilson, Maniplexes: Part 1: Maps, polytopes, Symmetry and Operators, *Symmetry* **4** (2012), 265–275.

Author Guidelines

Papers should be prepared in LaTeX and submitted as a PDF file.

Articles which are accepted for publication have to be prepared in LaTeX using class file amcjou.cls and bst file amcjou.bst (if you use BibTeX). These files and an example of how to use the class file can be found at

http://amc-journal.eu/index.php/amc/about/submissions#authorGuidelines

If this is not possible, please use the default LaTeX article style, but note that this may delay the publication process.

Title page. The title page of the submissions must contain:

- Title. The title must be concise and informative.
- Author names and affiliations. For each author add his/her affiliation which should include the full postal address and the country name. If available, specify the e-mail address of each author. Clearly indicate who is the corresponding author of the paper.
- Abstract. A concise abstract is required. The abstract should state the problem studied and the principal results proven.
- Keywords. Please specify 2 to 6 keywords separated by commas.
- Mathematics Subject Classification. Include one or more Math. Subj. Class. 2010 codes – see http://www.ams.org/msc.

References. References should be listed in alphabetical order by the first author's last name and formatted as it is shown below:

[1] First A. Author, Second B. Author and Third C. Author, Article title, *Journal Title* **121** (1982), 1–100.

[2] First A. Author, Book title, third ed., Publisher, New York, 1982.

[3] First A. Author and Second B. Author, Chapter in an edited book, in: First Editor, Second Editor (eds.), *Book Title*, Publisher, Amsterdam, 1999, 232–345.

Illustrations. Any illustrations included in the paper must be provided in PDF or EPS format. Make sure that you use uniform lettering and sizing of the text.

Subscription

Individual yearly subscription:	150 EUR
Institutional yearly subscription:	300 EUR

Any author or editor that subscribes to the printed edition will receive a complimentary copy of *Ars Mathematica Contemporanea*.

Subscription Order Form

Name: .....
E-mail: .....
Postal Address: .....
.....
.....
.....

I would like to subscribe to *Ars Mathematica Contemporanea* for the year 2014.

Individual subscription:	..... copies
Institutional subscription:	..... copies

I want to renew the order for each subsequent year if not cancelled by e-mail:

☐ Yes ☐ No

Signature: .....

Please send the order by mail, by fax or by e-mail.

By mail:	Ars Mathematica Contemporanea UP FAMNIT Glagoljaška 8 SI-6000 Koper Slovenia
By fax:	+386 5 611 75 71
By e-mail:	info@famnit.upr.si

Printed in Slovenia by Birografika Bori d.o.o. Ljubljana